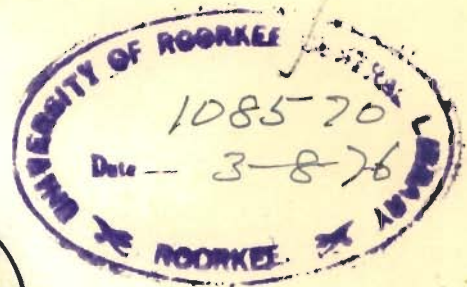# ANALYSIS OF CEMENT CONCRETE OVERLAYS
FOR
PAVEMENT SLABS

BY

S. M. AGRAWAL

A Thesis Submitted in Fulfilment of the Requirements
For the Degree of Doctor of Philosophy
in Civil Engineering

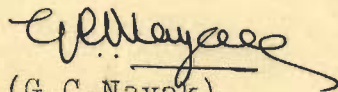### DEPARTMENT OF CIVIL ENGINEERING
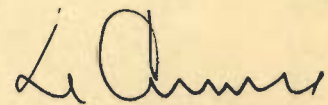UNIVERSITY OF ROORKEE
ROORKEE (INDIA)

September 1975

CERTIFICATE

Certified that thesis entitled 'ANALYSIS OF CEMENT CONCRETE OVERLAYS FOR PAVEMENT SLABS' which is being submitted by Mr. SHYAM MOHAN AGRAWAL in fulfilment of the requirements for the award of the Degree of DOCTOR OF PHILOSOPHY IN CIVIL ENGINEERING OF THE UNIVERSITY OF ROORKEE, is a record of student's own work carried out by him under our supervision and guidance. The matter embodied in this thesis has not been submitted for the award of any other Degree or Diploma.

This is further to certify that he has worked for a period of about three and a half years, from February 1972 to September 1975, for preparing the thesis at this university.

(G.C.Nayak)
B.E.(Hons),M.E.(Struct.)
Ph.D.(Wales),M.ASCE,MIE.,
Professor of Civil Engineering,
University of Roorkee,
Roorkee. U.P. India.

Dated September 10th,1975

(S.K.Khanna)
B.E.,M.E.,Ph.D.,F.I.E.,
Professor of Civil Engineering,
and Head of Highway and
Traffic Engineering Section,
University of Roorkee,
Roorkee.U.P. India.

ACKNOWLEDGEMENTS

Civil Engineering Department for their cordial attitude.

Help of Sri Ram Bahadur in tracing work and Sri Kishan Chand in compilation of thesis is gratefully acknowledged. Sri R.C.Sharma typed the thesis with diligence.

Lastly, several text books and research papers read that might have made indelible impressions but have gone un-mentioned in the list of references, are duly acknowledged.

S.M.AGRAWAL

C O N T E N T S

LIST OF APPENDICES

LIST OF TABLES

LIST OF FIGURES

NOTATIONS

Following notations are generally adopted, unless stated otherwise in the text. All figures, tables and equations are numbered in decimal system e.g. 4.5 refers to 5th figure of fourth chapter. However while refering to them in text of the same chapter it may be refered to as '5' for breivity.

A	=	Area
$[a]$	=	Coefficient matrix
$[B]$	=	Strain matrix
b	=	Super or subscript denoting a quantity relating to base
$[C]$	=	Elasticity matrix
$[D]$	=	Rigidity matrix
E	=	Modulus of elasticity
e_s	=	Shrinkage strain
$\{F\}$	=	Nodal forces
$\{f\}$	=	Vector of reactive forces,
G	=	Shear modulus, Second parameter of generalised foundation model
$\{g\}$	=	Influence field
h	=	Thickness
$H(x)$	=	Hermitian Polynomial
I_x, I_y	=	Moment of Inertia
$[K]$	=	Stiffness matrix

K_c = Fracture toughness

K = Stress intensity factor

k = Modulus of subgrade reaction

ℓ = Radius of relative stiffness

$\{\dot{M}\}$ = Moments

M = Moment

$[N]$ = Shape functions

0 = Super or subscript for denoting a quantity relating to overlay

$\{p\}$ = Active pressure

p = Subgrade reaction

Q = Shear force

q = Shear stress

r = Radius, radius vector

$[S]$ = Stress matrix

t = Temperature

ΔT = Temperature difference between top and bottom

$\{U\}$ = Displacement vector

u,v = Displacement at a point in a continuum

W_i, W_j = Weighting constants of quadrature rule

w = Deflection

x,y = Global coordinates

z = Distance from neutral plane

α = Coefficient of thermal expansion

β = $\sqrt{k/G}$

K_0, β_0 = Bessel's functions

ξ, η = Local coordinates,

$\{\delta\}$ = Nodal displacements

α_{ij} = Coefficient of explicitly integrated element for (i,j)th term

$\{\varepsilon\}$ = Strain components

θ = Temperature

ν = Poisson's ratio

$\{\chi\}$ = Curvature

ψ = Residual Force

$\{\sigma\}$ = Stress components

ε_o, σ_o = Initial strain or stress

τ = Shearing stress

γ = Shearing strain

S Y N O P S I S

Detailed finite element analysis with experimental
verification by model tests, have been carried out in
the present study for cement concrete overlays with
cracked or uncracked base slabs, representing subgrade
through several types of foundation models, for understand-
ing the behaviour of such pavement systems, and in turn
developing an analytical approach for suggesting design
parameters.

Idealised in plane strain, the analysis initially
reported here is to gain insight into the mechanics of
load-deformation and stress distribution of cracked base
with a fully bonded overlay and an overlay with bond
broken in the neighbourhood of the crack.

Based on plane strain analysis, a formulation
is presented for slabs by numerically integrated
Hermitian plate bending finite elements. Sub-element
concept is developed to model economically the crack,
non-uniformity in subgrade support and consistent
nodal loads. Capability to assess the stresses and
displacements due to hydro-thermal changes is also
incorporated in the computer program. Several tests
were applied to check the accuracy of the developed
technique and the computer program. Behaviour of
a single slab with a finite crack and a full length

crack with shear transfer is studied and the results are verified.

A formulation to modify this program for analysis of a bonded overlay is then presented to evaluate stresses and deflections under action of wheel loads, temperature differential and differential shrinkage. Analyses of some cases, with and without crack in the base is reported here to establish the feasibility of bonded overlays, estimate bond and flexural stresses, and study the mechanics of stress distribution.

'Reinforced Key Technique', a method to inhibit the menace of crack reflectance is suggested and its action is brought out based on this study, the fundamental principles of fracture mechanics, and the reported field results.

Similar modification is also formulated and incorporated to study the behaviour of sound or cracked slabs having an unbonded overlay. Comparative behaviour of bonded and unbonded overlays is studied.

The computer program was further modified to consider the subgrade not only as Winkler model but also an elastic continuum. Results of non-linear analysis to consider the subgrade as deformation dependent are presented. The comparison between Winkler and elastic solid models is made. An effective method to incorporate the generalized foundation model, such as due to Pasternak, is

suggested and included in the program. A simple procedure to estimate the second parameter of the two parameter foundation model is given.

Statistical evaluation of proposed method is reported, based on the model tests carried out.

Theory of influence surfaces is included by s a simple addition in the existing computer program to evaluate the critical load positions exactly and economically. It is shown that the same influence surface results can also be used to obtain the influence surfaces for temperature and shrinkage effects for different temperature distributions at any location in a pavement slab.

It is also shown that by adopting a modified procedure, the standard solutions e.g. Westergaard's equation or Pickett's influence charts can still be used for stress computations in rigid pavement slabs which have more than one layer of different properties in bonded or unbonded conditions. Similarly, a procedure is also suggested to correctly evaluate the stresses in base and overlay due to temperature differential by using Bradbury's solution in a modified form. Also, a similar procedure has been suggested for evaluating the shrinkage stresses. For estimating wheel load stresses in cracked base, a procedure based on beams on elastic foundation is suggested.

It is hoped that the present study would help in evolving rational design of rigid overlays for cement concrete pavements incorporating the effects of wheel loads, temperature and shrinkage with particular emphasis on the conditions of the base-overlay systems and their interfaces.

C H A P T E R   I

I N T R O D U C T I O N

1.1 PRACTICE AND PERFORMANCE OF SOME EARLY CEMENT CONCRETE ROADS IN INDIA

The first cement concrete pavement laid in India
was probably in 1920[1]. This was on the sharp curves of
Nainital-Kathgodam road. The thickness of the pavement
slab varied from 10 to 15 cm and the mix used was $1:2.3\frac{1}{2}$.
The foundation consisted of good metalled surface. In
1926-27 a small stretch of about 3/4 of a km is also
reported to have been constructed in Uttar Pradesh . The
thickened edge section adopted for this slab was 22.5 - 15 -
22.5 cm using 1:2:4 cement concrete mix. The foundation
again was of good existing metalled section, however, an
insulation layer of 1.25 cm, thickness is reported to have
been provided by spreading sand. It was realised that
use of this thickness was too conservative and therefore,
in a later construction of 1935-37, 40 km long stretch of
Ghaziabad- Bulandshahar road was concreted using 15-10-15 cm
section. Cross sections as thin as 7.5-5-7.5 cm are reported
to have been adopted in 1937 and later on it became a prac-
tice to provide a uniform thickness of about 10 cm using
proportion of 1:2:4 cement concrete mix . The foundation
always consisted of well compacted metalled section and the

slabs were directly laid on them. .Such slabs are termed as bonded concrete pavement slabs in India.

On Bombay-Poona and Bombay-Nasik roads concreted in 1937, 12.5 cm thick cement concrete slabs are reported to have been laid on 10 to 15 cm of good consolidated Water Bound Macadam section. The subgrade had CBR of 2 to 5 per cent. Each of the two lanes were 3.05 meters wide and the width of shoulders were 0.6 meter on either side. Though bonded concrete slabs were used , on certain portions of the road insulation by using paper was carried out[2].

The city roads of Hyderabad (1928), Chandni Chowk, Delhi (1936), Marine Drive, Bombay (1939) and Central Avenue, Calcutta (1940), carrying intensive traffic are some of the early examples of use of cement concrete for urban roads in India.

The performance of the concrete roads soon proved their usefulness and their construction gained pace. Though the early concrete roads were not designed to any accepted standards [3] and were initially carrying the then prevailing wheel loads, they were required to carry heavy traffic. In case of Bombay- Poona road, for example, which was carrying less than 10,000 tonnes per day[2] at the time of their conc-reting, had to cater for 40,000 tonnes per day in late 60's[4]. During this period of 25-30 years, the pavements performed well, specially looking to the fact that they sustained varied traffic conditions, both during war and peace and

under heavy, mixed (i.e. pneumatic tyred as well as iron tyred) traffic.

Thus, the early cement concrete pavements were having an excellent base, though in certain cases the sub-grade might have been poor, as the practice was to follow stage construction. Though they were relatively thin, they performed well under the prevailing traffic and environmental conditions.

As pointed out above the rapid growth in traffic, both with regard to number of wheel loads as well as its size, has given a new dimension to the problems for existing roads. The roads built. mostly in fourth or fifth decade of this Century, had to carry at the most a five tonner truck then.

The result of the phenomenal post war and post independence increase in traffic is reflected in the form of distress in pavements. To-day, as it stands, most of the cement concrete roads, which were built of 1:2:4 plain cement concrete on old metalled surface with thickness ranging from 7.5 cm to 13 cm , are distressed to varying degrees. There may be different causes or mechanisms that might have led to these manifestiations e.g., fatigue and environmental effects, apart from excessive load. The non-uniform support conditions created by widely existing expansive soils in India are also known to lead to longitudinal cracking[5,6].

1.2 STRENGTHENING OF EXISTING CONCRETE PAVEMENT

The old cement concrete roads and airfield pavements
mostly need strengthening. If it is already distressed, it
would need strengthening to provide safety and comfort to the
vehicular traffic and also to check further damage to the
road surface. If it is in sound condition, even then it
would need strengthening so that the pavement may cater
for the increasing demand of traffic and so that the adv-
antage of its strength can be taken for a longer period of
service. In either case, the answer to the problem is super-
imposing another good layer over the existing one. This
superimposed layer or the overlay, may be of cement concrete
or of bituminous mixtures.

1.2.1 Strengthening by Bituminous Overlays

Long term behavioural studies of composite pavements
have been carried out by Reyll and Corkill[7] in Canada on
stretches having different cross sections in order to
determine the best section. It has been concluded that
under the test conditions the best section had 8 cm of bitu-
minous concrete overlay on a 21cm thick base of unreinforced
cement concrete. It was further observed that a thickness
of upto 10 cm bituminous concrete was insufficient to
bridge the joints, but this did not hamper its riding quality.

Ghosh et. al.[8] found a thin bituminous overlay
upto 2.5 cm to be harmful for existing concrete slab which
requires strengthening, because the temperature differentials

in the slab are found to increase.

It is also shown, on the basis of cost analysis for Delhi region[8], that bituminous overlays are uneconomical. Incidentally. this cost analysis is on the basis of rates prevalent during pre-petroleum price hike period. As such the findings have become all the more valid.

It can therefore be said that a bituminous overlay does not appear to be economical from the point of view of strengthening a concrete slab, so as to save it from distress due to increased wheel loads. Even otherwise; for a cracked cement concrete pavement slab; the bituminous overlay may not be an answer, because in such a case, the overlay is found to fail again unless it is unusually thick[7,8,9,10] making the construction further uneconomical.

1.2.2 Cement Concrete Overlays

The cement concrete overlays enhance the load carrying capacity of the base by adding to its rigidity. There are two basic approaches which govern the construction of cement concrete overlays. One approach is to provide a bond between the base and overlay by a suitable bonding agent. This is termed as bonded overlay. The other approach termed as unbonded overlay is the one in which a thin seperation layer is provided to inhibit bond between the base and overlay. In bonded overlays the bond could be

achieved in many ways e.g. by using a, cementing agent like epoxy resin, giving a neat slurry wash or by acid treatment. Such constructions have been extensively used and have shown excellent performance[11,12].

In design method, the overlay thickness is determined by deducting the existing thickness from the required thickness calculated by standard methods. IRC[10] recommends provision of bonded overlays on 'sound' or 'slightly' cracked bases, but no allowance is suggested to account for cracked condition, even though 'slight'. Controversy also exists regarding the adequacy of bond. Whereas, it has been found that the asperities in base surface develop sufficient bond[13,14,15,16], bond failures in several cases are also reported[11,17], even when the bond strength was high. It is therefore, often felt that unless some mechanical methods to ensure bond are adopted, the bond failure is bound to occur and the bonded overlay can not be recommended[18]. Taneja[19] reports to have provided shear pegs on cracked bases constructed in 1969. The performance of overlay is claimed to be excellent.

Another aspect of bonded overlay is the reappearance of base crack on the overlay surface[11,12,17], like the one in bituminous surfaces. No definite mechanism is assigned to this manifestation. However, it is believed[12,20,21] that the reflection cracking takes place due to horizontal and vertical movements of the base slab.

It is also thought that reflection cracking can be avoided by adopting unbonded construction[20] and therefore, unbonded overlay is recommended on pavement slabs which are moderately cracked[10]. However, it appears that not many case studies are available to justify this recommendation. Besides this, the design methods give an allowance on an intuitional basis[10,19] in the existing base thicknesses to account for the cracks. The unbonded overlays are known to be heavy because of their independent entity. The cost of efforts required to inhibit bond[21] gets added up to the cost of additional concrete to make it even costlier. A minimum separation course of 5 cm thick bituminous material is recommended by IRC[10].

The intermediate category of cement concrete over-lays, known as partially bonded overlays are constructed on existing base without any special surface treatment except careful cleaning and washing. Though laboratory studies indicate sufficient shearing strength to develop in such cases[13,16], the required strength is not known. These overlays are recommended on fairly cracked bases[10]. Different agencies like, Portland Cement Association, U.S. Corps of Engineers, etc. have recommended different design formulae for this case because of the uncertainty of bond[20].

A method suggested for overlays on 'badly' cracked pavements is to completely break it up and lay the overlay

after broken slab is reseated by heavy rolling[22]. No
special design method is suggested because, probably
such a case only means a stiff elastic foundation. However,
it can be argued that breaking the old slab not only means
additional cost to be incurred on breaking but also loss
of residual strength.

1.3 EXISTING ANALYSIS FOR PAVEMENT SLABS

The existing solutions for the analysis of rigid
pavements can be classed in two categories, depending upon
the foundation model assumed to represent the interaction
of the slab with the subgrade. The model formulated by
Winkler[23] has been adopted by Westergaard[24] in his
classical analysis. The other model, in which the subgrade
is treated as an elastic half space has been adopted for
stress analysis by Biot, Pickett, Hogg, Hall, Losberg[25,26,27,28,29]
and others. Vesic and Saxena[30] observe that treating
the subgrade as elastic half space gives results which
are closer to reality, though values as obtained by
Winkler subgrade model are conservative.

Another distinction between the theories is the
basis of analysis. In those advanced by Westergaard,
Pickett, Hall, Hogg[24,26,27,28], the analysis is based
on elastic theory and the design on working stresses. On
the other hand Losberg, Mayerhof , Ghosh[29,31,32] have
adopted ultimate strength or yield line theories to obtain

the upper bound limit on loads. Such an analysis might have better applicability to reinforced concrete slabs where the loads are of the order sufficient to develop yielding in reinforcement under the load. It is corroborated by experimental results of Losberg[29] that for stresses of the order lesser than these the elastic theory is valid. Therefore, for the plain cement concrete slabs, as practised in India, the use of elastic theory seems to be valid.

One common feature of all these theories is the assumption of the pavement slab as a uniform, homogeneous and isotropic layer of infinite extent in horizontal plane resting on a uniform bed. Deviation from these assumptions have also been reported. Hudson and Matlock[33] have reported numerical solution of a pavement problem with actual panel dimensions. In this case the subgrade may have varying support characteristics at different places in a panel and there may be a void or a gap. The method suggested by them[33] treated the subgrade as a Winkler model. The discrete element method[34] is a variation of finite difference technique well known for plate problems[35,36]. The use of grillage or interconnected beam models has been usual for solving plate problems[37]. In the discrete element model, as well, the slab is represented by interconnected beams and bars. The foundation is represented by springs attached to crossing points of these beams and the wheel

loads are supposed to be acting as point loads at these points. This numerical method was extended by Saxena[38] for the subgrade regarded as uniform elastic continuum.

Discrete element method is also extended to solve the problem of lifting of the slab when acted upon by wheel loads[39]. Ayyash and Hudson[40,41] modified the earlier approach of Hudson and Matlock[33] to analyse a continuously reinforced concrete pavement (CRCP) slab containing cracks. Modelling of the crack was based on the assumption that the stress release has an effect upto a distance of 30 cm (one foot) and they found that the moments increased due to the presence of a crack. Findings of Niu[42] have also been similar . He has given a solution for the stresses and deflections due to a uniformly distributed load in a large slab resting on liquid subgrade and containing a crack which extends to infinity on both sides.

Moment distribution methods[43,44] and variational principles such as those due to Vlasov, Ressiner, Rayleigh-Ritz or Galerkin have also been adopted for solving the problems of beams and plates on plastic foundation[45,46,47].

1.4 THE PROBLEM ASSOCIATED WITH THE ANALYSIS OF RIGID OVERLAYS FOR PAVEMENT SLABS

There are two distinct cases in which the cement concrete overlay of any type discussed above need analysis, one is with uncracked base and the other containing cracks.

Some methods of analysis are available for the first case, but there is no report regarding the analysis of overlays of either type on cracked bases. Numerous field studies have reported frequent failures of overlays on cracked base[11,12,17,20] however no attempt seems to have been directed towards studying the mechanics.

In case of bonded overlays, the bond failure is often reported in overlays well bonded to the base, but explanations are lacking. The only remedial measures that appear to have been suggested to prevent failure of overlay on cracked base in flexure and bond appear to be either in designing the system as unbonded or in providing reinforcement. Even in this case how much and where the reinforcement should be provided is not well known. As regards unbonded overlays, while not many results of field studies are available to justify their recommendation, the theoretical treatment in this regard also lacks. The remedial measures adopted against bond failure depend mostly on intuition.

In another method suggested in which the cracked pavement is broken up and rolled, the controversy again exists regarding its effectiveness and economy. Since no method exists to analyse the overlay on cracked pavement, it is not possible to compare the advantages of providing unbonded overlays vis-a-vis breaking up the old slabs and reconstructing.

Even in case of overlays on bases free of distress, the rational methods of analysis and design do not exist by which distribution of flexural stresses could be estimated, specially where the elastic properties of base and overlay differ in bonded and unbonded construction. Rational estimation of interfacial shear stresses between base and overlay with due regard of temperature stresses in such pavement systems is also not possible.

The need therefore is to develop a realistic method for assessing the stresses and displacements of a rigid pavement system, which may be of one or more layers incorporating the following conditions :

(i)   The elastic properties and thicknesses of these layers need not necessarily be same.

(ii)   One or more of the layers may possess cracks of any size anywhere in the system.

(iii)   The interface between the layers may be either bonded or unbonded.

(iv)   The thickness of the layers may vary in section as in case of thickened edge pavement.

(v)   Any of the layers may have reinforcement either in its entire length or in a part of it.

(vi)   The subgrade may be regarded as a Winkler model Hookean model, nonlinear model or generalised

foundation model to account for shear interaction
in case of stiff subgrades.

(vii)   The wheel loads should be truly represented and
        may act anywhere on the system. It should be
        possible to take effect of gear configuration.

(viii) The effects of temperature changes should be given
        due cognizance.

1.5   METHOD OF APPROACH

As is true for any problem, the two alternatives
to study the structural response of a system could be
an experimental study or theoretical analysis. Some exper-
imental studies on full scale have already been carried
out [11,48]. However, there is still need to have studies
specially directed in this direction, with well instru-
mented slabs. The outcome may be enlightening and reliable
but the results may have their applications for the narrow
range of experimental conditions, as is the case with
empirical methods. A study based on sound theoretical
analysis and supplemented by experimentation is the best
course.

Nature of the problem as posed above is extre-
mely complicated even in its most simplified form. The
boundary conditions are too involved to be incorporated
in any closed or open form general solution. In recent
years, finite element method has emerged as a powerful
technique capable of handling complicated boundary conditions.

It is proposed to adopt this technique for evolving a suitable method for the solution of the present problem. An experimental verification is also intended to assess the validity of the formulation and its basic assumptions.

1.6 SCOPE OF THE STUDY

In the second chapter, some of the principles of the finite element method are described, studying the various forms and their applicability to the pavement problem, as the formulation of the intended solution is based on this.

The third chapter gives a description of basic studies carried out for some of the models of pavements in plane strain condition using finite element technique. The results of this study generate insight into the mechanics of stress distribution occurring in the vicinity of the crack. A method of "Reinforced Key Technique" is proposed to arrest the reflection cracking. The results of the basic study in third chapter is useful in formulating an economical model for solving a pavement system as plate resting on a suitable foundation. The formulation in detail is described in the fourth chapter to account for wheel loads, temperature stresses, cracks in slab etc, as realistically as possible to represent them through finite element model.

The stress analysis of a bounded overlay is taken up in the fifth chapter, while in the sixth chapter analysis of unbounded overlays are carried out. Formulation proposed in fourth chapter is modified to solve the problem of overlays. Flexural and interfacial shearing stresses are calculated and mechanics of their distribution and role is examined. A simple approach to determine these stresses rationally in sound base overlay system is proposed. A simplified procedure based on beams on elastic foundation theory is also proposed to get an idea about the magnitude of bond and flexural stresses in cracked systems.

The seventh chapter includes a detailed study of the implications of a foundation model[49]. Also the modification necessary in the proposed method is included for application to cases of Boussinesq type models, generalized foundation models and the nonlinear cases when loss of contact with foundation may take place due to wheel loads or environmental effects.

A comparison of the results of the proposed method to the observed behaviour of model slabs is shown in the eighth chapter in order to substantiate the theoretical formulation.

Realising that influence surfaces are economical tools for handling complex gear configurations, it is

attempted to indicate in the ninth chapter how the method can be applied for generating them.

Finally the conclusions of the study are listed in the last chapter.

CHAPTER II

BASIC CONCEPTS OF FINITE ELEMENT METHOD AND ITS APPLICATION TO PAVEMENT PROBLEM

2.1 DEVELOPMENT OF FINITE ELEMENT METHOD

Finite element method can be viewed in different perspective. Therefore, different authors have traced its development in different ways. Martin and Carey and Oden[51,52] attribute this development to ancient days when for measurement of the perimeter of a circle, the circle was approximated by a polygon. Thus, in those days attempts were made to determine the value of π by either an inscribed or a circumscribed polygon and depending on these either a lower bound or upper bound values were obtained. Naturally convergence was achieved by increasing the number of elements i.e., the sides of the polygon. Thus the view taken is, that the basis of finite element method is essentially going from 'Part to Whole[34].

Holland[53] credits Courant[55] as a pioneer in this field and Zienkiewicz[54] also acknowledges it. Courant solved the problem of torsion using a method, which in essence is similar to finite element method, viewed as based on energy principles. His work was followed by that of Prager and Synge[56].

The use of matrix methods for solution of structural engineering problems has been very well known. Engineers, developed the finite element method viewing it as another version of matrix method applied to continuum[57,58]. However, the credit of giving the final shape to this method is attributed to Turner, Clough , Martin and Topp[59].

There are three types of stiffness approaches in finite element method. These are based on

(a) displacement variation,
(b) stress variation, and
(c) mixed.

Though the initial application and development of the finite element method was for plane stress problems, like plates with in-plane forces, it soon became apparent that with only a minor change in material property representation, based on the theory of elasticity, the same could serve for plane strain problems as well. Similarly, development and application of the method to axisymmetric problems and problems of plate like models, subjected to out of plane loads, as well as for a three dimensional general solid followed the logical sequence.

The advancement continued in the direction to modify the more basic elements like constant strain triangles, so as to yield better efficiency, i.e. towards

-19-

developing such elements which will require handling of less number of equations so as to save on valuable computer time and space, the desired accuracy remaining the same. The attempts also continue to have elements of such shapes as to fit into arbitrary geometry, reducing the approximation and thus increasing the accuracy and efficiency. This search led to the elements with

    (i) improved interpolation functions including higher order polynomials,

   (ii) greater number of nodes and degrees of freedom per element,

  (iii) curved shapes.

2.2 APPLICATION OF THE METHOD

Apart from application to the problem of structural engineering and elasticity, the finite element method has been applied to problems like, fluid flow, creep, fracture, heat flow, electromagnetic fields, nuclear technology etc. The possibility of its application to the complex problems in these fields and many others, which involve nonhomogeneity, nonlinearity and discontinuity has attributed largely to the popularity of this method. The adoption of this method in such complex situations is possible, because the element system, called finite element mesh, can be so designed as to accommodate most of these arbitrary variations.

2.3 BASIC IDEAS

2.3.1 Stiffness

Fundamental to any matrix displacement method is the determination of the stiffness of the structural element or the load necessary for a unit displacement. The concept of 'spring stiffness' can be used to illustrate this basically.

If there is a bar, with one end fixed and other free the elongation Δ is given by

$$\Delta = K\ P$$

where, $K = A\ E/L$ = stiffness for uniform member of length 'L', cross-sectional area 'A' and modulus of elasticity 'E'.

The determination of the stiffness value 'K' may not be as straight forward for a two dimensional continuum element as for a single bar element. If an attempt is made on this basis, then the deformation along the common boundaries of the adjacent elements may not match, though they may match at the nodal points at which the elements are supposed to be connected like members in a frame work. This may lead to discontinuities, overlaps and stress concentrations. Therefore, the adjoining elements must act in unison, in a restricted manner. As such, a restriction is imposed on the deformation pattern by prescribing a shape function for each of the deformations or the degrees of freedom for a node.

2.3.2 Displacement Variation

This function is such that the displacement at any point within the element, including the boundaries is a function of the nodal displacement. These displacement patterns, known as shape functions, are the kernel of the method. Their choice greatly affects the efficiency of the analysis, because they form the foundation for establishing the necessary algebraic equations. These functions, which are nothing but an assumed functional for approximating the exact solution, are usually taken in the form of polynomials.

If the functional assumed is $[N]$, then for any element

$$\{U\} = [N]\{\delta\} \qquad \ldots 2.1$$

where,

$\{U\}$ = displacement of any point within the element boundaries,

$\{\delta\}$ = vector of nodal displacements.

As a general rule for interpolation, a higher order polynomial is a better approximation towards convergence, but the computation time increases. Therefore, a compromise between the two is the rule for obtaining an efficient mean. Generally the terms contained in the polynomial are such that following conditions are satisfied.

(i) The rigid body displacements should be realistically permitted.

(ii) Constant state of strain within the element should be possible to be represented.

(iii) The compatability of deformations with adjacent elements at their common boundaries must hold.

Veubeke[60] has shown that if the assumed functional satisfies the above requirements, then the strain energy of the whole system in the displacement model, represents the lower bound to the actual strain energy. This, in other words, means that the coefficients of the stiffness matrix as obtained by the variational principle applicable to the displacement model can be expected to be numerically a larger value and the obtained static influence coefficients smaller than their true value. However, it has also been shown that by increasing the total degrees of freedom of the system the two tend to converge. This result has been verified for any particular assumed functional by conducting numerical experimentations.[34,54]

It may not always be possible to adopt such displacement models which fully satisfy all above requirements. Some times it may be of advantage to use such formulations which are non-conforming[61] but then, the bound on the results can not be guaranteed.

2.3.3 Strain Displacement Relationship

If,

$\{\varepsilon\}$ = components of strain at a point which contributes to internal work,

$$\{\varepsilon\} = \left\{ \begin{array}{c} \dfrac{\partial u}{\partial x} \\[2mm] \dfrac{\partial v}{\partial y} \\[2mm] \dfrac{\partial v}{\partial x} + \dfrac{\partial u}{\partial y} \end{array} \right\} \qquad \ldots \; 2.2$$

then the individual strain components can be derived from strain-displacement relationship[62] and then, it is possible to write from equation 2.1 for a plane strain problem at any point (x,y) in the element, with reference to its local coordinate axes,

$$\{U\} = \left\{ \begin{array}{c} u \\ v \end{array} \right\} = [N]\{\delta\}$$

$$\{\varepsilon\} = \left\{ \begin{array}{c} \dfrac{\partial u}{\partial x} \\[2mm] \dfrac{\partial v}{\partial y} \\[2mm] \dfrac{\partial u}{\partial y} + \dfrac{\partial v}{\partial x} \end{array} \right\} \qquad \ldots \; (2.3)$$

$$= [B]\{\delta\} \qquad \ldots \; (2.4)$$

The matrix $[B]$ of equation 2.4 will be of the form

$$[B]_a = \left[\begin{array}{cc} \dfrac{\partial N_a}{\partial x} & 0 \\[2mm] 0 & \dfrac{\partial N_a}{\partial y} \\[2mm] \dfrac{\partial N_a}{\partial y} & \dfrac{\partial N_a}{\partial x} \end{array} \right] \qquad \ldots \; (2.5)$$

where, the subscript 'a' denotes that the quantities relate to the node 'a' of the plane strain element.

2.3.4 Stress-Strain Relationship

The stresses $\{\sigma\}$ at any point (x, y) in the element can again be written as

$$\{\sigma\} = [D]\{\varepsilon\} - [D]\{\varepsilon_0\} + \{\sigma_0\} \qquad \ldots 2.6$$

where $[D]$ = Elasticity matrix[62].

For a plane strain case proposed to be analysed in Chapter III

$$[D] = \frac{E(1-\nu)}{(1+\nu)(1-2\nu)} \begin{bmatrix} 1 & \frac{\nu}{(1-\nu)} & 0 \\ \frac{\nu}{(1-\nu)} & 1 & 0 \\ 0 & 0 & \frac{(1-2\nu)}{2(1-\nu)} \end{bmatrix} \qquad \ldots 2.7$$

where,

E = = modulus of elasticity of the continuum,

ν = value of its Poisson's ratio,

$\{\varepsilon_0\}$ = initial strains,

$\{\sigma_0\}$ = initial stresses.

It can therefore be seen that once the nodal displacements are known the displacements, strains and stresses at any point can be determined by using equations 2.1, 2.4 and 2.6 respectively.

2.3.5 Equilibrium Equations

The principle of Virtual Work can be applied.

From equations 2.1 and 2.4

$$d\{U\} = [N] \, d\{\delta\} \qquad \dots 2.8$$

and $\quad d\{\varepsilon\} = [B] \, d\{\delta\} \qquad \dots 2.9$

The work done by the applied nodal forces $\{F\}$ during any virtual displacement $d\{\delta\}$ must equal the internal work due to stresses $\{\sigma\}$ and distributed loads $\{p\}$. Therefore,

$$d\{\delta\}^T\{F\} = \int d\{\varepsilon\}^T\{\sigma\}dv - \int d\{U\}^T\{p\} \, dv,$$

$$= d\{\delta\}^T \int [B]^T\{\sigma\}dv - d\{\delta\}^T \int [N]^T\{p\} \, dv, \text{ from}$$

2.8 and 2.9.

Therefore, from equations 2.6 and 2.4,

$$\{F\} = \int [B]^T[D][B]dv\{\delta\} - \int [B]^T[D]\{\varepsilon_o\}dv$$

$$+\int [B]^T\{\sigma_o\}dv - \int [N]^T\{p\}dv \qquad \dots 2.10$$

2.3.6 Nodal Loads

The nodal forces based on work equivalency then become,

(i) Due to pressure loadings and body forces

$$\{F\}_p = -\int [N]^T\{p\}dv \qquad \dots 2.11$$

(ii) Due to initial strains like hydro-thermal strains in cement concrete pavements,

$$\{F\}_{\epsilon_0} = -\int [B]^T [D] \{\epsilon_0\} dv \qquad \ldots 2.12$$

(iii) Due to initial stresses like those due to excavation etc.

$$\{F\}_{\sigma_0} = \int [B]^T \{\sigma_0\} dv \qquad \ldots 2.13$$

The stiffness [K] then becomes

$$[K] = \int [B]^T [D] [B] dv \qquad \ldots 2.14$$

Determination of proper values of nodal forces is an important matter, because the loads as have been treated in the previous article are discrete values. It will seldom happen that the applied loads will lie on the nodes itself. One of the obvious possibilities of finding the nodal loads, is regarding them as static equivalent of neighbouring loads, lumped at nodes. Such a formulation is called 'lumped nodal load formulation'. Uncertainty of the bound of the results obtained by lumped nodal loads is its main defect.

A better approach therefore, is a 'consistent nodal load formulation' in which work equivalency is the basis of evaluation rather than static equivalence. Of course, the loads determined in this fashion must check for static equivalency also.

It can be noted here that if the pressure loading or body forces like pore pressures etc. of a particular value are acting only on a part of the element, then the integration needs to be performed only on that part.

2.3.7 Extension from 'Part to Whole'.

The solution of the problem in finite element method is obtained by combining the solution of its parts. But, it can be seen that there is no restriction in regarding the virtual work of a continuum as a sum of the virtual work of its parts. Further, it is found that on summing up the individual equilibrium equations for different regions, like eqn.2.10, the final set of equations are in a banded form, resulting in economy.

The procedure therefore, will be in general to

(i) evaluate element stiffness as per equation 2.14 for each element and form equilibrium equations,

(ii) add all such equations and solve for displacements $\{\delta\}$,

(iii) determine strains from relation 2.4 and stresses from equation 2.6.

To evaluate element stiffness efficiently, numerical integration procedure may be resorted to, a note on which is included in Appendix 2.A. For adding all equilibrium equations together, it is necessary that the stiffness of all the elements must be in the same frame work

of reference coordinates. A procedure for this is indicated in Appendix 2.B.

If the behaviour of the structure is load dependent e.g., loss of contact between the pavement and subgrade due to lifting up of the slab caused by wheel loads or hydro-thermal gradients, then it is necessary to adopt a procedure similar to that required for solving any non-linear problem.

2.4 ELEMENTS

2.4.1 Nomenclature of Elements

The different element names are based, as per their class, in different ways, e.g.,

(a) the shapes, such as triangular, rectangular, quadrilateral, tetrahedral etc.,

(b) degrees of freedom e.g. 8,12, or 16 DOF,

(c) the completeness of their displacement pattern, e.g., conforming or non-conforming,

(d) the displacement model used e.g. linear, parabolic cubic, and,

(e) the behaviour of the element, e.g., elements in plane stress, plane strain, axisymmetry, plate bending elements, joint elements etc.

2.4.2 Choice of Elements

The finite element method is essentially a method requiring engineering judgement. Therefore, personal skill

plays a dominant role in picking up a suitable element out of a galaxy of elements, which will best suit a particular situation. However, certain basic factors can be that

(i) the geometry of the structure shouldbe adequately represented by the element mesh, isoparametric elements can fit in almost any shape[54],

(ii) the choice will depend on the nature of the problem e.g., in situations like geotechnical problems, quadrilateral elements with 8 degrees of freedom are supposed to be enough[34], but the efficiency of higher order elements are better where flexural stresses predominate.

The grading of finite element mesh is also important[64,65] though it is difficult really to set up any norms. Use of two types of elements in a single problem is also found to be useful and economical[66].

2.5 ERRORS IN FINITE ELEMENTS ANALYSIS

It may be worth while to think over what might be the errors in finite element analysis so that it may lead to an insight into their sources. Due regard can then be given to them while planning the analysis.

Basically, finite element method being a numerical method, all the errors pertaining to a numerical method like numerical truncation etc., also necessarily hold for this method. Numerical round offs may be a potential

source of error, specially if the difference in the
coefficients of the matrix to be inverted for the solut-
ion of equilibrium equation is large. For this purpose
it is necessary to have elements, specially the adjacent
ones, of equal order of size. Melosh[67] has shown that
truncation errors can be of sizeable amount in certain
cases, thus, intermediate data generation and manipulation
is recommended in double precision. This will however,
significantly tax the computer memory and also the
computational time.

Apart from manipulation and truncation errors,
the other sources of error could be the error in modelling
say for example, a cut has to be imposed on depth as well
as width to model a semi-finite half space like a sub-
grade. Also, another example could be idealization of a
circular section by polygons or representation of a three
dimensional solid by finite elements in plane strain or
plane-stress etc. Similarly, modelling the circular loads
as equivalent square might be another source where errors
might creep in.

Errors can also be due to choice of improper dis-
critization e.g. use of coarse mesh, omission of certain
important degree of freedom e.g. the term of 'twist' in
plate bending element or omission of a certain term in
the assumed displacement model can also play mischief.

Averaging required to be done to find stresses at
node points or even at the area surrounding a Gauss point,

if Gaussian integration is used, may also introduce approximations.

These errors can be minimised if due care is taken and proper judgement is exercised in the **choice** of proper displacement model, discretization of structure and above all programming the computer code[68].

2.6 USE OF FINITE ELEMENT METHOD IN PAVEMENT ANALYSIS

The finite element method has been applied by Clough and Rashid[69] to the Boussinesq's problem[62] of stress distribution in a homogeneous, semi-infinite, isotropic, elastic half space. The results were found to compare well with the classical elastic solution.

Duncan et al.[70] applied this method to Burmister's problem[71] of stress distribution in an anisotropic layered media with linear as well as non-linear material properties. Kachroo[72] also studied a similar problem and showed that by adopting finite element analysis the results obtained are closer to measured values.

Wilson[73] analysed the transient and steady state temperature distribution in plane and axisymmetric bodies. Cheung and Nag[74] analysed the problem of lifting of a plate resting on elastic foundation using finite element method. Sargious et al.[75] have applied the method, using STRUDEL program to compare the field observations on rigid pavements and conclude that finite element

method is a potential method for analysis of pavement problems.

Smith[76] has used triangular finite element in axisymmetry to analyse plates on elastic foundation and has compared the results with the model tests.

Wang, Sargious and Cheung[77] have used the rectangular, 12 degrees of freedom, plate bending element to study the effect of foundation model on stresses in pavement slabs and have later extended this study to investigate the stresses when the slab has an opening of rectangular shape similar to a manhole[78].

Huang and Wang[79] reported to have developed a finite element program to study the effect of load transfer efficiency of joints in concrete pavements on the stresses and deflections of rigid pavements and have shown to have obtained an excellent correlation with AASHO road test results. The method used to simulate a joint is by assigning a pre-determined efficiency value for load transfer from a node on one side of joint to the one which is on other side. Thus, the load applied to a node on one side of the joint is distributed among the two nodes in proportion to the load transfer efficiency.

In another paper[80] the authors apply the analysis to the problem of non-uniformity of subgrade support, in which the subgrade reaction is supposed to be lumped at nodal points and in the event of contact loss this

reaction is supposed to be absent.

Pitorius[81] has used the 'Prismatic Solid' program for determining the stresses in pavements with cement treated base. For this purpose, the three dimensional problem is converted into a two dimensional one by representing the wheel loads with the help of harmonic analysis. Fossberg[83] has also used the same program, reported, to have been developed by Wilson[82] to determine the stresses in the slab containing a long crack parallel to the centre-line.

In the next chapter, considerations are given to generating a suitable model for analysing a distressed pavement slab, overlaid by another layer.

APPENDIX 2.A

NUMERICAL INTEGRATION

Numerical integration technique becomes a necessity for integrating complex functions[84]. In finite element method the numerical integration technique is getting increasingly popular because of its versatile nature to accommodate arbitrary variations in geometric and material properties of the element.

The basis of this technique is replacing the integration by summation. There are various methods of numerical integration. The one suited and more popular in finite element technique is Gaussian Integration.

$$I = \int_{-1}^{+1} f(x)dx = \sum_{i=1}^{n} W_i f(z_i) \qquad \ldots 2.15$$

where,

  n = order of integration rule, i.e. number of sampling points,

  W_i = weight coefficient for ith sampling point,

  z_i = abscissa of ith sampling point

$f(x), f(z_i)$ = function

$$I = \int_{-1}^{+1} f(x)dx = Af(a) + B.f(b) + Df(d) + \ldots \qquad \ldots 2.16$$

For two dimensional integration

$$I = \int_{-1}^{+1} \int_{-1}^{+1} f(x,y)dx.dy$$

$$= \sum_{i=1}^{n} \sum_{j=1}^{n} W_i W_j f(z_i, u_j) \qquad \ldots 2.17$$

$$I = A^2 f(a,a) + A.B.f(a,b) + A.C.f(a,c)$$
$$+ A.B.f(b,a) + B^2.f(b,b) + B.C.f(b,c)$$
$$+ C.A.f(c,a) + C.B.f(c,b) + C^2.f(c,c) \qquad \ldots \ 2.18$$

while, one function say z_i, is kept constant the other u_j is varied and summed for each value of i thus, if n = 3 then there will be total 9 operations.

Numerically Integrated Finite Element (NIFE) are more exact, though integration itself is not, and give better results towards convergence. They are economical and efficient as they allow the representation of geometric and material properties that may vary arbitrarily.

APPENDIX 2.B

COORDINATE TRANSFORMATION

Stiffness generation process requires the assembly of stiffness of individual elements. The stiffness of each element is in terms of its local coordinates. The origin of the local coordinate system may be any convenient point like the centre of the element or one of its nodes. When adding stiffnesses together for assembly, the coordinates of all the elements must be on the same system. As such the transformation becomes necessary.

Let the local coordinate system, in two dimensions, be ξ and η, and that of global x and y.

Then, it is required to convert the shape functions say $[N_i]$ for any node i in an element, from local to global.

$$N_i = f(\xi, \eta)$$

also $$x = f_1(\xi, \eta)$$

and $$y = f_2(\xi, \eta)$$

For the calculation of $[K]$, $\int [B]^T [D] [B] dv$ is required as per equation 2.14 and $[B_i]$ in $[B]$, say, for the case of plane strain is,

$$[B_i] = \begin{bmatrix} \dfrac{\partial N_i}{\partial x} & 0 \\ 0 & \dfrac{\partial N_i}{\partial y} \\ \dfrac{\partial N_i}{\partial y} & \dfrac{\partial N_i}{\partial x} \end{bmatrix}$$

As per chain rule of partial differentiation

$$\left\{ \begin{array}{c} \dfrac{\partial N_i}{\partial \xi} \\[2ex] \dfrac{\partial N_i}{\partial \eta} \end{array} \right\} = \left[\begin{array}{cc} \dfrac{\partial x}{\partial \xi} & \dfrac{\partial y}{\partial \xi} \\[2ex] \dfrac{\partial x}{\partial \eta} & \dfrac{\partial y}{\partial \eta} \end{array} \right] \left\{ \begin{array}{c} \dfrac{\partial N_i}{\partial x} \\[2ex] \dfrac{\partial N_i}{\partial y} \end{array} \right\} \qquad \ldots\ 2.19$$

$$[J] = \left| \begin{array}{cc} \dfrac{\partial x}{\partial \xi} & \dfrac{\partial y}{\partial \xi} \\[3ex] \dfrac{\partial x}{\partial \eta} & \dfrac{\partial y}{\partial \eta} \end{array} \right| \qquad \ldots\ 2.20$$

$\dfrac{\partial N_i}{\partial \xi}$ and $\dfrac{\partial N_i}{\partial \eta}$ are local derivatives and are known. It is required to find global derivatives. Above equation can also be rewritten as,

$$\left\{ \begin{array}{c} \dfrac{\partial N_i}{\partial x} \\[2ex] \dfrac{\partial N_i}{\partial y} \end{array} \right\} = [J]^{-1} \left\{ \begin{array}{c} \dfrac{\partial N_i}{\partial \xi} \\[2ex] \dfrac{\partial N_i}{\partial \eta} \end{array} \right\} \qquad \ldots\ 2.21$$

where $[J]$ is known as Jacobian Matrix and its inverse is required to determine the global derivatives. Also it can be shown that[85]

$$dx.dy = | J.| d\xi\ d\eta \qquad \ldots\ 2.22$$

Now, $x = \displaystyle\sum_{i=1}^{n} x_i N_i(\xi, \eta)$ and $y = \displaystyle\sum_{i=1}^{n} y_i N_i(\xi, \eta)$

Therefore, on differentiation the Jacobian matrix becomes,

$$[J] = \begin{bmatrix} \sum x_i \frac{\partial N_i}{\partial \xi} & \sum y_i \frac{\partial N_i}{\partial \xi} \\ \sum x_i \frac{\partial N_i}{\partial \eta} & \sum y_i \frac{\partial N_i}{\partial \eta} \end{bmatrix} \qquad \ldots 2.23$$

Thus the Jacobian matrix can be evaluated, local derivative of shape function being known and numerically inverted in the computer at every point of Gaussian integration (ξ, η). This by equation 2.21 will then yield required global values.

In case of plate bending elements the matrix $[B_i]$ comprises of the second partial derivative of $[N_i]$, as such coordinate transformation will require determination of analogous matrix known as Hessian.

CHAPTER-III

STUDY OF THE BEHAVIOUR OF A CRACKED SLAB WITH AN OVERLAY

3.1 MODELING OF PAVEMENT STRUCTURE

In reality, even a simple three dimensional analysis may not be an answer to a pavement problem which essentially involves layered system with variable boundary conditions and variable material properties, subjected to wheel loads and environmental effects. Such an analysis is obviously not possible at the present time due to the limitation of computing facilities. Analysis of pavement idealised as two dimensional plane, axisymmetric or a plate with suitable foundation model appear to be feasible. Selection regarding material constants, geometry, boundary conditions and nature of loading are crucial.

Truly speaking there is no material the behaviour of which is linearly elastic at all the stress levels even in the working range[86]. Yet, it is found that assumption of linear elasticity for several construction materials have always resulted in behaviour quite satisfactory from the point of view of engineering design. Similarly, the behaviour of practically all the materials is time dependent and in many cases also dependent on stress path or history dependent. Again, the assumptions like isotropy and homogeneity of the materials are open to question.

The idealisation regarding configuration of the structure is made to reduce the computation, wherever it is found that this would not adversely affect the result, e.g. considering the problem of a retaining wall or a dam as a plane problem is usual. Similarly, a slab, if not very thick, is regarded as a thin plate problem. The problem of central loading of a homogeneous axi-symmetric body can be converted into a simpler problem by regarding it as axisymmetric. In theoretical methods, the plate on elastic foundation of limited dimensions is treated as semi-infinite whereas, in numerical methods it is just the otherway. Boundaries need to be assigned to the depth and width of the subgrade.

A cement concrete pavement some times can not be treated as an axisymmetric structure, because loading at the edge or corner can not be simulated then. When it is intended to consider a slab having a crack, which usually is non-circular, such consideration is ruled out.

Considering the pavement as a two dimensional plane structure like a plane strain model, has the difficulty in truly assigning the wheel loads, though the cracks can be considered as long straight ones. These kinds of difficulties, have been overcome by Wilson[82] and Nayak and Jain[87] through the use of Fourier's terms and such a method has also been applied by Pitorius[81] and Fossberg[83] to pavements. However, the main features of this analysis

are:

(a) 8 to 10 times costlier on computer time as compared to an ordinary plane, elastic analysis,

(b) variation of geometric and material properties in the longitudinal direction can not be incorporated.

(c) corner loading can not be simulated.

(d) the crack can only be regarded as a long, straight crack and always in the longitudinal direction.

(e) non-linearity in material properties can not be considered.

The only advantage of such an analysis is proper representation of the wheel load which is essential for for true assessment of stresses and deflections. However, for qualitative assessment of transverse behaviour of pavement with longitudinal crack, the plane strain analysis is quite satisfactory.

Modelling, a pavement slab as a thin plate on elastic foundation is a justified conventional procedure (24,26-33,38,40,42,43,45) and is also intended in this work. However, before doing so, it is proposed to model the pavement slab with a long, longitudinal crack and an overlay as a body in plane strain.

3.2 AIM OF THE STUDY

The object of this study is to gain an insight into the mechanism of load deformation and stress distribution

of layered, cracked and uncracked pavement system.
Therefore, to fulfil this, the model chosen is the
plane strain study of a pavement slab with an overlay
considered as bonded to the base which has a long crack
parallel to its centre line. The behaviour is studied
under a load near the centre line. It is thought that
the proper insight into the mechanism will help in
modeling the pavement slab correctly, so as to truly
assess the parameters of importance in design, through
an analysis.

For this purpose, the crack is modeled by a hinge.
This is reasonable, as it is found by actual load tests
that through a full depth crack the shear transfer does
take place though the moments can not be transferred[88].
This attribute is considered to be due to the aggregate
interlock[89], and perhaps rightly so, because the
formation of crack surface in cement concrete is at the
expense of the energy rather than a slip mechanism[90].

3.3 PROGRAMME OF INVESTIGATION

3.3.1 A study of following models in plane strain condi-
tion is proposed to investigate their behaviour:

    (i) A sound pavement slab,

    (ii) A pavement slab with a full depth crack modeled
        in accordance with the requirements of para 3.2.

    (iii) A slab having an overlay fully bonded.

(iv) A slab having a fully bonded overlay but a crack in the base.

(v) A slab with a crack in the base and having an overlay but with bond broken in the vicinity of the crack.

3.3.2 The main considerations in designing this numerical experimentation to understand the mechanics, have been:

(i) to make the experimentation as simple as possible, in order to make the results apparent, clear and meaningful. With this end in view the elastic properties of the base and overlay were assumed to be identical.

(ii) to have the dimensions and properties of all the parameters as realistic as possible so as to simulate the actual conditions. Details of all these parameters and justification of their adoption is discussed in the following paragraphs.

(iii) to perform basic study and not the parametric study. From this view point all the parameters were kept constant. However, two sets of studies were performed by only drastically changing the subgrade properties so as to have confirmation of the results of both sets qualitatively. Incidentally, this gives the additional information regarding the parameter' effect of subgrade quality.'

3.3.3 Finite Element Analysis

The element chosen to generate the plane strain model was an isoparametric[54] quadrilateral element with

8 nodes and 16 degrees of freedom per element. It has already been mentioned in last chapter that the selection of an element and its arrangement to discretize a structure is a matter of engineering judgement. The decision to adopt this element has been on the following bases:

(i) This element is reported to be efficient.[91]

(ii) As the pavement slab is to be represented, which is a long and thin structure, the aspect ratio of the elements has to be kept high to achieve economy and a superior element is therefore, required.

(iii) The bending effects predominate in the case of a pavement slab and these can be better evaluated by an isoparametric element[54].

The computer simulation and analysis of these plane strain models were carried out by an efficient and well tested finite element program with the acronym 'PSPSAS' (Plane Stress, Plane Strain, Axi-symmetric Program)[92], using IBM 360/44 Data processing System at Delhi University.

3.3.4 Numerical Assignment

For numerical analysis of the cases described in Table 3.1, it is necessary to prepare data in accordance with clause(ii) para 3.3.2. Following values have therefore been adopted.

(a) The Elastic Properties of the Slab

For structural concrete, I.S.: 456-1964[93] does
not provide an explicit relationship for determination
of modulus of elasticity, although an equation of the
form: $E = 750 fc$, where fc is the compressive strength
gives an approximate estimate for the grade of concrete.
Paving concretes have lower w/c ratios and therefore,
it is natural to have higher strength. At the same time
the relation given by above authority are known for its
lower bound values[94]. Therefore, considering even
M 150 structural concrete the value obtained of
$11.25x10^4$ kg/cm^2 is a lower value for the concrete of
about one month age.

Orchard, et.al[95] have discussed about relationship
between static and dynamic values of modulus of elast-
icity and find that dynamic values are slightly higher
than static values for concrete and other materials.
Considerations for the use of dynamic modulus is relevant
under moving wheel loads.

Keeping the above facts in view, the modulus of
elasticity of concrete is taken as $E_c = 150x10^3$ kg/cm^2,
and Poisson's ratio, $\nu = 0.15$.

It is recognised that the elastic properties of
concrete increase with age, though at a very slow rate
later[94]. On the other hand it could decrease as
well under fatigue.[96] On these counts the elastic

properties of the base and overlay should be taken as different values. However, as clarified in clause (i) of para 3.3.2 they are taken as same values.

(b) The Properties of the Subgrade:

The elastic properties of the subgrade are chosen so as to have two widely different values. The values of elastic properties should be high because as discussed in first chapter the old concrete pavement slabs normally were founded on good base as a result of stage construction. The following ratios of modulus of elasticities of concrete and subgrade are therefore chosen, (i) $E_c/E_s = 200$, (ii) $E_c/E_s = 2000$. The second value is chosen in accordance with clause (iii) of para 3.3.2. In both the cases the Poisson's ratio is taken as 0.45.

According to Vesic and Saxena[97] and McIlough and Boedecker[98] they fall in the range of modulus of subgrade reaction K = 0.5 to 10 kg/cm^3, approximately.

(c) Slab Dimensions

For the purpose of numerical analysis the thickness of the pavement slab is taken as 22.5 cm and that of overlay as 15 cm. The width of the slab, however, was fixed from the consideration that it should be so much as not to effect the behaviour at the point of maximum stress. The best way, therefore, was to adopt such values as to simulate infinite slab effect or in other

words the full basin shape should develop. Following
the Ohio River Division Laboratory[99] recommendations
the slab width is assumed as thrice the radius of
relative stiffness, $\sqrt[4]{D/K}$, $D = E_c h^3/12(1-\nu^2)$ and h = slab
thickness.

According to these requirements the width of the
slab for the combination of base and overlay on weaker
subgrade was assumed as 900 cm.

(d) Subgrade Dimensions:

The consideration in deciding the width and the
depth of the subgrade was such that the size effect was
minimised in making the comparative study. As per
Vesic and Saxena[97] the depth could be considered
infinite if for the values adopted in this study, the
subgrade is deeper than 660 cm. The depth of elastic
continuum was taken as 720 cm. The width of the sub-
grade was taken as 1300 cm which is about 1.5 times the
width of the pavement.

Figure 3.1 shows the finite element idealization
of the pavement structure. The subgrade is represented
by elements 1 to 14. The cement concrete slab is divided
into 8 elements, i.e. element members 15 to 22. Thus,
there are a total of 22 elements, each with 8 nodes. Total
number of nodes are 85. As the pavement is considered
to be symmetric about centre line, only the right hand
half is considered for analysis, effecting a saving in

computer time. Thus 15 nodes, which are on the centre
line, are considered as restrained horizontally. Five
nodes on the bottom boundary of the subgrade are consi-
dered as restrained vertically, whereas, another five on
the right hand boundary on which cut as discussed above,
are restrained horizontally. Thus, total 23 nodes are
restrained.

(e) The Crack

The attributes of the crack are already described
in article 3.2. To simulate the crack, same point was
assigned two node numbers i. one node which is on the
crack is split into two. But this was not done for all
the nodes along the depth of crack. One of the nodes,
the uppermost in the crack was intact, in order to
simulate a hinge. The location of crack was parallel
to the centre line of the slab at a distance of 60 cm from
it. This distance was however taken arbitrarily. This
is shown in figure 3.2(a).

(f) Bond Condition

The bond is considered to hold between the base
and the overlay i.e. it is assumed that full strain
compatibility exists at the interface. However, in
Case V, as described in Table 3.1, the bond is assumed
to be broken for a distance of 15 cm on either side of

the crack in order to investigate the change in mechanism of stress distribution if the bond is broken. The representation of this in finite elements is shown in Figure 3.2(b).

(g) Load

Like all other parameters in the study, an attempt was made to simulate the load also as realistically as possible. Lewis and Harr[100] report to have determined a value of 125 lbs/in. to be equivalent to a standard axle load of 18,000 lbs for a 12 ft. wide pavement. Taking this result as a guide, the load was taken as 30 kg/cm. However, it was found that this load induces very little stress specially in Set I, as per Table 3.1. Therefore, the load was taken as 300 kg/cm.

3.4 ANALYSIS AND DISCUSSION OF RESULTS

The results of the finite element analysis carried out on the cases as described in article 3.3 are presented in figures 3.3 to 3.13.

3.4.1. Studies on Single Slab with and without a Crack (Case I and II)

Figure 3.3(a) shows, how this crack is modelled by finite elements. Figure 3.3(b) shows the variation of bending moment in Case I of Set I i.e. a 22.5 cm slab and compares it with that with a fully cracked one. The

effect of crack across which only shear is transferred is evident. The moment at cracked section becomes zero as now there is no section available to resist it. Moment on the right hand side becomes negative due to shear transfer. The situation can then be compared with those of beams on elastic foundation[101]. Figure 3.3(c) compares the deflections in Case I and II of Set I and shows increase in maximum deflection on cracking. But the deflected basin resembles like one of a more flexible slab.

3.4.2 Studies on Slabs with Overlays (Cases III, IV and V)

3.4.2.1 Deflection Studies

Deflected profiles for cases III, IV and V, of set I as defined in Table 3.1, are plotted in figure 3.4. It can be seen that the maximum deflection of the slab with a crack is about 5 percent more than that without a crack. However, the effect of loss of bond in the crack zone is to increase the deflection further by 7 percent. Figure 3.5 shows these very variations for Set II, i.e. when $E_c/E_s = 2000$. It is evident from the figure that the deflection patterns are exactly identical to those in figure 3.4 for Set I. But in Set II i.e. where the subgrade is weaker the deflection increases by approximately 20 per cent for cracked case and about 40 per cent in case of bond loss accompanying a crack. This observation

leads to the conclusion that the cracking of a pave-
ment base slab on a weaker subgrade, induces dis-
proportionally severe conditions in the pavement
structure. This also gives an indication that at the
crack location, when the base is unable to carry any
moments, the overlay will have to play a much more
important role specially if the subgrade is weak.
Reactive pressures are also drawn in the figure 3.5
and they do approximately testify that the theory of
modulus of subgrade reaction i.e. the Winkler's model
is not very incorrect as in the neighbourhood of the
load the reactive pressures are more or less proportional
to the deflections. A detailed discussion of this is
however, included in the Chapter VII.

3.4.2.2 Effect of Crack and Bond Loss on Stresses.

Figure 3.6 is an instructive diagram, drawn to
show the variation of bending stresses at different
typical cross-sections of the pavement slab for Set I.
Diagram (i) shows this variation at a section near to
the crack of case V i.e. when bond is lost, while
diagram (iii) is for Case IV and diagram (iv) is for
Case III, the location being the same. These three
diagrams have three distinct forms. The diagram (iv)
which is for a sound base shows a continuous and smooth
stress variation. (This however, is incidentally because

the elastic properties of the overlay are taken to
be same as base deliberately, just for making analysis
more clear). These stress distributions can be regarded
as equivalent to three moments as analysed in diagram(iii)
for case IV i.e. when the bond is intact near the crack.
One moment is in the overlay, the other is in the base
and the third one is generated by forming a couple due
to bond. This analysis can also be done for case V i.e.
when bond is lost. However, there can not be any moment
resisting couple in the vicinity of the crack due to bond
as in this case the bond is supposed to be broken. The
small forces are only the balancing forces from the zone
beyond the zone of bond loss where such a couple does
form.

The pattern of stress distribution in diagrams
(i) and (iii) are different and effect of bond is clear.
The bond makes the stress variation at interface contin-
uous in diagram (iii).

Diagram (ii) is for case V but at a section which
is at a distance from the crack equal to about twice the
depth of crack. The pattern of this variation is identical
to diagram (iv) and therefore, indicates that the dis-
turbances created by the presence of crack have subsided
in this zone. Beeby[104] observed that in controlled
constant curvature tests on reinforced cement concrete
members, the spacing of the cracks were about twice their
size. Thus, he inferred that in the spirit of St. Venant's

principle the effect of crack should extend upto a distance equal to the depth of crack on its either side.

The diagram (iii) and diagram (iv) are for the same locations of Case IV and III respectively. Diagram (iii) shows an increase in the compressive overlay stress by about 15 per cent. However, the effect of crack which extends upto this distance (6.75 cm) has an effect of stress release and therefore, the base stress is less. This observation is similar to that of Fossberg[83]. He has shown variations of stresses at the crack location and at a distance of 15 cm from crack. These are reproduced in figure 3.7. It is seen that at the crack the base is free of stress due to stress release. However, at 15 cm from the crack (i.e. the depth of largest crack in this case) the disturbance is almost over.

The inferences that can be drawn from figure 3.6 are:

(i)   the cracking causes stress release in the base and the section available to resist moments at this location is only that of overlay.

(ii) The effect of stress release is local. However, it does extend upto a certain distance, which based on this study, those of Fossberg[83] and Beeby[104] and also in the spirit of St.Venant's principle[62], can be taken as equal to the depth of cracks in the base.

(iii) Bond loss in the vicinity of the crack puts the overlay under heavy stress, because of lack of moment resisting couple due to bond

and reduction in lever arm between tension
and compression areas.

3.4.2.3 Effect of Bond Loss on Moments

Figure 3.8 illustrates the variation of bending
moment in overlays in Cases III, IV and V of Set I.
It is clear from this diagram that the overall behaviour
of these cases are similar to reduction in radius of
relative stiffness in Cases III, IV and V progressively.
Figure 3.9 shows the forces generated due to bond which
form a couple, even though the slab may contain a crack.
This diagram pertains to Case IV of Set I. It is seen
that the forces generated in the base are generally
lower than in the overlay. This is, in fact because
of the reason that the subgrade is also considered as
bonded to the base in the finite element analysis. But,
while computing these forces from stresses, the effect
of subgrade is neglected.

The results plotted for Set II are exactly of same
nature and there is no difference except in numerical
magnitudes. They are therefore not repeated for para-
meters similar to those shown in figure 3.6, 3.8 and 3.9.

Figure 3.10 shows, how the bending moments are
shared between base and fully bonded overlay in Case IV
of set I. It is clear that at the location of the crack
the overlay has to carry a large amount of moment. The
overlay is therefore, very highly stressed in this zone.

Every where else, the base carries a larger portion of the load, its rigidity (i.e. 'EI') being more. The same observation is true for set II shown in figure 3.11, but in this case the bending moment carried by the overlay in the vicinity of the crack is proportionately large, due to higher deformations, as noticed in figure 3.5.

Figure 3.12 is drawn to compare the magnitudes of moments carried by the overlays in fully bonded case and in case when bond is broken. The numerical values are for set I in this figure and for Set II in figure 3.13. It is seen from both these figures that the moments in overlay leaving the zone of the crack with bond broken are somewhat lesser than that with full bond. This is because it can be noticed from figure 3.8 that the slab with broken bond behaves as a more flexible slab than one with full bond at the cracks. However, at the crack and in its vicinity the situation is the otherway, the stress resultants are very heavy in case when the bond is broken. This is also seen from figure 3.6(i) and (iii) where stress variation is drawn and the reasons for heavy stress resultants are clear from this diagram. It is also seen that overlay with broken bond is taxed much severely in case of weaker subgrade as in figure 3.13. The reason is explained by increased deformations as shown in figures 3.4 and 3.5. In case of figure 3.5 the increase of deformations due to bond

loss are thrice as much as in figure 3.4.

3.4.3 Discussions based on experimental studies [96,102-105]

Observations on some of the performance studies reported, are pertinent in this regard. Prasad, Sharma and Jain[102] in an experimental field investigation found that reflection cracking did not occur on rigid overlays bonded to rigid base, using Araldite (an epoxy compound of good quality used for bonding).However, it did soon occur on slabs where reliance was placed on bonding by priming with rich mortar after etching with acid.

Observations of Gillette[103] on Selfridge Air Force Base are also applicable in this regard. Gillette, reporting, that bonded cement concrete overlay was provided on the apron to cover various defects in cement concrete pavement including numerous cracks, writes:

" Since construction of bonded overlay, this apron has been continually used for parking jet fighter aircraft. A loss of bond has been experienced in approximately 10 per cent of the area with practically the entire amount occuring along joints or cracks that have reflected through the overlay from the base pavement".

His observations for Standiford Field Airport are also similar.

Felt[105] gives his observations on many overlay projects. In all of these projects one feature that was

common, was of crack reflectance. In about half a dozen of these projects, bond loss in the area adjoining a reflected crack is reported, even though the bond strength of all the core samples taken were sufficiently high.

It can be argued on the basis of above reports that bond loss and crack reflectance does appear to have a bearing on one another. One is the manifestation and other the mechanism. This leads to the dilemma like 'egg and chicken'. However, the findings of Prasad, Sharma and Jain[102] does lead to an answer and results through figure 3.9 confirm this. The tensile forces transferred through the bond at the location of the crack are of the order 150 kg/cm length of the pavement. These forces would have been of greater magnitude, had the load been nearer to the crack. This tensile force will act at the point considered as hinge at the inter-face and its tendency will be to destroy bond and induce 'slip'. If the full bond strength of the inter-face is mobilized, bond failure is liable to occur. Even if it is not mobilized in single load application, damage is likely to take place under repeated load applications. However, it is difficult to say, whether these forces will act as concentrated line loads at the cracks or in what manner they may be distributed in the overlay.

A similar observation can be made with regard to bond stresses considered as complimentary shearing

stresses. If actual values of the moments obtained at the sampling points, located on either side of the crack are taken from figure 3.8, the change in moment is found to be 4100 kg.cm/cm over an average distance of 13.25 cm. It is difficult to say, how the shearing stresses will be distributed in the neighbourhood of the crack. But if it is argued that at some point in this zone the neutral axis lies at the interface (and this is not very unlikely), then, perhaps the distribution of shear stresses can be assumed as if in a rectangular section with depth equal to twice the overlay thickness. In such a case the shear stresses work out to be roughly 15 kg/cm^2 at the interface which is quite a high value and can threaten the bond.

Findings of Sinno and Furr[96] are of significance in respect of bond. They report to have performed repeated load tests on reinforced precracked beams of 8" x 8" (20 cm x 20 cm) size overlaid with $1\frac{1}{2}$" and 2" (3.75 cm and 5 cm) bonded overlay, bonding being done with epoxy and also by cement grouting in some cases. The load applied was of such a level as to induce 20,000 psi (1400 kg/cm^2) tensile stress in steel bars in all cases. No bond or any other kind of failure occured in any of the beams even under 2×10^6 load cycles, though the deformations increased due to fatigue. The load was then increased to 150 per cent and no failure occured even under additional 1×10^6 load applications. Thereafter,

for additional load cycles, the tensile cracks in
the overlay were observed above the crack in base beam.

Here, it can be observed that the force in the base
at the crack location must have been carried by the steel
bars, relieving the bond at base overlay interface.

The conclusion can therefore, be drawn, that if
the overlay is to be saved from failure over the crack
then bond must not be allowed to break, this being specially
necessary in case of weaker subgrades.

3.5 REMEDIAL MEASURES FOR BOND FAILURE IN PLAIN CONCRETE SLAB WITH A CRACK

As it is noticed that the bond failure can endanger
the serviceability of the overlay, it is a fact that a
measure against this is essential. Figure 3.14 shows
the path of stresses diagramatically. In diagram (i) the
base pavement does not contain any irregularity whereas
in diagram (iii) the disturbance is created due to a dis-
continuity in the path as a result of a crack in the
base. The tensile forces will have to take a path through
the interface at the point of discontinuity. An obvious
way to avoid this is to generate an additional path
through which these stresses can pass the discontinuity.
This can perhaps be done by inserting a steel bar at the
level shown in diagram (iii).

Based on these concepts a method named as 'Reinforced
Key Technique' is suggested. The steps involved in this

method are:

(i) As a steel bar is to be inserted in the base at about its mid-depth, it is necessary to cut a groove in the slab, across the crack. The depth of the groove may be about half the depth of the slab and its width can be about 3 to 4 times the size of aggregate. The length of the groove will have to be kept equal to the bond length on either side of the crack or joint. The spacing of the grooves will be based on the force it is expected to carry(150 kg/cm length of slab in case of set I analysed above). The plan of the grooves cut in this way are shown in figure 3.15 (i).

(ii) The reinforcement, the size and spacing of which can be calculated from the consideration of axial force/unit length is placed in the groove, figure 3.15 (ii).

(iii) The groove can be concreted along with the overlay. figure 3.15 (iii).   A section of completed overlay along a crack.is shown in figure 3.15(iv).

Iyenger[+] is of the view that this method has its recognized merits as a crack arrester, but he feels that making the cut in the pavement may not be practical and therefore, suggests the use of reinforcement at the

---

+ Personal communication from C.L.N.Iyengar, The Concrete Association of India, Bombay.

interface rather than in the groove. His contention is, that if the deflection is not too much, then the rein- forcement provided at either place will not make much difference.

According to Ghosh[+] a method very similar to the proposed one is already in extensive use in Germany. While agreeing with the theoretical findings on stress conditions in rigid overlays, he felt that method may not be economical.

The groove can be cut by a concrete cutting hammer. The hammer is developed by concrete section of Structural Engineering Research Centre of Roorkee. The replaceable cutting tool of tempered steel is fixed along with the hammer which weighs about 2 kg and can be operated by one hand. One manl can normally cut about 3-4 grooves in a working day, as has been experienced in the tests performed in the laboratory. The advantage of this hammer is that a worker can use only one hand at a time.

However, a much faster and economical method of cutting these grooves is by power driven tools. These may be either electrically operated or may be operated by an oil engine mounted over it. Depending upon the tool used and the efficiency of the operator, a groove can be cut in

[+] Personal communication from Dr.R.K.Ghosh, Head of Rigid Pavement Division, Central Road Research Institute of India, New Delhi.

between 7 to 20 minutes time.

Obviously the groove, cut in any manner, will seldom have smooth faces and as such a good bond between the base and the overlay can be expected.

Alternatives

Some alternatives to Reinforced Key Technique can be proposed, with a view to achieve greater efficiency and economy.

(i) a groove can be cut along the crack and reinforcement placed longitudinally, in a manner similar to that done at right angles to it. This would impart far more strength to the bond and cater for any breakage likely from stress concentrations at the corners of joint between crack and transverse grooves.

(ii) Fibre reinforcement[106,107] is gaining popularity as an alternative[108,109]. Overlay of fibre reinforced concrete exhibited far better performance on airport pavements[110] as compared to usual overlays. The alternative that could be suggested are:

(a) Use of fibre reinforced concrete in grooves cut in 'Reinforced Key Technique', as proposed with overlay

of usual concrete.

(b) Use of fibre reinforced concrete in groove cut along and perpendicular to the crack and overlaying with unreinforced concrete.

(c) Using fibre reinforced concrete for groove filling, as in above two cases as well as for entire overlaying.

3.6 CONCLUSIONS

The study, therefore, leads to the following conclusions:

1. Deformations increase on development of a crack and are further increased if the bond in its neighbourhood is lost.

2. This increase in deformations are disproportionately high on very weak subgrades.

3. Stresses decrease in the base due to stress release on cracking, and it is reasonable to assume this zone as equal to twice the depth of crack.

4. Stresses in the overlay increase at the crack location and tensile stresses also develop in it which may not be there in the uncracked case.

5. Bonding of the interface has a great effect as a larger portion of moment of resistance of a bonded overlay is due to this quality.

6.   The interfacial bond is liable to fail in case of cracked base unless special measures are adopted to check it.

7.   Failure of interfacial bond at the crack, increases the overlay stress further, specially it develops large tensile stresses at the bottom of the overlay slab. Therefore, if the overlay is to be saved from failure, it is necessary to ensure that the bond does not fail.

8.   Though the base may be cracked but still it is an advantage as the tensile stresses developed in fully bonded overlay are of low order.

9.   Findings of Ohio River Division Laboratory with regard to size of slab for infinite action does appear to be reasonable as by having adopted these the complete basin shaped trough did develop.

10.   Three types of remedial measures to check reflection cracking have been suggested to arrest bond and flexural failures. Field feasibility studies of these measures are however required to be carried out.

TABLE 3.1

CASES STUDIED.

Set No.	Case No.	$\dfrac{E_c}{E_s}$	Base condition	Base thickness	Overlay thickness	Remarks
I	I	200	Sound	22.5 cm	–	
	II	200	Cracked at 60 cm from centre line	22.5 cm	–	
	III	200	Sound	22.5 cm	15 cm	
	IV	200	Cracked at 60 cm from centre line	22.5 cm	15 cm	
	V	200	Cracked at 60 cm from centre line	22.5 cm	15 cm	Bond broken for 15 cm on either side of the crack
II	I	2000	Sound	22.5 cm	–	
	II	2000	Cracked at 60 cm from centre line	22.5 cm	–	
	III	2000	Sound	22.5 cm	15 cm	
	IV	2000	Cracked at 60 cm from centre line	22.5 cm	15 cm	
	V	2000	Cracked at 60 cm from centre line	22.5 cm	15 cm	Bond broken for 15 cm on either side of the crack.

Ȼ 300 kg/cm

XIX   XX   XXI   XXII

XV   XVI   XVII   XVIII   SUBGRADE LEVEL

XIV   XI

X   XII   XIII

IX

VI   VII   VIII

V

III   IV

NO. OF PARABOLIC
ELEMENTS NE = 22
NODE POINTS NP = 85
BOUNDARY POINTS NB = 23
NO. OF MATERIALS
     NMAT   = 2

SCALE _ 1cm = 30cm

I   II
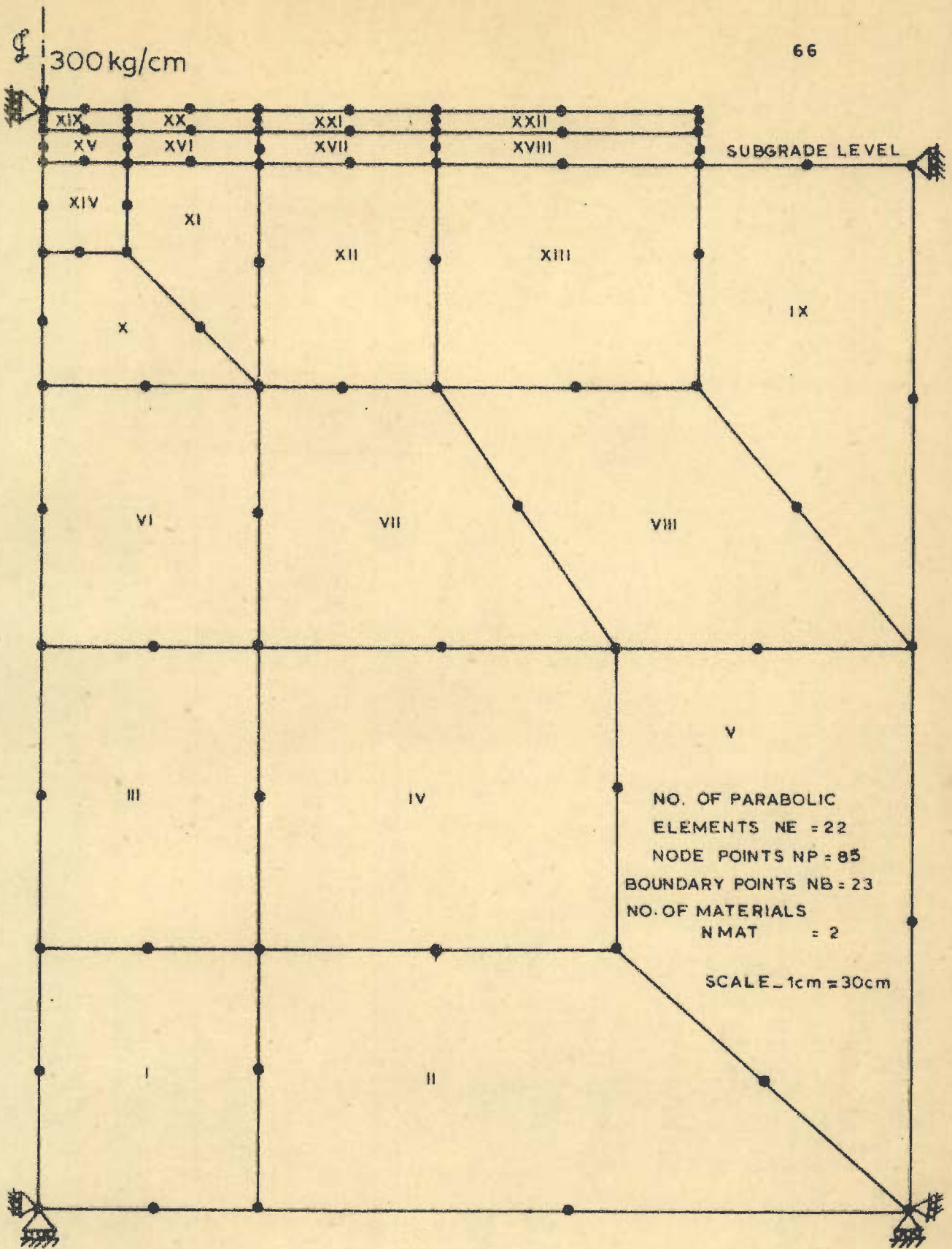
FIG. 3.1 _ FINITE ELEMENT IDEALISATION OF PAVEMENT
IN PLANE STRAIN

NE = 22   NP = 88

a_ WITH FULL BOND

NE = 28   NP = 127

b_ WITH BOND LOST NEAR THE CRACK
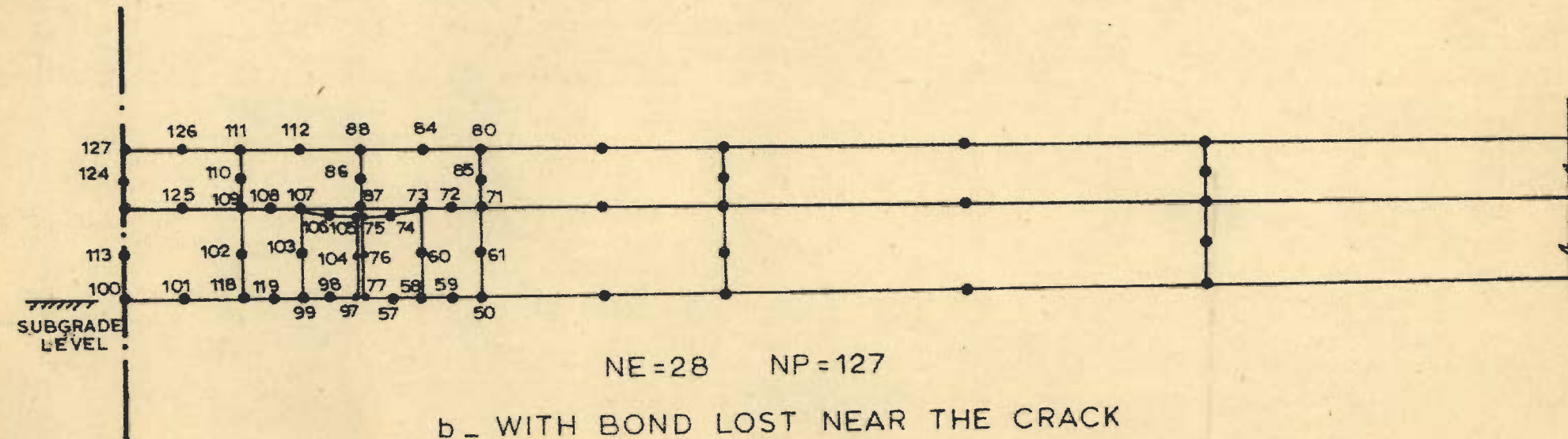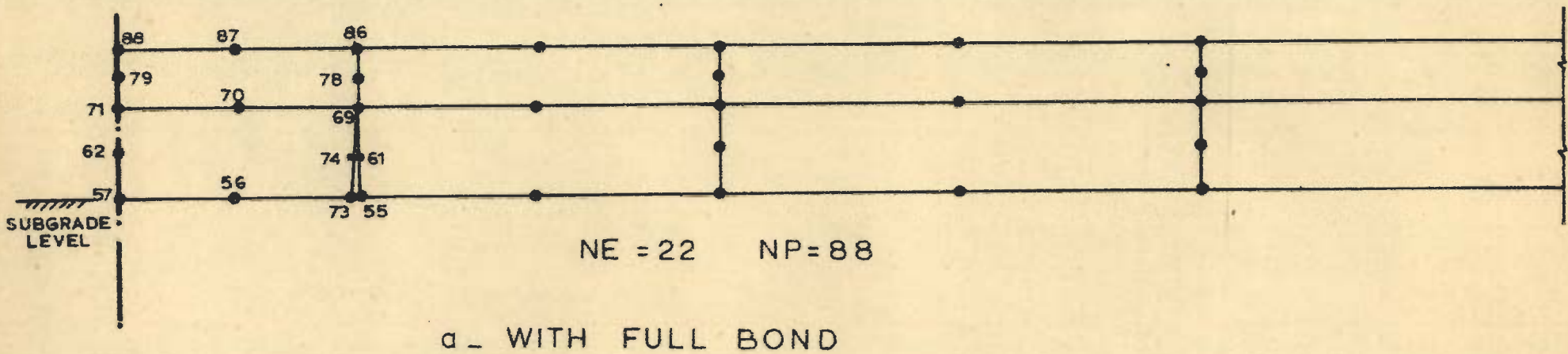
FIG. 3. 2 _IDEALIZATION OF CRACKED BASE WITH OVERLAY

300 kg/cm

a _ FINITE ELEMENT DISCRETIZATION
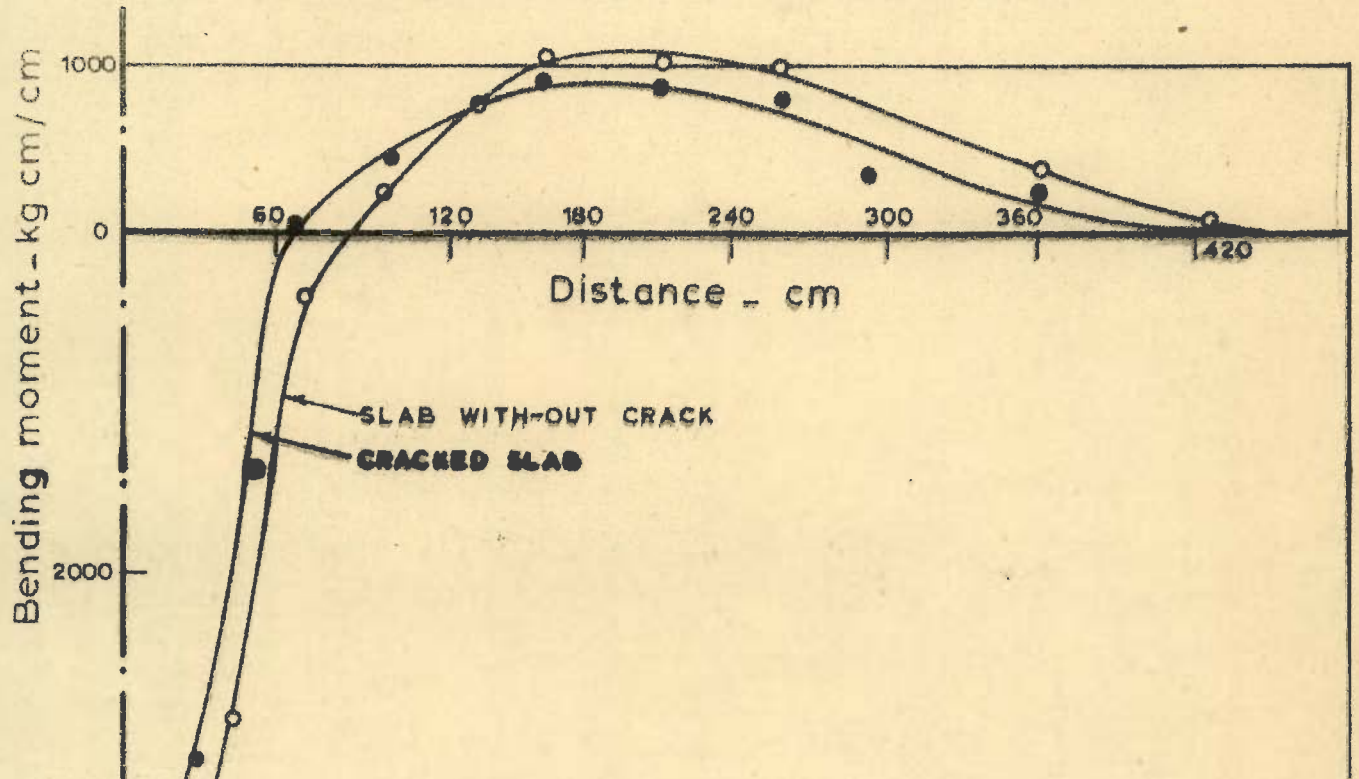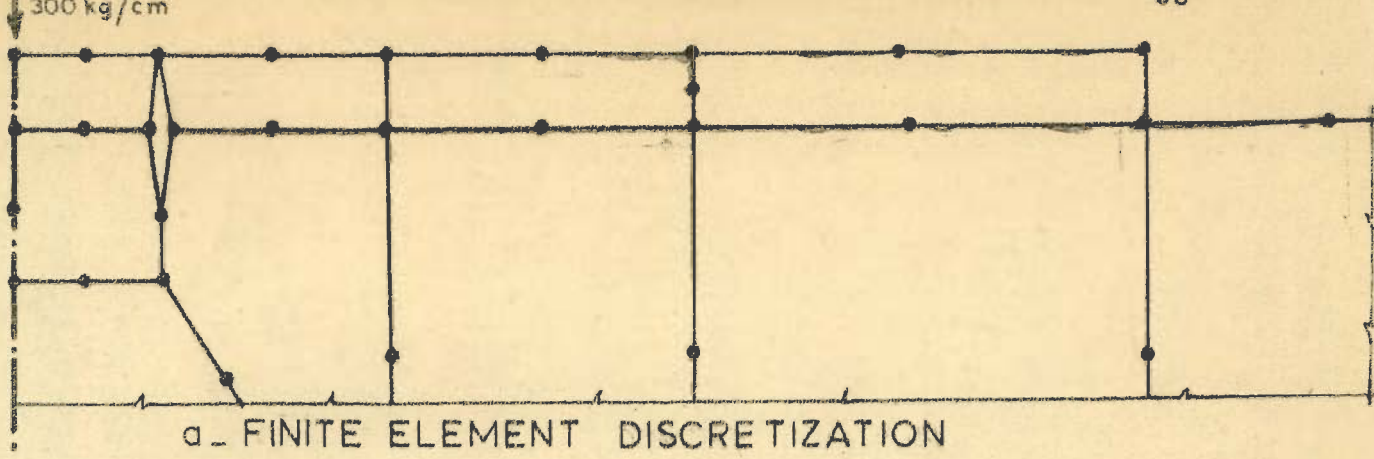
b _ BENDING MOMENT VARIATION

SLAB WITH-OUT CRACK

CRACKED SLAB

c _ DEFLECTION VARIATION

CRACKED SLAB

SLAB WITHOUT CRACK

Bending moment _ kg cm/cm

Deflection _ cm

Distance _ cm

Distance _ cm
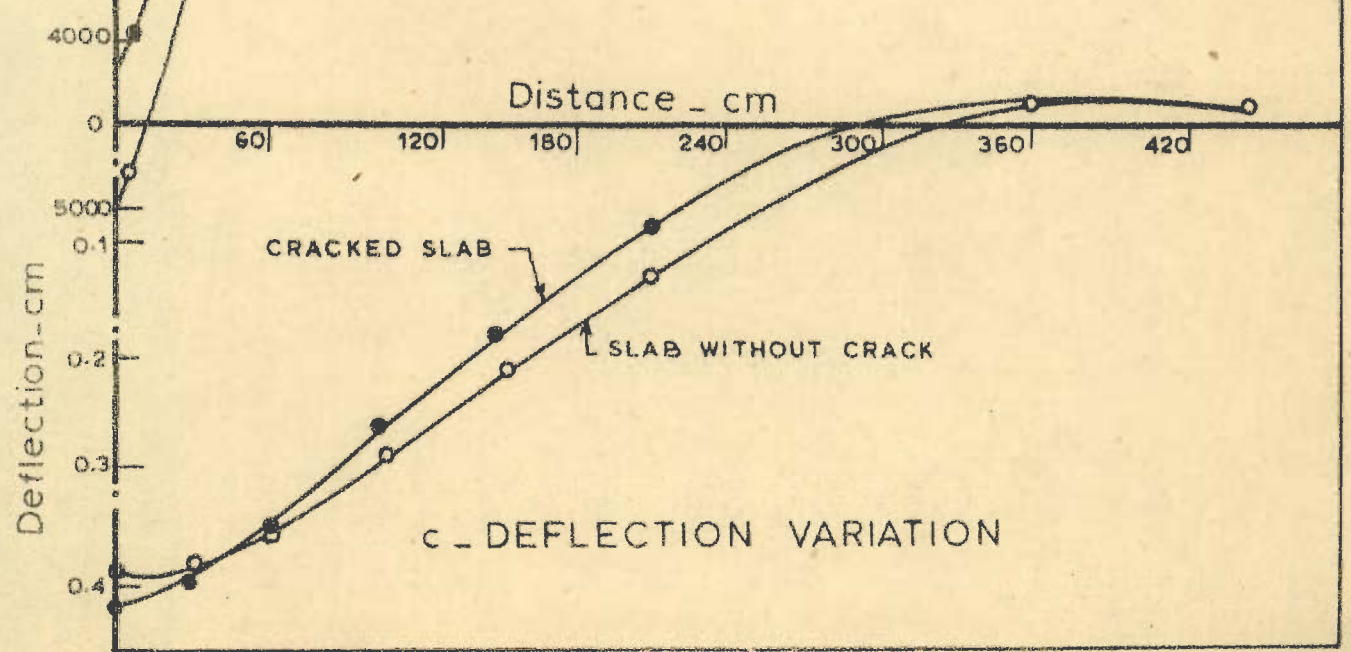
FIG.3.3_ SINGLE SLAB WITH AND WITHOUT CRACK
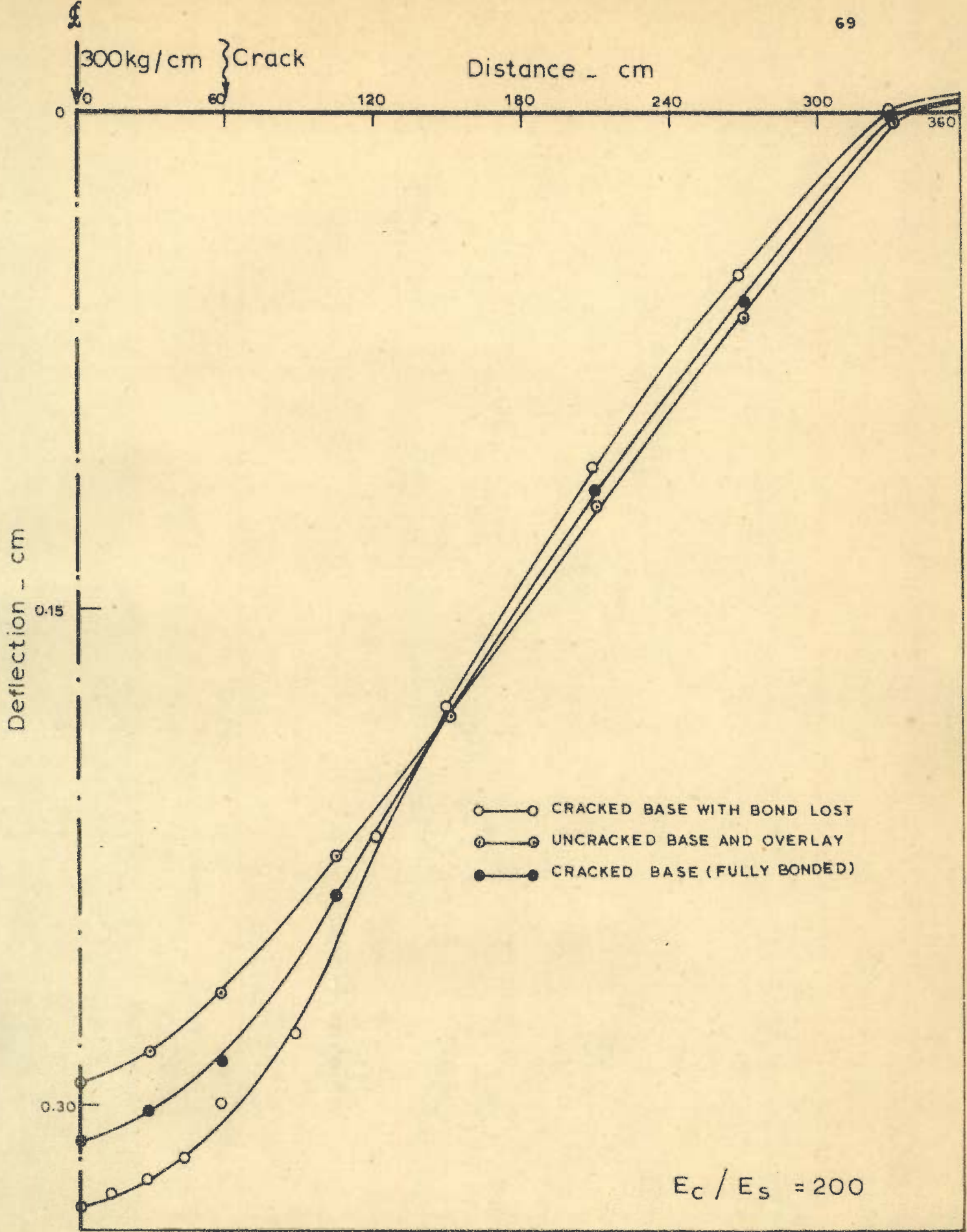
FIG. 3.4 _ DEFLECTION OF PAVEMENT SLAB
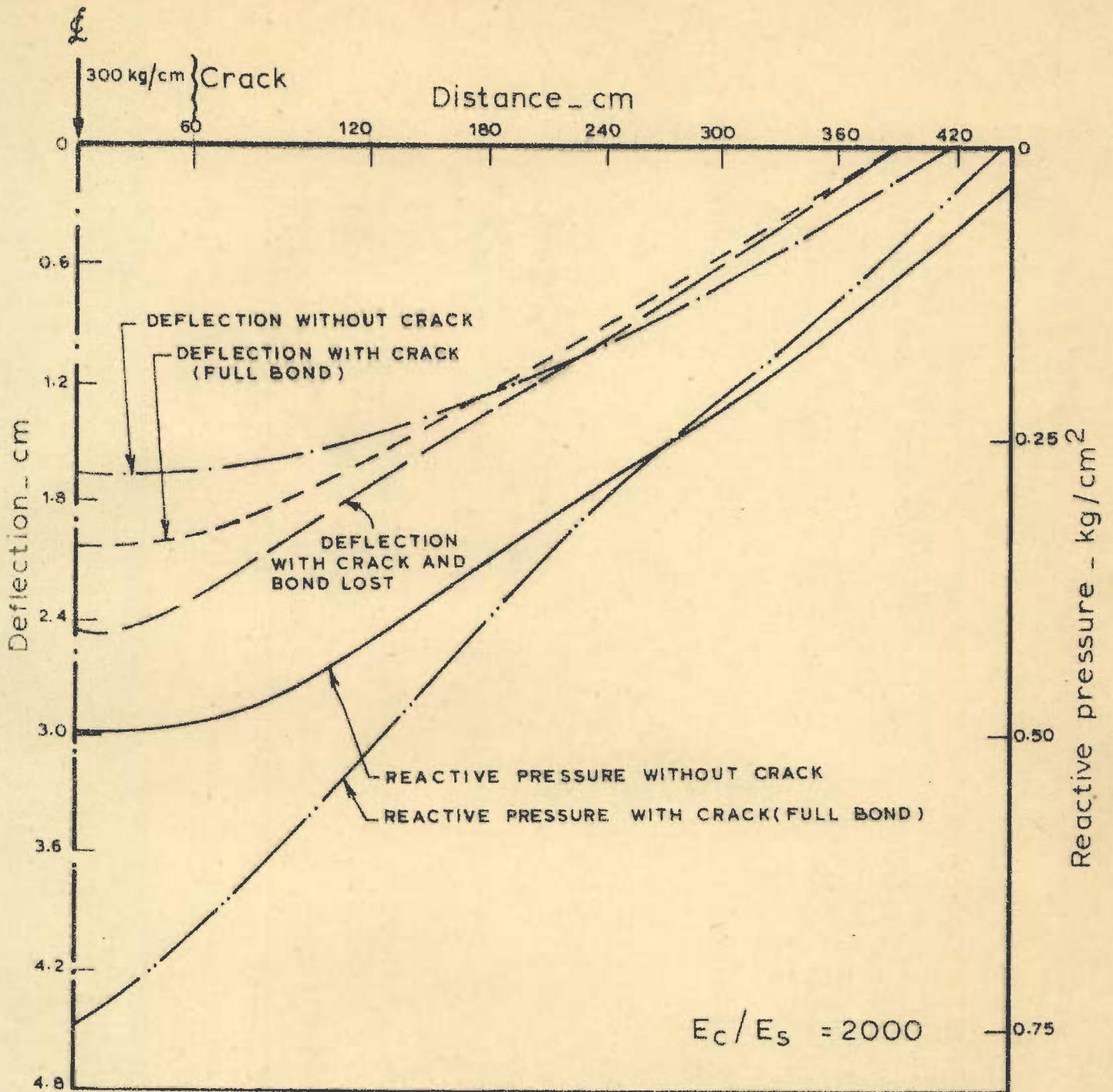
FIG. 3.5 – DEFLECTION AND REACTIVE PRESSURE DISTRIBUTION IN PAVEMENT SLABS WITH BASE AND OVERLAY

i_SECTION AT 3.4cm
FROM THE CRACK

ii_SECTION AT 33 cm
FROM CRACK (THE
ZONE IN WHICH THE
BOND IS INTACT)

IV_ STRESS DISTRIBUTION IN
PAVEMENT SLAB
(OVERLAY+BASE) WITHOUT
CRACK

BOND BROKEN NEAR THE CRACK

Scale _ 1cm = 25kg/cm^2

$E_c/E_s = 200$

III _ SECTION AT 6.75 cm FROM THE CRACK IN CASE
WHEN BOND IS NOT BROKEN
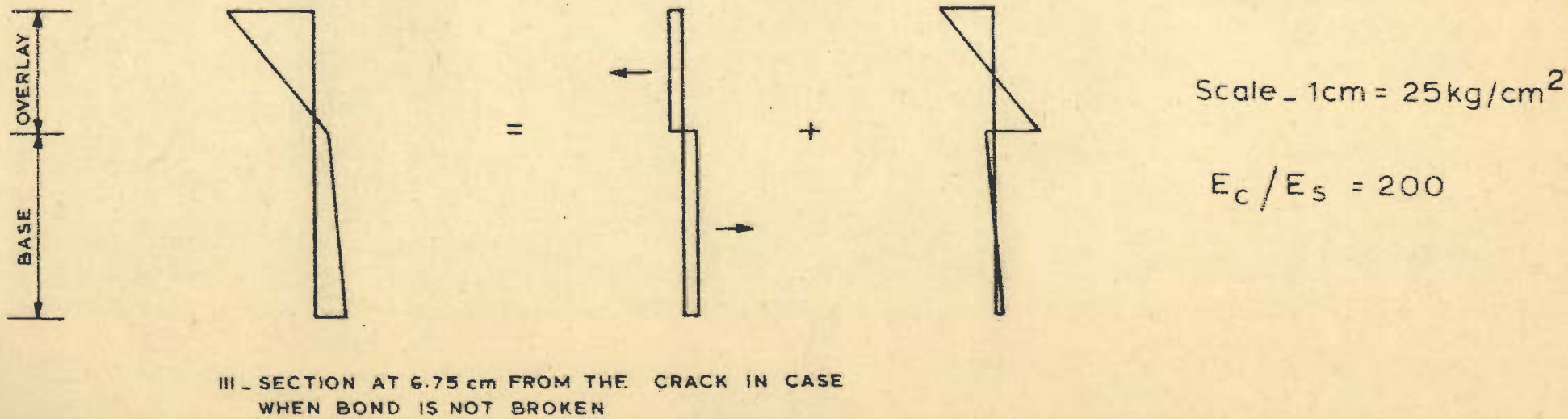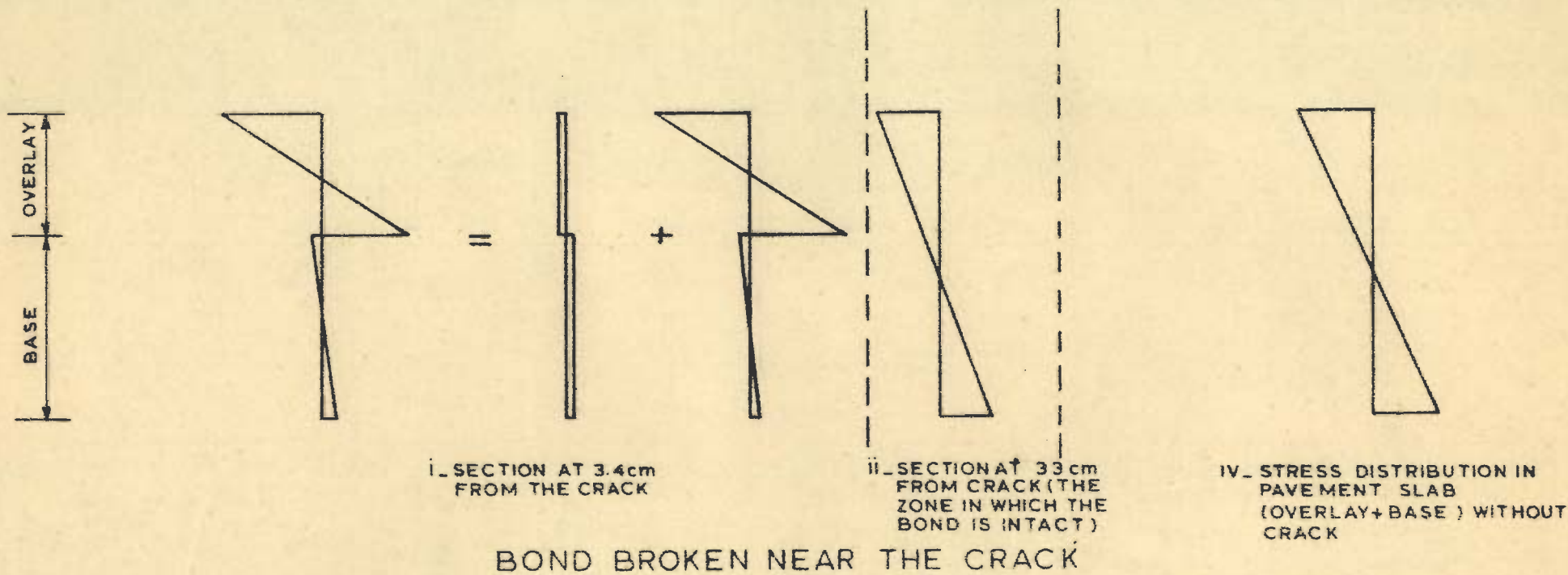
FIG. 3.6 _ STRESS DISTRIBUTION IN SLABS

71

Compressive stress kg/cm^2

~ 22.5 cm   0   2.5   5.0   7.5   10

Tensile stress   kg/cm^2

10   7.5   5.0   2.5   0   DEPTH OF CRACK FROM BOTTOM

a _ AT CRACK

O———O   NO CRACK
X——X   3.75 cm
●———●   7.5 cm
△——△   11.25 cm
+   15 cm

Compressive stress   kg/cm^2

~ 22.5 cm   0   2.5   5.0   7.5   10

10   7.5   5.0   2.5   0

Tensile stress   kg/cm^2

b _ AT 15cm FROM CRACK
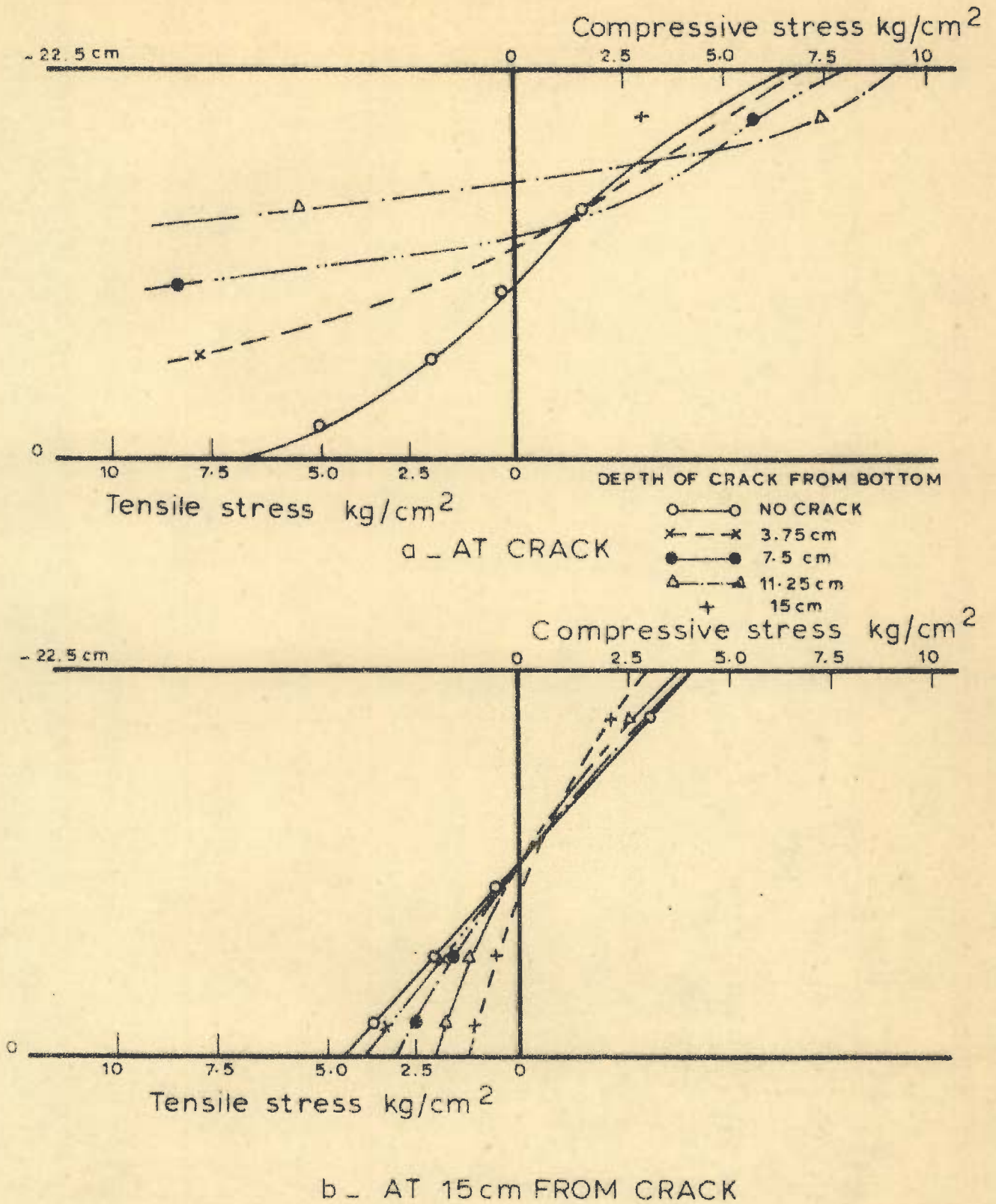
FIG. 3.7 _ STRESS VARIATION FOR DIFFERENT CRACK
          DEPTHS (83)
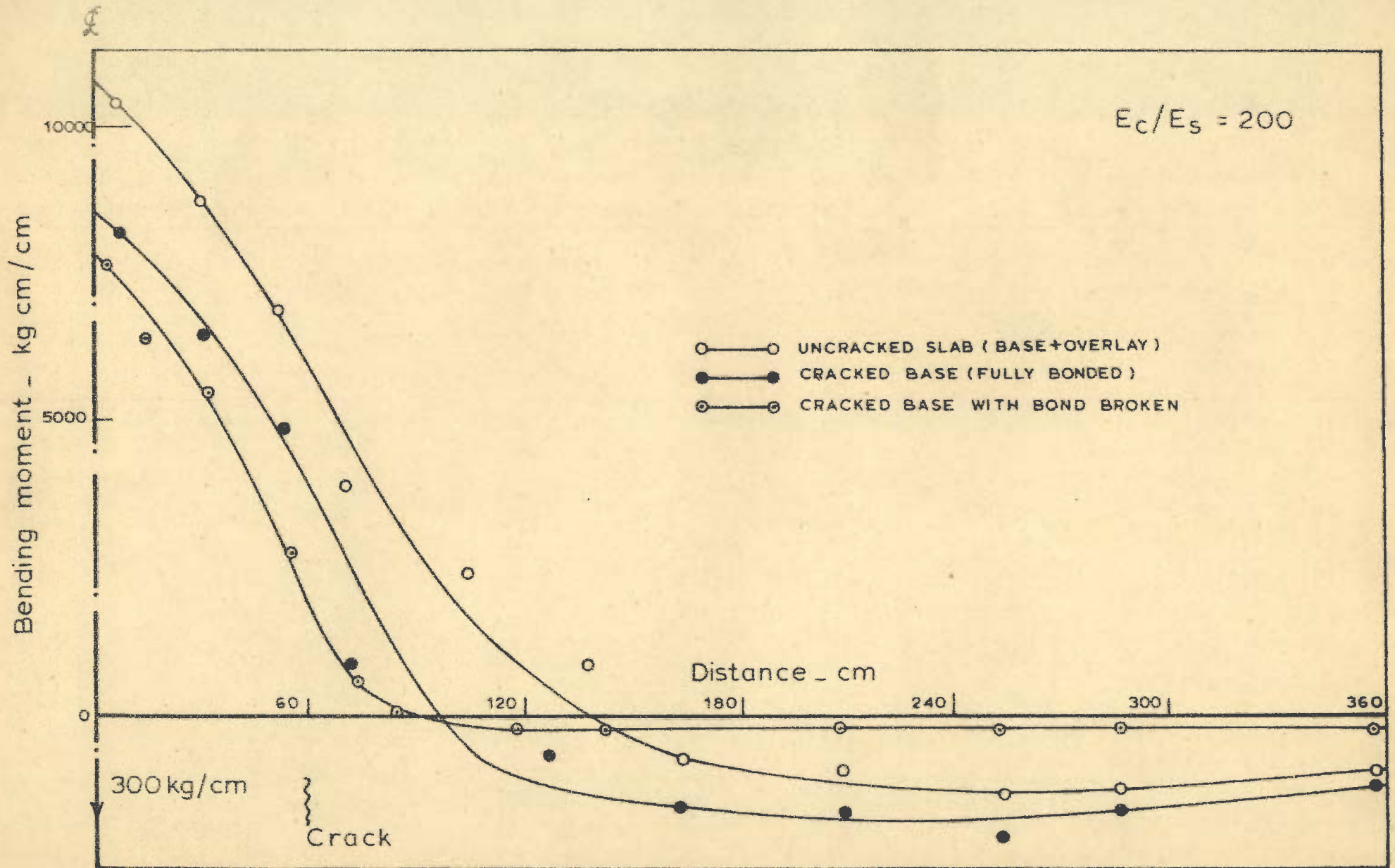
FIG. 3.8 _ VARIATION IN BENDING MOMENT IN SLABS WITH OVERLAY
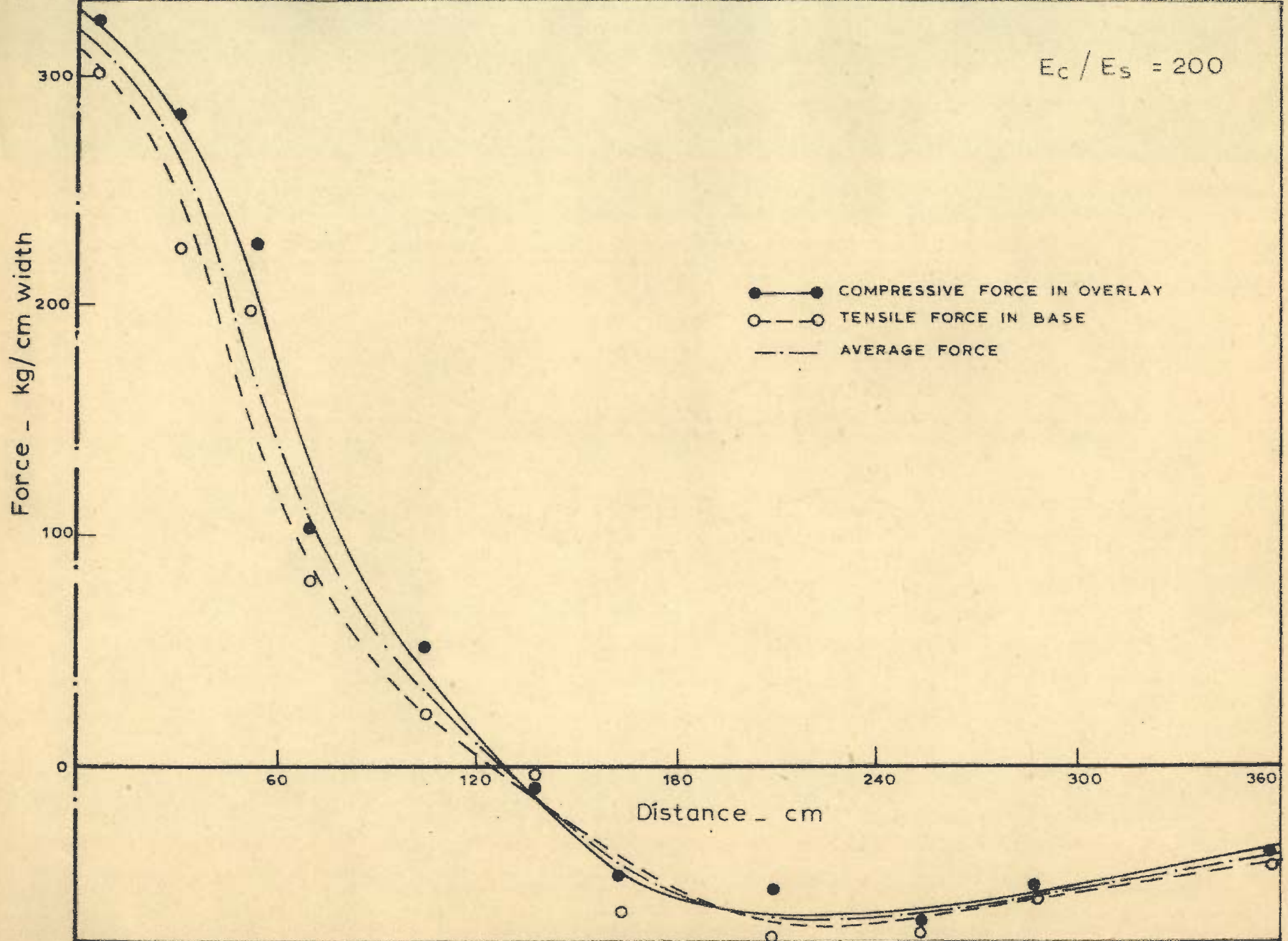
FIG 3.9   DIRECT FORCE IN OVERLAY AND CRACKED BASE WITHOUT LOSS OF BOND
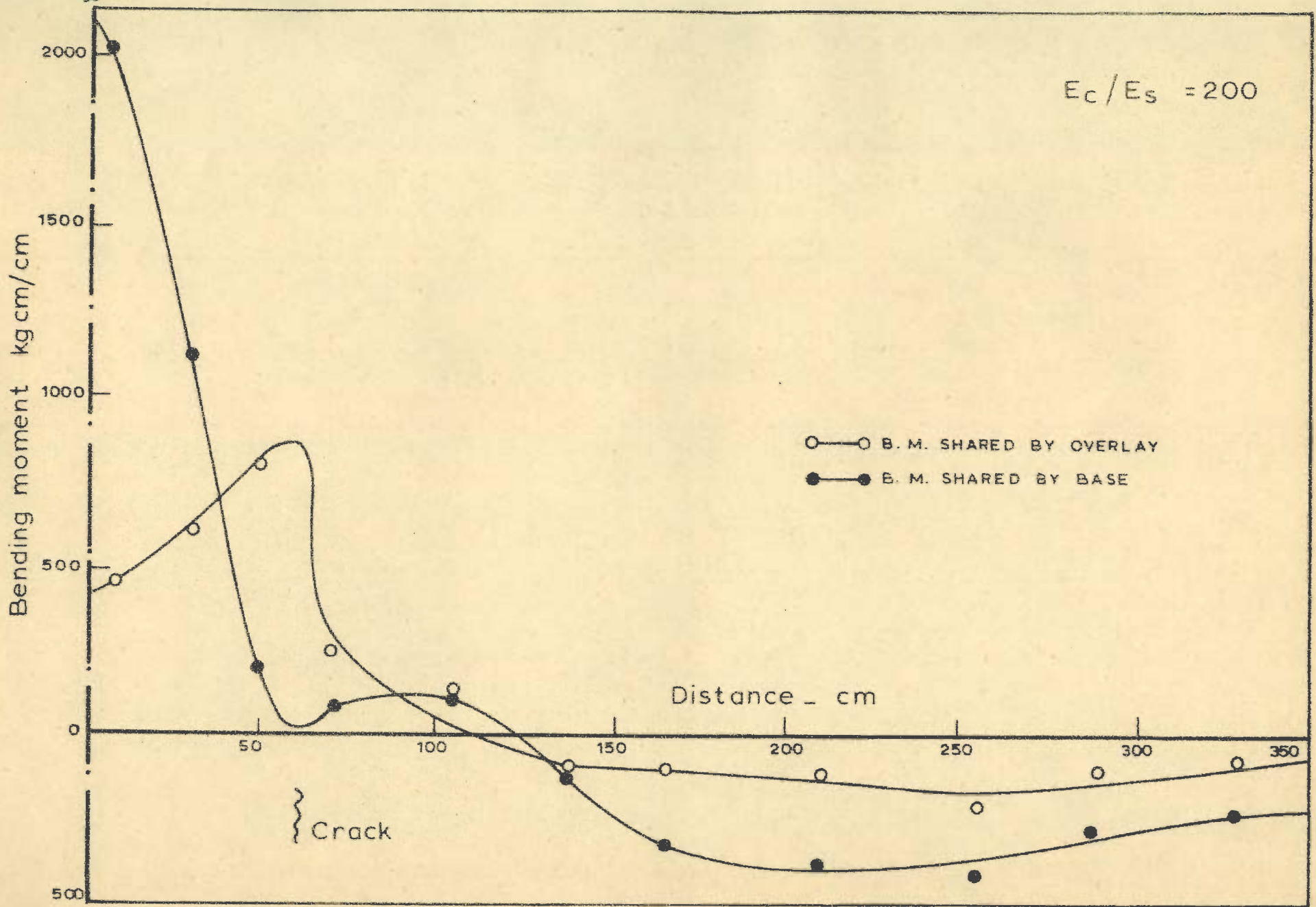
FIG. 3.10 _ SHARING OF BENDING MOMENTS BY OVERLAY AND CRACKED BASE
SLAB WITHOUT LOSS OF BOND
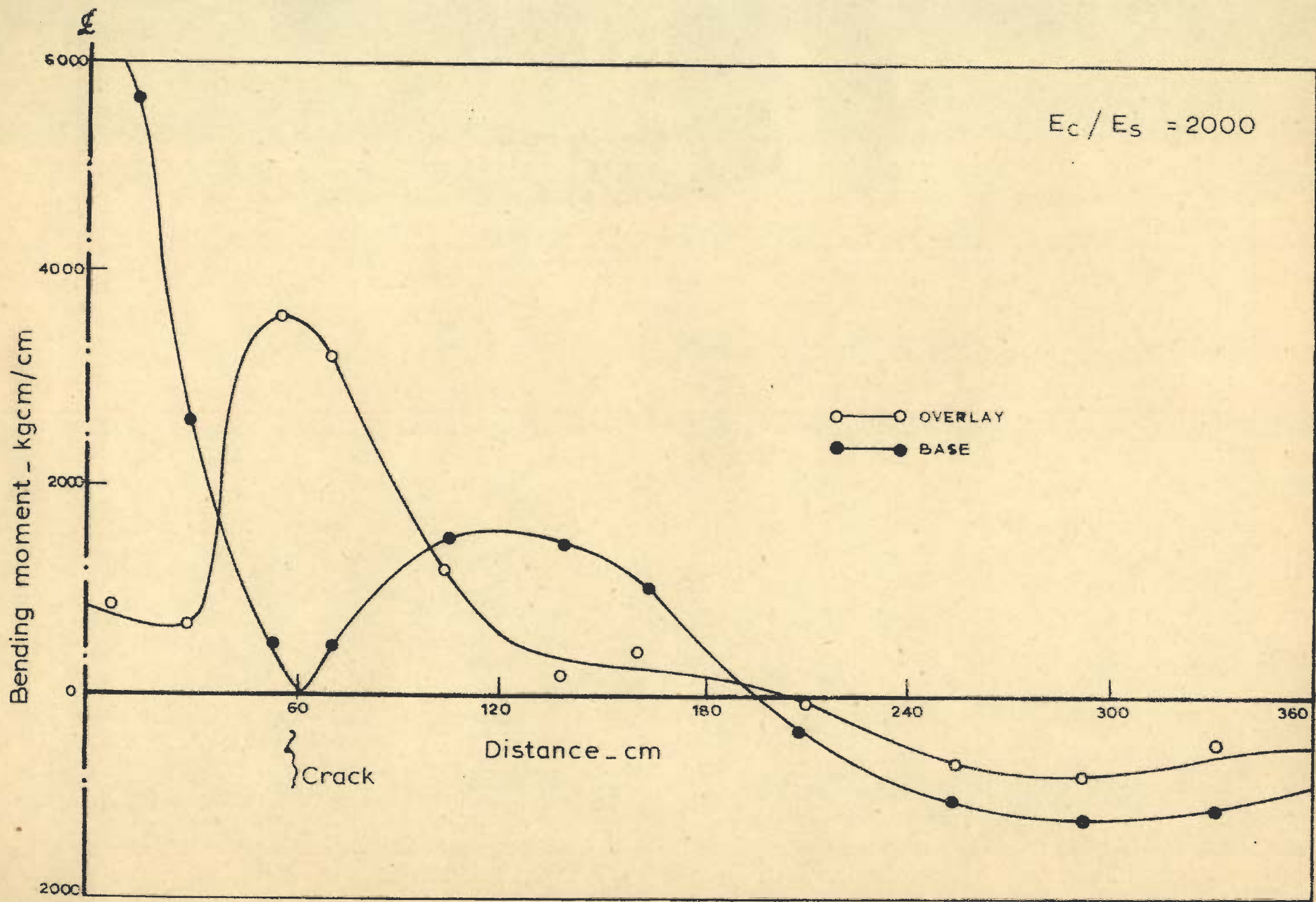
FIG. 3.11 — SHARING OF BENDING MOMENTS BY OVERLAY AND CRACKED BASE WITHOUT LOSS OF BOND

$E_C / E_S = 200$

Bending moment – kg cm/cm

◦———◦ WITHOUT LOSS OF BOND
●———● BROKEN BOND

Crack

Distance – cm
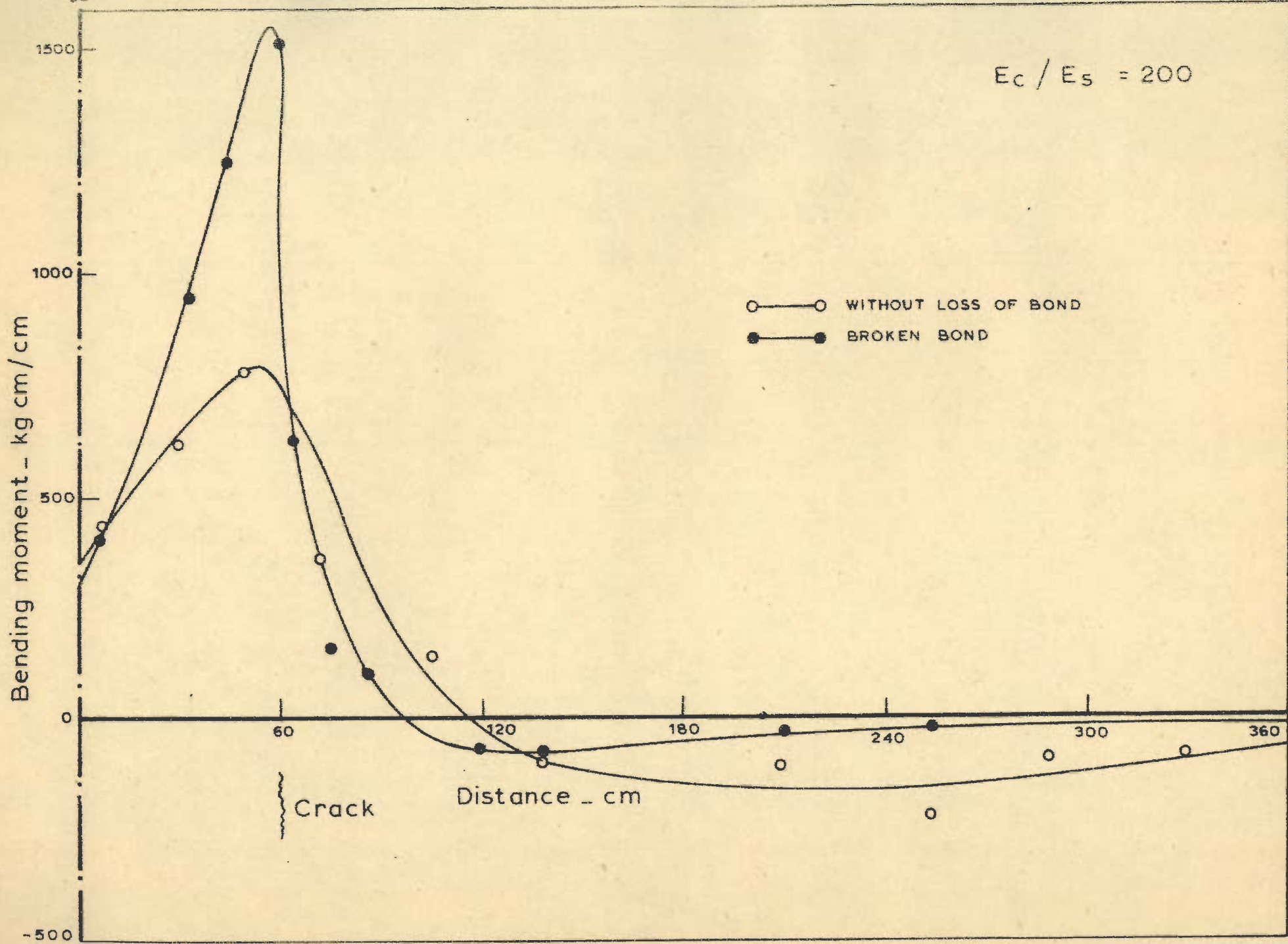
FIG. 3.12 – COMPARISON OF BENDING MOMENTS IN OVERLAY SLABS

77

$E_C / E_S = 2000$

o———o WITHOUT LOSS OF BOND

●———● BROKEN BOND

Bending moment _ kg cm/cm

Distance _ cm
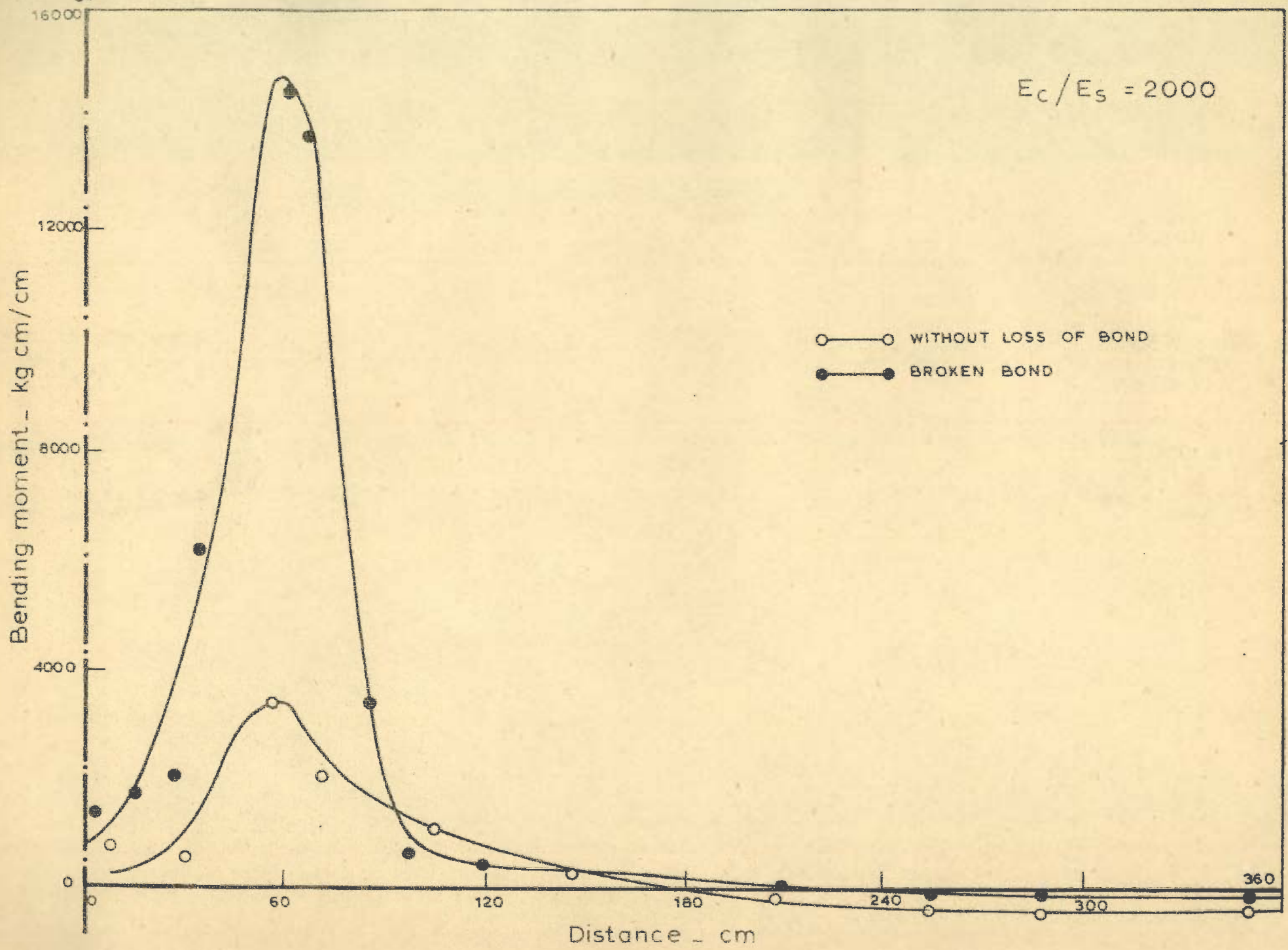
FIG. 3.13 _ COMPARISON OF BENDING MOMENTS IN OVERLAY SLABS

WHEEL LOAD
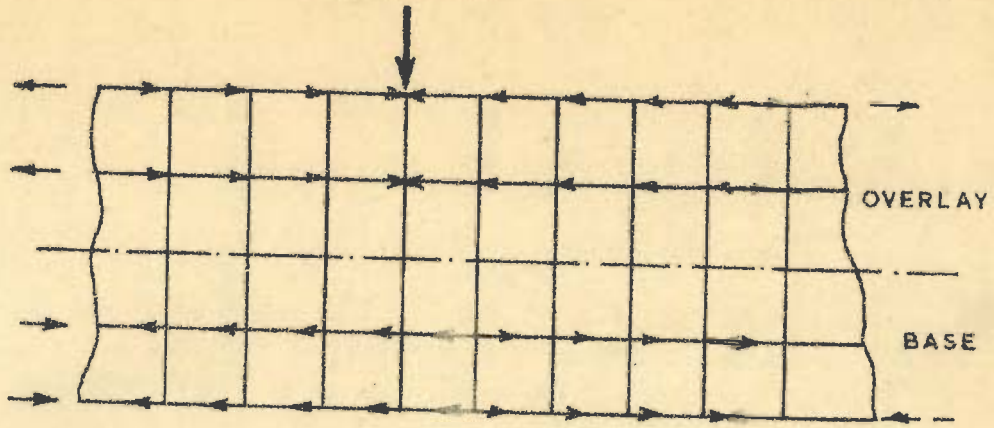
OVERLAY

BASE

I _ UNCRACKED BASE WITH OVERLAY

WHEEL LOAD

OVERLAY

BASE
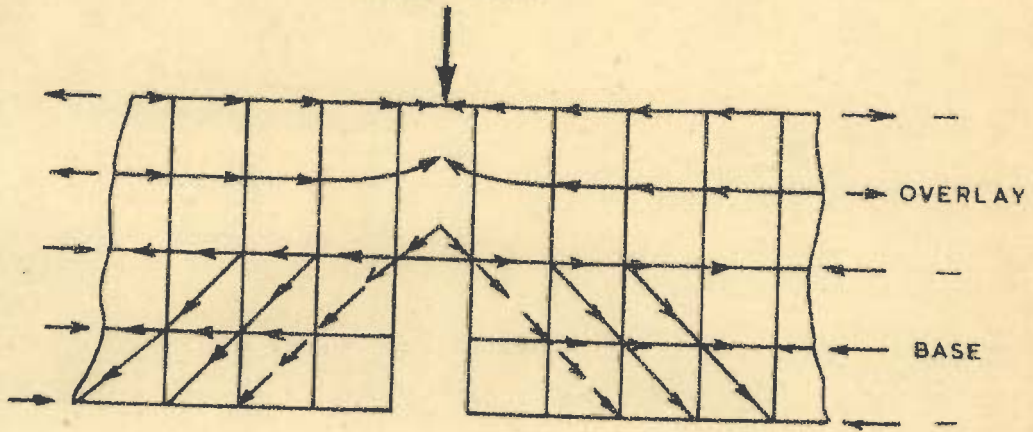
II _ DISTURBANCE DUE TO CRACK

WHEEL LOAD

OVERLAY

BASE

R
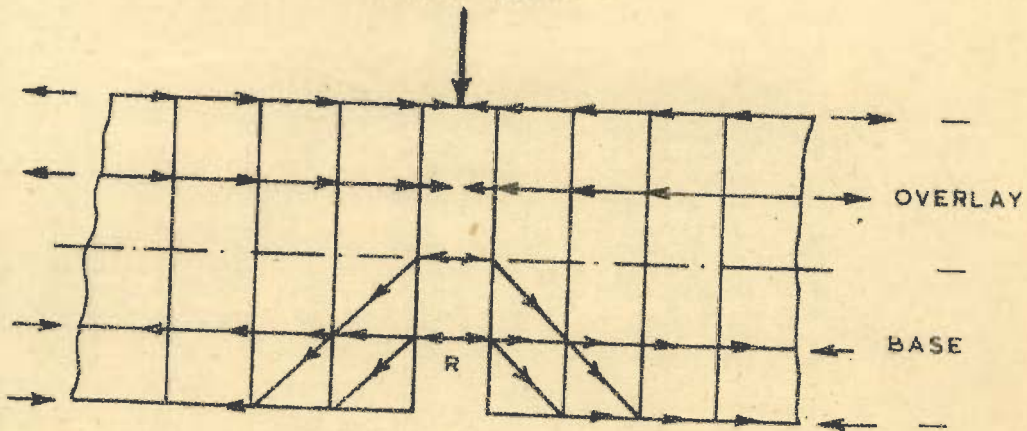
R _ REINFORCEMENT

III _ CORRECTION BY REINFORCEMENT

FIGURE _ 3.14
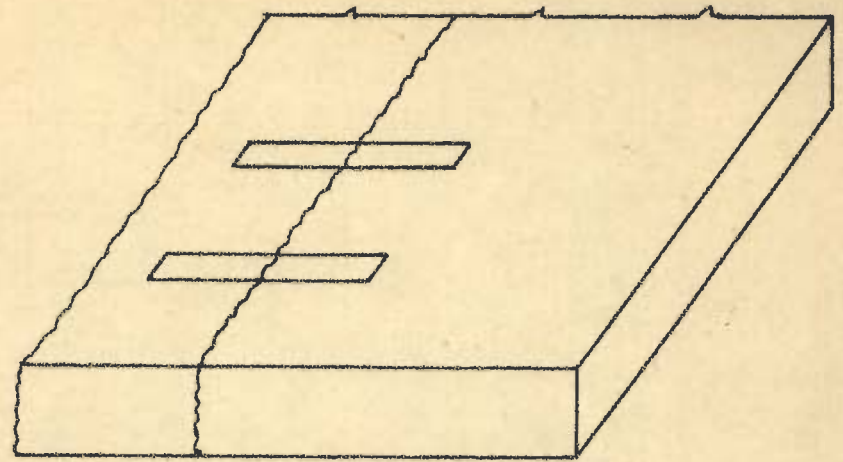
I _ Plan of grooves
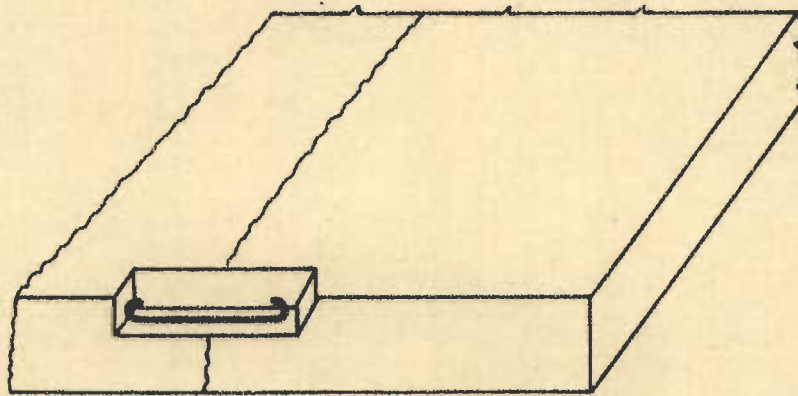
II _ Groove with reinforcement
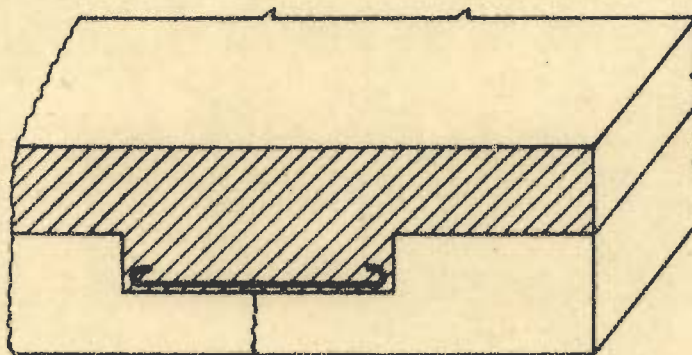
III _ Overlay concreted with groove

5cm

22.5cm

12cm
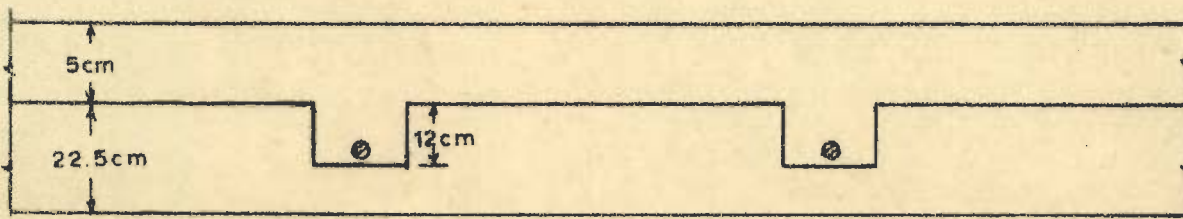
IV _ Section of completed overlay along crack

FIG. 3.15 _ REINFORCED KEY TECHNIQUE

CHAPTER IV

FORMULATION FOR ANALYSIS OF PAVEMENT SLAB
WITH CRACKS

4.1 INTRODUCTION

As has already been mentioned, truly, a three
dimensional analysis is required for determining the
stresses and displacements in a pavement slab which has
a layered construction and also possesses discontinui-
ties. However, for reasons pointed out in last chapter,
it becomes necessary to handle only a two dimensional
analysis. It was decided that out of several possible
two dimensional conversions, e.g., considering the
problem as a plane-strain, plane stress or axisymmetric
case, the one in which the pavement slab is considered
as a transversely loaded plate on a suitable foundation
is the most appropriate one. In such a model, it is poss-
ible to account the effect of important parameters like
load placements, temperature differential etc., on a
realistic basis. It is quite natural that this conversion
of a three dimensional problem into two dimensional one,
will call for certain assumptions and approximations.
One such approximation is that the subgrade can not be
treated as a continuum and has to be represented by a
mathematical model such as Winkler[23], Biot[25],
Pasternak[45] or any other type.[111]

4.2 GENERAL ASSUMPTIONS

Following assumptions are regarded as valid for making the two dimensional analysis of a cement concrete pavement possible:

1. The material of the cement concrete pavement behaves as an elastic homogeneous mass in accordance with the Hooke's law. The validity of such an assumption has already been discussed.

2. It is assumed that the pavement slab behaves as a plate. This means,

   (a) that at any cross-section, the normal boundary stresses are linearly distributed, and

   (b) that the deformations are small enough so as not to give rise to any appreciable amount of stretching at the neutral plane.

The validity of this assumption stems from the fact that the thickness of the pavement slab is small in comparison to its other dimensions and that deformations have to be limited in order to prevent cracking.

A corollary of this assumption is the validity of bending theory and therefore, it is implied that the usual assumptions of the theory of bending are valid, viz.

   (c) The points lying initially on the normal to neutral plane, in the undeformed state, remain on the same normal in the deformed state also.

(d) The transverse deformation of all points on
a normal to the middle plane are same i.e.,
the stresses normal to the neutral plane and
the change in thickness can be disregarded.

The validity of these assumptions can be supported
through the analysis using continuum elements reported
in Chapter III.

3. The loads acting are either considered as
transverse loads or as moments. The body forces
are disregarded, but they can be considered as
a part of applied transverse loads.

4. It is assumed that the subgrade can be adequately
represented by a suitable foundation model. If
the subgrade is represented by dense liquid
as adopted by Westergaard[24] the following
usual implications apply:

(a) the reaction of foundation at each point
is supposed to be proportional to the
deflection of the slab at that point.

(b) the reaction is assumed to be vertical.

(c) the reaction at a point is independent of
the reactions at its neighbouring points.

(d) the pavement slab and the foundation are
in contact at every point.

4.3 MATERIAL CHARACTERIZATION

The most important point in stress-deformation analysis is proper modeling of the actual material behaviour. On being subjected to load, the material of the body undergoes deformations or displacements. These deformations in case of cement concrete pavements, are small and therefore it is reasonable to adopt a linear definition of strain with respect to the original configuration of the point under consideration i.e., the Cauchy's definition. Thus, [112]

$$\varepsilon_{ij} = \frac{1}{2}(\frac{\partial u_i}{\partial x_j} + \frac{\partial u_j}{\partial x_i}) \qquad (i,j=1,2,3) \qquad ... \ 4.1$$

where, ε, u and x relate to strain, displacement and position, respectively.

Stress will be induced due to these nine strain components. For a general material the stress is a function of time and temperature and as such, the constitutive relationship to describe stress can be written as:

$$\sigma_{ij} = F(\varepsilon_{ij}, x, T, t) \qquad (i,j = 1,2,3) \ ... \ (4.2)$$

where, σ, T and t relate to stress, temperature and time, respectively.

The material presently under consideration is cement concrete and the loading is a moving wheel load. The temperature changes to which the material is to be

subjected is only atmospheric temperature variations.
Since the time of load application is small and it is
also known that the moment diagram has a steep peak under
the load,[113] it is reasonable to assume that the
material behaviour is independent of time and temperature.
The stress at a point therefore becomes dependent on the
strain and the position of the point.

Thus,

$$\sigma_{ij} = F(\varepsilon_{ij}, x) \qquad (i, j = 1, 2, 3) \quad \ldots \ 4.3$$

These nine components reduce to only six because
of the symmetry of the stress tensor[112].

Also, according to the assumption (ii)(d) of article 4.2,
the stress in the transverse direction i.e. z direction
of the pavement is negligible. This means,

$$\sigma_z = \tau_{xz} = \tau_{yz} = 0 \qquad \ldots \ (4.4)$$

Therefore, the stress-strain relationship can
be written as,

$$\begin{Bmatrix} \sigma_x \\ \sigma_y \\ \tau_{xy} \end{Bmatrix} = \begin{bmatrix} C_{11} & C_{12} & C_{13} \\ C_{12} & C_{22} & C_{23} \\ C_{13} & C_{23} & C_{33} \end{bmatrix} \begin{Bmatrix} \varepsilon_x \\ \varepsilon_y \\ \gamma_{xy} \end{Bmatrix} \qquad \ldots \ (4.5)$$

It is seen that if the coordinate axes are chosen
in such a manner that the principal direction of
orthotropy coincides with them, then

$$C_{13} = C_{23} = 0$$

and $\qquad \tau_{xy} = C_{33}\gamma_{xy}$

For orthotropic material in plane stress[37]

$$\left\{ \begin{array}{c} \sigma_x \\ \sigma_y \\ \tau_{xy} \end{array} \right\} = \frac{1}{1-\nu_x\nu_y} \left[\begin{array}{ccc} E_x & \nu_x E_y & 0 \\ \nu_y E_x & E_y & 0 \\ 0 & 0 & (1-\nu_x\nu_y)G_{xy} \end{array} \right] \left\{ \begin{array}{c} \varepsilon_x \\ \varepsilon_y \\ \gamma_{xy} \end{array} \right\}$$

$$\dots \ (4.6)$$

where, E_x, E_y, ν_x, ν_y and G_{xy} are elastic constants for the orthotropic material.

or, $\qquad \{\sigma\} = [C]\{\varepsilon\}$ $\qquad\qquad\qquad \dots \ (4.7)$

It is necessary to give an explicit definition to $\{\varepsilon\}$.

From figure 4.1 which shows the deformed shape of the slab in accordance with the assumption (ii)^2 of Article 4.2.

$$u = -z \frac{\partial w}{\partial x} \, ,$$

and $\qquad v = -z \frac{\partial w}{\partial y}$

the strain $\varepsilon_x = \dfrac{\partial u}{\partial x} = -z \dfrac{\partial^2 w}{\partial x^2}$

$$\varepsilon_y = \dfrac{\partial v}{\partial y} = -z \dfrac{\partial^2 w}{\partial y^2}$$

$$\dots \ (4.8)$$

and $\qquad \gamma_{xy} = \dfrac{\partial u}{\partial y} + \dfrac{\partial v}{\partial x} = -2z \dfrac{\partial^2 w}{\partial x \partial y}$

On substituting these values in equation 4.6

$$\sigma_x = -C_{11} \cdot z \frac{\partial^2 w}{\partial x^2} - C_{12} z \frac{\partial^2 w}{\partial y^2}$$

$$\sigma_y = -C_{12} z \frac{\partial^2 w}{\partial x^2} - C_{22} z \frac{\partial^2 w}{\partial y^2} \qquad \dots (4.9)$$

$$\tau_{xy} = -2z\, C_{33} \frac{\partial^2 w}{\partial x \partial y}$$

Bending moments M_x, M_y, and M_{xy} can be obtained by integrating the moments of stresses

$$M_x = \int_{-h/2}^{h/2} \sigma_x z \, dz$$

$$= -\frac{h^3}{12}\left(C_{11} \frac{\partial^2 w}{\partial x^2} + C_{12} \frac{\partial^2 w}{\partial y^2}\right)$$

Similarly,

$$M_y = -\frac{h^3}{12}\left(C_{12} \frac{\partial^2 w}{\partial x^2} + C_{22} \frac{\partial^2 w}{\partial y^2}\right) \qquad \dots (4.10)$$

and following (114)

$$M_{xy} = M_{yx} = \int_{-h/2}^{h/2} -C_{33} \tau_{xy} z \, dz$$

$$= \frac{2h^3}{12} C_{33} \frac{\partial^2 w}{\partial x \partial y}$$

Therefore, it is possible to write

$$\begin{Bmatrix} M_x \\ M_y \\ M_{xy} \end{Bmatrix} = \begin{bmatrix} D_{11} & D_{12} & 0 \\ D_{12} & D_{22} & 0 \\ 0 & 0 & D_{33} \end{bmatrix} \begin{Bmatrix} -\dfrac{\partial^2 w}{\partial x^2} \\ -\dfrac{\partial^2 w}{\partial y^2} \\ 2\dfrac{\partial^2 w}{\partial x \partial y} \end{Bmatrix} \qquad \dots (4.11)$$

The formulation can be extended to problems with varying flexural rigidities along x and y directions. However, the formulation becomes uncertain due to the Poisson's ratio. A better proposition therefore, is to treat the material as isotropic but its flexural properties different in x and y directions. Thus, defining $[D]$ as[114, 115]

$$D_{11} = \frac{E}{(1-\nu^2)} \, I_x$$

$$D_{22} = \frac{E}{(1-\nu^2)} \, I_y$$

$$D_{12} = \nu \sqrt{D_{11} D_{22}}$$

$$D_{21} = D_{12}$$

and $$D_{33} = \frac{1-\nu}{2\nu} D_{12}$$

... (4.12)

where E = modulus of elasticity of concrete

ν = Poisson's ratio for concrete

and I_x, I_y= moment of inertia per unit length of the equivalent section about its neutral axis, in x and y directions respectively.

4.4 MODELING OF PAVEMENT BY FINITE ELEMENTS
4.4.1 Selection of Element

It is now observed that with the basic assumptions stated in article 4.2, the pavement can very well be modeled by plate bending elements[34, 51, 54]. There are a number of elements of plate bending type with triangular,

rectangular, quadrilateral or parallelogram configuration. There is no restriction imposed on the element shape because the straight forward geometry of the pavement can be accurately modeled by elements of any shape.

Also the elements of the plate bending type could be classified as a conforming or a non-conforming one. The main implication of non-conforming element is with respect to the minimization of the strain energy of the system and its bound towards achieving monotonic convergence as the total degree of freedom of the system is increased. It is shown[116] that in case of 'plate bending elements' if 'constant strain' criterion is satisfied and if the displacement function chosen is such that with decrease in element size the continuity condition becomes more and more complete, then it is possible to achieve convergence with non-conforming displacement function.

However, it is well known that the solutions in which continuity is also maintained, leads to a proper bound on the true strain energy of the system[117]. From this point of view, it is straight forward to adopt a conforming formulation as it has been reported, that in many nonconforming plate models, the convergence is not achieved as the mesh size is reduced[118].

Bogner, Fox and Schmit[120] have shown that a conforming displacement function for a rectangular plate

bending element can be generated by using Hermite interpolation polynomial. This element has four corner nodes and each node is assigned four degrees of freedom, viz., lateral deflection 'w', two orthogonal slopes '$\partial w/\partial x$' and '$\partial w/\partial y$' and the twist '$\partial^2 w/\partial x \partial y$'. The Hermite interpolation polynomial uses the function value and the value of the first derivative at each point. Thus the polynomial is tangent to the function at every point[121]. The transverse displacement 'w' is represented by the function and its tangents are slopes '$\partial w/\partial x$' and '$\partial w/\partial y$'. Gallagher[122] commenting on the efficiency of the Hermitian polynomial states,

"--The results obtained with complete and
compatible function were of superior accuracy
at any given level of refinement for the case
studied'.

These observations and also those of Argyris and William[123], institute sufficient confidence to adopt this element. The only probable disadvantage of this element is that of its shape because of which all corners must contain a right angle and as such the element size can be increased only in one direction. The effect of this constrain is on the aspect ratio which tends to be high as element size is increased and limiting the aspect ratio results in loss of economy. A compromise between economy and accuracy is therefore imperative.

4.4.2 Evaluation of Element Stiffness for Orthotropic Slab

The explicitly d rived coefficients of the element stiffness matrix for a 4 noded rectangular element, with 16 degrees are for isotropic plate bending element. However, in the present formulation it is necessary to treat the element as orthotropic, so as to properly model the cracked pavement slab. It is therefore, necessary to completely derive the stiffness coefficients for such an element.

The Hermitian Polynomials defined for interval (o, a) are:

$$
\left.
\begin{aligned}
H_{01}(x) &= \frac{1}{a^3}(2x^3 - 3ax^2 + a^3) \\[2mm]
H_{02}(x) &= \frac{1}{a^3}(3ax^2 - 2x^3) \\[2mm]
H_{11}(x) &= \frac{1}{a^2}(x^3 - 2ax^2 + a^2 x) \\[2mm]
H_{12}(x) &= \frac{1}{a^2}(x^3 - ax^2)
\end{aligned}
\right\}
\qquad \cdots \ (4.13)
$$

Then,

$$
w(x,y) = \sum_{i=1}^{2} \sum_{j=1}^{2} \Big[H_{oi}(x) \cdot H_{oj}(y) \cdot w_{ij} + H_{1i}(x) \cdot H_{oj}(y) \cdot w_{xij}
$$
$$
+ H_{oi}(x) \cdot H_{1j}(y) \cdot w_{yij} + H_{1i}(x) \cdot H_{1j}(y) \cdot w_{xyij} \Big]
$$

where,

$w(x,y)$ = d flection of the slab at any point (x,y) within the el ment, including its boundari s.

w_{ij} = deflection of node (i,j) according to figure 4.2.

w_{xij} = slope in local 'x' direction at node (i,j)

w_{yij} = slope in local 'y' direction of node (i,j)

w_{xyij} = twist at node (i,j).

Also, from equation 2.1

$$w(x,y) = [N]\{\delta\} \qquad \dots (4.15)$$

where,

$[N]$ = matrix containing shape functions with proper coordinate values, and

$\{\delta\}$ = list of nodal degrees of freedom taken in proper order.

Equation 4.15 can be written explicitly as:

$$
w(x,y) = \frac{1}{a^3b^3}
\begin{Bmatrix}
(2x^3-3ax^2+a^3)(2y^3-3by^2+b^3) \\
a(x^3-2ax^2 + a^2x)(2y^3-3b^2y+b^3) \\
b(2x^3-3ax^2+a^3)(y^3-2by^2+b^2y) \\
ab(x^3-2ax^2+a^2x)(y^3-2by^2+b^2y) \\
(3ax^2-2x^3)(2y^3-3by^2+b^3) \\
a(x^3-ax^2)(2y^3-3b^2+b^3) \\
b(3ax^2-2x^3)(y^3-2by^2+b^2y) \\
ab(x^3-ax^2)(y^3-2by^2+b^2y) \\
(3ax^2-2x^3)(3by^2-2y^3) \\
a(x^3-ax^2)(3by^2-2y^3) \\
b(3ax^2-2x^3)(y^3-by^2) \\
ab(x^3-ax^2)(y^3-by^2) \\
(2x^3-3ax^2+a^3)(3by^2-2y^3) \\
a(x^3-2ax^2+a^2x)(3by^2-2y^3) \\
b(2x^3-3ax^2+a^3)(y^3-by^2) \\
ab(x^3-2ax^2+a^2x)(y^3-by^2)
\end{Bmatrix}^{T}
\begin{Bmatrix}
w_{11} \\
w_{x11} \\
w_{y11} \\
w_{xy11} \\
w_{12} \\
w_{x12} \\
w_{y12} \\
w_{xy12} \\
w_{22} \\
w_{x22} \\
w_{y22} \\
w_{xy22} \\
w_{21} \\
w_{x21} \\
w_{y21} \\
w_{xy21}
\end{Bmatrix}
$$

$i=2, j=1$

$\dots (4.16)$

where,

a = dimension of the element along x direction,

and b = dimension of the element along y direction.

now, let $\xi = x/a$ and $\eta = y/b$ ... (4.17)

therefore,

$$\frac{\partial \xi}{\partial x} = \frac{1}{a} \quad \text{and} \quad \frac{\partial \eta}{\partial y} = \frac{1}{b} \qquad ... (4.18)$$

also

$$\frac{\partial w}{\partial x} = \frac{\partial w}{\partial \xi}\frac{\partial \xi}{\partial x} = \frac{1}{a}\frac{\partial w}{\partial \xi}$$

... (4.19)

and $\quad \dfrac{\partial w}{\partial y} = \dfrac{\partial w}{\partial \eta}\dfrac{\partial \eta}{\partial y} = \dfrac{1}{b}\dfrac{\partial w}{\partial \eta}$

Again

$$\frac{\partial^2 w}{\partial x^2} = \frac{\partial}{\partial x}\left\{\frac{\partial w}{\partial x}\right\} = \frac{1}{a^2}\frac{\partial^2 w}{\partial \xi^2}$$

$$\frac{\partial^2 w}{\partial y^2} = \frac{1}{b^2}\frac{\partial^2 w}{\partial \eta^2}$$

and $\quad \dfrac{\partial^2 w}{\partial x \partial y} = \dfrac{\partial}{\partial x}\left(\dfrac{\partial w}{\partial y}\right) = \dfrac{1}{ab}\dfrac{\partial^2 w}{\partial \eta d\xi}$ ... (4.20)

It can also be seen that

$$\partial \xi \partial \eta = \frac{1}{ab} dx\, dy \qquad ... (4.21)$$

Therefore from equations 4.8 and 4.11,

$$\{\chi\} = \left\{\begin{array}{c} -\dfrac{\partial^2 w}{\partial x^2} \\[2mm] -\dfrac{\partial^2 w}{\partial y^2} \\[2mm] 2\dfrac{\partial^2 w}{\partial x \partial y} \end{array}\right\}$$

$$
= \begin{bmatrix} -\dfrac{1}{a^2} & 0 & 0 \\[2mm] 0 & -\dfrac{1}{b^2} & 0 \\[2mm] 0 & 0 & \dfrac{2}{ab} \end{bmatrix} \begin{Bmatrix} \dfrac{\partial^2 w}{\partial \xi^2} \\[2mm] \dfrac{\partial^2 w}{\partial \eta^2} \\[2mm] \dfrac{\partial^2 w}{\partial \eta \partial \xi} \end{Bmatrix} \qquad \ldots (4.22)
$$

or $\quad \{\chi\} = [A]\{\overset{*}{\chi}\}$

Similar to equation 2.2 the curvature-displacement relationship can be

$$
\{\chi\} = [B]\{\delta\} = [A][B^{*}]\{\delta\} \qquad \ldots (4.23)
$$

where $[B]$ for plate bending case will be

$$
\underset{3 \times 16}{[B]} = \begin{bmatrix} -\dfrac{\partial^2 N_1}{\partial x^2}, & -\dfrac{\partial^2 N_2}{\partial x^2}, & -\dfrac{\partial^2 N_3}{\partial x^2} & \cdots\cdots\cdots -\dfrac{\partial^2 N_{16}}{\partial x^2} \\[3mm] -\dfrac{\partial^2 N_1}{\partial y^2}, & -\dfrac{\partial^2 N_2}{\partial y^2}, & -\dfrac{\partial^2 N_3}{\partial y^2} & \cdots\cdots\cdots -\dfrac{\partial^2 N_{16}}{\partial y^2} \\[3mm] 2\dfrac{\partial^2 N_1}{\partial x \partial y}, & 2\dfrac{\partial^2 N_2}{\partial x \partial y}, & 2\dfrac{\partial^2 N_3}{\partial x \partial y} & \cdots\cdots\cdots 2\dfrac{\partial^2 N_{16}}{\partial x \partial y} \end{bmatrix}
$$

and $[B^{*}]$ in local coordinates can be explicitly written as,

$$[\mathbf{B}^*]^T = \begin{bmatrix}
6(2\xi-1)(2\eta^3-3\eta^2+1) & 6(2\xi^3-3\xi^2+1)(2\eta-1) & 36(\xi^2-\xi)(\eta^2-\eta) \\
a(6\xi-4)(2\eta^3-3\eta^2+1) & 6a(\xi^3-2\xi^2+\xi)(2\eta-1) & 6a(3\xi^2-4\xi+1)(\eta^2-\eta) \\
6b(2\xi-1)(\eta^3-2\eta^2+\eta) & b(2\xi^3-3\xi^2+1)(6\eta-4) & 6b(\xi^2-\xi)(3\eta^2-4\eta+1) \\
ab(\xi-4)(\eta^3-2\eta^2+\eta) & ab(\xi^3-2\xi^2+6)(6\eta-4) & ab(3\xi^2-4\xi+1)(3\eta^2-4\eta+1) \\
6(1-2\xi)(2\eta^3-3\eta^2+1) & 6(3\xi^2-2\xi^3)(2\eta-1) & 36(\xi-\xi^2)(\eta^2-\eta) \\
a(6\xi-2)(2\eta^3-3\eta^2+1) & 6a(\xi^3-\xi^2)(2\eta-1) & 6a(3\xi^2-2\xi)(\eta^2-\eta) \\
6b(1-2\xi)(\eta^3-2\eta^2+\eta) & b(3\xi^2-2\xi^3)(6\eta-4) & 6b(\xi-\xi^2)(3\eta^2-4\eta+1) \\
ab(6\xi-2)(\eta^3-2\eta^2+\eta) & ab(\xi^3-\xi^2)(6\eta-4) & ab(3\xi^2-2\xi)(3\eta^2-4\eta+1) \\
6(1-2\xi)(3\eta^2-2\eta^3) & 6(3\xi^2-2\xi^3)(1-2\eta) & 36(\xi-\xi^2)(\eta-\eta^2) \\
a(6\xi-2)(3\eta^2-2\eta^3) & 6a(\xi^3-\xi^2)(1-2\eta) & 6a(3\xi^2-2\xi)(\eta-\eta^2) \\
6b(1-2\xi)(\eta^3-\eta^2) & b(3\xi^2-2\xi^3)(6\eta-2) & 6b(\xi-\xi^2)(3\eta^2-2\eta) \\
ab(6\xi-2)(\eta^3-\eta^2) & ab(\xi^3-\xi^2)(6\eta-2) & ab(3\xi^2-2\xi)(3\eta^2-2\eta) \\
6(2\xi-1)(3\eta^2-2\eta^3) & 6(2\xi^3-3\xi^2+1)(1-2\eta) & 36(\xi^2-\xi)(\eta-\eta^2) \\
a(6\xi-4)(3\eta^2-2\eta^3) & 6a(\xi^3-2\xi^2+\xi)(1-2\eta) & 6a(3\xi^2-4\xi+1)(\eta-\eta^2) \\
6b(2\xi-1)(\eta^3-\eta^2) & b(2\xi^3-3\xi^2+1)(6\eta-2) & 6b(\xi^2-\xi)(3\eta^2-2\eta) \\
ab(6\xi-4)(\eta^3-\eta^2) & ab(\xi^3-2\xi^2+\xi)(6\eta-2) & ab(3\xi^2-4\xi+1)(3\eta^2-2\eta)
\end{bmatrix}$$

$$\dots \quad (4.24)$$

because of the relationships shown in tabular form below

Hermitian Polynomial	H	$\frac{dH}{d\xi}$	$\frac{d^2 H}{d\xi^2}$	$\frac{d^3 H}{d\xi^3}$
$H_{01}(\xi)$	$(2\xi^3 - 3\xi^2 + 1)$	$6(\xi^2 - \xi)$	$6(2\xi - 1)$	12
$H_{02}(\xi)$	$(3\xi^2 - 2\xi^3)$	$6(\xi - \xi^2)$	$6(1 - 2\xi)$	-12
$H_{11}(\xi)$	$a(\xi^3 - 2\xi^2 + \xi)$	$a(3\xi^2 - 4\xi + 1)$	$a(6\xi - 4)$	6a
$H_{12}(\xi)$	$a(\xi^3 - \xi^2)$	$a(3\xi^2 - 2\xi)$	$a(6\xi - 2)$	6a

It is now possible to determine the element stiffness for plate alone $[K_p]^e$ which according to equation 2.14 is

$$[K_p]^e = \int_0^a \int_0^b [B]^T [D] [B] \, dx.dy$$

Using equation 4.23, this can be also written as

$$[K_p]^e = ab \int_0^1 \int_0^1 [B^*]^T [A] [D] [A] [B^*] d\xi \, d\eta$$

$$\ldots (4.25)$$

Value of $[B^*]$ can be substituted from equation (4.24) and that of $[D]$ from equation 4.12.

This equation can be evaluated explicitly or the integral value can be obtained by numerical integration (Appendix 2.A).

The general form of an element 'K_{ij}' of 16x16 matrix $[K_p]^e$ is

$$K_{ij} = \frac{a^{\alpha^1_{ij}} b^{\alpha^2_{ij}}}{a.b} \left[D_{11} \alpha^3_{ij} (b/a)^2 + D_{22} \alpha^4_{ij} (a/b)^2 + D_{12} \alpha^5_{ij} + D_{33} \alpha^6_{ij} \right]$$

$$\ldots (4.26)$$

These coefficients $\alpha^1, \alpha^2, \alpha^3, \alpha^4, \alpha^5$ and α^6 for each value of i and j are given in the table 4.1. For a linear system to which Maxwell-Betti theorem(124) is applicable, the matrix $[K_p]^e$ must be symmetric. The coefficients are therefore given for only lower triangular matrix.

4.4.3 Properties of Slab with Subgrade

4.4.3.1 Reactive Forces due to Subgrade

The slab is resting on an elastic bed and it is assumed that the two are having full bearing at every point. Thus, at each point of contact, there will be a reactive force acting on the slab due to the foundation. In order to reduce the problem to a degree of determinacy, it is necessary to assume a mathematical correlation between this reactive force and the slab deformation. The simplest and usually assumed model among these is the Winkler's model[23].

In the linear Winkler foundation model, it is assumed that the subgrade behaves as a dense liquid of density 'k' such that the reactive pressure 'f' at any point, where deflection is 'w' is given by

$$f = -kw$$

4.4.3.2 Lumped Foundation Stiffness

These reactive pressures can be regarded as nodal forces and treated as a concentrated force acting at nodal point. The formulation in such a treatment is straight

forward and the equation of equilibrium i.e. equation
2.10 can be modified as

$$([K_p] + k[a])^e | \delta |^e = |F|^e \qquad \qquad \ldots (4.27)$$

where,

$[K_p]$ = stiffness matrix of pavement, and

$[a]$ = a diagonal matrix, the diagonal terms
represent the area under command of a
node over which the subgrade reaction
is supposed to be uniformly distributed.
It may be noted that $[a]$ contains zero
terms corresponding to derivatives of w.
This is an approximation. Moreover terms
corresponding to 'rotational stiffness, if
and   any, can not be included.

$|F|$ = vector of nodal forces due to applied loads.

Such a formulation is reported to have been
successfully adopted by Huang and Wang[79,80].
Obviously, adopting this procedure will mean, replacing
infinite number of springs by a finite number with one
spring attached to each node with the assumption that
there is constant deflection at all the points surround-
ing a node.

4.4.3.3 Consistent Foundation Stiffness

It is more appropriate to treat the subgrade
reaction at each point as variable, consistent, with
the deformation 'w' and its derivatives, if any, at
that point, and apply the principle of virtual work[124].
This will make the behaviour of the pavement certain

and a bound will be assured.[117]

In general, the reactive forces $\{f\}$ due to Winkler foundation due to (nx1) deformation vector $\{w\} = \{w, \frac{\partial w}{\partial x}, \frac{\partial w}{\partial y} \ldots \}^T$ can be written as

$$\underset{nx1}{\{f\}} = -\underset{nxn}{[k]}\underset{nx1}{\{w\}}$$

where $[k]$ is a constant diagonal matrix at a point and $n = 1$ for ordinary Winkler foundation.

The internal virtual work done by the reactive forces can be equated to the work done by its equivalent nodal forces $\{F\}_W$ during virtual nodal displacement $d\{\delta\}$.

$$-\iint d\{w\}^T \{f\} dS = d\{\delta\}^T \{F_W\} \qquad \ldots (4.28)$$

Substituting the deformation at a point

$$\underset{nx1}{\{w\}} = \underset{n \, x16}{[N]}\{\delta\} \quad \text{and} \quad d\{w\}^T = d\{\delta\}^T [N]^T$$

the equivalent nodal forces

$$\{F\}_W = -\left[\iint [N]^T [k] [N] dS \right] \{\delta\} = -[K_s]\{\delta\} \quad \ldots (4.29)$$

where,

$[K_s] = $ stiffness matrix of subgrade.

The final equation of equilibrium then reduces to

$$\{F\} = [K_p]\{\delta\} + [K_s]\{\delta\}$$
$$= [K]\{\delta\}$$

$$\ldots (4.30)$$

where $[K]$=stiffness of the pavement (slab+subgrade combined).

For n = 1, the stiffness matrix of the subgrade becomes

$$[K_s] = \iint [N]^T k [N] ds \qquad \ldots (4.30)$$

Thus, in this manner, the stiffness of the sub-grade is to be added to the stiffness of the pavement slab.

If K_{sij} is the element (i,j) of the matrix $[K_s]$ then, it is possible to write an explicit integration of equation 4.30.

$$K_{sij} = a^{\alpha^1_{ij}} . b^{\alpha^2_{ij}} . k . \alpha^7_{ij} \qquad \ldots (4.31)$$

The values of α^1, α^2 and α^7 are given in Table 4.1 for different values of (i,j). Again, since $[K_s]$ has to be symmetric, only lower triangular values of coeff-icients need to be evaluated.

4.4.4 Evaluation of Nodal Forces

4.4.4.1 Consideration for representing the Wheel Loads

The main considerations for realistic representation of wheel loads to obtain their influence on the pavement are:

(a) The wheel load is not static but is moving. This fact gives rise to two main considerations:

(i) The consideration of time effect on material behaviour:

   With the increase in the speed of the vehicle the loading time is reduced. Therefore, as a result of a narrow and steep force time curve obtained in pavements, the material character tends to become independent of time factor. This is specially true for cement concrete which does not appreciably exhibit visco-elastic characteristic during short-term loadings. Even for flexible pavements it is observed that the effects are negligible[72]. However, the usefulness of dynamic modulus of elasticity of concrete as obtained by Orchard, Walker and Stewart[95] is useful.

(ii) The consideration of dynamic or the inertial effects due to wheel movement:

   Such effects are a function of several variables like, speed of the movement, suspension system of the vehicle[125,126], tyre conditions, inflation pressure, pavement roughness etc. These variables make the assessment difficult and it is recommended[127] that a further study is warranted. However, Sargious et al.[75] based on actual measurement observe that,

   "....The negligible dynamic effect observed
   lends support to current design practice of
   considering static load only".

   According to Jones, Lister and Thower[128], the effect of moving wheel loads is essentially of quasi-static

type in which inertial forces have negligible effect due to a large difference in velocity of wave propagation in pavement material and the speed of the moving vehicle

(b) The second consideration in wheel load representation stems from the wheel load location. Again, there are two points worth considering:

(i) The absolute position of a wheel load on the pavement slab. From this point of view it is conventional to consider three locations viz., interior, edge and corner, of a slab. However, the critical location may be other than one of these due to the presence of a crack or a discontinuity. Therefore, it should be possible to determine the influence of the wheel load located any where on the slab.

(ii) A point may not be influenced by the position of a single wheel load but may also be under the influence of another adjoining load. Thus, the relative locations of wheel loads also become important. Though, it may not always be necessary to consider the location of adjoining wheel load due to the fact that the stress distribution in the pavement is highly localized because, it is known that the stress distribution curve has a steep peak below the wheel load[113]. The true representation of dual tyre load is important.

(c) As the stresses in the pavement slab are highly sensitive to the location and the distribution of the wheel load, contact pressure on the pavement surface needs due consideration. Once again, the two points that arise are:

    (i) The distribution of contact pressure- It has been found that the distribution of contact pressure is a function of type of tyre (number of ply rating), inflation pressure, tyre condition type of road surface, load coming on the tyre and also the speed of the vehicle. Markwick and Starks[129] observed that for normally loaded tyres the pressure is greater at the centre but for overloaded tyres it is greater under the walls. According to Bones and Kuhn[130], the modern automobile tyre is more like a overloaded one. Also, the centre of the reactive tyre pressure must fall ahead of the centre of axle in the direction of motion so as to give rise to rolling resistance[131].

    A method is therefore, required which can economically represent these variations, within the practical limitations, as realistically as possible.

    The interfacial shear stresses will also be present, specially at the instant when brakes

are applied. However, as is often the pract-
ice, these are not given importance for the
analysis.

(ii) The Shape of Contact Area:

In the analysis it has been usual to regard it as
circular or semi-circular[24,26,29]. However, for a loaded
wheel of a heavy highway vehicle or an aircraft the contact
area more closely resembles a rectangle with rounded
corners[132], where the imprint is taken on an unyielding
surface. This, therefore, holds true for rigid pavement.

It is therefore, appropriate to represent the contact
area by a rectangular geometry.

4.4.4.2 Evaluation of Nodal Forces due to Wheel Loads

In Chapter II. it was resolved that the consistent
load vector is one which is based on work equivalency,
rather than on statical equivalency alone. Therefore,
from equation 2.11 with the notations as defined

$$\{F\} = \int_A [N]^T \{p\} \, dA$$

This integration can be explicitly evaluated or
the integral value can be obtained by numerical integra-
tion.

If F_i is the ith term of vector $\{F\}$ then on
explicit integration it is seen that it is possible to

write, for the element under consideration

$$F_i = p \; a^{\alpha_i^8} \; b^{\alpha_i^9} \; / \; \alpha_i^{10} \qquad \qquad \dots \; (4.32)$$

where, α^8, α^9 and α^{10} are given in Table 4.2 for each value of it.

However, a limitation of such a formulation is that the whole of the element has to be treated as loaded and that too with a uniform pressure. This means that the element size is governed by the loaded area and becomes an over-riding factor in structural idealisation. However, the numerical integration technique provides a flexibility in the solution.

A weighted quadrature rule like Gaussian quadrature[133] can be used. As per details of numerical integration (Appendix 2.A), the summation sign can replace the integration sign and accordingly,

$$\{F\} = ab \sum_{i=1}^{n} \sum_{j=1}^{n} \; [N_{i,j}]^{T} \, |p_{ij}| \; W_i \; W_j \qquad \dots \; (4.33)$$

where,

i,j = sampling point in x and y direction respectively.

n = order of the quadrature rule,

p_{ij} = contact pressure between tyre and pavement in the sub-interval supposed to be under command of sampling point (x_i, y_j),

W_i, W_j = ith and jth weighting constants respectively in accordance with the adopted quadrature rule[133].

As a numerical example the equivalent nodal loads
are given in Table 4.3 for the case of an element of
3mx3m size which is divided in 9 areas and each area is
successively loaded with a pressure of 1000 kg/m^2.

Say, for example if part I (figure 4.3) is loaded,
then from Table 4.3 values of equivalent nodal forces
can be obtained for i=1, j=1 taking moments about the
centre of element in x direction is $\sum M_x = 0$.

It is seen that,

$$\text{moment of nodal forces} = \begin{aligned}&(646.36-23.61-0.86+23.61)\times 1.5\\&-178.34+22.65+0.83-6.51\end{aligned}$$

$$= 806.85$$

and

$$\text{moment of applied load} = (\tfrac{5}{18}\times 3)(\tfrac{5}{18}\times 3)(1000\times 0.387\times 3)$$

$$= 806.25$$

Similarly, it can be seen that,

$$\sum M_y = 0.$$

Also, sum of nodal forces in vertical directions must
equal to the applied load

$$\text{applied load} = (\tfrac{5}{18}\times 3)(\tfrac{5}{18}\times 3) \times 1000$$

$$= 694.44.$$

$$\text{sum of vertical nodal forces} = 646.36+23.61+23.61+0.86$$

$$= 694.74.$$

Thus, the static equilibrium conditions hold good.

4.4.4.3 Evaluation of Nodal Forces due to
         Temperature Changes

The effect of temperature and moisture changes
are essentially similar in nature. Therefore, the effects
of one is convertible into the equivalent effects of
other by introducing a factor. Hence, it is appropriate
to deal with only one say thermal effects.

Considerations to following points are necessary
to evaluate thermal effects.

The changes in pavement temperature can be treated
in two parts-

(1) Changes in average temperature which will cause
    the slab to expand or contract. This expansion
    or contraction will be resisted by frictional
    stresses at the bottom of the slab. The coeff-
    icient of friction will thus play an important
    role.

(2) Non-uniformity in temperature through the pave-
    ment cross-section will result in differential
    expansion and contraction between the top and
    bottom fibers of the slab. This will result in
    warping.. The weight of the slab will restrain
    warping. It is reported[134] by actual field
    measurements that warping does occur. However,
    it is conventional to assume full restrain
    in the analysis[135-139]. Therefore, keeping

in line with these, full subgrade restrain
is again assumed as valid in the present
analysis.

The stresses will depend on temperature gradient,
subgrade stiffness, pavement slab stiffness and coeff-
icient of thermal expansion of the slab.

The slab is continuously in motion due to temperat-
ure changes and therefore, it can be termed as 'quasi-
static[140] since the stresses are changing at every
instant. But at a particular instant, the instant which
will give the worst effect, they can be treated as cons-
tant because of the slow rate of change. Thus, a static
analysis is appropriate. The problem becomes a thermo-
elastic problem because the temperature field in non-
uniform through the cross-section and the pavement is
treated as an elastic body. For solution, it is necessary
to convert the temperature field into the stress field.

Under the assumption of full restrain, the net
strains are bound to be zero[141]. It is usual to assume
the temperature as same at all the points lying on a plane
parallel to the middle and the distribution of temperature
through the cross-section is linear. Therefore,

$$\varepsilon_x' = \varepsilon_x^o - z\frac{\partial^2 w}{\partial x^2} = \alpha \theta + \frac{1}{E}(\sigma_x - \nu\,\sigma_y) = 0$$

$$\varepsilon_y' = \varepsilon_y^o - z\frac{\partial^2 w}{\partial y^2} = \alpha \theta + \frac{1}{E}(\sigma_y - \nu\sigma_x) = 0$$

$$\gamma'_{xy} = \gamma^o_{xy} - 2z\, \frac{\partial^2 w}{\partial y^2} = \frac{2(1+\nu)}{E}\, \tau_{xy} = 0 \qquad \Bigg\} \qquad \ldots \text{(4.34)}$$

where,

$\varepsilon'_x, \varepsilon'_y$ and γ'_{xy} are net strains,

$\varepsilon^o_x, \varepsilon^o_y$ and γ^o_{xy} are the corresponding values for restrained thermal strains,

σ_x, σ_y and τ_{xy} are the stresses developed.

α = coefficient of thermal expansion, and

θ = fall of temperature at a point which is at a distance 'z' from neutral plane.

Solving equation 4.34

$$\sigma_x = \sigma_y = \frac{E\alpha\theta}{(1-\nu)}$$

and $\qquad\qquad \tau_{xy} = 0 \qquad\qquad \ldots \text{(4.35)}$

Therefore, to convert the thermoelastic problem into an elastic problem it is necessary to apply these stresses at every point. This will however, violate the conditions of equilibrium. Thus it is necessary to apply a moment at the edges to satisfy this condition. Therefore,

$$M_x = \int_{-h/2}^{h/2} \sigma_x\, z\, dz$$

$$= \left(\frac{E\alpha}{1-\mu}\right) \int_{-h/2}^{h/2} \theta z.dz \qquad \ldots \text{(4.36)}$$

and similarly

$$M_y = \left(\frac{E\alpha}{1-\mu}\right) \int_{-h/2}^{h/2} \theta z.dz$$

Putting $\theta = \frac{\Delta T}{h}.z$ and integrating equation 4.36

$$M_x = M_y = \frac{E \alpha \Delta T h^2}{12(1 - \mu)} \qquad \ldots (4.37)$$

where,

    ΔT = difference of temperature between top and bottom of slab, and

    h = thickness of slab

Thus, the system of forces which are equivalent to thermal non-uniformity are completely defined. The procedure will be to

    (i) apply moments at all edges as given by equation 4.37.

    (ii) subtract the stress given by equation 4.35 from the stresses developed due to applied edge moments.

The equivalent nodal forces due to applied moments are to be evaluated so that they may form the part of the load vector in equation of equilibrium (equation 2.10)

These edge moments are once again to be applied in the form of consistent nodal loads. The value of these nodal loads have to be obtained by principle of virtual work as was done in Chapter II.

Therefore, from equation 2.12

$$\{F\} = \iint [B]^T [D][\varepsilon] \, dA \qquad \ldots (4.38)$$

Again, as usual the equation can be explicitly evaluated or the integral value can be obtained by numerical integration. The explicit integration yields,

$$F_i = p \, \alpha_i^{11}(a^{\alpha_i^{12}} + b^{\alpha_i^{13}}) \qquad \ldots \ (4.39)$$

where, F_i = ith term of vector $\{F\}$

α_i^{11} = multiplying coefficient

a = dimension of element parallel to axis of x

b = dimension of element parallel to y axis

α^{12}, α^{13} = exponential coefficients of a and b respectively,

and,

$$p = \frac{Eh^3}{12(1-\nu^2)} \cdot \frac{\alpha.\Delta T}{h}$$

It may be recognised that,

$$\frac{Eh^3}{12(1-\nu^2)} = D$$

= rigidity of the pavement slab

and $\quad \dfrac{\alpha.\Delta T}{h} = X_0$

= curvature of slab due to temperature differential

4.5 MODELING OF CRACKED SLAB

A crack forms a discontinuity in the stress field and can be regarded as analogous to obstruction in fluid flow. This is demonstrated in figure 4.4. For a plate in bending, a crack would effect in loss of bending stiffness in the direction perpendicular to the crack. This will be as a result of loss of the capacity of the fibers to resist imposed moments and as such they will undergo greater rotation. However, in the other direction, i.e., the one parallel to the crack, the situation will not alter very much. An obvious method to model the crack is therefore, to simulate its effect by orthotropic properties i.e., by taking different moment curvature relationships in the two orthogohal directions.

Difficulty now arises in characterising the loss of rigidity of the cracked section. Not much could be said with certainty regarding the rigidity of the section perpendicular to the crack, in case of plain cement concrete slabs, However, there is enough evidence to feel convinced that the rigidity of this plane could be correctly assessed in case of reinforced cement concrete slabs. This is based on studies performed by Branson[142], Yu and Winter[143], Beeby[144] and several others.

4.5.1 Modeling the Crack through Finite Elements

Attempts are reported to have been made towards characterising the crack in plate bending finite element

model by treating the element as cracked[145,146]. Bell[147] later stated that treating the element as partly cracked has become unsuccessful and therefore suggested the case of an element which is wholly cracked. To find the moment-curvature relationship, the author prefers using the method suggested by Priestley[148].

Plane continuum elements have often been used to simulate crack[149-152]. This is often done by disconnecting the nodal points which are on the common boundary of the crack. A procedure similar to this has been adopted in Chapter III.

It has been shown[115] by using 20 noded, three dimensional isoparametric elements that in case of beams, good correlation exists between the observed behaviour and predicted values.

An iterative scheme has been suggested[153] in which layers of finite elements go on successively cracking as the load is incremented. It is stated that the modified EI approach, as adopted by Jofriet and McNiece[154,155] does not yield good results. By taking the experimental values for the slab obtained by Jofriet and McNiece , the authors[153] show that their results converge.

Jofriet and McNiece[155] conclude that Beeby's method[104] yields results which show excellent agreement with the experimental observations. Beeby's method is based on modifying the rigidity i.e. EI of the cracked section in

the direction perpendicular to the plane containing the crack.

This method is simple and economical. Moreover, it is directly applicable to the case of pavement slabs where the cracks are known as a priori. The only problem is to model them and this can be done by using Beeby's recommendations for reinforced concrete slabs. Beeby suggests modification in 'EI' of the cracked part by taking value of 'E' as 0.57 of that of the uncracked part and 'I' is the value of moment of inertia of the cracked section. However, no recommendation of this kind is known for the plain cement concrete and therefore, pending extensive investigation, the safest recourse seems to consider total loss of rigidity for the entire crack depth.

It can therefore, be said that based on the work reported by several investigators, the method of modeling a crack in the slab by assigning orthotropic properties to the element appears to be appropriate. While Beeby's method for determination of the constitutive law in the direction perpendicular to the crack, seems to be applicable for reinforced cement concrete, for plain cement concrete, all the stiffness of the cracked part may be neglected. This fact is also backed by the limited studies of cracked slab, reported in the previous chapter, when it was observed that at the crack section the part, which is cracked does not participate in carrying the stress.

Another very important issue in modeling the
crack is with regard to the width of the crack. The crack
width itself may be very small. In case of plane conti-
nuum elements i.e., in case of plane stress, plane strain
or even in axisymmetric or three dimensional elements, the
crack can be easily represented by splitting a node into
two. Both these nodes may have same coordinates but just
form a discontinuity in between the element boundaries
and additional degrees of freedom are assigned. This is
simple and straightforward. But in case of plate elements
the continuity of slope must exist in the direction of
the crack, so also, the deflection of the two adjoining
nodes on a crack must be same due to dowel action of the
aggregates. Therefore a modeling by splitting the nodes
will lead to inaccurate results in plate bending. There
is ample evidence to believe that substantial load transfer
is possible across the crack due to aggregate inter-
locking[88,89,153]. This is because the formation of a
crack in concrete is not a phenomenon based on slip but
is because of the energy used up in causing fracture like
one in brittle material[156].

Among the earlier work done in this direction, to
model the crack in finite element in plate bending,
Jofriet and McNiece[154,155] have not stated anything
about the size of the element in their work. Bell and
Elms[147] have also not touched this point, though they
mention that, should the mesh size appear to be improper

in the course of load increments, the mesh geometry may have to be changed. However, no specific definition to this statement is given.

Beeby[104] observed that in a controlled constant curvature test, the cracks in the beams are spaced at a distance of approximately twice the depth of the crack. This he attributes to the effect of stress release due to the crack, which in the spirit of St.Venant's principle should exist for a distance equal to the depth of crack on either side of it because in case of a uniform stress field, which was adopted in his test, the crack will only have an effect of a local disturbance in an otherwise undisturbed surroundings. Similarly, the tests based on photoelastic studies carried out by Post[157] and several others, using interferometric isopachic technique, indicate the isochromatic fringe pattern supporting that in the case of beams the zone adjoining the crack is almost free of stress upto a distance equal to about the depth of crack. Post's work was later substantiated by Williams[158], who gave a theoretical explanation for the observed stress distribution pattern.

It therefore appears to be appropriate to take the effect of stress release within a zone equal to one to two times the depth of cracks. It is to be agreed that more extensive investigations on cracked pavement slabs are necessary to uncover the truth. However, the observations based on the limited numerical experimentation

described in Chapter III endorse this judgement.

4.6 NUMERICAL INTEGRATION

Apart from programming advantages and quick implementation for nonlinear situations numerical integration is proposed with the following advantages in view:

1. In case of explicit formulation, the stresses are obtained at nodal points, whereas, in numerical integration procedure stresses and displacements can be readily obtained at sampling points of numerical integration scheme. These are more reliable.

2. It has already been shown that by using numerical integration scheme it is possible to load only a part of element and obtain the consistent nodal loads. This leads to a great deal of economy.

3. By a similar argument, it can be shown that sub-grade discontinuities, in a part of an element can also be accommodated, without resorting to modification of structural idealization.

4. Advantage can be taken of reduced integration technique. It has already been mentioned that since the mathematical foundation of the finite element method is based on minimization of potential energy by variation of shape, the

obtained solution tends to be stiff[60]. A
method of improving the result is to provide
greater number of degrees of freedom to the
system. However, this tends to uneconomy.
Reduced integration technique is therefore
suggested in which by adopting a quadrature
rule of an order one less than the exact,
it is claimed that results significantly
improve[159,160]. Incidentally there is also
a significant saving in computational time
because of the reduced computations.

5. Earlier attempts to model partially cracked
    element in bending have not been very success-
    ful. But by adopting a numerical integration
    scheme such a possibility exists as the
    variation of material constants across the
    element can be considered without any complica-
    tion.

6. Numerical integration can in general be more
    economical. Nayak[161] has shown that by use of
    the concept of generalised modulus matrix the
    use of $[B]$ matrix can be avoided and $[B^*]$
    is to be calculated only once for the parent
    element at all the integrating points.

4.7 REPRESENTATION OF LOSS OF CONTACT WITH THE SUBGRADE

The basis of coupling of subgrade reaction with the pavement slab is same as that of determination of consistent loads, both being based on work principles. Thus, the subgrade stiffness, given by equation 4.30

$$[K_s] = \iint [N]^T k [N] ds$$

can also be evaluated by numerical integration and it can be argued that if a part of subgrade has lost contact with the pavement, then the work done by the remaining part can be obtained by numerical integration performed on the remaining subintervals.

Loss of contact or variation in subgrade modulus known as a priori, because of reasons like pumping, shrinkage, swelling etc. [162,163,164] can therefore be realistically taken into account, without much restriction being imposed on the geometry of the finite element idealisation. Earlier, loss of contact have been taken into account in finite element method by Huang and Wang[80]. This was done by removing the spring supposed to be attached to the relevant node.

4.8 EVALUATION OF THE PROPERTIES OF PARTLY CRACKED ELEMENT

Though it will usually be possible to adjust the element size in such a way that an entire element may

represent the crack as per the resolutions made in last article. However, some times it may so happen that this may not be possible, for reasons of economy. In such cases it may be necessary to treat only a part of the element as cracked. This appears to be possible, through numerical integration procedure. Nayak[165] has shown that it is possible to assign different constitutive relationships to different parts of an element (sub-element), each part having its centre at the Gauss point and area equal to the weightage corresponding to that Gauss point. Thus, the procedure becomes similar to the one adopted for partial loaded element.

This means that if,

$[D_{ij}]$ = rigidity of the slab corresponding to the sampling point (i,j)

$\{M\}$ = stresses corresponding to that point,

$\{\chi\}$ = strains corresponding to that point

$[B_{ij}]$ = $[B]$ matrix with coordinates of Gaussian sampling point (i,j)

then,

$$\{M_{ij}\} = [D_{ij}]\{\chi\} \qquad \qquad \dots (40)$$

and

$$\{\chi_{ij}\} = [B_{ij}]\{\delta\} \qquad \qquad \dots (4.41)$$

will still hold good. The implication of this formulation is that the strain remains to be continuous, though the stress will become discontinuous. However, there cannot be any objection to writing the strain energy of the

element as

$$S_c = \frac{1}{2} \int_A \{\chi\}^T \{M\} dA$$

the only difference being that the integral is not
continuous and therefore has to be done in parts. By
usual numerical integration procedure

$$S_c = \frac{1}{2} \sum_{i=1}^{n} \sum_{j=1}^{n} \{\chi_{ij}\}^T \{M_{ij}\} W_i W_j \qquad \qquad .. \ (4.42)$$

where,

W_i, W_j = weighting constants of the adopted weighted
quadrature rule.

By equating this to the work done by external forces as
in article 2.3.2.2 it can still be proved that

$$\{F\} = ab(\sum_{i=1}^{n} \sum_{j=1}^{n} [B_{ij}]^T [D_{ij}][B_{ij}])\{\delta\} W_i W_j \qquad .. \ (4.43)$$

Thus, it is possible to arrive at the proper stiffness
of the element which is

$$[K_p] = ab \sum_{i=1}^{n} \sum_{j=1}^{n} [B_{ij}]^T [D_{ij}][B_{ij}] W_i W_j \qquad \qquad .. \ (4.44)$$

Use of equation 40 will be necessary in stress
calculations and in this formulation it becomes obligat-
ory to calculate stresses on these very sampling points.

4.9 ANALYSIS OF AN INCLINED CRACK

The transformation of flexural rigidity matrix
[D] will be necessary if the direction of crack does

not coincide with the direction of local coordinates.

If M_x', M_y' and M_{xy}' are moments in transformed direction (parallel and perpendicular to the crack) and if α is the angle between these two sets of directions measured clockwise positive from x direction, then it can be shown that the relationship between M' and M is

$$[M'] = \begin{bmatrix} \cos^2\alpha & \sin^2\alpha & -2\sin\alpha\cos\alpha \\ \sin^2\alpha & \cos^2\alpha & 2\sin\alpha\cos\alpha \\ \sin\alpha\cos\alpha & -\sin\alpha\cos\alpha & \cos^2\alpha-\sin^2\alpha \end{bmatrix} \{M\}$$

$$= [T_1]\{M\} \qquad \qquad \dots (4.45)$$

This follows directly from well known stress transformation law of elasticity.[114] A similar operation on curvature can yield

$$[\chi'] = \begin{bmatrix} \cos^2\alpha & \sin^2\alpha & -\sin\alpha\cos\alpha \\ \sin^2\alpha & \cos^2\alpha & \sin\alpha\cos\alpha \\ 2\sin\alpha\cos\alpha & -2\sin\alpha\cos\alpha & \cos^2\alpha-\sin^2\alpha \end{bmatrix} \{\chi\}$$

$$[T_2]\{\chi\} \qquad \qquad \dots (4.46)$$

These transformation matrices are such that

$$[T_1]^{-1} = [T_2]^T \qquad \qquad \dots (4.47)$$

Therefore,

$$[D] = [T_2]^T [D'] [T_2] \qquad \qquad \dots (4.48)$$

where, all the dashed quantities refer to coordinates which coincide with principle directions of orthotropy and those without prime refer to local coordinate axis of element.

A comparison of explicitly multiplied transformed flexural rigidity matrix with Hearmon[166] or Lekhnitskii[167] proves its correctness.

A numerical integration process does not present any difficulty in either stiffness formulation or stress computation for any arbitrary direction of crack. Through explicit integration formulation this may be an uneconomical process.

4.10 FORTRAN IV CODING AND DEBUGGING

The only computer available at Roorkee is IBM 1620 model I at S.E.R.C. Roorkee. This has a punched card input/output system. This however, proved to be a boon in disguise. Because of the memory limitations it is not possible to run the whole program in a single go on this system, even for a smallest test problem. The program was therefore split up in three parts. The output of the first part was read in the second part and so on. In the first part the geometry of the idealised slab was read in and the stiffness of the slab was computed and taken as output.

In the second part this stiffness was read in. The

applied loads were also read in and got converted into equivalent nodal loads. The equilibrium equations were then formed and the solutions for displacements were obtained by Gaussian Elimination process. These displacements were obtained as punched output.

The third part of course was simple and did not mobilize much of memory either. The displacement were fed in and the stresses at each Gaussian point was obtained for the whole slab. The whole process was cumbersome and time consuming too, as it required practically 10 to 15 days for getting a single problem solved, but was admittedly advantageous on two counts. Firstly, because it provided lot of insight in the processes, which might have gone hidden up in a fast computer and secondly, it saved lot of precious time of a fast computer.

Three problems were tried in this way-

(i) A simply supported square isotropic plate of 5m x 5m size, the quarter of which was considered because of double symmetry. The quarter of this plate was divided into 4 elements.

(ii) Above slab with fixed edges instead of simply supported.

(iii) A 4m x 4m slab on winkler foundation.

The results of (i) and (ii) were compared with standard solution of Timoshenko[114] and the difference

was within 2%. . In case of (iii) the values of stresses given by the program under the load were 4.5% higher than those given by Westergaard[24] in the corresponding semi-infinite slab in interior load position.

The three parts of the program were then combined into a single one. The uneconomical statement to suit the constrains of IBM 1620 computer were changed. Results were obtained on IBM 360/44 Data Processing System at Delhi University Computer Centre. The total program runs in some 1000 FORTRAN statements at this stage and takes about 220 sec. to compile it. This time includes the time required for printing the FORTRAN listing and location MAP, the printer being an on-line type, directly coupled with the CPU. Some of the details of this program are given in the final form (i.e., after addition of layers analysis of bonded or unbonded type, Elastic Solid type foundation, two parameter foundation, foundation with loss of contact and the required modification for influence surfaces) in the Appendix 'A'.

Test runs were conducted with the program on IBM 360/44 with a view to check the correctness of the formulation with minimum expenditure of computer time. Three important aspects were looked in for-

(i) Comparison with existing solutions in cases
    where this is possible, e.g. by Westergaard's

solution[24] or for cracked slab by solution given by Niu and Picket[168].

(ii) Static check in all cases particularly those for which solution does not exist for comparison.

(iii) Physical feel.

Following material properties have been taken in all test cases:

E_c - modulus of elasticity of concrete
30×10^4 kg/cm^2

ν_c - Poisson's ratio for concrete = 0.15

k - Modulus of subgrade reaction = 12 kg/cm^2

The justification for adopting these properties have already been discussed earlier.

Test Case I- Comparison with Westergaard's solution

The slab of following dimensions

Length of slab = 6 meter,
Width of slab = 6 meter.
Thickness   = 23.0 cm

was considered.

The reason for adopting a square panel was to simulate the semi infinite slab conditions for comparison with Westergaard's interior load solution. Size 6mx6m was considered as a slab with enough size to satisfy

the conditions sought.

A load of 8000 kg was considered to be acting on 120 cm x 120 cm area in the exact centre of this panel. Only one quarter of the panel was analysed because of the double symmetry. The finite element mesh was graded to achieve maximum economy with minimum loss of accuracy. The basis of this was however, only the physical judgement. In calculations by Westergaard's equation, the load was taken of equal magnitude and radius of contact was taken as equal to half the width of the square contact area.

Figure 5(c) shows the plan of this quarter slab, Figure 5(a) indicates variation of bending moment M_y along section A-A'. Variation of M_y along section B-B' is shown in figure 5(b). Figure 6(a) shows the variation of moment M_x along AA'. Deflections along Y-axis and X-axis are shown in Figure 6(b) and Figure 6(c) respectively.

It is to be noted that-

(i) Stresses deflections and slopes must be symmetrical about the diagonal.

(ii) When compared with Westergaard's solution[24] the maximum moment works out to be 590 kg.cm./cm. as compared to 610 kg.cm./cm. given by the analysis.

(iii) Static check must apply. Static equilibrium may

be checked from two considerations-

(a) Sum of all reactive forces must equal the applied loads. For this purpose, a weightage is given to each node corresponding to the area it is supposed to represent. This is similar to lumped nodal reaction formulation discussed earlier and adopted by Huang and Wang[79,80]. It is an approximate method and in present case the error in static equilibrium is 2.8% even though it is a very symmetrical case with least possibility of approximation in assigning the weightages.

(b) Another method of checking the statics is to consider the equilibrium of a part of the slab. The applied loads and the reactive forces must be in equilibrium with the side shears and moments as shown in figure 7(a). The distribution of reactive forces has to be guessed again. But this time, by taking only a small part this guess may be more correctly approximated by a linear interpolation. The error is therefore , less and is within 1% for all different sections to which these checks have been applied in x as well as in y direction.

Case II- Checking correctness of Part Loading
            Formulation.

Same slab as tested in Case I, but for testing
the partly loaded element formulation, was analysed.

The loaded area was represented by Gauss point
No.1 as shown in figure 7(b) i.e. by an area of 33.33 cm
by 33.33 cm which gives a load of 5540 kg This gives
a maximum moment of 972 kg.cm./cm. which when extra-
polated for centre of the loaded area gives 990 kg.cm/cm
The calculated value of maximum moment as per Wester-
gaard's equation works out to be 1030 kg.cm/cm for the
load of 5540 kg and radius of contact 16.65 cm.

The static equilibrium, when checked as per para
(iva) of case I gives sum of reactive forces as 5663 kg.
i.e. an error of 2.2% .

Case III. Testing of Fully Cracked Element

A finite crack of 120 cm length across the centre
along x-axis of the kind already discussed in article 4.5
was considered in the slab with other condition identical
to that in case I. The crack was supposed to have an
effect upto 60 cm i.e. whole element width.

Direct comparison of this with standard solution
is not possible. The other tests, therefore, have to
be applied.

The sum of all reactive forces add upto 7648 kg.
as against 8000 kg applied load. The equilibrium of

different parts compare with ±2.5% difference. The difference is specially more near the cracked part because of the uncertainty of the reactive pressure distribution.

Case IV. Testing of Partly Cracked Element Formulation.

All the conditions were kept same as in Case III except that in this case the crack was supposed to have an effective zone of stress release as equal to that of the weightage of the Gauss Point No.1 in the element. This amounts of taking the zone of stress release as 33.33 cm.

Remarks for Case III also hold for this case.

4.11 DISCUSSION OF RESULTS

In absence of a standard solution and having ascertained that the static equilibrium conditions are satisfied within reasonable limits, the physical feel, which can be called a 'qualitative check' as compared to 'quantitative check', will at least provide a confidence in correctness of the formulation. Variations of M_y, M_x and deflections are drawn in figure 5(a,b,c) and 6(a,b,c). These diagrams are very instructive as well.

These figures indicate that behaviour of partly cracked element is essentially same as that of fully

cracked one and its effect is lesser than the fully cracked element. This is quite justified.

Figure 4.5a shows reduction in stresses in the crack zone due to stress release. However, these stresses are bound to be diverted in the sound part, which is ahead of the crack tip, and as such a concentration of stresses can be expected in that zone. This is schematically depicted in figure 4.5(c) and the crack is analogous to obstruction in stream lined fluid flow shown in figure 4.4. The shaded zone of stress release shown in figure 4.5(c) being similar to wake zone in figure 4.

Stresses can be expected to increase in magnitude at the crack tip if the centre of loaded contact area coincides with it. This, however, has not been studied quantitatively as it is besides the main theme of the present work . However, it is illustrative that the crack, once formed, is liable to progress due to stress concentration as shown in figure 4.5(c).

Figure 4.5(b) presents the variation of moment, M_y in y- direction. The effect of stress release in direction perpendicular to the crack is clear. This is equivalent to applying a released moment in that direction.

Figure 4.6(a) shows that cracking increases the moment in x direction because, higher load is shared in that direction due to its higher rigidity. Looking upon from the considerations of statics this is justified because

in cracked state the deflections in direction of crack
increases. This is agreeable with the findings of Niu
and Pickett[168] as also of Abou Ayyash and Hudson[40,41]
though their findings are for long cracks. Figure 6(b)
and (c) show that deflection along the crack have increased
on cracking while in the orthogonal direction the inc-
rease is only local. This is truly so because in direct-
ion perpendicular to the crack the slope becomes higher
due to loss of rigidity.

Case V- Comparison of Stresses and Deflection
        with the Solution given by Niu[42].

To simulate the conditions of a long crack the
slab dimensions were taken as 11 meters x 11 meters. A
straight transverse crack along centre of the pavement
was considered. This crack was simulated by a partly
cracked element (article 4.8) along its central Gaussian
point of 3 point Gaussian integration which means that
zone of stress release was taken as 24 cm wide. The other
material properties were same as in Case I.

The loading was simulated by partly loading this
cracked element on its corner Gaussian point, of 5 point
integration rule.

The maximum bending moment as determined by inter-
polation from Niu[42] is 52.2 kg cm/cm whereas, that
found under load by finite element analysis was
58.5 kg.cm/cm. The deflection as per Niu is 0.665×10^{-3} cm

and that obtained was 0.56×10^{-3} cm. Thus it is seen that the moment is more while deflection is lesser. The reason that can be attributed to this greater rigid behaviour of the pavement slab could be:

(i) Finite length of slab.

(ii) The rigidity is not supposed to be totally lost in crack zone in crack direction but is taken as 1% of the original.

(iii) The width of the zone of stress release is taken arbitrarily as 24 cm.

(iv) Interpolation from Tables might have also contributed to differences in the values.

The results are plotted in figure (8). Figure 8(c) is the plan of the slab showing crack and load position and finite element idealisation of the central part. Figure 8(a) shows variation of bending moments along Gaussian sampling points which are 3.63 cm away from the line of symmetry. Influence of crack on bending moment M_y can be seen from this figure. It is also seen that the moment M_x is still almost symmetrical about load. Similar effect is also evident on deflections plotted in figure 8(b). These patterns show remarkable resemblance to those obtained from the analysis of plane continuum element observed in Chapter III.

Case VI   Uncracked Slab with (i) temperature gradient and self load, (ii) temperature gradient alone.

Both these were analysed on pavement slab the particulars of which are given in Case I. Both these cases give

identical results as regards stresses, indicating that
gravity loads have no effect on linear analysis with
Winkler foundation.

The results of maximum stresses obtained with temp-
erature gradients are within $4\frac{1}{2}\%$ of those given by
Bradbury's solution for edge stresses but for interior
stresses the results tally within 1%.

4.12 OBSERVATIONS FROM STUDY OF TEST PROBLEMS

It can be observed from above discussion that

i) The formulation yields results which are in
close agreement with those due to Westergaard[24],
for similar conditions.

ii) The results are comparable with those due to
Niu[42] when the load is placed near a long
straight crack.

iii) The static equilibrium conditions in all the
cases hold within reasonable limits of accuracy.

iv) All the results can be given a physical inter-
pretation and are therefore justifiable.

v) The temperature stresses calculated by the
formulation agree very well with those given by
Bradbury for a sound slab.

The observations can incidentally also be drawn
with regard to some aspects of the behaviour of pavement

slab e.g.,

   i) Stresses ahead of crack increase as a result of
      the presence of a finite crack and thereby, if
      cracking is once initiated it is likely to progress
      under variable and variably placed wheel loads.

  ii) Behaviour of the crack is analogous to the flow
      of fluid.

 iii) The effect of a crack is to release the stress in
      direction perpendicular to it. However, the stresses
      in orthogonal direction increase.

  iv) The effect of width of stress release zone taken
      quantitatively different by whole element and by
      part element is essentially similar in nature.
      However, the effect is more pronounced when the
      width is greater.

TABLE-4.1

EXPLICIT COEFFICIENTS FOR COMBINED STIFFNESS OF SLAB AND SUBGRADE

i	j	α^1	α^2	$\alpha^3 \times 35$	$\alpha^4 \times 35$	$\alpha^5 \times 25$	$\alpha^6 \times 25$	$\alpha^7 \times 1225$
1	1	0	0	156	156	72	144	169
2	1	1	0	78	22	36	12	143/6
2	2	2	0	52	4	8	16	13/3
3	1	0	1	22	78	36	12	143/6
3	2	1	1	11	11	61/2	1	121/36
3	3	0	2	4	52	8	16	13/3
4	1	1	1	11	11	11/2	1	121/36
4	2	2	1	22/3	2	4	4/3	11/18
4	3	1	2	2	22/3	4	4/3	11/18
4	4	2	2	4/3	4/3	8/9	16/9	1/9
5	1	0	0	-156	54	-72	-144	117/2
5	2	1	0	-78	13	-6	-12	169/12
5	3	0	1	-22	27	-36	-12	33/4
5	4	1	1	-11	13/2	- 3	- 1	143/72
5	5	0	0	156	156	72	144	169
6	1	1	0	78	-13	6	12	-169/12
6	2	2	0	26	-3	-2	-4	-13/4
6	3	1	1	11	-13/2	3	1	-143/72
6	4	2	1	11/3	-3/2	-1	-1/3	-11/24
6	5	1	0	-78	-22	-36	-12	-143/6

Table 4.1 continued

i	j	α^1	α^2	α^3x35	α^4x35	α^5x25	α^6x25	α^7x1225
6	6	2	0	52	4	8	16	13/3
7	1	0	1	-22	27	-36	-12	33/4
7	2	1	1	-11	13/2	-3	-1	143/72
7	3	0	2	-4	18	-8	-16	3/2
7	4	1	2	-2	13/3	-2/3	-4/3	13/26
7	5	0	1	22	78	36	12	143/6
7	6	1	1	-11	-11	-61/2	-1	-121/36
7	7	0	2	4	52	8	16	13/3
8	1	1	1	11	-13/2	3	1	-143/72
8	2	2	1	11/3	-3/2	-1	-1/3	-11/24
8	3	1	2	2	-13/3	2/3	4/3	-13/36
8	4	2	2	2/3	-1	-2/9	-4/9	-1/12
8	5	1	1	-11	-11	-11/2	-1	-121/36
8	6	2	1	22/3	2	4	4/3	11/18
8	7	1	2	-2	-22/3	-4	-4/3	-11/18
8	8	2	2	4/3	4/3	8/9	16/9	1/9
9	1	0	0	-54	-54	72	144	81/4
9	2	1	0	-27	-13	6	12	39/8
9	3	0	1	-13	-27	6	12	39/8
9	4	1	1	-13/2	-13/2	1/2	1	169/144
9	5	0	0	54	-156	-72	-144	117/2
9	6	1	0	-27	22	36	12	-33/4
9	7	0	1	13	-78	-6	-12	169/12
9	8	1	1	-13/2	11	3	1	-143/12

Table 4.1 continued

i	j	α^1	α^2	α^3x35	α^4x35	α^5x25	α^6x25	α^7x1225
9	9	0	0	156	156	-72	144	169
10	1	1	0	27	13	-6	-12	-39/8
10	2	2	0	9	3	2	4	-9/8
10	3	1	1	13/2	13/2	-3	-1	-169/144
10	4	2	1	13/6	3/2	1/6	2/6	-13/48
10	5	1	0	-27	22	36	12	-33/4
10	6	2	0	18	-4	-8	-16	-3/2
10	7	1	1	-13	11	3	1	-143/72
10	8	2	1	13/3	-2	-2/3	-4/3	13/36
10	9	1	0	-78	-22	-36	-12	143/6
10	10	2	0	52	4	8	16	13/3
11	1	0	1	13	27	-6	-12	-39/8
11	2	1	1	13/2	13/2	-1/2	-1	-169/144
11	3	0	2	3	9	2	4	-9/8
11	4	1	2	3/2	13/6	1/6	1/3	-13/48
11	5	0	1	-13	78	6	12	-169/12
11	6	1	1	13/2	-11	-3	-1	143/72
11	7	0	2	-3	26	-2	-4	-13/4
11	8	1	2	3/2	-11/3	1	1/3	11/24
11	9	0	1	-22	-78	-36	-12	-143/6
11	10	1	1	11	11	61/2	1	121/36
11	11	0	2	4	52	8	16	13/3
12	1	1	1	-13/2	-13/2	1/2	1	169/146
12	2	2	1	-13/6	-3/2	-1/6	-1/3	13/48

Table 4.1 continued

i	j	α^1	α^2	$\alpha^3 x\ 35$	$\alpha^4 x35$	$\alpha^5 x\ 25$	$\alpha^6 x25$	$\alpha^7 x1225$
12	3	1	2	-3/2	-13/6	-1/6	-1/3	13/48
12	4	2	2	-1/2	-1/2	1/18	1/9	1/16
12	5	1	1	13/2	-11	-3	-1	143/72
12	6	2	1	-13/3	2	2/3	4/3	-13/36
12	7	1	2	3/2	-11/3	1	1/3	11/24
12	8	2	2	-1	2/3	-2/9	-4/9	-1/12
12	9	1	1	11	11	11/2	1	121/36
12	10	2	1	-22/3	-2	-4	-4/3	-11/18
12	11	1	2	-2	-22/3	-4	-4/3	-11/18
12	12	2	2	4/3	4/3	8/9	16/9	1/9
13	1	0	0	54	-156	-72	-144	117/2
13	2	1	0	27	-22	-36	-12	33/4
13	3	0	1	13	-78	-6	-12	169/12
13	4	1	1	13/2	-11	-3	-1	143/72
13	5	0	0	-54	-54	72	144	81/4
13	6	1	0	27	13	-6	-12	-39/8
13	7	0	1	-13	-27	6	12	39/8
13	8	1	1	13/2	13/2	-1/2	-1	-169/144
13	9	0	0	-156	54	-72	-144	117/2
13	10	1	0	78	-13	6	12	-169/12
13	11	0	1	22	-27	36	12	-33/4
13	12	1	1	-11	13/2	-3	-1	143/72
13	13	0	0	156	156	72	144	169

Table 4.1 continued

i	j	α^1	α^2	$\alpha^3 . x35$	$\alpha^4 \times 35$	$\alpha^5 \times 25$	$\alpha^6 . x\ 25$	$\alpha^7 x1225$
14	1	1	0	27	-22	-36	-12	33/4
14	2	2	0	18	-4	-8	-16	3/2
14	3	1	1	13/2	-11	-3	-1	143/72
14	4	2	1	13/3	-2	-2/3	-4/3	13/36
14	5	1	0	-27	-13	6	12	39/8
14	6	2	0	9	3	2	4	-9/8
14	7	1	1	-13	-13	1/2	1	169/144
14	8	2	1	13/6	3/2	1/6	1/3	13/48
14	9	1	0	-78	13	-6	-12	169/12
14	10	2	0	26	-3	-2	-4	-13/4
14	11	1	1	11	-13/2	3	1	143/72
14	12	2	1	-11/3	3/2	1	1/3	11/24
14	13	1	0	78	22	36	12	143/6
14	14	2	0	52	4	8	16	13/3
15	1	0	1	-13	78	6	12	-169/12
15	2	1	1	-13	11	3	1	143/72
15	3	0	2	-3	26	-2	-4	-13/4
15	4	1	2	-3/2	11/3	-1	-1/3	-11/24
15	5	0	1	13	27	-6	-12	-39/8
15	6	1	1	-13/2	-13/2	1/2	1	169/144
15	7	0	2	3	9	2	4	-9/8
15	8	1	2	-3/2	-13/6	-1/6	-1/3	13/48
15	9	0	1	22	-27	36	12	-33/4

Table 4.1 continued

i	j	α^1	α^2	α^3x35	α^4x35	α^5x25	α^6x25	α^7x1225
15	10	1	1	-11	13/2	-3	-1	143/72
15	11	0	2	-4	18	-8	-16	3/2
15	12	1	2	2	-13/3	2/3	4/3	-13/36
15	13	0	1	-22	-78	-36	-12	143/6
15	14	1	1	-11	-11	-61/2	-1	121/36
15	15	0	2	4	52	8	16	13/3
16	1	1	1	-13/2	11	3	1	-143/72
16	2	2	1	-13/3	2	2/3	4/3	-13/36
16	3	1	2	-3/2	11/3	-1	-1/3	-11/24
16	4	2	2	-1	2/3	-2/9	-4/9	-1/12
16	5	1	1	13/2	13/2	-1/2	-1	-169/144
16	6	2	1	-13/6	-3/2	-1/6	-1/3	13/48
16	7	1	2	3/2	13/6	1/6	1/3	-13/48
16	8	2	2	-1/2	-1/2	1/18	1/9	1/16
16	9	1	1	11	-13/2	3	1	143/72
16	10	2	1	-11/3	3/2	1	1/3	11/24
16	11	1	2	-2	13/3	-2/3	-4/3	13/36
16	12	2	2	2/3	-1	-2/9	-4/9	-1/12
16	13	1	1	-11	-11	-11/2	-1	-121/36
16	14	2	1	-22/3	-2	-4	-4/3	-11/18
16	15	1	2	2	22/3	4	4/3	11/18
16	16	2	2	4/3	4/3	8/9	16/9	1/9

Table concluded

TABLE 4. 2

EXPLICIT COEFFICIENTS OF NODAL LOAD

i	α^8	α^9	α^{10}
1	1	1	4.0
2	2	1	24.0
3	1	2	24.0
4	2	2	144.0
5	1	1	4.0
6	2	1	-24.0
7	1	2	+24.0
8	2	2	...-144.0
9	1	1	4.0
10	2	1	-24.0
11	1	2	-24.0
12	2	2	144.0
13	1	1	4.0
14	2	1	24.0
15	1	2	-24.0
16	2	2	-144.0

TABLE 4.3

EQUIVALENT NODAL LOADS FOR ELEMENT LOADED IN PARTS

i	j	Node	Equivalent Nodal Loads Corresponding to				Area in Fig. 3 $=w_i \times w_j$ (sq.m)
			w	$\dfrac{\partial w}{\partial x}$	$\dfrac{\partial w}{\partial y}$	$\dfrac{\partial^2 w}{\partial x \partial y}$	
1	1	1	646.35985	178.3392	178.3392	49.2091	I, area$=(\frac{5}{18}x3)(\frac{5x3}{18})$
		2	23.611106	-22.6520	6.5146	-6.2500	$=25/36$
		3	0.862498	-0.8275	- 0.8275	0.7988	
		4	23.611106	6.5146	-22.6520	-6.2500	
1	2	1	1182.336500	326.2222	580.3217	160.1184	I+II area
		2	43.189986	-41.4356	21.1987	-20.3377	$= \frac{25}{36} + \frac{5x3}{18} \times \frac{8x3}{18}$
		3	20.441378	-19.6111	-15.5162	14.8815	$= 65/36$
		4	559.587760	154.3976	-424.6345	-117.1622	
	3	1	1205.947600	332.7368	602.9737	166.3684	I+II+III area
		2	44.052480	-42.2631	22.0264	-21.1355	$= \frac{65}{36} + \frac{25}{36} = \frac{90}{36}$
		3	44.052480	-42.2631	-22.0264	21.1355	
		4	1205.947500	332.7368	-602.9737	-166.3684	
2	1	1	1741.924200	734.7193	750.8567	277.2806	I+II+III+IV area
		2	580.029140	-444.2456	169.9092	-132.0438	$= \frac{90}{36} + \frac{40}{36} = \frac{130}{36}$
		3	63.631360	-56.9472	-40.8098	35.2192	
		4	1225.526300	347.4209	-621.7573	-180.4561	
	2	1	2186.368600	1068.0526	1084.1900	527.2805	I+II+II+IV+V area
		2	1024.473500	-777.5789	503.2425	-382.0438	$= \frac{130}{36} + \frac{64}{36} = \frac{194}{36}$
		3	508.075800	-390.2806	-374.1431	285.2192	
		4	1669.970700	680.7543	-955.0906	-430.4561	
	3	1	2205.9474	1082.7367	1102.9735	541.3683	I+II+III+IV+V+VI, area $= \frac{194}{36} + \frac{40}{36} = \frac{234}{36}$
		2	1044.0523	-792.2631	522.0261	-396.1315	
		3	1044.0523	-792.2631	-522.0261	396.1315	
		4	2205.9473	1082.7367	-1102.9735	-541.3683	

Table 4.3 continued

i	j	Node	Equivalent nodal loads corresponding to				Area in Fig.3 $= w_i \times w_j$
			w	$\frac{\partial w}{\partial x}$	$\frac{\partial w}{\partial y}$	$\frac{\partial^2 w}{\partial x \partial y}$	
	1	1	2229.5585	1105.3887	1109.4884	547.6183	I+II+III+IV+V+VI+VII
		2	1690.4120	-970.6022	700.3653	-445.3376	area $= \frac{234}{36} + \frac{25}{36} = \frac{259}{36}$
		3	1067.6634	-798.7776	-544.6782	402.3815	
		4	2206.8097	1083.5641	-1103.8010	-542.1622	
3	2	1	2249.1373	1124.1722	1124.1722	561.7060	I+II+III+IV+V+VI+VII+VIII
		2	2226.3886	-1118.4852	1102.3477	-556.2499	area $= \frac{259}{36} + \frac{40}{36} = \frac{299}{36}$
		3	1603.6400	-946.6606	-946.6606	513.2937	
		4	2226.3885	1102.3476	-1118.4856	-556.2493	
	3	1	2249.9999	1124.9996	1124.9996	562.4998	I+II+III+IV+V+VI+VII+VIII+IX
		2	2249.9997	-1124.9998	1124.9997	-562.4999	area $= \frac{299}{36} + \frac{25}{36} = 9$
		3	2249.9997	-1124.9998	-1124.9998	562.4999	
		4	2249.9997	1124.9996	-1124.9997	-562.4999	

TABLE 4.4

COEFFICIENTS FOR LOAD VECTOR DUE TO TEMPERATURE
DIFFERENTIAL

i	α^{11}	α^{12}	α^{13}
1	0	-	-
2	1/2	-	1
3	1/2	1	-
4	1/12	2	2
5	0	-	-
6	-1/2	-	1
7	1/2	1	-
8	-1/12	2	2
9	0	-	-
10	-1/2	-	1
11	-1/2	1	-
12	1/12	2	2
13	0	-	-
14	1/2	-	1
15	-1/2	1	-
16	-1/12	2	2

FIG. 4·1 _ DEFORMATION OF PAVEMENT SLAB
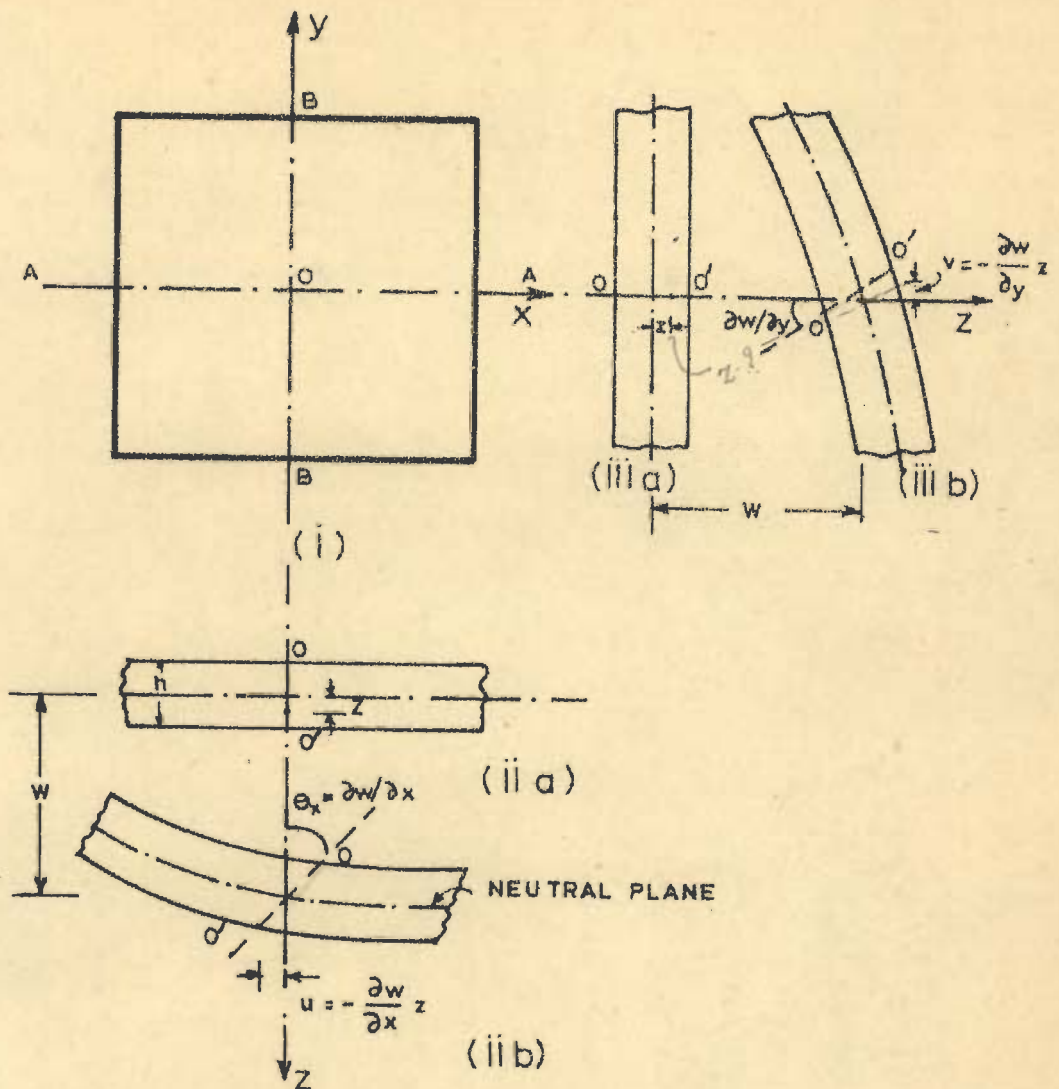
i _ PLAN OF AN UNDEFORMED SLAB PART

ii a _ SECTION ALONG A-A IN UNDEFORMED STATE

b _ SECTION ALONG A-A IN DEFORMED STATE

iii a _ SECTION ALONG B-B IN UNDEFORMED STATE

b _ SECTION ALONG B-B IN DEFORMED STATE
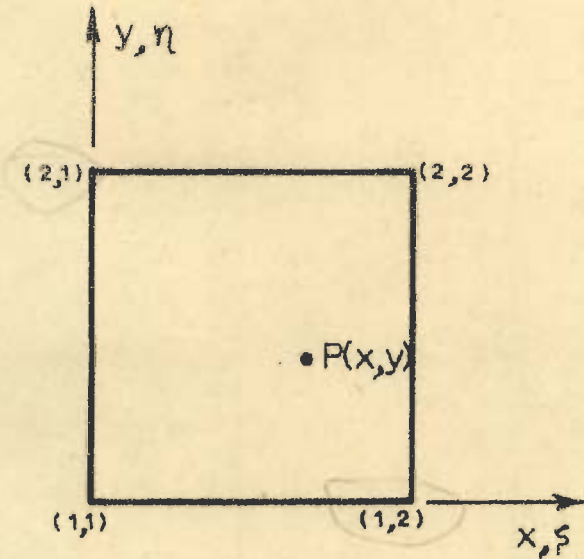
FIG. 4.2 _ HERMITIAN PLATE
ELEMANT
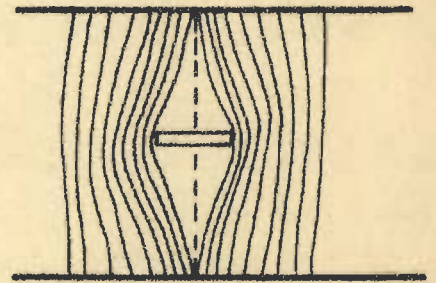
FIG. 4.4 _ ANALOGY BETWEEN
FLUID FLOW AND
STRESS- PATHS
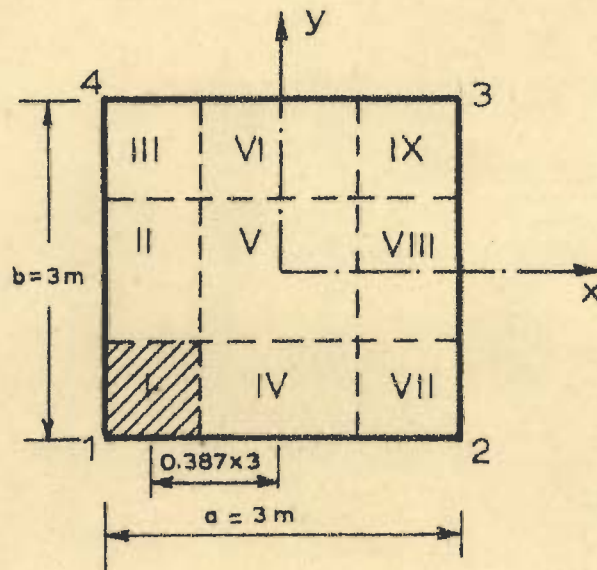
FIG. 4.3 _ RECTANGULAR ELEMENT DEVIDED
INTO SUBELEMENTS

a_ VARIATION OF My ALONG A A'

b_VARIATION OF My ALONG B B'   c_ PLAN OF SLAB (Quarter)
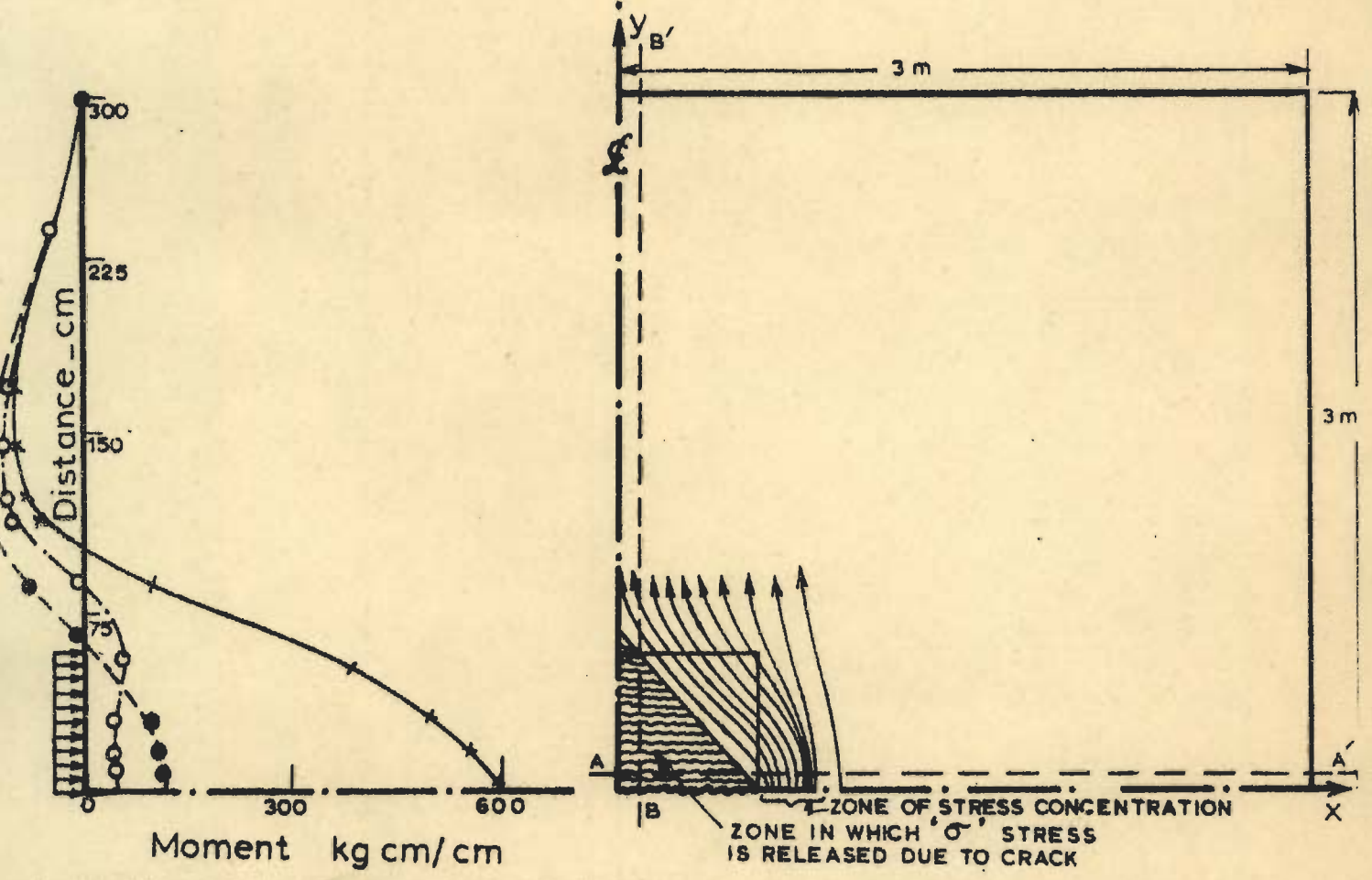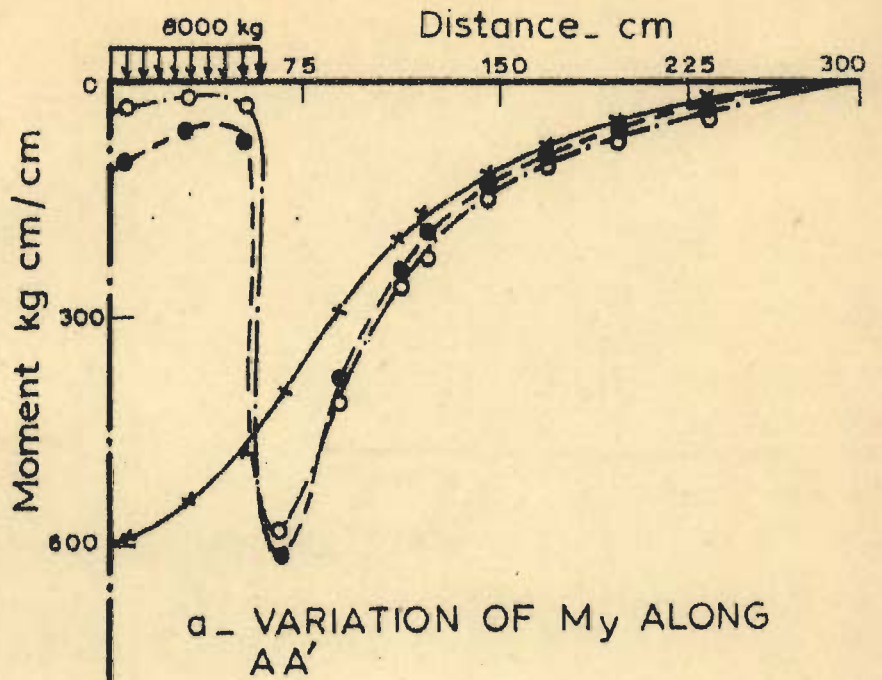
FIG. 4.5_ 6 x 6m SLAB IN CRACKED AND UNCRACKED CONDITION

a _ BENDING MOMENT ALONG A A'

b- DEFLECTION ALONG X=0

c _ DEFLECTION ALONG Y = 0
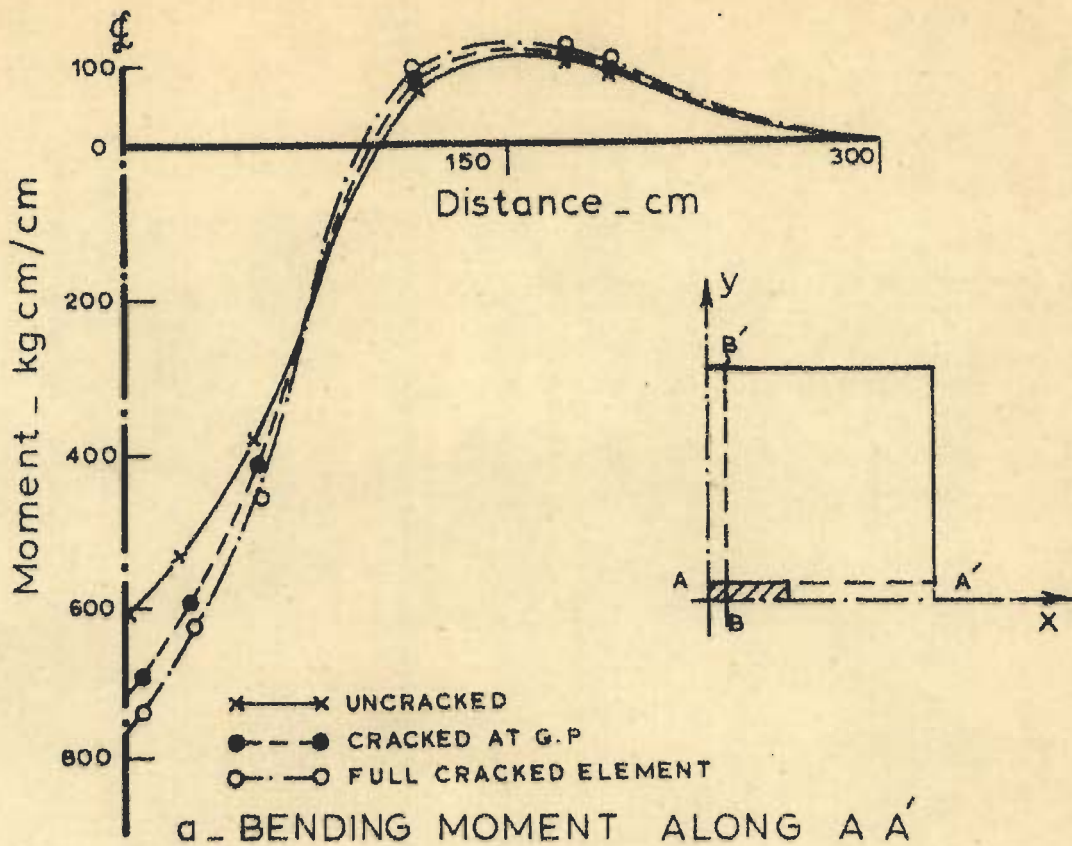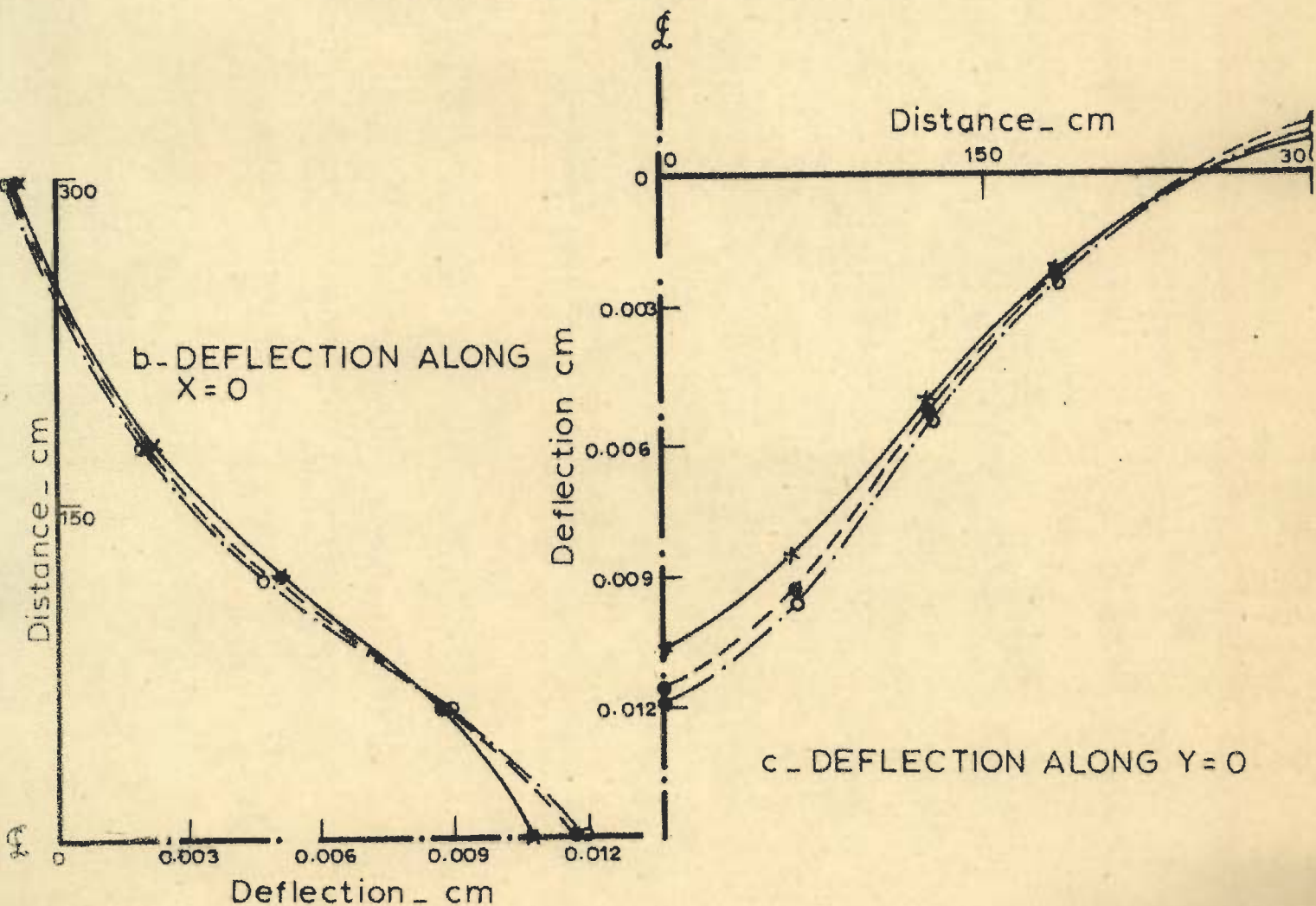
FIG. 4·6 _ SLAB WITH FINITE CRACK

Legend:
- ×——× UNCRACKED
- ●——● CRACKED AT G.P
- ○——○ FULL CRACKED ELEMENT
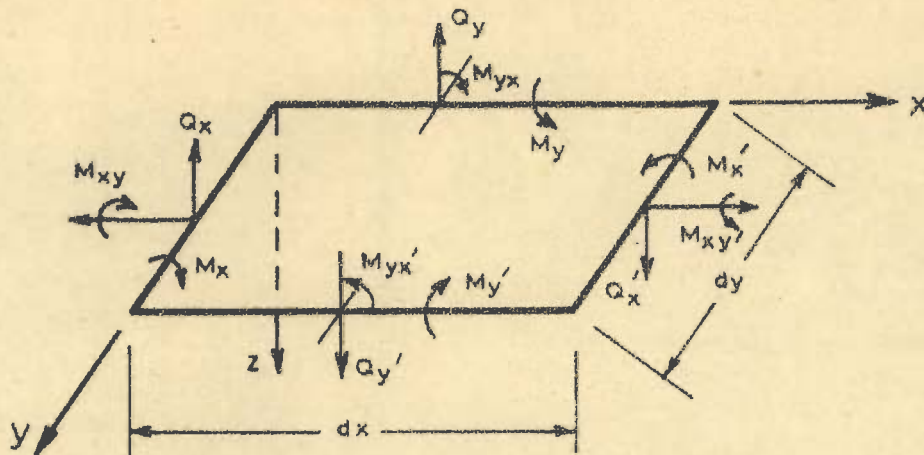
$$(Q_x - Q_x') \, d_y + (Q_y - Q_y') \, d_x + F = 0$$

WHERE, F = REACTIVE FORCE

$$Q_y = \frac{\partial M_y}{\partial y} - \frac{\partial M_{xy}}{\partial x}$$

$$Q_x = \frac{\partial M_x}{\partial x} + \frac{\partial M_{xy}}{\partial y}$$

a _ STATIC EQUILIBRIUM OF PLATE ELEMENT
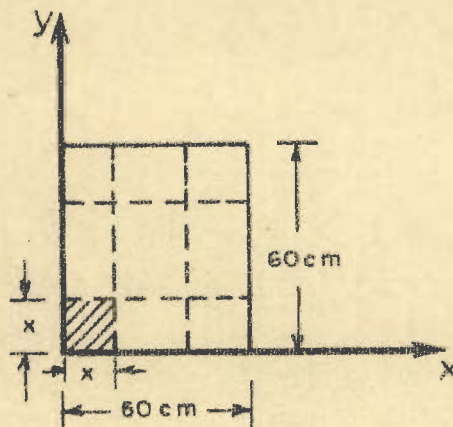
◿ LOADED PART OF ELEMENT

$$x = \frac{60 \times 5}{18} = \frac{50}{3} \text{ cm}$$

b _ LOADING OF SUB ELEMENTS

FIG. 4·7

£ of crack

My

Mx

0

20

40

60 — Distance — cm

a — VARIATION OF Mx AND My ALONG A A'
3.63 cm FROM CENTRE LINE

180   120   60   0   60   120   180

b — DEFLECTION ALONG CENTRE
LINE OF SLAB

0.275

CRACK

£

A.   3.63 cm
A

y

x
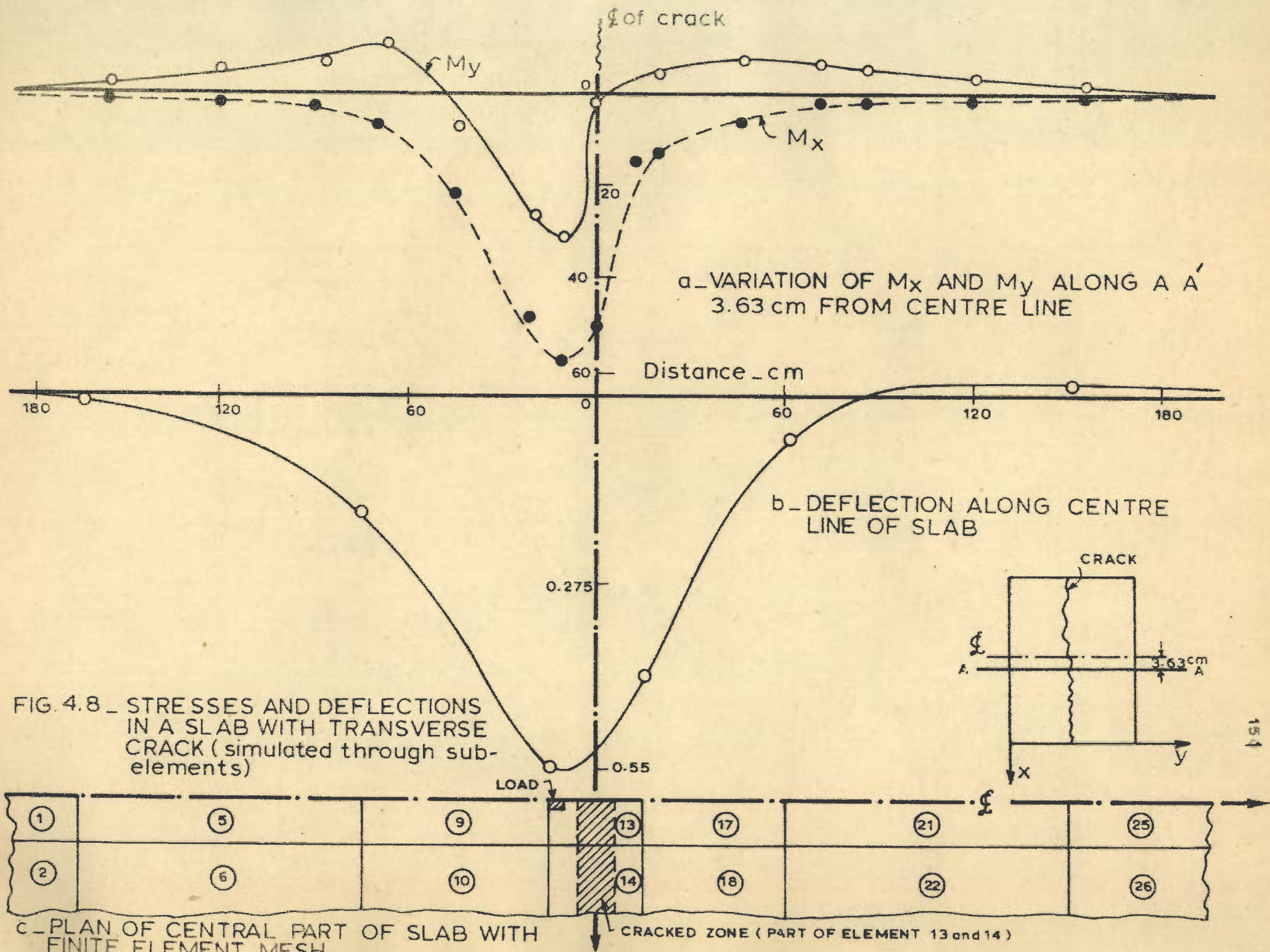
FIG. 4.8 — STRESSES AND DEFLECTIONS
IN A SLAB WITH TRANSVERSE
CRACK (simulated through sub-
elements)

0.55

LOAD

① 5 ⑨ 13 17 ㉑ ㉕

② 6 ⑩ 14 18 ㉒ ㉖

C — PLAN OF CENTRAL PART OF SLAB WITH
FINITE ELEMENT MESH

£

CRACKED ZONE (PART OF ELEMENT 13 and 14)

CHAPTER V

ANALYSIS OF BONDED CONCRETE OVERLAYS

5.1 INTRODUCTION

Tests of cement concrete slabs laid directly on old cement concrete pavements proved that the load which they were able to cater, without distress, was far in excess of what could have been expected[48, 103, 105]. This observation instituted confidence that overlay slabs can behave as a monolithic unit with the base and thereby enhance the load carrying capacity to a large extent.

Later, tests conducted by superficial observations, e.g. soundings[103, 169] as well as those detailed ones, in which cores were cut out of the in-service pavements with overlays[11, 105] showed that the interfacial bond remained intact in the normal circumstances. However, it appears, that the controversy continued to exist, whether the bond developed was enough for full shear transfer, necessary for efficiency of the bonded overlay, or not. This may have been due to the fact that many field observations did report bond failure. But a critical search of the reports reveal that most of these reported bond failures were only in the limited areas, adjoining the reflected cracks or joints or in the neighbourhood of the free edges[103, 105]. In certain cases it has been recognised that the bond failure has been the result of improper

construction technique or substandard work[102].

5.2 EFFECTIVENESS OF BONDING

A common question that has often been asked is whether a bonded overlay is feasible at all. Doubts have often arisen that unless some specific measures, like provision of shear pegs etc., are adopted, the base and the overlay can not act as a single unit[18]. Fear, also appears due to the reason that the repeated loadings or fatigue might destroy the bond and slipping at the interface might occur. Warping is also thought of as a cause that could separate the overlay from the base[170].

However, the field[11,48,102,103,105,169] as well as laboratory studies[16,96] provide conclusive evidence in favour of bonded overlays. The fact that most of the covered areas (90 percent or more) is often found to retain bond intact even after a number of years of in-service life[11,12,17], itself establishes a point in favour. Further full scale tests were performed on pavements slabs overlaid by bonded overlays, to verify whether full shear transfer takes place at the interface. The results of these well instrumented tests indicate that full strain compatibility conditions did hold true at the interface of base and overlay, which means that full shear transfer was taking place[48]. On the other hand tests were also performed on base

slab overlaid by concrete overlay with bonding prevented
and the results indicate that there was no transfer of
shear at the interface.

Laboratory tests carried out on beams by Sharma[16]
indicate that even when reliance is placed on asperities
of old and new slab to develop friction like bond, the
action of the two beams, one placed on the other is mono-
lithic. However, by grouting method a sufficiently high
quality of bond can be developed, its value being as high
as 75 percent of the value of monolithic beam, casted as
a single unit.

Sinno and Furr[96] conducted a series of laboratory
tests to study the effect of repeated load application
on bond failure. Two kinds of bonding methods were used,
the grouting and the epoxy bonding. An observation of signi-
ficance was that the cracks in the old pre-cracked beams
developed vertically through the overlay as well, but
not under the normal repeated designed loading. It was
only after increasing the designed loading to 150 percent
that this failure was observed under load cycling. Keeping
the fact in view that in all cases the beam in the base
was reinforced with 4 steel bars, this fact is significant
from the point of view of the findings reported in
Chapter III.

5.3 PROBLEMS OF BONDED OVERLAY

The problem of running of the base crack or reflection cracking in bonded overlay, is a menace, that has bothered the highway engineers to a great extent and has instituted doubt in the supremacy of the bonded overlays. Because of this reason, some agencies like Indian Roads Congress[10] do not recommend a bonded construction on a significantly cracked base slab.

Crack reflectance is not the only minus point discrediting the bonded overlay, although it is a major one. Special considerations are often necessary to ensure effective and durable bonding, as the success of the whole system lies in it. This adds to the cost of overlay concrete. The temperature differential between the top of the overlay and the bottom of the base is likely to be higher due to greater thickness. This fact may, therefore, offset the advantage gained by bonding to some extent. Apart from this, the differential shrinkage might take place between the overlay and base. Had there been no bond, this differential movement would have been unrestrained and there would have been very little stress. But, when overlay is bonded to base, the restraint offered by the base will generate stresses in both overlay and base.

On these counts, it becomes necessary to pay due consideration to thermal and shrinkage stresses in case of bonded overlays, apart from wheel load stresses.

5.4 METHODS OF ANALYSIS

5.4.1 Existing Methods

The existing methods of analysis of rigid overlays on rigid bases are due to P.C.A. and U.S.Corps of Engineers.[21] Field observations as well as controlled strain and deflection measurements have shown that the overlay bonded to base acts as a monolithic system. Therefore, for the purpose of analysis, it is logical to take the sum of the base and overlay thickness as the thickness of the pavement slab and find the stresses.

However, this will hold good only in case when overlay and base have identical material characteristics. Generally, even if the material composition is same (i.e. mix proportion and ingredients), the elastic properties of the old and new cement concrete may notbe same as a result of difference of age[171]. Apart from this, if the materials of base and overlay are différent , then the elastic properties of the two are bound to be different. In such cases, analysis by existing methods is not possible.

It seems that no attempts have been reported to consider the temperature effects on the base-overlay system. However, Ghosh et al[172,173] have considered the effect of differential drying shrinkage between the overlay and base following the initial strain approach as given by Birkeland[174] for precast beams, overlaid by cast-in-situ slabs.

5.4.2 Considerations for Analysis

It, therefore, appears that it is necessary to evolve a suitable method of analysis which could, on sound theoretical basis, give due recognition to the difference in elastic properties of the base and overlay for calculation of stresses and deflections in whole of the pavement structure for wheel loads placed any where on it. Not only this, the method should also be able to assess the stresses and displacements in the pavement when it is subjected to environmental influences. Also, it is possible that the old base might contain cracks. It is proposed to extend the method of Chapter IV by which the stresses and deflections can be calculated with fair degree of accuracy when the cracked pavement is overlaid by a bonded overlay.

5.5 GENERAL FORMULATION FOR THE ANALYSIS OF BONDED OVERLAY ON SOUND OR CRACKED BASE DUE TO WHEEL LOADS, THERMAL GRADIENTS AND DIFFERENTIAL SHRINKAGE.

5.5.1 General Assumptions:

1. It is assumed that all the plate theory assumptions stated in article 4.2 are also valid for this analysis.

2. It is assumed that condition of perfect bond exists at the base overlay interface i.e. at this face, full shear transfer takes place and the condition of full strain compatibility

holds good. The justification of this assumption is based on field observations, instrumented full scale tests and laboratory results as discussed in article 5.2.

3. Due to orthotropic properties the centroidal axes of the cross-sections along the orthogonal directions will not lie in the same plane. Effects due to this will however be neglected.

4. The temperature distribution in the pavement cross-section is assumed to be linear.

5. It is assumed that, as discussed and formulated in Chapter IV, the effect of the crack can be simulated by the orthotropic properties.

6. It is also assumed that the coordinate axis taken as reference frame coincides with the principal directions of orthotropy. However, if they do not, then the expressions can be obtained using rotation matrix as described in Chapter IV.

7. Shrinkage is assumed to be constant across the depth of the overlay.

5.5.2 General Formulation

It is seen from equations of Chapter IV that for

an orthotropic slab:

$$\left\{ \begin{array}{c} \varepsilon_x \\ \varepsilon_y \\ \gamma_{xy} \end{array} \right\} = z \left\{ \begin{array}{c} \dfrac{\partial^2 w}{\partial x^2} \\ \dfrac{\partial^2 w}{\partial y^2} \\ -2\dfrac{\partial^2 w}{\partial x \partial y} \end{array} \right\} \qquad \ldots (5.1)$$

and from equation 4.6

$$\left\{ \begin{array}{c} \sigma_x \\ \sigma_y \\ \tau_{xy} \end{array} \right\} = \left[\begin{array}{ccc} C_{11} & C_{12} & 0 \\ C_{21} & C_{22} & 0 \\ 0 & 0 & C_{33} \end{array} \right] \left\{ \begin{array}{c} \varepsilon_x \\ \varepsilon_y \\ \gamma_{xy} \end{array} \right\} \qquad \ldots (5.2)$$

Let the superscript 'o' relate to overlay and superscript 'b' relate to base.

Also let:

t_m = mean temperature rise or fall (with fall taken as positive)

e_s = differential shrinkage strain i.e. difference of strain in overlay and base,

Δt = difference of temperature between top and bottom surfaces,

 z = distance from centre of gravity of composite section,

 h = thickness of pavement (i.e. base and overlay),

*h_1 = distance of top of overlay from the centre of gravity of the composite section,

---

* values will be different in different orthotropic directions.

$^{*}h_2$ = distance of the bottom of overlay from the centre of gravity of the composite section,

$^{*}h_3$ = distance of the bottom of the base from the centre of gravity of the composite section,

α^o, α^b = coefficient of thermal expansion of the material of overlay and base.

Then, from 5.2

$$
\begin{Bmatrix} \sigma_x^o \\ \sigma_y^o \\ \tau_{xy}^o \end{Bmatrix} = \begin{bmatrix} C_{11}^o & C_{12}^o & 0 \\ C_{21}^o & C_{22}^o & 0 \\ 0 & 0 & C_{33}^o \end{bmatrix} \begin{Bmatrix} \varepsilon_x + \dfrac{\alpha^o z \, \Delta t}{h} + e_s \\ \varepsilon_y + \dfrac{\alpha^o z \, \Delta t}{h} + e_s \\ \gamma_{xy} \end{Bmatrix} \qquad \ldots (5.3)
$$

Similar expressions can be written for the base

$$
\begin{Bmatrix} \sigma_x^b \\ \sigma_y^b \\ \tau_{xy}^b \end{Bmatrix} = \begin{bmatrix} C_{11}^b & C_{12}^b & 0 \\ C_{21}^b & C_{22}^b & 0 \\ 0 & 0 & C_{33}^b \end{bmatrix} \begin{Bmatrix} \varepsilon_x + \dfrac{\alpha^b z \, \Delta t}{h} \\ \varepsilon_y + \dfrac{\alpha^b z \, \Delta t}{h} \\ \gamma_{xy} \end{Bmatrix} \qquad \ldots (5.4)
$$

The stress resultants can be obtained by integrating the stresses in the respective direction, over the depth. Accordingly,

$$
M_x = \int_{h_1}^{h_2} \sigma_x^o \, z \, dz + \int_{h_2}^{h_3} \sigma_x^b \, z \, dz \qquad \ldots (5.5)
$$

Putting the values from equation 5.3 and 5.4,

---

* values will be different in different orthotropic directions.

$$M_x = \int_{h_1}^{h_2} C_{11}^o \left[\varepsilon_x + \frac{\alpha^o z \, \Delta t}{h} + e_s \right] z \, dz$$

$$+ \int_{h_1}^{h_2} C_{12}^o \left[\varepsilon_y + \frac{\alpha^o z}{h} \Delta t + e_s \right] z \, dz$$

$$+ \int_{h_2}^{h_3} C_{11}^b \left[\varepsilon_x + \frac{\alpha^b z \, \Delta t}{h} \right] z \, dz$$

$$+ \int_{h_2}^{h_3} C_{12}^b \left[\varepsilon_y + \frac{\alpha^b z \, dt}{h} \right) \right] z \, dz \qquad \ldots (5.6)$$

By putting appropriate values of ε from equation 5.1, integrating, simplifying and rearranging

$$M_x = \frac{1}{3}(h_1^3 - h_2^3) \left[C_{11}^o \left(-\frac{\partial^2 w}{\partial x^2} + \alpha^o \cdot \frac{\Delta t}{h} \right) + C_{12}^o \left(-\frac{\partial^2 w}{\partial y^2} + \frac{\alpha^o \Delta t}{h} \right) \right]$$

$$+ \frac{1}{2}(h_1^2 - h_2^2) e_s (C_{11}^o + C_{12}^o)$$

$$+ \frac{1}{3}(h_2^3 - h_3^3) \left[C_{11}^b \left(-\frac{\partial^2 w}{\partial x^2} + \alpha^b \frac{\Delta t}{h} \right) \right.$$

$$\left. + C_{12}^b \left(-\frac{\partial^2 w}{\partial y^2} + \alpha^b \frac{\Delta t}{h} \right) \right] \qquad \ldots (5.7)$$

If all 'C' are given their appropirate values and they are combined with $(h_1^3 - h_2^3)$ and written as:

*

$$D_{11}^o = \frac{1}{3}(h_1^3 - h_2^3) C_{11}^o$$

$$D_{22}^o = \frac{1}{3}(h_1^3 - h_2^3) C_{22}^o$$

$$D_{12}^o = \frac{1}{3}(h_1^3 - h_2^3) C_{12}^o$$

$$D_{33}^o = \frac{1}{3}(h_1^3 - h_2^3) C_{33}^o$$

$$D_{12}^b = \frac{1}{3}(h_2^3 - h_3^3) C_{12}^b$$

$$D_{22}^b = \frac{1}{3}(h_2^3 - h_3^3) C_{22}^b$$

* Depending upon the orthotropic elastic constants h_1, h_2, h_3 will be different

$$D_{11}^b = \frac{1}{3}(h_2^3 - h_3^3)C_{11}^b$$

$$D_{33}^b = \frac{1}{3}(h_2^3 - h_3^3)C_{33}^b$$

$$D_{11}^{o\,'} = \frac{1}{2}(h_1^2 - h_2^2)C_{11}^o$$

$$D_{12}^{o\,'} = \frac{1}{2}(h_1^2 - h_2^2)C_{12}^o$$

$$D_{22}^{o\,'} = \frac{1}{2}(h_1^2 - h_2^2)C_{22}^o$$

$$\dots \quad (5.8)$$

Equation 5.7 becomes

$$M_x = -(D_{11}^o + D_{11}^b)\frac{\partial^2 w}{\partial x^2} - (D_{12}^o + D_{12}^b)\frac{\partial^2 w}{\partial y^2} + (D_{11}^o + D_{12}^o)\,\alpha^o\,\frac{\Delta t}{h}$$

$$+(D_{11}^b + D_{12}^b)\alpha^b\,\frac{\Delta t}{h} + (D_{11}^{o\,'} + D_{12}^{o\,'})e_s \qquad \dots \quad (5.9)$$

Similarly, it can be written,

$$M_y = -\left[(D_{22}^o + D_{22}^b)\frac{\partial^2 w}{\partial y^2} + (D_{21}^o + D_{21}^b)\frac{\partial^2 w}{\partial x^2}\right]$$

$$+(D_{22}^o + D_{21}^o)\alpha^o\,\frac{\Delta t}{h} + (D_{22}^b + D_{21}^b)\alpha^b\,\frac{\Delta t}{h}$$

$$+e_s(D_{22}^{o\,'} + D_{21}^{o\,'}) \qquad \dots \quad (5.10)$$

and

$$M_{yx} = 2\left[D_{33}^o + D_{33}^b\right]\frac{\partial^2 w}{\partial x \partial y} \qquad \dots \quad (5.11)$$

Equation 5.9, 5.10 and 5.11 can be written in a compact

form as:

$$
\begin{Bmatrix} M_x \\ M_y \\ M_{xy} \end{Bmatrix} =
\begin{bmatrix} D_{11}^o & D_{12}^o & 0 \\ D_{21}^o & D_{22}^o & 0 \\ 0 & 0 & D_{33}^o \end{bmatrix}
\begin{Bmatrix} -\dfrac{\partial^2 w}{\partial x^2} + \alpha^o \dfrac{\Delta t}{h} \\ -\dfrac{\partial^2 w}{\partial y^2} + \alpha^o \dfrac{\Delta t}{h} \\ 2\dfrac{\partial^2 w}{\partial x \partial y} \end{Bmatrix}
$$

$$
+ \begin{bmatrix} D_{11}^b & D_{12}^b & 0 \\ D_{21}^b & D_{22}^b & 0 \\ 0 & 0 & D_{33}^b \end{bmatrix}
\begin{Bmatrix} -\dfrac{\partial^2 w}{\partial x^2} + \alpha^b \dfrac{\Delta t}{h} \\ -\dfrac{\partial^2 w}{\partial y^2} + \alpha^b \dfrac{\Delta t}{h} \\ 2\dfrac{\partial^2 w}{\partial x \partial y} \end{Bmatrix}
$$

$$
+ \begin{bmatrix} D_{11}^{o'} & D_{12}^{o'} & 0 \\ D_{21}^{o'} & D_{22}^{o'} & 0 \\ 0 & 0 & 0 \end{bmatrix}
\begin{Bmatrix} e_s \\ e_s \\ 0 \end{Bmatrix}
$$

$$\dots \ (5.12)$$

It is found that aggregate type is an important factor on which the coefficient of thermal expansion depends[175]. As the aggregate type is likely to remain same in a locality, it is reasonable to assume that, $\alpha^o = \alpha^b = \alpha$.

Equation 5.12 can be written in a further simplified form as:

$$\begin{Bmatrix} M_x \\ M_y \\ M_{xy} \end{Bmatrix} = \begin{bmatrix} D_{11}^o + D_{11}^b & D_{12}^o + D_{12}^b & 0 \\ D_{21}^o + D_{21}^b & D_{22}^o + D_{22}^b & 0 \\ 0 & 0 & D_{33}^o + D_{33}^b \end{bmatrix} \begin{Bmatrix} -\dfrac{\partial^2 w}{\partial x^2} + \alpha\dfrac{\Delta t}{h} \\ -\dfrac{\partial^2 w}{\partial y^2} + \alpha\dfrac{\Delta t}{h} \\ 2\dfrac{\partial^2 w}{\partial x \partial y} \end{Bmatrix}$$

$$+ \begin{bmatrix} D_{11}^{o\,'} & D_{12}^{o\,'} & 0 \\ D_{21}^{o\,'} & D_{22}^{o\,} & 0 \\ 0 & 0 & 0 \end{bmatrix} \begin{Bmatrix} e_s \\ e_s \\ 0 \end{Bmatrix} \qquad \ldots (5.13)$$

At this stage if effects of shrinkage are separated out,
then writing

$$\begin{aligned}
D_{11} &= D_{11}^o + D_{11}^b \\
D_{12} &= D_{12}^o + D_{12}^b \\
D_{21} &= D_{21}^o + D_{21}^b \\
D_{22} &= D_{22}^o + D_{22}^b \\
D_{33} &= D_{33}^o + D_{33}^b
\end{aligned} \qquad \ldots (5.14)$$

Equation 5.13 becomes

$$\begin{Bmatrix} M_x \\ M_y \\ M_{xy} \end{Bmatrix} = \begin{bmatrix} D_{11} & D_{12} & 0 \\ D_{21} & D_{22} & 0 \\ 0 & 0 & D_{33} \end{bmatrix} \begin{Bmatrix} -\dfrac{\partial^2 w}{\partial x^2} + \alpha\dfrac{\Delta t}{h} \\ -\dfrac{\partial^2 w}{\partial y^2} + \dfrac{\Delta t}{h} \\ 2\dfrac{\partial^2 w}{\partial x \partial y} \end{Bmatrix} \qquad \ldots (5.15)$$

Again this can be written symbolically as

$$\{M\} = [D]\{\chi\} + [D]\{\chi_o\} \qquad \ldots (5.16)$$

where the constitutive relation matrix of equation 4.11
holds.

If the direction of orthotropy and reference axis is not coincident then using equation (4.48), the $[D]$ is modified and in such a case all the terms in $[D]$ will be non-zero terms.

If Q denotes out-of-plane shear then[114]

$$Q_x = \frac{\partial M_x}{\partial x} + \frac{\partial M_{xy}}{\partial y}$$

Therefore, from equations 5.9 and 5.10

$$Q_x = -\left[D_{11} \frac{\partial^3 w}{\partial x^3} + D_{12} \frac{\partial^3 w}{\partial x \partial y^2} - 2D_{13} \frac{\partial^3 w}{\partial x^2 \partial y} \right]$$
$$- \left[D_{31} \frac{\partial^3 x}{\partial x^2 \partial y} + D_{32} \frac{\partial^3 w}{\partial y^3} - 2D_{33} \frac{\partial^3 w}{\partial x \partial y^2} \right] \quad \ldots (5.17)$$

and similarly

$$Q_y = -\left[D_{21} \frac{\partial^3 w}{\partial x^2 \partial y} + D_{22} \frac{\partial^3 w}{\partial y^3} - 2D_{23} \frac{\partial^3 w}{\partial x \partial y^2} \right]$$
$$- \left[D_{31} \frac{\partial^3 w}{\partial x^3} + D_{32} \frac{\partial^3 w}{\partial y^2 \partial x} - 2D_{33} \frac{\partial^3 w}{\partial x^2 \partial y} \right] \quad \ldots (5.18)$$

However, if coordinate axis are chosen such that plane xz and yz are planes of elastic symmetry, then

$$D_{13} = D_{31} = D_{23} = D_{32} = 0$$

and equations 5.17 and 5.18 are modified accordingly.

5.5.3 Determination of Stresses and Deflections at a Point:

The procedure of determination of statical influences can follow the same procedure as in the previous Chapter

since the basic relationship given by equation 5.16 is in a form readily adaptable to finite element method, the important feature of the previous article being to express the equation of base with overlay in the same form as for the single slab if the shrinkage effects are not considered.

Having known the modified constitutive law the equations of equilibrium can be formed, in the usual manner as given by equation 4.30. From the solution of these simultaneous equations, the unknown displacements, i.e. slopes and deflections at various points can be obtained. The strains can then be calculated by use of equation 2.4 as they are derivatives of displacements.

Having obtained the strains, the stresses in the overlay and base can be calculated by using the fundamental equations 5.3 and 5.4 respectively.

5.5.4 Determination of the Interfacial stress.

Figure 5.1(a) shows an infinitismal element of the pavement slab of dimensions dx, dy. For brevity, all the stress components are not shown.

Applying the method of sections and considering the equilibrium in x and y direction respectively,

$$\int_{h_1}^{h_2} \sigma_x^0 \, dy \, dz + \int_{h_1}^{h_2} \tau_{xy}^0 \, dx \, dz = \tau_{zx} \, dx \, dy + \int_{h_1}^{h_2} (\sigma_x^0 + \frac{\partial \sigma_x^0}{\partial x} \, dx)$$

$$+ \int_{h_1}^{h_2} (\tau_{xy}^0 + \frac{\partial \tau_{xy}^0}{\partial y} \, dy) dx \, dz$$

where, τ_{zx} = interfacila shear stress, and other quantities are as defined in article 5.5.2.

Therefore,

$$\tau_{xz}dx\,dy = -\int_{h_1}^{h_2} \frac{\partial \sigma_x^o}{\partial x} \, dx\,dy\,dz - \int_{h_1}^{h_2} \frac{\partial \tau_{xy}^o}{\partial y} \, dx\,dy\,dz \quad \ldots \quad (5.19)$$

But from equation 5.3 values of σ_x^o and τ_{xy}^o can be obtained and substituted in equation (5.19) on simplification,

$$\tau_{xz} = \int_{h_1}^{h_2} z \begin{bmatrix} C_{11}^o & C_{12}^o & C_{13}^o \end{bmatrix} \begin{Bmatrix} \dfrac{\partial^3 w}{\partial x^3} \\[2mm] \dfrac{\partial^3 w}{\partial y^2 \partial x} \\[2mm] -2\dfrac{\partial^3 w}{\partial x^2 \partial y} \end{Bmatrix} dz$$

$$+ \int_{h_1}^{h_2} z \begin{bmatrix} C_{31}^o & C_{32}^o & C_{33}^o \end{bmatrix} \begin{Bmatrix} \dfrac{\partial^3 w}{\partial x^2 \partial y} \\[2mm] \dfrac{\partial^3 w}{\partial y^3} \\[2mm] -2\dfrac{\partial^3 w}{\partial x \partial y^2} \end{Bmatrix} dz$$

On integration,

$$\tau_{xz} = \frac{1}{2}[h_1^2 - h_2^2]\left[\begin{bmatrix} c_{11}^o & c_{12}^o & c_{13}^o \end{bmatrix} \left\{\begin{matrix} \dfrac{\partial^3 w}{\partial x^3} \\ \dfrac{\partial^3 w}{\partial y^2 \partial x} \\ -2\dfrac{\partial^3 w}{\partial x^2 \partial y} \end{matrix}\right\}\right.$$

$$\left.+\begin{bmatrix} c_{31}^o & c_{32}^o & c_{33}^o \end{bmatrix} \left\{\begin{matrix} \dfrac{\partial^3 w}{\partial x^2 \partial y} \\ \dfrac{\partial^3 w}{\partial y^3} \\ -2\dfrac{\partial^3 w}{\partial x \partial y^2} \end{matrix}\right\}\right] \qquad \dots (5.20)$$

Similarly, it can be proved that:

$$\tau_{yz} = \frac{1}{2}[h_1^2 - h_2^2]\left[\begin{bmatrix} c_{21}^o & c_{22}^o & c_{23}^o \end{bmatrix} \left\{\begin{matrix} \dfrac{\partial^3 w}{\partial x^2 \partial y} \\ \dfrac{\partial^3 w}{\partial y^3} \\ -2\dfrac{\partial^3 w}{\partial x . \partial y^2} \end{matrix}\right\}\right.$$

$$\left.+\begin{bmatrix} c_{31}^o & c_{32}^o & c_{33}^o \end{bmatrix} \left\{\begin{matrix} \dfrac{\partial^3 w}{\partial x^3} \\ \dfrac{\partial^3 w}{\partial x \partial y^2} \\ -2\dfrac{\partial^3 w}{\partial y \partial x^2} \end{matrix}\right\}\right] \qquad \dots (5.21)$$

Now, in order to determine the interfacial shear stresses from equations 5.20 and 5.21, it is necessary to know the derivative of the curvatures i.e. the third partial derivatives of the deflections at various points.

The second derivatives of deflections are already known as derived in equation 4.22. Exactly, similar procedure of obtaining local derivatives can be adopted for obtaining the third derivatives.

Though, the procedure of local derivatives is accurate and straightforward, it is a burden on costly computer time. Also, it is taxing on the memory which is falling short in case of elastic solid type foundation. It is therefore, proposed to determine the derivatives by finite difference melhhod using forward difference technique. This method becomes exceedingly economical without excessive loss of accuracy.

5.5.5 Determination of Stresses due to Differential Shrinkage:

Viest[176] and others have treated the problem of the determination of stresses due to differential shrinkage in a cast-in-situ slab over a pre-cast beam. All of them consider the problem as one dimensional. Approach of Birkeland[174] is basic and a modification of all these, but in this approach too the problem is regarded as a beam problem. Zuk[177] has also analysed the same problem, but it is a further modification on Birkeland's analysis because in this approach he considers the effect of transverse shrinkage of the cast-in-situ slab, which was neglected by Birkeland.

Figure 5.1(b) illustrates the mechanics of differential shrinkage

As shown in diagram (i) the magnitude of shrinkage stress

$$P = e_s A_o E^o \qquad \qquad \ldots (5.28)$$

where A_o = cross-sectional area of overlay.

The self-equilibrating system of forces are shown in diagram (iv). These forces will generate stress at top and bottom of overlay and base as shown in diagram (v).

If,

f_1 = stress at top of overlay,

f_2 = stress at bottom of overlay,

f_3 = stress at top of base, and

f_4 = stress at bottom of base

then, these are given by

$$f_1 = P\frac{E_o}{E_b}\left[\frac{1}{A_o'} - \frac{1}{A} - \frac{C(C + \frac{h^o}{2})}{I} \right]$$

$$f_2 = P\frac{E_o}{E_b}\left[\frac{1}{A_o'} - \frac{1}{A} - \frac{C(C - \frac{h^o}{2})}{I} \right]$$

$$f_3 = -P\left[\frac{1}{A} + \frac{C(C - \frac{h^o}{2})}{I_b} \right], \text{ and}$$

$$f_4 = -P\left[\frac{1}{A} + \frac{C - (h + \frac{h^o}{2})}{I} \right] \qquad \ldots (5.29)$$

where,

A_o' = equivalent cross-sectional area of overlay,

A = equivalent cross-sectional area of base and overlay

I = equivalent moment of inertia of the section, and

C = distance between centre of gravity of overlay and composite.

These forces can also be viewed as direct forces and couples as shown in diagram (vi).

Birkeland's approach in its original form has also been applied for determination of stresses in bonded concrete overlays over concrete pavement slabs by Ghosh et.al[166,167].

However, the equilibrium of the self-equilibrating force system will get modified due to the presence of reactions of elastic foundation which are bound to come into play.

Therefore, it is necessary to adopt the finite element formulation as was proposed in equation 5.13.

On examining equation 5.13 it can be seen that it is not necessary to perform the finite element analyses exclusively for shrinkage if it is already done for temperature stresses and vice-versa. The conversion factor can be determined as follows:-

From equations 5.13 and 5.15,

$$\left\{ \begin{matrix} M_x \\ M_y \end{matrix} \right\}^t = \frac{\alpha \Delta t}{h} \begin{bmatrix} D_{11} & D_{12} \\ D_{21} & D_{22} \end{bmatrix} \left\{ \begin{matrix} 1 \\ 1 \end{matrix} \right\} \qquad \ldots (5.30)$$

and

$$\left\{ \begin{matrix} M_x \\ M_y \end{matrix} \right\}^s = e_s \begin{bmatrix} D_{11}^{o'} & D_{12}^{o'} \\ D_{21}^{o'} & D_{22}^{o'} \end{bmatrix} \left\{ \begin{matrix} 1 \\ 1 \end{matrix} \right\} \qquad \ldots (5.31)$$

where superscript 't' denotes temperature and 's' stands for shrinkage.

In isotropic case $M_x = M_y$.
In can therefore be seen that

$$\frac{M_x^t}{M_x^s} = \frac{\alpha \, \Delta T}{h \, e_s} \left[\frac{D_{11} + D_{12}}{D_{11}^{o'} + D_{12}^{o'}} \right] \qquad \ldots \text{(5.32)}$$

which on substitution of appropriate values from equation 5.14, 5.8 and 4.6 and simplification becomes,

$$\frac{M^t}{M^s} = \frac{2}{3} \frac{\alpha \, \Delta T}{h \, e_s} \left[\frac{h_1^3 - h_2^3}{h_1^2 - h_2^2} + \frac{E^b}{E^o} \frac{1-\nu^o}{1-\nu^b} \frac{h_2^3 - h_3^3}{h_1^2 - h_2^2} \right] \qquad \ldots \text{(5.33)}$$

The shrinkage of overlay will give rise to axial forces and moments as shown in figure 5.1(b). The stresses due to moments can be evaluated by equation 5.33. If the stresses generated due to axial forces in base and overlay are represented by primed quantities and if 'e' is the elastic strain generated in the base-overlay interface due to these forces then,

net strain in the overlay $= e_s - e$ $\qquad \ldots \text{(5.34)}$

Therefore, the stresses due to axial forces in overlay will be

$$\begin{Bmatrix} \sigma_x^{o'} \\ \sigma_y^{o'} \end{Bmatrix} = \frac{E^o}{1-\nu^{o^2}} \begin{bmatrix} 1 & \nu^o \\ \nu^o & 1 \end{bmatrix} \begin{Bmatrix} e_s - e \\ e_s - e \end{Bmatrix} \qquad \ldots \text{(5.35)}$$

or

$$\sigma_x^{o\,'} = \frac{E^o}{1-\nu^o}(e_s - e) \qquad \ldots (5.36)$$

and stresses due to axial forces in base will be

$$\begin{Bmatrix} \sigma_x^{b\,'} \\ \sigma_y^{b\,'} \end{Bmatrix} = \frac{E^b}{1-\nu^{b2}} \begin{bmatrix} 1 & \nu^b \\ \nu^b & 1 \end{bmatrix} \begin{Bmatrix} -e \\ -e \end{Bmatrix} \qquad \ldots (5.37)$$

or $\qquad \sigma_x^{b\,'} = -\dfrac{E^b}{1-\nu^b}\cdot e \qquad \ldots (5.38)$

Also from the considerations of statics

$$\frac{E^o h^o}{1-\nu^o}(e_s - e) - \frac{E^b h^b}{1-\nu^b}\, e = 0$$

Therefore, $\qquad e = \dfrac{\dfrac{E^o h^o}{1-\nu^o}}{\dfrac{E^o h^o}{1-\nu^o} + \dfrac{E^b h^b}{1-\nu^b}}\, e_s \qquad \ldots (5.39)$

Therefore, the net stresses at any point in the base overlay system will be a combination of the effects due to axial forces and moments. Stresses due to moments can be either determined directly by using equations 5.31 and then applying the procedure as outlined in Chapter IV for determination of equivalent nodal forces for temperature stresses or could also be determined indirectly from equation 5.33 from temperature stresses.

The stresses due to axial forces can be determined from equations 5.36, 5.38 and 5.39.

5.6 MODELING OF CRACKED BASE

The rigidity of the base slab is expressed in equation 5.16 in such a form which represent the orthotropic conditions, i.e. the rigidities in two orthogonal directions need not be same. This condition suits modeling of crack amicably. If the direction of crack coincides with one of the coordinate axis, the equation 5.15 can directly be used. However, if the direction of crack is arbitrary, transformation as given by equation 4.48 is necessary.

If the base has a crack, the effect of the crack will be to release stresses in the base in the direction perpendicular to the crack alignment. As has already been discussed in article 4.5, the effect of this stress release will extend upto a certain distance on either side of the crack, which can reasonably be assumed as equal to the depth of crack on either side. The rigidity of the orthogonal direction can be assumed as unaffected.

The rigidities for the cracked transformed section can be determined by equation 4.12.

5.7 MODIFICATION OF COMPUTER PROGRAM

5.7.1 In Chapter IV, it is reported, that the program is coded, debugged and tested for a single layer of pavement slab resting on Winkler foundation. The slab may be isotropic, homogeneous or may have arbitrary cracks. The wheel loads acting on the slab can be represented by

rectangular contact area and the stresses due to temperature differential can be evaluated.

In the first stage of modification of this very program, the solution algorithm for bonded overlays, is included as discussed hitherto. Following changes are incorporated:

(i) An identification procedure is set so as to select the calculation procedure according to the number of layers.

(ii) An identification procedure is also built to select the operations, in accordance with the condition of the base i.e. whether sound or cracked.

(iii) If the base is cracked, then it is again necessary to select operations according to whether the crack extends on the whole element or only a partly cracked element is used as discussed in article 4.8.

(iv) If the crack orientation makes an angle with the reference frame, then constitutive laws have to be modified, the ability to do so already exists.

(v) The stresses at top and bottom of overlay and base are required. The interfacial stress is also to be evaluated as discussed in article 5.5.4. A modification in this respect

is also incorporated.

5.7.2 Testing of Program with Modification

The modified program, incorporating the operations as mentioned above for determination of stresses and displacements has to be checked for its correctness on the lines of article 4.10.

For this purpose the cases to be analysed are as shown in Table 5.1. The details of this analysis is discussed below. For all the cases following properties are taken:

(i) Base thickness = 10 cm

(ii) Overlay thickness= 8 cm

(iii) Wheel load of 4500 kg. is simulated in FEM analysis through dual-tyre assembly with contact area 25 cm x 10 cm with a gap of 16 cm in between. In interior location, this assembly is located with its centre coincident with centre of the pavement. In the edge region, the exterior edge of the outer tyre is supposed to be over the pavement edge.

(iv) For comparison with Westergaard's solution, the wheel load is taken as 4500 kg acting over a circular contact area of 850 sq.cm. giving same pressure.

(v) Modulus of subgrade reaction is taken as
12 kg/cm^2.

(vi) Size of the pavement slab is assumed as
3.5mx9m for finite element analysis.

(vii) The difference of temperature between top
of overlay and bottom of base is assumed
as 13°C.

(viii) The modulus of elasticity of the material of
the base which is assumed as isotropic, is
taken as 30x10^4 kg/cm^2 and its Poisson's ratio
as 0.15.

(ix) Coefficient of thermal expansion is taken as
0.8x10^{-5} per degree centigrade for overlay
as well as for base.

Case I: In addition to above conditions the modulus of
elasticity of the overlay is taken to be same as base
i.e. 30x10^4 kg/cm^2. Three cases are analysed:

(a) Wheel load is placed at the centre of the pave-
ment slab. When compared with Westergaard's
solution[24], the difference in maximum stress
under the wheel load is found to be 1.285 per-
cent as shown in Table 5.1.

(b) With the wheel load placed at edge position as
described in para (iii) above, the maximum
moment as determined by the present formulation

differs by 0.92 percent as compared to that
found by Westergaard's equation.

(c)   A temperature difference of $13^\circ C$ is supposed to
exist between top and bottom slab. The stress
developed due to this is determined by finite
element analysis and is compared with the interior
stress as given by Bradbury's solution. As shown
in Table 5.1 the results are within 1.2 percent.

It may be noted that the 10 cm base fully bonded
to 8 cm overlay, will be equivalent to 18 cm pavement
slab when the elastic properties of base and overlay are
considered to be the same. The results of the present
formulation also confirms this, because the results of
Westergaard's solution with 18 cm thick slab agree,
reasonably with the numerical results.

Case II: In this case the elastic properties of the
overlay are supposed to be different than that of the
base. The modulus of elasticity of the overlay is assumed
as half of that of base i.e. 15×10^4 kg/cm^2. The Poisson's
ratio is taken as 0.2. Each layer is considered as having
isotropic properties.

It is not possible to directly apply the Wester-
gaard's solution to this case. Therefore, a modification to
solution is done. Accordingly, based on the formulation
discussed in article 5.5.2, the value of radius of

relative stiffness 'l' is determined for using Wester-
gaard's equation, for the combined base-overlay system.
Three cases are again solved:

(a) In this case the wheel load is placed at
the interior region and the maximum stress
as determined by finite element solution
differs by 0.8 percent with the one deter-
mined by modified Westergaard's solution.

(b) The wheel load is placed at the edge. The
maximum stress under the wheel load parallel
to the edge as found by the finite element
program differs by 1.31 percent as compared
to modified Westergaard's solution.

(c) The Bradbury's equation is also modified by
computing the equivalent radius of relative
stiffness in exactly the same way and the
stress due to temperature differential, as
given by finite element program is compared
to those calculated by Bradbury's procedure.
The results are found to differ by 1.26 percent.

Modified Bradbury's procedure is given in appendix
5C and modified Westergaard procedure is described in
Appendix 5B. It is therefore observed that:

(i) If the modulus of elasticity of the base and
overlay does not differ, then the existing

practice of taking the combined thickness
of base and overlay as a single thickness is
justified.

(ii) If the elastic properties of base and overlay
differ, then it is possible to evaluate the
maximum stress using a modified Westergaard's
solution procedure for wheel load stresses and
modified Bradbury's solution for temperature
stresses.

5.8 ANALYTICAL INVESTIGATION

A very large number of variables are involved for
truly examining the behaviour of a cement concrete
overlay laid on a base slab, with the assumption of full
strain compatibility of the interface. To name a few
variables:

(i) Thickness of base

(ii) Thickness of overlay

(iii) Properties of subgrade

(iv) Modulus of elasticity of base

(v) Modulus of elasticity of overlay

(vi) Wheel load positions, size, spacing,
magnitude

(vii) Thermal effects

(viii) Shape, size, location and spacing of cracks

(ix) Size of pavement panel

(x) Effect of differential shrinkage.

An analysis which involves a study of all these variables will no doubt create a true insight into the behaviour. Such a study can only be carried out by using the finite element method which has a provision to consider them. The only other requirement, then, for such a parametric study would be, availability of computer effort and also availability of time for analysis and interpretation and parametric correlations. However, presently following analysis is proposed:

(i) Base Thickness:

3 base thicknesses are considered i.e. 8 cm, 12 cm and 16 cm. The reason for choosing these thicknesses is, as was discussed in chapter I, that most of the existing highway pavements, that need overlays fall in this range.

(ii) Thickness of Overlay:

To study the effect of overlay thickness economically only two overlay thicknesses are considered i.e. 10 cm and 6 cm. These thicknesses are however, adopted rather arbitrarily, though bonded overlays that are normally adopted in practice may have, somewhat similar value.

(iii) Subgrades may have widely variable properties:

The subgrades with a base course layer on them is however a typical of an existing concrete road cross-section in the country. For this reason the value of

modulus of subgrade reaction chosen for analysis is 12 kg/cm^3. Only one value is chosen, so as to limit the computations.

(iv) Modulus of elasticity of Overlay:

Modulus of elasticity of the overlay is taken as 15x10^4 kg/cm^2. The justification of taking such a value has already been discussed in chapter III. Again, to limit the computations, this factor is not taken as a parameter for study. Poisson's ratio is taken as 0.2.

(v) Modulus of Elasticity of Base:

Modulus of elasticity of base has been assumed as 30x10^4 kg/cm^2 and only one value is taken for the reason stated above. The higher value is adopted because it is known that modulus of elasticity of cement concrete increases with time, though at a very slow rate. The old base, being considered, may be as old as 25-30 years, as most of cement concrete roads built in the country which need strengthening, are that old. Many times a lower value of modulus of elasticity is also adopted to take the effect of fatigue into consideration. However, since cracking is given due regard in the present analysis in the form of stress release a value lower than its initial value may not be justified. The Poisson's ratio is taken as 0.15.

(vi) Wheel Load Position:

Wheel loads may vary in size, shape and pressure

of contact. They may also differ in magnitude, spacing and location with respect to pavement. The three critical positions, as proposed by Westergaard viz., interior, edge and corner are well known. However, for a pavement slab with arbitrary cracks, these may not be true.

The wheel load taken in the analysis is a dual tyre load, loaded with 4500 kg. which is a standard value for highway loading. The size of the contact area and spacing of tyres is taken on the basis of actual measured area of the tyre print of a loaded highway truck. It was found that the areas of each of the two tyres of a dual tyre assembly were more or less same. The shape resembled a rectangle with rounded edges. On the basis of this the size of each tyre was taken as a rectangular strip of 25 cm x 17 cm with a gap of 16 cm in between the two tyres.

The load is positioned, at the edge loading position, with an intention that this might perhaps be the most serious location, although more loading positions can be tried. Analysis for each successive load position takes only 1/4 to 1/5 of the time for the first position. This is because, the time of reading data, stiffness generation and partly of inversion is saved. For every subsequent loading the partially inverted and stored stiffness matrix is used for solution of equilibrium equations. However, the printing time of the on-line printer is

large and perhaps can not be avoided. Thus, only one load position is considered. Further, to economise, the load is taken at the centre of the edge, so that the structure may become symmetrical and only half will require analysis.

(vii) Thermal Effect:

The thermal effect considered is that due to temperature differential set up between the top of the pavement slab and the bottom of base due to the difference in the ambient temperature of top and bottom. This temperature difference will cause unequal expansions or contractions of top and bottom fibres leading to curling. The coefficients of thermal expansion of concrete for base and overlay both are taken as 8×10^{-6} per degree centigrade. The value of this differential is taken from IRC[178] which is based on the thickness of the slab and the regions in which road is situated and is shown in Figure 5.18. It is assumed that the variation of temperature within the pavement slab is linear. This is justified, because, the thermal properties of hardened cement concrete does not change very much with the age and therefore, the base and overlay are likely to act as a single thickness.

(viii) Crack:

Out of various parameters like crack size (length), location, shape (orientation) etc., it is aimed at

studying the behaviour of the slab when there is an isolated transverse crack in a long panel. To economise on computer effort, it is assumed that this crack bisects the slab, so that advantage of symmetry may be obtained. The crack is assumed to be a full depth crack in base slab and to traverse throughout the pavement width.

(ix) Size of pavement panel:

The lateral and longitudinal dimensions of the slab exhibit influence on the stresses and deflections. It is not proposed to study this influence. Therefore, the transverse dimension of a panel is assumed as 3.5 meter. This value is taken on the basis, that normally for a dual carriageway of a highway, this value would approximate the width of the slab. The length of the slab is taken as 9 metre.

(x) Differential Shrinkage:

The contraction of two layers, i.e. the base and overlay are bound to be different due to difference in age. In fact, the shrinkage in the overlay itself may not be uniform. The water held in the calcium silicate gel structure which is known to be similar to the mineral tobermorite[179], formed on hydration of cement may dry out faster at the surface than the interior. This transient state may exist for a considerable time. This would

lead to upward warping causing compression at the
base. The analysis of such a variation is easily possi-
ble by appropriate modification of shrinkage strain $'e_s'$
in equation 5.3. However, this will be subject to relia-
ble data. In the present analysis, as formulated in
equation 5.3, the steady state condition is assumed.

The value of restrained differential shrinkage is
taken as 0.0002 as recommended by Branson[142] and adopted
by Ghosh et.al.[172,173] and Cement Concrete Association[13].

5.9 RESULTS AND DISCUSSIONS

The results of analysis for the cases described
in article 5.8 are presented in the form of figures and
tables and are discussed below. Figure 5.2 shows the
general finite element idealisation for pavement slab.
The double hatched zone indicates the load placement as
discussed in article 5.7.2.

5.9.1 Analysis of Stresses and Deflections in
Pavement Slabs With Overlay on Sound
Base, Under Wheel Load at Edge.

Figure 5.3 is drawn to compare variation of deflec-
tion along edge of pavements having 10 cm overlay on
8 cm and 16 cm base. It is seen that the deflection of
8 cm base under wheel load is higher than 16 cm base. But
the deflected basin is of greater radius on stiffer slab.
The reason for this behaviour is clear from figure 5.4
which shows the variation of slope along edge. It is seen

from this figure that slope as well as rate of change
of slope is higher for pavement slab which is less
rigid.

Variation of deflection along perpendicular direct-
ion to the edge for above two cases is plotted in
figure 5.5. Again it is seen that deflection for stiff-
er slab is lesser, under the load but is greater else-
where. This is because the slope in this direction, as
shown in figure 5.6 is greater for less stiffer slab
and is constant under loaded area which is approximately
50 cm. Thus, cantilever like deflection pattern perpend-
icular to the edge is evident from these figures which
causes tensile flexural stresses at the top of the pave-
ment slab at a certain distance resulting in cracking
under ultimate load[29,31,32].

Again, in figure 5.4, the slope first increases
and then decreases causing positive and negative curvat-
ures respectively. The effect of this on moment is reflected
in Figure 5.7, which compares the variation of moment 'M_y'
(parallel to the edge) along the edge. The three curves
relate to moments in pavements having 10 cm overlay on
8 cm, 12 cm and 16 cm base. All these curves show that
the moments are very high under the load but they decrease
at a very fast rate due to high stress gradients and soon
acquire a negative value. This justifies the considera-
tion of a single wheel load. It is also seen that moment
in a stiffer slab is greater, though the deflections,

slope and rate of change of slope were lesser as seen from figures 5.3 and 5.4. This is because higher moment is necessary to cause same curvature in a stiffer slab. Also since the deflection basin, as seen from figures 5.3 and 5.5 is larger in case of stiffer slab, the greater moment can be expected in this case from the consideration of statics.

Stress gradients are slightly higher in a less stiffer slab. Therefore, the shearing forces will be larger in their case.

Table 5.2 compares the maximum bending moments M_y for different combinations of base and overlays, as determined by finite element method to those determined by modified Westergaard's equation. The maximum moment will occur under the centre of the loaded area, in the direction parallel to the edge. Since, in the finite element analysis the sampling point is slightly off the centre of the loaded area, the maximum moment is to be determined by extrapolation in the region where gradients of stresses are high.

As stated earlier, the Westergaard's equation is applied to the base overlay system by adopting equation 5.16 for determination of the value of 'ℓ' i.e. the radius of relative stiffness of the pavement. It is seen that the two values are in close agreement and therefore, the maximum wheel load stresses can be determined very

economically by using this modified procedure.

It is also seen that for the values adopted in the study the maximum values of moments are almost equal in pavement slabs having equal overlay and base thickness combination i.e. moments for say 10 cm overlay on 8 cm base is almost equal to moment in 6 cm overlay on 12 cm. base the combined thickness of both being 18 cm. This is because there is not much difference in the radius of relative stiffness, which is proportional to the fourth root of the stiffness. The values of radius of relative stiffness is 54.19 and 54.71 respectively. However, the maximum compressive stresses at the top of the overlay differ by about 6 percent, which is because of the difference in strains, which are function of curvature and distance from neutral axis. It is also seen that as expected the value of stresses at the bottom of overlay is exactly half, of that at the top of base. This is because full strain compatibility between base and overlay holds. Thereby the strains at the bottom of overlay and top of base become equal. But the stresses in overlay are half because the modulus of elasticity of the overlay material is assumed to be half of that of the base.

5.9.2 Analysis of Stresses and Deflections Due to
        Wheel Load in Pavement Slabs having Cracked Base:

5.9.2.1 Effect of Cracking:

Comparison of variation in deflection, along

edge for 10 cm overlay on 12 cm base when the base is
sound with that when the base contains a crack is made
in Figure 5.8. A similar comparison for slopes is made
in Figure 5.9. As can be expected, the deflection in
the central part, is more when the base has a crack. The
slope also increases and as a result the deflection acquires
a smaller value for cracked slab at a small distance from
the load. The rate of change of slope is very high in the
vicinity of the crack.

Figure 5.10 compares the variation of moment along
the edge for the case of a 10 cm overlay on 12 cm base to
that when this overlay is on a base of same thickness
but containing a full depth transverse crack centrally.
It is seen that the positive moment developed at the
centre of the load is very much reduced in cracked case.
This is as a result of stress release in the base due to
cracking, which is taken to be effective for a distance
equal to the depth of the crack on either side of it, as
already discussed. This figure has striking resemblance
with Figure 3.8 where the pavement structure was idealised
in plane strain and curves were plotted for moments on
sound base with overlay to compare it with the case when
the base is cracked. Thus, this provides a 'qualitative
check'. A solution procedure based on the theory of beams
on elastic foundation is developed and described in
Appendix 'A' to VI chapter, for a rough check as truly

speaking a slab cannot be compared to a beam.

Figure 5.11 shows the variation of deflection along the direction perpendidular to the edge for a 10 cm overlay on 12 cm. base and compares it with the case when the base contains a crack. Figure 5.12 compares the slope for above two cases in the same direction. It is seen that the deflection in case of cracked base is higher under load but unlike in the direction parallel to the edge, it continues to be higher even away from the edge. This is because the slope, as shown in Figure 5.12 has same rate of change in cracked case as in uncracked case, though numerically the slope is slightly higher. The moments 'M_x' in the direction perpendicular to edge can be expected to remain unchanged in the two cases as the two curves in figure 5.12 are parallel.

5.9.2.2 Comparison of Cracked Bases

Figure 5.13 compares the moments along edge for the case when the base of 8 cm, 12 cm and 16 cm, under the 10 cm. overlay is having a crack. It can be seen from this figure that the base thickness has a beneficial effect as the maximum moment developed in the overlay at the crack is lesser for the base of larger thickness. Same observation is valid for the case of 6 cm overlay on 8 cm. 12 cm and 16 cm base having a crack. The variation

of moment 'M_y' along the edge for this condition is plotted in figure 5.14.

A comparison of figure 5.13 and 5.14 indicates that the maximum moment at crack is greater in 10 cm overlay as compared to 6 cm overlay for any particular base thickness. However, variation of flexural stress at the top fibre of the overlays is plotted in figure 5.15. This variation is along the pavement edge. In both the cases the base is 16 cm thick having a crack. It is seen that though as shown in figure 5.13 and 5.14 the moment is higher in 10 cm overlay, the flexural stress is higher in 6 cm overlay, when the base is same in the two cases.

Figure 5.16 compares the top fibre bending stresses in 10 cm overlay on 8 cm, 12 cm and 16 cm base. On comparing the numerical values from figure 5.15 and 5.16, it is observed that a 4 cm increase in overlay thickness has a more beneficial effect than the same increase in base thickness, though the rigidity of the overlay is half that of base. This shows that the damaged base and sound overlay can not be compared on the same basis.

Moreover, comparison of stresses as shown in figure 5.16 needs further discussion. The stress in 10 cm overlay on 8 cm base is higher than the stress in 10 cm overlay when the base is 12 cm and on the basis of normal stress yield criterion (Appendix 5.A) the latter system is safer. But it may not necessarily be so according to

the concepts of fracture mechanics. A 12 cm cracked base has c/d ratio of 12/22 = 0.545 while that of a 8 cm base will be (8/18) = 0.444. A higher c/d i.e. crack depth to total depth ratio means a higher stress concentration.

As per Kaplan[180] the average value of critical strain energy release rate 'G_c' has been found as 0.024 kg.cm/cm^2 for three different kinds of cement concrete mixes.

Adopting this average value as a guide, the determination of critical overlay stress 'σ_c^o' in a 10 cm overlay on 8 cm cracked base, will be as follows:

The stress concentration factor f(c/d) for a ratio of c/d = 0.44 is found as 0.48 approximately[181].

Therefore, according to equation 5.47 (Appendix 5.A).

$$G_c = \pi \sigma_c^{o^2} \frac{h}{E} f(c/d)$$

On substituting E = 15x10^4 kg/cm^2
and   h = 10 cm.

$$\sigma_c^o = 27 \text{ kg/cm}^2$$

Moment 'M_c' corresponding to this critical stress is 450 kg.cm/cm. $M = f z = \frac{27 \times 10^2}{6} = 450$

Salam and Monismith[182] have adopted the following equation due to Bueckner[183]

$$K_\tau = \frac{6M}{(d-c)^{3/2}} g(\frac{c}{d})$$

where K_{-} = stress intensity factor in opening mode,

and $g(c/d)$ = function dependent on c/d as reproduced in figure 5.23.

c/d	0.05	0.1	0.2	0.3	0.4	0.5	0.6
$g(\frac{c}{d})$	0.36	0.49	0.6	0.65	0.69	0.72	0.73

Therefore if, M is taken as M_c i.e. the critical moment, then the corresponding value of critical stress intensity factor will be K_{-c} which is defined as 'fracture toughness'. Fracture toughness is a material property, related to G_c by

$$K_c = \sqrt{\frac{G_c}{E}}$$

If suffix '1' relates to 10 cm overlay on 8 cm cracked base and '2' refers to 10 cm overlay on 12 cm cracked base, then

$$\frac{6 \, M_{c2}}{(d_2-c_2)^{3/2}} \, g(\frac{c_2}{d_2}) = \frac{6M_{c1}}{(d_1-c_1)^{3/2}} \, g(\frac{c_1}{d_1})$$

But $d_1-c_1 = d_2-c_2 = 10$ cm. and from figure 5.23,

$$g(c_1/d_1) = 0.7$$
and $$g(c_2/d_2) = 0.725$$
$$M_{c_1} = 450 \text{ kg. cm./cm.}$$

Accordingly, M_{c_2} = 437.5 kg.cm/cm.

Similarly, M_{c_3}, relating to 10 cm.overlay on 16 cm base = 431.5 kg.cm./cm.

Thus it is seen that as the thickness of the cracked base increases, the critical moment decreases. This is because, the moment release in a thicker cracked base will be higher, i.e. numerically the value of $\beta.a$ in figure ? (Appendix 5.A) will be larger. The result of this will be that there will be a higher stress concentration at the root of crack causing greater distress in the material at that point.

However, it can be seen from structural analysis that a larger thickness of cracked base will give higher support and therefore, will undergo lesser deformation. The result of this will be lesser stress in overlay. Therefore, the larger thickness will be an advantage, but perhaps not as much as expected by normal yield criterion (Appendix 5A). This is clear from figure 5.24.

It may be argued that base and overlay have different modulus of elasticity. However, the value of 'G_c' may not be effected very much due to this. But the effect of higher modulus of elasticity of cracked base on stress intensity factor may be worse than expected. The standard value of stress intensity factor for such an anisotropic structure is not known. However, use of finite element method can be made[184,185,186] to determine this accurately.

However, the above discussions based on qualitative

analysis is useful to show that it is very important to reduce stress concentration. This is possible through provision of 'Reinforced Key' at the crack as shown in figure 3.14 and 3.15.

Figure 5.17 shows the variation of flexural stresses at the top of overlay. This variation is along the edge for a 10 cm overlay.on 12 cm base for the cracked and uncracked base. It is seen that the stresses in the overlay at the crack location are almost doubled in case when base is cracked. However, elsewhere the overlay on cracked base is having lesser stresses. This is because the cracking makes the pavement more flexible and as a result the moments are reduced. Similar result was observed in analysis of pavement slab in Chapter III.

5.9.3 Analysis of Pavement Slab Subjected to Temperature Variation:

Figure 5.18 shows the variation of temperature differential for different thickness of concrete pavement slabs. This is based on 'General Report on Road Research in India"[178]. As Roorkee is situated in Northern region, the curve pertaining to this region is adopted for data.

Table 5.3 shows the maximum temperature differential for different pavement thickness and also the maximum moments and stresses due to it. It is seen that the temperature differential and moment increases with pavement

thickness, however, there is not much difference in stresses. This indicates that there is practically no beneficial effect of overlay on temperature stresses.

Figure 5.19 compares the deflection of 10 cm overlay on 8 cm base for cracked and uncracked conditions under a temperature differential of 13°C between top of overlay and bottom of base. It is seen that the deflections in these two cases significantly differ only in the central part, i.e. in the vicinity of the crack. Elsewhere, they are practically the same. This indicates that the effect of crack, assumed in the transverse direction along the centre line of the pavement, is only local.

Figure 5.20 shows the contours of the deflected profile for the uncracked case of 10 cm overlay on 8 cm base. From the diagram it can be seen that the corners and the edges tend to warp up, while the central part maintains contact with the subgrade. The figure also shows that the slope is gradual along longitudinal centre line while along transverse centre line it is steep. This is because the values of M_x and M_y generated due to temperature differential are equal but the transverse dimension of slab is lesser than the longitudinal dimension.

Figure 5.21 shows variation of stress parallel to edge due to wheel load and temperature differential for 10 cm overlay on 8 cm base. It can be seen that the

thermal stresses remain practically constant in the
central part of the edge (at the end of the edges the
stresses are bound to be zero to satisfy the static equil-
ibrium) and their magnitude is practically half of the
maximum wheel load stress at the centre of the edge.

Figure 5.22 compares the bending moments developed
due to temperature gradient along the longitudinal centre
line of the pavement slab having 10 cm overlay on 8 cm
base to that when the base has a central transverse crack.
The curve for moment in case of sound pavement slab is
exactly similar to that obtained by Wiseman, Harr and
Leonards[189]. From this figure it may be seen that the
moments are unaffected by crack at all places except over
the crack itself where it drops down. This is due to the
reason that the applied loads due to temperature gradients
which are in the form of moments applied at the edges
do not cause an appreciable increase in curvature of the
slab due to the crack which is in the central part of the
slab, i.e. away from the transverse edge '   . Thus,
the moment due to this curvature is reduced at the crack
due to reduction in stiffness at that location. However,
to satisfy statics, this would result in increase in shear-
ing forces.

5.9.4 Shrinkage Effects

Table 5.4 compares the stresses developed due to
differential shrinkage in sound base-overlay systems at

the top and bottom of base and overlay, by the Birkelands approach and by finite element analysis. It can be noticed that the results generally agree for the values at top of base and bottom of overlay. However, they differ significantly for top of overlay and bottom of base. It is also seen that the values are generally higher.

While formulating the analysis earlier in this chapter, it was seen that the shrinkage effects were considered in two parts viz. one due to direct forces and other due to moments developed because of the eccentricity of the centre of shrinkage force. The subgrade has no part to play in case of direct forces. Therefore, the magnitudes of these forces are almost same in Birkeland's approach and **in finite** element analysis, except that in the later analysis effect of Poisson's ratio is taken into consideration while the earlier is for beams and therefore neglects it.

However, the subgrade restraint has to play an important role in cases of moments. Therefore flexural stresses differ in two case i.e. one in which subgrade restraint is taken into account and in another where subgrade is supposed to be absent, and the stresses will naturally be higher when the restraint is considered.

The reason of agreement in stresses at the interface is that the interface is close to neutral axis and therefore at that location, only the axial stresses

predominate.

It can also be seen from table 5.5 that though the contribution from shrinkage in interfacial stresses is largest still the values are within the permissible limits.

Flexural, direct tensile and interfacial stresses in overlay are tabulated in table 5.6 in case of cracked base. It is seen that the tensile stresses are very heavy in the case of thin overlays on thin bases, but they tend to come down in the permissible range as the base or overlay thickness increases. The reason for this is that the stresses due to moment component reduces on account of cracking (it can be observed to be reverse of that in uncracked condition. Also the effect due to moment component is similar to moments due to wheel loads). However, the axial stress component increases with base thickness due to greater restraint. Not much change of axial stress component can be expected in cracked and uncracked conditions, because this component induces tension in overlay and compression in base. However, if a gap is generated at the crack then the values obtained can be regarded as conservative.

It can therefore be said that there could be two possible alternatives to reduce these stresses. One is to provide unbonded overlay at the cost of increased

overlay thickness or to develop moment resisting capacity in cracked base. The latter appears to be a better alternative.

5.9.5 General Discussions

It can be observed from the table 5.6 that an increase in base thickness reduces the overlay stress. However, the same increase in overlay thickness reduces the stress even more.

It was seen in para 5.9.1 that the pavements of equal total thickness give almost same moments for un-cracked base. But this is not true when the base contains a crack. This is obviously because of the difference in the size of crack.

These stresses can be defined as nominal stress values, as they are calculated from bending theory[190]. However, the stress in the bottom of the overlay may be quite different at the crack location. This is due to the fact that stress concentrations are bound to occur at that point, due to the presence of crack. The amount of stress concentration will depend upon the depth of crack, being more for deeper crack[191]. Not only this, the stress concentration also depends on the proximity of another crack. Another crack in its neighbourhood reduces the stress concentration, by making the stress path more stream lined[190]. Neuber[191] has found that

for beams, with deep notch the value of stress (maximum stress) at the crack tip, may be as much as 3 to 4 times the nominal stress values. Thus yield and plastic flow is likely to occur in a small zone ahead of crack tip. It is possible that during the course of repeated load application the zone of plastic flow may extend leading to propagation of crack. It has been found that bolts with single groove had lesser life in fatigue than those of same size with many threads[192]. This shows the effect of stress concentration on fatigue life.

Many alternatives to reduce stress concentrations in highway pavement with a view to avoid reflection cracking, could therefore be:

(i) providing multiple cracks by breaking up the pavement slab is many times suggested[21,22]. It is however, seen that the presence of a crack in the base, increases the overlay stress considerably. Thus, breaking up of the base would mean:

(a) further increase in overlay stress due to reduced rigidity of base and therefore a thicker overlay would be required. However, it is a point to be seen for any particular base-overlay combination whether reduction in stress concentration factor[190] has an overriding influence on this increase in nominal stress value, caused by loss of base rigidity.

(b) cost incurred in pavement breaking.

(ii) provide unbonded overlay: Providing unbonded
overlay would mean expenses to be incurred
on:

     (a) increased overlay thickness as the
        advantage of moment resisting couple
        due to bonding (Chapter III) is
        not being taken, and

     (b) providing separation course or other
        methods to prevent any bond from
        occuring due to friction.

(iii) provide thicker overlay so as to have lesser
stress concentration which would mean greater
cost,

(iv) provide reinforcement in overlay, which would
mean increased cost and infact this would
act more like a crack arrest mechanism
rather than a mechanism to reduce stress.

(iv) adopt reinforced key technique as described
in Chapter III which would effectively reduce
stress concentration.

It is also seen from table 5.6 that stress due to
temperature differential decreases with the increasing
thickness of base for any overlay thickness. However,
reverse is the effect on shearing stresses at the inter-
face. This is due to the fact that on a thicker cracked
base the rate of decrease of moment is higher, due to
greater amount of stress release. The moment in the
uncracked part is also higher. Therefore, this results

in greater shearing forces. When shearing stresses
are computed from these shearing forces, they also
work out to be higher (though higher shearing force
may not necessarily mean higher shearing stresses at
the interface). The shearing stresses are of signi-
ficant magnitude, specially those due to thermal
differential and differential shrinkage. The magni-
tude of total shearing stresses are enough to threaten
bond failure. Interfacial shearing stresses due to
wheel loads are of nominal magnitude and by them-
selves insignificant. Failure of bond would mean
further loss of rigidity of base overlay system in
the vicinity of the crack. This further loss of
stiffness would result in further increase in deflect-
ions, slopes and curvatures as seen in chapter III.
Thus, it is possible that a well designed overlay, in
which full reliance is placed on effective bonding,
might crack at the location of the old crack due to
overstressing. This explains the phenomenon observed,
in which bond failure is found to exist at the location
of reflected cracks or joints in the overlay[103,105].

It can be pointed out that 'Reinforced Key
Technique' not only acts as a measure against stress
concentration it is an effective method of ensuring
bond at the location of a crack.

Superimposing deflections due to gravity load
at 2.35 kg/cm^3 on those of fig.5.20, it can be seen
that curling[134] does occur.

5.10 CONCLUSIONS

Following conclusions can be drawn out of the limited numerical experimentation reported in this Chapter:

1. The formulation as proposed in this chapter forms a suitable and efficient system for realistically assessing the statical influence parameters like, moments, shear, deflections etc. at any point in the system under following conditions:

   (a) The wheel load may be represented by a rectangular tyre print. Any number of such wheel loads may be placed at any location in the pavement. Dual tyre load can be realistically represented.

   (b) The base may contain a bonded overlay.

   (c) The base may have elastic properties signi-ficantly different as compared to overlay. This makes the solution procedure applicable to semirigid pavements with overlays, the rational analysis of which was not possible hitherto.

   (d) The base or overlay may contain any number of cracks of any size or shape and at any location.

   (e) Due regard can be paid to temperature stresses in above system.

(f) Differential shrinkage, that is likely
to take place due to age difference
of base and overlay will give rise to
stresses, which can be evaluated by
finite element method and also by a
modification of Bradbury's solution
as given in Appendix '5.C'

2. By adopting the proposed approach for deter-
mination of equivalent stiffness of sound base
overlay system, it is possible to determine the
maximum wheel load stresses by use of Wester-
gaard's equation which is applicable for single
layer. This is given in Appendix '5.B'.

3. Similarly, by using the same stiffness, it is
possible to use Bradbury's solution for stresss
due to temperature differential.

4. It is observed that on cracking the deflections
and slopes increase in the direction of the
crack as well as in the orthogonal direction,
under the action of wheel load. However, the rate
of change of slope does not increase appreciably
in the direction of crack while in the direction
orthogonal to the crack there is a significant
increase.

5. Increase in base thickness, which is cracked,
as well as increase in overlay thickness, tend

to decrease the stress in overlay at the crack location. However, the increase in overlay thickness has much more significance than an equal increase in base thicknesses, though the rigidity of the overlay material is assumed as half that of base material.

6. The cracking gives rise to high interfacial shearing stress due to temperature differential which is further increased due to differential shrinkage. So much so that the bond is likely to break under repeated load cycling.

7. It is seen by stress analysis that reflection cracking is very much likely to occur in bonded overlays.

8. From the considerations of points 6 and 7 above, the usefulness of 'Reinforced Key Techniques' as proposed in Chapter III is emphasised.

9. Interfacial bond stresses occuring in an overlay laid on a sound base is of very nominal order both due to wheel load as well as temperature gradients. As such a bonded overlay on a sound base is very much feasible and advisable beyond any point of controversy.

10. Curling[134] under temperature and self load is seen to occur.

APPENDIX 5.A

Failure of any material is conventionally supposed to be governed by one of the many strength theories like Von Mises, Tresca, Mohr-Coulomb. These failure criteria are based on triaxiality of stresses and failure is supposed to take place by a slip mechanism along a plane on which the stress combinations are such that they satisfy the yield conditions.

The simplest among these is the normal or square yield criterion, according to which, the failure occurs in a multi-axial system when either the principal tensile or compressive stress reaches the uniaxial tensile or compressive strength. For brittle material; as also for concrete, the ultimate tensile strength σ_{ut} is considerably smaller than the ultimate compressive strength σ_{uc}. In the Figure 5.25, which represents biaxial conditions, with σ_1 and σ_2 principal stresses and $\sigma_3 = 0$, the normal stress criterion is represented by square CFHJ.

The strength of a bar under uniaxial tension is OB as shown in the figure. However, it can be noticed that the presence of any orthogonal tensile or compressive principal stress does not alter this strength.

Mohr's yield criterion for biaxial stress field

is also illustrated in figure 5.25 superimposed on the square yield criterion. It is based on the principle that the failure occurs when the shear stress reaches some critical value τ_f on a plane such that this stress is a function of the normal stress σ_n on that plane. Usually this function is expressed as:

$$\tau_f = C + \sigma_n \tan\phi \qquad \ldots (5.40)$$

where,

C and ϕ are constants for the material.

Investigations carried out by Kupfer et al.[193] and Liu and others[194] indicate that biaxial stress field does effect failure of concrete. Based on their investigations the authors have suggested the failure criterion of concrete which is somewhat similar to Mohr's failure criterion. Applicability of Mohr-Coulomb theory to concrete is often verified[195,196].

Apart from these failure theories, Griffth[197] postulated another theory, according to which, every material contains flaws or voids and these flaws act as stress raisers or pockets of stress concentrations. In cement concrete microcracks develop during setting and hardening or during subsequent loading[198]. These cracks may form due to shear or tensile stresses and may exist at mortar-aggregate interface or in the mortar itself[199]. Griffth suggested that the strain energy of the system decreases as the crack length increases, under any applied

stress. This happens because energy is used up in creating new surfaces formed during fracture.

If γ = surface energy per unit area,

   U = strain energy released per unit thickness (in plane stress given by 1/2 x stress x strain x area)

   $= -\frac{1}{2} \sigma \frac{\sigma}{E} \beta a^2$ as shown in figure 5.26(a),

   β = a constant for zone in which the stress 'σ' is supposed to be released, and

   E = Modulus of Elasticity,

Therefore, for an increase in crack length 'da',

$$\frac{dU}{da} = -\frac{\sigma^2}{E} \beta\ a$$

According to Griffth's accurate analysis,

$$U = -\frac{1}{2} \frac{\sigma^2 \pi\ a^2}{E}$$

While, $\quad \frac{dU}{da} = -\frac{\sigma^2 \pi\ a}{E}$, in plane stress $\qquad \ldots (5.41)$

The total energy 'W' in plane stress is given by

$$W = -\frac{1}{2} \frac{\sigma^2 \pi a^2}{E} + 2\gamma a \qquad \ldots (5.42)$$

This is shown in Figure 5.26(b). As the crack extends, its surface energy increases because new surface is formed. But this is at the cost of reduced strain energy.

The maximum in total energy curve is given by

$$\frac{dW}{da} = 0$$

$$\gamma = \frac{\sigma^2 \pi a}{2E} \qquad\qquad \text{.. (5.43)}$$

Thus in figure 5.26(b) the line of strain energy release rate and surface energy line intersect at a point where a_c is the crack length. This crack length is the critical length of the crack i.e. such a value at which the crack will grow under applied stress system.

Thus,

$$\text{fracture strength } \sigma_F = \sqrt{\frac{2E\gamma}{\pi a}} \qquad \text{... (5.44)}$$

In other words if the strain energy release rate exceeds a critical value then growth of crack will take place.

No consideration has yet been given to stress concentration at the crack tip. Due to the fact, that the crack acts as stress raiser, the stress at the crack tip will be higher than at other points in an otherwise uniform stress field 'σ' and it is usual to express this as:

$$\sigma = \frac{K}{\sqrt{2\pi r}} \qquad \text{for } r \ll a \text{[200]} \qquad \text{... (5.45)}$$

where, r = distance of point from crack tip

K = stress intensity factor, and

σ = nominal stress e.g. value given by the equation

$$\sigma = \frac{6M}{bh^2} \qquad\qquad \text{... (5.46)}$$

in a beam in bending.

However, the stress level at the crack tip will be a function of the (a/d) ratio,

where,   d = depth of beam

or in other words it may be possible to write:

Strain energy release rate = G

Winne and Wundt[181] derived expression for f(a/d). This has been used by Kaplan[180] and Salam and Monismith.[182]

It has been found that the critical strain energy release rate 'G_c' is a fundamental property of a brittle material and is constant like modulus of elasticity[201].

Kaplan[180] has evaluated G_c for three different mixes of cement concrete and has found that the values are fairly constant. Blight[202] has given some methods which can be used for determination of G_c.

Determination of stress intensity factor is a complex problem even for the simplest geometries[201]. Finite element method is extensively being applied for its evaluation for cases where standard solution do not exist[184,185,186,203,204]. Beuckner[183] has used boundary collocation method to determine the stress intensity factor in case of cracked beams in bending and this method has also been adopted by Ramsamooj[205]. The

standard values of stress intensity factors derived are for the simply supported, isotropic, homogeneous beams containing a crack. These could only very approximately be applied for the qualitative purposes to the analysis of anisotropic plates as presently under study.

Failure of concrete is often studied as a fracture mechanism. Glucklich[206] concludes that law of fracture mechanics are applicable to concrete though according to him the energy released is higher than energy of surfaces created because prior to cracking, there are many microcracks which absorb released energy. Also, the reason for low strength of concrete is due to the fact that rate of energy release increases with crack length in tension whereas it is constant in compression.

Naus and Lott[207] have studied the parameters that influence the value of fracture toughness 'K_c' of concrete and state that bigger size aggregate act as crack arresters. Applicability of the laws of fracture mechanics to concrete are also investigated by many other workers[90,204, 208-210].

Although the applicability of the laws of fracture mechanics is being justified[211,212], it is felt that data is not enough to put it on an accurate quantitative footing[187,188,213].

APPENDIX 5.B

SIMPLIFIED PROCEDURE FOR MAXIMUM WHEEL LOAD
STRESS DETERMINATION

It is seen that the maximum stresses obtained by finite element analysis can be compared with Westergaard's closed form solution by adopting a very simple modification.

For any section modulus $= \frac{h_c^2}{6}$ of a pavement slab having a base and overlay,

$$M_j = \sigma_j \frac{h_c^2}{6}$$

where σ_j = maximum stress for any load position 'j' like interior, edge, or corner as given by Westergaard's equation[162],

e.g. for interior, (with all the assumptions of Westergaard taken valid)

$$M_i = \frac{0.316P}{6}\left[4\log_{10}\frac{\ell}{b} + 1.069\right] \qquad \ldots \ (5.48)$$

where,

P = load,

b = equivalent radius of resisting section,

$= \sqrt{1.6a^2 + h^2} - 0.675$ for $\frac{a}{h} < 1.724$

Otherwise, b = a,

where, a = radius of contact, and

ℓ = radius of relative stiffness $= \sqrt[4]{\frac{D}{K}}$

Since, 'D' the rigidity, can be determined for base slab
with bonded overlay as described in preceding articles
of this chapter, it is possible to calculate moment.

The curvature can now be determined from equations
5.9 and 5.10 and therefore it is possible to determine
strain by equation 5.1 and stress from relation 5.2.

Note: 1. The modified procedure for determination of the
value of radius of relative stiffness is general
and same procedure can be adopted for determina-
tion of the value of 'ℓ_b' for use in Pickett's
equation and charts[214] for both Winkler as well
as elastic solid models.

2. The same value of 'ℓ' can be used to determine
deflections as well   by usual formulae.

3. A flow diagram is included here.

4. Table 5.7 compares the deflections as computed
by finite element method to those given by
Westergaard's solution

FLOW CHART
FOR

Program for Calculation of Moments and Stresses in bonded and unbonded base-overlay systems with different elastic constants based on Modified Westergaard's approach.

Description

N BOND = Bond condition

= 0 for no bond or single slab

= non-zero for bonded overlay

HO = Overlay thickness,

HB = Base thickness,

EO, AMUO = Modulus of Elasticity Poisson's ratio over Overlay

EB, AMUB = Modulus of Elasticity Poisson's ratio overlay Base

AK = Modulus of subgrade reaction,

P = Load,

A = Radius of contact of tyre print

OUT-PUT:

Punches out moments below load and stresses due to it at

(i) top of overlay
(ii) bottom of overlay
(iii) top of base
(iv) bottom of base

```
                        ( START )
              ┌──────────────────────────┐
              │ READ, NBOND, HO, HB,     │
              │ EO, EB, AMUO, AMB,       │
              │ AK, P, A                 │
              └──────────────────────────┘
                          │
                          ▼
                      ◇ IF                NO
                        BOND- ──────────────────────┐
                        ED                           │
                          │                          ▼
                    YES   │                ┌──────────────────┐
                          ▼                │  CALCULATE D     │
              ┌──────────────────┐         └──────────────────┘
              │ CALCULATE        │                  │
              │ NEUTRAL          │                  │
              │ AXIS             │                  │
              └──────────────────┘                  │
              ┌──────────────────┐                  │
              │ CALCULATE        │                  │
              │ 'D'=Rigidity     │                  │
              └──────────────────┘                  │
                          │◀─────────────────────────┘
                          ▼
              ┌──────────────────┐
              │ CALCULATE        │
              │ 'ℓ'=radius       │
              │ of relative      │
              │ stiffness        │
              └──────────────────┘
                          │
                          ▼
              ┌──────────────────┐
              │ CALCULATE        │
              │ MOMENTS AT       │
              │ EDGE, INTER-     │
              │ IOR AND          │
              │ CORNER           │
              └──────────────────┘
                          │
                          ▼
                      ◇ IF                NO
                        BOND- ──────────────────────┐
                        ED                           │
                          │                          ▼
                    YES   │                ┌──────────────────┐
                          ▼                │ CALCULATE        │
              ┌──────────────────┐         │ STRESSES         │
              │ CALCULATE        │         └──────────────────┘
              │ STRESSES         │         ┌──────────────────┐
              └──────────────────┘         │ PUNCH TITLE      │
              ┌──────────────────┐         └──────────────────┘
              │ PUNCH TITLE      │                  │
              └──────────────────┘◀─────────────────┘
                          │
                          ▼
              ┌──────────────────┐
              │ PUNCH RADIUS OF  │
              │ RELATIVE STIFF-  │
              │ NESS, MOMENTS AND│
              │ STRESSES         │
              └──────────────────┘
                          │
                          ▼
                       ( STOP )
```
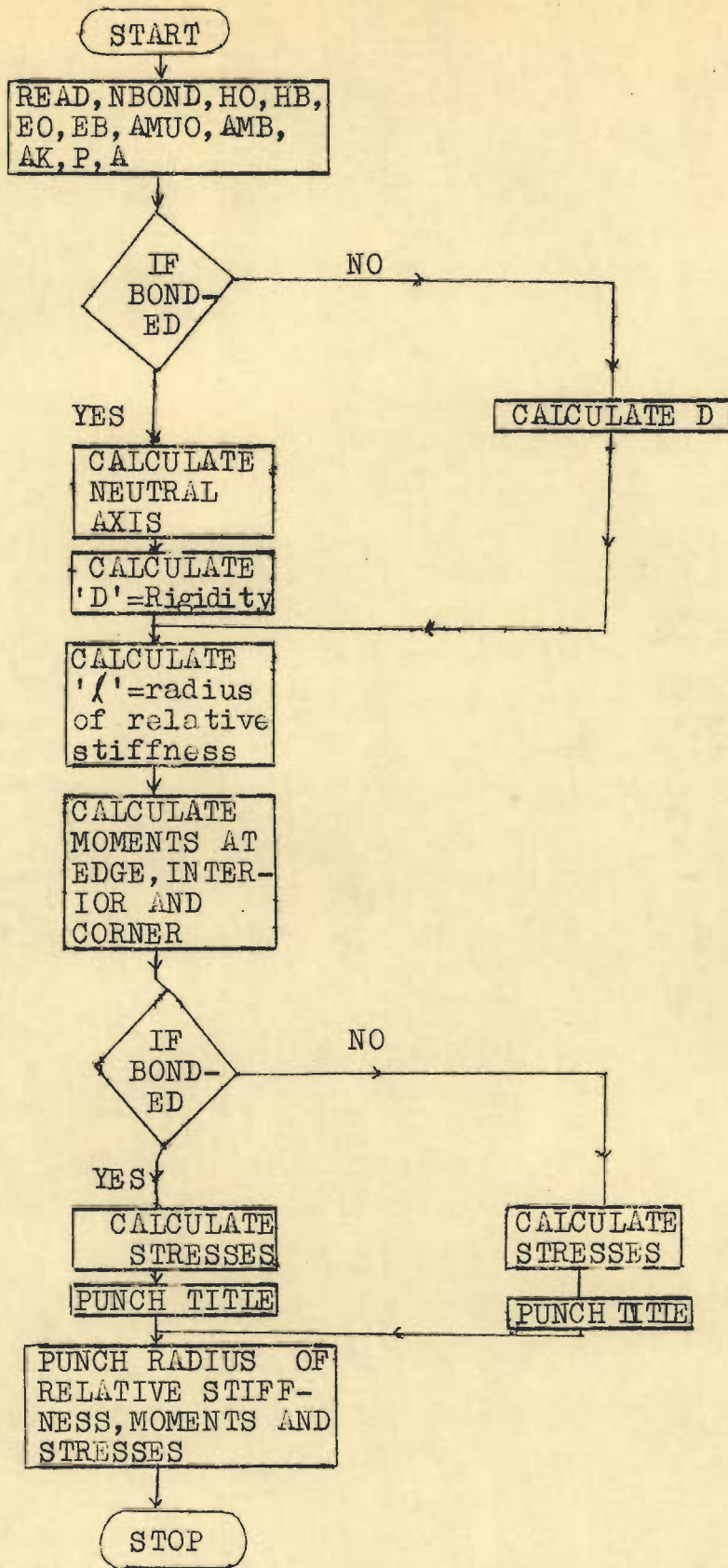
APPENDIX 5.C

SIMPLIFIED PROCEDURE FOR MAXIMUM TEMPERATURE STRESS EVALUATION

A procedure similar to that described in Appendix 5.B can be adopted to evaluate temperature.

The value of radius of relative stiffness can be evaluated and the values of warping stress coefficients C_1 and C_2 [136] determined from the graph.

Bradbury's equation can be written as[162]:

$$\sigma = C . \frac{E \alpha \Delta T}{2} \qquad \dots (5.49$$

where,

$C = C_1$ for edge, and

$C = \left(\dfrac{C_1 + \nu \, C_2}{1 - \nu^2} \right)$, for interior

The value of C can be evaluated if it is assumed that

$$\nu = \nu^o = \nu^b$$

It is possible to write for moment

$$M = C . \frac{\alpha . \Delta T}{h^o + h^b} . D \qquad \dots (5.50)$$

because, it can be recognised that $\dfrac{\alpha . \Delta T}{h^o + h^b}$ is the curvature due to temperature differential 'ΔT'[114] in slab of thickness $(h^o + h^b)$, based on assumptions stated in article. Thereafter, procedure for determination of stresses can

be identical as stated in Appendix 5.B.

APPROACH FOR SHRINKAGE STRESSES

As described in text the shrinkage stresses can
be regarded in two parts. The effect of moment part can
be evaluated by finding the appropriate ratio as described
in equation 5.33 and the stresses can be evaluated by
superimposing the axial stresses given by equations
5.36 and 5.38.

TEMPERATURE STRESSES IN CRACKED SLAB WITH OVERLAY

Table 5.8 compares the moments as calculated by
modified Bradbury's approach for the case when the base
contains a crack as adopted in the present study. Since
the crack adopted in the present study was one which is
away from the edge, it was seen during the course of
analysis that the maximum principal curvature due to
'initial strain' remained constant even after cracking.
Thus, the procedure that could be adopted is:

(i) determine maximum moments for uncracked slab due to
     temperature gradients,

(ii) determine curvature from relation

$$\chi = \frac{M}{D}$$

(iii) determine moment in overlay at the cracked part
from

$$M = \frac{D_c}{\lambda}$$

where,

$$D_c = \frac{E^o h_o^3}{12(1-\nu^2)}$$

<u>Note</u>: Same procedure can be applied for shrinkage stress
determination at crack.

TABLE-5.1

COMPARISON OF MAXIMUM MOMENTS FOR LAYERED
PAVEMENT SLABS

S. No.	Loading	Thickness(cm)		Modulus of Elasticity(kg/cm³)		FEM	Modified Westergaard/ Bradbury	% Difference
		Base	Overlay	Base	Overlay			
Case I (a)	Interior	8	10	30×10^4	30×10^4	893.0	881.522	1.285
(b)	Edge	8	10	30×10^4	30×10^4	1306.0	1293.983	0.92
(c)	Temperature	8	10	30×10^4	30×10^4	789.4	799.000	1.20
Case II (a)	Interior	8	10	30×10^4	15×10^4	873.0	866.028	0.80
(b)	Edge	8	10	30×10^4	15×10^4	1280.0	1263.185	1.31
(c)	Temperature	8	10	30×10^4	15×10^4	780.2	790.000	1.26

TABLE-5.2

COMPARISON OF MAXIMUM MOMENTS DUE TO WHEEL LOADS ON EDGE

S.No.	Thickness (cm)		Mod.of Elasticity (kg/cm^2)		Moments (kg.cm/cm)		Stresses[++] (kg/cm^2)			
	Overlay	Base	E^o	E^b	FEM[+]	Modified Wester-gaard	Overlay		Base	
							Top	Bottom	Top	Bottom
1.		8	15x10^4	30x10^4	1280	1263.18	19.30	0.98	1.97	-27.33
2.	10	12	15x10^4	30x10^4	1340	1353.20	13.64	2.90	5.90	-19.74
3.		16	15x10^4	30x10^4	1480	1414.80	9.90	3.30	6.50	-14.80
4.		8	15x10^4	30x10^4	1105	1129.70	27.90	7.2	14.40	-40.70
5.	6	12	15x10^4	30x10^4	1253	1270.40	18.10	7.4	14.90	-27.60
6.		16	15x10^4	30x10^4	1397	1365.40	12.40	6.3	12.65	-19.66

+   Values extrapolated from nearest Gauss point to centre of loading,

++ Stresses are computed by Modified Westergaard's solution

-ve Sign indicates tension.

TABLE 5.3

MOMENTS AND STRESSES AT THE CENTRE IN PAVEMENTS WITH BONDED OVERLAY DUE TO
TEMPERATURE DIFFERENTIAL

(Finite Element Results, $\alpha = 8\times10^{-6}/°C$)

S. No.	Thickness (cm) Base	Thickness (cm) Overlay	Temperature Differential	Maximum Moment (kg/cm/cm)	Stress Overlay Top	Stress Overlay Bottom	Stress Base Top	Stress Base Bottom+
1.	8	10	13.0°C	780	11.07	0.58	1.16	-17.05
2.	12	10	13.8°C	1048	11.02	2.38	4.76	-15.80
3.	16	10	14.5°C	1573	11.44	3.76	7.52	-16.88

TABLE 5.4

COMPARISON OF SHRINKAGE STRESSES BY FEM
AND BIRKELAND'S APPROACH

| Case | Net Stress by Birkeland's Approach | | | | Total stress by FEM | | | |
| | Overlay | | Base | | Overlay | | Base | |
	Top	Bottom	Top	Bottom	Top	Bottom	Top	Bottom
10 on 8	7.6	-17.00	25.68	-13.65	14.19	-16.75	26.4	-27.3
10 on 12	3.9	-15.82	28.08	-17.29	7.82	-14.90	30.6	-23.3
10 on 16	-1.29	-15.60	28.45	-17.82	4.39	-13.80	32.2	-25.9

TABLE -5.5

INTERFACIAL SHEARING STRESSES AT EDGE IN BONDED OVERLAY AND UNCRACKED BASE DUE TO WHEEL LOADS, TEMPERATURE DIFFERENTIAL AND DIFFERENTIAL SHRINKAGE

S. No.	Thickness (cm)		Interfacial shearing stresses (kg/cm^2)		Differential Shrinkage	Total Stress (kg/cm^2)
	Base	Overlay	Wheel Load	Temperature Differential		
1.	8	10	1.89	0.48	1.440	3.810
2.	12	10	1.43	0.41	1.080	2.920
3.	16	10	0.98	0.33	0.786	2.096
4.	8	6	1.30	0.52	6.500	8.320
5.	12	6	1.06	0.46	4.100	5.620
6.	16	6	0.58	0.43	3.03	4.040

TABLE-5.6

STRESSES IN BOTTOM OF OVERLAY ON CRACKED BASE AT THE CENTRE OF THE EDGE

S. No.	Overlay Thick- ness (cm)	Thick- ness of cracked Base (cm)	Flexural stresses(kg/cm^2)			Axial Stress due to shrinkage	Shearing stresses(kg/cm^2)		
			Wheel Load	Tempera- ture	Shrinkage		Wheel Load	Temperature	Shrinkage
1	6	8	41.7	7.10	81.33	6.0	0.63	4.80	54.90
2	6	12	37.5	5.60	49.90	7.5	1.32	5.30	47.20
3	6	16	33.3	4.50	31.60	8.6	1.67	7.00	47.50
4	10	8	31.2	6.03	78.00	18.4	1.38	6.80	20.05
5	10	12	27.6	4.60	12.10	21.1	1.79	9.85	25.92
6	10	16	24.0	3.20	7.62	22.8	2.15	10.10	24.05

TABLE 5.7

COMPARISON OF DEFLECTIONS OBTAINED BY FEM WITH CLOSED FORM SOLUTION

Case	l (cm)	Position of Loading	Type of Loading (radius of contact) (cm)	Load (kg)	Deflection		% Difference
					Closed Form Solution (cm)	Finite Element Solution (cm)	
25 cm slab	76.20	Interior	Distributed radius = 30 cm	1818	0.00025	0.00024	5.74
25 cm slab	76.20	Interior	Distributed radius = 60 cm	7272	0.00093	0.00091	1.80
10 cm overlay on 8 cm base (unbonded)	38.41	Edge	Point Load	4500	0.10990	0.10660	3.10
10 cm overlay on 16 cm base (unbonded)	55.97	Edge	Distributed 25x50 cm	4500	0.05180	0.03498	48.00
10 on 8(bonded)	54.19	Edge	Distributed 25x50 cm.	4500	0.05530	0.03754	47.00
10 on 16	71.75	Edge	Distributed 25x50 cm.	4500	0.03150	0.0249	26.50

Note: 1. $K = 12.0$ kg/cm^3 in all cases

2. For interior load $= w_i = \dfrac{P \cdot l^2}{8D}\left[1-\left(\dfrac{a}{l}\right)^2\left(0.217-0.367\log\dfrac{a}{l}\right)\right]$

3. For edge load $= w_e = \dfrac{1}{\sqrt{6}}(1+0.4\nu)\cdot\dfrac{P}{Kl^2}$

4. Large Difference obtained in 'edge case' is because the closed form solution does not take load distribution into account.

TABLE -5.8

COMPARISON OF STRESSES AT THE BOTTOM OF OVERLAY
OVER CRACK (FEM SOLUTION VS MODIFIED BRADBURY)
(APPENDIX 5.C)

S. No.	Overlay Thickness	Base Thickness	Finite Element Solution (kg/cm)	Modified Bradbury (kg/cm^2)	%. Difference
1.	10 cm	8 cm	6.03	5.92	1.66
2.	10 cm	12 cm	4.60	4.33	5.87
3.	10 cm	16 cm	3.20	3.08	3.75
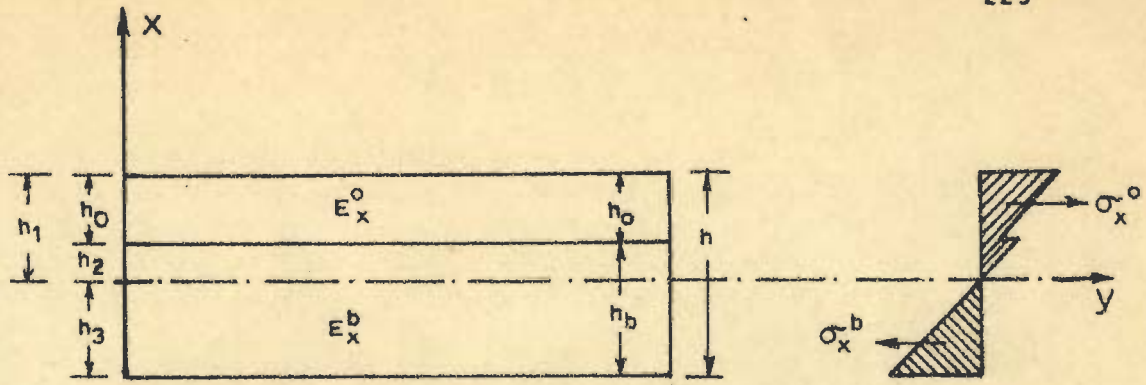
SECTION   X = CONSTANT

$$E_x^o < E_x^b$$

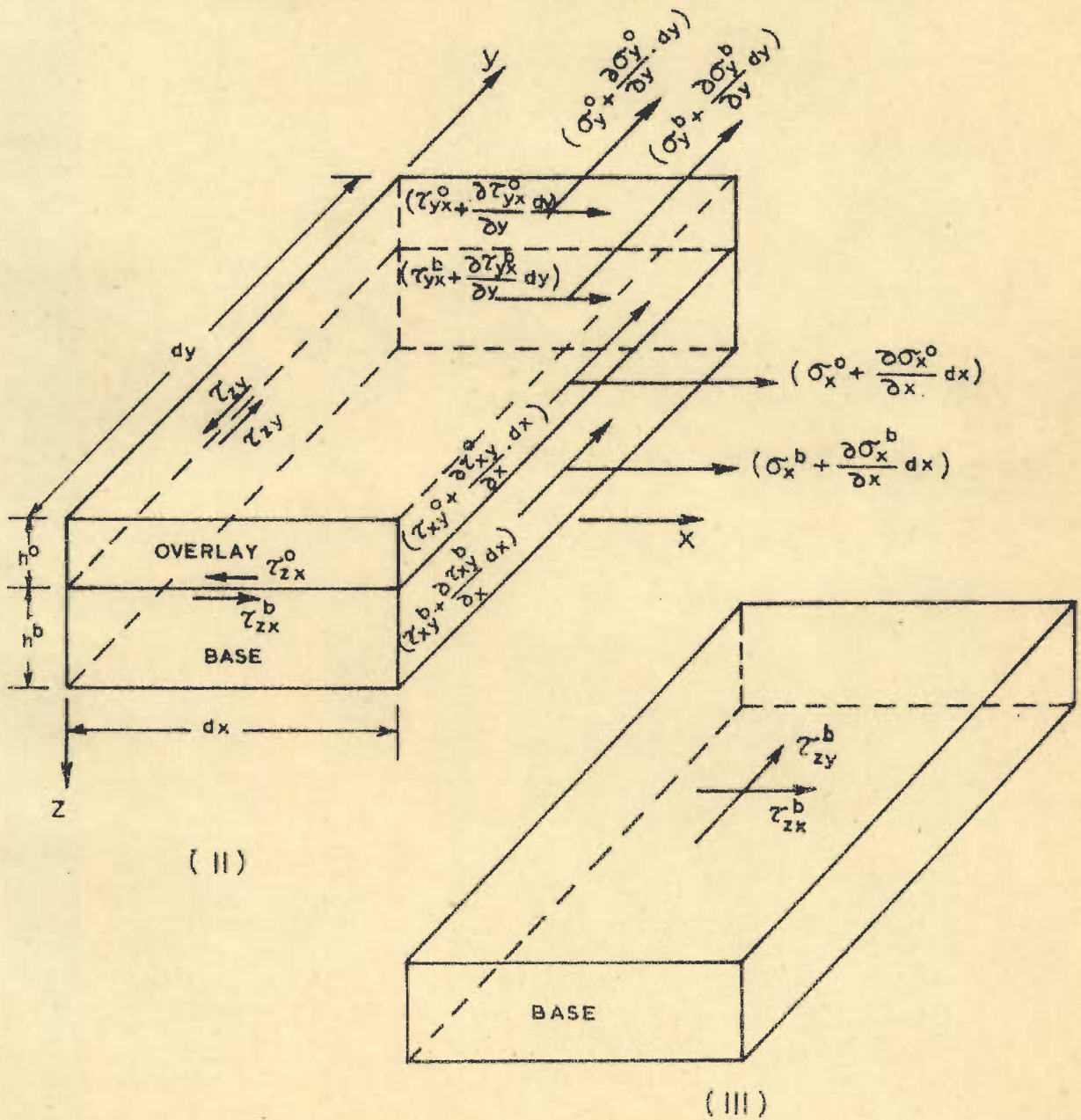## (I)_ BENDING STRESSES IN BASE SLAB WITH OVERLAY

(II)

(III)

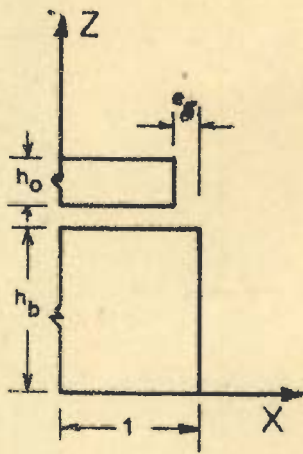## FIG. 5.1 a _ INTERFACIAL SHEARING STRESSES
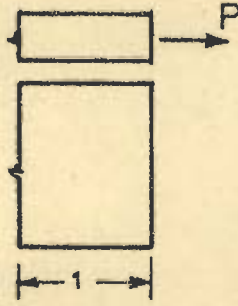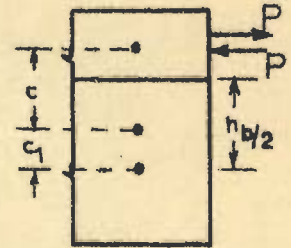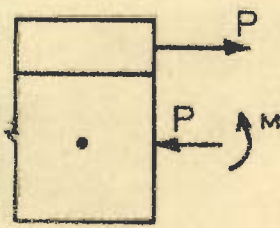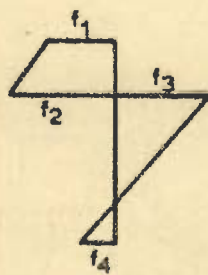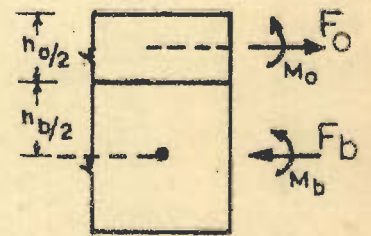
FIG. 5.1 b _ SHRINKAGE STRESSES

NP = 35, NE = 24, NB = 7
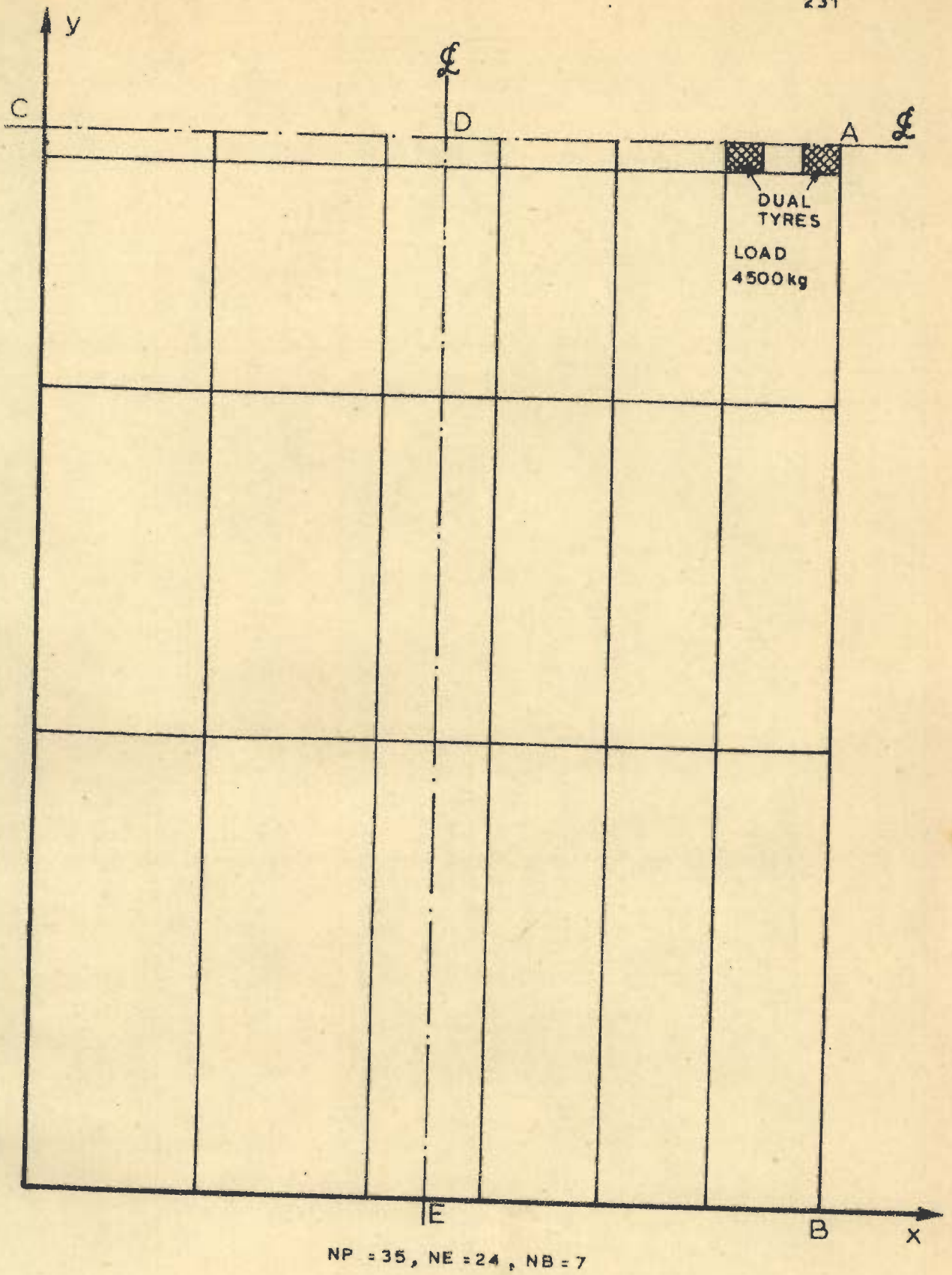
FIG. 5.2 — A TYPICAL FINITE ELEMENT IDEALIZATION OF PAVEMENT SLAB BY RECTANGULAR PLATE BENDING ELEMENTS

Distance — cm

10 cm OVERLAY ON 16 cm UNCRACKED BASE
10 cm OVERLAY ON 8 cm UNCRACKED BASE

FIG. 5.3 — VARIATION OF DEFLECTION ALONG AB
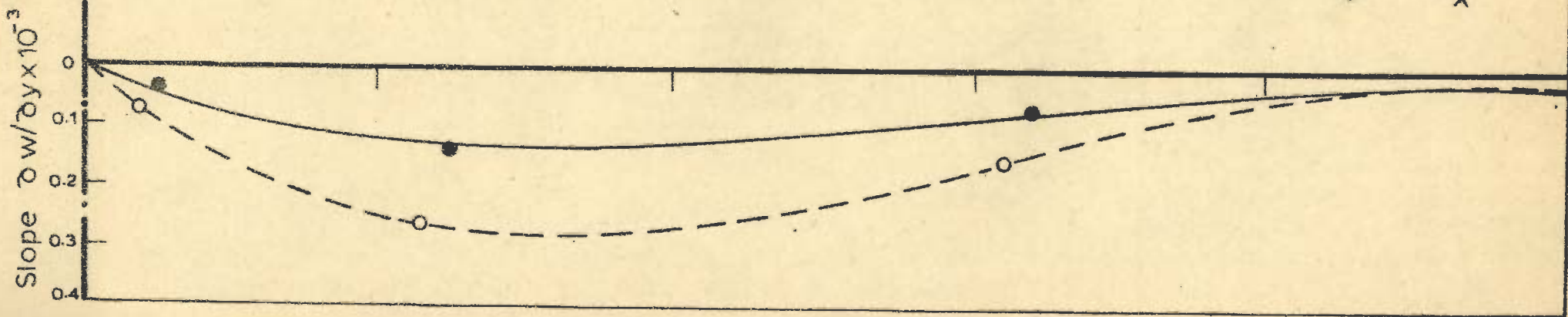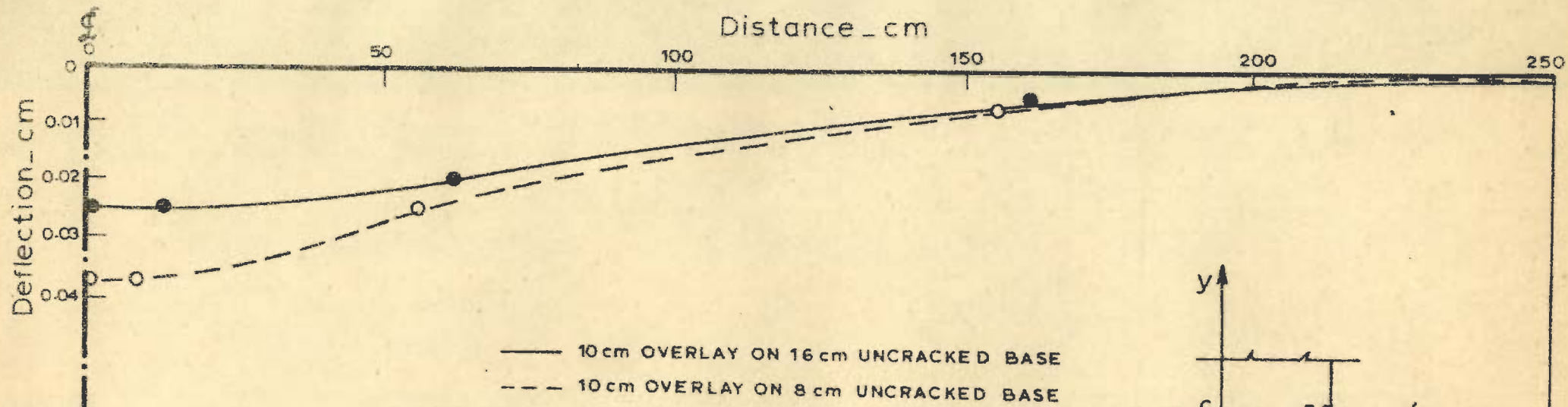
FIG. 5.4 — VARIATION OF SLOPE ALONG AB

FIG. 5.5_ VARIATION OF DEFLECTION ALONG AC

——— 10 cm OVERLAY ON 16 cm UNCRACKED BASE
– – – 10 cm OVERLAY ON 8 cm UNCRACKED BASE
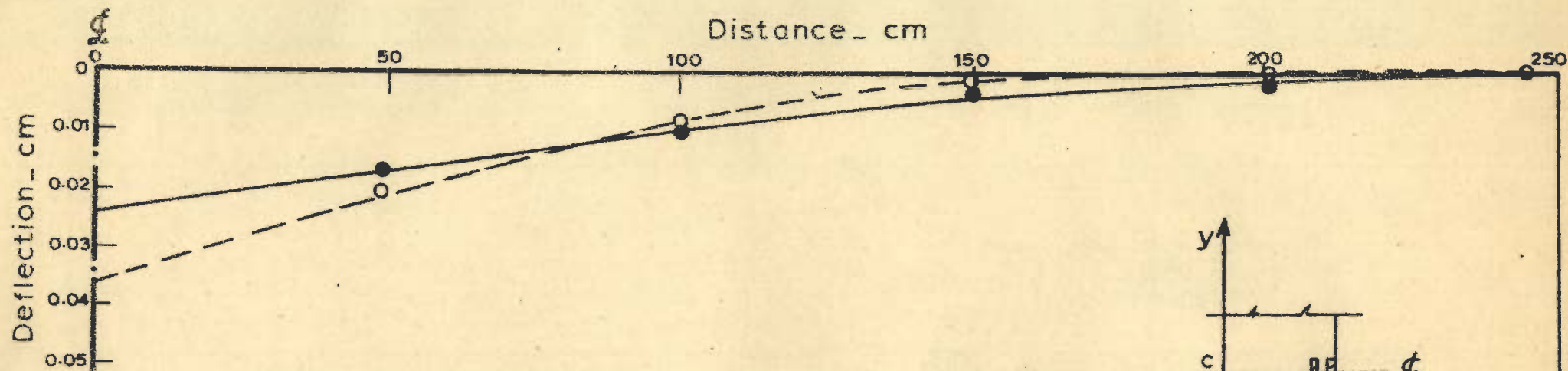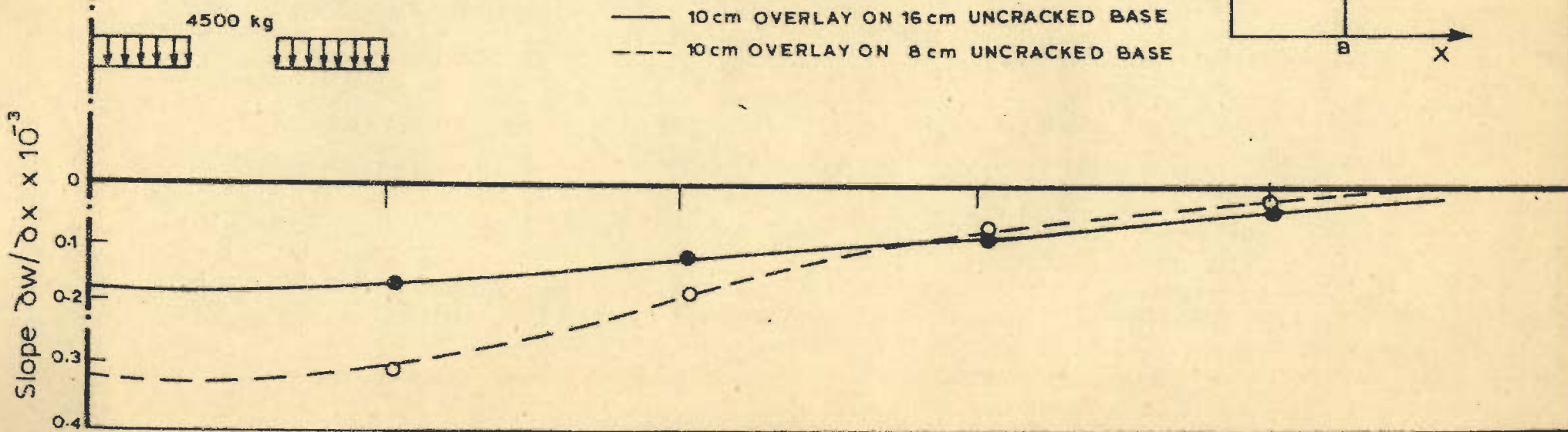
FIG. 5.6_ VARIATION OF SLOPE ALONG AC
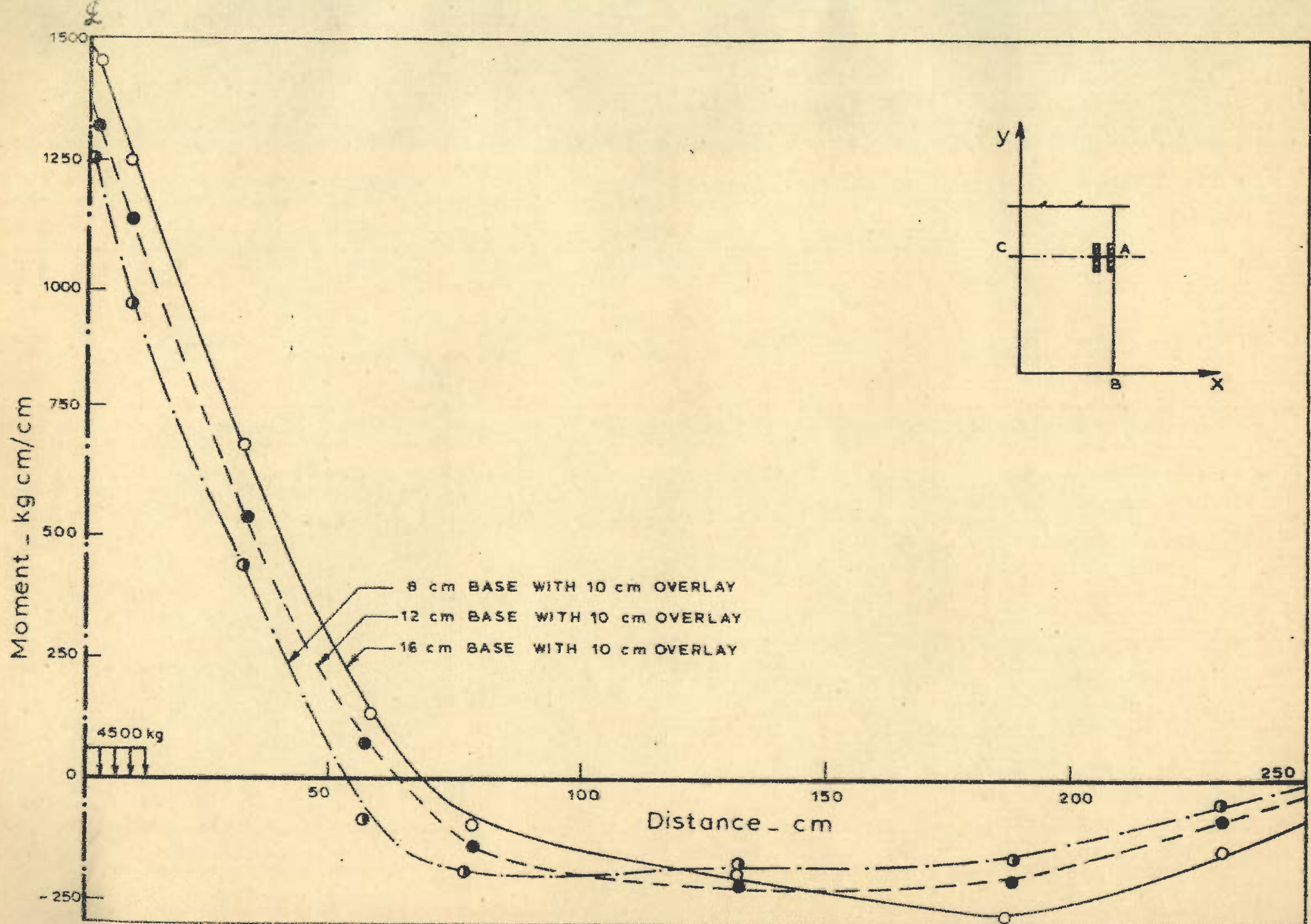
FIG. 5.7 _ VARIATION OF MOMENT My ALONG A B FOR PAVEMENT SLABS WITH 10 cm
OVERLAY ON UNCRACKED BASE

8 cm BASE WITH 10 cm OVERLAY
12 cm BASE WITH 10 cm OVERLAY
16 cm BASE WITH 10 cm OVERLAY

4500 kg

Moment _ kg cm/cm

Distance _ cm

234

FIG. 5.8 _ DEFLECTION ALONG AB

FIG. 5.9 _ VARIATION OF SLOPE ALONG A B

Distance _ cm

Deflection _ cm

Slope ∂w/∂y × 10⁻³

——— 10 cm OVERLAY ON 12 cm UNCRACKED BASE
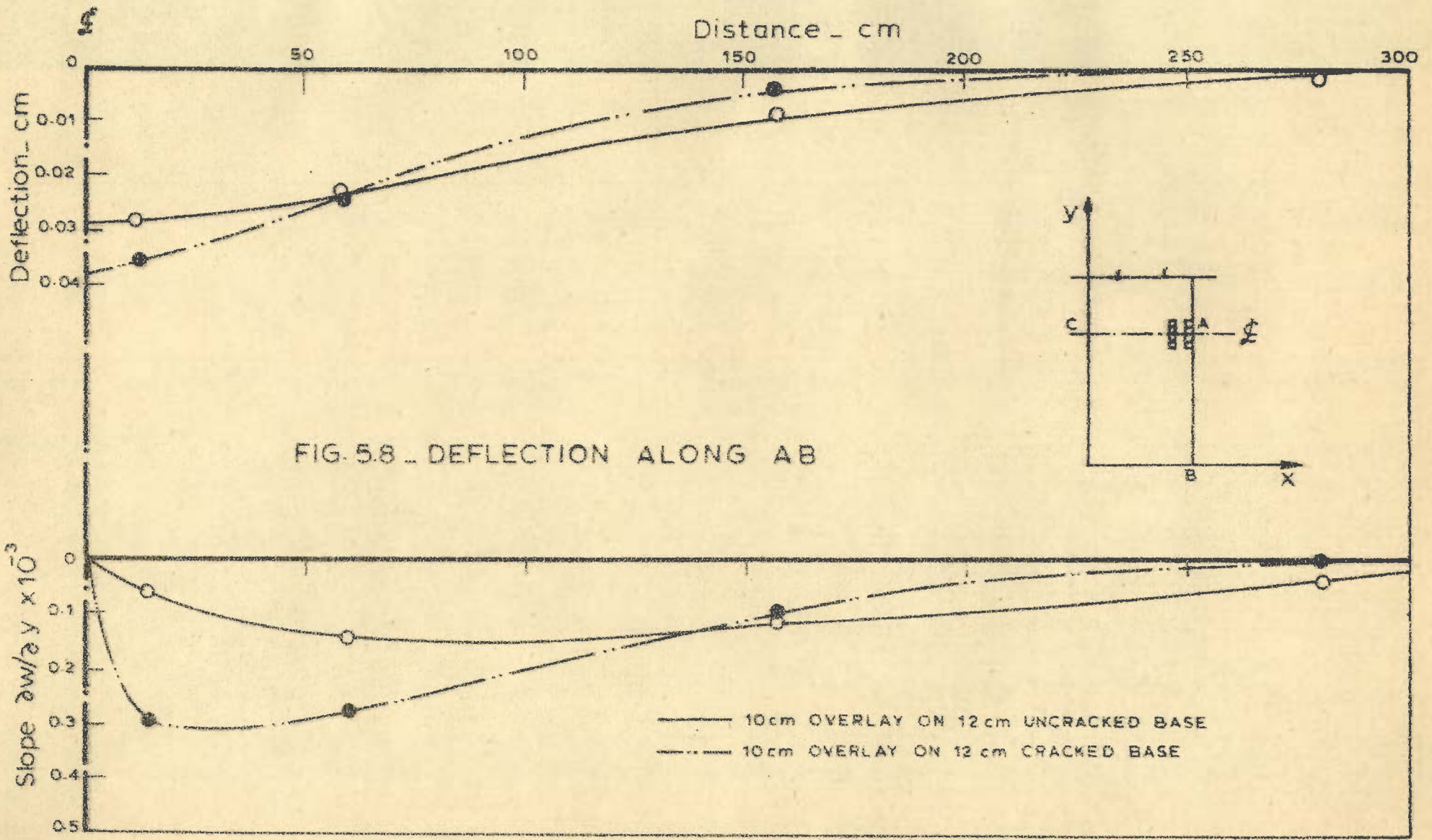
—·—·— 10 cm OVERLAY ON 12 cm CRACKED BASE
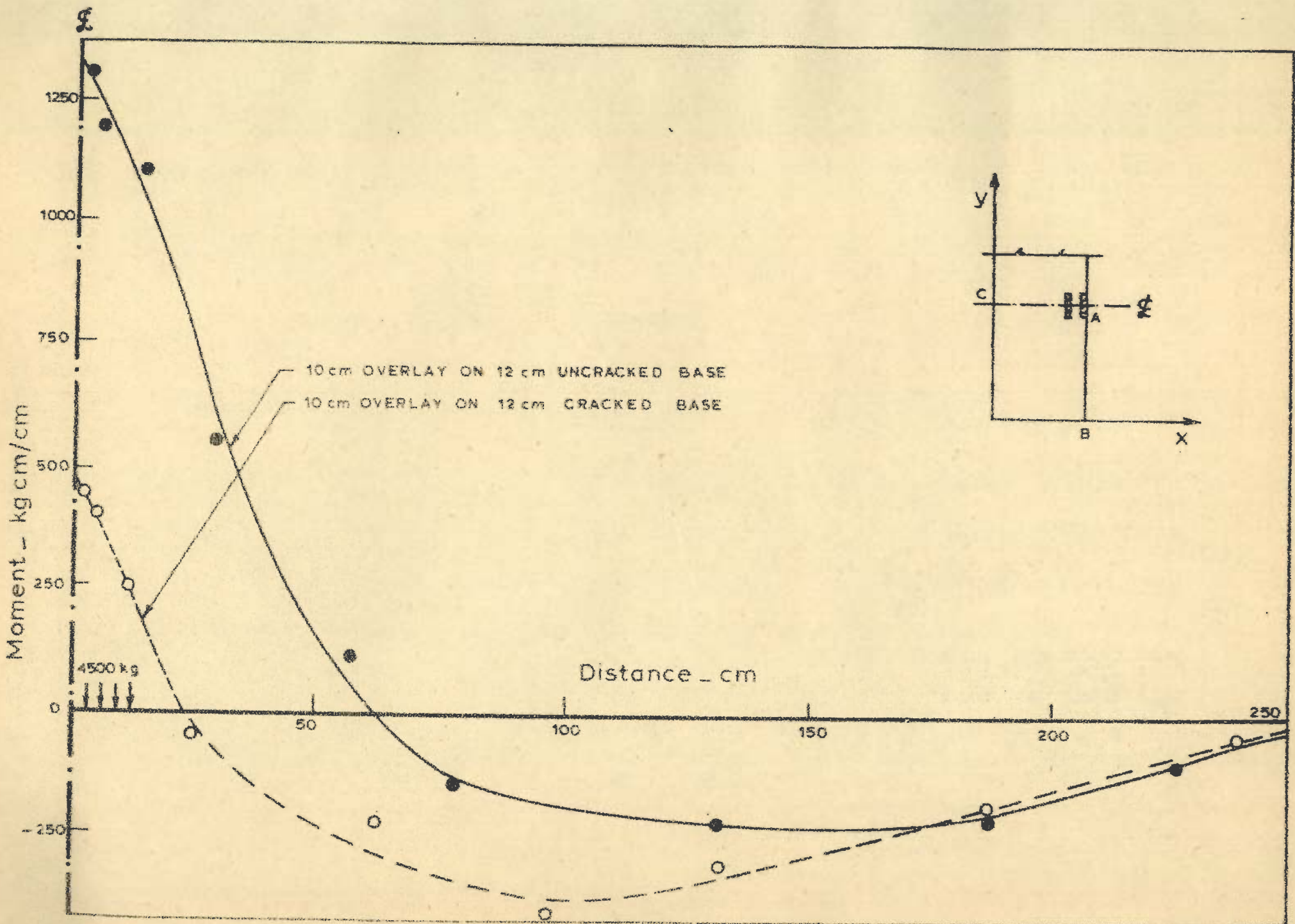
FIG 5.10 _ VARIATION OF MOMENT ALONG AB

Moment _ kg cm/cm

Distance _ cm

10 cm OVERLAY ON 12 cm UNCRACKED BASE

10 cm OVERLAY ON 12 cm CRACKED BASE

4500 kg

236

Distance _ cm

FIG. 5.11 _ VARIATION OF DEFLECTION ALONG AC

——————— 10 cm OVERLAY ON 12 cm UNCRACKED BASE

— — — — 10 cm OVERLAY ON 12 cm CRACKED BASE

FIG. 5.12 _ VARIATION OF SLOPE ALONG AC

237
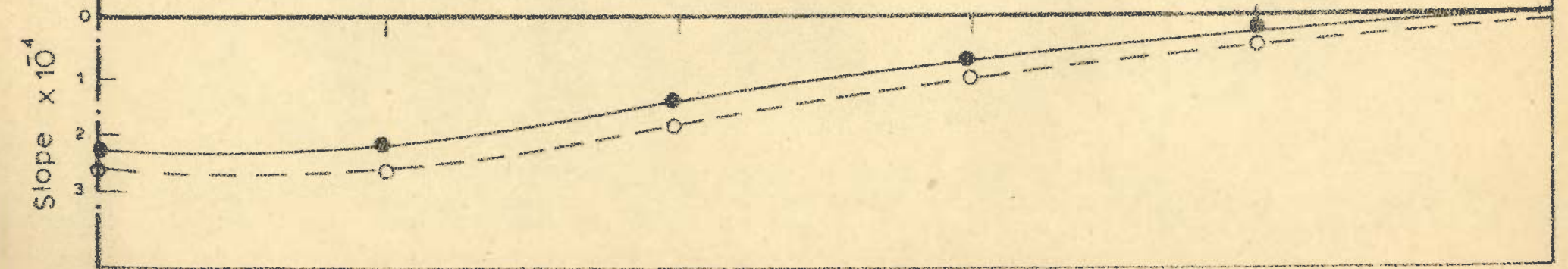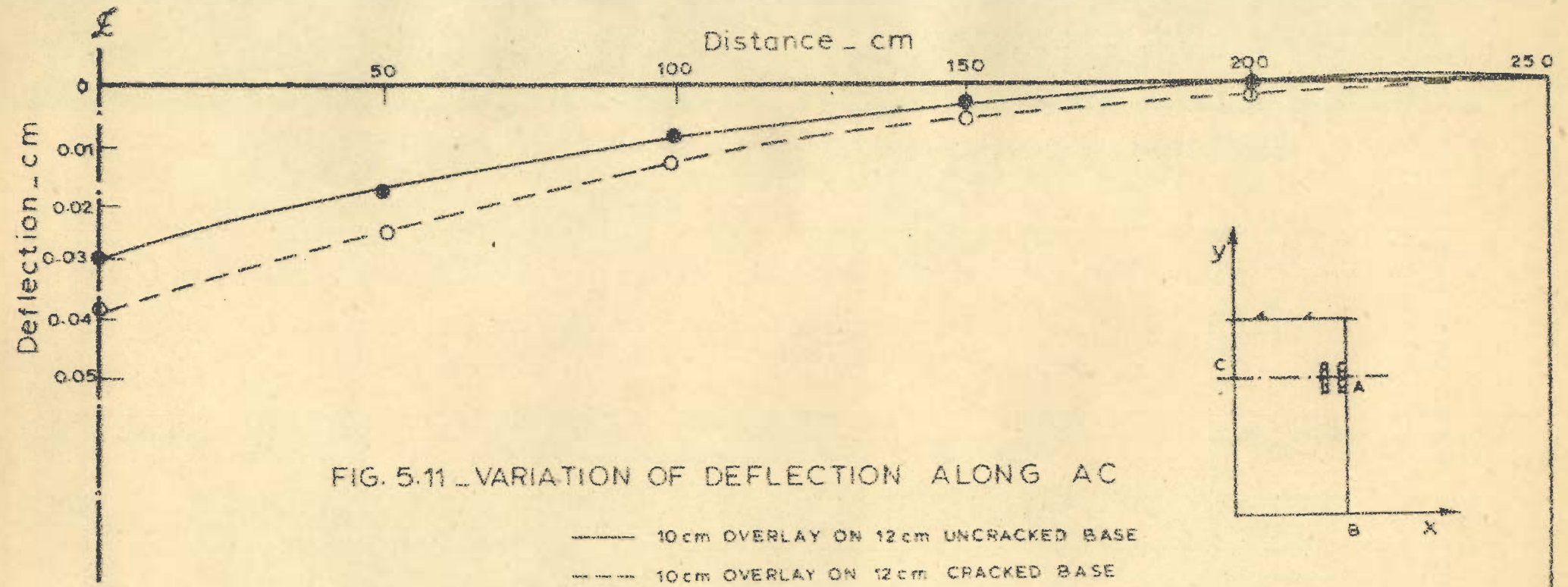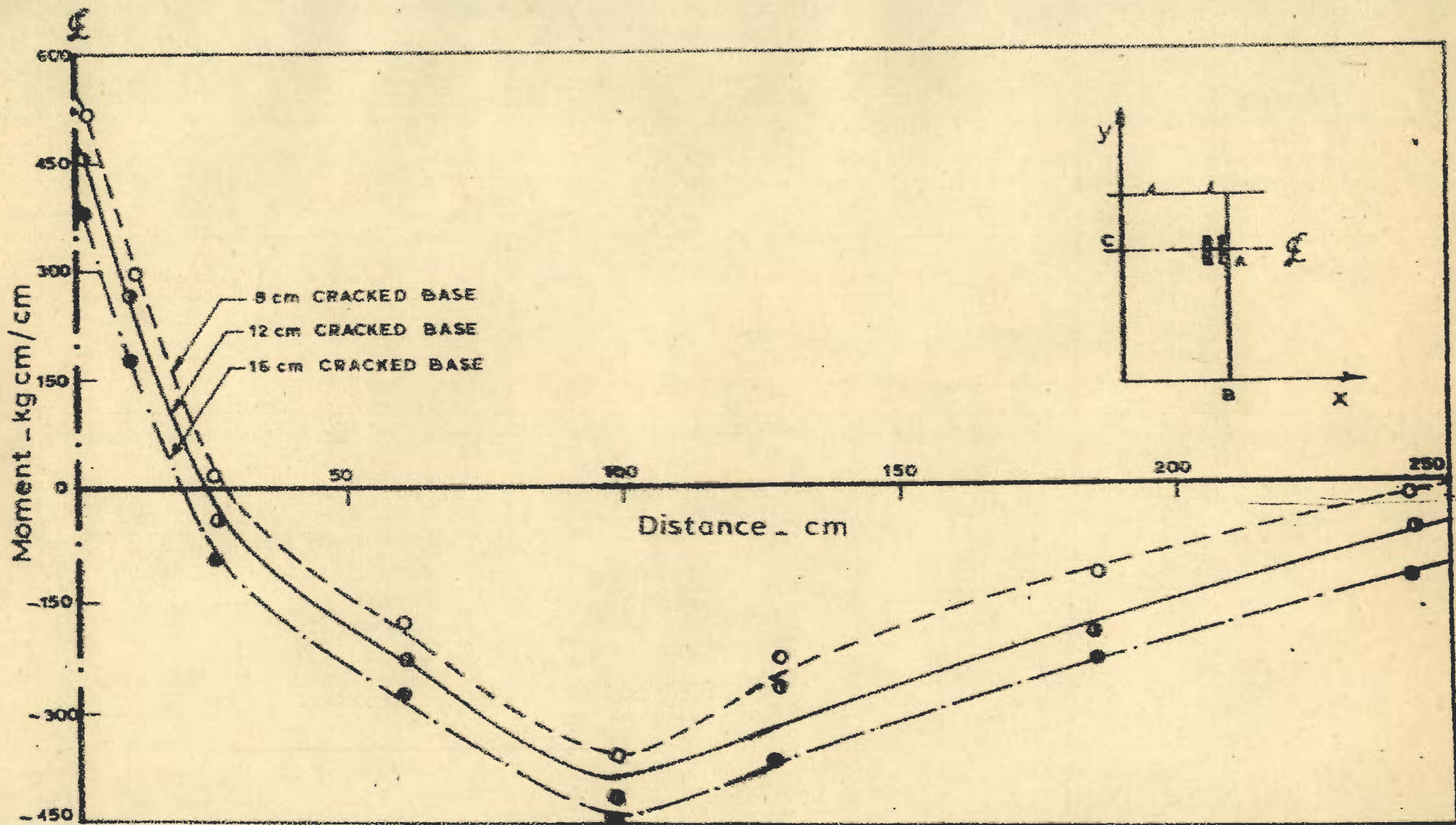
FIG. 5.13 — VARIATION OF MOMENT My ALONG AB 10 cm OVERLAY ON CRACKED BASE
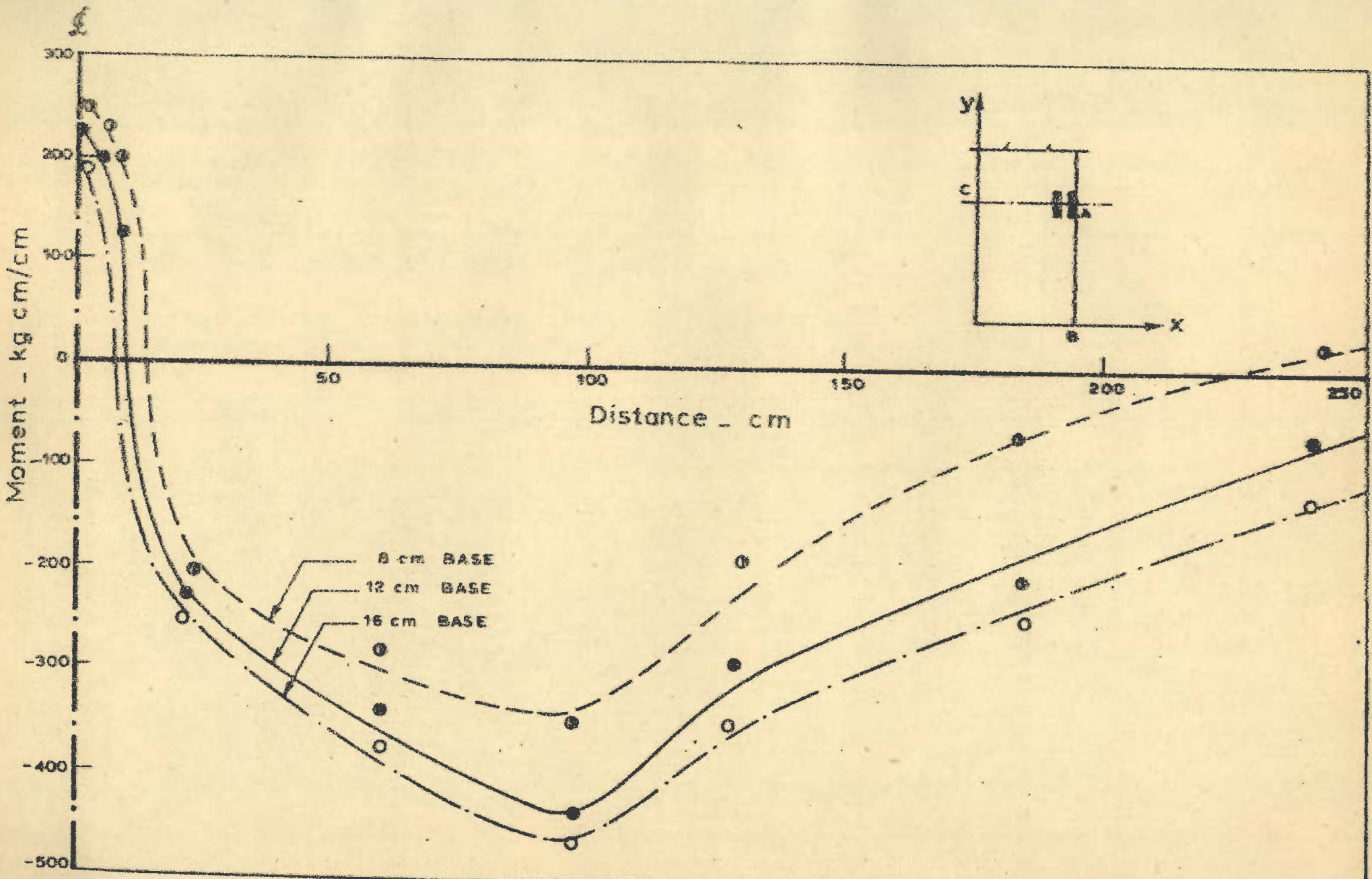
FIG. 5.14 - VARIATION OF MOMENT M_y ALONG AB 6 cm OVERLAY ON CRACKED BASE

8 cm BASE

12 cm BASE

16 cm BASE

Moment - kg cm/cm

Distance - cm

239
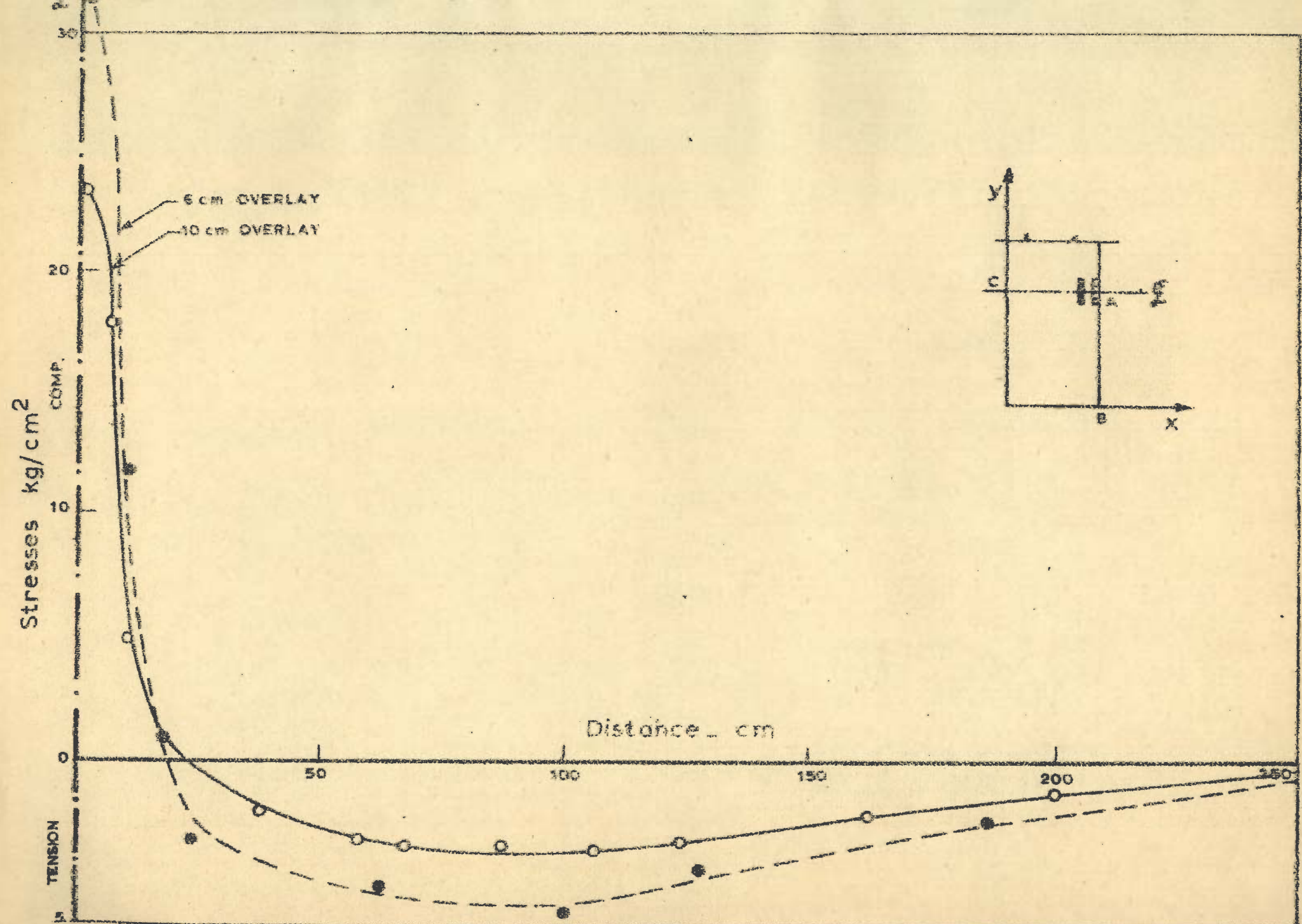
FIG. 5.15 – VARIATION OF FLEXURAL STRESSES IN THE TOP OF OVERLAY, 16 cm CRACKED BASE ALONG AB
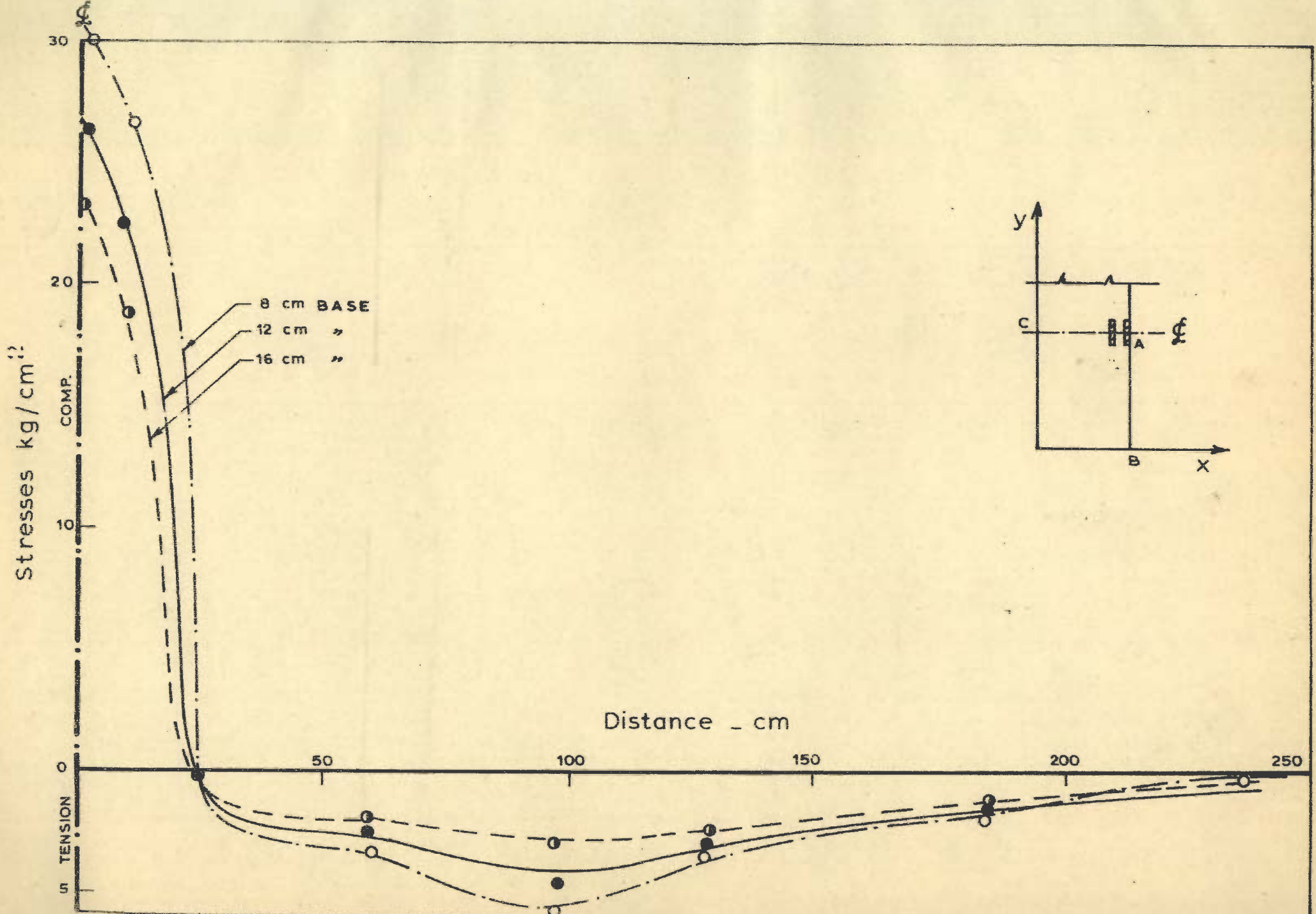
FIG. 5.16 _ VARIATION OF FLEXURAL STRESSES IN THE TOP OF 10 cm OVERLAY (CRACKED BASE) ALONG AB
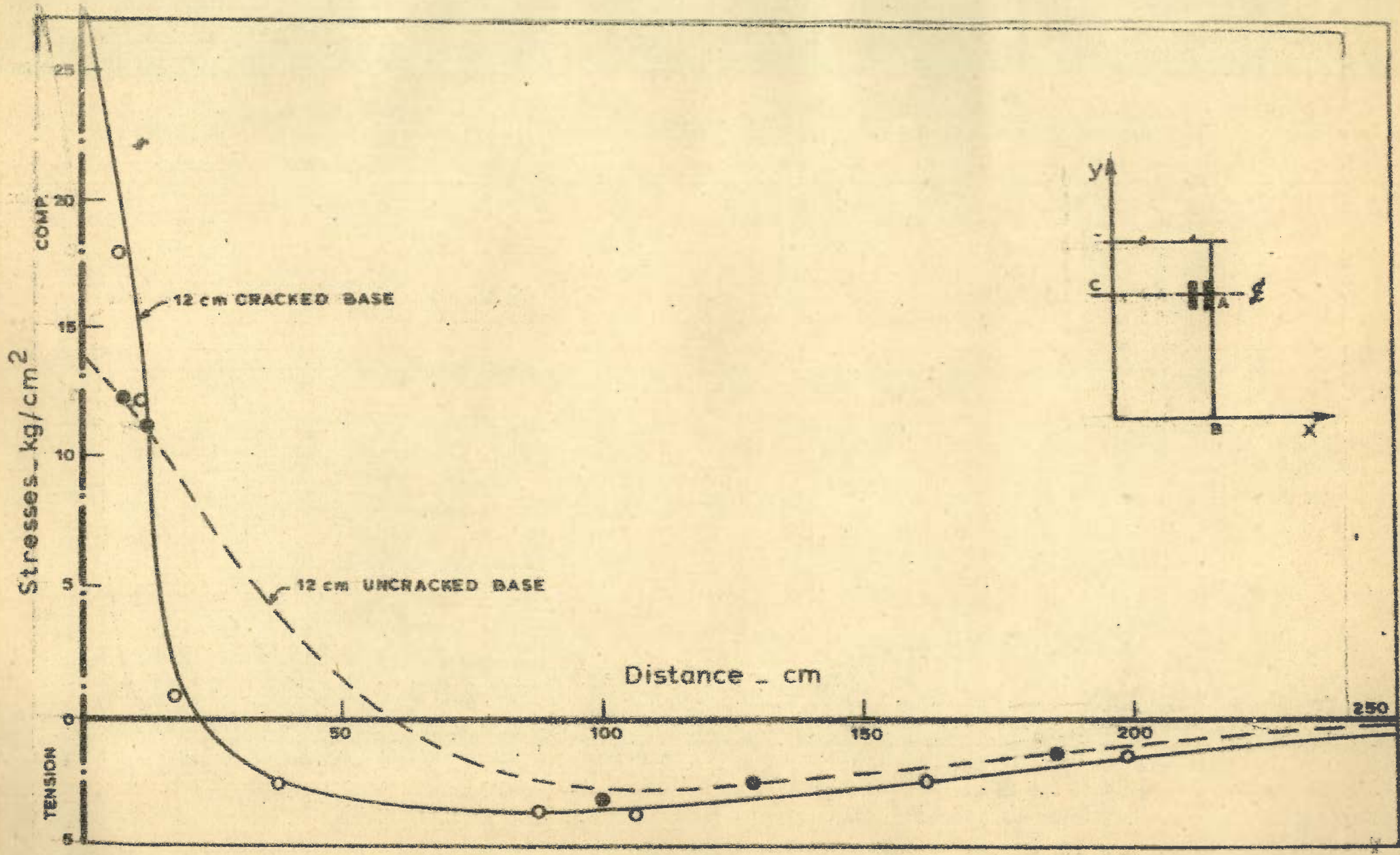
FIG. 5.17 _ VARIATION OF FLEXURAL STRESSES IN THE TOP OF 10 cm OVERLAY ALONG AB
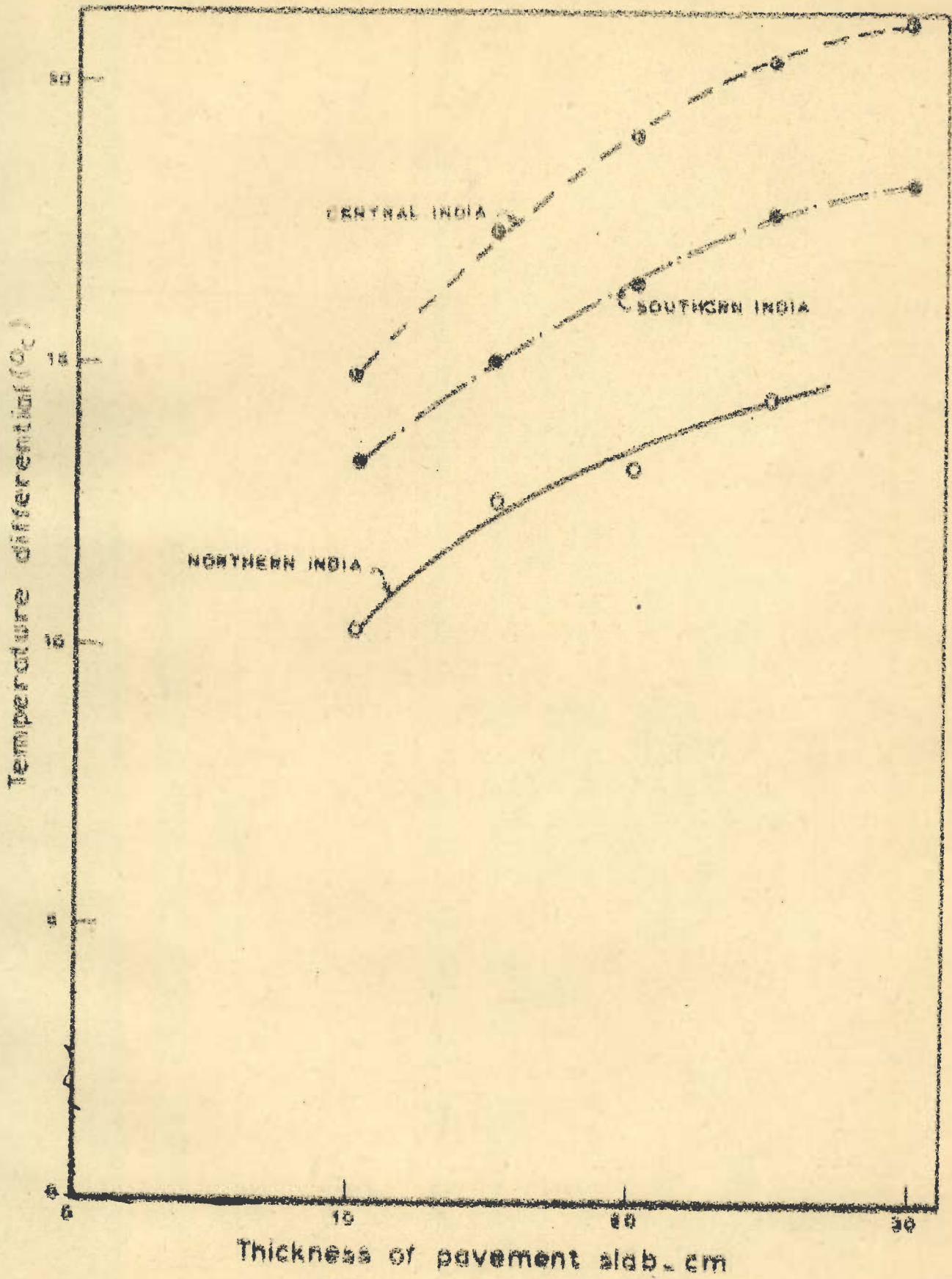
FIG. 5.18 _ TEMPERATURE DIFFERENTIAL IN PAVEMENT SLAB[178]

10 cm OVERLAY ON 8 cm BASE

CRACKED BASE
SOUND BASE

Distance – cm
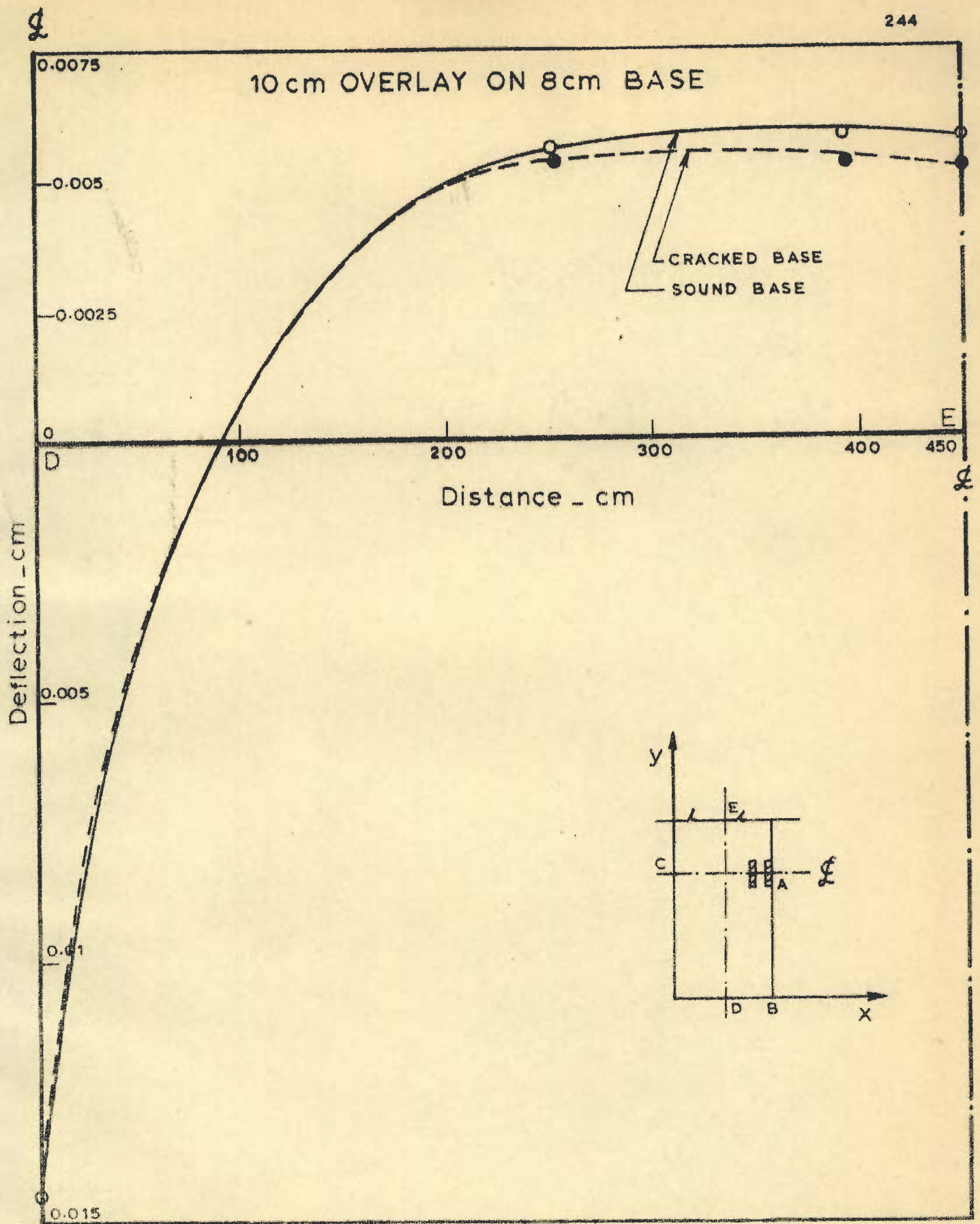
Deflection – cm

FIG. 5·19 – VARIATION OF DEFLECTION ALONG LONGITUDINAL
CENTRE LINE DE DUE TO TEMPRATURE DIFFERENTIAL
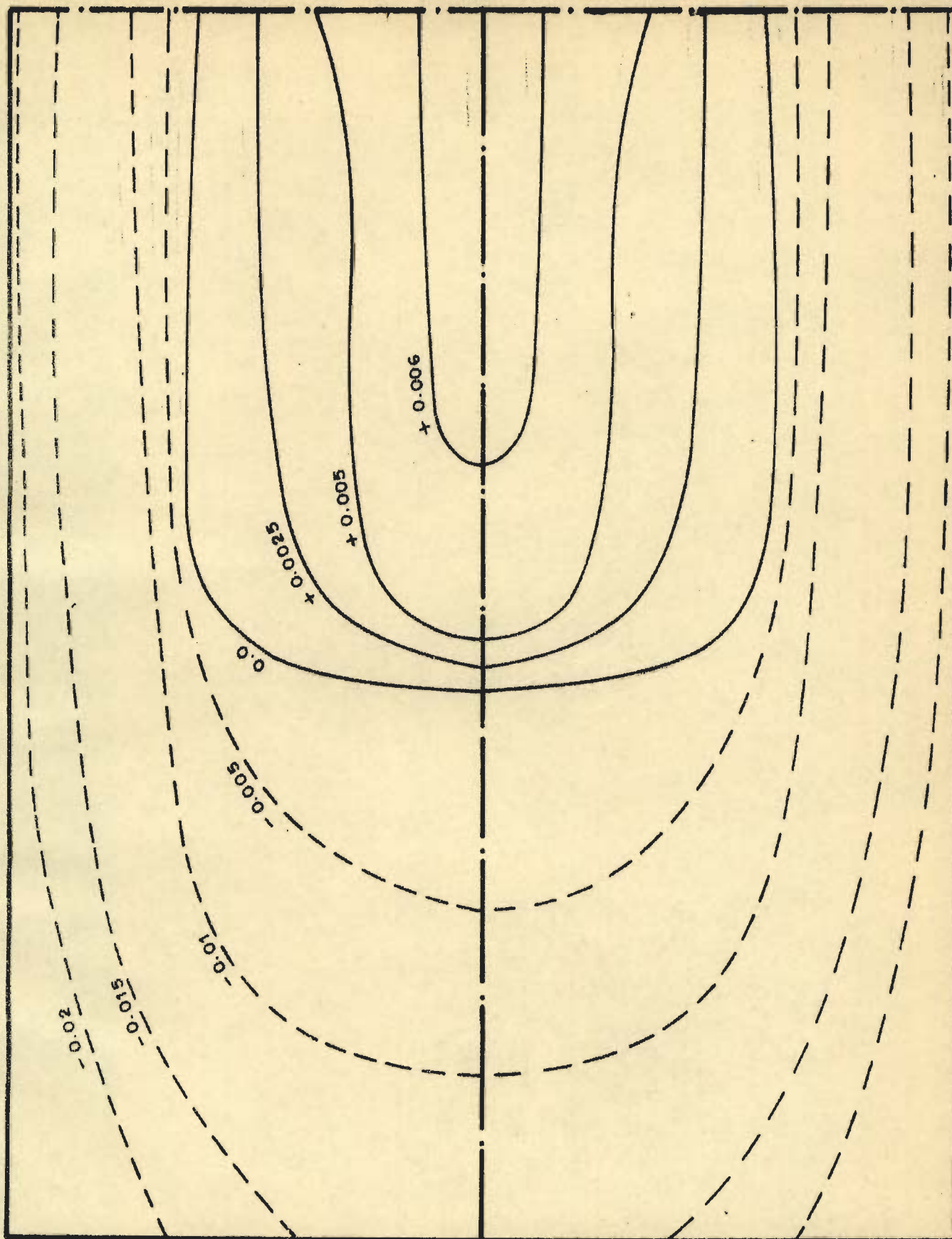
FIG. 5. 20_ CONTOURS OF DEFLECTION DUE TO TEMPRATURE
DIFFERENTIAL IN 10 cm OVERLAY AND 8 cm BASE
PAVEMENT SLAB
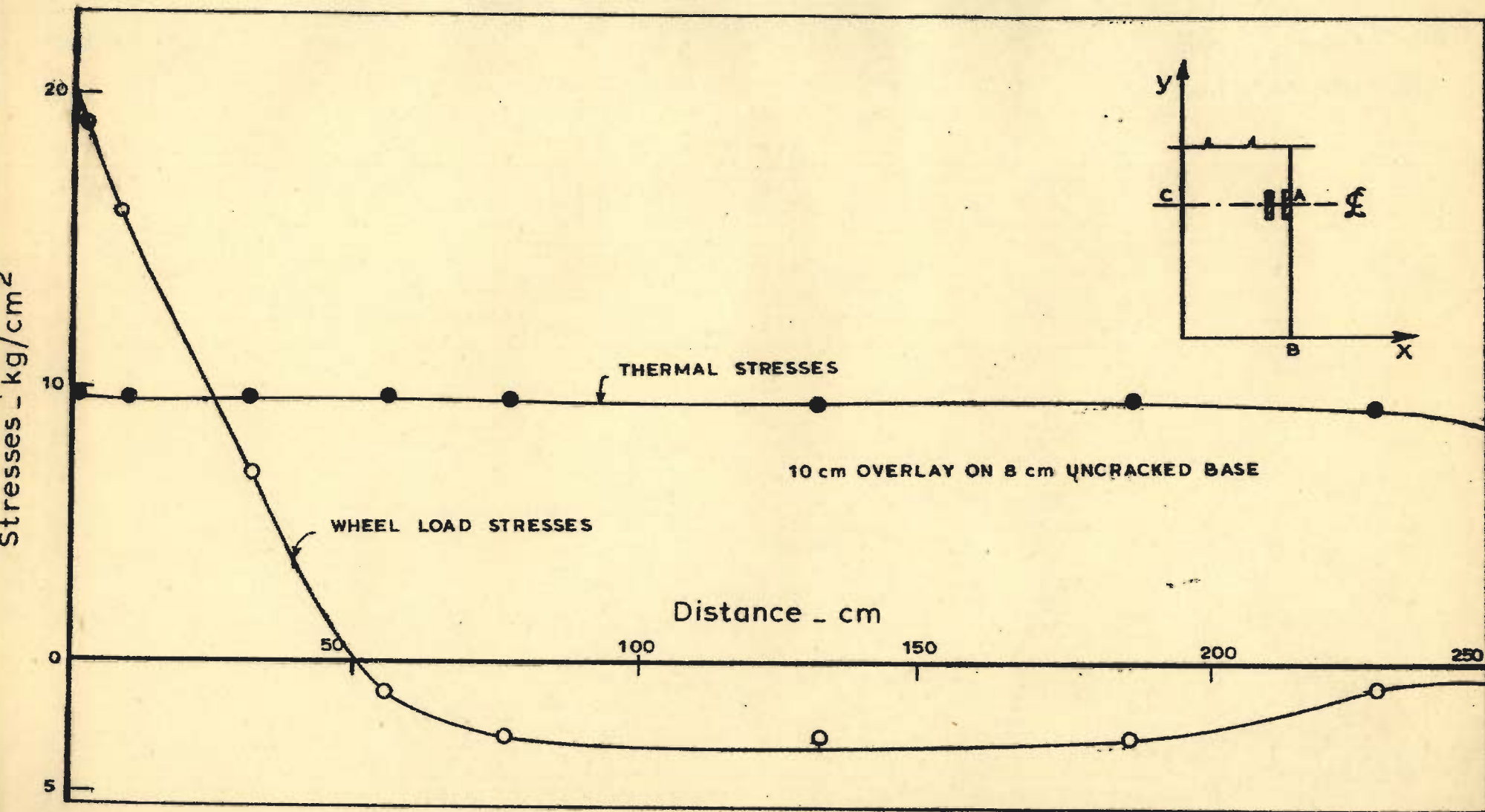
FIG. 5.21 _ VARIATION OF STRESSES AT THE TOP OF OVERLAY ALONG AB
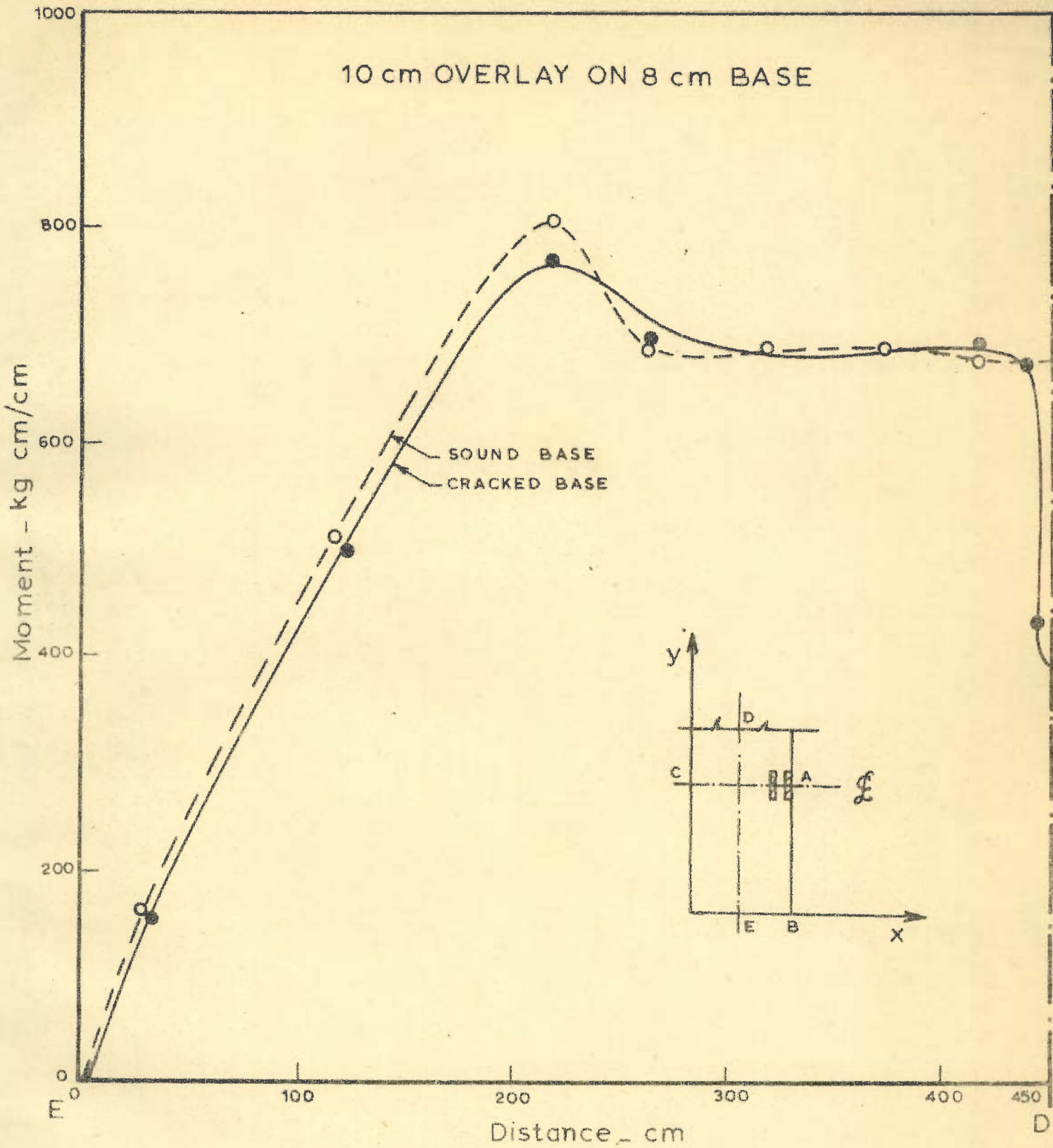
FIG. 5.22 _ VARIATION OF MOMENT ALONG LONGITUDINAL CENTRE
LINE D E OF PAVEMENT DUE TO TEMPERATURE GRADIENT
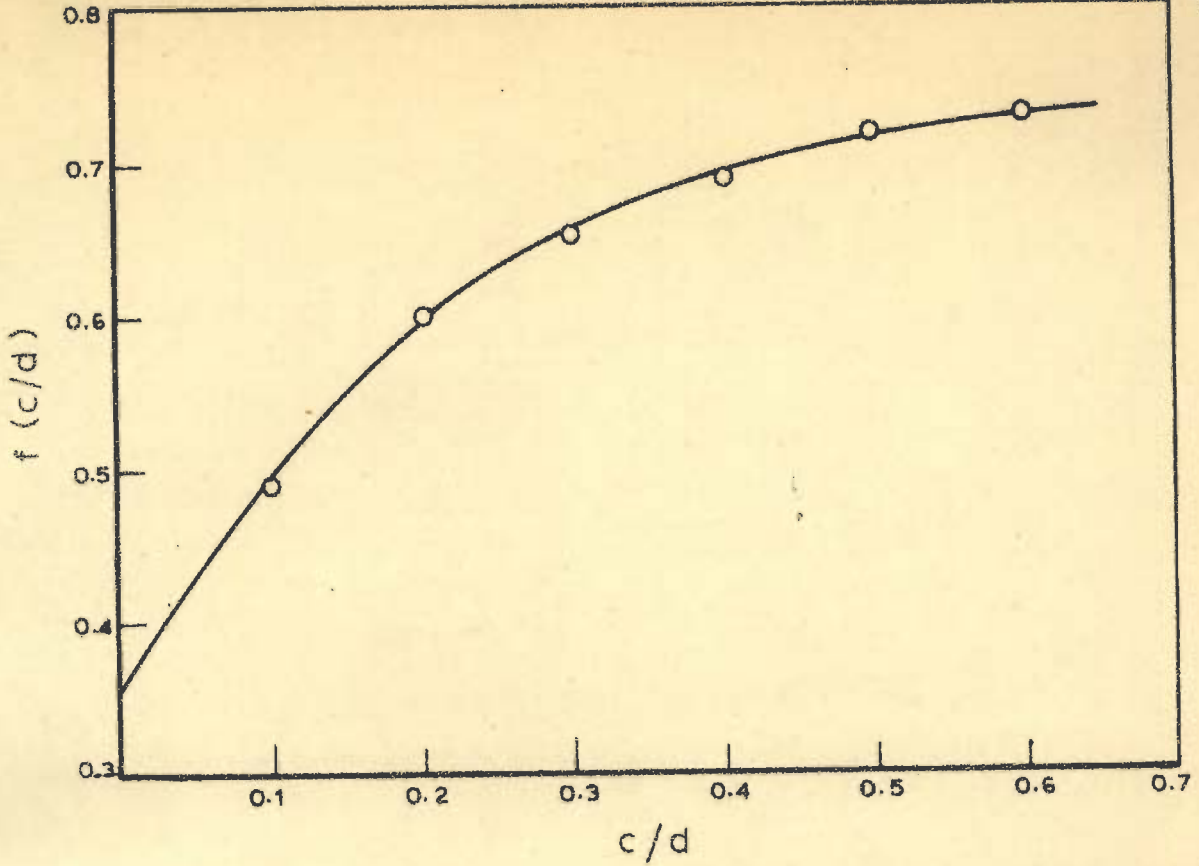
FIG. 5.23 — VALUES OF f(c/d) FOR DIFFERENT (c/d) RATIOS[179]
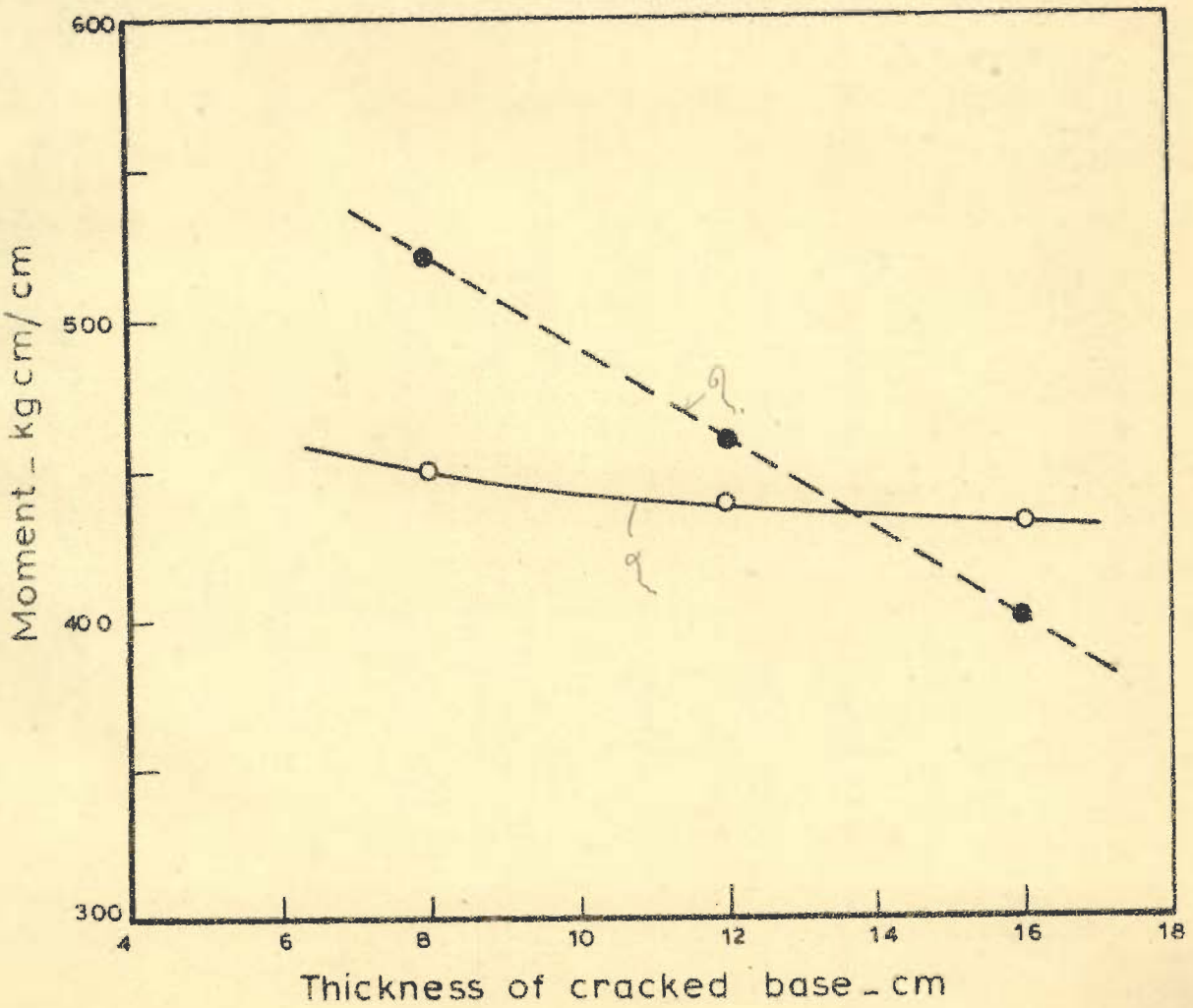
FIG. 5.24 — CRITICAL AND DEVELOPED MOMENTS
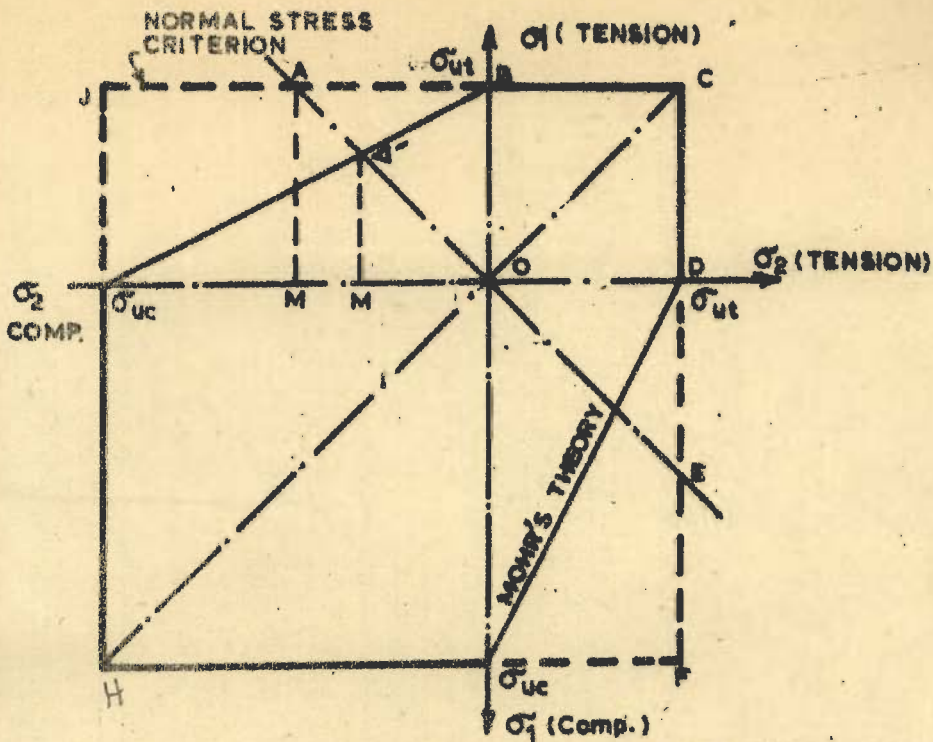
FIG. 5.25 _ NORMAL STRESS AND MOHR'S YIELD CRITERION

FIG. 5.26 a _ STRAIN ENERGY RELEASED DUE TO CRACK

FIG. 5.26 b _ VARIATION OF ENERGY WITH CRACK LENGTH

CHAPTER-VI

ANALYSIS OF UNBONDED OVERLAYS

6.1 INTRODUCTION

Analysis of bonded cement concrete overlays on base of cement concrete or any other material that satisfies the bending theory is dealt in Chapter V . It was seen that in bonded overlays the condition of full strain compatibility is assumed. As a result of this condition the slip between overlay and base is restricted while bending. A high moment resisting couple develops due to bonding.

However, two counts on which the bonded overlay becomes a liability are the efforts required to ensure bond and secondly, as per theory postulated by Griffith[197] the cracks, if any, produces inherent weakness in pavements due to stress concentrations. Indian Roads Congress[10] therefore, recommends unbonded overlay slabs on significantly cracked pavements.

Whereas, it was a problem to ensure bond between base and overlay in case of bonded system, it is also taken as a problem to inhibit bond in the other system[215] and expenses are supposed to be incurred on this item. Moreover, it is argued in favour of the previous system that the cost incurred on extra thickness required in

unbonded overlay is many times more than the expenditure on bonding.

From the considerations of analysis the unbonded overlay is free from the problem of stresses due to differential shrinkage, interfacial shear stresses and to a certain extent problem of stress analysis due to temperature differential. This is because difference of temperature between top and bottom of overlay are to be treated on the basis similar to single pavement slab[216]. However, rational evaluation of wheel load stresses in the unbonded overlay and base that may have cracks does pose a problem.

6.2 UNBONDED CONSTRUCTION

A layer of concrete simply overlaid on the other layer that does not contain any structural defects may not essentially behave as an unbonded overlay. This is because the interfacial shearing stresses in such a system may not be of significant magnitude, as shown in Chapter V. Also, it is found by laboratory testing that sufficiently good amount of strength can develop[13,16] even when no special interfacial treatment is given.

Therefore, special treatment is necessary if bond is to be prevented. This would call for the necessity of providing an intermediate layer of sand asphalt, paper or other similar material. However Mellinger[48] reports the

findings of experiments carried out at Sharonville Heavy Load Tracks[217]. The overlay was cast on the base which was cured using membrane curing compound. The strain meters provided at the top and bottom of overlay as well as top and bottom of base indicated that there was no shear transfer at the interface because the membrane curing compound was not removed before casting the overlay and this prevented the formation of any bond between the two layers of cement concrete.

6.3 EXISTING METHODS FOR DESIGN AND ANALYSIS

The basis of design of overlay on rigid pavements has been mostly empirical. The method suggested by Corps of Engineers, Civil Aeronautical Administration and P.C.A. fall under this category[21,218,219].

According to Corps of Engineers formulae:

$$h_o^2 = h^2 - Ch_c^{b^2} \qquad \qquad \ldots (6.1)$$

where, h^b = thickness of existing slab,

h_o = thickness of overlay slab,

h = design slab thickness for a single slab placed directly on subgrade,

C = a coefficient depending upon the condition of existing slab,

= 1 for sound slab,

= 0.75 for slabs having initial cracks,

C = 0.35 for badly cracked slab.

I.R.C.[10] has suggested values of C for five different categories of distress in base slab,

Burmister's layered theory[71] is also often used to determine the overlay thickness. This use is however, indirect. Bose has[220,221] suggested a method in which the value of modulus of subgrade reaction 'k' is determined by use of plate load test on subgrade. The modulus of elasticity of subgrade from Burmister's equation[71] is given by

$$E_s = 1.18 x r_o x k \qquad \qquad \dots (6.2)$$

where,

E_s = modulus of elasticity of subgrade,

r_o = radius of test plate = 37.5 cm.

This value was then used to determine the coefficient 'F_w' which is based on the E_s/E_b and h_b a ratio,

E_b = modulus of elasticity of existing concrete slab, and

a = radius of contact.

The modulus of elasticity of the combined system could be determined from:

$$E_{(s+b)} = \frac{E_s}{F_w} \qquad \qquad \dots (6.3)$$

The equivalent modulus of subgrade reaction for the

base and overlay could be then found by use of equation 6.2. The overlay could now be designed by using Westergaard's method[24] or Pickett design charts[214] assuming this value of subgrade reaction.

A similar method has been used by Lemcoe and Mahala[222] to determine the modulus of subgrade reaction to be adopted for analysis of overlay stresses.

In the method by Bose[220,221] the value of radius of contact 'a' is taken as standard plate radius. However, Lemcoe and Mahala[222] take it as actual contact radius plus the depth of overlay slab, assuming 45° distribution through the overlay.

Another assumption on the method proposed by Lemcoe and Mahala is taking an arbitrary value of slab thickness to account for distress in existing slab. Bose[220], however, does not propose any such assumption and the applicability of the method is restricted to sound existing slab only.

It is also a point worth considering that how far can the Burmister method[71] be applied to determine the support value of base slab when the region under study is the edge or corner, being more important locations. However, a plea for unified approach has already been made by McCllough and Beodecker[98].

U.S. Navy Department has adopted the recommendations

of Marcus and Palmer[223]. According to this method:

$$f_0' = f_0 \frac{E^o h^{o3}}{E^b h^{b3} + E^o h^{o3}} \qquad \ldots (6.4)$$

and

$$f_b' = f_b \frac{E^b h^{b3}}{E^b h^{b3} + E^o h^{o3}} \qquad \ldots (6.5)$$

f_0' = maximum stress in overlay under a given
applied load when new slab rests on the
base slab,

f_0 = maximum stress in overlay when overlay is
directly resting on subgrade without base slab,

f_b' = maximum stress in the base when the load is
applied on overlay,

f_b = maximum stress in the base when the base acts
alone,

It can be seen that the values of f_0 and f_b can
be obtained by using Westergaard's equation or design
charts as per conventional procedure. Therefore, the
stresses in base and overlay can be analysed.

Mellinger[48] has suggested the following formula
for use in determining the equivalent base thickness 'h_{eb}',
for edge loading,

$$h_{eb} = \left[\frac{R_b h^{b2} (1+\nu^o)(3+\nu^b)}{R_o (1+\nu^b)(3+\nu^o)} \right]^{1/2} \qquad \ldots (6.6)$$

and for interior loading

$$h_{eb} = \left[\frac{R_b h^{b2} (1+\nu^o)}{R_o (1+\nu^b)} \right]^{1/2} \qquad \ldots (6.7)$$

The formulae is based on the rupture strength of

base and overlay. The effect of Poisson's ratio can be
seen to be small.

R_b and R_0 denote modulus of rupture of base
and overlay.

These formulae are based on model analysis[224].
A need for experimental verification has been emphasised.[218]

Shackel[225] reported experimental investigation
on beams having a separation course interposed. The
comparison with theory based on Marcus and Palmer[223]
indicated acceptable prediction, proving the justification
of the assumptions made in the theory.

6.4 CONSIDERATION FOR ANALYSIS

It is therefore, necessary to evolve a suitable
method of analysis which could, on sound theoretical basis,
give due recognition to the difference in elastic propert-
ies of base and overlay for the calculation of stresses
and displacement in whole of the pavement structure for
wheel loads placed anywhere on it. The method should have
its applicability to the general case when the overlay
is laid on a cracked base as the main aim of providing
an unbonded overlay is to cover a distressed base rather
than simply enhance its structural capacity.

A formulation for such an analysis is proposed
in following paragraphs.

6.5 GENERAL FORMULATION FOR THE ANALYSIS OF THE UNBONDED OVERLAY ON SOUND OR CRACKED BASE.

6.5.1 General Assumptions made are as under:

1. All the assumptions relating to plate theory as stated in article 4.2 are also valid for the analysis of unbonded overlays.

2. The interface between base and overlay is perfectly smooth and therefore, no interfacial shear stresses develop.

3. Under the action of wheel load the deflection of base and overlay are same.

4. As discussed and formulated in chapter IV, the effect of crack can be simulated by assigning orthotropic properties.

5. The coordinate axis taken as reference frame coincides with the principal direction of orthotropy. However, if they do not, then expressions can be obtained using rotation matrix as described in chapter IV.

6. The temperature gradient is assumed as linear throughout the depth of pavement.

Assumptions 2 and 3 as stated above need clarification. Assumption 2 imposes a condition which is only true in theory. In reality, the interface between base and overlay can not be free of any interfacial shear, though it is

possible that slippage might occur between base and over-
lay after a certain value of stress is exceeded. This
would impose a condition of partial bonding. Though an
attempt for analysis of partial bonding is reported[226,227,228],
a rational analysis for such a condition would not have
much value in the absence of reliable data[13,229]. It
is also seen that an assumption neglecting any shear res-
istance at interface gives the other extreme case.

It is difficult to say how far could the assumption 3
be valid for every point on the interface. However, it may
be argued that the truth of assumption, under the action
of wheel can not be violated in the neighbourhood of the
load. However, it is possible that it may not be valid for
the zones away from the load. Fortunately, the effect of
this will not adversely effect the stresses and displace-
ment in the base-overlay system in the vicinity of the load.
The point of interest, is generally the neighbouring area
around the centre of gravity of the wheel load, this being
the most severely stressed location. The validity of this
assumption can be upheld on these grounds.

6.5.2 General Formulation

A general formulation, incorporating evaluation of
stresses and displacement in base and unbonded overlay
having different elastic properties and discontinuities,
is proposed based on the assumptions as stated in article
6.5.1.

From equation 4.5

$$\left\{ \begin{matrix} \sigma_x \\ \sigma_y \\ \tau_{xy} \end{matrix} \right\} = \begin{bmatrix} C_{11} & C_{12} & 0 \\ C_{21} & C_{22} & 0 \\ 0 & 0 & C_{33} \end{bmatrix} \left\{ \begin{matrix} \varepsilon_x \\ \varepsilon_y \\ \gamma_{xy} \end{matrix} \right\} \qquad \dots (6.8)$$

where,

$$\left\{ \begin{matrix} \varepsilon_x \\ \varepsilon_y \\ \gamma_{xy} \end{matrix} \right\} = -Z \left\{ \begin{matrix} \partial^2 w/\partial x^2 \\ \partial^2 w/\partial y^2 \\ -2 \dfrac{\partial^2 w}{\partial x. \partial y} \end{matrix} \right\} + \left\{ \begin{matrix} \alpha \dfrac{\Delta T}{h} Z \\ \alpha \dfrac{\Delta T}{h} Z \\ 0 \end{matrix} \right\} \qquad \dots (6.9)$$

If superscript 'o' refers to overlay and 'b' to base, then from equation 6.8,

$$\left\{ \begin{matrix} \sigma_x^o \\ \sigma_y^o \\ \tau_{xy}^o \end{matrix} \right\} = \begin{bmatrix} C_{11}^o & C_{12}^o & 0 \\ C_{21}^o & C_{22}^o & 0 \\ 0 & 0 & C_{33}^o \end{bmatrix} \left\{ \begin{matrix} \varepsilon_x \\ \varepsilon_y \\ \gamma_{xy} \end{matrix} \right\} \qquad \dots (6.10)$$

and by validity of assumption 3,

$$\left\{ \begin{matrix} \sigma_x^b \\ \sigma_y^b \\ \tau_{xy} \end{matrix} \right\} = \begin{bmatrix} C_{11}^b & C_{12}^b & 0 \\ C_{21}^b & C_{22}^b & 0 \\ 0 & 0 & C_{33}^b \end{bmatrix} \left\{ \begin{matrix} \varepsilon_x \\ \varepsilon_y \\ \gamma_{xy} \end{matrix} \right\} \qquad \dots (6.11)$$

Equation 6.10 and 6.11 are for the case when the principal direction of orthotropy are coincident with coordinate axis. However, if the two are different then equation 4.48 can be used to modify them.

The stress resultants can be obtained by integrating the stresses over the depth with base and overlay taken separately. Treating assumption 2 as valid, the stress distribution along depth will be as shown in Figure 6.1(a):

$$M_x = \int_{-h^o/2}^{h^o/2} \sigma_x^o \, Z \, dZ + \int_{-h^b/2}^{h^b/2} \sigma_x^b \, Z \, dZ \qquad \ldots (6.12)$$

By substituting proper values of σ_x^o and σ_x^b from equation 6.10 and 6.11

$$M_x = \int_{-h^o/2}^{h^o/2} (C_{11}^o \epsilon_x + C_{12}^o \epsilon_y) Z \, dZ$$
$$+ \int_{-h^b/2}^{h^b/2} (C_{11}^b \epsilon_x + C_{12}^b \epsilon_y) Z \, dZ$$

On substituting values of ϵ_x and ϵ_y from equation 6.9, integrating, simplifying and rearranging,

$$M_x = - \frac{h^{o3}}{12} \left[C_{11}^o \left(\frac{\partial^2 w}{\partial x^2} + \alpha \frac{\Delta T}{h} \right) + C_{12}^o \left(\frac{\partial^2 w}{\partial y^2} + \frac{\alpha \, \Delta T}{h} \right) \right]$$
$$- \frac{h^{b3}}{12} \left[C_{11}^b \left(\frac{\partial^2 w}{\partial x^2} + \alpha \frac{\Delta T}{h} \right) + C_{12}^b \left(\frac{\partial^2 w}{\partial y^2} + \frac{\alpha \, \Delta T}{h} \right) \right] \quad \ldots (6.13)$$

Similarly

$$M_y = - \frac{h^{o3}}{12} \left[C_{21}^o \left(\frac{\partial^2 w}{\partial x^2} + \alpha \frac{\Delta T}{h} \right) + C_{22}^o \left(\frac{\partial^2 w}{\partial y^2} + \frac{\alpha . \Delta T}{h} \right) \right]$$
$$- \frac{h^{b3}}{12} \left[C_{11}^b \left(\frac{\partial^2 w}{\partial x^2} + \frac{\alpha . \Delta T}{h} \right) + C_{22}^b \left(\frac{\partial^2 w}{\partial y^2} + \frac{\alpha . \Delta T}{h} \right) \right] \quad \ldots (6.14)$$

and

$$M_{xy} = \frac{h^{o^3}}{12} C_{33}^{o} \frac{2\partial^2 w}{\partial x \partial y} + \frac{h^{b^3}}{12} C_{33} \frac{\partial^2 w}{\partial x \partial y} \qquad \ldots (6.15)$$

All 'C' and 'h' of these equations can be combined to be written in a more compact form as:

$$D_{11} = \frac{h^{o^3}}{12} C_{11}^{o} + \frac{h^{b^3}}{12} C_{11}^{b}$$

$$D_{12} = \frac{h^{o^3}}{12} C_{12}^{o} + h^{b^3} C_{12}^{b} = D_{21}$$

$$D_{22} = \frac{h^{o^3}}{12} C_{22}^{o} + h^{b^3} C_{22}^{b}$$

$$D_{33} = \frac{h^{o^3}}{12} C_{33}^{o} + h^{b^3} . C_{33}^{b} \qquad \ldots (6.16)$$

The equations can then be written as

$$M_x = -D_{11}\left(\frac{\partial^2 w}{dx^2} + \frac{\alpha . \Delta T}{h}\right) - D_{12}\left(\frac{\partial^2 w}{\partial x^2} + \frac{\alpha . \Delta T}{h}\right)$$

$$M_y = -D_{21}\left(\frac{\partial^2 w}{\partial x^2} + \frac{\alpha . \Delta T}{h}\right) - D_{22}\left(\frac{\partial^2 w}{\partial y^2} + \frac{\alpha . \Delta T}{h}\right)$$

and

$$M_{xy} = 2D_{33} \frac{\partial^2 w}{\partial x \partial y} \qquad \ldots (6.17)$$

Equations 6.17 can be written in matrix form as

$$\begin{Bmatrix} M_x \\ M_y \\ M_{xy} \end{Bmatrix} = \begin{bmatrix} D_{11} & D_{12} & 0 \\ D_{21} & D_{22} & 0 \\ 0 & 0 & D_{33} \end{bmatrix} \begin{Bmatrix} -\frac{\partial^2 w}{\partial x^2} + \frac{\alpha \Delta T}{h} \\ -\frac{\partial^2 w}{\partial x^2} + \frac{\alpha \Delta T}{h} \\ 2\frac{\partial^2 w}{\partial x \partial y} \end{Bmatrix} \qquad \ldots (6.18)$$

Or symbolically,

$$\{M\} = [D]\{\chi\} + [D]\{\chi_0\} \qquad \ldots (6.19)$$

Thus, it is seen again that equation 6.19 is of the same form as equation 4.11 or equation 5.16. Therefore the formulation proposed in those chapters after these equations are also valid hereafter.

6.5.3 Modeling of Cracked Base

The modelling of cracked base can be done exactly in the way described in article 5.6 for bonded overlays. However, in the present case there is no bond at the interface between the overlay and base. Therefore, it is possible that the effect of stress release in the base might extend for a larger distance than equal to the thickness of the cracked base. This distance can be incorporated in the analysis, based on further detailed investigations, as carried out by Beeby[104] for slabs and beams which is applicable to monolithic construction i.e. bonded overlay.

However, in the present analysis the zone of stress release is supposed to extend upto a distance equal to the depth of crack on its either side.

6.6 MODIFICATION AND TESTING
6.6.1 Modification of Computer Program

First stage of modification of the computer program reported to have been coded in Chapter IV was described in Chapter V, wherein modification required for

incorporating bonded overlays was aimed. Modification for incorporating unbonded overlays is exactly on the same lines.

6.6.2 Testing of Modified Program

It is proposed to test the program directly by comparing the results of proposed analytical investigations with those of modified Westergaard's solution. Westergaard's solution procedure is modified by finding the value of rigidity by equation 6.16 and determining the value of 'ℓ' i.e. radius of relative stiffness from this. The comparative values of these two sets are shown in Table 6.1.

The material properties for overlay and base, the pavement dimensions in length and width, the wheel loads and the subgrade properties are assumed identical to those adopted in chapter V. The finite element discretisation was similar to that shown in Chapter V.

6.7 ANALYTICAL INVESTIGATIONS

The analytical investigations proposed are similar to that described in article 5.8. Based on the experience of article 5.9, a 6 cm unbonded overlay is too thin to be a practical proposition and the limitation of computer time for this study only one overlay thickness i.e. of 10 cm is analysed by finite element method. 6 cm overlay is analysed by modified Westergaard's and Bradbury's approach

to compare the values with bonded overlays.

6.8 RESULTS AND DISCUSSIONS

The results of analyses for the cases described above are presented in the form of graphs and tables and are discussed below:

6.8.1 Analysis of Stresses and Deflections in Pavement Slabs with Overlay on Sound Base, Under Wheel Load at Edge.

Figures 6.1(b) and 6.1(c) compare the variation of deflection and slope along edge of the pavement having 10 cm overlay on 8 cm base with that having the same overlay on 16 cm base when the wheel load is placed at the centre of the edge in both the cases.

Figure 6.2 shows the variation of moments along edge in a pavement with 10 cm overlay on 8 cm base to one with 16 cm base. Similarity between this figure and figure 7 of Chapter V is obvious. The remarks relating to these figures made in article 5.9.1 also hold here.

Table 6.2 is made on the basis of modified Westergaard's method (Appendix 5.B). It is seen from Table 6.1 that the results of finite element method agree well with those of modified Westergaard's approach. Results in Table 6.2 can therefore be regarded as acceptable. It is seen from this table that the maximum moment value increases as the base thickness increases for bonded

as well as for unbonded case. It is also seen that the
values of maximum moments for 10 cm overlay on 12 cm
base is close to that of 6 cm overlay on 16 cm base in
bonded case as was discussed in article 5.9.1. However,
this is not so in unbonded case. On the contrary, in
unbonded case the maximum moment on pavement slab with
10 cm overlay with 12 cm base and that on 6 cm overlay
on same base is very nearly the same. The reason for this
is that the increase in rigidity is very slight due to
extra 4 cm of unbonded overlay the modulus of elasticity
of which is only half of that of base. As a result, the
radius of relative stiffness in the two cases are 46.7 and
44.5 cm respectively in unbonded case. These values
for bonded case are 63.1 and 54.7 cm respectively. Thus,
it is seen that whereas the modulus of elasticity of the
overlay has relatively less effect in bonded overlay
and the dimension is more important, in unbonded construct-
ion the modulus of elasticity is important. It could also
be stated that in case of unbonded overlays, the pavement
behaviour is governed more by the layer which is of greater
rigidity.

Also, comparing maximum values of moments in 10 cm
overlay on 16 cm base with the pavement slab where overlay
is 6 cm, it is seen that the value for 6 cm overlay on
16 cm base is greater than 10 cm overlay on 16 cm base.
The values of radius of relative stiffness 'ℓ' are 54.7
and 55.9 cm respectively. However, in Westergaard's

equation the stress is a function of 1/b, where 'b' is equivalent radius of contact[24]. Accordingly, the values of 1/b for the two cases work out as 4.26 and 4.32 respectively. This explains why the value of maximum moment is greater in case of 6 cm overlay on 16 cm base than 10 cm overlay on 16 cm base.

Table 6.2 also shows that the values of maximum moment in pavement slabs with unbonded overlay in above two cases is almost same, and the stresses in the thicker overlay is more although the base thickness is same. This can be viewed as follows.

According to basic moment-curvature relationship:

$$\frac{M}{EI} = \frac{1}{R} = \text{curvature}$$

Since, curvature is constant as per assumption 3,

$$\frac{M_o}{M_b} = \frac{E_o I_o}{E_b I_b} \qquad \dots (6.20)$$

and

$$M_o + M_b = M \qquad \dots (6.21)$$

Therefore moments are distributed among overlay and base in proportion to their rigidities. Thus 10 cm overlay carries moment in proportion of 1:8.192 whereas the 6 cm overlay will carry 1:38.

If analysed by the method proposed by Marcus and Palmer[223] the stresses in the overlay are 5.776 and 2.59 kg/cm^2 for 10 and 6 cm overlay respectively on 16 cm base slab.

By adopting proposed Modified Westergaard's procedure these are 8.0 and 5.32 kg/cm^2 respectively. The values as obtained from Marcus and Palmer formulae are given in Table 6.3.

If a comparison is sought between bonded and unbonded overlays, it may be seen that moments in bonded overlay for any combination of base and overlay is higher. But the maximum tensile stress at the bottom fibre of the base is far in excess in unbonded case. Moreover, in the range of proposed analytical study (article 5.8 and 6.7), the tensile stresses do not develop in the bonded overlay.

It can also be seen that except for 10 cm overlay on 8 cm and 12 cm base, the maximum compressive stresses in the top fibre of the overlay have greater magnitude in case of bonded overlays than unbonded overlays. This probably is again due to the facts that in unbonded case the overlay gets less share of moment (equation 6.20) in all above cases and also that the stress is function of distance from neutral axis. This distance is small in unbonded overlay.

6.8.2 Temperature Stresses

It is realised that Bradbury's approach can be applied to determine temperature stresses. Table 6.3 shows the moments and stresses generated in base and overlay due to this. It is seen that the overlay stresses

decrease as the base thickness increases.

6.8.3 Effect of Cracked Base on Stresses

Figures 6.3a and 6.3b compares the deflections
and slopes in 10 cm overlay on 16 cm base for cracked
and uncracked conditions. It is seen that the deflect-
ion under load has increased due to existance of crack.
Also the slope as well as the rate of change of slope
has become high, thus increase in curvature will take
place.

Figure 6.4 compares moments developed along the
edge of pavement slab having 10 cm overlay on 8 cm base
for cracked and uncracked conditions. Figure 6.5 is
for the case when base is 16 cm thick. It is seen that
in both the cases the value of maximum positive moment
developed under the wheel load reduces on having cracked.
Whereas, in case of 10 cm overlay on 8 cm base the
ratio of uncracked to cracked moment is 0.8, that in
case when base is 16 cm thick is 0.487. This indicates
that the reduction in moment is greater on a thick base
when it gets cracked. This is due to the fact that on
having cracked the thick base which was carrying greater
moment loses it moment carrying capacity. This is some-
what similar to moment release due to cracking (article
5.9.2.1) observed in case of bonded overlays. Physically,
this phenomenon means that greater support is provided
by a thicker slab than a thinner one even in cracked

conditions.

Principles of 'Beams on Elastic Foundation'[101]
can be applied to those cases i.e. to the cases when the
beam is supposed to have two layers of similar thicknesses
as base and overlay and their material properties are
also supposed to be same as those of the layers of pave-
ment slab. However, the load representation does pose
difficulty and therefore, it is assumed that the load is
of same magnitude as wheel load. It is applied as knife
edge load with width equal to dual tyres i.e. 50 cm. The
width of the beam is also assumed to be 50 cm. The formula-
tion and solution is described in Appendix 'A'.

Figures 6.6 and 6.7 show the comparison of stresses
at the top of 10 cm overlay when it is resting on 12 cm
and 8 cms bases in uncracked and cracked conditions. It
can be seen that there is a tremendous increase in the
maximum top fibre stress of the overlay when the base is
considered as cracked. Comparing it with the Figure 5.17
where variations were plotted for same conditions but
for bonded interfacial condition, it is seen that the
increase in stress on cracking is far more in unbonded
condition than in the bonded condition. This observation
is also in line with the findings of Chapter III where it
was observed that the stress increase on cracking was
far more when in the analysis the bond was supposed to
have been lost in the vicinity of the crack.

Figure 6.5 compares the variation of moments along edge in pavement slabs having 10 cm overlay on 8 cm cracked base to that when the cracked base is of 16 cm thickness. Figure 6.8 compares the variation of top fibre stress in overlay for these two cases. It is seen that as stated above, the thickner base has a beneficial effect and an increase of 8 cm in base thickness, though cracked, reduces overlay stress by almost 12 kg/cm^2 which is about 30 percent of the maximum stress.

6.9 CONCLUSIONS

The results as discussed in article 6.8 leads to following general conclusions regarding overlays:

1. The formulation envisaged in this chapter is a realistic and rational method for determination of wheel load stresses in an overlay provided on a sound or cracked base with a thin separation course in between to act as a bond breaker. The pavement slab may have any dimension, the overlay and base may have different sizes and different elastic properties, the wheel loads can be of any size and magnitude and any number of them can be placed anywhere and the crack may have any size, shape or location.

2. It is seen that a modification, which is based on 'equivalent radius of relative stiffness' can be used to determine the maximum stresses in an unbonded base

overlay system. A flow diagram of a small and economical computer program is included in appendix 5.B which is applicable for bonded as well as for unbonded overlays.

3. It is shown for the case of sound base, and overlay that a thicker overlay may not necessarily result in reduction of stresses in the overlay. Same statement is also true for base i.e. if the overlay is much more rigid than the base, then a slight increase in base thickness may not reduce the stresses in it, on the other hand it may increase. But the stresses in overlay would reduce in that case.

4. If the base is cracked then the above conclusion does not hold. An overlay on a thicker base positively has less stresses.

5. Stresses greatly increase in the overlay when the base is considered as having a crack. This increase is far more in excess than that where the base and overlay was considered as bonded.

6. Even in case of sound base and overlay the maximum stresses at the section reduce considerably when the overlay is considered as bonded to the base. From these considerations, it may be safe to allow the bond to develop of its own, if it does so, when the overlay is designed on the basis of no bond at interface.

7. It is shown in Appendix 6A that it is possible to derive expressions to solve the problem of 'Cracked

Beams on Elastic Foundation' and its behaviour is exactly similar to that of 'Cracked Slab'. Therefore, the procedure described in Appendix '6.A' can be used as a guide, both for bonded as well as unbonded case and for both the condition i.e. when base is sound and when it is cracked.

8. Bradbury's solution can be adopted to determine stresses in overlay and base , by the procedure as proposed in Appendix 5.C.

APPENDIX 6.A.

ANALYSIS OF CRACKED BEAM WITH OVERLAY ON ELASTIC FOUNDATION

Figure 6.9 shows a beam having two layers and resting on an elastic foundation. Following general assumptions are supposed as valid:

1. Assumptions (i), (ii) and (iv) stated in article 4.2 with respect to slab is also supposed to hold good for beams.

2. Load is assumed as knife edge load acting at the centre of the beam.

3. The crack is in one of the beams, at its centre and extends for its entire depth.

4. The crack can be modeled as discussed in articles 4.5 and 5.6.

5. The origin of coordinates is assumed at centre of the beam.

The differential equation governing the deformation and equilibrium of the beam on elastic foundation, under the validity of the assumptions 1, 2 and 5 stated above is: [101]

$$EI \frac{d^4 w}{dx^4} = -wK\beta \qquad \qquad \dots (6.22)$$

where, w = deflection of any point 'x' of the beam

B = width of the beam,

K = modulus of subgrade reaction,

P = load at centre.

= characteristic length

$$\frac{1}{\lambda} = \sqrt[4]{\frac{4EI}{K.B}}$$ ... (6.23)

EI = rigidity of beam.

The solution of equation 6.22 is,

$$w = e^{\lambda x}(C_1 \cos\lambda x + C_2 \sin\lambda x) + e^{-\lambda x}(C_3 \cos\lambda x + C_4 \sin\lambda x)$$
... (6.24)

But it is known that

$$\frac{e^{-\lambda x} + e^{\lambda x}}{2} = \cosh \lambda x$$

and $$\frac{e^{\lambda x} - e^{-\lambda x}}{2} = \sinh\lambda x$$

Therefore, $e^{\lambda x} = \cosh \lambda x + \sinh \lambda x$

and $e^{-\lambda x} = \cosh \lambda x - \sinh \lambda x$

Substituting these values in equation (6.24)

$$w = A \cosh \lambda x \cos \lambda x + B \cosh \lambda x \sin \lambda x + C \sinh \lambda x \cos \lambda x$$
$$+ D \sinh \lambda x \sin \lambda x$$ ... (6.25)

where, $A = C_1 + C_2$,

$B = C_2 + C_4$,

$C = C_1 - C_3$ and

$D = C_2 - C_4$ ... (6.26)

If for $a < x < b$

A,B,C,D= constants in equation (6.26)

M = moment at any section

θ = slope

S = shear to the left of any section and for
0 < x < a

λ = characteristic length

K_1 = subgrade reaction
= modulus of subgrade reaction x width of the beam

w_1 = deflection

$E_1 I_1$ = rigidity of the overlay

A_1, B_1, C_1, D_1 = constants in equation 6.26

$θ_1$ = slope

M_1 = moment at any section

then, for a < x < b

by differentiating equation 6.25 w.r.t. x and rearranging

$$θ = slope = \frac{dw}{dx} = -\left[(A-D)\cos h\,λx.\,\sin λx - (A+D)\sinh λx\,\cos λx\right.$$
$$\left. -(B+C).\cosh λx\,\cos λx - (B-C)\,\sinh λx.\sin λx\right]$$

... (6.27)

and curfature,

$$\frac{d^2w}{dx^2} = -2λ^2\left[A.\sinh λx.\sin λx - B.\sinh λx\,\cos λx\right.$$
$$\left. +C.\cosh λx.\sin λx - D.\cosh λx.\cos λx\right] ... (6.28)$$

Similarly, further differentiating equation (6.28)
w.r.t. x and rearranging,

$$\frac{d^3w}{dx^3} = -2\lambda^3 \left[(A+D)\cosh \lambda x . \sin \lambda x + (B+C).\sinh \lambda x.\sin \lambda x \right.$$
$$\left. -(B-C).\cosh \lambda x.\cos \lambda x+(A-D).\sinh \lambda x.\cos \lambda x \right] \dots (6.29)$$

Now, considering the part between x = 0 to x = a. In this part it is assumed that on account of the stress release due to the crack, the base does not carry any stress. The value of 'a' would be equal to 'h_b' where 'h_b' is base thickness. This is in line with the discussions of article 4.5 and 5.6.

The equation 6.26 for this part can be written as

$$w = A_1.\cosh \lambda_1 x.\cosh \lambda_1 x + B_1\cosh \lambda_1 x.\sin \lambda_1 x+C_1.\sinh \lambda_1 x.\cos \lambda_1 x$$
$$+D_1\sinh \lambda_1 x.\sin \lambda_1 x.$$

It can be seen from the assumptions that 'w' has to be a symmetric function 'x',

Therefore,

$$B_1=0 \; ; \; C_1= 0, \text{ and}$$

$$w_1 = A_1\cosh\lambda_1 x.\cos\lambda_1 x + D_1\sinh\lambda_1 x.\sin\lambda_1 x \qquad \dots (6.30)$$

By differentiating w.r.t. 'x' and rearranging,

$$\theta_1 = \frac{dw_1}{dx} = \lambda_1 \left[(A_1 +D_1).\sinh\lambda_1 x.\cos\lambda_1 x - (A_1-D_1)\cosh\lambda_1 x.\sin\lambda_1 x \right] \dots (6.31)$$

$$\frac{d^2w_1}{dx^2}= 2\lambda_1^2 \left[D_1\cosh\lambda_1 x.\cos\lambda_1 x-A_1.\sinh\lambda_1 x.\sin\lambda_1 x \right] \dots (6.32)$$

It can be seen that there are six unknowns, viz.

A,B,C,D,A_1,D_1.

Following boundary conditions can now be applied to evaluate the unknowns,

     (1) at x = a,   w = w_1

     (2) at x = a, $\theta = \theta_1$

     (3) at x = a,   M = M_1

     (4) at x = b,   M = 0

     (5) at x = b, shear force S = 0 and

     (6) for equilibrium sum of all vertical forces
         must vanish, accordingly $\sum v = 0$

     Applying, these conditions

     from condition (1) at x = a, w = w_1, therefore from equations (6.25) and (6.30).

A.coshλa.cosλa+B.coshλa.sinλa+C.sinhλa.cosλa
+D.sinhλa.sinλa

= A_1.coshλ_1a.cosλ_1a+D_1.sinhλ_1a.sinλ_1a   ... (6.33)

From condition (2), at x = a, $\theta = \theta_1$
therefore from equations 6.27 and (6.31),

λ[(D-A).coshλa.sinλa+(A+D).sinhλa.cosλa+(B+C)coshλa.cosλa
   +(B-C).Sinhλa.sinλa]

= λ_1[(A_1+D_1).sinhλ_1a.cosλ_1a+(D_1-A_1)coshλ_1a.sinλ_1a]

                                         ... (6.34)

From condition (3), at x = a, M = M_1,
Therefore, from equations (6.28) and (6.32)

$$-2EI\lambda^2 [A.\sinh\lambda a.\sin\lambda a - B.\sinh\lambda a.\cos\lambda a + C.\cosh\lambda a.\sin\lambda a$$
$$-D.\cosh\lambda a.\cos .\lambda a]$$

$$= -2E_1 I_1 \lambda_1^2 [A_1 \sinh\lambda_1 a.\sin\lambda_1 a - D_1.\cosh\lambda_1 a.\cos\lambda_1 a]$$

$$\ldots (6.35)$$

From condition (4), at x = b, M = 0,

Therefore from equation (6.28),

$$-2EI\lambda^2 [A.\sinh\lambda b.\sin\lambda b - B.\sinh\lambda b.\cos\lambda b + C.\cosh\lambda b.\sin\lambda b$$
$$-D.\cosh\lambda b.\cos\lambda b]$$

$$= 0 \qquad\qquad \ldots (6.36)$$

From condition (5) at x = b, S = 0,

Therefore from equation (6.29):

$$(D-A).\sinh\lambda b.\cos\lambda b - (A+D)\cosh\lambda b.\sin\lambda b + (B-C).\cosh\lambda b.\cos\lambda b$$
$$+(B+C).\sinh\lambda b.\sin\lambda b$$

$$= 0 \qquad\qquad \ldots (6.37)$$

From condition (6), $\sum v = 0$ i.e. sum of all reactive forces to the right hand side of x = 0 must equal to half the active force.

Therefore,

$$K_1 \int_0^a w_1 dx + K \int_0^b w.dx = \frac{P}{2}$$

or

$$K_1 \int_0^a [A_1.\cosh\lambda_1 x.\cos\lambda_1 x + D_1.\sinh\lambda_1 x.\sin\lambda_1 x].dx +$$

$$K \int_0^b [A.\cosh\lambda x.\cos\lambda x + B.\cosh\lambda x.\sin\lambda x + C.\sinh\lambda x.\cos\lambda x$$
$$+D.\sinh\lambda x.\sin\lambda x].dx$$

$$= \frac{P}{2} \qquad\qquad \ldots (6.38)$$

On integrating and rearranging

$$\frac{K}{2\lambda} \big[(A+D)(\cosh\lambda b . \sin\lambda b - \cosh\lambda a . \sin\lambda a) + (A-D)(\sinh\lambda b . \cos\lambda b$$

$$-\sinh\lambda a . \cos\lambda a) + (B+C)(\sinh\lambda b . \sin\lambda b - \sinh\lambda a . \sin\lambda a)$$

$$-(B-C)(\cosh\lambda b . \cos\lambda b - \cosh\lambda a . \cos\lambda a) \big]$$

$$+ \frac{K_1}{2\lambda_1} \big[(A_1+D_1)\cosh\lambda_1 a . \sin\lambda_1 a.$$

$$+(A_1-D_1)\sinh\lambda_1 a . \cos\lambda_1 a \big]$$

$$= P/2 \qquad\qquad\qquad \dots (6.39)$$

Equations 6.33 to 6.39 can be rearranged and written
in the form:

$$[L]\{L_1\} = \{R\} \qquad\qquad \dots (6.40)$$

where, $[L]$ = coefficient matrix of known values,

$\{L_1\}$ = matrix of unknowns,

$\{R\}$ = vector of knowns

Values of $\{L_1\}$ can be obtained by finding inversion of $[L]$.

The appropriate value of deflection, slope, moment
or shear can then be determined by using equation 6.25 to
6.32.

Note:

1. Because of the large disparity in the numerical
   magnitudes between coefficients of matrix $[L]$,
   it is necessary to use double precision in
   floating point.

2.   Recognising that $\ell = 4\sqrt{\dfrac{D}{K}}$

      where D = rigidity 'D_{11}' as determined by either equation 5.14 or equations 6.16. The formulation has its applicability for beams with bonded as well as unbonded overlays.

3.   By choosing $K_1 = K$, the formulation becomes applicable to case when subgrade reaction is uniform all through the length of beam,

4.   By adopting $\lambda_1 = \lambda$, the formulation becomes applicable to uncracked beams.

5.   The applicability of this formulation to pavement slabs is more 'qualitative than quantitative'. However, use of beam action hypothesis to pavement slabs is already discussed (230). This formulation provides a rational procedure for solution of stresses and displacements in such a case.

6.   The formulation is particularly useful for determination of nominal stresses (Appendix '5.A') at the crack section in a beam on elastic foundation, being tested for crack propagation and fatique life studies. However, limitation due to assumption 4 must be accorded due recognition.

7.   Flow diagram for determination of moments and deflections at an interval of b/5 is included.

ANALYSIS OF SOME CASES OF NON-PRISMATIC
BEAMS IN BONDED AND UNBONDED CONDITIONS

Figure 6.10 shows the flow chart of computer program based on formulation discussed above.

The analysis is proposed on beams of same length, thickness and properties as the base and overlay of the pavement slab. The width of the beam is assumed as

50 cm., being the width of dual tyre and the load is
900 kg/cm.

Figure 6.11 is drawn to compare the 10 cm un-
bonded overlay to a base beam of 8 and 12 cm thickness.
It is seen that as observed earlier in case of pavement
slabs the moment in beam with 12 cm base is more. The
variation of moments along length of beam is similar to
that observed in case of moment along edge in pavement
slab with edge load. To have a check on formulation,
comparison is also shown in this figure with a standard
solution of an infinitely long beam. The characteristic
length 'λ' is determined for the non-prismatic beam
as in case of overlays (Appendix '5.B'). The length of
finite beam is 9 meters which fall in the category of
long beams[101]. The close agreement of the two curves in
the figure shows the correctness of the formulation for
uncracked beams with non-prismatic properties.

Figure 6.12 represents deflections in beams with
10 cm overlay having 8 cm base in sound and cracked
conditions. The trend of these curves are similar to
figures 5.8 and 6.3(b).

Moments for beams with 10 cm overlay and 8 cm
base in uncracked condition is compared for 2 cases in
figure 6.13, viz.   bonded case and unbonded case. These
are also compared to results of finite element analysis
for a pavement slab with 10 cm unbonded overlay on 8 cm

base. The moments are plotted along the edge for the edge loading. It can be seen that for beams, the maximum moment in bonded case is greater than in unbonded beam. This observation also holds for pavement slabs. Comparison with unbonded slab shows that the moments in slab is still lower but the nature of the variation of moment along the edge is same.

Figure 6.13 also shows the comparison between moments in beams with 10 cm overlay on 8,12 and 16 cm base. These curves are similar to those in figure 5.7.

Figure 6.14 compares moments in beams with 10 cm bonded overlays when base beam of 8,12 and 16 cm haing a central cracks. It is again seen that the diagram is similar to figure 5.13. Chapter V and remarks made there are upheld. The variation of moments along edge in pavement slab with 10 cm bonded overlay on 12 cm cracked base is also shown. The moments in cracked slab is lesser than in beam, though the behaviour in both the cases is similar.

The maximum negative moment in cracked beam acquires a high value, due to the moment that is released on cracking. In case of slabs. These values do not acquire such a magnitude.

In figure 6.15 a comparison is attempted between beam and slab with unbonded overlays of 10 cm thickness

when the base is having a crack. The variation in moments
for slabs, as obtained by finite element analysis, having
8 and 16 cm base is plotted and are compared with 'modified
moments' of beams. The modified moments are calculated
as follows.

The maximum moment 'M_s' as calculated by the modi-
fied Westergaard's approach for edge load given in
Appendix 5.B is determined in pavement slab with sound
base. The maximum moment, M_b and M_{b_1}, in beam with same base-
overlay combination in cracked and uncracked condition
respectively are also determined. The ratio $M_s : M_b$ is
calculated and the moment in beam in cracked condition
i.e. M_{b_1} is reduced in this proportion to determine
$M_{b_1} \times \frac{M_s}{M_b}$. This is termed as modified moment and plotted in
figure 6.15.

It can be seen that maximum values of modified
moments in beam and the maximum moment in cracked slab
match fairly well.

Table 6.4 gives moments in beams with overlays
in cracked and uncracked conditions ·

It is therefore, seen that by adopting this
simple procedure. The maximum moment in overlay on a
cracked base slab can be estimated from beam analysis.
Beam results are higher. In pavement the distribution of

bending moment along the other direction reduces the
deflections and bending moment. These factors can be
worked out only in simple cases such as edge loading
or at the centre.

TABLE 6.1

COMPARISON OF MAXIMUM MOMENTS BY MODIFIED
WESTERGAARD AND FEM

S.No.	Thickness (cm)		Moments (kg.cm/cm)	
	Overlay	Base	Modified Westergaard	FEM*
1	10	8	1006.72	1012
2	10	12	1129.67	1135
3	10	16	1229.70	1250

* Maximum values determined by extrapolation to the
centre of loaded area.

TABLE-6.2[*]
COMPARISON OF MOMENTS AND STRESSES

S. No.	THICKNESS (cm) Over-lay	Base	MAXIMUM MOMENT Bonded	Unbonded	STRESS IN[**] BONDED OVERLAY Top	Bottom	UNBONDED OVER-LAY Top	Bottom	STRESS IN[**] BONDED BASE Top	Bottom	UNBONDED BASE Top	Bottom
1	10	8	1263.2	1006.7	19.3	1.0	30.20	-30.20	1.9	-27.3	47.18	-47.18
2	10	12	1353.2	1129.7	13.6	2.9	15.21	-15.21	5.9	-19.7	36.50	-36.50
3	10	16	1414.8	1229.7	9.9	3.2	8.00	- 8.00	6.5	-14.8	25.618	-25.618
4	6	8	1129.7	919.5	27.9	7.2	26.51	-26.51	14.4	-40.7	87.58	-87.58
5	6	12	1270.4	1116.2	18.1	7.4	10.94	-10.94	14.9	-27.6	43.77	-43.77
6	6	16	1365.4	1247.3	12.4	6.3	5.32	- 5.32	12.6	-19.6	28.48	-28.48

* Based on modified Westergaard's results
** -ve sign indicates tension

TABLE 6.3

COMPARISON OF STRESSES BY MARCUS AND PALMER
WITH MODIFIED WESTERGAARD'S
PROCEDURE (Appendix 5.B)

S. No.	Case	Marcus and Palmer fomulae (kg/cm^2)		Modified Westergaard's Procedure (kg/cm^2)	
		Overlay	Base	Overlay	Base
1.	10 on 8	±26.23	±42.49	±30.20	±47.18
2.	10 on 12	±11.91	±36.26	±15.21	±36.50
3.	10 on 16	±5.77	±26.80	± 8.00	±25.62
4.	6 on 8	±17.58	±69.35	±26.51	±71.19
5.	6 on 12	± 5.94	±44.00	±10.94	±43.77
6.	6 on 16	± 2.59	±29.30	± 5.32	±28.40

TABLE 6.3A

MOMENTS AND STRESSES AS PER MODIFIED
BRADBURY'S APPROACH (APPENDIX 5.C)

S. No.	Case	ΔT(°C)	Total Moment	Moment		Stresses	
				Overlay	Base	Overlay	Base
1.	10 on 8	13°	221	109.0	112.0	±6.5 kg/cm^2	±10.50
2.	10 on 12	13.8	421	94.6	326.0	±6.67	±13.60
3.	10 on 16	14.5	770	83.7	684.0	±5.02	±16.06

TABLE 6.4

COMPARISON WITH BEAMS ON ELASTIC FOUNDATION

S.No.	Case	Westergaa- rd's value M_s	M_b	M_{b_1}	$M_{b_1} \times \frac{M_s}{M_b}$	Actual
1.	6 on 8 bonded	1130	1492	580	440	380
2.	6 on 12 bonded	1270	1864	384	262	350
3.	6 on 16 bonded	1365	2236	280	-	300
4.	10 on 8 bonded	1263	1770	1114	800	530
5.	10 on 12 bonded	1353	2108	893	560	460
6.	10 on 16 bonded	1414	2450	500	290	380
7.	10 on 8 unbonded	1006	1300	1170	900	820
8.	10 on 12 unbonded	1130	1640	890	612	706
9.	10 on 16 unbonded	1230	1856	1005	670	602

Note: M_s = values of moments obtained by Modified Westergaard's solution for uncracked case

M_b = values of moments obtained for beam in uncracked case,

M_{b_1} = value of moment obtained by 'cracked beam' formulation

$\frac{M_{b_1} \times M_s}{M_b}$ = Estimated value of moment in slab with cracked based obtained by simplified procedure,

Actual = value of moment in crack case obtained by finite element method
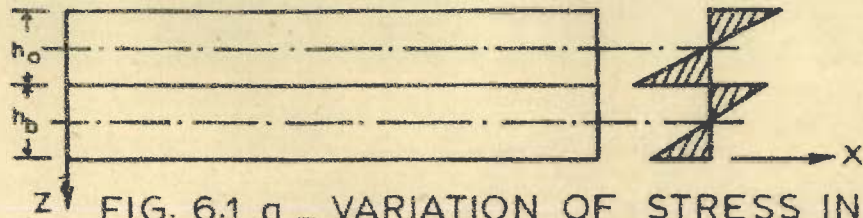
FIG. 6.1 a _ VARIATION OF STRESS IN CROSS SECTION OF BASE AND OVERLAY

O———O 10 cm OVERLAY ON 16 cm BASE
X———X 10 cm   „   „   8 cm   „

FIG. 6.1 b _ VARIATION OF DEFLECTION ALONG AB

Deflection _ cm

Distance _ cm

Slope x 10⁻³

FIG. 6.1c _ VARIATION OF SLOPE ALONG AB
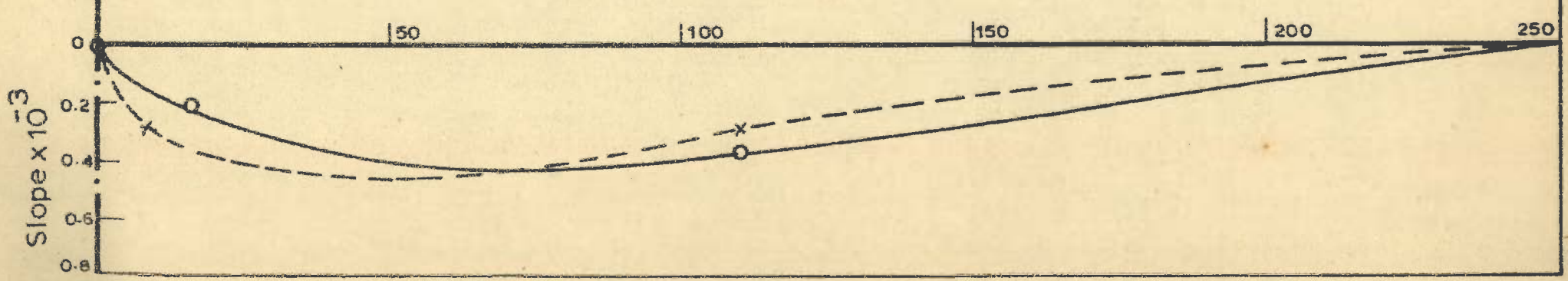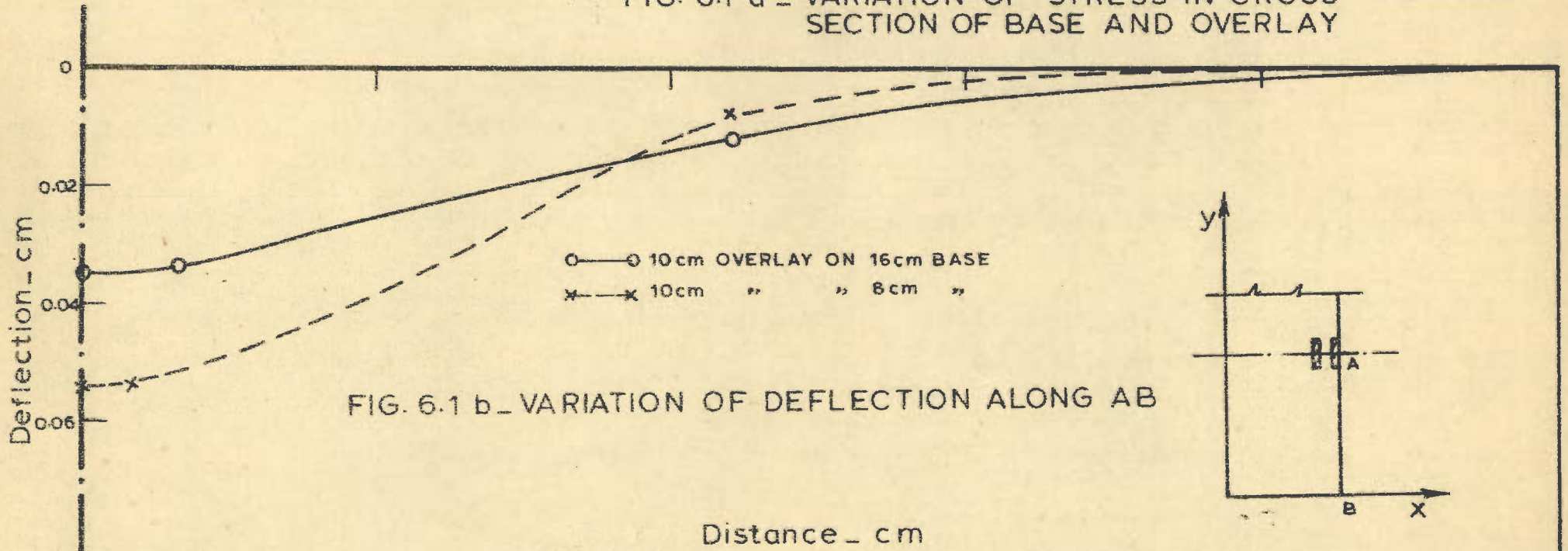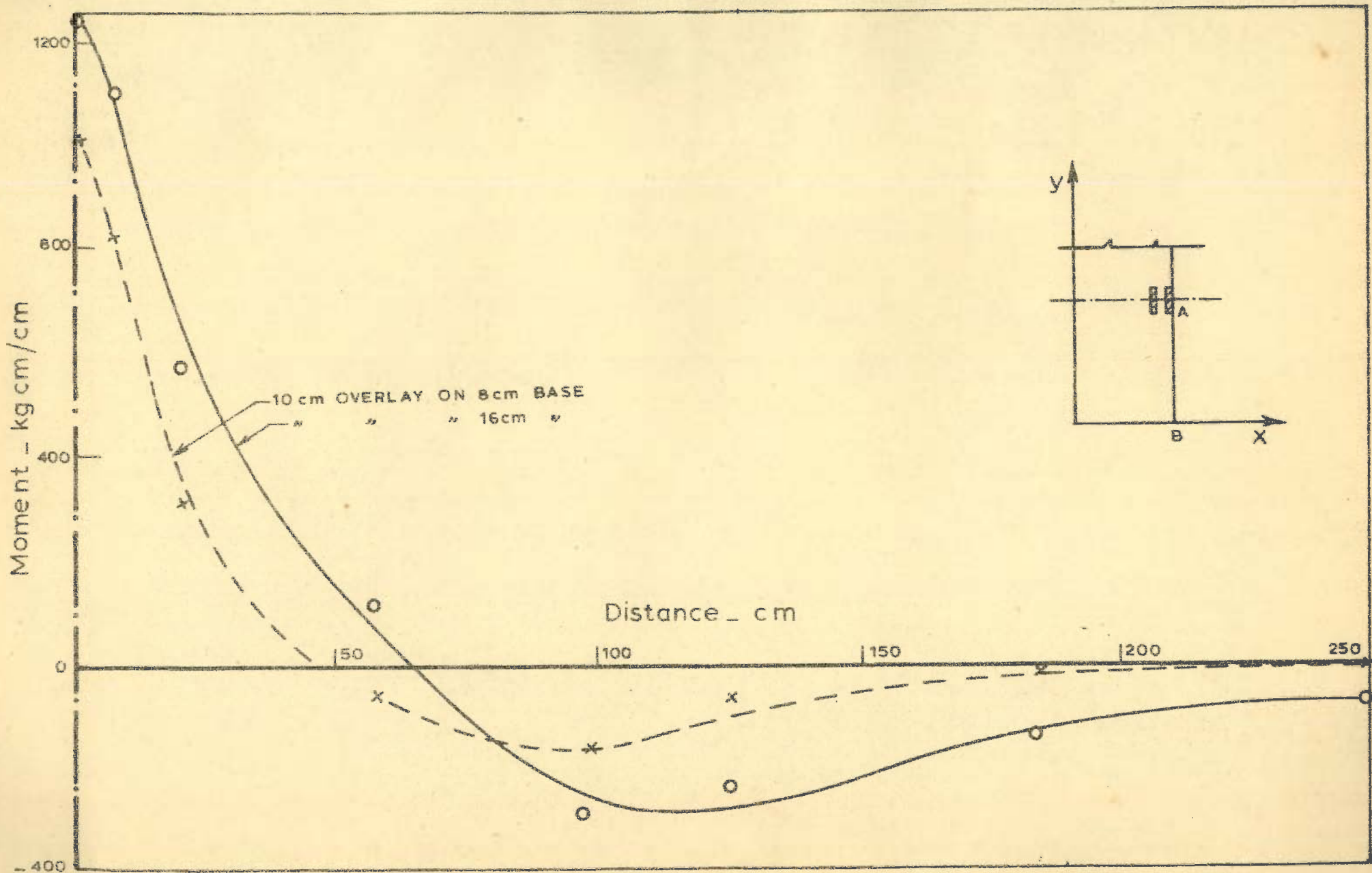
FIG. 6.2 _ VARIATION OF MOMENT M_y ALONG AB UNCRACKED BASE

Within the figure:

Moment _ kg cm/cm

1200

800

400

0

_ 400

Distance _ cm

50   100   150   200   250

10 cm OVERLAY ON 8cm BASE

"   "   "   16cm   "

y

x

A

B

Distance _ cm

Deflection _ cm

O————O 10cm OVERLAY ON 16cm SOUND BASE
✕——✕ 10cm ,,   ,, 16cm CRACKED BASE
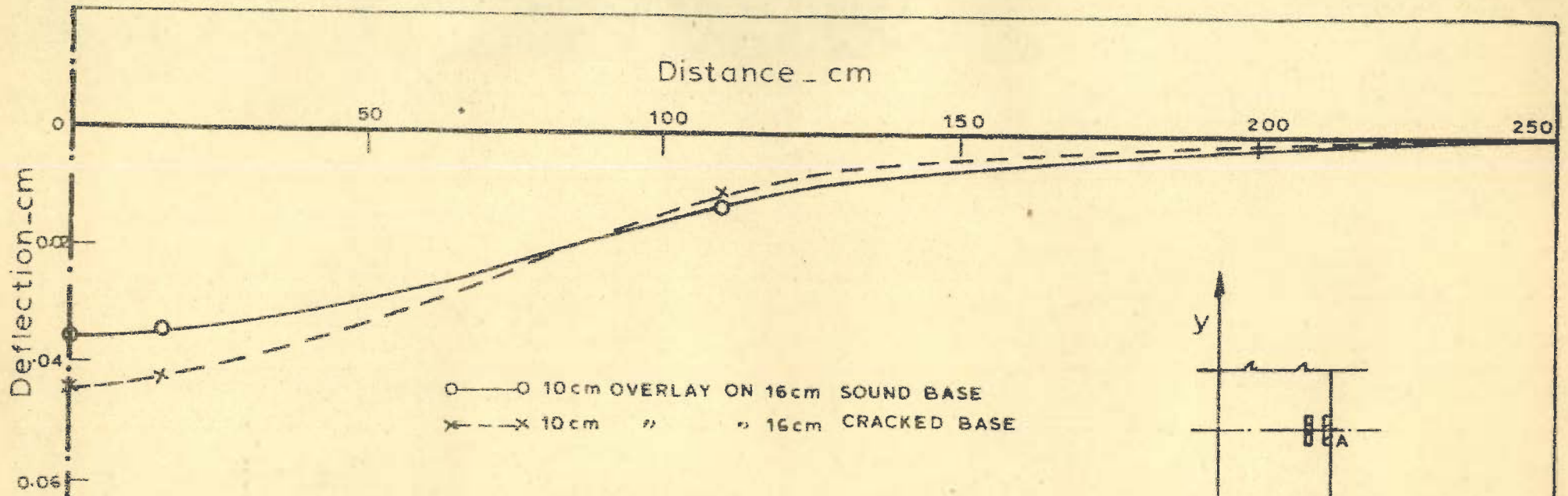
FIG. 6.3a_ VARIATION OF DEFLECTION ALONG AB

Slope x10⁻³
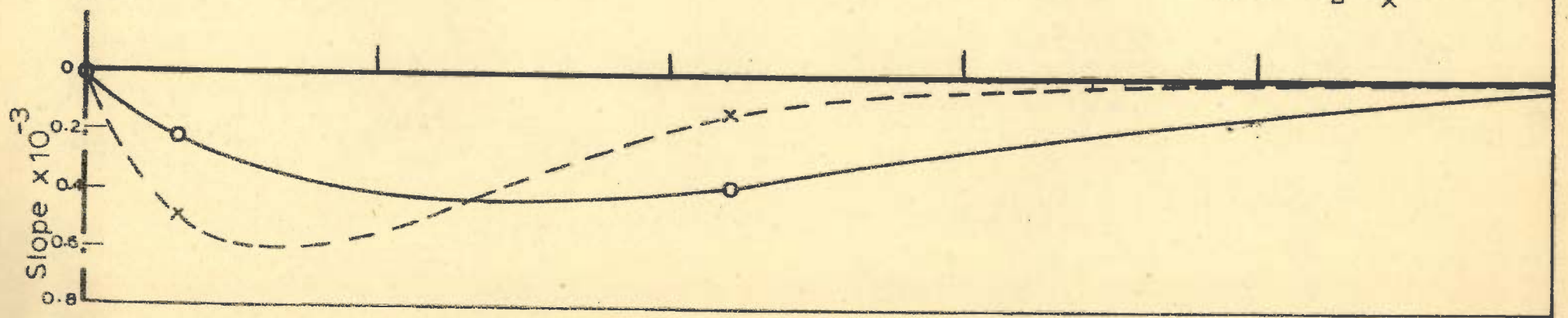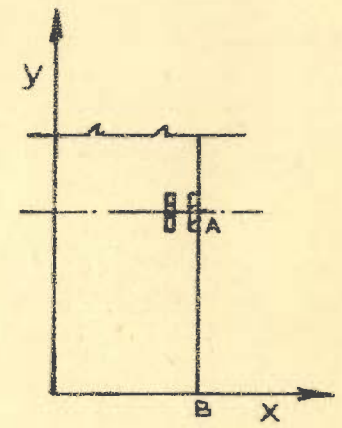
FIG. 6.3 b _ VARIATION OF SLOPE ALONG AB
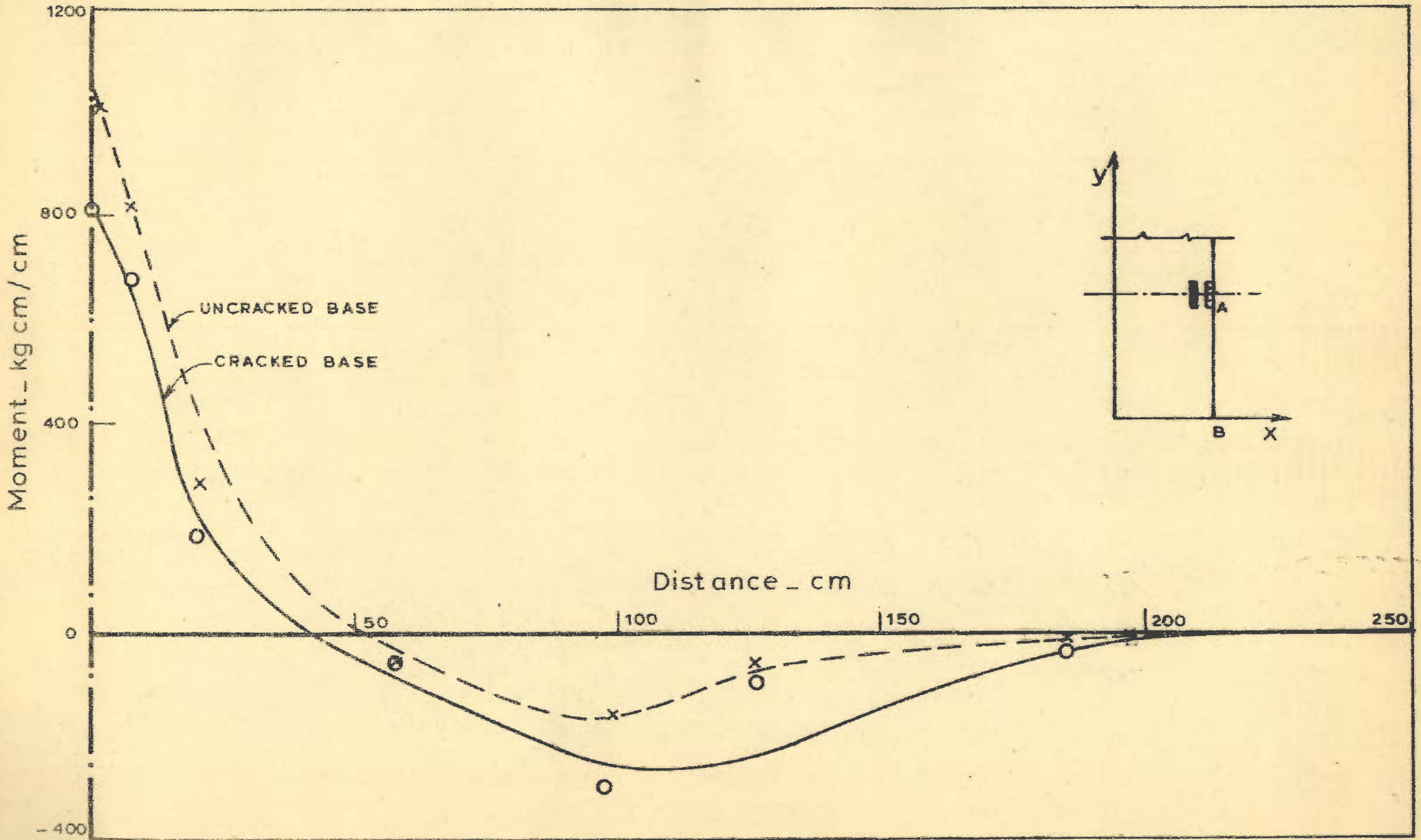
FIG. 6.4 _ MOMENTS IN 10 cm OVERLAY ON 8 cm UNBONDED BASE
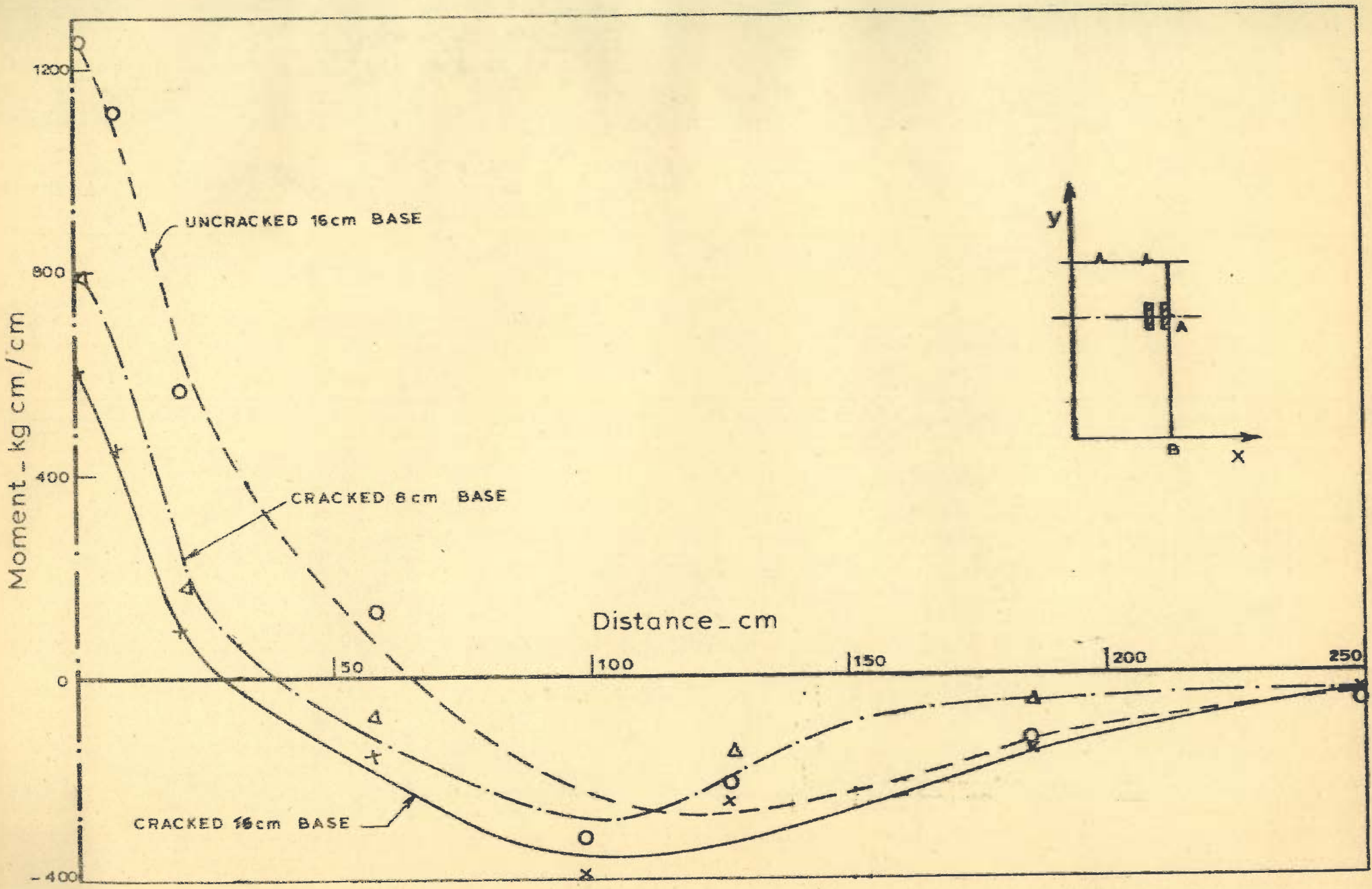
FIG. 6.5 _ MOMENT IN SLAB WITH 10cm OVERLAY ALONG A B.
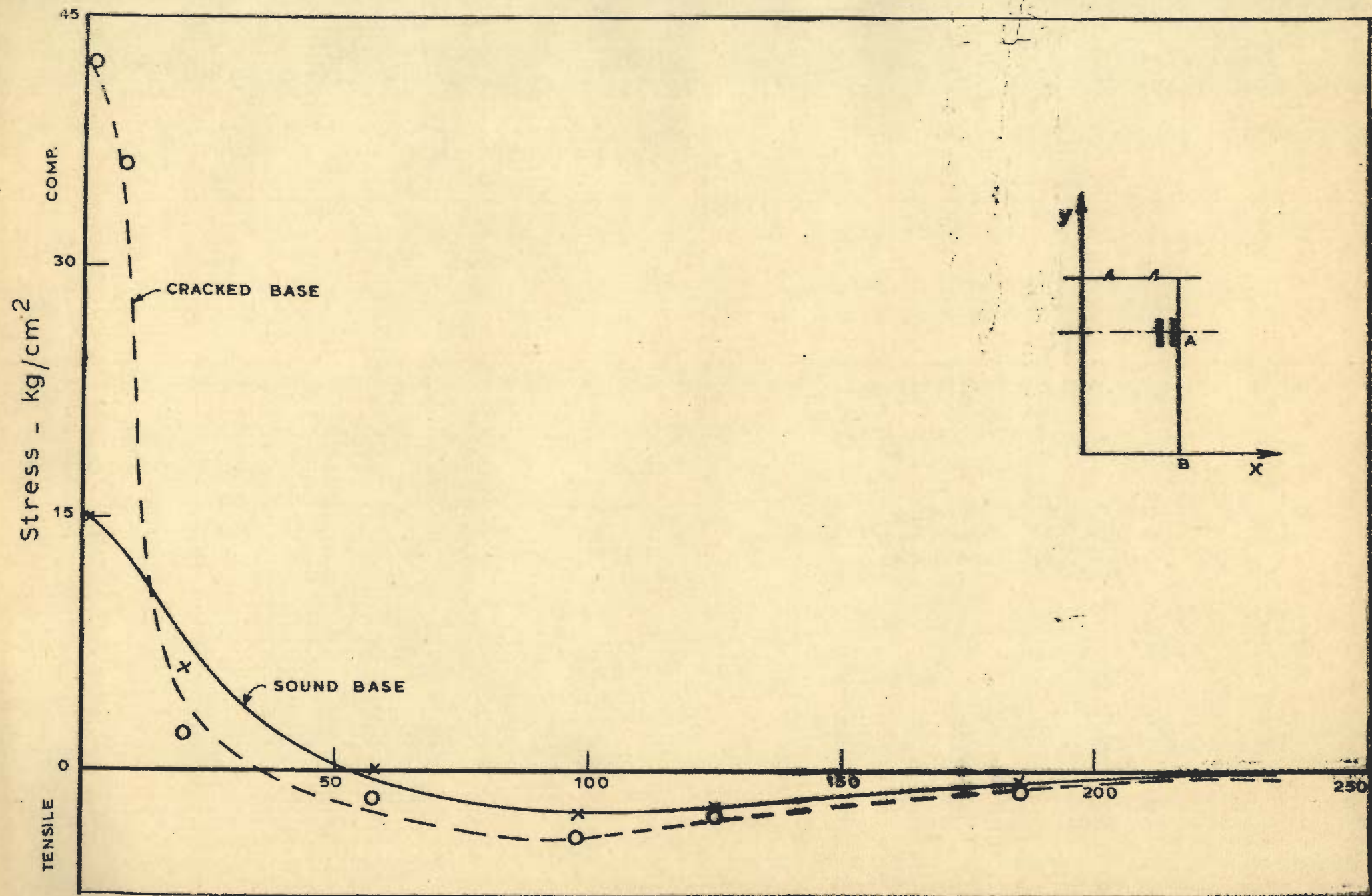
FIG. 6.6 _ FLEXURAL STRESS IN THE UNBONDED OVERLAY, 10 cm THICK ON 12 cm BASE
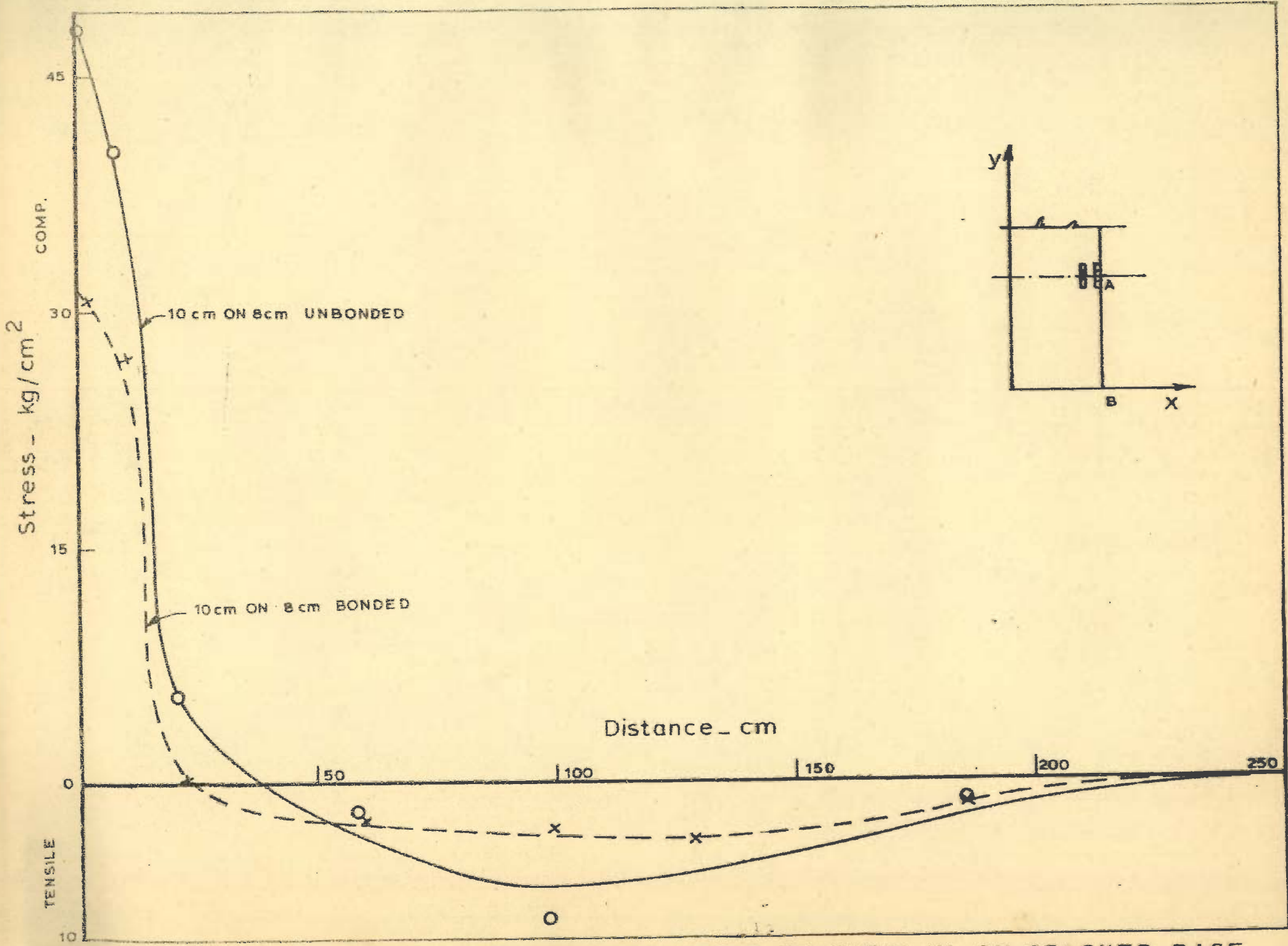
FIG. 6.7 _ FLEXURAL STRESSES AT THE TOP OF OVERLAY ON CRACKED BASE

295
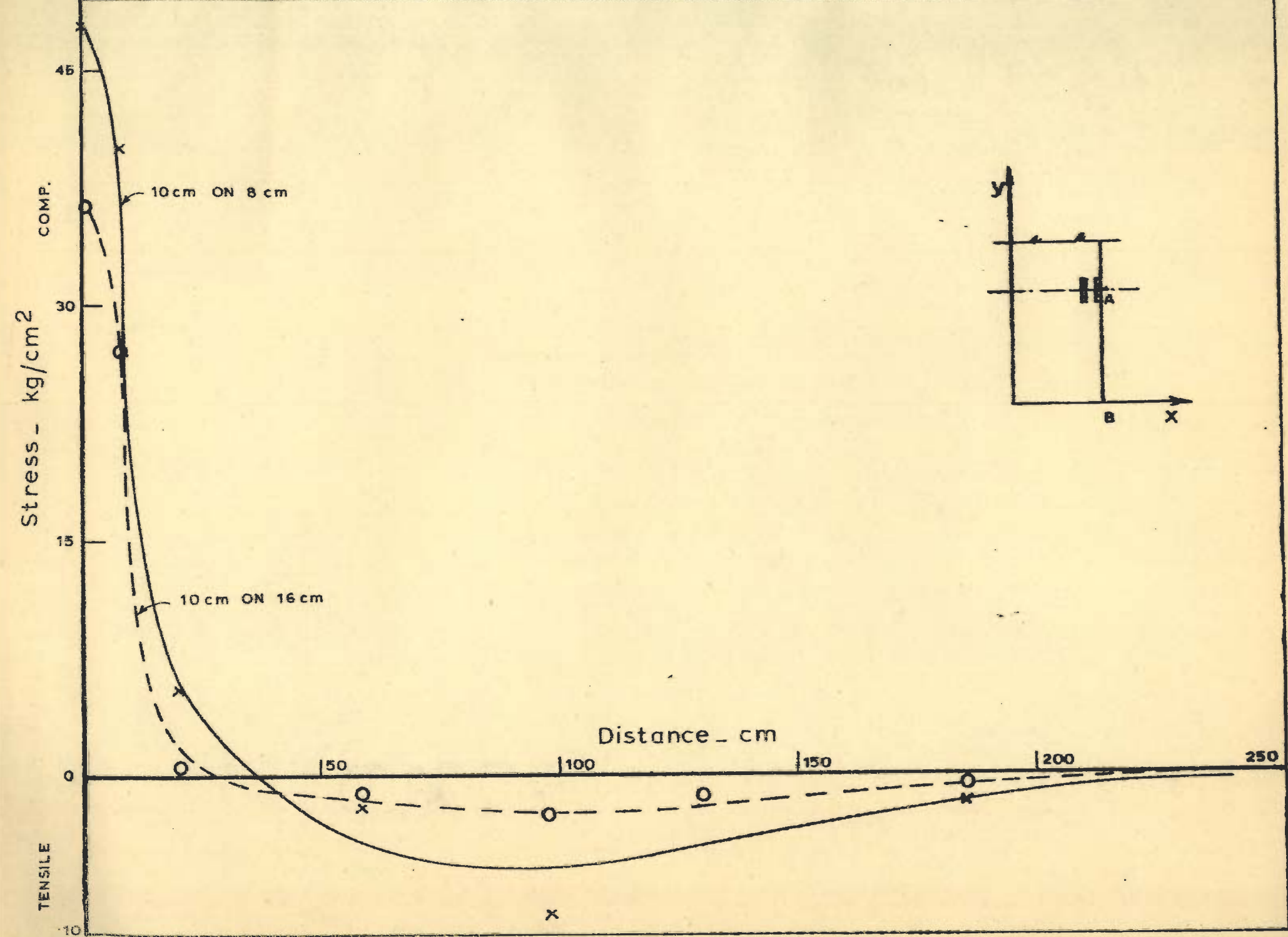
FIG. 6·8 - FLEXURAL STRESSES AT THE TOP OF UNBONDED OVERLAY ON CRACKED BASE
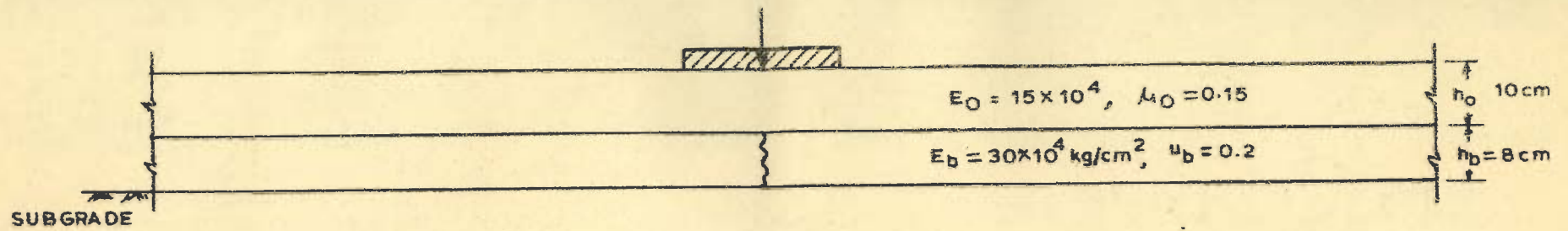
I — Section of pavement slab with overlay and cracked base
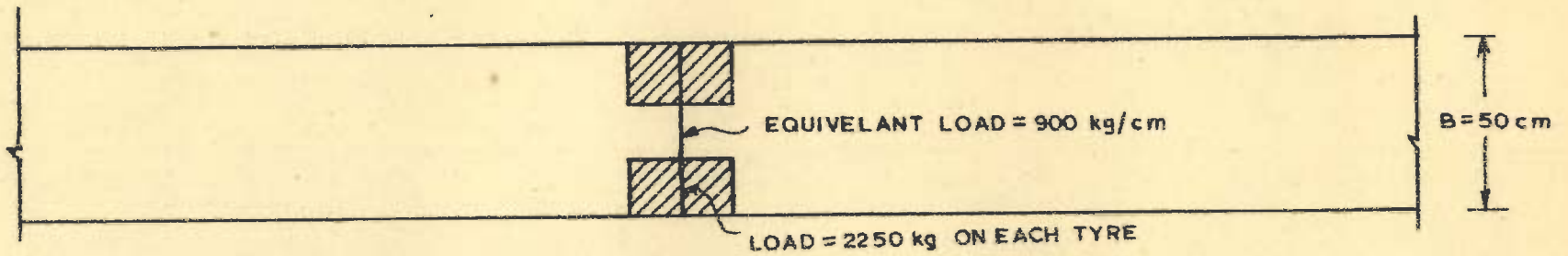
II — Plan of beam with load
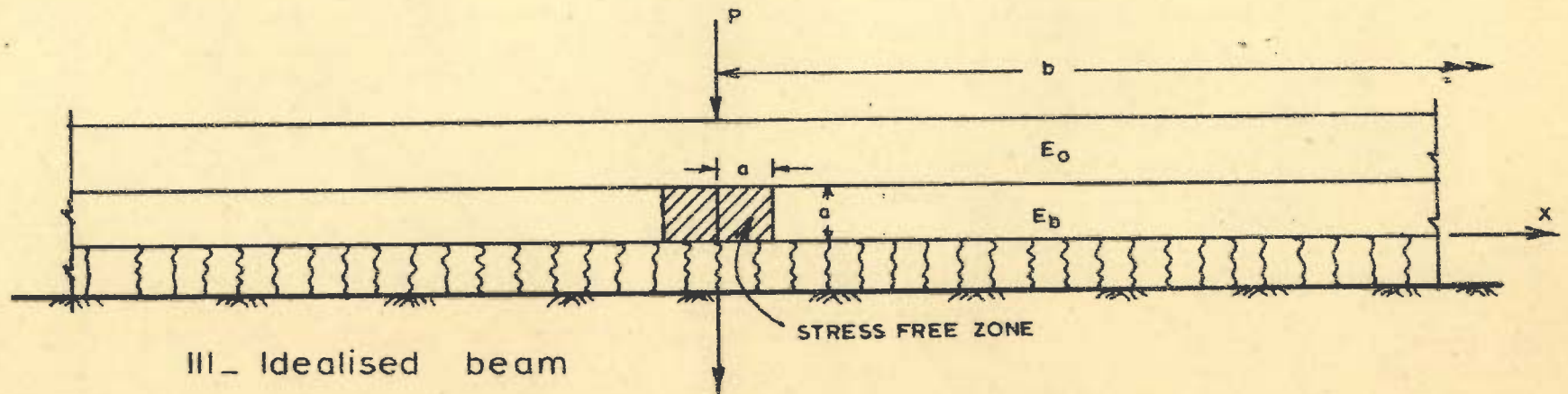
III — Idealised beam

FIG. 6.9 — CRACKED NON-PRISMATIC BEAM ON WINKLER FOUNDATION

FLOW CHART FOR 'CRACKED BEAM ON ELASTIC FOUNDATION' PROGRAM

START

READ, NC, NB, HO, HB, E^o, E^b, AK, B, AL, P

IF BONDED — NO

YES

IF CRACKED

IF CRACKED — NO

YES

NO

YES

CALCULATE 'EI' OF CRACKED AND UNCRACKED PART

CALCULATE 'EI'

CALCULATE 'EI'

CALCULATE 'EI' OF CRACKED AND UN-CRACKED PARTS

PUNCH TITLE

PUNCH TITLE

PUNCH TITLE

PUNCH TITLE

CALCULATE CHARACTERISTIC LENGTH λ AND λ_1

FORM EQUATION $[L]\{L_1\} = \{R\}$

DETERMINE $[L]^{-1}$

DETERMINE $\{L_1\}$

A

```
      ( A )
        |
        v
┌────────────────────┐
│ BACK SUBSTITUTE IN │
│ EQUATIONS          │
└────────────────────┘
        |
        v
┌────────────────────┐
│ DETERMINE MOMENTS  │
│ AND DEFLECTIONS AT │
│ AL/5, INTERVALS    │
└────────────────────┘
        |
        v
┌────────────────────┐
│ PUNCH, DEFLECTIONS │
│ AND MOMENTS AT     │
│ ALL POINTS         │
└────────────────────┘
        |
        v
    ( STOP )
```

FIGURE -6.10 FLOW CHART FOR 'CRACKED
BEAM ON ELASTIC FOUNDATIONS

DESCRIPTION- NC = Crack condition,

= 0, for no crack

= non-zero for crack at centre,

NB = bond condition

= 0, for no bonded or single beam

= non-zero for bonded

HO = thickness of overlay, E^o=modulus of elasticity
of overlay

HB = thickness of base, E^b = modulus of elasticity
of base

AK = Modulus of subgrade fraction

B = Width of beam,

AL = Length of beam

EI = Rigidity of beam

[L] = Coefficient Matrix of equation (6.40) in
text

{L} = Unknown vector

{R} = Active Load Vector

OUTPUT- Punches out moments and deflections at (i) centre
(ii) HB from centre,(iii) at every AL/5 distance from
centre.
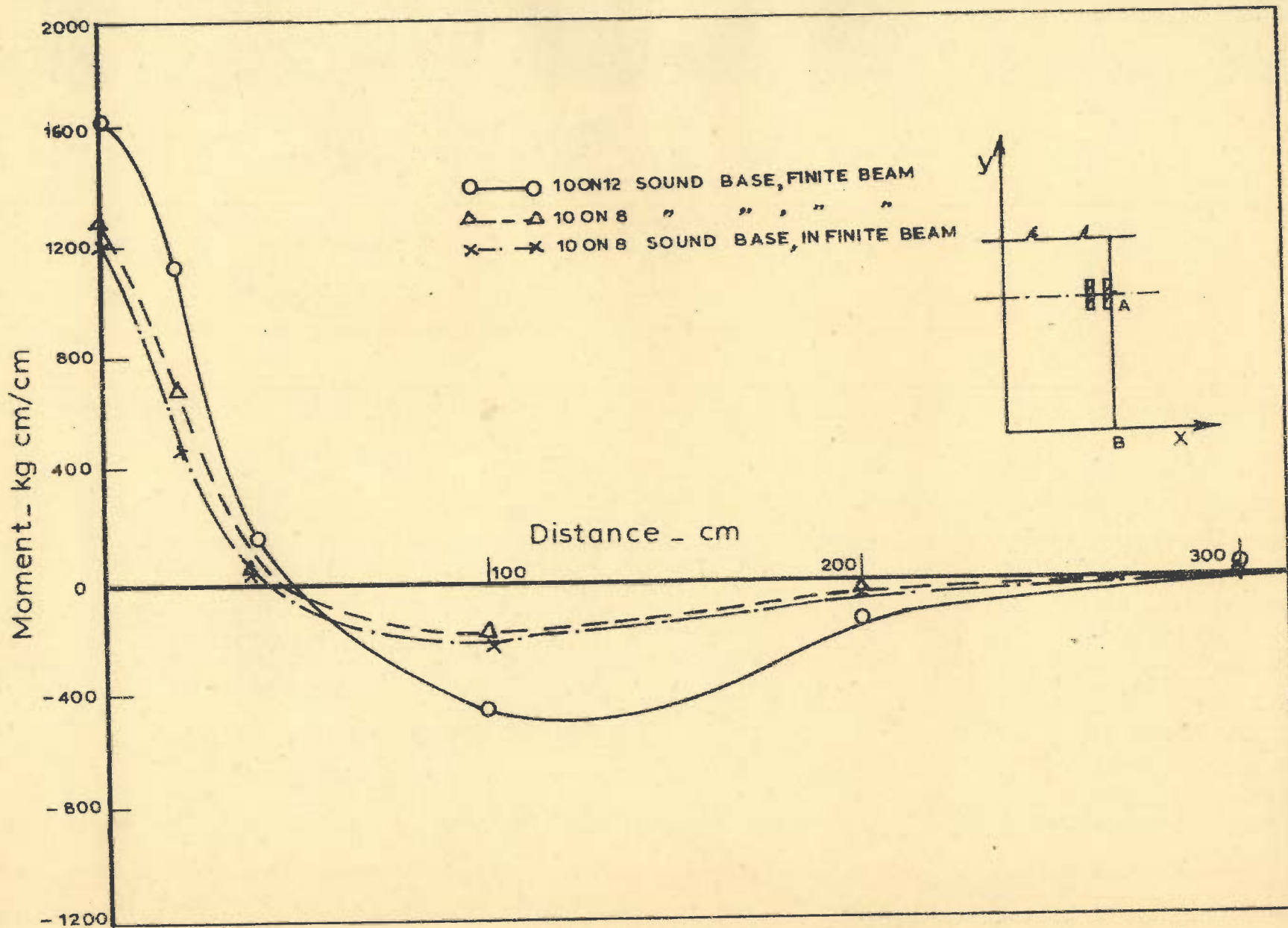
FIG. 6·11 _ MOMENTS IN LAYERD BEAMS IN UNBONDED CONDITION
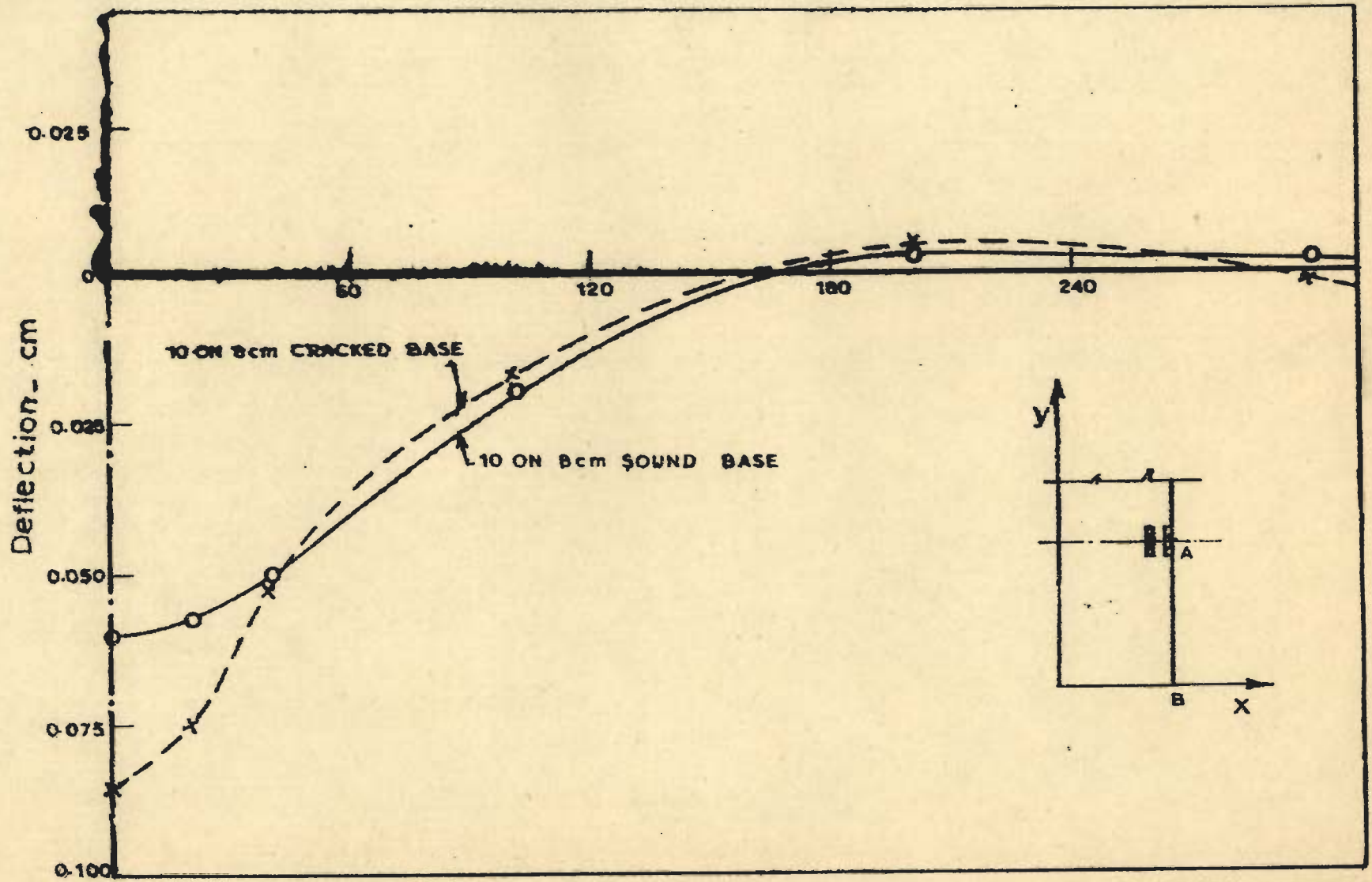
FIG. 6.12 _ DEFLECTION IN BEAM WITH CRACKED AND UNCRACKED BASE, BONDED OVERLAY
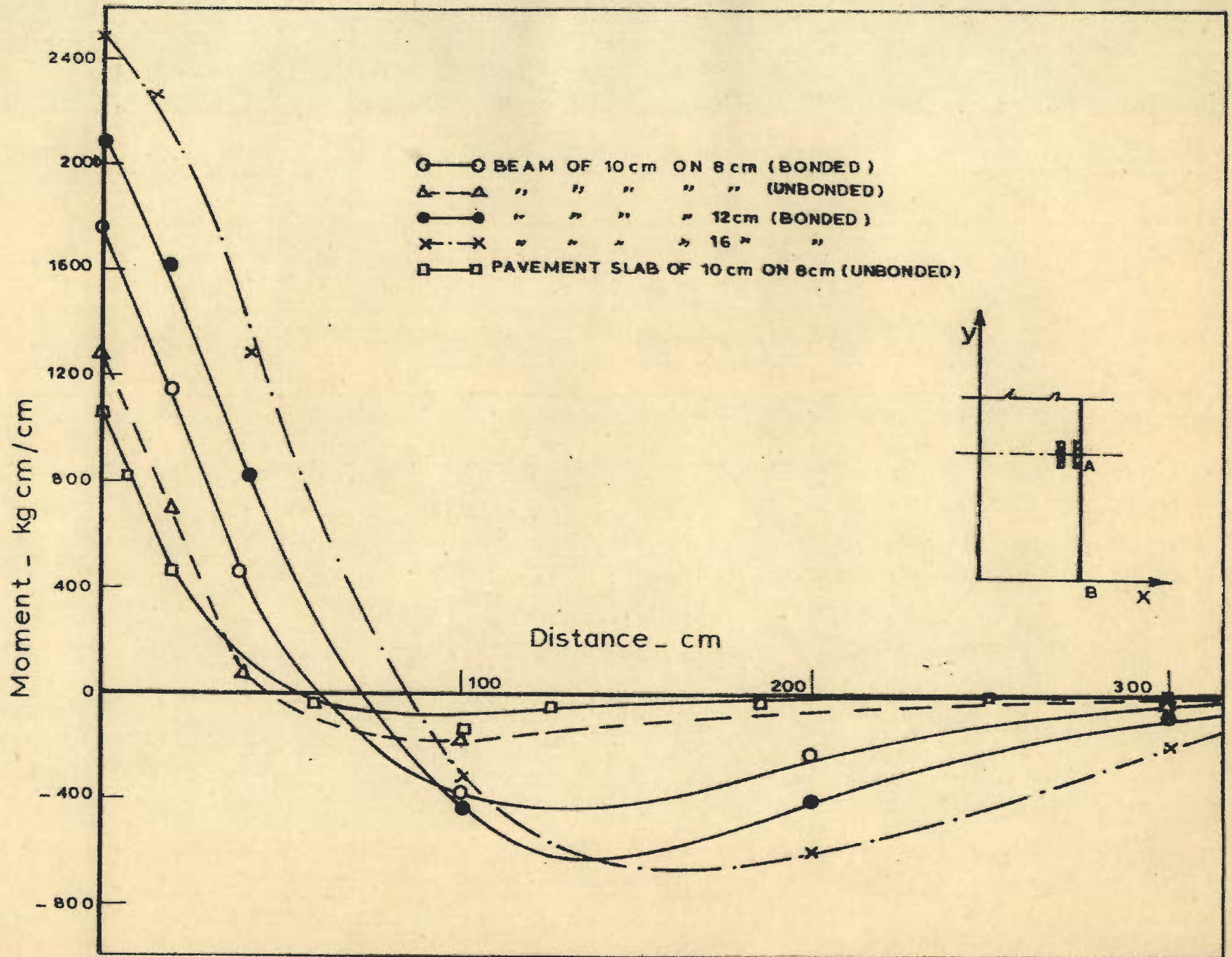
FIG. 6.13 _ COMPARISON OF LAYERED BEAM AND SLAB ON SOUND BASE

Legend:

○——○ BEAM OF 10 cm ON 8 cm (BONDED)
△——△ ,,   ,,   ,,   ,,   ,, (UNBONDED)
●——● ,,   ,,   ,,   ,, 12 cm (BONDED)
✗—·—✗ ,,   ,,   ,,   ,, 16 ,,   ,,
□——□ PAVEMENT SLAB OF 10 cm ON 8 cm (UNBONDED)

Moment _ kg cm/cm

Distance _ cm
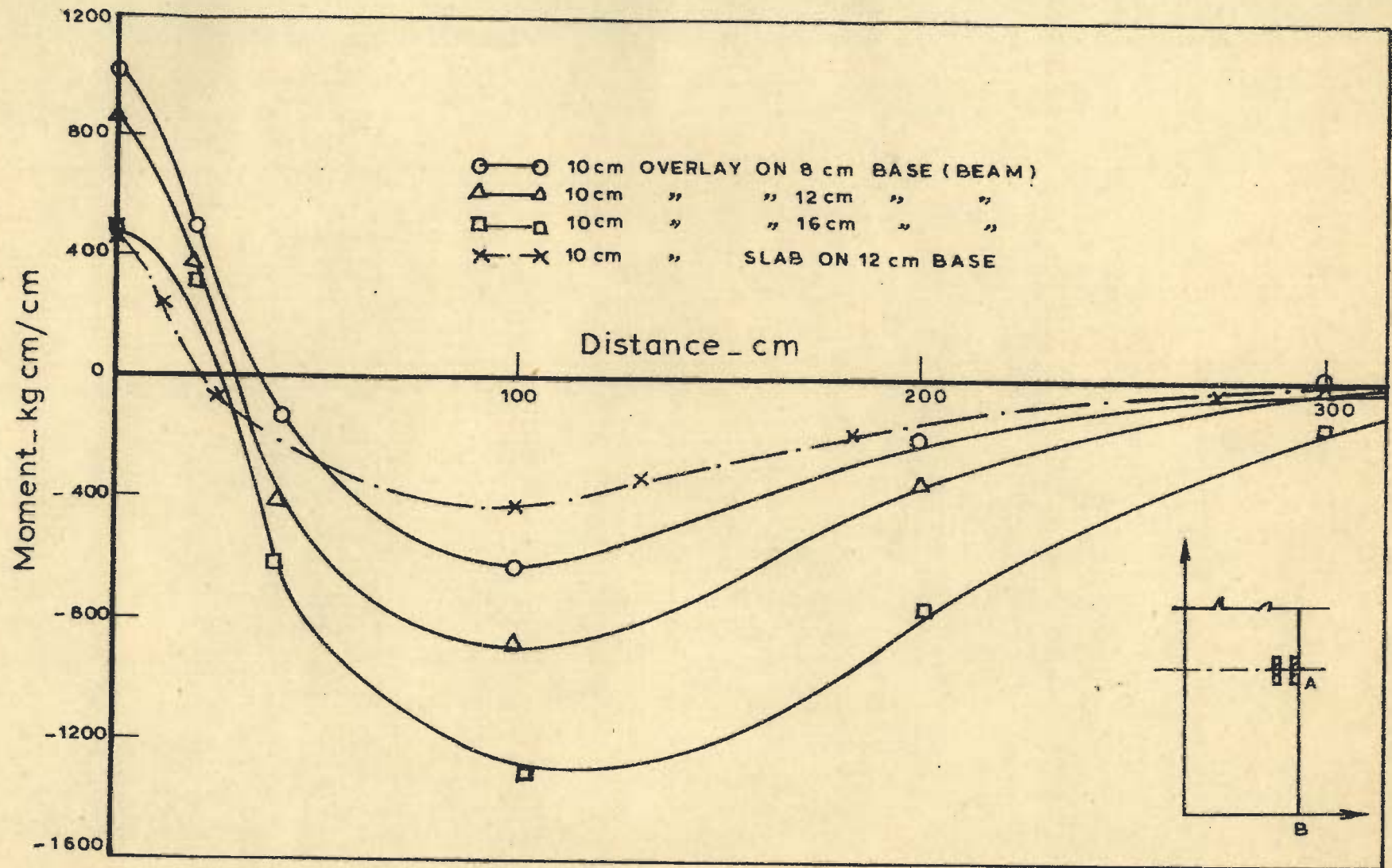
FIG. 6.14 _ VARIATION OF MOMENT BEAM WITH BONDED OVERLAY ON CRACKED BASE

Legend (within figure):

- O——O 10 cm OVERLAY ON 8 cm BASE (BEAM)
- △——△ 10 cm „ „ 12 cm „ „
- □——□ 10 cm „ „ 16 cm „ „
- ✕—·—✕ 10 cm „ SLAB ON 12 cm BASE

Y-axis: Moment _ kg cm / cm
X-axis: Distance _ cm
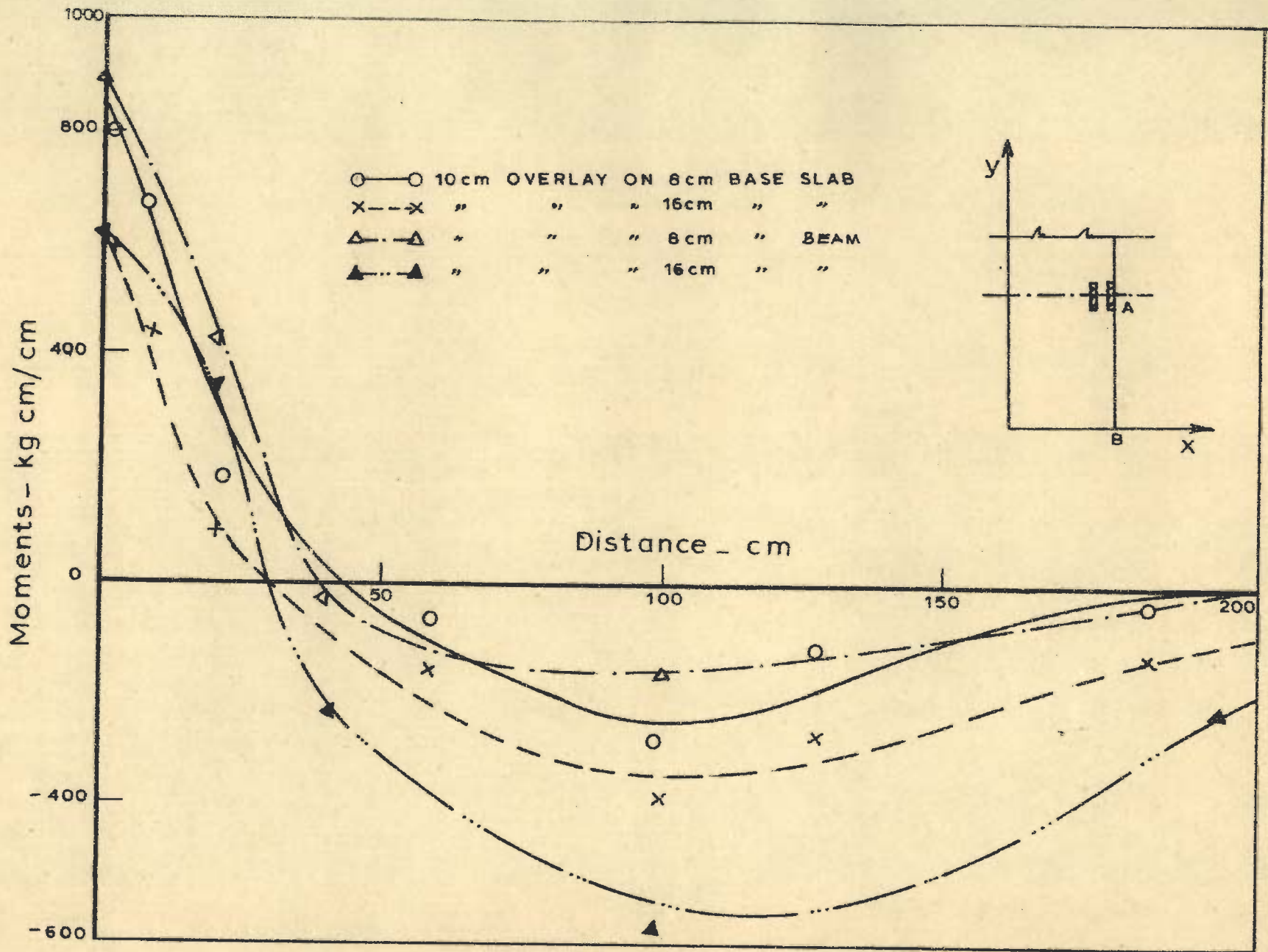
FIG. 6·15 _ MOMENTS IN CRACKED CASES BEAMS VS SLAB IN UNBONDED CONDITION

CHAPTER-VII

INFLUENCE OF SUBGRADE MODEL

7.1 NEED FOR A MODEL

The pavement slab is assumed to be continuously resting on the 'subgrade'. The wheel load induces deformations in the pavement slab and because of the assumption of continuous support, the same deformations occur in subgrade as well. Forces are also generated at the pavement-subgrade interface. The sum of these reactive forces need to be in equilibrium with the active forces. However, the exact distribution of these reactions is yet a guess work. A relation is therefore sought, through a 'sub-grade model' to give a definite shape to this so that distribution of reactions can be obtained. This would reduce highly indeterminate problem of slab on subgrade to a degree of determinacy.

7.2 PAVEMENT SUBGRADE MODELS

Various 'Subgrade models' are thus, put forward for the primary response analysis of a pavement slab.

The model suggested by Winkler[23] was the earliest one among such models and is still quite in vogue. Simplicity is the most attractive characteristics of this model and perhaps the other reason why it could stand the

test of time is the often repeated phrase: "for all
practical purposes it gives sufficiently accurate results".
The impact of this phrase on the exactitude and economy
of analysis is often questioned. This was principally
the reason why by the end of the first half of this
century, investigators were prone to improve upon this
subgrade model.

7.2.1 Dense Liquid Subgrade
Implications of Winkler's model are:

(1) The reaction at the slab-subgrade interface
at a point of contact is supposed to be proportional to
the movement of the slab perpendicular to the interface: The
implication   of this in turn is that if the component
of displacement perpendicular to the interface is 'w'
then the reaction:

$$p = k.w$$

where, k = a constant, called modulus of subgrade
             reaction.

The further implication of this assumption is that
this reaction is independent of stress level and the size
of loaded area. Extensive investigation with various plate
diameters have revealed that load-deformation curve is
non-linear. Fortunately, the magnitude of subgrade reac-
tion is quite low in a cement concrete pavement. Therefore
use of a constant value of 'k' does appear justified.
This, however, is not the case with plate diameter 'k'

relationship. The value of modulus of subgrade reaction 'k' changes significantly with plate diameter. A relation of the form $k = a + b/B$, with 'a' and 'b' as constants and 'B' plate width, was suggested by Engesser[231] based on experimental study. Goldbeck et al.[232] also observed similar behaviour. Arlington tests resulted in the conclusion that since the change in value of 'k' is insignificant after a plate diameter of about 75 cm this size should be regarded as standard. The reason for the variation of 'k' with plate diameter is explained by Terzaghi[231], based on pressure bulb. Another explanation that can be accorded to it, could be from the consideration, which labels this model as artificial. In reality, on being loaded the plate and the area covered by it is not the only zone that undergoes displacement, but the adjoining mass as well deforms. This is because, in reality the subgrade is not the aggregate of infinite number of closely spaced, individual springs, as propounded by the theory, but does behave in a manner, as if there is an interconnection between them. Thus, on being subjected to a specified displacement 'w_o' the adjoining mass offers a certain resistance, the value of which depends on the shape of deflected profile, but this could be somewhat a constant value. Thus, with increase in plate size, the relative effect of this resistance becomes minor.

Thus, adopting a value of 'k' corresponding to 75 cm

diameter may be safe but inaccurate.

(2)   The subgrade reaction is supposed to be perpendicular to the interface. This means that in case of pavement slabs no shearing forces exist at the slab subgrade interface. Analysis by Cheung and Nag[74] has shown that significant change in stresses can be expected if due consideration is given to horizontal forces that are generated due to vertical loads in footings. However, validity of this for pavement slabs, where loads transferred to subgrade is relatively on a large area is yet to be verified.

.(c)   Continuous contact is assumed between the pavement slab and the subgrade. This however, may not always be true. Loss of contact along edges or corners may take place due to wheel loads and/or temperature differential. Agrawal and Hudson[39] have found lifting to occur in model steel plate resting on clay subgrade. They assign this reason to explain the large difference between observed and calculated values of stresses. They therefore recommend 'No tension analysis'. However, the no-tension or bilinear subgrade model has been adopted by Tsai and Westman [233]. They show that such a model is hardly significant and the results of two models are not very different. Sargious[134] and Lall[216] conclude that loss of contact due to temperature warping does occur.

Earlier observations of Hveem[164] and Geldmacher et al.[234] were also similar. Based on this Leonard and Harr[235] suggested a theory to account for loss of contact in circular slab. Later, Lewis and Harr[100] solved the problem of partial contact in a pavement slab resting on viscoelastic foundation subjected to a moving line load. Huang and Wang[80], in a recent paper, have applied finite element method to evaluate static influence due to a wheel load when contact is lost either due to warping or is known as a-priori.

Loss of contact can be adopted on priori basis if it is known that a certain zone has sunk due to some reason or the other like, settlement due to repeated load[237] or due to moisture movement[238,239,240] or adjoining ground movement etc. Richart and Zia[240], Brown[241] and Laytton and Meyer[163] have attempted to deal with such conditions.

The subgrade is thus supposed to behave as an ideal viscous fluid and therefore, the term 'Dense Liquid Subgrade' is given to such a subgrade model.

7.2.2 Elastic Solid Subgrade

Looking to the artificial nature of the Winkler's model, it is often thought that regarding the subgrade as an isotropic, homogeneous, linearly elastic half space, like one treated by Bossinesq[62] may be .

closer to reality. However, following points arise.

(a) Determination of the value of elastic
parameters E and ν of the subgrade requires
elaborate equipment like triaxial cell[242]
etc. Moreover, the procedure is cumbersome,
time consuming and requires good measurements
which can not be reliably done in field.

(b) The elastic parameters are not constants but
are stress dependent[243] and also depend on
the method of experimentation[30].

(c) The subgrade may not be homogeneous. The
elastic properties may vary with depth[76].
It is also possible that the subgrade may
consist of natural or artificial layered
deposits having different elasticity for diff-
erent layer. Characterising such a condition
as isotropic may be erroneous. On the other
hand treating it as such may be difficult
because of difficulty in computations and also
because of detailed soil-survey that may be
required. However, Mednikov[224] has given a
method by which a single equivalent value of
'E' and 'ν' can be obtained for known layer
thicknesses.

(d) Any loss of contact between slab and subgrade

may present greater difficulty in such a model.

(e) Elastic solid model is a function of depth[97,214,245] which may not always be assessable easily.

Yet, it is found that the elastic solid subgrade model is a better representation of the subgrade[30]. Attempts are therefore reported to have been directed towards comparing these two models[30,76,77,97,98,248]. However, results of different authors in this regard differ so much that definite inferences can not be drawn.[49,247]

Because of all these drawbacks it is considered that Winkler model may be better specially if something could be done to improve its drawbacks as mentioned above.

7.2.3 Generalised Subgrade Model

Attempts were therefore directed towards evolving such a foundation model which will improve upon the dense liquid model and may be free from the drawbacks of the elastic solid model. This follows the suggestions by Hetenyi, Filonenko-Borodich, Reissner, and Pasternak[248]. Aim of all these models have been to develop analogy with springs in such a way that not only those springs; which are directly under the load are displaced, but the adjacent springs which are not loaded, are also involved.

In case of Pasternak's model shear interaction
is assumed between spring elements. Physically, this
could be imagined by an interconnection between adjoin-
ing springs through an incompressible beam. Figure 7.1
shows the deflected surface profile of a subgrade due to
a load placed at a distant point. It is supposed to be
made up of the elements, as shown in the figure. A shear
force exists between them which pulls them down. For the
load-deformation relation, the vertical equilibrium of
the element in figure 7.2 may be considered.

If G = shear modulus of the subgrade

$$\tau_{xz} = G \ \gamma_{xz} = G(\frac{\partial w}{\partial x} + \frac{\partial u}{\partial z})$$
and
$$\tau_{yz} = G \ \gamma_{yz} = G(\frac{\partial w}{\partial y} + \frac{\partial v}{\partial z}) \qquad \dots \ (7.1)$$

where,

w = deflection of surface of subgrade

If N_x = shear force/unit length in x-direction,

N_y = shear force/unit length in y-direction,

$\partial u/\partial z$ and $\partial v/\partial z$ are horizontal components and can
be neglected.

$$N_x = \int_0^1 \tau_{xz} \cdot dz = G \ \frac{\partial w}{\partial x}$$
and
$$N_y = \int_0^1 \tau_{yz} \cdot dz = G \cdot \frac{\partial w}{\partial y} \qquad \dots \ (7.2)$$

Considering, the equilibrium of the element in vertical

direction, figure 1.

$$\frac{\partial N_x}{\partial x} + \frac{\partial N_y}{\partial y} + f - p = 0 \qquad \qquad \dots (7.3)$$

Substituting the values from equation (2)

$$f = -G(\frac{\partial^2 w}{\partial x^2} + \frac{\partial^2 w}{\partial y^2}) + p$$

where,

f = applied surface pressure,

and   p = subgrade reaction

= kw

$$f = kw - G(\frac{\partial^2 w}{\partial x^2} + \frac{\partial^2 w}{\partial y^2}) \qquad \qquad \dots (7.4)$$

For an axisymmetric case like a loaded circular plate it is better to convert equation 7.4 (r,z) coordinate system and write it as

$$f = k \cdot w - G(\frac{\partial^2 w}{\partial r^2} + \frac{1}{r} \cdot \frac{\partial w}{\partial r}) \qquad \qquad \dots (7.5)$$

The general solution of the equation is

$$w(r) = AK_0(\beta \cdot r) + BI_0(\beta r) \qquad \qquad \dots (7.6)$$

where, $\beta = \sqrt{\frac{k}{G}}$

I_0 = modified Bessel's function of first kind and zero order,

K_0 = modified Bessel's function of Second kind and zero-order.

A, B = constants

By applying the boundary condition that at $r = \infty$, $w(r) = 0$, $B = 0$

therefore, $w(r) = A.K_0(\beta.r)$ ... (7.7)

This is the solution of the damping curve generate due to deflection w_0 at $r = r_0$

Thus,

$$w_0 = A.K_0(\beta.r_0) \qquad \qquad ... (7.8)$$

and $\dfrac{w(r)}{w_0} = \dfrac{K_0(\beta.r)}{K_0(\beta.r_0)}$ ... (7.9)

Thus, the equation 7.9 is in non-dimensional form.

The general differential equation of a plate on elastic foundation therefore, gets modified, in accordance with equation 7.4, to

$$D_{11} \frac{\partial^4 w}{\partial x^4} + D_{22} \frac{\partial^4 w}{\partial y^4} + 2D_{12} \frac{\partial^4 w}{\partial x^2 \partial y^2} = Q - kw - G\left(\frac{\partial^2 w}{\partial x^2} + \frac{\partial^2 w}{\partial y^2}\right) \quad ... (7.10)$$

where, Q = surface loads,

and D_{11}, D_{22}, D_{12} = usual plate rigidities.

A procedure for determination of 'G' is developed in Appendix 7.A.

7.3 MODELING OF PAVEMENT SLAB WITH SUBGRADE AS ELASTIC CONTINUUM

The modeling of a pavement slab with subgrade assumed as dense liquid has been described in Chapter IV

in accordance with the Winkler's assumptions. It was
supposed therein that the load at a point causes inf-
luence at that point only and all other points are free.
However, in case of an elastic half space, the distur-
bance at a point will result in displacements at all the
points lying on its surface, theoretically even upto an
infinite distance. Thus the force-displacement relation-
ship is a stiffness matrix in this case rather than a
stiffness coefficient as in Winkler's case. Moreover,
as the effect of one point is on all other points, this
stiffness matrix will naturally be full rather than
sparse[77,249].

Deflection at point 'j' due to a load at point 'i'
is given by Boussinesq's equation[244],

$$w_{ij} = \frac{P(1-\nu_s^2)}{\pi \, E_s d_{ij}} \qquad \qquad \dots \ (7.11)$$

where, w_{ij} = deflection at 'j' due to load at 'i'

d_{ij} = distance between points i and j

P = load at i

E_s and ν_s = elastic parameters for subgrade

All the assumptions in this case are same as those
of Boussinesq[62] and their validity is already discussed
in last article.

The deflection at the centre of the uniformly
loaded rectangular area can be obtained by treating the

pressure P/ab over an area $d\xi.d\eta$ as a concentrated load 'P' in equation 7.11 as shown in Figure 7.3.

$$w_{ii} = 2\int_{\xi=0}^{\xi=a/2}\int_{\eta=0}^{\eta=b/2}\frac{P(1-\nu_s^2)}{ab}\frac{d}{\pi E_s}\frac{d}{\sqrt{\xi^2+\eta^2}}$$

Solving this elliptical integral and placing the limits

$$w_{ii} = \frac{P(1-\nu_s^2)}{\sqrt{A.E_s}} \times f \qquad\qquad \dots (7.12)$$

where, f are the coefficients as given in Table 7.1.

Now in the finite element formulation if it is assumed that a node is the centre of uniform pressure then its deflection due to this pressure can be obtained from equation 7.12. Also, deflection at any other nodal point due to this nodal pressure can be obtained from equation 7.11.

Since the assumption of linear elasticity is supposed to hold, the law of reciprocal deflection must also be valid and therefore it is possible to write:

$$\{F_s\} = [K_s]\{\delta\} \qquad\qquad \dots (7.13)$$

where,

$\{F_s\}$ = reactive forces at nodes due to the nodal displacements $\lfloor\delta\rfloor$

and $[K_s]$ = stiffness matrix of subgrade containing coefficients, the diagonal ones being derived from equation 7.12 and the off-diagonal from equation 7.11 with proper application of Maxwell's law of reciprocal deflection.

A = Area of rectangle with side a and b

Equation 7.13 is directly in the form of equation of equilibrium as derived in equation 4.29 and therefore total nodal forces and displacements can be summed up to write.

$$\{F\} = \{F_p\} + \{F_s\}$$
$$= [K_p]\{\delta\} + [K_s]\{\delta\} \qquad \ldots (7.14)$$

where, $\{F_p\}$ = nodal forces of pavement slab,

$\{K_p\}$ = stiffness of pavement slab.

Since, law of reciprocal deflection holds $[K_s]$ will be symmetric like $[K_p]$ and by choosing the nodal points in such a way that they coincide for slab and sub-grade the size of $[K_p]$ and $[K_s]$ will be same. Therefore, equation 7.14 becomes

$$\{F\} = [K]\{\delta\} \qquad \ldots (7.15)$$

which is a standard form in finite element algorithm. But, restrictions on usual finite element procedures are now imposed and they are:

1. $[K]$ is fully populated and therefore, the usual finite element assembly and solution algorithms do not hold.

2. Since there is interaction between each and every point it is not possible to take advantage of symmetry even for the most symmetric

case. Huang[49] has however, treated this

as a symmetric problem. This was later pointed

out by Wang et al.[247]

These restrictions have a tremendous impact on
economy. Both due to full (triangular) matrix storage
requirement, as well as full structure geometry to be
analysed, the memory falls short for a sizeable problem.
The computation time also increases.

7.4 MODELING OF PAVEMENT SLAB INCORPORATING LOSS OF CONTACT

Loss of contact between subgrade and pavement
slab, at their interface, may occur due to various
reasons. The reasons for these have been discussed in
para 3 of article 7.2.1. The problem of loss of contact
can be of two types. One in which the loss of contact
is due to such reasons, that the zone of contact loss
can be determined before commencement of the analysis.
The problem in this case is of linear nature and the
procedure that could be adopted has already been for-
mulated and discussed in article 4.7.

Other problem associated with loss of contact is
a non-linear one. The loss of contact at a point may
occur due to a wheel load placed at some distant point
or due to curling, resulting from hydro-thermal gradients.
Thus the zone of contact loss is not known at the instant

of taking up the analysis as it depends on the behaviour
of the pavement structure subjected to inputs. There-
fore, the procedure of non-linear analysis becomes
a necessity. Various usual procedures for non-linear
analysis and their relative merits have been discussed
in Appendix 7.B. The procedure selected for the present
analysis is that of constant stiffness type because
of its advantages stated therein of calculating invers-
ion of stiffness matrix once for all.

The equation governing the solution algorithm
is therefore equation 7.18 in which unbalanced forces
i.e. the difference between forces assumed before
starting the analysis and after completion of the first
cycle is found on the basis of displacement level
achieved in the first cycle. Thus, if there is any
negative deflection (i.e. loss of contact due to lift-
ing), the unbalanced forces will be affected, because
according to the new constitutive law, these reactive
forces will have to be taken as zero, whereas, in the
first cycle they are causing a downward reaction. Thus
an equal and opposite force has to be applied. These
forces are again taken as applied nodal loads in accor-
dance with the concept of consistent nodal loads. The
stresses and displacements due to this are found and
are added to the original. The process is repeated till
the additional stresses generated are insignificant.

7.5 PAVEMENT SLAB ON TWO PARAMETER SUBGRADE MODEL

The equation 7.4 gives reactive pressure for two parameter subgrade model. This has to be incorporated now in equation 7.14. Accordingly, the equation 7.14 can be written as

$$\{F\} = [K_p]\{\delta\} + [K_s]\{\delta\} + [K_2]\{\Delta\} \qquad \ldots (7.16)$$

where,

$[K_2]$ = stiffness coefficient matrix for second term in equation 7.4.

$[K_s]$ = stiffness matrix, same as that for Winkler subgrade,

$\{\Delta\}$ = curvatures corresponding to second term of equation 7.4.

This formulation is though possible[250], but does not appear to be good, as it is uneconomical. Therefore, another formulation is attempted. It is noticed that as vector $\{\Delta\}$ contains small quantities as such the effect of the third term in equation 7.16 is small. An iterative scheme is proposed in which the solution to equation 7.16 is sought with third term i.e. shear interaction of foundation is neglected. This is as usual for Winkler foundation. Then the unbalanced forces are calculated as in article 7.4 for the deformations obtained with due consideration of shear interaction in the subgrade. This modifies the forces which would have otherwise balanced. Thus unbalanced forces, which are obtained are again applied and statical

influences are determined, their net value being the sum
of this and the earlier one. Iterations are again performed
till convergence is obtained between two consecutive
cycles. The stiffness matrix is once calculated and kept
constant. Therefore the assembled stiffness matrix is once
partially inverted and kept stored on tape. The procedure
is thus similar to the one adopted for analysis when
material property of the structure is changing with level
of deformation.

Mednikov[251] has given a procedure by which the
equivalent values of 'k' and 'G' for use in equation 7.4
can be obtained for a multilayered subgrade, the height
and elastic properties of each layer being known.

7.6 DISCUSSION ON VALIDITY OF WINKLER'S MODEL AND
ITS EQUIVALENCE WITH CONTINUUM MODEL

Figure 7.4 shows the variation of pressure within
the subgrade, under a 38 cm thick concrete slab when
subjected to 1500 kg/cm knife edge load. The contours
are for same vertical stress. These contours very much
resemble the pressure bulbs under a strip footing[252].
The ratio of surface pressure and deflection can be used
to evaluate 'k' i.e. the modulus of subgrade reaction.
The variation of 'k' along the length of the slab for the
case of 38 cm and 23 cm slabs are shown in figure 7.5.
This is for the case when E_c/E_s i.e. modulus of elasticity
of concrete to subgrade is taken as 2000. It is seen that

in the neighbourhood of the load the value of **'k'** is fairly constant for one particular slab rigidity. However, it does appear to change slightly with rigidity of the slab.

Figure 7.6 shows the variation of 'k' along the slab length for the above two cases when E_c/E_s = 200. In this the variation along slab length is large, meaning thereby that the value of **'k'** is not constant throughout the slab length. This behaviour is also indicated for a 38 cm thick circular slab considered as loaded by 4000 kg and the variation of 'k' is plotted in figure 7.6 along radial distance from the centre. Therefore, it can be concluded that 'k' varies not only with the elastic properties of soil and the rigidity of the slab as has been pointed out by Vesic and Saxena, but it also varies with pressure. Details regarding calculation of 'k' are given in table 7.2.

Vesic and Saxena[30] conclude that there is no unique value for 'k' of a particular soil. The value of **'k'** corresponding to any particular value of 'E_s' is different for deflection and moment. However, McCllough and Boedecker[98] give a unique value of 'k' for any value of 'E_s'. Values of 'k' as computed by data from finite element analysis are averaged for a particular slab rigidity and 'E_s'. This is then compared with those given by Vesic and Saxena[30] as per their computation of equivalent **'k'** value for infinite

subgrade depth on the basis of deflections. This is
because, in the analysis the subgrade is taken as
deeper than the restriction imposed on them. This
comparative statement along with the values given by
McCllough and Boedecker[98] is shown in Table 7.3.

In a thin slab like a 23 cm one the pressure and
deflection under the load is higher than a 38 cm slab,
but due to the higher rate of change of slope they
acquire a lower value away from the load. The value
of "K" then falls below that for 38 cm slab. On this
basis, the value of "K" for given $'E_s'$ appears to be a
function of pressure.

It is a matter of uncertainty as yet that how
does the value of modulus of subgrade reaction, as
determined by the standard perfectly rigid 75 cm dia-
meter plate, fits into the case of flexible cement
concrete slabs. Thus, the value of 'k' is infact not
standard. On the other hand the standard value of
$'E_s'$ determined by a certain procedure; like triaxial
test, plate load test, Vander poels stiffness factor,
or any other method; is not a constant either[30]. Not
only this, the value of same subgrade soil is a funct-
ion of confining pressure[243] as well as stress
level[72]. Therefore, this value is more non-standard.
Apart from this the point against use of elastic solid
subgrade mentioned in article 7.2.2 and also by Arora[253]

has to be borne in mind. This apart from the fact that the slight variation in support characteristics of the subgrade has negligible effect on the pavement stresses[24,231] puts the Winkler's model on a superior footing.

However, the foundation model incorporating the shear interaction as proposed by Pasternak[248] or a similar one, certainly is a better proposition.

7.7 MODIFICATION OF PROGRAM

The third stage of modification in the program was mentioned in the last chapter in which the modification was done to incorporate unbonded overlays. In the fourth stage, modification was done to incorporate different kinds of foundation models. The modification to incorporate Pasternak's model as well as Winkler's model where tension in the foundation is not allowed, are very similar as mentioned in article 7.4 and 7.5. An identification system was built in so that proper model out of the three could be chosen. If Pasternak's model is to be adopted then value 'G' in equation 7.4 has to be defined. If 'G' is taken as zero, then it amounts to adopting Winkler's model with loss of contact (article 7.4).

However, the elastic solid model is not included in the same program. The reason being that the memory

limitations in this program is very severe due to reasons mentioned in article 7.3. The stiffness assembly and solution algorithm is also different for this case because of fully populated nature of the stiffness matrix. Thus, it is separately programmed.

However, the procedure for solution of bonded and unbonded overlays remains same without any change and all kinds of analysis possible on Winkler's model are possible on these three models as well.

7.8 ANALYSIS AND RESULTS

A 23 cm cement concrete pavement slab with following properties are analysed:

E_c = modulus of elasticity of concrete = 15×10^4 kg/cm^2

ν_c = Poisson's ratio for cement = 0.2

E_s = modulus of elasticity of subgrade = 750 kg/cm^2

ν_s = Poisson's ratio for subgrade = 0.45

L = length of slab = 600 cm

B = width of slab = 400 cm

P = Load = 4500 kg

A = loaded area
= 44x56 cm in case of interior loading,
= 44x28 cm in case of edge loading.

Figure 7.7 shows variation of moments along edge in case of edge loading. In case of interior load, the moments in direction parallel to edge are plotted along

longitudinal centre line in same figure.

Results of non-linear analysis are shown in table 7.4 and 7.5. It is clear from these tables that the effect of lifting caused due to wheel load at edge is negligible on stress resultants. Findings of Tsai and Westman [233] have also been similar. Though the convergence is slow, all checks for convergence are satisfied.

APPENDIX-7.A

DETERMINATION OF SECOND PARAMETER OF TWO
PARAMETER FOUNDATION MODEL

It is necessary to know the value of parameter 'G'
in order to use the Pasternak's foundation model. A
simple mechanical procedure is developed based on theory
of coupled spring foundation[254] which is same as general-
ised foundation model[248].

For a rigid plate pressed down, by a pressure 'p'
through a distance 'w_0' the modulus of subgrade reaction
will be

$$K = \frac{p}{w_0}$$

If the deflection 'w' are known for some points
then it is possible to determine the ratio w/w_0 at these
points and plot them against the nondimensionalized dis-
tance $\frac{r}{r_0}$.

where, $2r_0$ = diameter of the standard test plate = 75 cm

and   r = distance of the point at which deflection is
            'w' measured from the edge of the plate.

If the scale of this plot is matched with that of
figure 7.8 and the plot is on a piece of transparent
paper, then this curve can be matched with the curves in
the figure   and a value of 'β' can be interpolated.

Recognising that 'k' is found and that $\beta = \sqrt{k/G}$, the parameter 'G' can be found. However, if the experimental curve falls outside the range of the graph given in the figure 7.8 , it would be necessary to first plot more graphs using equation 7.92.

APPENDIX 7.B

NON-LINEAR ANALYSES

(Modification of material properties based on
deformations)

Changes in geometrical or material properties of the
system with deformations require recourse to special tech-
nique. On examining the equation of equilibrium equation
4.30, it can be noted that deformations are functions
of loads as well as stiffness. Thus, the changes in
material properties will affect the stiffness and thereby
deformation. The deformations in turn will affect the
stresses.

Incremental Method

A straight forward, approach to nonlinear solution
is therefore obvious, in which the load is applied in
parts. During each small load increment the properties
are supposed to be constant and for each increment new
stiffness matrix is generated and inverted. The stresses
as obtained by previous load increment are treated as
initial stresses in equation 2.10.

Iterative Methods

Under this category a procedure that is direct is
variable stiffness procedure. Full load is applied and
stiffness matrix is determined based on non-linear

constitutive law for initial modulus i.e. zero displace-
ment. Based on this stiffness the displacements are
calculated. The constitutive law will now give another
stiffness for the deformations new cycles are thus per-
formed, each time with a new stiffness matrix.

Both of the above procedures require updating of
stiffness matrix at each step and are therefore costly.

Constant Stiffness Method

A procedure is therefore better in which constant
initial slope is used for stiffness calculations. However,
the stresses are calculated from the constitutive law
corresponding to the strain level achieved. Since now,
there is a difference between the elastic solution and
the stresses level achieved the equilibrium conditions will
fail to hold and there will be an 'unbalanced force'. This
unbalanced force is required to be redistributed till
balance is obtained.

If $\{\psi\}$ = vector of unbalanced nodal forces,
then the difference of internal and external work done dur-
ing virtual displacement $d\{\delta\}$ will give

$$d\{\delta\}^T\{\psi\} = \int_V d\{\varepsilon\}^T\{\sigma\}dv - d\{\delta\}^T\{F\} \qquad \ldots (7.17)$$

But $\{\varepsilon\} = [B]\{\delta\}$ as per eqn.2.4

$\therefore d\{\varepsilon\} = [B]\{d\}\{\delta\}$

or $d\{\varepsilon\}^T = d\{\delta\}^T [B]^T$

$\therefore \{U\} = \int_V [B]^T \{\sigma\} dv - \{F\}$

$\qquad \qquad \qquad \qquad \qquad \qquad \qquad \qquad \ldots (7.18)$

The process is similar to Newton-Ralphson type in which initial tangent stiffness is generated (and also kept constant) and trial values of $\{\delta\}$, are obtained. These are used then to calculate the unbalanced forces as given by Eqn.7.18. These forces are now taken as applied loads and are redistributed. In other words difference between elastic solution and the true stress level is found at the end of each trial, and the process continues till the unbalanced force is negligible.

The process requires larger number of iterations but each iteration may require only a fraction of time as compared to iteration of variable stiffness if the initial stiffness is once generated and stored after partial inversion for use in every iteration.

However, for better results a combination of above two procedures can be used.

TABLE 7.1

VALUE OF COEFFICIENT 'f' (equation 7.12)
FOR VALUES OF a/b

a/b	1	2	3	4	5	6
f	0.95	0.92	0.88	0.82	0.71	0.37

TABLE 7.2

COMPUTATION OF MODULUS OF SUBGRADE REACTION FOR
ELASTIC CONTINUUM

No.	Case	Distance from centre of slab	Deflection 'w'	Subgrade Reaction p	Modulus Subgrade Reaction K=p/ω	Average 'K'
1	2	3	4	5	6	7
I	Plane Strain 38 cm slab E_c/E_s=2000	0.0	1.706	0.494	0.276	
		30.48	1.676	0.501	0.299	
		61.00	1.646	0.480	0.291	
		106.70	1.524	0.446	0.292	0.301
		152.40	1.372	0.409	0.298	
		213.40	1.128	0.341	0.302	
		274.00	0.823	0.289	0.351	
II	Plane Strain 23 cm slab E_c/E_s=2000	0.0	2.524	0.749	0.297	
		30.48	2.480	0.754	0.304	
		61.00	2.370	0.685	0.289	
		106.70	2.110	0.587	0.278	0.29
		152.40	1.770	0.488	0.275	
		213.40	1.290	0.348	0.270	

Table 7.2 continued

1	2	3	4	5	6	7
III	Plane strain 38 cm slab $E_c/E_s = 200.00$	0.0	0.301	0.965	3.20	
		30.48	0.293	0.973	3.32	
		61.00	0.273	0.801	2.93	
		106.70	0.232	0.611	2.64	2.82
		152.40	0.182	0.473	2.60	
		213.40	0.118	.266	2.25	
IV	Plane Strain 23 cm slab $E_c/E_s = 200.00$	0.0	0.387	1.472	3.80	
		30.48	0.369	1.415	3.83	
		61.00	0.329	0.976	2.96	3.245
		106.70	0.250	0.597	2.39	
V	Axisymmetric 38 cm slab $E_c/E_s = 200.00$	0.0	0.0128	0.0556	4.340	
		30.48	0.0119	0.0556	4.670	
		61.00	0.0107	0.0439	4.103	
		106.70	0.0085	0.0283	3.330	3.730
		152.40	0.0067	0.0219	3.270	
		213.40	0.0045	0.0120	2.66	

Table concluded.

TABLE 7.3

COMPARISON OF MODULUS OF SUBGRADE REACTION

S. No.	Method of Computing	Modulus of Subgrade Reaction(kg/cm³)			
		$E_c/E_s = 2000$		$E_c/E_s = 200.00$	
		SLAB THICKNESS		SLAB THICKNESS	
		38 cm	23 cm	38 cm	23 cm
1.	Vesic and Saxena[30] (based on moments)	0.221	0.3456	4.750	7.435
2.	Vesic and Saxena[30] (based on deflection)	0.093	0.1450	1.995	3.122
3.	McCllough and Boedecker[97]	1.710	1.7100	13.12	13.120
4.	Finite Element Analysis	0.301	0.2930	2.820	2.658

TABLE 7.4

RESULT OF NON-LINEAR ANALYSIS TO ACCOUNT FOR LIFTING DUE TO LOAD POSITION

Iteration Number	Maximum Sagging Moment (kg.cm/cm)	Maximum Hogging Moment kg.cm/cm	Maximum (+ive) Deflection cm	Maximum (-ve) Deflection cm
1	1247.97	322.00	349.83×10^{-4}	5.93×10^{-4}
2	1248.74	321.00	351.13×10^{-4}	10.07×10^{-4}
3	1249.50	320.75	352.06×10^{-4}	13.34×10^{-4}
4	1250.05	318.88	352.82×10^{-4}	16.07×10^{-4}

TABLE 7.5

CALCULATION OF NORMS

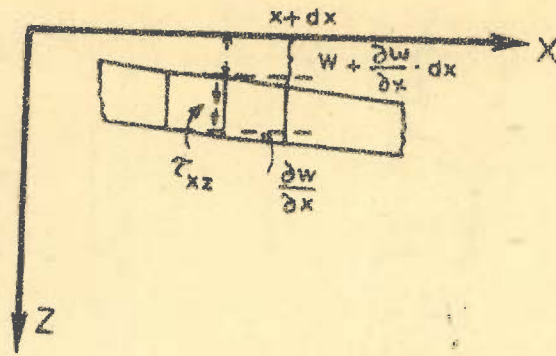| CYCLE	NORM DUE TO LOAD			NORM DUE TO DEFLECTION		
	$R^2 = \sum \text{Residue}^2$	$P^2 = \sum \text{Load}^2$	$\text{LNORM} = \sqrt{\dfrac{R^2}{P^2}} \times 100$	$C^2 = \sum \text{CORRECTION}^2$	$D^2 = \sum \begin{array}{l}\text{TOTAL} \\ \text{DEFLECTION}^2\end{array}$	$\text{DNORM} = \sqrt{\dfrac{C^2}{D^2}} \times 100$
1.	13714.6426	1254400.00	10.465%.	1.9236×10^{-6}	3678.717×10^{-6}	2.286%
2.	Print-out not obtained			1.8233×10^{-6}	3698.807×10^{-6}	2.210%.
3.	6498.1200	1254400.00	7.197%	1.3062×10^{-6}	3718.401×10^{-6}	1.874%

FIG. 7.1 – DEFLECTION IN SUBGRADE AWAY
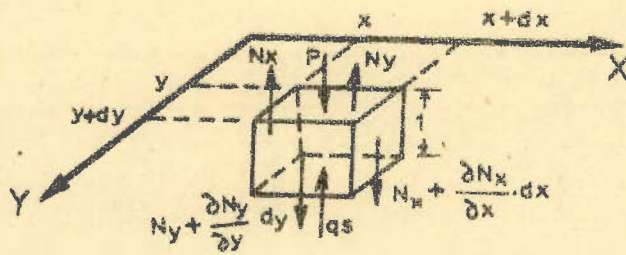FROM LOAD

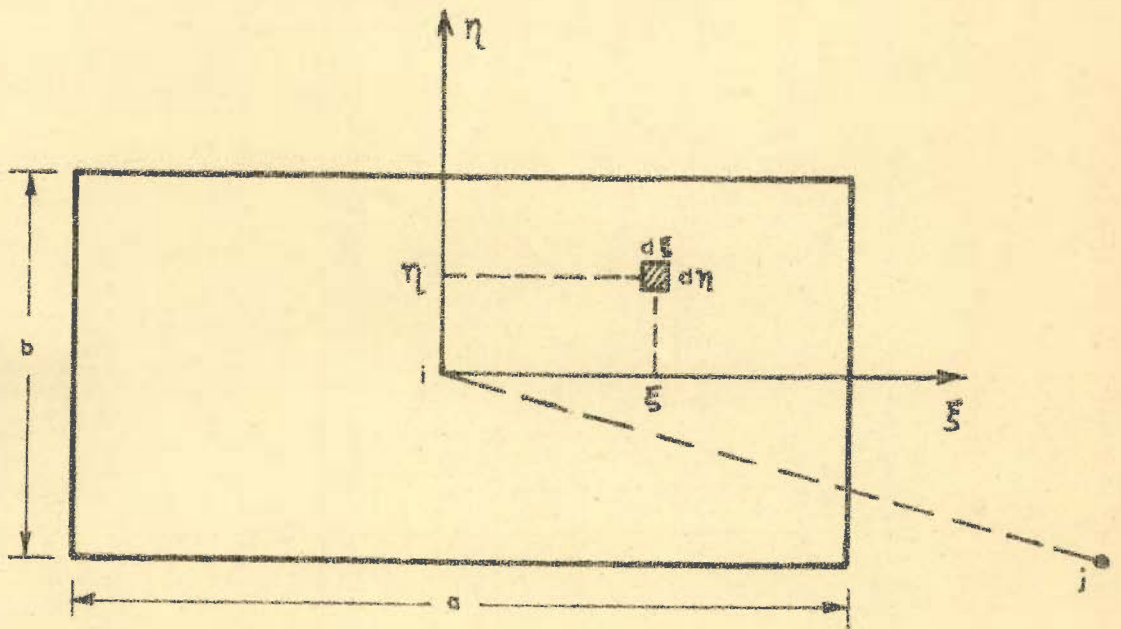FIG. 7. 2 – EQUILIBRIUM OF AN ELEMENT OF
SUBGRADE

FIG. 7.3 – REFERENCE FIGURE FOR ELASTIC SOLID
SUBGRADE
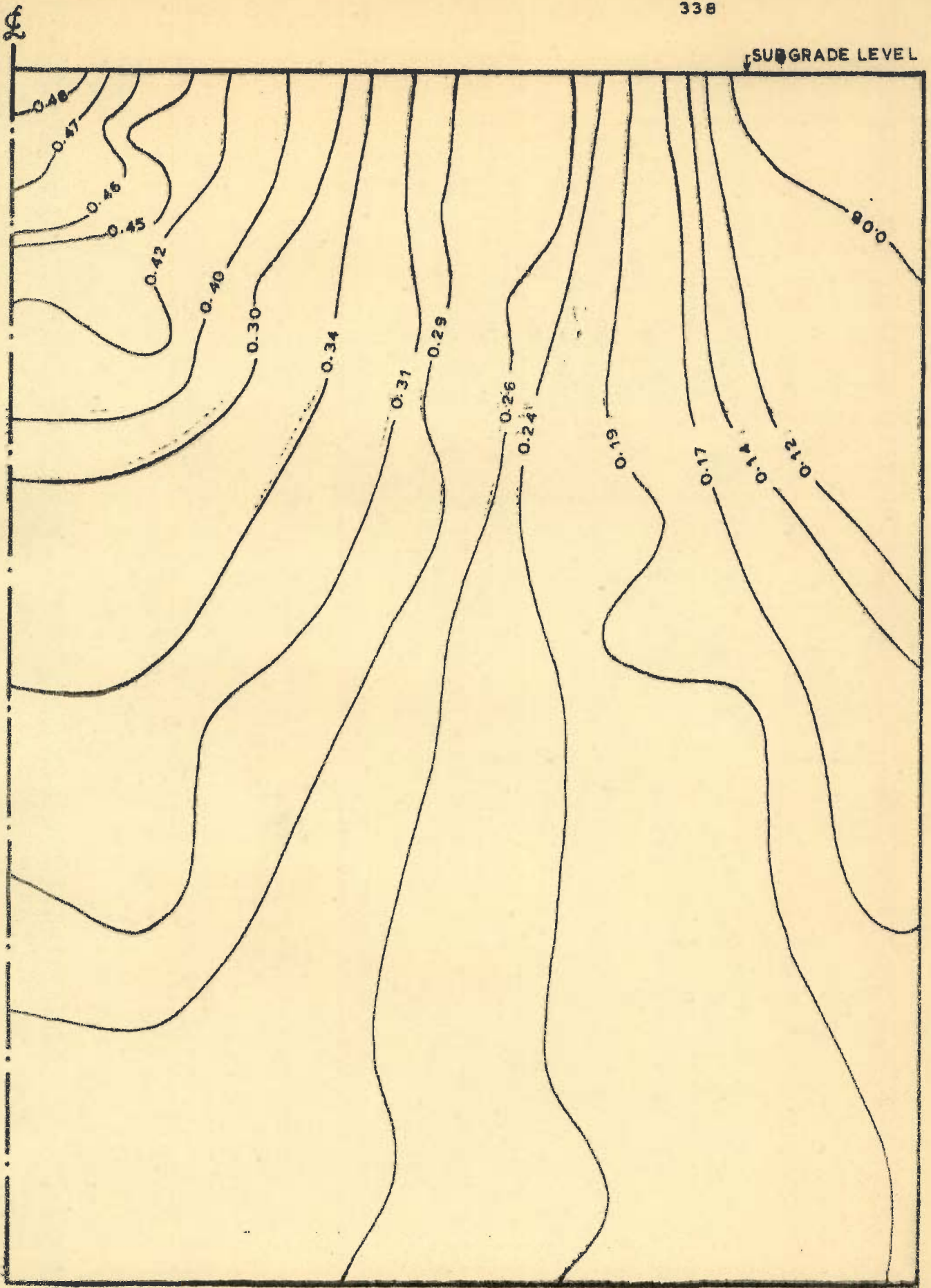
FIG. 7.4_ CONTOURS OF PRESSURE IN SUBGRADE , (kg/cm²)
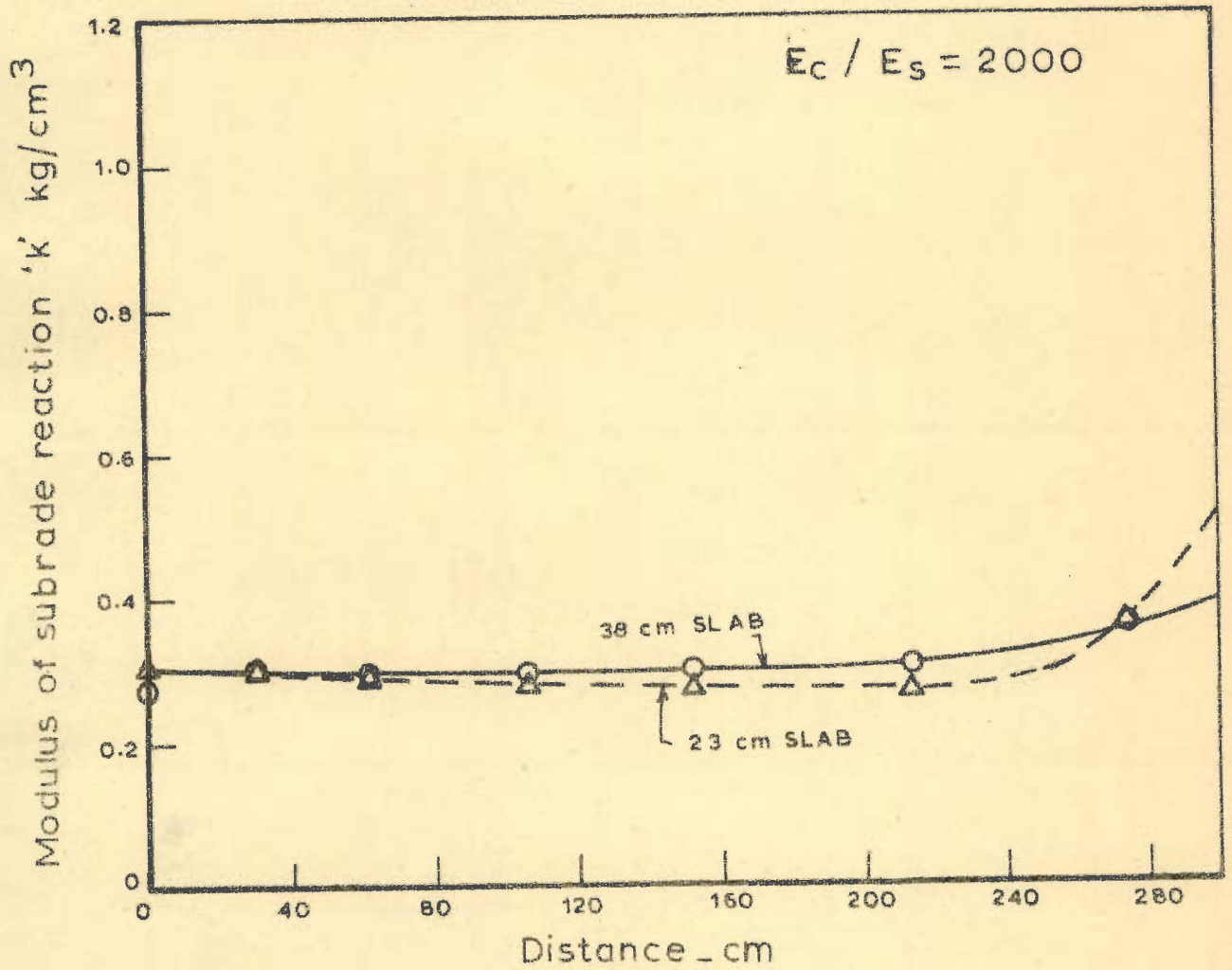
FIG. 7.5 _ VALUE OF k DETERMINED BY FINITE
ELEMENT RESULTS
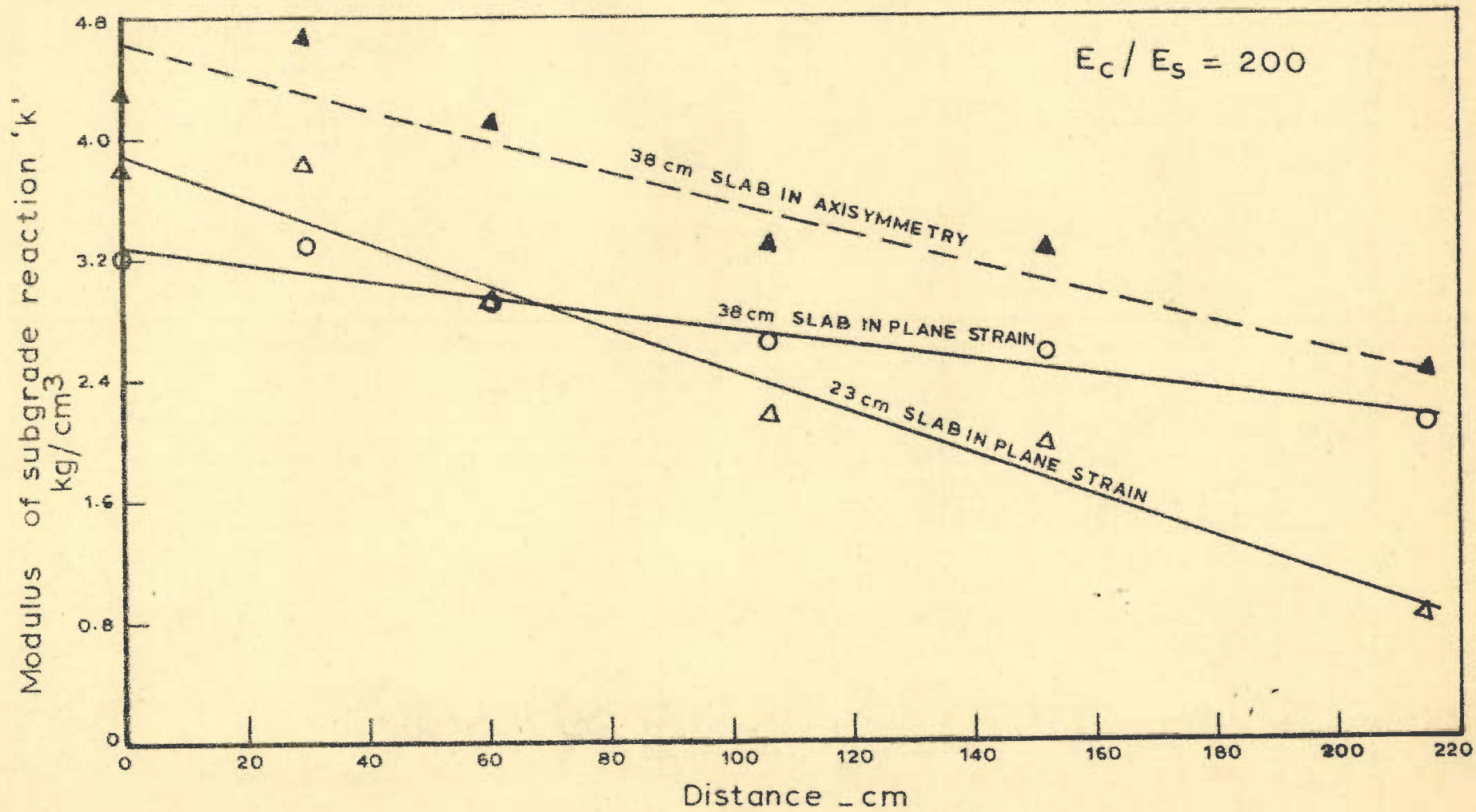
FIG. 7·6 _ VALUE OF k DETERMINED BY FINITE ELEMENT RESULTS

Chart details:
- Y-axis: Modulus of subgrade reaction 'k' kg/cm³ (values: 0, 0.8, 1.6, 2.4, 3.2, 4.0, 4.8)
- X-axis: Distance _ cm (values: 0, 20, 40, 60, 80, 100, 120, 140, 160, 180, 200, 220)
- $E_c / E_s = 200$
- 38 cm SLAB IN AXISYMMETRY
- 38 cm SLAB IN PLANE STRAIN
- 23 cm SLAB IN PLANE STRAIN

340

FIG.7.7 SLAB ON ELASTIC SOLID SUBGRADE

$E_c = 15 \times 10^4$ kg/cm^2

$E_s = 750$ kg/cm^2

SLAB THICKNESS = 23 cm

EDGE, MOMENT 'M$_y$' ALONG EDGE

INTERIOR, MOMENT 'M$_y$' ALONG ℄ PARALLEL TO EDGE

Moment kg cm/cm

Distance - cm

341
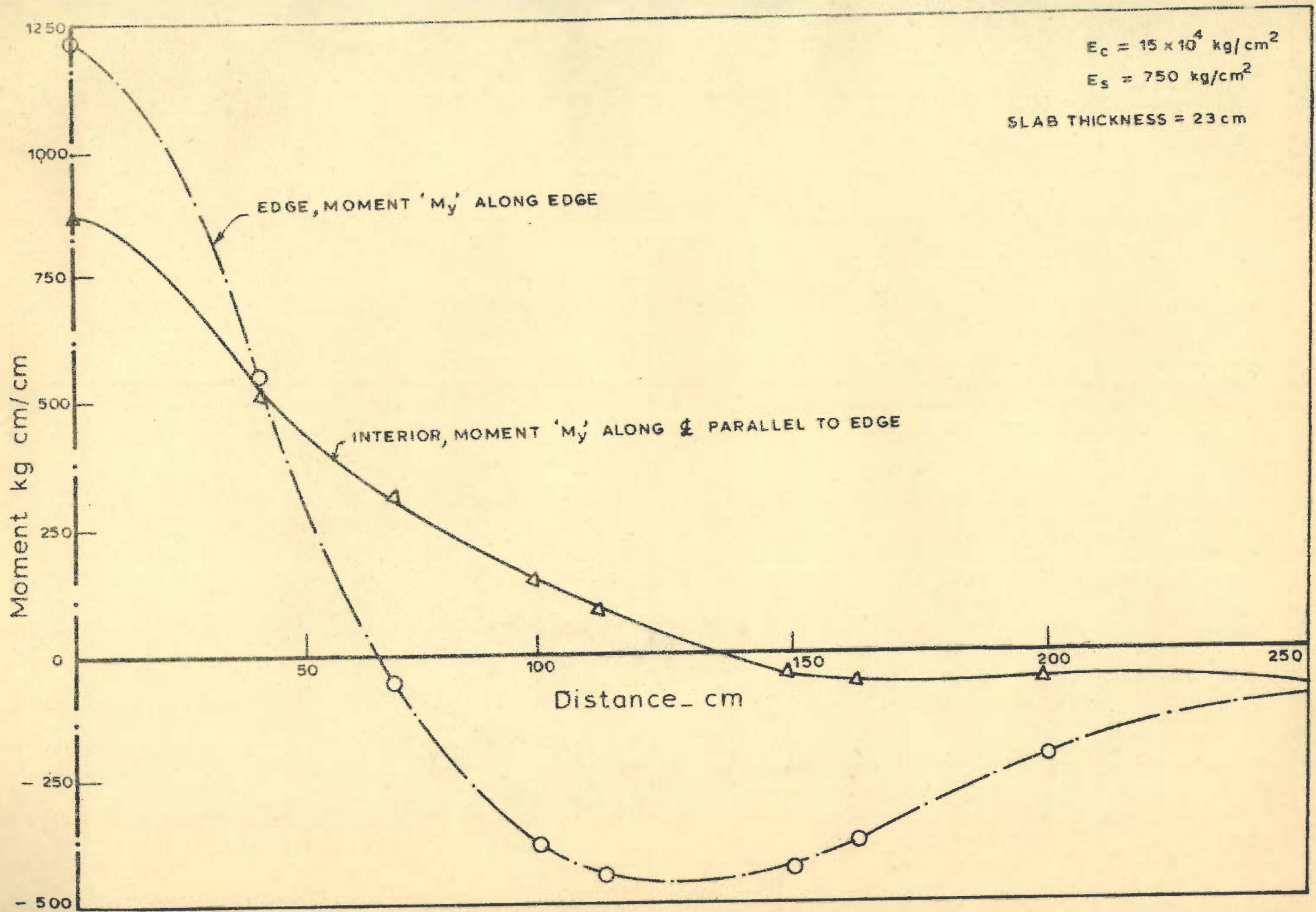
FIG. 7. 8 _ NON-DIMENSIONALISED DEFLECTIONS TO
DETERMINE SECOND PARAMETER

CHAPTER-VIII

EXPERIMENTAL VERIFICATION OF
FINITE ELEMENT SOLUTION

8.1 INTRODUCTION

There can be no doubt regarding the perfection
of the theoretical treatment viz. the finite element
method. However, the chances of deviation from reality
do exist. This is because it is very difficult to
assess 'nature' through theoretical treatment. There-
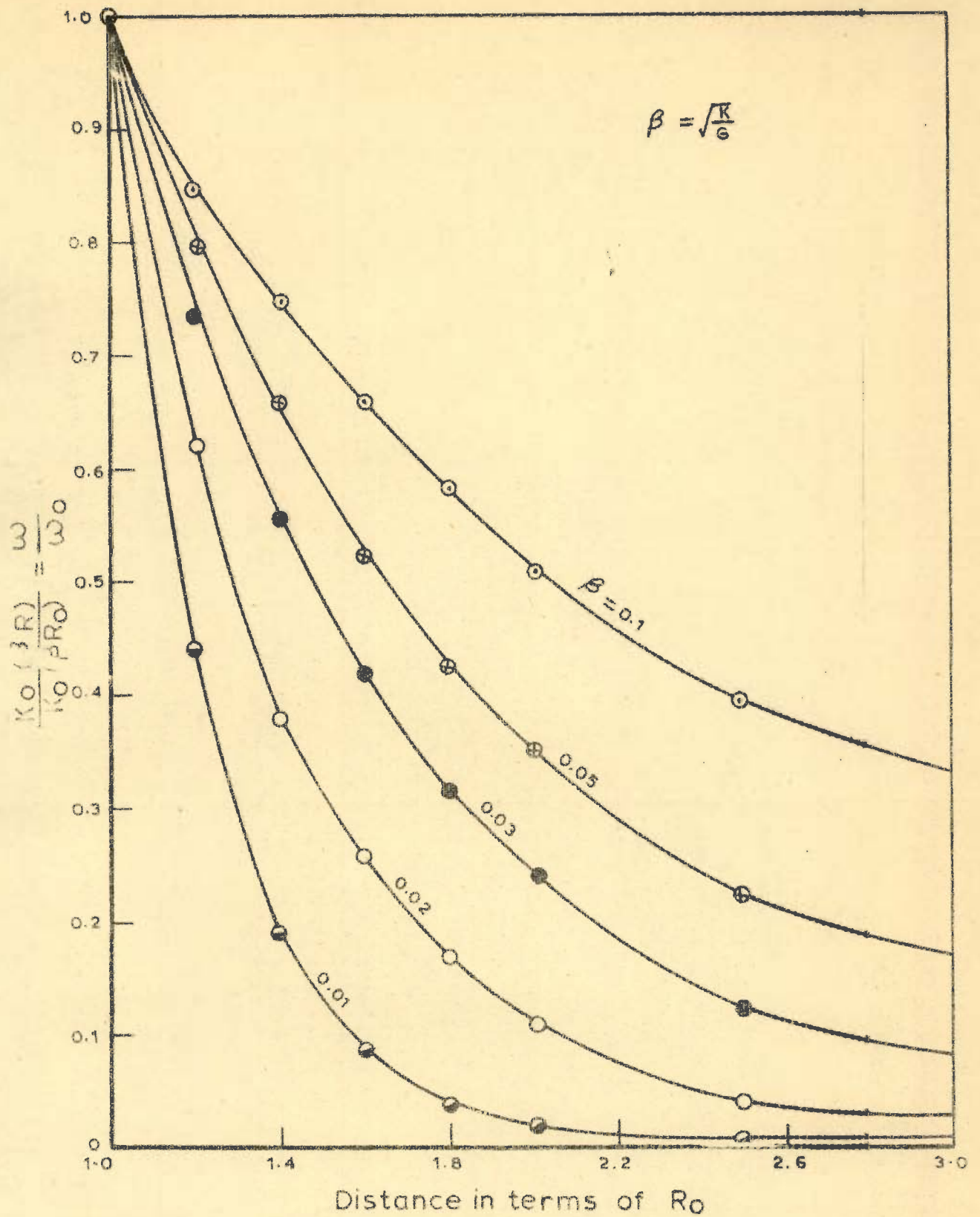fore some simplifying assumptions are always involved.
The assumptions involved in the present theoretical
analysis are listed in relevant chapters. Secondly,
there could be an error in the new program which runs
in some 1600 statements. However, the results given
by the program is tested in various ways, e.g. checking
the statics, physical interpretation of the results
or quantitative and qualitative comparisons with other
existing solutions wherever possible. This has already
been done and therefore possibility of error in programm-
ing is eliminated. The only doubt then, that might arise
is due to the assumptions, especially those which are
made to solve such cases, the solution of which are not
available for comparison. These are particularly with
respect to validity of assumptions of full bonding at
interface in case of bonded overlays, continuous

contact in case of unbonded overlays and stress release
at 45° in case of a crack. Apphysical verification of
statical influence will institute perfect confidence
in the solution system.

8.2 CHOICE OF METHODS AND THEIR LIMITATIONS

A wide choice of possibilities exist for veri-
fication. These range from actual field tests for
establishing the pavement behaviour to controlled model
simulation. The field tests are naturally the best.
However, they require elaborate testing over a long
period by a group of researchers. Full scale laboratory
testing is another possibility. But the main drawback
of this procedure is that the development of desired
conditions may be doubtful e.g. simulation of a crack
in the base. Moreover, the time of testing increases
for a number of cases to be studied. In case of model
testing a number of conditions can be studied with rel-
ative ease. The choice of model testing then opens up
the desired avenue.

Models are usually defined as[255] a device which
is so related to a physical system, known as prototype
that the observations on the model may be used to accura-
tely predict the performance of the prototype. The model
envisaged here is not strictly a model according to this
definition. This is because the purpose of testing here
is different. The theoretical analysis can be substantiated

on any device that simulates the required conditions, without necessarily being related to a prototype. However, it can still be called a model because the proposed tests are made with an ultimate aim of representing the pavement system.

The chief advantages of selecting such a test are:

(i) Control over simulation is possible. It helps to develop condition of full bonding by cementing the layers. Similarly, by adopting smooth surfaces at interface, 'no bond condition' can be developed. Idealised subgrade conditions as well as simulation of a crack or joint in the base is possible.

(ii) In many cases, time is saved by adopting a model. This is particularly true under the present circumstances because time of curing the test slab for each case and its overlay as well, in every case would have required prolonged periods, the test site always being the same.

(iii) Large quantities of material are required in full scale pavement testing. In models it is not so.

(iv) The number of cases studied could be more in case of model tests, because of ease of handling and saving in time and cost.

(v) Keeping the aim of the present tests
i.e. verification of the finite element
solution in view, the model tests have quali-
tative superiority over the full scale tests.

8.3 REQUIREMENTS OF THE MODEL

The model should be such that it should represent
the pavement properties as closely as possible. With
this end in view following requirements need to be
satisfied:

(i) The subgrade of the pavement slab is usually
supposed to be simulated by a mathematical
model like that of Winkler type. The test
model should simulate the same.

(ii) The pavement slab can be assumed to be made
up of elastic material (article 3.1). The
model material should also behave similarly,
within the range of testing.

(iii) The full bonded and unbonded conditions should
be possible to be simulated.

(iv) It may however, be mentioned that no restrict-
ion need be applied to geometrical properties
of the model, because in the proposed method,
analysis is possible for any geometry.

8.4 SELECTION OF MODEL MATERIAL

A wide range of materials can be considered for the preparation of model which will satisfy the above constraints. These could be:

(a) For Subgrade:

    (i) Clayey soil with controlled moisture content [256]

    (ii) Dry sand [257]

    (iii) Synthetic subgrade made out of sand-bitumen-latex or similar other combinations [258]

    (iv) Rubber subgrade [259]

    (v) Closely spaced uniform springs [260]

    (vi) Dense liquid [261]

    (vii) Liquid in an elastic container [262]

(b) For Pavement Slab:

    (i) Metallic plate e.g. steel, copper, aluminium or any other metal [256].

    (ii) Micro concrete [263]

    (iii) Plaster of Paris, Hydrostone Gypsum Cement Mortar. [264]

    (iv) Perspex or similar plastics.

The materials selected are:

    (a) Dry sand: The reasons of selecting dry sand as a model material are:

    (i) It is possible to obtain uniform density even in a very loose state. [257,265]

    (ii) The properties of local sand are already well known. [265]

(iii) Formulation for elastic solid model can be tested through this medium.

(b) Closely spaced uniform springs: This type of subgrade was selected for truly representing the Winkler subgrade model as assumed in the theory.

(c) Perspex was selected for simulating the pavement slab, with following advantages in view:

    (i)   Uniformity of thickness,

    (ii) Elastic, homogeneous and isotropic material properties.

    (iii) Large measurable strains can be expected even under small loads[266]. This has a specific advantage in case of pavement model because it is known that stress gradients are very high in the vicinity of the loaded area, therefore error in recording are minimised. Moreover, away from the load, the strains are very low and in a stiff material these may be too small to be measured unless heavy loads are applied.

    (iv) Bond conditions at interface can be developed easily. The surface of perspex is smooth enough to simulate unbonded condition when one layer is placed on another. Bonding can easily be done by araldite mixed with acetone as thinner or chloroform.

However, it is also known that this material contains certain drawbacks. These are:

    (i)   The deformation in perspex is time dependent.

(ii) Modulus of elasticity changes with temperature, age and moisture content.

(iii) Perspex assumes curvature under its own weight and therefore if the sheets are not stored properly for a long time, it is possible that the surface of the perspex sheet may contain initial curvature.

The effect of time dependent deformation can usually be avoided[263,266]. The change in elastic properties due to ambient conditions and age do not pose a problem because, it was proposed to complete the testing in a season when temperature remains fairly uniform. To be specific the strain measurements were done in the month of March and a part of April. All possible efforts to reduce the time of testing was made by proper planning.

8.5 PROPOSED INVESTIGATIONS

Following cases were studied on Winkler subgrade

(a) Single slab on subgrade,

(b) Base slab with unbonded overlay,

(c) Unbonded overlay with base slab having a discontinuity.

(d) Bonded overlay with base having a discontinuity.

(e) Bonded overlay with sound base.

All above five cases were also studied on sand subgrade.

A comparison with Finite Element solution for all above ten cases was proposed. It was also decided to test the model under two load positions, viz. interior and edge loadings.

8.6 FABRICATION OF THE MODEL

8.6.1 Selection of Model Dimension

(i) Slab

As the finite element analysis is possible for any slab size, the size of the perspex slab had no constraint. Therefore, from the considerations of ease of handling and proper instrumentation, the size of perspex slab was kept as 60 cm x 60 cm. The square plate was adopted to take the advantage of double symmetry so that number of strain gauges could be reduced. This was necessary not only to reduce the cost, but also from the point of feasibility as this would have exceeded the capacity of the multichannel switching unit. The thickness should be such that it should be small as compared to slab dimension, a requirement as per the assumption of plate theory (article 4.2). Based on this requirement and availability the thickness of the perspex sheet selected was 0.63 cm. The perspex sheet used was from ICI, a standard make.

The overlay was also kept of same dimensions. The crack was simulated by cutting the perspex sheet in the base into two pieces. Since the overlay is placed on its top and the load over it, it can be visualized that shear transfer as envisaged in modelling the crack (article 4.5) will take place. This was done with due cognizance of the aim i.e. verification of the effect of main assumptions involved in finite element formulation on the stresses in the base overlay system, specially the overlay.

(ii) Winkler Subgrade

The subgrade was made of high tensile steel, helical springs of 5 cm length and 1.75 cm dia. with a pitch of 5 mm. The wire diameter was 1.5 mm. This spring was selected out of several springs examined for their suitability. The springs were placed on a rigid mild steel plate of 6 mm thickness and size 62x62 cm. The plate was supported on a rigid frame with cross under support to ensure its rigidity. Holes of 1.25 cm diameter were drilled 5.0 cm apart to accommodate the spring guides. Springs were placed on these holes with spring guides inserted. The spring guide ends were provided with threads and nuts to enable adjustment of the spring height by ± 2 mm. This was essential because an earlier attempt was foiled where springs were directly fixed on a firm base and the perspex sheet

was placed on it. It was observed that only 60 percent
of the springs maintained contact with the plate. This
could have been because of the slight curvature in
the plate due to self-weight or the other reason
could be unequal height of the springs due to improper
fixing on the firm base. The adjustment of the spring
height by the sleeve and nut arrangement enabled the
assurance of perfect contact between the subgrade
and the slab. A drawback of this system was that the
adjustment caused unequal precompressions in certain
springs. However, the precompression was negligible
and only a minority of springs were subjected to it.
Thus the total effect of this precompression on the
average value of modulus of subgrade reaction was
considered to be negligible.

The details of the final subgrade model are
shown in figure 8.1. Also the view of this arrangement
is shown in figure 8.2.

(iii) Sand Subgrade:

Same perspex plate was used on sand subgrade also.
The sand was filled in the container by rainfall method[265]
with 1 metre height of fall. The container was made of
2 cm. thick wooden planks. Its dimensions were 1 x 1
meter in plan and depth was 30 cm. The decision to keep
this depth was based on approximate calculations to
simulate the semi-infinite subgrade conditions.
Formula given by Vesic and Saxena[38] was taken as a

guide. The horizontal dimensions were taken as $1\frac{1}{2}$ times the plate dimensions with an intention that the boundaries will be significantly away to have any influence on semi-infinite conditions adopted in Boussinesq's equation. The arrangement for elastic solid model is shown in figure 8.3.

8.6.2 Instrumentation

8.6.2.1 Strain gauges

The survey of available, electrical resistance strain gauges indicated that the gauges with following specifications could be procured for use in the present study:

1. Type   : bonded wire strain gauge, helical coil

2. Size   : (a) 5 mm
                  (b) 10 mm

3. Resistance : (a) 121.4±0.2 ohms
                  (b) 120.8±0.2 ohms

4. Gauge factor:(a) 2.05±2 percent
                  (b) 2.05±2 percent

8.6.2.2 Location of the Strain Gauges:

The fact that the stress gradients are high in the neighbourhood of the load, was kept in mind in deciding the location of the strain gauges. As it was decided to perform tests under interior and edge load

positions the strain gauges were fixed at close spacing
towards these locations. The strain gauges used in the
vicinity of these load positions were of smaller size
so that the average strain recorded by the gauge may be
accurate enough. Also, this would permit closer spacing
and larger number of gauges to be fixed. Another const-
raint in fixing the strain gauges was that it was decided
that the test plate in the base after performing the
Case (a) and (b) on both the spring and the sand
subgrade, would be cut to simulate the cracked base.
It was, therefore, necessary to shift the position of
strain gauges by 0.5 cm towards one side of the centre
line.

Figure 8.4 shows the placement of the strain gauges
in the base slab. The locations of the strain gauges in
the overlay is shown in the figure 8.5. These along with
the connecting leads is also shown in figure 8.6. It may
be noted that the strain gauges between points O and E
in Figure 8.4 and O'-E' in figure 8.5 are placed in
pairs at right angles to each other. This was done to
enable the stress computation with due consideration of
Poisson's effect. Strain gauges were also placed between
O-A, O-C and C-E in the base.

8.6.2.3 Fixing of Strain Gauges

The location of the strain gauges were accurately
marked on the perspex plate to be used as base as well as

that which was to be adopted as overlay. This was as
per the details shown in figure 8.4 and 8.5. The surface
were now thoroughly cleaned and slightly roughened by
fine sand paper. A thin layer of 'Araldite' was applied
on the surface of the perspex at the location of the
gauges and also to the back side of the gauge. The
gauges were fixed and kept under a constant pressure of
about 5 kg/cm^2 for 24 hours. Leads were connected to
them thereafter, each lead being marked simultaneously
with a number tag corresponding to the number shown
in the figures 8.4 and 8.5 to ease their identification.
The leads were bunched and taped together neatly to avoid
interference with the springs. The appropriate arrange-
ment of bunching is shown in figure 8.6. The side of the
base plate on which strain gauges were fixed was kept
in contact with the subgrade, whereas, the strain gauges
were fixed on the top of the overlay. This was necessary
to have good contact at the interface.

8.6.3 Loading Arrangement

It was decided to adopt square contact area, since
simulation of square or rectangular loaded area is simple
in finite element method. There isnno restriction about
the size of loaded area. Therefore the size of contact
area was adopted as 3 cm by 3 cm. Incidentally, the
results of Paxon[267] indicate that for pavement slab

the shape of contact area does not have significant
influence. The load was applied by keeping standard
weights of 2 kg and 4 kg. over the stiff rubber pads
of 3x3 cm size so as to achieve as uniform a pressure
distribution as possible. The rubber pad, through which
the load was applied, was firmly secured to the position
of loadings so that during subsequent loading and un-
loading the position of the pad does not change.

8.6.4 Strain Measuring Bridge

The strain measuring bridge used was manufactured
by National Aeronautical Laboratory, Bangalore. The bridge
can sense the magnitude of strain of the electrical resis-
tance gauges of 120 to 1000 ohms directly. Gauge factor
range varies from 1.5 to 4.5. The total range is 0 to
$\pm$10,000 microstrains with a least count of a unit micro-
strain. The instrument has a built in power supply regu-
lator/unit for stable operation on 230 volts 50 cycle
A/C mains.

8.6.5 Multichannel Switching Unit

Multi-channel switching unit facilitates the
reading of a number of strain gauges in sequence by
connecting the relevant gauge and the dummy with the
strain measuring bridge through a knob control. The
available multichannel switch was of local make with

an arrangement to accommodate 50 strain gauges at a
time. During trials, it was found that the contact
resistance of the switch varied on each manipulation
of the knob control. This necessitated due precautions
while using it.

8.7 EXPERIMENTAL PROCEDURE

8.7.1 Determination of Slab and Subgrade Properties

Since the deformation in the perspex plate are
time dependent, it was, therefore, necessary to eliminate
the error that might creep in due to this behaviour.
Roll[263] has mentioned two methods to account for the
error due to time dependent behaviour. He however, sugg-
ests that waiting for a period of 20 to 30 minutes after
loading would eliminate the errors due to creep. The
strain vs time relationship was studied before the
commencement of the experimentation and strain-time
curve is shown in figure 8.7. It can be observed that
under the range of loading adopted for present study,
the change in strain reading after a lapse of 5 minutes
was only of the order of 1 micro-strain. It was, there-
fore, decided that for all loadings the readings of strain
be taken after lapse of 5 minutes.

Slab Properties

It is necessary to know the elastic properties
i.e. modulus of elasticity and Poisson's ratio of the

slab material, for computation of stresses. These values were determined by simply supported beam tests under two point symmetrical loading. It was also seen that the strain occuring in the beam had a time dependent variation. This in turn shows that the value of 'E' is time dependent. Therefore due precaution in accordance with the preceding paragraph was taken. The average values obtained were:

$$E = \text{modulus of elasticity} = 24000 \text{ kg/cm}^2$$
$$\nu = \text{Poisson's ratio} = 0.3$$

Subgrade Properties

(a) Modulus of Subgrade Reaction of Spring Subgrade

The average value of modulus of subgrade reaction was obtained by centrally loading, rigid plates of sizes 10x10 cm, 16x16 cm and 20x20 cm. It was noticed that there was practically no difference between the k values so determined. The average value obtained was 0.65 kg/cm^3.

(b) Modulus of Elasticity of Dry Sand Subgrade

The elastic properties under various confining pressures have been determined by Srivastava[265] for local sand. The method of sand filling adopted by him was same as in the present case. The confining pressure under the test slab will be low. Therefore, adopting his results for low confining pressures the value of

modulus of elasticity was taken as 25 kg/cm^2 and Poisson's ratio as 0.25.

8.7.2 Strain Recording Under Loaded Condition

The strain measuring bridge was calibrated, initially balanced and set for the gauge factor as per the instruction manual of the bridge. The connection of the measuring bridge to multichannel switching unit was made.

Strain recording for various strain gauges was commenced serially. The knob switch of the multichannel unit was set to the proper gauge. Initial reading of the strain measuring bridge was taken by balancing the bridge. The load of 2 kg was then placed at the proper location. The strain measuring bridge was again balanced after giving a time gap of five minutes to allow for the termination of time-deformation effect as decided in article 8.7.1. The load was then increased to 4 kg, 5 minutes were allowed again and thereafter the strain recording was done.

The load was removed and again a time gap of 5 minutes was given for the strains to recover. The initial reading of the balanced strain measuring bridge for the second strain gauge connected through the multichannel switching unit was recorded. The load was again

placed in position taking due precaution that there was no impact loading. The procedure similar to that adopted for recording the strain in the first gauge was repeated for this and all subsequent recordings.

A detailed precautionary investigation was carried out to ensure accuracy of results, by checks and rechecks. This detailed preinvestigation was necessary because of the temperamental functioning of the multichannel switching unit, because of which it was necessary to carry out the arduous procedure described above, consuming about 12 hours for each test.

8.7.3 Sequence of Testing

The following sequence was adopted to carry out the testing of the various cases enumerated in article 8.5.

Case I SINGLE LAYER

The single layer perspex sheet was first placed on Winkler subgrade and was tested as stated above for edge and interior load positions.

The single slab was then placed on dry sand bed and was tested at interior and edge locations.

CASE II- UNBONDED OVERLAY ON UNCRACKED BASE:

Second layer of perspex sheet was carefully

placed on the first layer to simulate unbonded overlay on uncracked base and the strains were measured on dry sand for interior and edge load positions. The set up was then removed. It was placed carefully on the spring bed, and was tested under interior and edge loadings.

CASE III- UNBONDED OVERLAY ON CRACKED BASE

The set up was removed and the base slab was cut as planned in article 8.6 to simulate a straight transverse crack. This slab along with the overlay was placed back on the spring subgrade and tested for interior and edge load positions. It was then removed and placed on the sand bed and tested for interior and edge load positions.

Case IV- BONDED OVERLAY ON CRACKED BASE

The set up was removed and the two halves of the base were bonded to the overlay with a mixture of 'Araldite' and Acetone to give thin consistency for uniform bonding. The two were kept under a pressure of about 5 kg/cm^2 for 24 hours. Thereafter it was removed and was placed on the sand bed and tested for interior and edge load positions. The testing for interior and edge load positions on Winkler subgrade was done thereafter.

CASE V-BONDED OVERLAY ON UNCRACKED BASE

Another set of two plates of 60x60 cm and 0.63 cm thickness were taken and bonded together as described

above. The system of strain gauges were fixed to the
bottom of the base and top of the overlay by adopting
a similar procedure as described earlier. This set up
after due drying and setting was placed first on
spring subgrade to test for interior and edge load
positions and thereafter on sand subgrade to test the
strains generated in base and overlay when the load
was placed in the centre and edge of the overlay.

8.7.4 Precautions during Testing

Besides careful observation of every aspect
following precautions were taken.

1. At each time of shifting of the respective
pavement system from spring subgrade to sand subgrade
and vice-versa it was ensured that the subgrade was in
full contact with the base. It was usually noticed that
on spring subgrade one or two springs required slight
readjustment. In case of sand subgrade no difficulty
was faced. After placing the plate on the sand a slight
manipulation of the plate ensured full contact.

2. In case of unbonded overlays the interface
was cleaned and a thin layer of french chalk powder was
uniformly sprinkled on the top of the base. The overlay
was then placed on it to observe the pockets of lack
of contact, at the interface. It was observed that the
lack of contact towards one of the edges did exist, though

it was only in a small zone. This was considered as negligible.

3. Care to avoid impact during loading and unloading was ensured.

4. To ensure that there was no effect of loading and unloading on the strains, sample of the readings were rechecked after completion of the full strain measurement. It was seen that there was practically no difference between the two sets.

5. All precautions necessary for strain measuring as per Perry and Lissner[268] and the operating manual of the strain measuring bridge manufacturers were taken.

8.8 ANALYSIS

The primary aim of the analysis is to verify the results of finite element analysis for various base overlay systems with the model experimentation. For the analysis following procedure was followed:

(a) Stress Computations from Model Tests:

The strain readings at any point were converted into stresses by the following formula,

$$\sigma_x = \frac{E}{(1-\nu^2)} - (\varepsilon_x + \nu\,\varepsilon_y) \qquad \ldots (8.1)$$

$$= \frac{E}{(1-\nu^2)} |\varepsilon_y + \nu\varepsilon_y| \qquad \ldots (8.2)$$

$$\sigma_y = \frac{E}{1-\nu^2}(\varepsilon_y + \nu\varepsilon_x)$$

Along the edge the strain gauges were fixed only in the direction parallel to the edge. This is because stress σ_y in the direction perpendicular to the edge is zero. Therefore from equation 8.1 and 8.2,

$$\sigma_x = \varepsilon_x . E \qquad\qquad ... 8.3$$

(b) Finite Element Analysis:

(i) Data Preparation; the finite element idealisation of the slab is as shown in figure 8.8 for Winkler subgrade. The data with relevant properties was prepared for the finite element program and the computer results were obtained on IBM 36/44. As shown in the figure the advantage of double symmetry along the centre lines was taken. This can be done for edge loading only if there is no effect of edge load beyond y-axis. This was confirmed by experimental tests. Therefore, it was decided that the advantage of double symmetry could be taken to reduce the computer time.

8.9 ANALYSIS OF RESULTS AND DISCUSSION

The results of the finite element analysis have been compared with the experimental observations. These comparisons are shown in the form of graphs. All the stresses are for unit load of one kg on 3 x 3 cm area. For experimental values, these stresses are computed by using equation 8.1, from the strain measurements taken.

The analytical values are obtained from the finite element results. The finite element results give moments at the Gaussian sampling points of the 3 point Gaussian integration value for an element[133]. These moments were converted into stresses and are then plotted in the figures. The distance are measured from the centre of the load in each case. The direction in all the figures are with reference to figure 8.4.

8.9.1 Comparison of Results of Single Slab

Figures 8.9 to 8.12 relate to comparison of stresses at the bottom of base as computed by Finite Element method to those found by measurements. In Figure 8.9, the loading is at the centre of the slab, the subgrade is of springs and the stresses are σ_y varying from O to E as given in figure 8.4.

Figure 8.10 relates to comparison of stresses along E B parallel to the edge for σ_x stresses on spring subgrade with edge loading. Figure 8.11 is for same conditions as figure 8.9 for sand subgrade. The close agreement of the nature as well as numerical magnitude can be seen from these figures. However, in case of figure 8.11, the behaviour of the experimental slab as compared to the analytical one is similar to one with higher radius of relative stiffness. The behaviour of sand is highly dependent on confining pressure and it is not known what

might be the confining pressure in the present case.
Therefore, the value of 'E_s' adopted from Srivastava[265]
may be on higher side, causing the discrepancy.

Another reason why stresses measured are lower than
the calculated in case of interior loading (figure 8.9)
is the 'saucer action'. It is believed that in-plane
forces come into play when the order of deflections
increase above 25-30 per cent of the plate thickness[165].
Incidentally the deflection under maximum test load of
4 kg do reach these values in case of single slab and
therefore the chances of presence of in-plane forces
increase in actual experiment. However, in finite element
solution; these forces are not taken into account because,
in actual cement concrete pavement slabs, the deflection
of this order never develops.

In case of figure 8.10 i.e. when the load is at the
edge, the two curves are matching. As the edges are free,
the in-plane forces are not prominent, though in this case
the deflections are of that magnitude.

Figure 8.12 related to the sand subgrade with edge
load shows an excellent correlation between observed and
calculated values.

8.9.2 Comparison of Unbonded Overlay on Uncracked Base

Figures 8.13 to 8.16 are for this condition, with
figure 8.13 relating to interior loading on spring subgrade,

figure 8.14 to edge loading on same subgrade. Figure 8.15
and 8.16 relate to sand subgrade with interior and
edge loadings respectively. Strains are measured at the
top of the overlay and bottom of the base, as such under
the load they are compressive and tensile, respectively.
Since the base and the overlay are of same rigidity, the
stresses at their top and bottom, respectively should be
equal in magnitude and opposite in nature, if the curvature
of both remain the same all throughout. This is assumed
in finite element analysis and therefore the analytical
curves in these figures are exactly symmetrical about the
distance axis. Regarding the symmetry of experimental
curves in figures 8.13 to 8.16 it can be seen that it
exists almost in all cases in the vicinity of the load.
Away from the load the symmetry does appear to be dis-
turbed. This indicates that in these cases there could
be a difference in curvatures of base slab and overlay
at locations away from the load. However, in all the
cases, the maximum stresses which are occuring under the
load are agreeing with the finite element results. This
indicates that the differences in curvature that might
exist away from the load does not affect the magnitude
of maximum stresses which occur under the load, where,
due to the presence of load the curvatures in base and
overlay become the same. This was also argued in
Chapter VI and therefore the contention on which the
formulation was based is found to be correct by experimental

verification.

The fact that the experimental and theoretical curves are matching gives confidence for the theoretical approach for unbonded overlays.

8.9.3 Comparison of Bonded Overlays on Uncracked Base:

Figures 8.17 and 8.18 relate to bonded overlays with uncracked base resting on spring beds under interior and edge loading conditions, respectively. Figure 8.19 and 8.20 are corresponding figures for sand subgrade. It is seen that in all cases the experimental and calculated values tally fairly well excepting figure 8.19 which is the case of interior loading on sand subgrade. The experimentally observed values are generally lower than expected ones. Moreover the curves are perfectly symmetrical. This proves the applicability of the bending theory.

The validity of the solution for bonded overlays is thus checked.

8.9.4 Cracked Base with Unbonded Overlay

Figure 8.21 and 8.22 shows the variation of stresses in base and overlay in the direction perpendicular to the crack when the load is in the centre of the slab. Figure 8.21 is for spring subgrade and figure 8.22 for sand subgrade. It is seen from figure 8.21 that the stress in the vicinity of the crack is reduced. However, the value

of stress in the neighbourhood of the crack is much less
than expected. This has disturbed the symmetry of the
base and overlay stresses as well. However, it can be
observed in the figure that the maximum stress measured
in the overlay is still agreeing with the expected value.
The maximum value in overlay is obtained from experi-
mental curve by extrapolating the observations and as
the trend of the experimental and theoretical curves are
same in the neighbourhood of the load, the extrapolation
is reasonable.

Same observations are also applicable to figure 8.22
which relates to sand subgrade. However, in this case, the
stress released in the vicinity of the crack is not so
much. It therefore appears that the greatly reduced values
observed in figure 8.21 could be due to the subgrade supp-
ort being discrete in that case, as the distance of spring
support from the crack is about 2 cm.

Figure 8.23 is for edge loading condition on spring
subgrade. The stress release has similar nature as in
figure 8.21 causing disturbance in symmetry. Not only
this, the maximum overlay stress, as observed is also
less in this case by about 20 percent.

Figure 8.24 is once again similar to figure 8.22
both being for the case of sand subgrade. The behaviour
of discrete springs are distinct from continuous subgrade.

However, this does not disqualify the Winkler model which
considers infinite number of springs rather than finite,
as adopted in the model study. The analysis is based on
Winkler model and therefore, there is difference in stress
magnitudes as observed and as calculated for the case of
cracked slab.

Figure 8.25 compares stresses parallel to the
direction of crack. All the curves are drawn based on the
experimental data. Comparison is made between the stresses
in slabs in cracked and uncracked conditions. The diff-
erence in base stresses can be observed, though the
overlay stresses increase on cracking, the base stresses
decrease. The reason for the lesser values of stresses
obtained for cracked base could be the Poisson's effect.
Due to stress release, the stress in other direction is
reduced in the base slab all along the crack. However,
the overlay is a separate entity and the crack in the base
has no direct connection with the material of the overlay.
As such due to the increase in deformations after cracking,
the stresses in the overlay increase. The magnitude of this
increase is not much as can be seen from the figure.

8.9.5 Bonded Overlay on Cracked Base

Comparison of calculated and observed values of
stresses in base and overlay slabs under interior loading

condition is made in figures 8.26 and 8.27 for spring
bed and sand subgrade, respectively. The behaviour of
cracked base on spring subgrade is different in the
bonded case as compared to the unbonded case observed
earlier. The stresses observed in unbonded base were
seen to be very small in the vicinity of the crack when
the subgrade was a bed of springs. However, in bonded
case, the bond does not allow the stresses to decrease
very much. Still the predicted and observed stresses
are different even in the bonded case. The overlay
stresses however match in both the figures.

Figures 8.28 and 8.29 are analogous to figure 8.26
and 8.27 respectively for edge loading conditions. The
observations applicable to those figures are also applicable
for these.

Figure 8.30 compares the experimentally observed
values of stresses in the direction of crack, in base
slab and overlay for cracked and uncracked conditions. The
figure is similar to figure 8.25 which was for unbonded
condition. In this case also the increase in overlay
stresses and decrease in base stresses can be observed
as was seen in unbonded case. Figures 8.31 and 8.32
compare the results of observations and the finite elements
solution analogous to figures 8.25 and 8.30 respectively.
It can be seen that the finite element solution gives
results which agree quite well with the experimental values.

It could therefore be inferred that the crack simulation by orthotropic properties, as are assumed in the theoretical formulation, is reasonable.

8.10 CONCLUSIONS

This experimentation confirms the validity of the finite element analysis and the assumptions made therein. Specifically, the following conclusions can be drawn for both interior as well as edge load positions:

(i) The results of the finite element analysis for the slab on elastic foundation are valid for Winkler as well as elastic solid foundation models.

(ii) The observed stresses and those calculated for bonded and unbonded OVERLAYS agree for sound as well as cracked overlays in case of both types of foundations.

(iii) The observed stresses in the bonded and unbonded BASE for the sound condition agree with finite element solution in both the foundation models.

(iv) In case of cracked base with unbonded overlay the observed stresses in the base are very small as compared to finite element solution. However, in case of sand subgrade the difference is reasonable though still their magnitude is small.

(v) In case of bonded overlays on cracked base also, the stress measured in base is small as compared to that calculated by finite element method. However, the difference is reasonable in both types of foundation.

(vi) For true assessment of stresses in the base near the crack, further studies are warranted.

(vii) Representation of crack in the slab by orthotropic properties is reasonable.

(viii) The statistical analysis for goodness of fit between experimental and analytical values as shown in Table 8.1 reveal that

(a) for single slab and cases of overlays with uncracked base the curves fit within 99 percent degree of confidence.

(b) for cases of overlays with cracked base the curves fit within 90 percent degree of confidence.

TABLE 8.1

STATISTICAL ANALYSIS FOR GOODNESS OF FIT BETWEEN EXPERI-
MENTAL AND ANALYTICAL STRESS-DISTANCE CURVES

Serial Number	Case	layer	Degree of freedom $\nu = N-1$	χ^2 cal-culated value	χ^2 table value for 99% confidence	Difference significant Insignificant
1	2	3	4	5	6	7
1.	Single layer-interior load spring subgrade	⌣	6	0.823	0.872	Insignificant
2.	Single layer-edge load spring subgrade		6	0.399	0.872	Insignificant
3.	Single layer-interior load. Sand subgrade		6	0.447	0.872	Insignificant
4.	Single Layer-Edge Load Sand Subgrade		6	0.137	0.872	Insignificant
5.	Uncracked Base with Unbonded Overlay Interior Load-Spring Subgrade	Base	6	0.042	0.872	Insignificant
		Overlay	6	0.016		Insignificant
6.	Uncracked Base with Unbonded Overlay Edge Load Spring Subgrade	Base	6	0.119	0.872	Insignificant
		Overlay	6	0.251		Insignificant
7.	Uncracked Base with Unbonded Overlay Interior Load S·nd Subgrade	Base	6	0.597	0.872	Insignificant
		Overlay	6	0.383		Insignificant
8.	Uncracked Base with Unbonded Overlay Edge Load, Sand Subgrade.	Base	6	0.233	0.872	Insignificant
		Overlay	6	0.009		Insignificant
9.	Uncracked Base with Bonded Overlay Interior Load Spring subgrade	Base	6	0.227	0.872	Insignificant
		Overlay		0.095		Insignificant

1.	2	3	4	5	6	7
10.	Uncracked Base with Bonded Overlay Edge Load Spring Subgrade	Base Overlay	6 6	0.023 0.032	0.872	Insignificant Insignificant
11.	Uncracked Base with Bonded Overlay Interior Load Sand Subgrade	Base Overlay	6 6	0.153 0.245	0.872	Insignificant Insignificant
12.	Uncracked Base with Bonded Overlay Edge Load Sand Subgrade	Base Overlay	6 6	0.049 0.160	0.872	Insignificant Insignificant

χ^2 Table value for 90% confidence

13.	Cracked Base with Unbonded Overlay Interior Load Spring Subgrade	Base Overlay	7 7	0.933 0.236	2.833	Insignificant Insignificant
14	Cracked Base with Unbonded Overlay Interior Load Sand Subgrade	Base Overlay	7 7	1.080 0.485	2.833	Insignificant Insignificant
15.	Cracked Base with Unbonded Overlay Edge Load Spring Subgrade	Base Overlay	7 7	1.760 2.85	2.833	Insignificant Significant
16.	Cracked Base with Unbonded Overlay Edge Load Sand Subgrade	Base Overlay	7 7	1.032 2.770	2.833	Insignificant Insignificant
17.	Cracked Base with Bonded Overlay Interior Load Spring Subgrade	Base Overlay	7 7	0.264 0.184	2.833	Insignificant Insignificant

1	2	3	4	5	6	7
18.	Cracked Base with Bonded Overlay Interior Load Sand Subgrade	Base Overlay	7 7	0.389 0.550	2.833	Insignificant Insignificant
19.	Cracked Base with Bonded Overlay Edge Load Spring Subgrade	Base Overlay	7 7	0.318 1.392	2.833	Insignificant Insignificant
20.	Cracked Base with Bonded Overlay Edge Load Sand Subgrade	Base Overlay	7 7	0.360 0.676	2.833	Insignificant Insignificant
21.	Cracked Base with Unbonded Overlay Interior Load Spring Subgrade	Base Overlay	7 7	0.255 0.154	2.833	Insignificant* Insignificant
22.	Cracked Base with Bonded Overlay Interior Load Spring Subgrade	Base Overlay	7 7	0.312 0.283	2.833	Insignificant* Insignificant

* Stresses along the crack

Note: Six degrees of freedom were considered for statistical analysis for single layer and cases of overlay on uncracked base, at equal distances of 5 c.m. each. However, because of the large variation in base stresses in the vicinity of the crack an additional point was taken at a distance of 1 cm. from the point of loading to give 7 degrees of freedom.

|←1·75cm→|

5mm

5cm
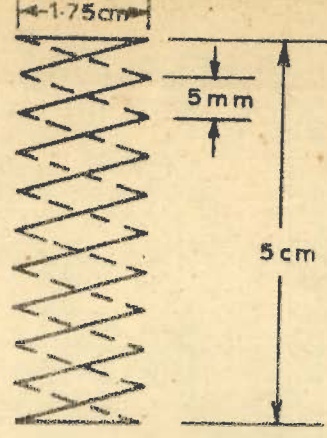
SPRING

SQUARE
WASHER 1mm
2.5 x 2.5 cm

5mm

5cm

7cm

5mm

SCALE FULL SIZE

|←1cm→|

GUIDE

ALL SQUARE
WASHERS WITH
SAME PLAN

↑A

62 cm

M. S. FLAT 6mm x 2cm
FOR PLATE SUPPORT

←——— 62cm ———→
PLAN

SCALE_1cm = 5cm

←5cm→   M. S. PLATE 6mm THICKNESS
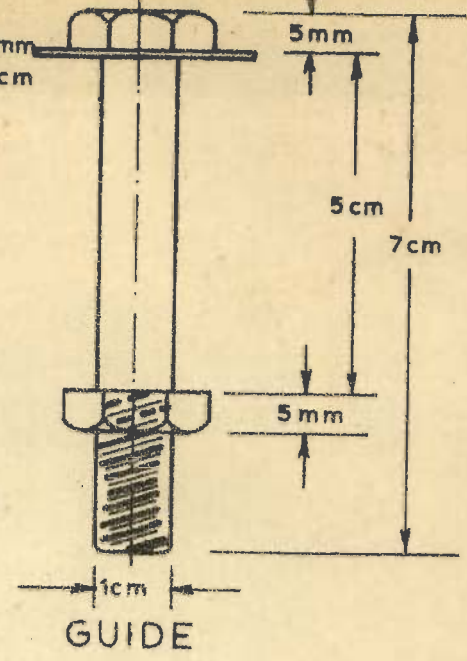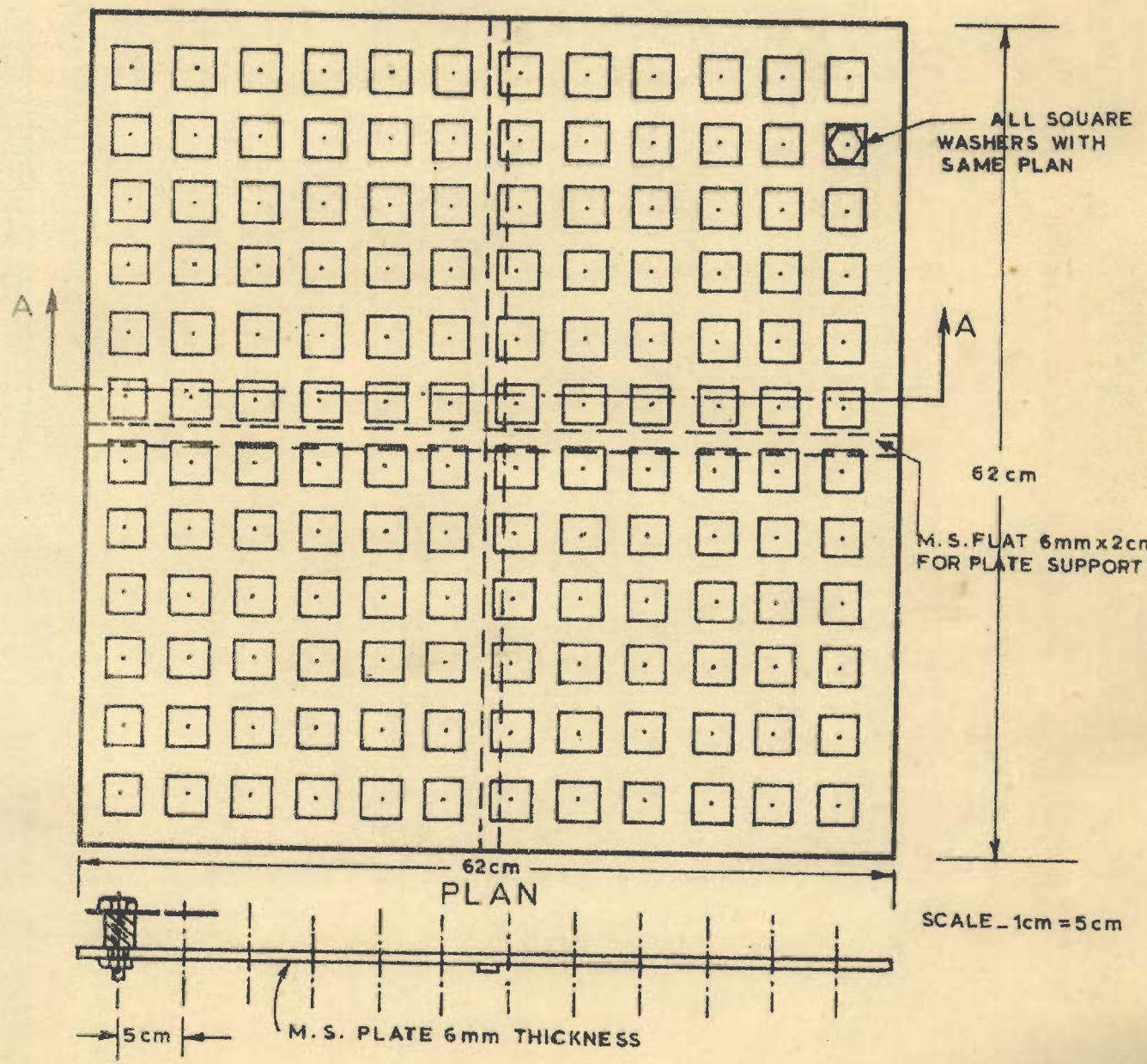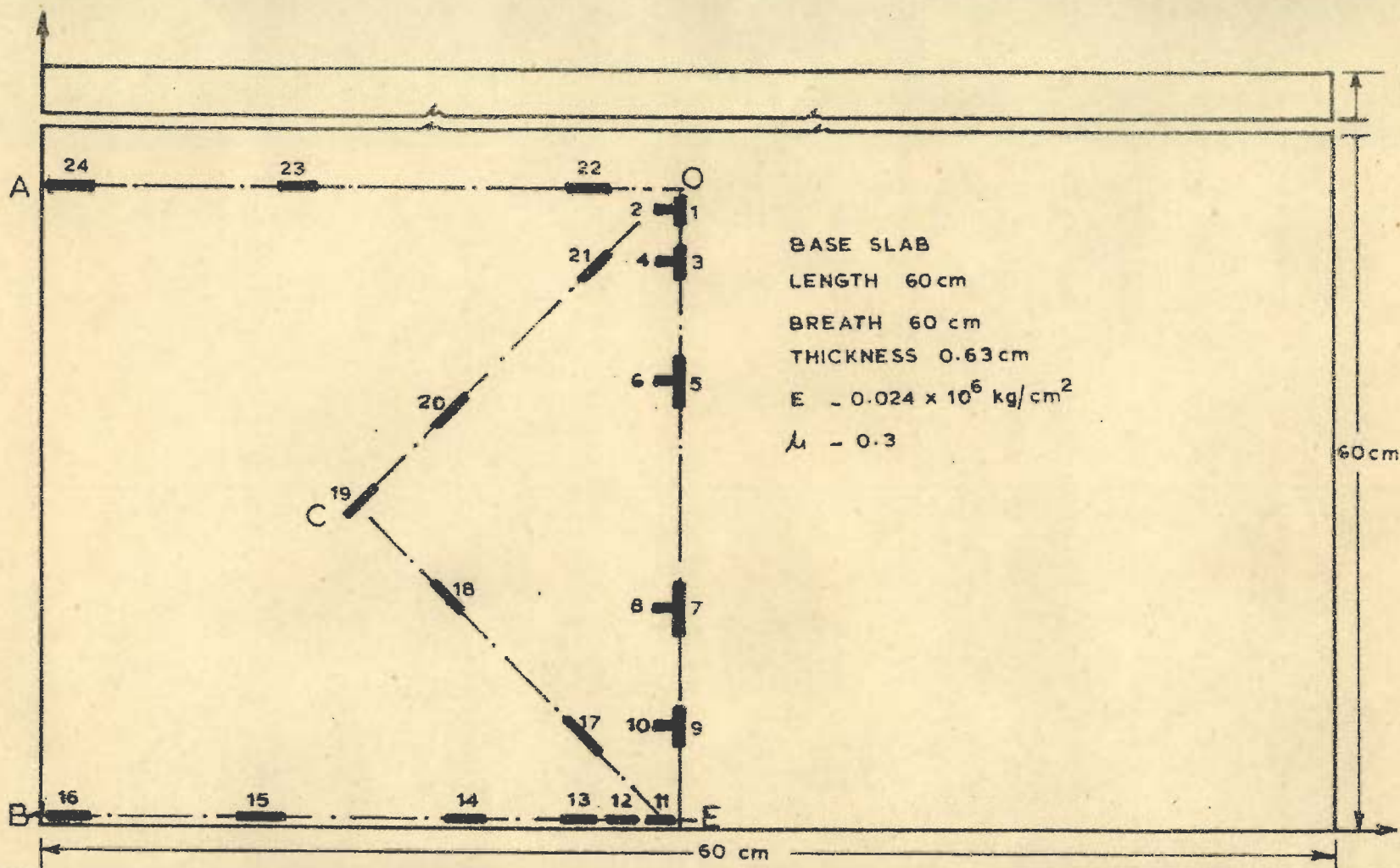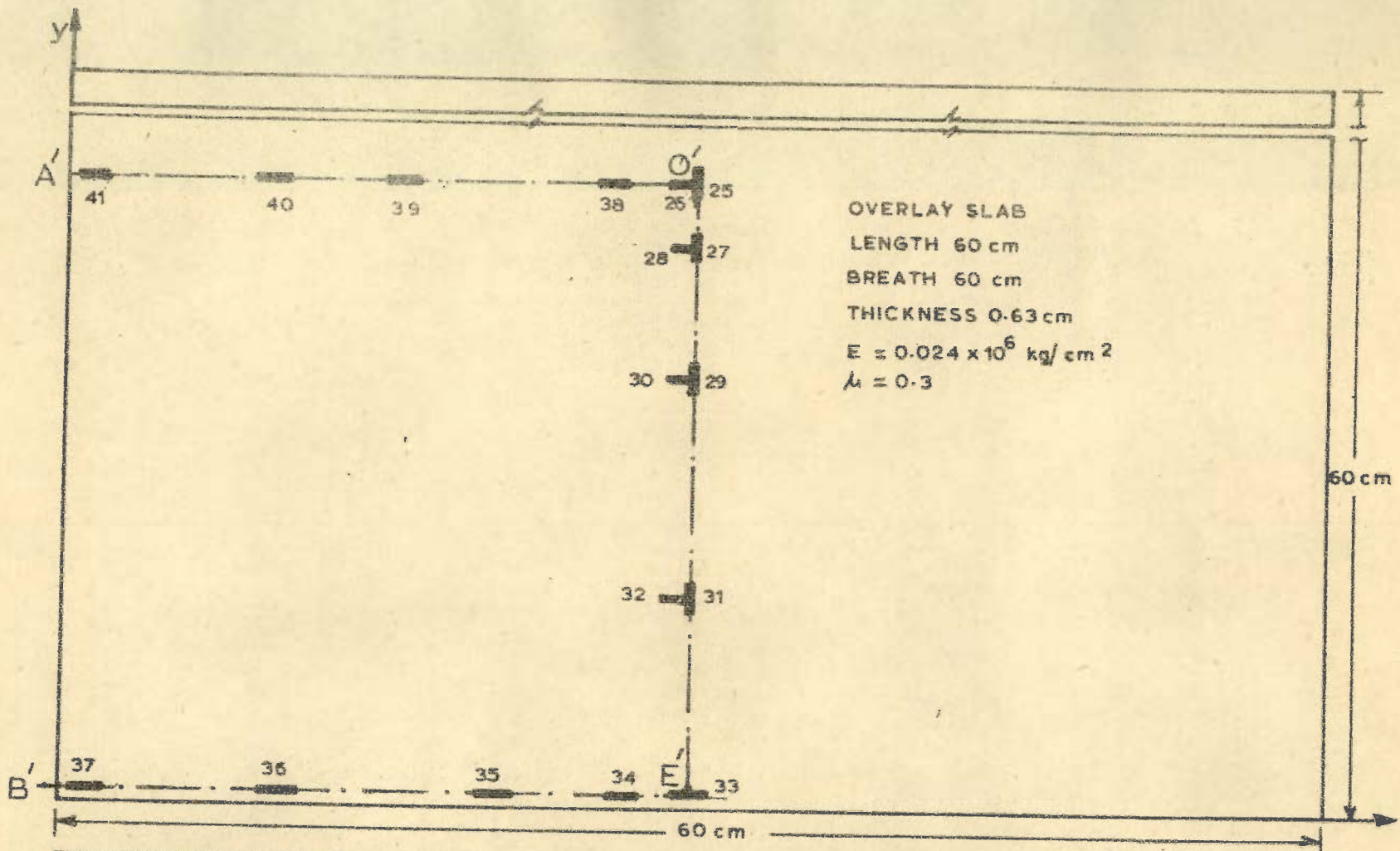
FIG. 8.1 _ DETAILS OF SPRING SUBGRADE
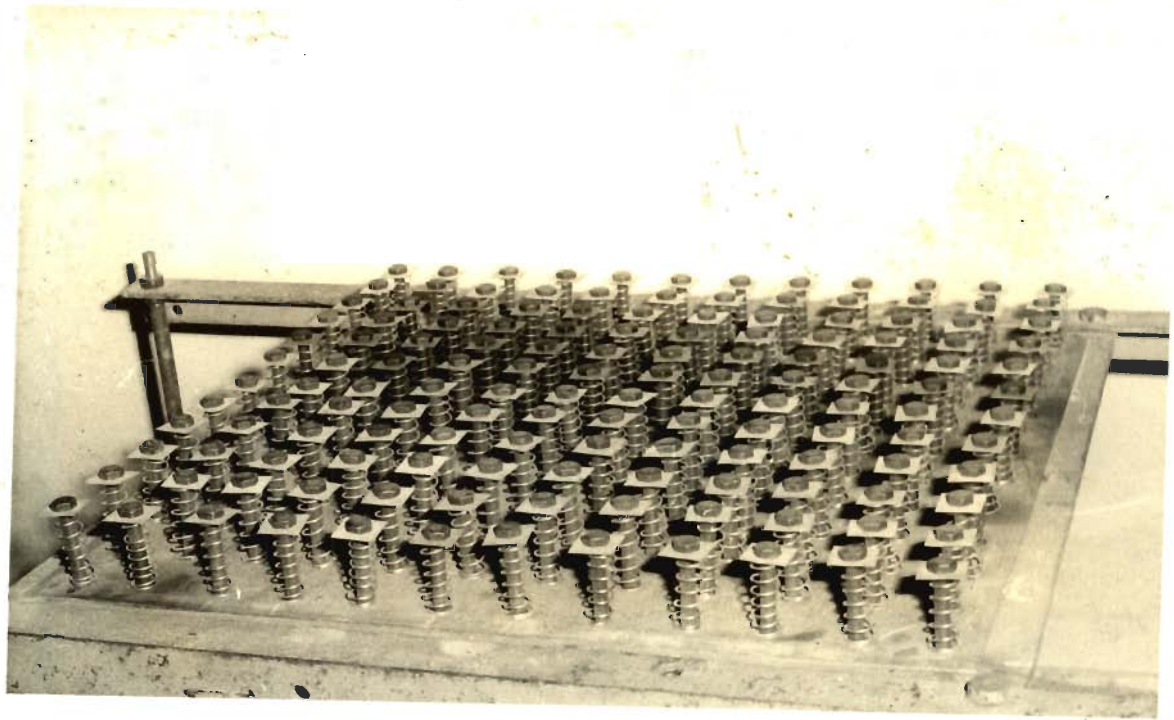
FIG. 8.2   SPRING SUBGRADE

FIG 8.3   WINKLER MODEL

BASE SLAB

LENGTH 60 cm

BREATH 60 cm

THICKNESS 0.63 cm

$E = 0.024 \times 10^6$ kg/cm^2

$\mu = 0.3$
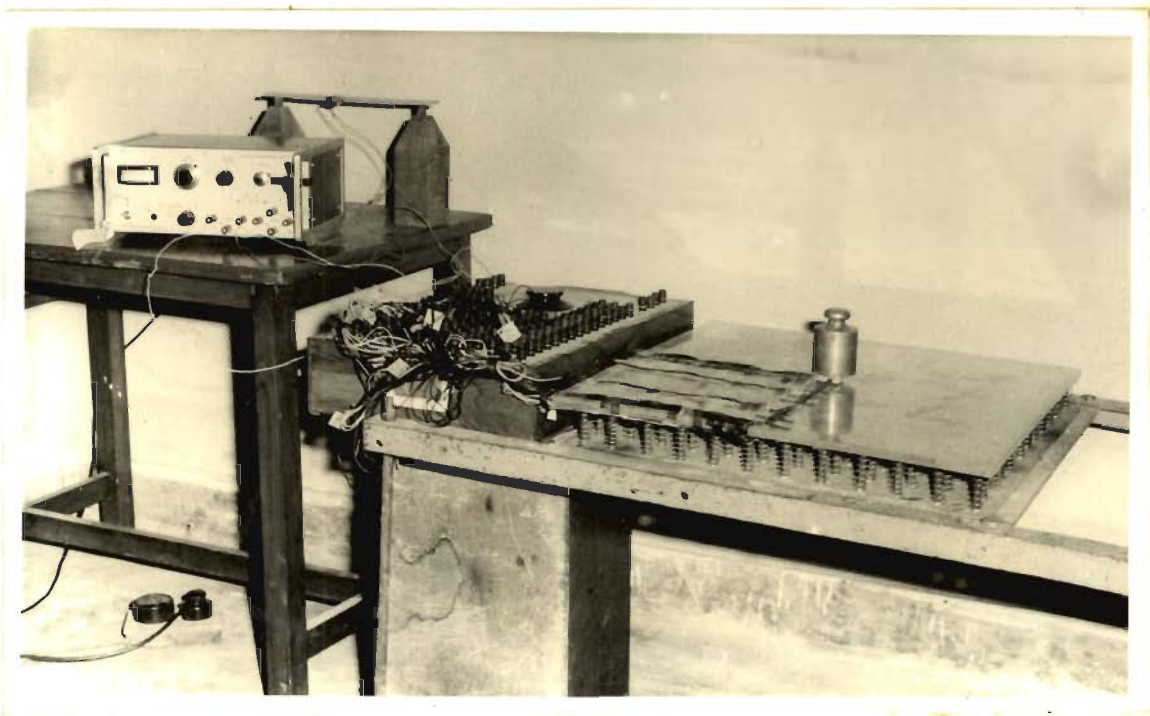
STRAIN GAUGE NO.	DISTANCE FROM O ALONG OE	TYPE	S.G. NO.	DISTANCE FROM O ALONG OE AND OC	TYPE	S.G. NO.	DISTANCE FROM E ALONG EB AND EC	TYPE	S.G. NO.	DISTANCE FROM O ALONG OA	TYPE	REMARKS
1	1·0	SA5	8	20·0	SA10	11	0.5	SA5	1	0.5	SA 5	
2	1.0	,,	9	26.0	SA 5	12	2.5	,,	2	1.0	,,	
3	4.0	,,	10	26.0	,,	13	4.0	,,	22	4.0	,,	
4	4.0	,,	11	29.5	,,	14	10	,,	23	14.0	SA10	
5	10·0	SA10	21	5.0	,,	15	20	SA 10	24	29.5	,,	
6	10·0	,,	20	15.0	SA 10	16	29.5	,,				
7	20·0	,,	19	20.0	,,	17	5.0	SA 5				
						18	15	SA10				

FIG. 8.4 _ DETAILS OF STRAIN GAUGE ARRANGEMENT ON BOTTOM OF BASE SLAB

y

A'
41   40   39   38 26 25   O'

OVERLAY SLAB
LENGTH 60 cm
BREATH 60 cm
THICKNESS 0.63 cm
$E = 0.024 \times 10^6$ kg/cm^2
$\mu = 0.3$

28 27

30 29

32 31

B'
37   36   35   34 E' 33

60 cm

60 cm

STRAIN GAUGE NO.	DISTANCE FROM O' ALONG O'E'	TYPE	STRAIN GAUGE NO.	DISTANCE FROM E' ALONG E'B'	TYPE	STRAIN GAUGE NO.	DISTANCE FROM O' ALONG O'A'	TYPE	REMARKS
25	0.0	SA5	33	0.0	SA5	26	1.0		
26	0.0	„	34	3.0	,,	38	3.0		
27	3.0	„	35	10.0	,,	39	10.0		
28	3.0	„	36	20.0	SA10	40	20.0		
29	10.0	SA10	37	29.5	SA10	41	29.5		
30	10.0	,,							
31	20.0	„							
32	20.0	„							
33	29.5	SA5							

FIG. 8.5 _ DETAILS OF STRAIN GAUGE ARRANGEMENT ON TOP OF OVERLAY SLAB
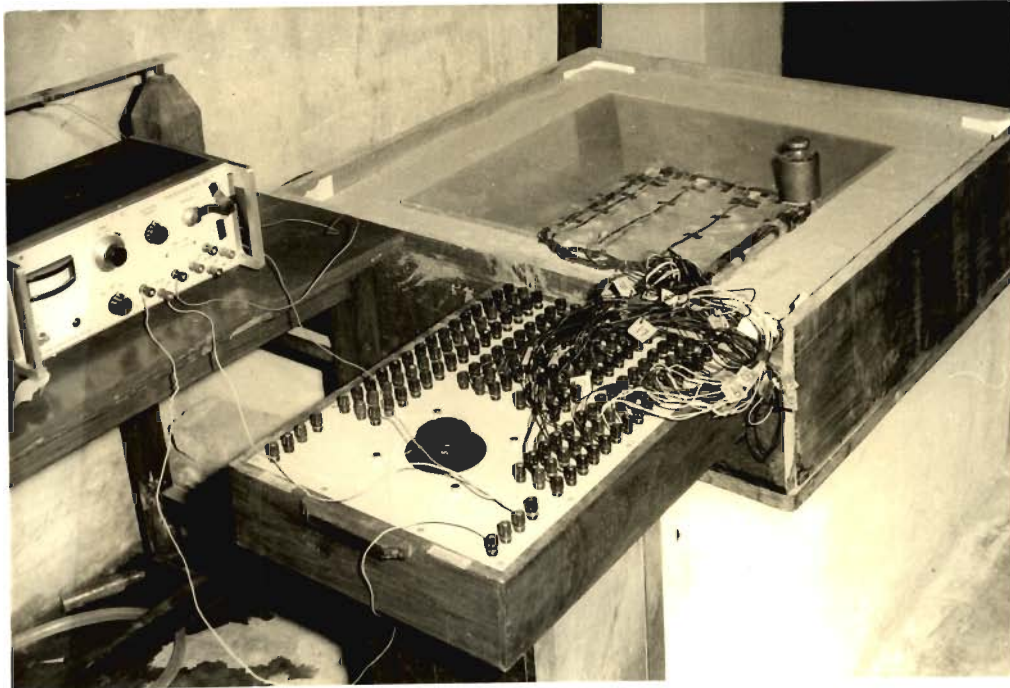
FIG. 8.6   ELASTIC SOLID MODEL
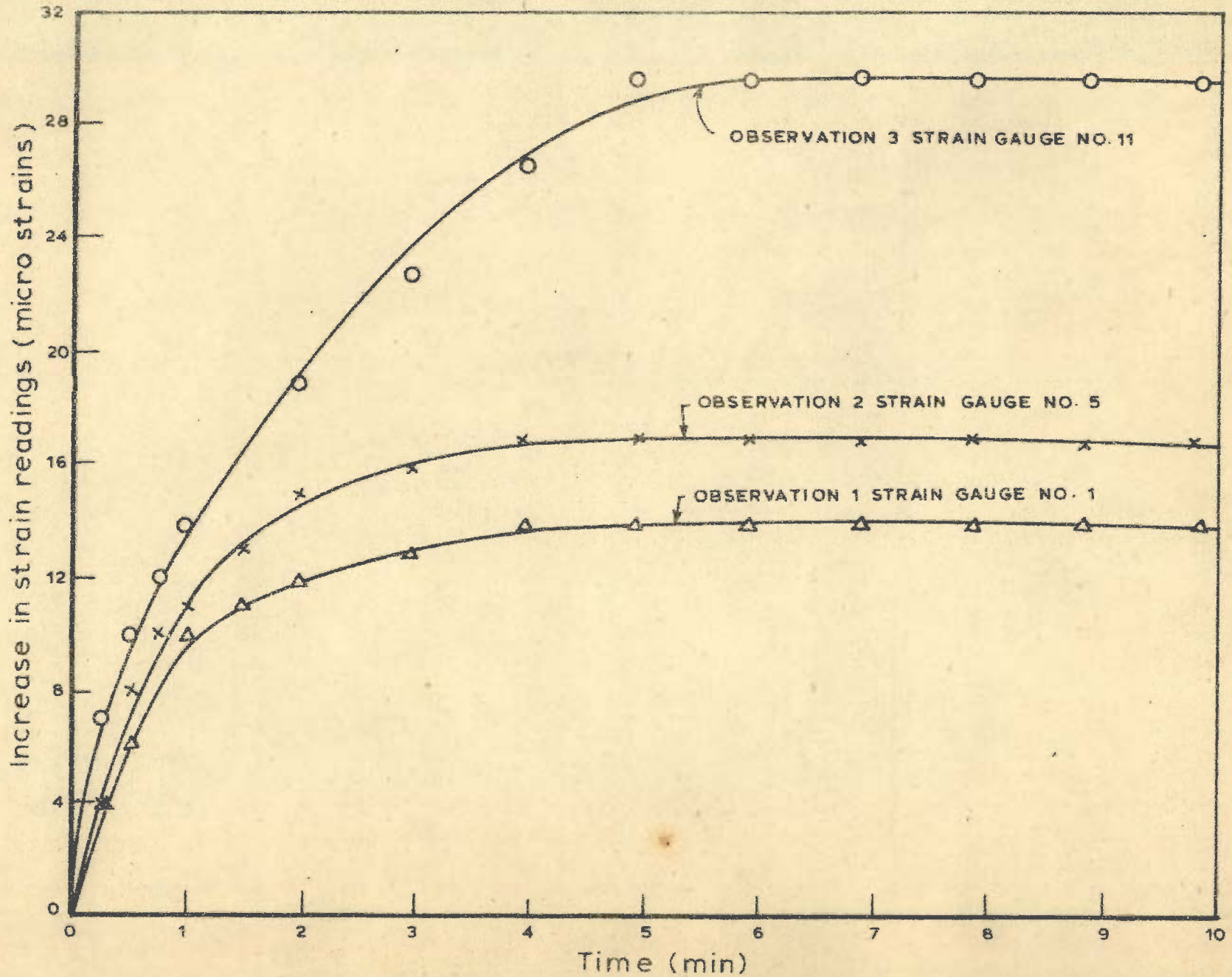
FIG.8.7 _ TIME DEPENDENT INCREASE IN STRAIN AFTER LOADING
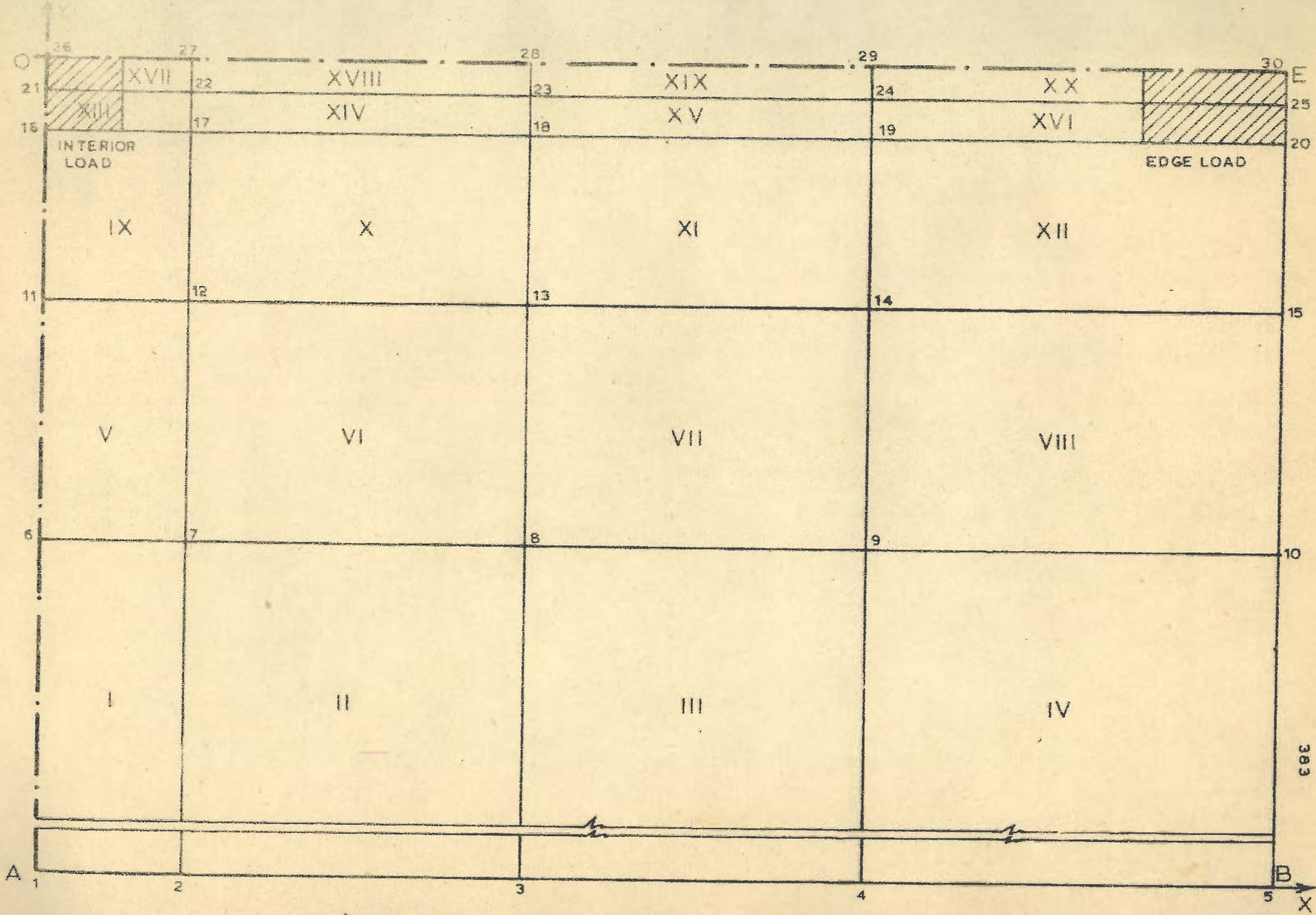
FIG.8.8 _ FINITE ELEMENT IDEALISATION OF QUARTER SLAB ON WINKLER SUBGRADE
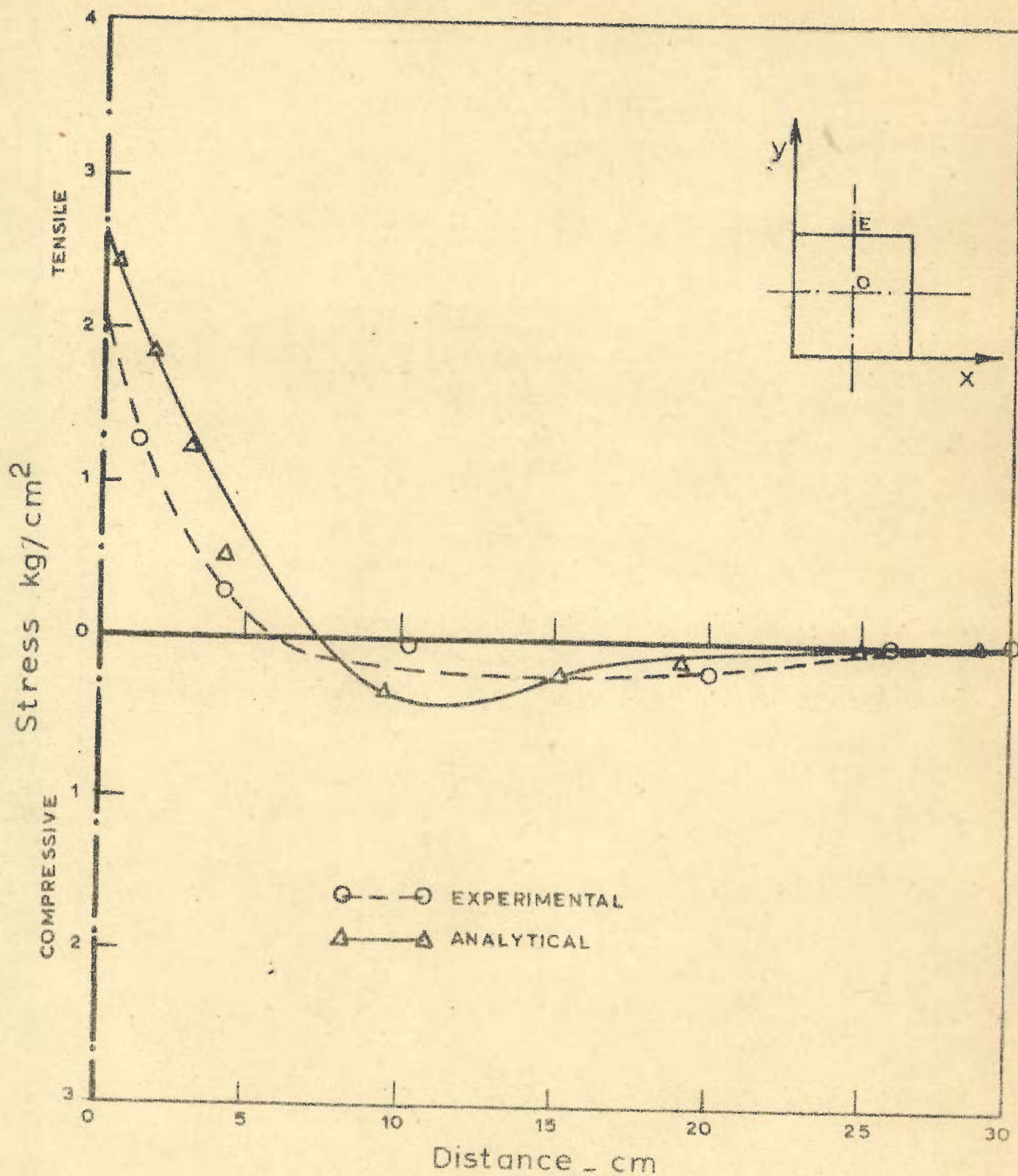
FIG. 8.9. VARIATION OF STRESS σ_y ALONG OE IN
BOTTOM FIBRE OF SINGLE LAYER, INTERIOR
LOAD, SPRING SUBGRADE.
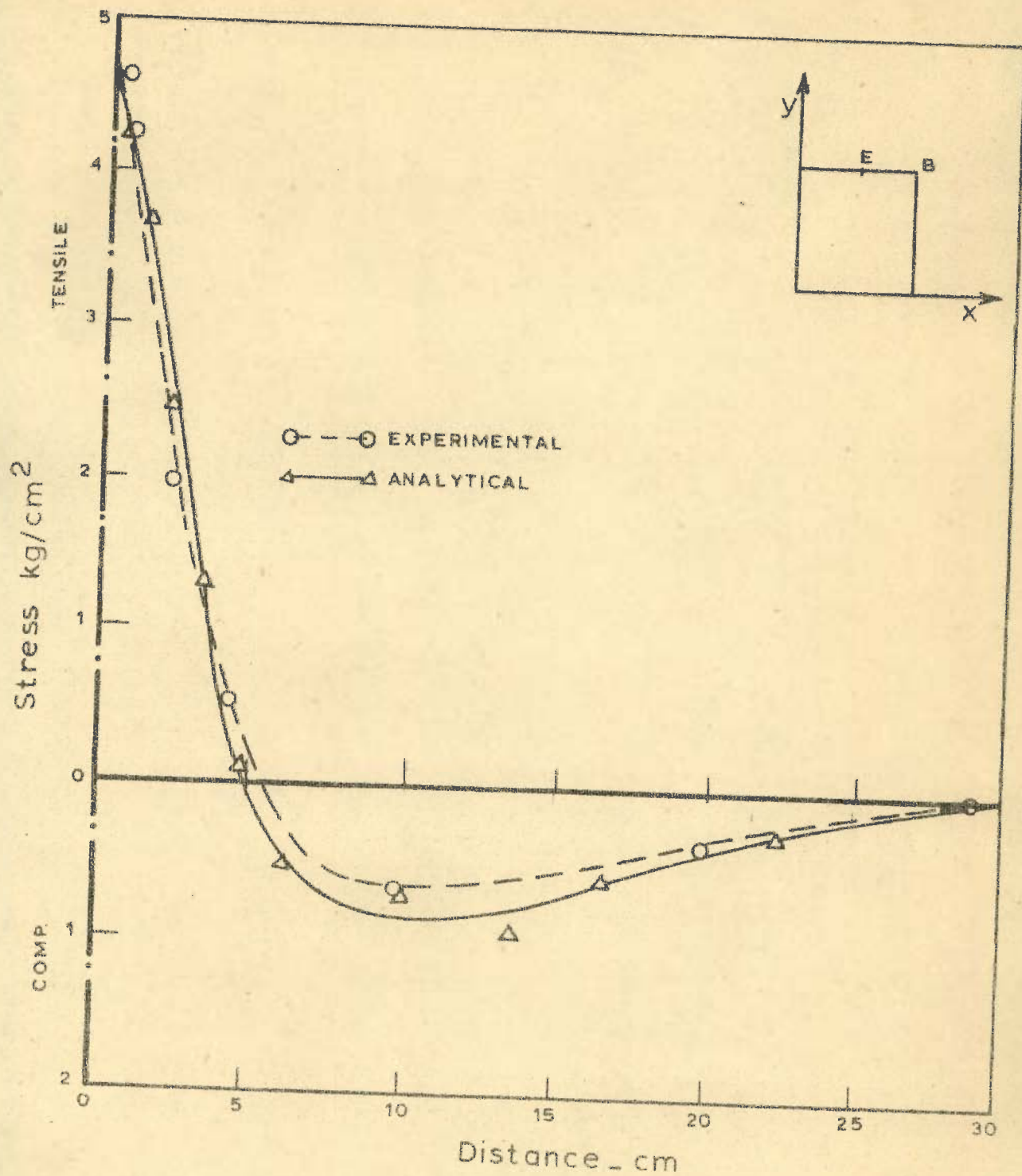
FIG. 8.10 _ VARIATION OF STRESSES σ_x ALONG EB IN BOTTOM FIBRE OF SLAB, EDGE LOAD, SPRING SUBGRADE.
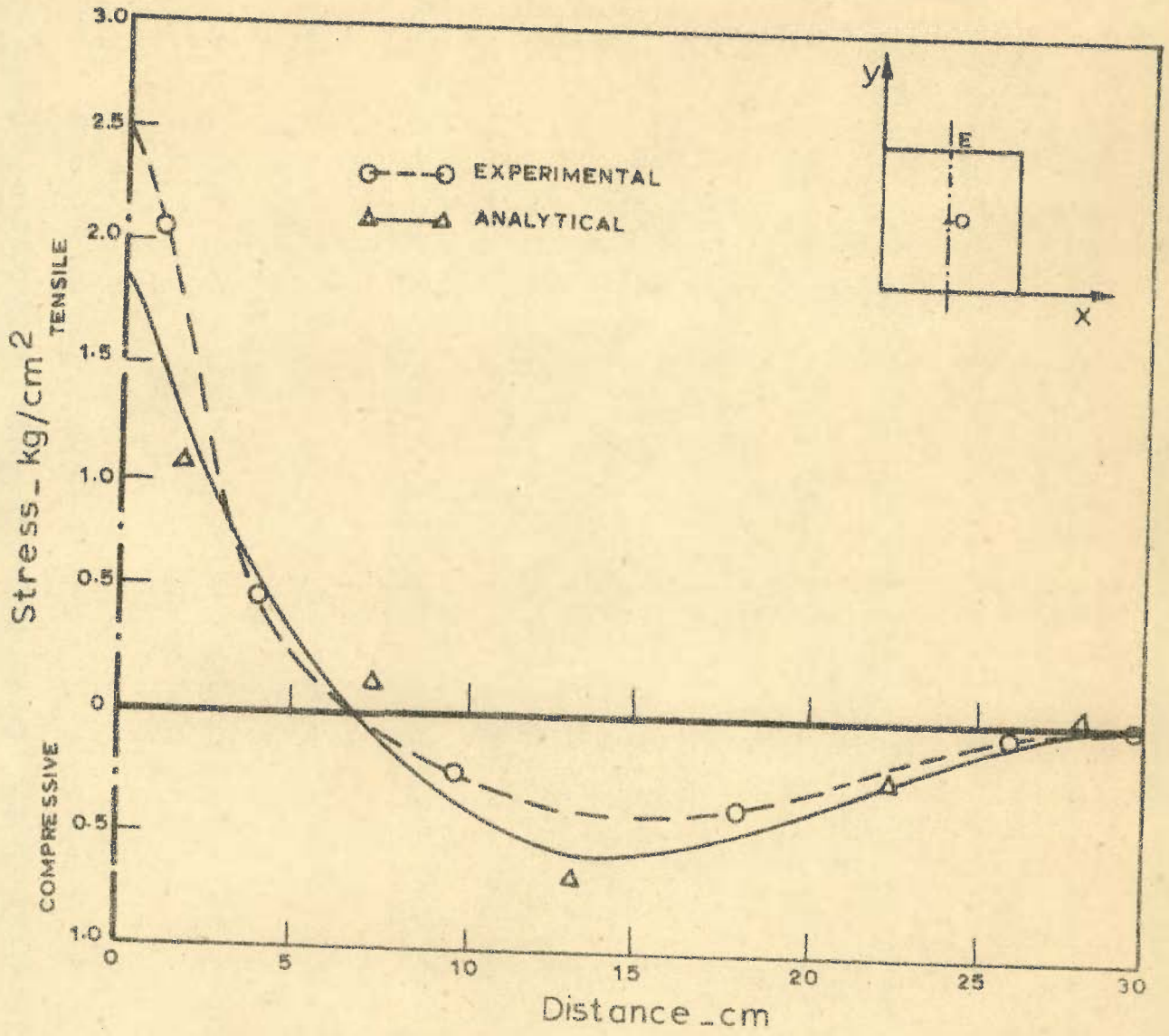
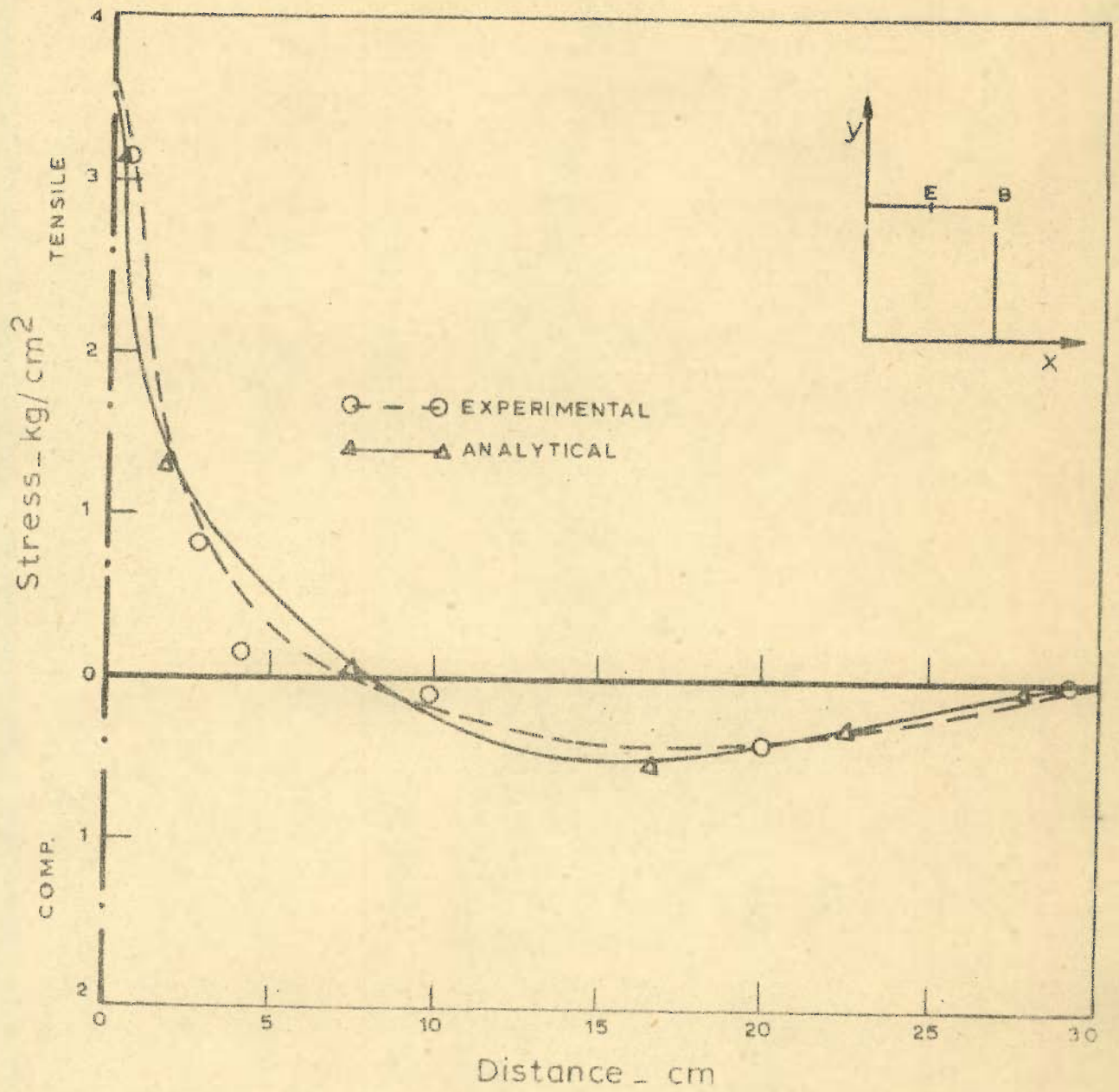FIG. 8.11 _ BOTTOM FIBRE STRESS IN SLAB ALONG OE,
INTERIOR LOAD, SAND SUBGRADE

FIG. 8 .12 _ VARIATION OF STRESS σ_x ALONG EB IN BOTTOM
FIBRE OF SLAB ON SAND SUBGRADE, EDGE LOAD
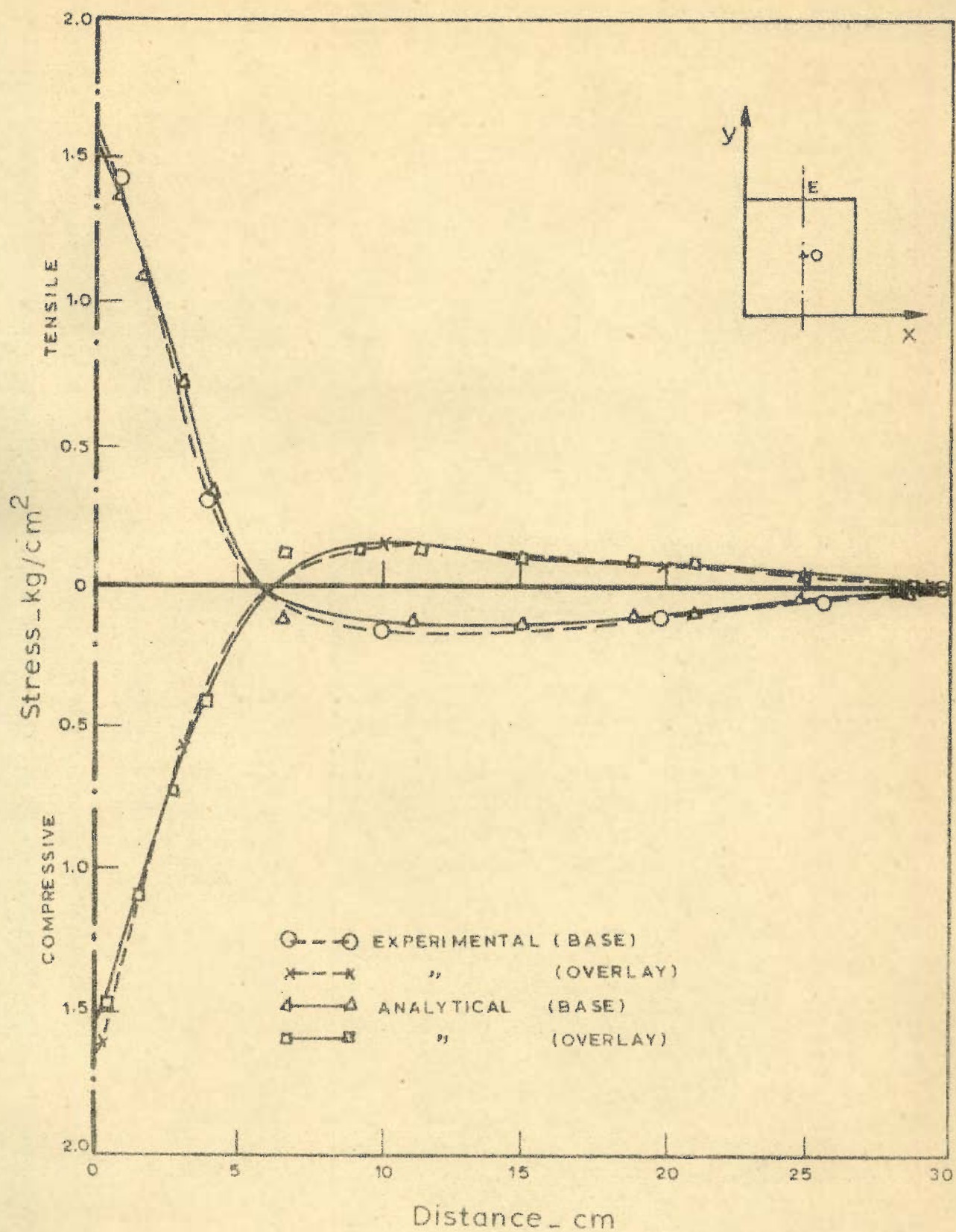
FIG. 8.13 _ UNCRACKED BASE WITH UNBONDED OVERLAY
INTERIOR LOAD , SPRING SUBGRADE , σ_y ALONG
O E
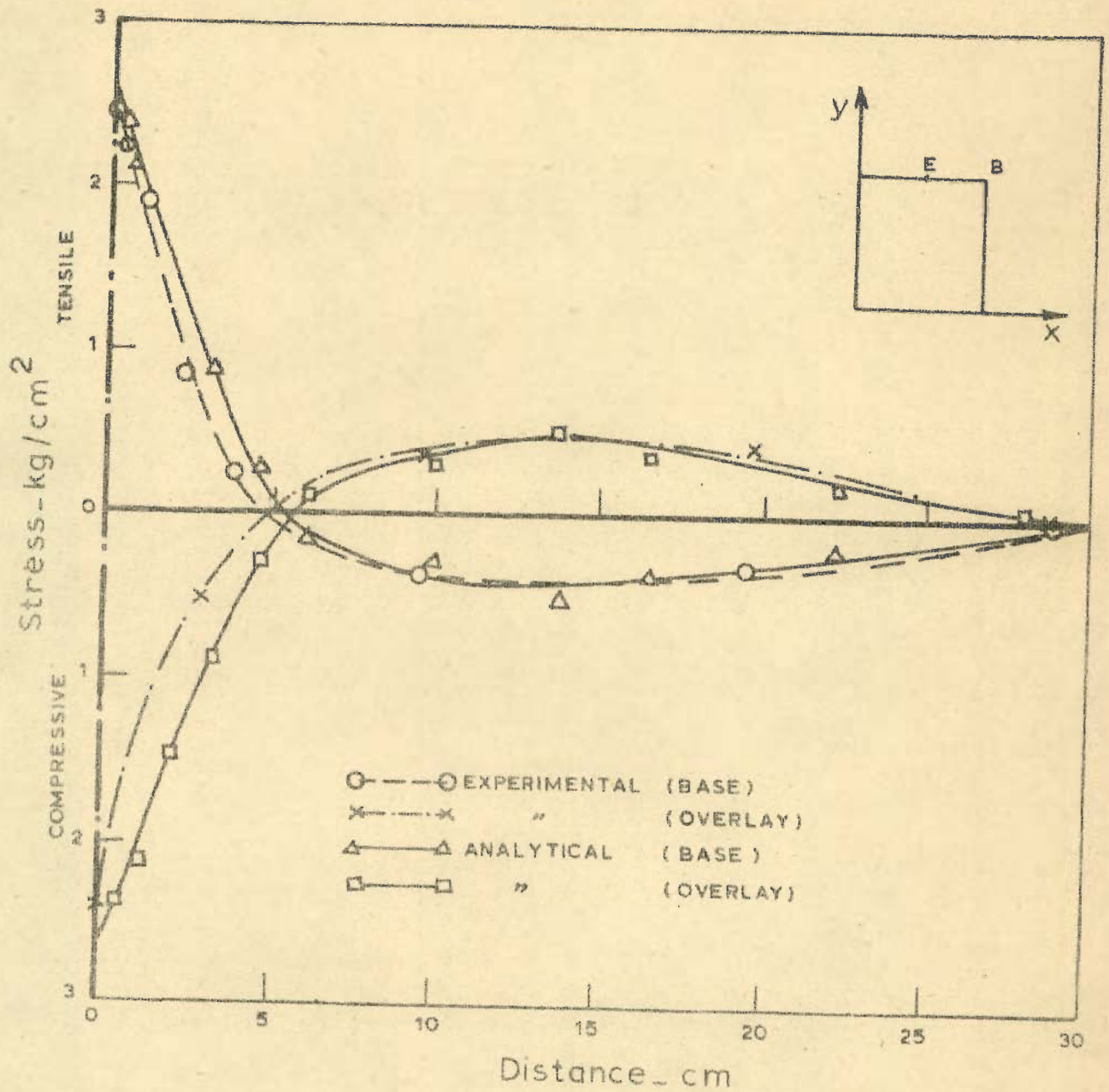
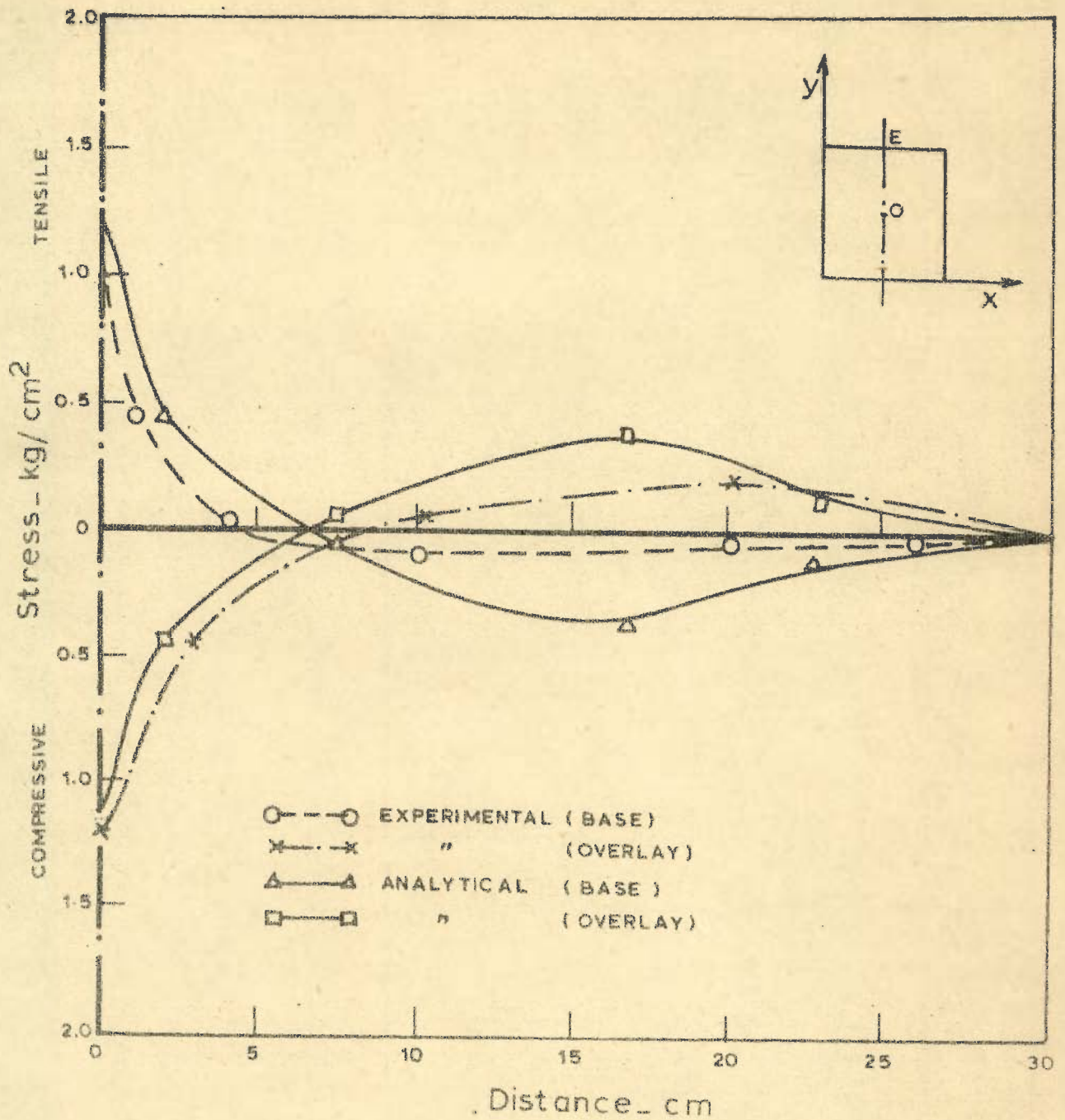FIG. 8 .14 _ UNCRACKED BASE WITH UNBONDED OVERLAY, EDGE LOAD, SPRING SUBGRADE, σ_x ALONG EB

FIG. 8.15 _ UNCRACKED BASE WITH UNBONDED OVERLAY,
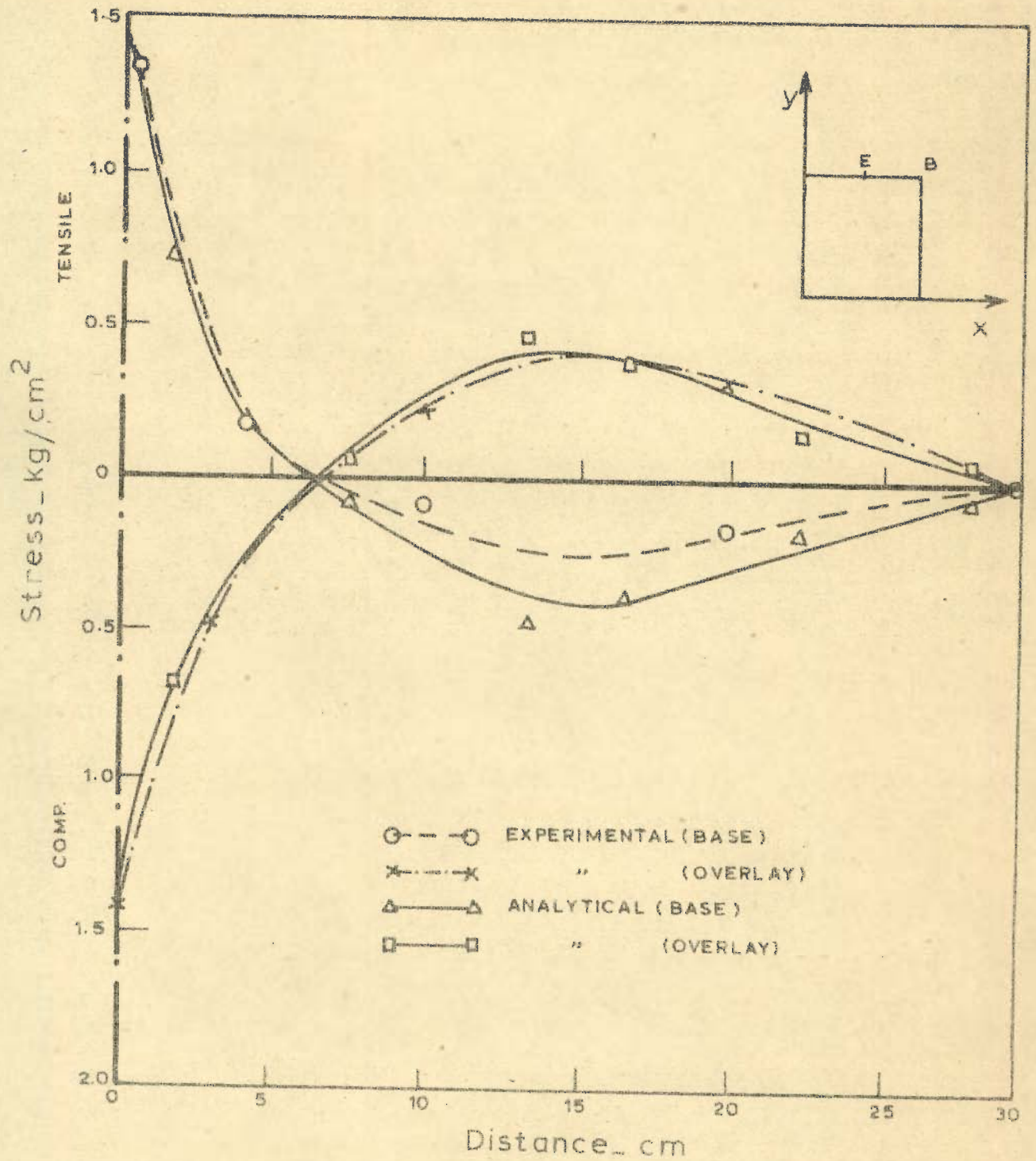INTERIOR LOAD, SAND SUBGRADE, σ_y ALONG OE

FIG. 8 16 _ UNCRACKED BASE WITH UNBONDED OVERLAY,
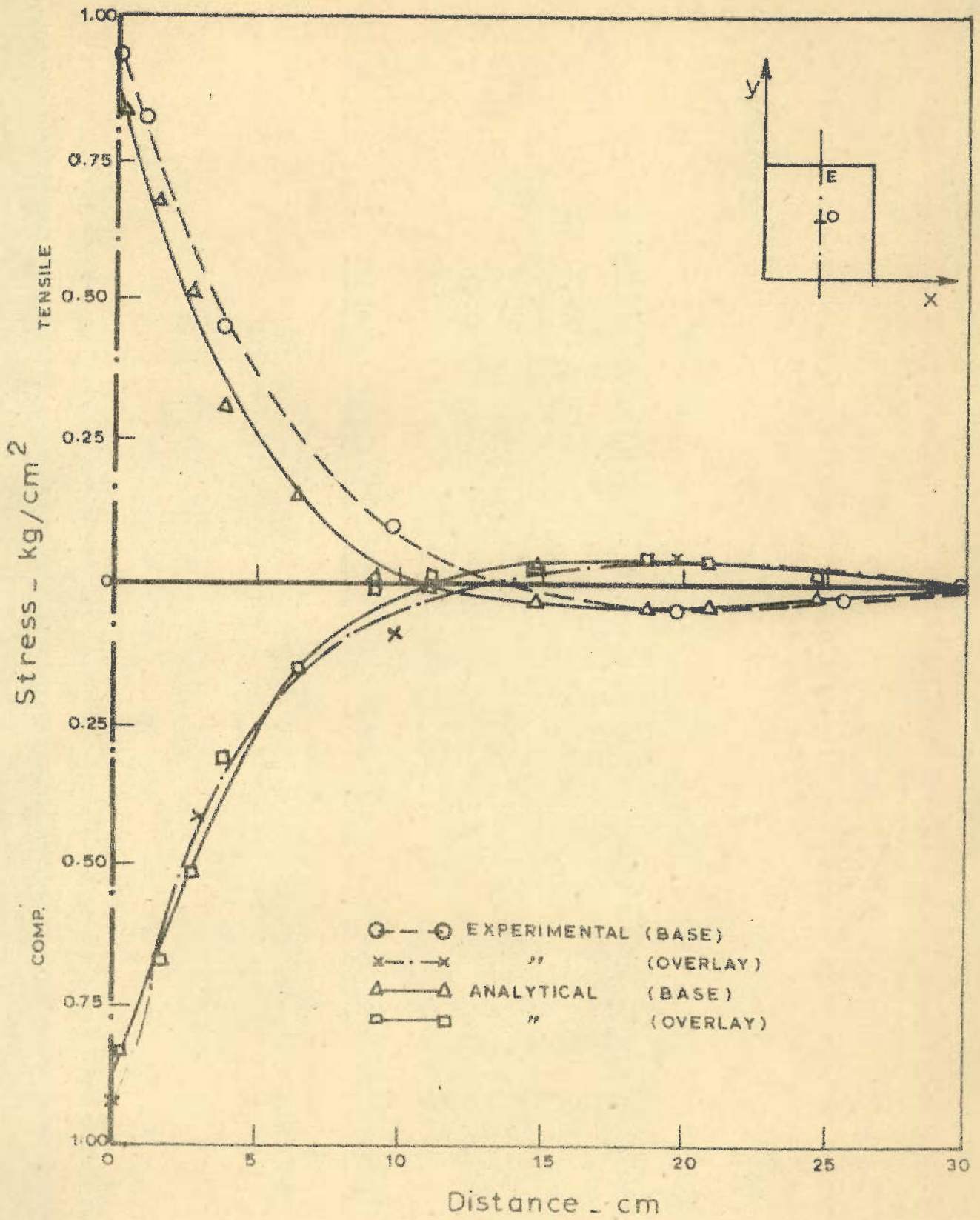SAND SUBGRADE, EDGE LOAD, σ_x ALONG EB

FIG. 8.17 — UNCRACKED BASE WITH BONDED OVERLAY, INTERIOR LOAD, SPRING SUBGRADE, σ_y ALONG OE
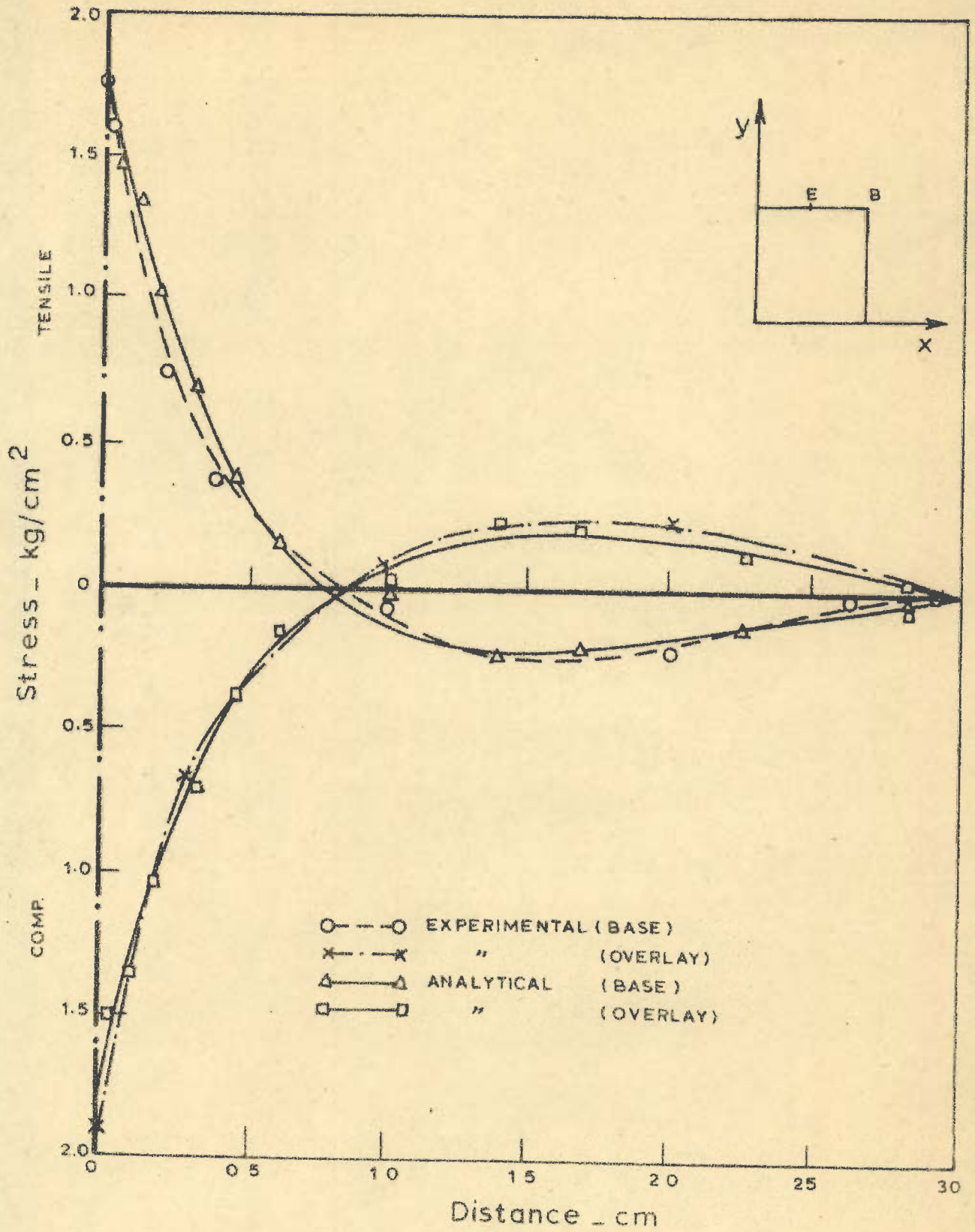
FIG. 8.18 _ UNCRACKED BASE WITH BONDED OVERLAY,
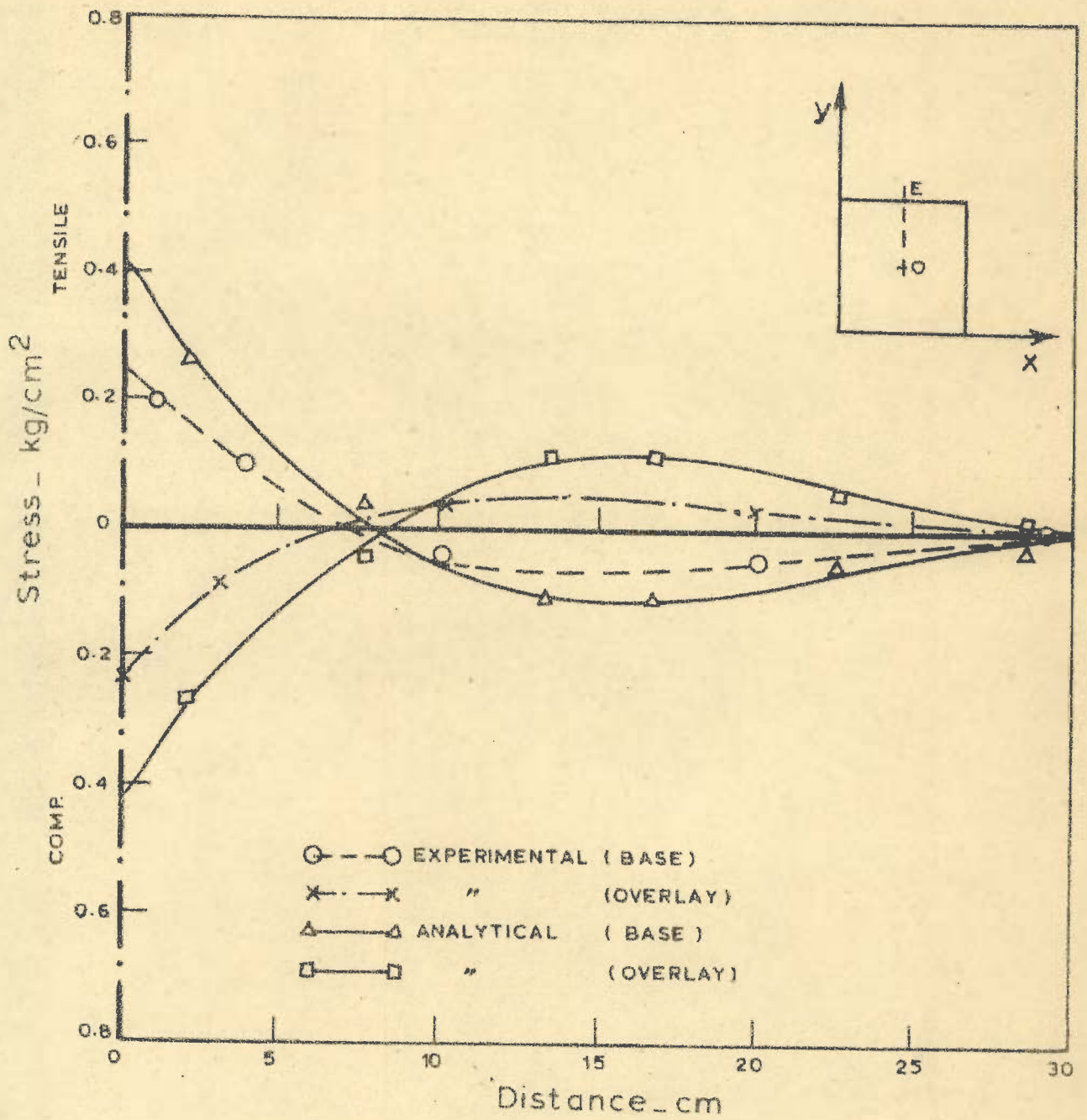EDGE LOAD, SPRING SUBGRADE, σ_x ALONG EB

FIG. 8.19 _ UNCRACKED BASE WITH BONDED OVERLAY,
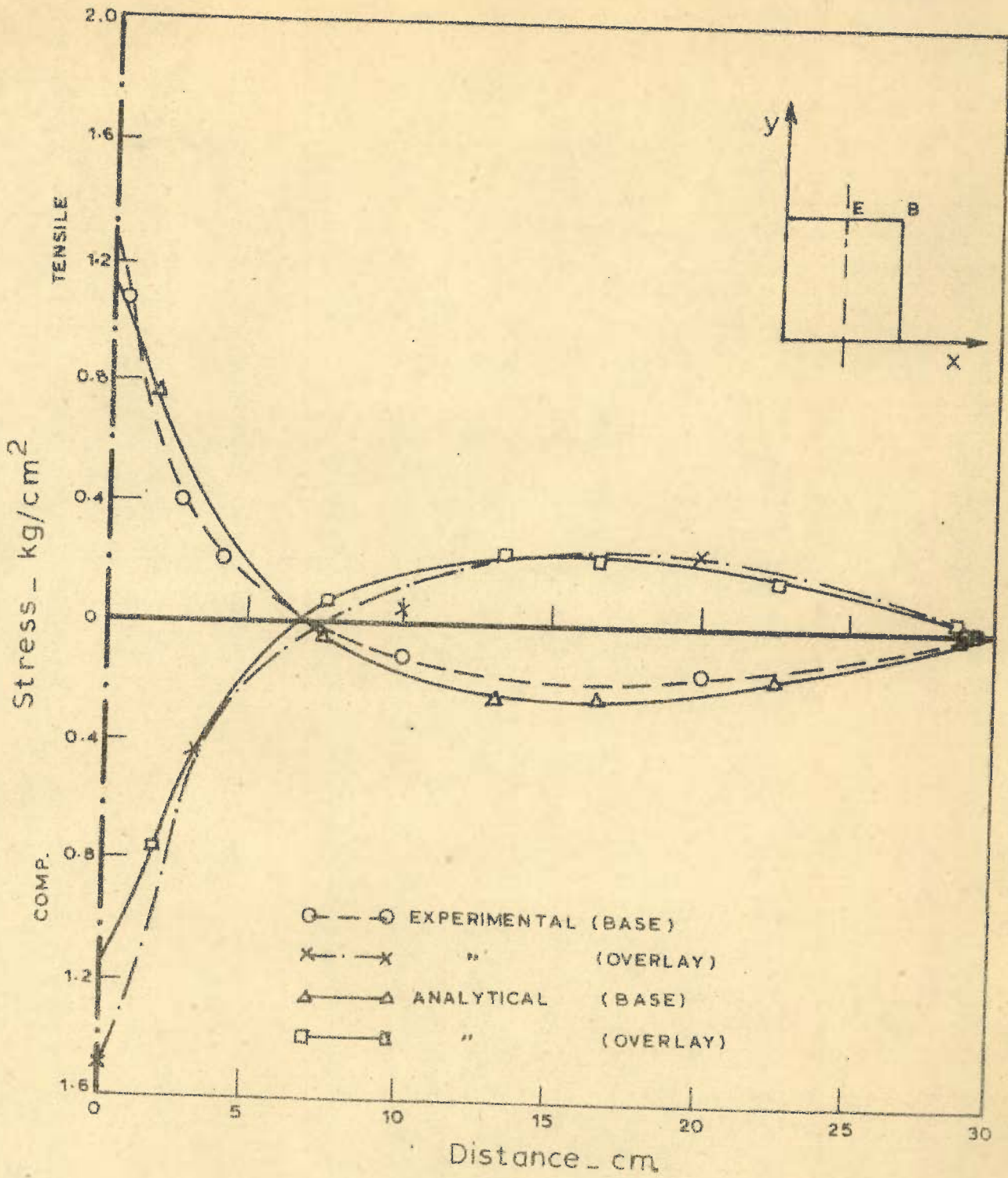INTERIOR LOAD, SAND SUBGRADE, σ_y ALONG OE

FIG. 8.20 _ UNCRACKED BASE WITH BONDED OVERLAY,
EDGE LOAD, SAND SUBGRADE, σ_x ALONG EB

FIG. 8.21 _ CRACKED BASE WITH UNBONDED OVERLAY,
INTERIOR LOAD, SPRING SUBGRADE, STRESSES
PERPENDICULAR TO CRACK, σ_x ALONG OA.

FIG. 8·22 _ CRACKED BASE WITH UNBONDED OVERLAY, INTERIOR LOAD, SAND SUBGRADE, σ_x ALONG OA

FIG. 8.23 _ CRACKED BASE WITH UNBONDED OVERLAY,
EDGE LOAD, SPRING SUBGRADE, σ_x ALONG E B.

FIG. 8.24 – CRACKED BASE WITH UNBONDED OVERLAY,
EDGE LOAD, SAND SUBGRADE, σ_x ALONG E B

FIG. 8.25 _ COMPARISON OF EXPERIMENTAL ANALYSIS,UNCRACKED BASE WITH UNBONDED OVERLAY VS CRACKED BASE WITH UNBONDED OVERLAY,INTERIOR LOAD,SPRING SUBGRADE, σ_y ALONG OE
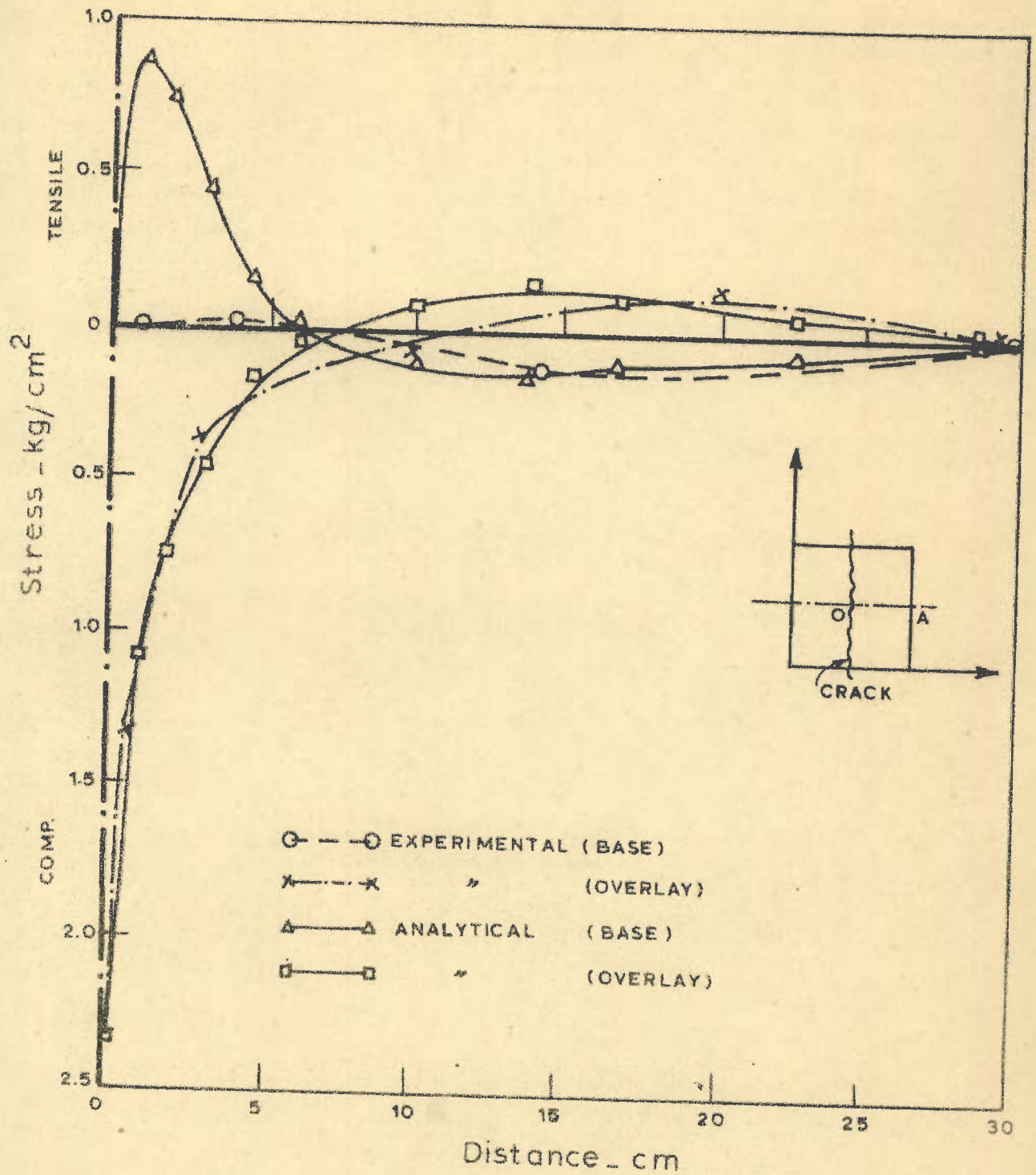
FIG 8 .26 _ CRACKED BASE WITH BONDED OVERLAY, INTERIOR LOAD, SPRING SUBGRADE, STRESSES PERPENDICULAR TO THE CRACK, σ_x ALONG OA
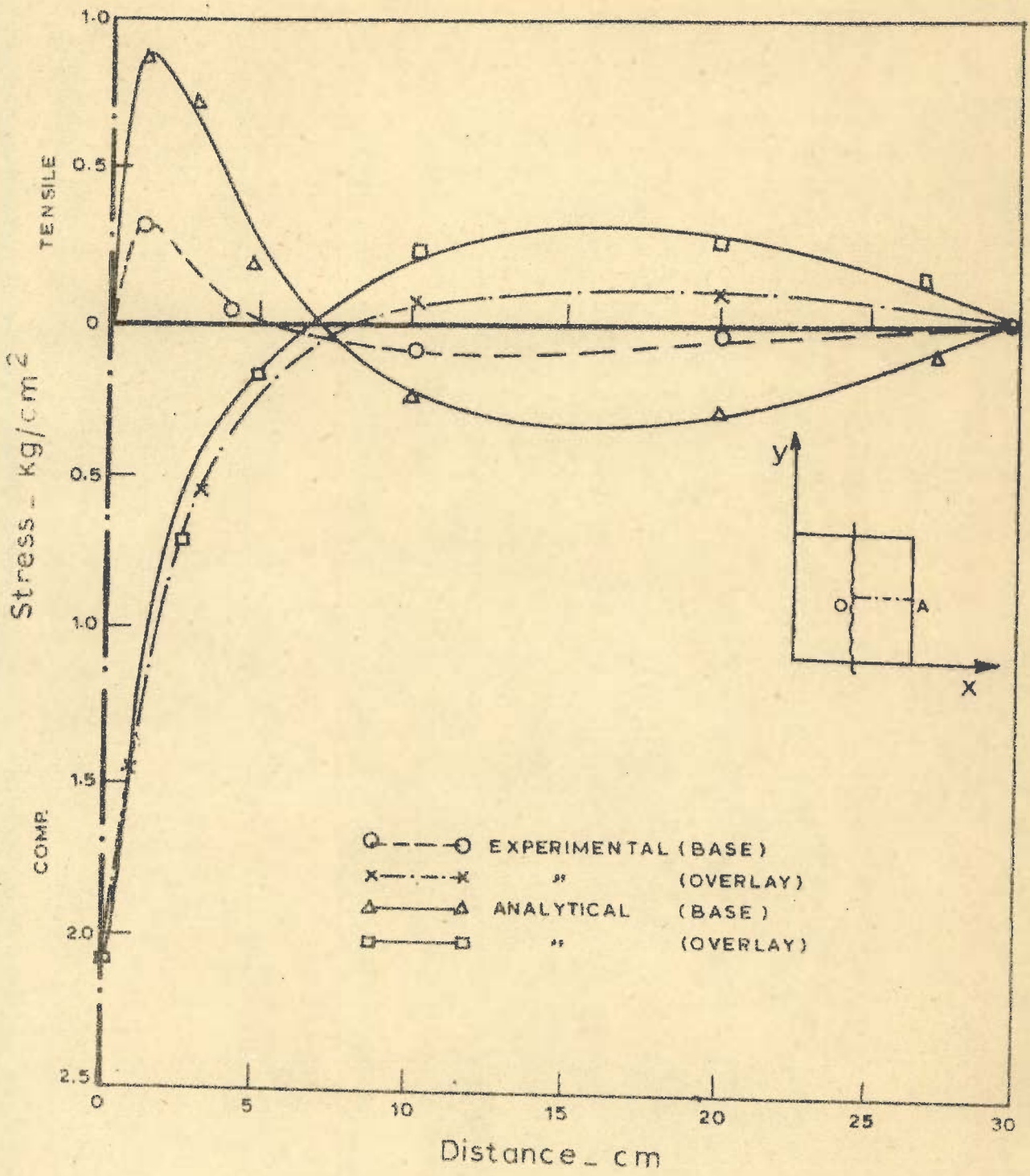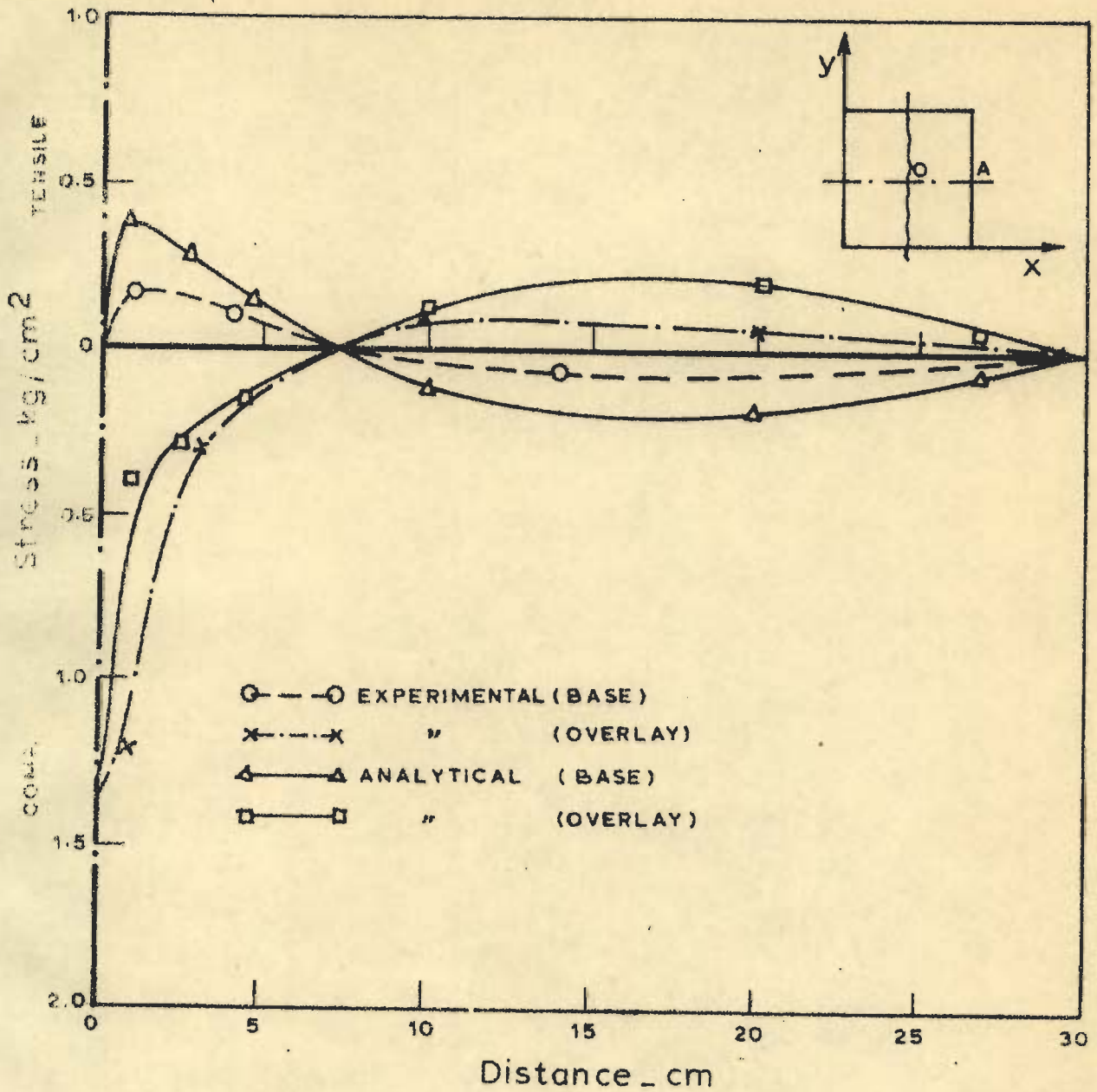
FIG. 8.27 – CRACKED BASE WITH BONDED OVERLAY, INTERIOR LOAD, SAND SUBGRADE, σ_x ALONG OA
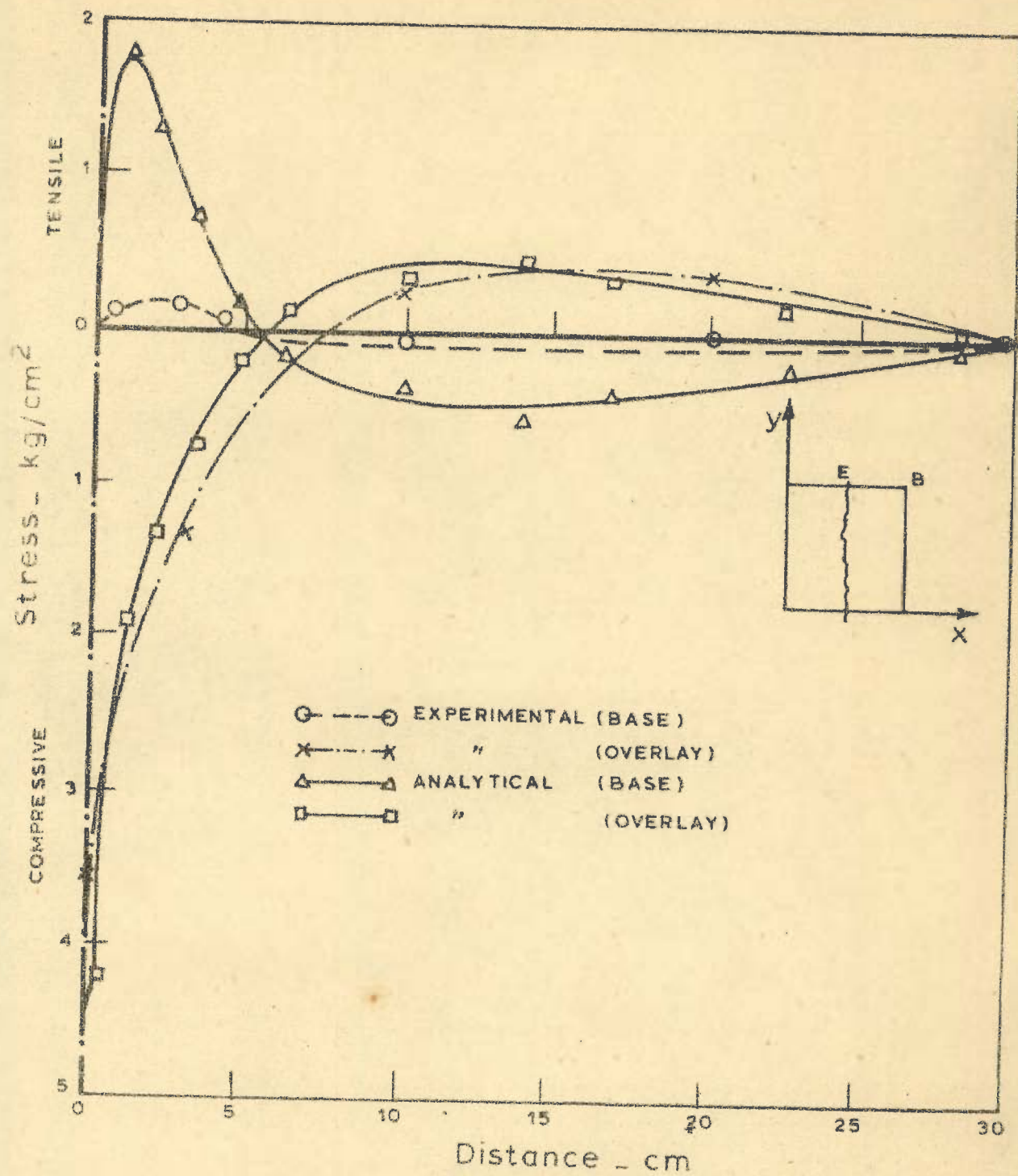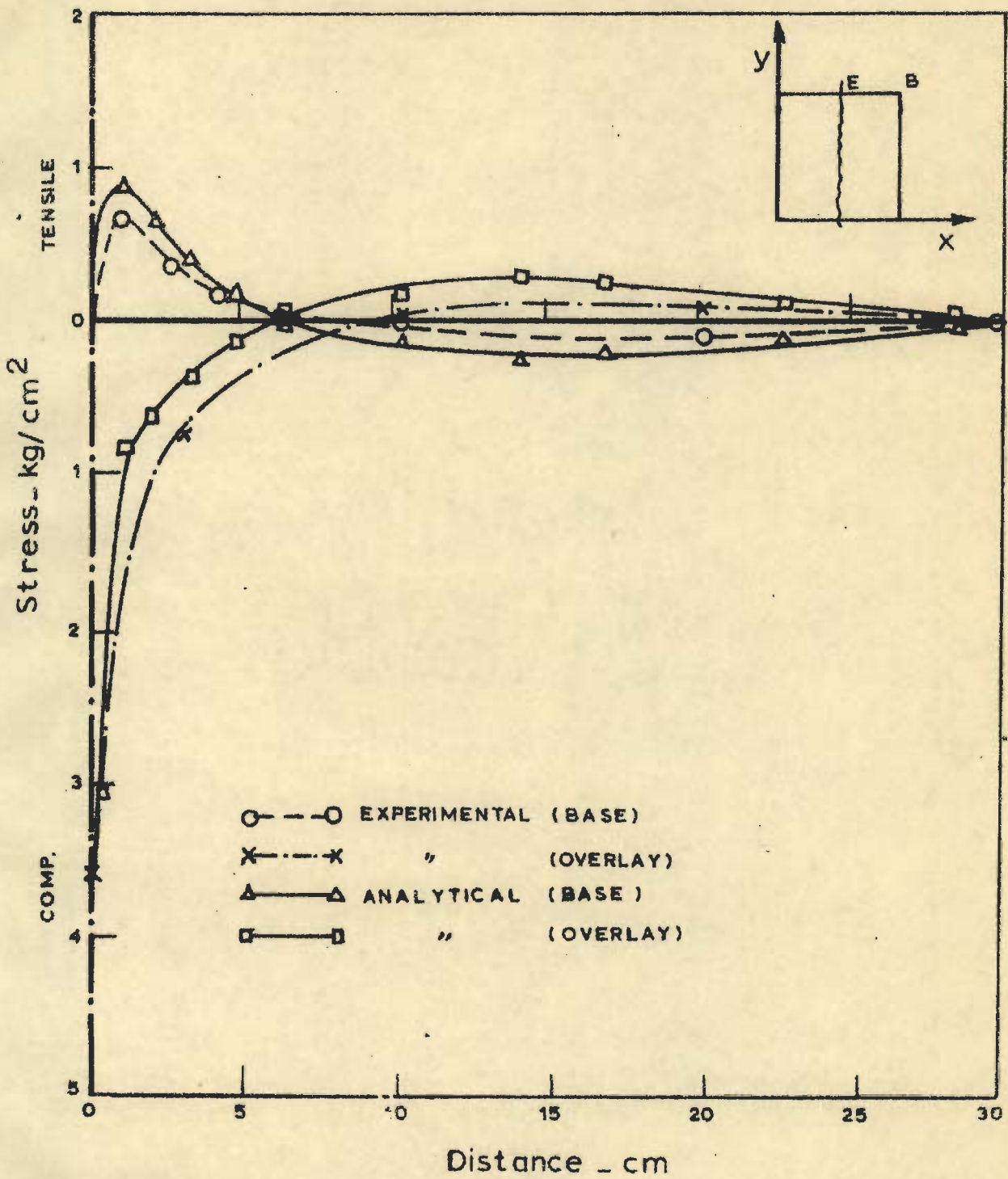
FIG. 8.28 _ CRACKED BASE WITH BONDED OVERLAY, EDGE LOAD, SPRING SUBGRADE, σ_x ALONG E B
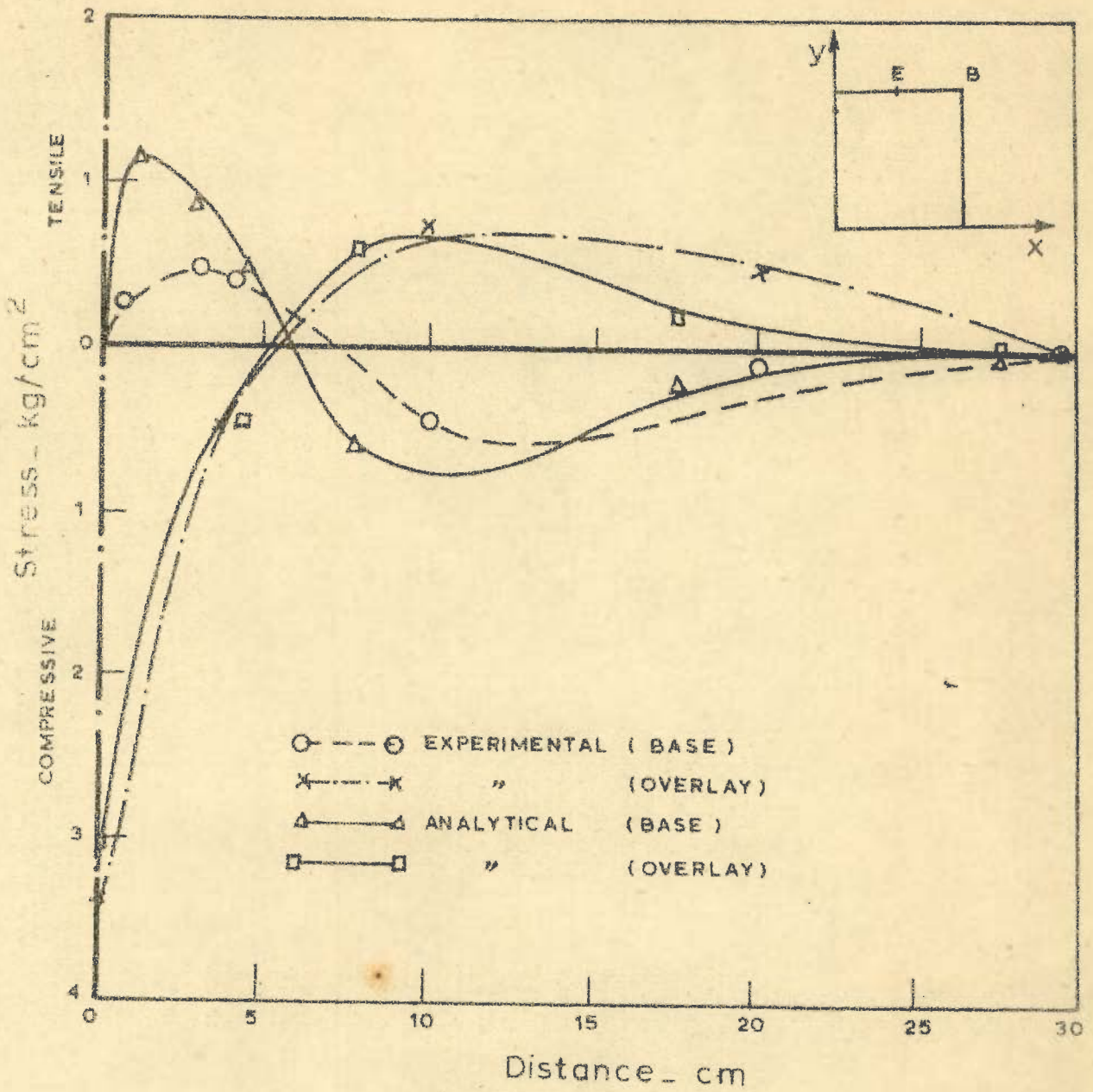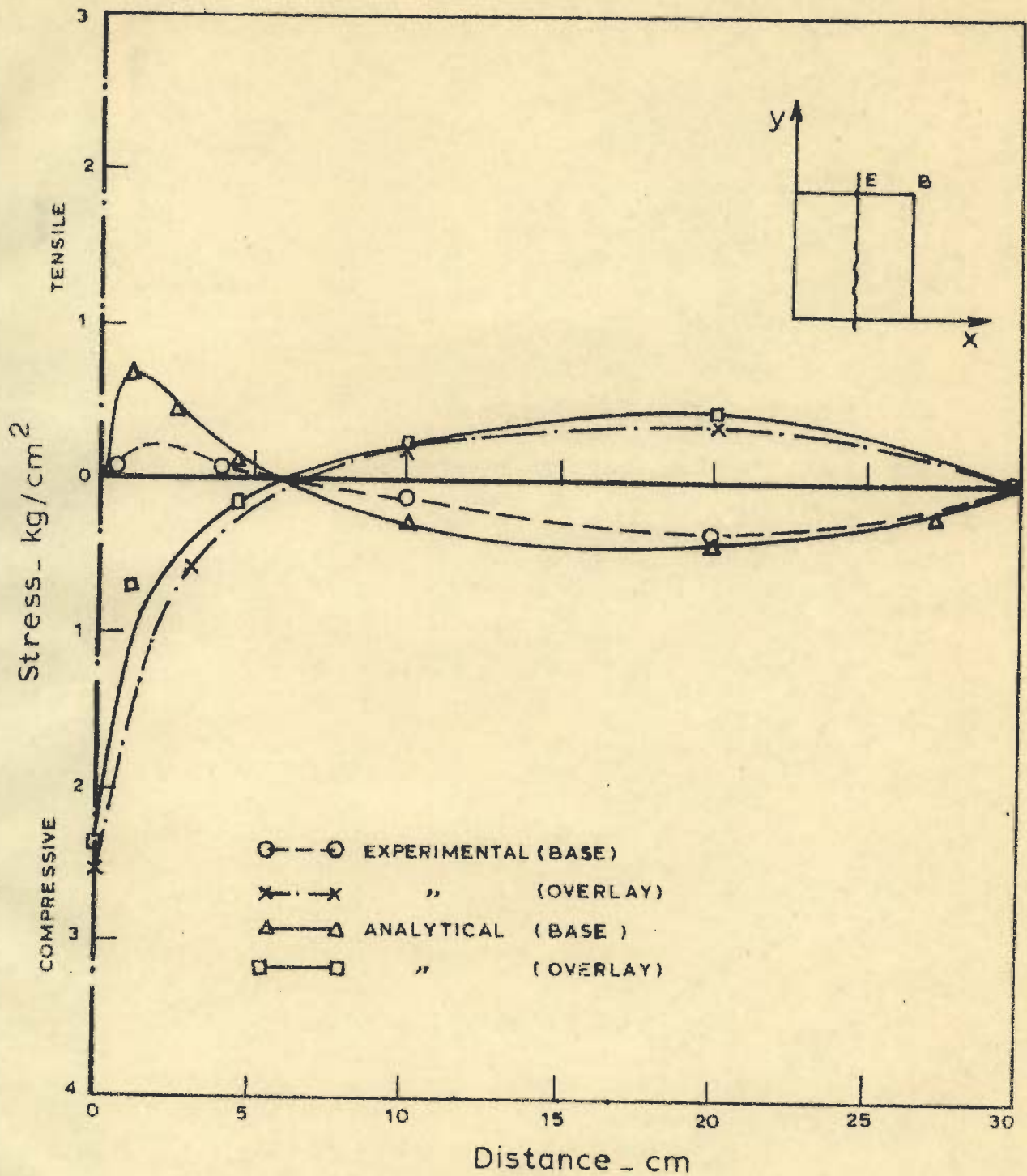
FIG. 8.29 - CRACKED BASE WITH BONDED OVERLAY, EDGE
LOAD, SAND SUBGRADE, σ_x ALONG EB
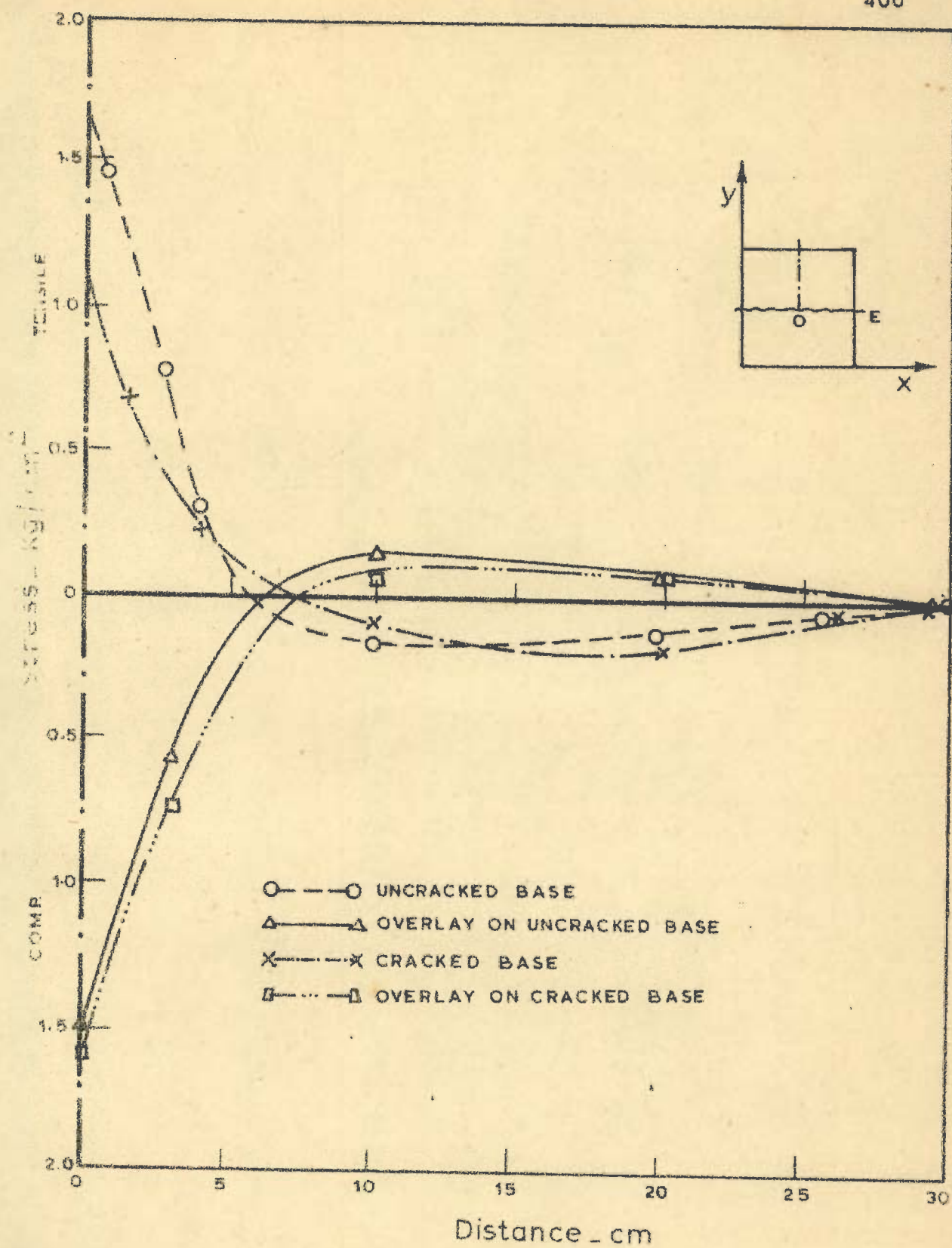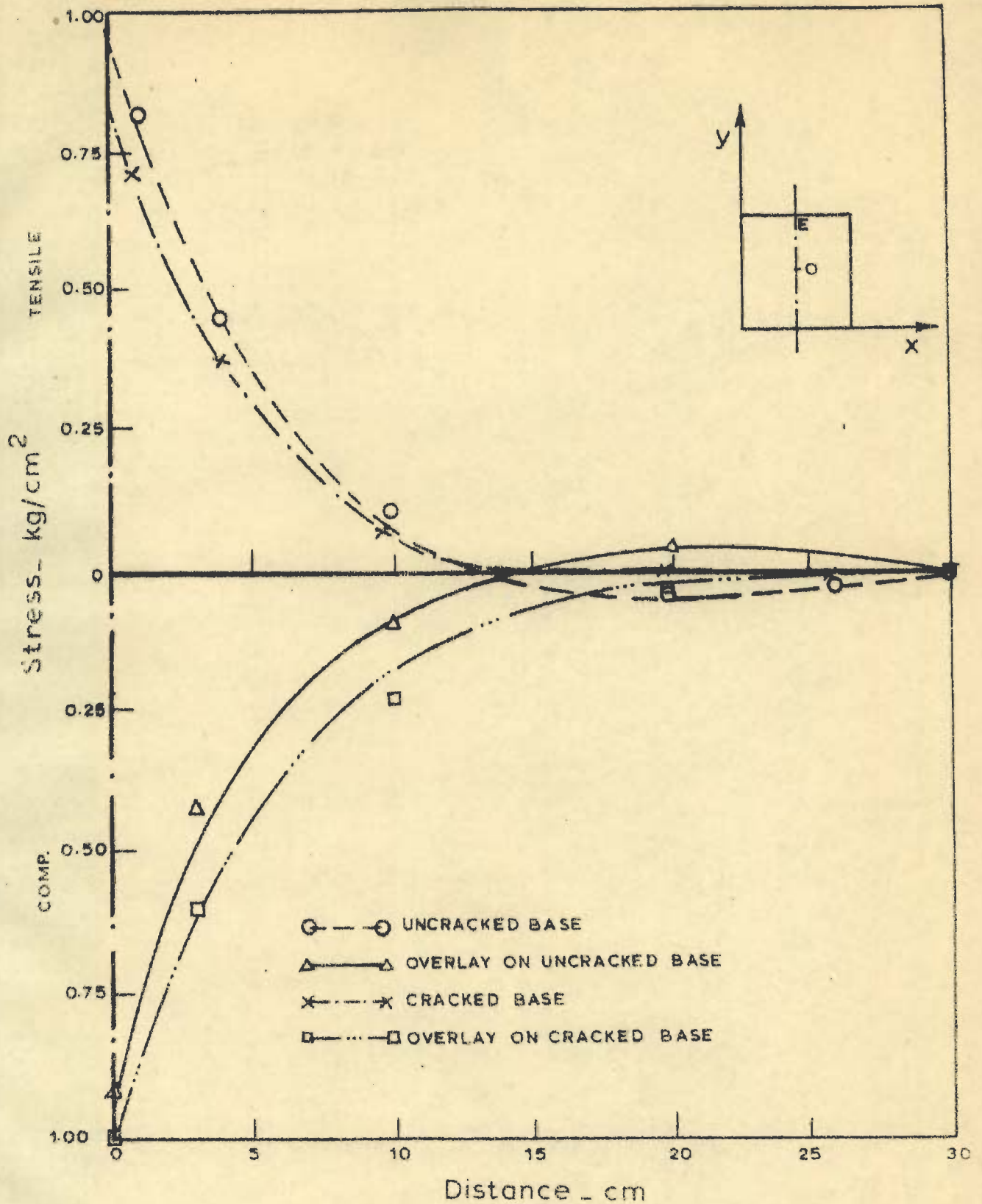
FIG. 8.30 _ COMPARISON OF EXPERIMENTAL ANALYSIS
UNCRACKED BASE WITH BONDED OVERLAY VS
CRACKED BASE WITH BONDED OVERLAY.
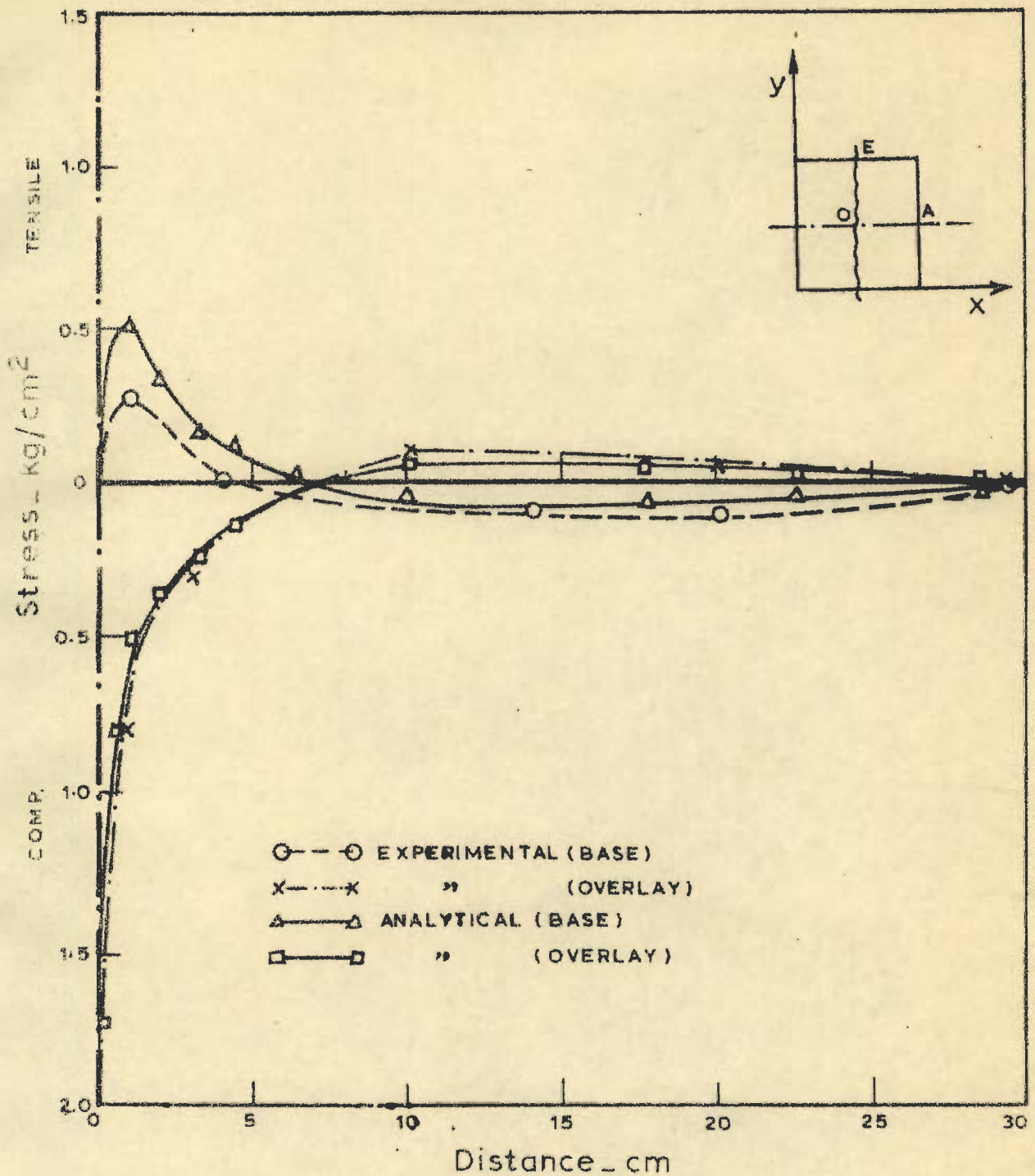INTERIOR LOAD , SPRING SUBGRADE , σ_y ALONG
O E
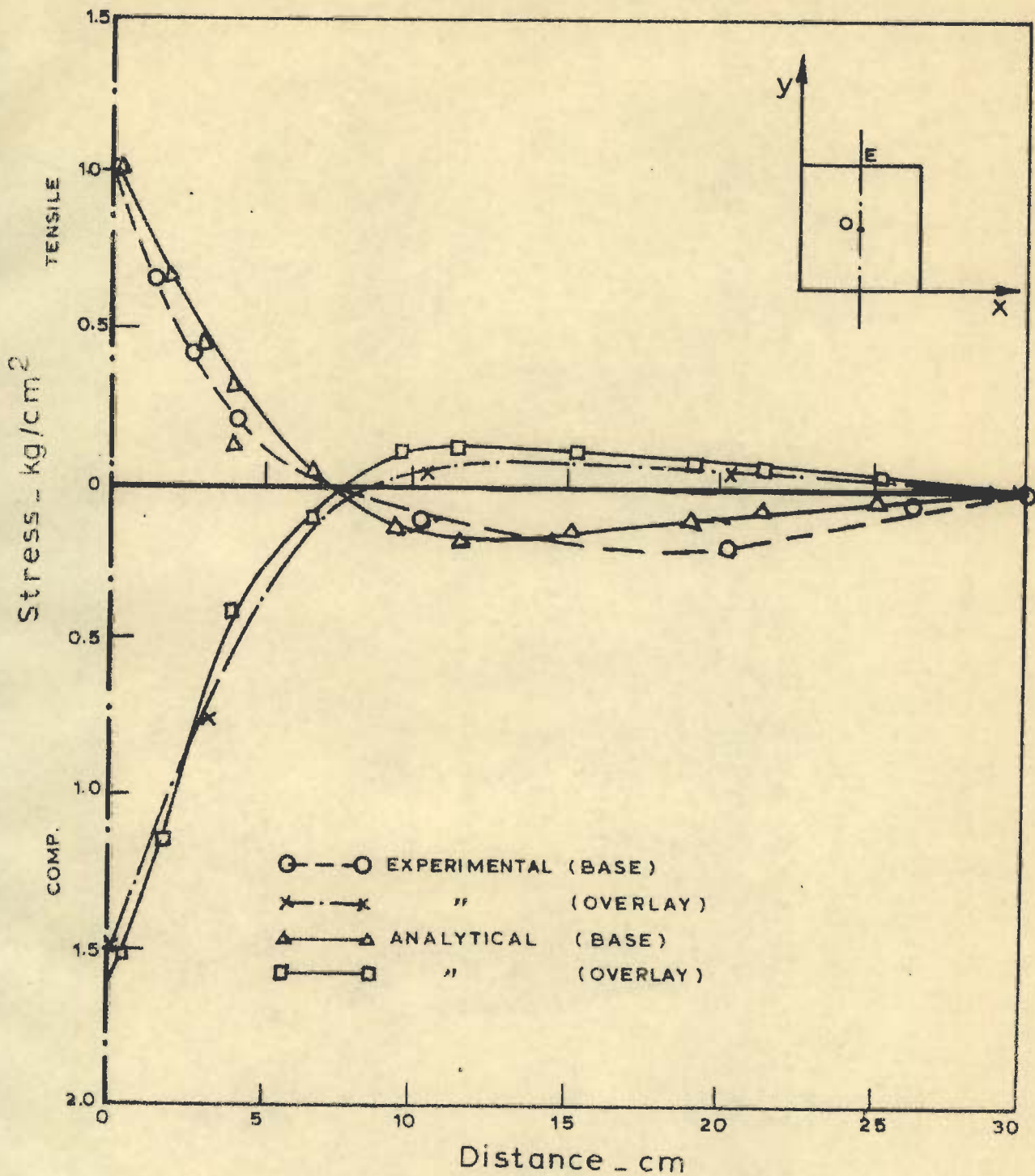
FIG.8.31 – CRACKED BASE WITH UNBONDED OVERLAY, INTERIOR LOAD, SPRING SUBGRADE, σ_y ALONG O E
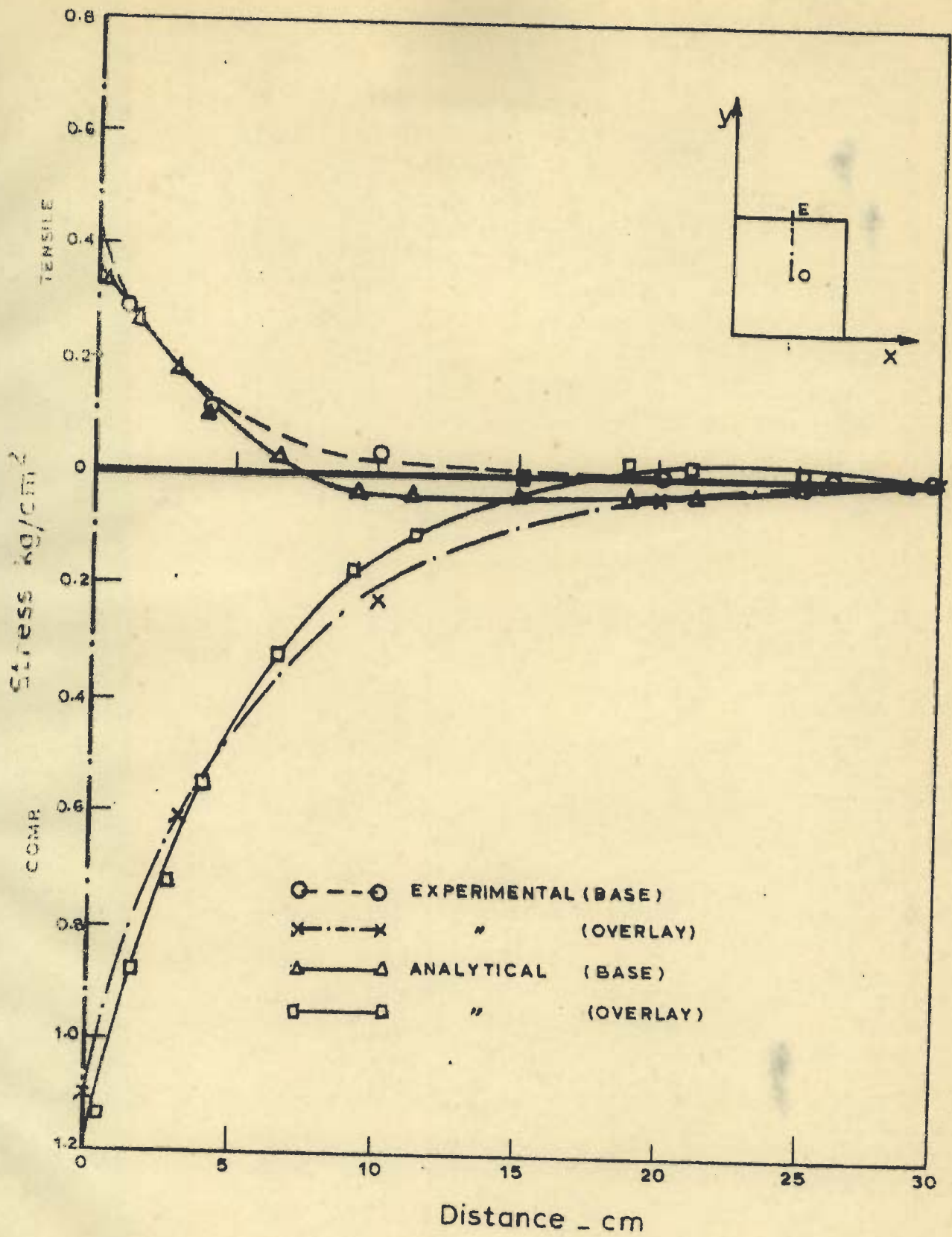
FIG. 8.32 _ CRACKED BASE WITH BONDED OVERLAY, INTERIOR LOAD, SPRING SUBGRADE, σ_y ALONG O E

CHAPTER-IX

INFLUENCE SURFACES

9.1 INTRODUCTION

Influence lines[269] have their well established identity in the cases where effects of a moving load is to be studied for determination of its maximum value in a one-dimensional structure like a beam or a truss[269]. Influence surfaces are their extension for two dimensional structures like plates or shells. Essentially, the determination of the influence field is possible for only a linear system, to which Maxwell-Betti-theorem is applicable.

Influence surfaces for plates have earlier been analytically obtained by Pucher[270] and Krug and Stein[271] for isotropic and orthotropic rectangular plates by using singular and regular solutions. A large group of workers at University of Illinois have used finite difference method for obtaining influence surfaces for various types of bridges[272]. Influence surfaces have also been obtained by using model tests[273].

Nayak and Davies[274] have extended the finite element method for obtaining the influence surfaces for bridge slabs. The finite element provides a suitable

unified approach to the determination of influence
fields in elastic continua[275].

The pavement slab on elastic foundation can be
similarly treated. The cases of multiple wheel loads,
temperature and shrinkage effects in the part or whole
of the slab can be analysed with ease. The method is
essential for cases where it is difficult to find the
critical load positions such as in pavement with open-
ings and overlay-pavement slab with multiple known
cracks in the base slab.

The technique of calculating the influence field
is a simple alteration in the existing finite element
program. In essence, a set of prescribed forces are
applied around the observation point to cause an 'elastic
pinch' and the resulting body deformations serve as
influence fields for the quantity required at the obser-
vation point.

In a pavement problem a set of self-equilibrating
'pinch' loads are applied to calculate any one of the
moments M_x, M_y, M_{xy}, and shears Q_x and Q_y around an
observation point. The resulting deformations w, $\frac{\partial w}{\partial x}$,
$\frac{\partial w}{\partial y}$ serve as influence fields. The wheel load effect is
calculated by using the vertical displacement w as inf-
luence field. The temperature and shrinkage effects are
calculated by using the slopes $\frac{\partial w}{\partial x}$ and $\frac{\partial w}{\partial y}$ corresponding
to the equivalent moments caused by any varying thermal

and shrinkage effects.

Finally there are the two main problems of getting influence fields accurately and the use of influence fields for the calculation of design values.

The details regarding the accuracy of influence coefficients, suitable self-equilibrating 'pinch' loads with respect to an observation point and the use for calculating design values are given in reference [274,271]. However, the theory of influence surfaces for pavements and its use for calculating wheel loads, thermal and shrinkage effects are given hereafter.

9.2 THEORY OF INFLUENCE SURFACES

Let

$$\{g(x_k, \xi_k)\} = \begin{Bmatrix} g_1 \\ g_2 \\ g_3 \end{Bmatrix} \qquad \dots (9.1)$$

define the influence function for a required quantity $M_i(x_k)$ at an observation point x_k of a pavement and ξ_k defines the point at which vertical loads P and unit couples m_x and m_y defined by a vector $\{1,1,1\}^T$ is applied.

When general distributed surface loads $\{p\} = \{p, m_x^o, m_y^o\}$, line loads $\{q\} = \{q, m_x, m_y\}$ and concentrated loads $\{P\}_i = \{P, \bar{M}_x, \bar{M}_y\}$ are acting

$$M_i(x_k) = \int_A \{p\}^T \{g\} dA + \int_S \{q\}^T \{g\} dS + \sum_{i=1}^{n} \{P\}_i^T \{g\}_i \qquad \dots (9.2)$$

It is required to prove that the influence function $\{g\}$ may be represented by a set of displacements $\{U\} = \{w, \frac{\partial w}{\partial x}, \frac{\partial w}{\partial y}\}^T$ defining the influence field due to a set of elastic pinch loads arround observation point x_k.

In a finite element formulation as described in chapters II and IV, for a point in an element e,

$$\{U\} = [N][\delta]^e \qquad \qquad \dots (9.3)$$

due to a set of nodal forces $\{F\}$ causing displacements $\{\delta\}$. The nodal displacements and forces are linked by

$$\{\delta\} = [K]^{-1}\{F\} \qquad \qquad \dots (9.4)$$

and the inversion of the stiffness matrix is the basis of standard finite element solution programs. The solution may be repeated for many values of $\{F\}$. In the absence of any initial effects, the moments at a point in the element are given by

$$\{M\} = [D]\{\chi\} = [D][B]\{\delta\}^e = [S]\{\delta\}^e \qquad \dots (9.5)$$

where $[S]$ is the element stress matrix.

Equation 9.5 is not required directly in an influence field program but may be used indirectly to determine 'elastic pinch' loads to be applied near the observation point in order to simulate the deformation discontinuities at the point x_k corresponding to M_i and cause a set of deformations $\{U\} = \{w, \frac{\partial w}{\partial x}, \frac{\partial w}{\partial y}\}^T$ throughout the pavement.

From equation 9.5

$$M_i(x_k) = \{S_i\}^T \{\delta\}^e = \sum_{j=1}^{n} S_{ij}\delta_j \qquad \ldots (9.5a)$$
$$\phantom{M_i(x_k) = \{}\underset{1 \times n}{\phantom{\{S_i\}}}\ \underset{n \times 1}{\phantom{\{\delta\}}}$$

where n is the number of generalised displacement components for element e.

By applying unit load component $\{P_m\}^T = \{1,0,0\}$ at any point m defined by ξ_k. From reciprocal theorem the nodal displacement δ_j of $\{\delta\}^e$ due to unit load $\{P_m\}$ is given by

$$\begin{matrix} P_m = \left\{\begin{matrix}1\\0\\0\end{matrix}\right\} & F_j = 1 \\ \delta_j & = w_m \end{matrix} \qquad \ldots (9.6)$$

or

$$\begin{matrix} P_m = \left\{\begin{matrix}1\\0\\0\end{matrix}\right\} & F_j = S_{ij} \\ S_{ij}\delta_j & = w_m \end{matrix} \qquad \ldots (9.6a)$$

Therefore,

$$\left[\sum S_{ij}\delta_j\right] \overset{P_m = \left\{\begin{matrix}1\\0\\0\end{matrix}\right\}}{} \{F\} = \{S_i\} \atop = w_m \qquad \ldots (9.7)$$

and from equation 9.5a

$$M_i(x_k) = \{S_i\}^T \{\delta\} \overset{P_m = \left\{\begin{matrix}1\\0\\0\end{matrix}\right\}}{=} w_m \begin{matrix}\{F\} = \{S_i\}\end{matrix} \qquad \ldots (9.8)$$

Similarly for $\{P_m\} = \{0,1,0\}^T$ and $\{P_m\} = \{0,0,1\}^T$

$$M_i(x_k) = \left(\frac{\partial w}{\partial x}\right)_m^{\{F\}=\{S_i\}} \quad \text{and} \quad M_i(x_k) = \left(\frac{\partial w}{\partial y}\right)_m^{\{F\}=\{S_i\}} \qquad \ldots (9.9)$$

Therefore, according to equation 9.1 for $\{P_m\} = \{1,1,1\}$

$$\{g\} = \left\{\begin{matrix} w \\ \frac{\partial w}{\partial x} \\ \frac{\partial w}{\partial y} \end{matrix}\right\} = \{U\}^{\{F\}=\{S_i\}} \qquad \ldots (9.10)$$

The 'elastic pinch' loads for $M_i(x_k)$ defined by $\{F\} = \{S_i\}$ can be determined automatically from the stress matrix already available within the program.

9.3 USE OF EXISTING PROGRAM

It is clear from equation 9.8 that the 'elastic pinch' loads can be determined by using stress matrix given by

$$[S] = [D][B] \qquad \qquad \ldots (9.11)$$

Both $[D]$ and $[B]$ matrices at any point are already available in existing program as these are required for calculating stiffness matrix, equivalent nodal forces due to thermal and shrinkage effects and stresses at any point. If the observation point is located at a node, appropirate 'weighting' of the pinch loads applied to the set of nodes around the observation point may be used[274]. The influence field represented by the deformation field $\{U\}$ will be 'correct' (determined by the accuracy for the finite element idealisation of the pavement) at all the points except within the pinch zone around the observation point. With reasonably graded mesh lines, this zone will be small as compared to the size of the pavement. The modifications in the existing program are necessary to generate 'pinch' loads by using $[D]$ and $[B]$ matrices with suitable 'weighting' and to terminate the program after the determination of displacement only. It is usual

to do simple averaging for calculating influence sur-
faces at a node point connecting several elements.

Further it is economical to calculate several
influence surfaces in one run by using the resolution
process similar to the process of solving a problem
of multiple right hand sides. This is done by keeping
the inverted stiffness matrix calculated once for all.

In order to use the influence surfaces at various
points the various sets of influence surfaces are usually
stored on magnetic discs.

In a pavement problem the nodal displacement vectors
will also contain slopes and twisting curvatures. The
slopes and twisting curvatures are useful for calculating
the temperature and shrinkage effects.

9.3.1 Wheel Load Effect

For obtaining the stress value due to a wheel
load having a pressure 'p' and elliptical contact area
the tyre point can be placed at appropriate position. The
area can be divided into small rectangular patches and
the influence coefficient for each patch may be deter-
mined by interpolation. Influence of the load on the
patch at the observation point can then be determined
by multiplying this influence coefficient by area of
the patch and the contact pressure. Sum of all such
influences will give the total influence of the wheel

load on the desired stress at the observation point.
Similarly several wheel loads in different positions
can be considered to obtain the maximum value of stress
at a desired point.

9.3.2 Thermal and Shrinkage Effect

The direct method of analysis for thermal and
shrinkage along with the results is given in Chapter .V.
In this analysis the equivalent nodal loads due to
thermal and shrinkage effects are calculated as

$$\{F\}_t = -\int_A [B]^T [D] \{\lambda_0\} dA \qquad \ldots (9.12)$$

where $\{\lambda_0\}$ is resulting initial strain curvature due to
thermal and shrinkage. For thermal effect

$$\{\lambda_0\} = \begin{Bmatrix} \alpha_x \frac{\Delta t}{h} \\ \alpha_y \frac{\Delta t}{h} \\ 0 \end{Bmatrix} \qquad \ldots (9.13)$$

Equivalence of shrinkage with thermal effect for bending
analysis has already been established in Section 5.5.5
Therefore we can treat only the thermal effect. Let

$$\{M_0\} = \begin{Bmatrix} M_{xo} \\ M_{yo} \\ 0 \end{Bmatrix} = [D] \{\lambda_0\} \qquad \ldots (9.14)$$

The equivalent nodal forces due to the constant
vector $\{M_0\}$ on a rectangular area are the edge couples

marked on the Fig.9.13a. If the thermal effect vector $\{M_o\}$ is constant over the Hermitian rectangular element then the equivalent nodal forces as shown in Fig.9.13b can be obtained as

$$\{F\}_t^T = -\{0, X_o, Y_o, XY_o, 0, -X_o, Y_o, -XY_o,$$
$$0, -X_o, -Y_o, XY_o, 0, X_o, Y_o, -XY_o\}^T \quad \ldots (9.15)$$

where,

$$X_o = \frac{M_{xo}b}{2}, \quad Y_o = \frac{M_{yo}a}{2}, \quad XY_o = \frac{M_{xo}b^2}{12} + \frac{M_{yo}a^2}{12}$$

The results of Fig.9.13 can be used as an ordinary applied load vector similar to wheel load effect. The initial strain effect is then added according to

$$\{M\} = [D]\{\chi + \chi_o\} \quad \ldots (9.16)$$

The total effect from influence surface only gives $[D]\{\chi\}$ to which known $[D]\{\chi_o\}$ is to be added.

9.4 APPLICATION TO PAVEMENT SLABS WITH OVERLAYS

The overlay pavement on cracked or uncracked base slab is modeled in the same way as described in Chapters V and VI by using orthotropic properties and the problem is treated as a linear one. Therefore, the results obtained by using the influence surface technique will be identical to those obtained in Chapter V and VI by direct solutions for particular wheel load positions and temperature gradients. However, the influence surface results are

more general because the stress values can be obtained for any other load positions.

Special advantage may be expected in case of pavement slabs with crack or cases when bonded or unbonded overlays are existing on base slab containing single or multiple cracks and when the multiple wheel load configurations are to be considered. Influence surface for several locations can be economically obtained through a single inversion operation as mentioned above. These locations have to be decided by judgement and experience.

Similar use of influence surface in case of pavement slabs can be in situations when the slab contains an opening of square or any other shape like those adopted as manholes or for underground drainage of surface water.

Use of influence fields can also be emphasized for cases of temperature stresses when a part of a slab panel may be in shade and other subjected to direct action of atmosphere. Similarly, cases of non-uniform shrinkage can arise in case of pavement slab having non-uniform thickness.

9.5 RESULTS

The various cases studied are shown in Table 9.1. The influence surfaces plotted for these cases are plotted in Fig.9.1 to 9.12.

Checks have been applied by comparing the results
obtained by direct solution programs of Chapters V and
VI and by using the influence surface fields for calculat-
ing the wheel load, temperature and shrinkage effects
as discussed in Section 9.3.1 and 9.3.2.

The influence surface results are more general and
can be used for other positions of wheel loads and diff-
erent   thermal gradients which are likely to occur
in the pavement

9.6 DISCUSSIONS AND CONCLUSIONS

A simple method of finding the influence surfaces
for pavements by using the existing finite element
program has been presented. The simultaneous use of
slopes $\partial w/\partial x$ and $\partial w/\partial y$ for calculating thermal and
shrinkage effects on any part of pavement slab has been
established.

It is well known that the influence surface tech-
nique is not very popular with the pavement designers
despite its versatility and computational efficiency.
A pavement designer usually requires critical values of
stresses only at reasonably selected points. The attract-
ive features of influence methods of predicting the
effect of wheel loads placed any where on the pavement
and complex thermal gradients and shrinkage effects

are overshadowed by the availability of direct solutions for simpler cases and also the direct solution programs.

In this chapter only the influence surfaces for various cases of bonded and unbonded overlays on un-cracked and cracked base slabs have been presented to illustrate this technique. Checks have been made with the results obtained by direct solution programs.

Finally in the conclusion it is recommended that the influence surface programs should not be used to produce tables and charts as has been done in this chapter and elsewhere[270,271]. Instead every problem may be treated as 'one off' and the influence field data for various observation points stored on magnetic discs. These then can be used to find the critical wheel load, thermal and shrinkage effects and critical magnitudes of stresses needed for design purposes. In order to gain confidence on influence surface technique it is recommended that the simultaneous use of direct programs may be made. The present program contains both of these facilities.

TABLE 9.1

CASES STUDIED

Case	Thickness		Location of observation Point	Parameter	Fig.No.
	Base cm.	overlay cm.			
1. Single slab	20 (U.C)	—	Centre	M_x, M_y, M_{xy}	9.1 to 9.3
2. Bonded overlay	8(U.C)	10	Centre	M_y	9.4
			Edge	M_y	9.5
3. Unbonded	8(U.C.)	10	Centre	M_y	9.6
			Edge	M_y	9.7
4. Bonded	16(U.C)	10	Centre	M_y	9.8
			Edge	M_y	9.9
5. Bonded	16(C)	10	Centre	M_x, M_y	9.10, 9.11
			Edge	M_y	9.12

U.C. - stands for uncracked base,
  C - stands for cracked base.
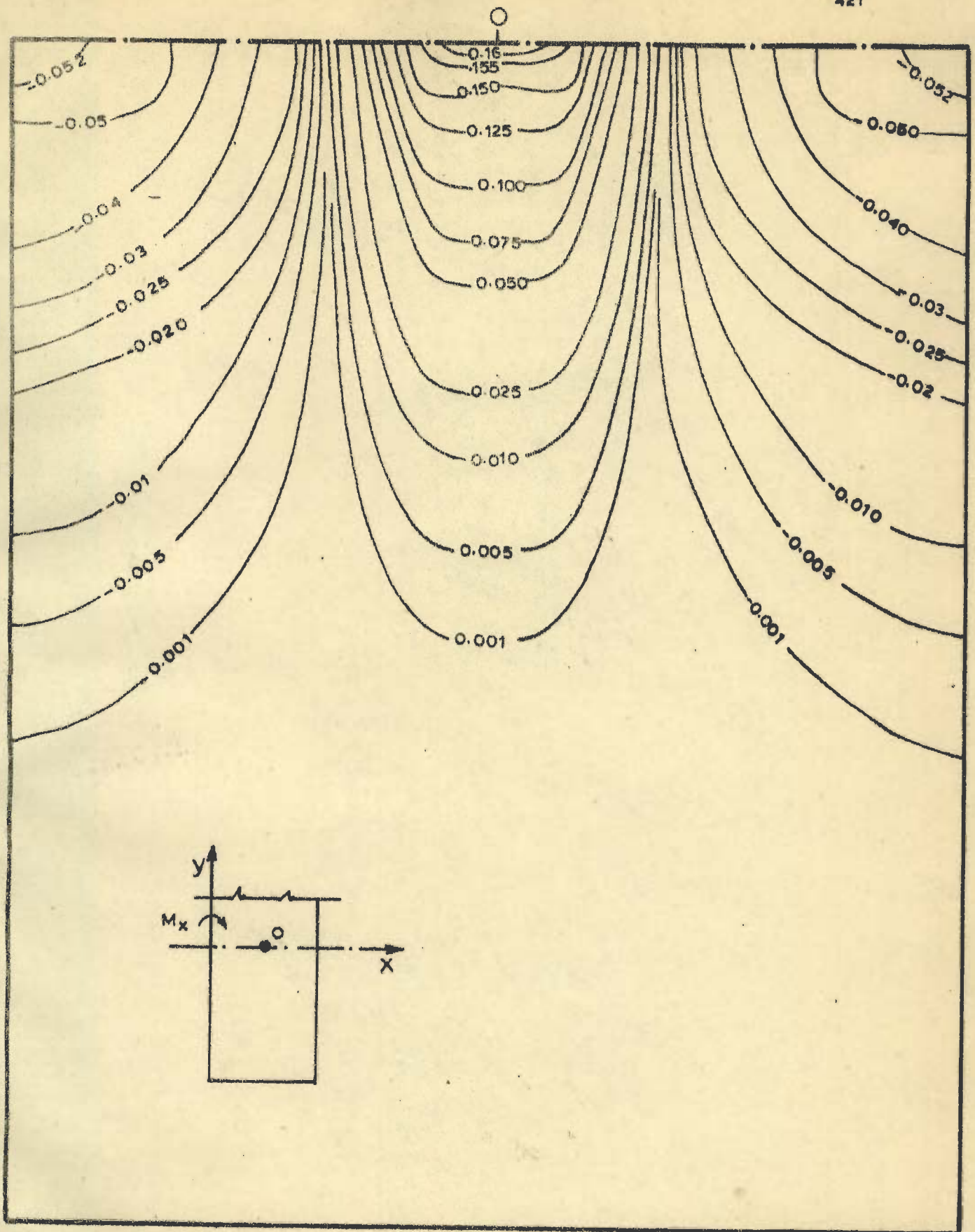
FIG. 9.1 _ INFLUENCE SURFACE FOR MOMENT M$_x$ AT POINT 'O'
IN 20 cm PAVEMENT SLAB
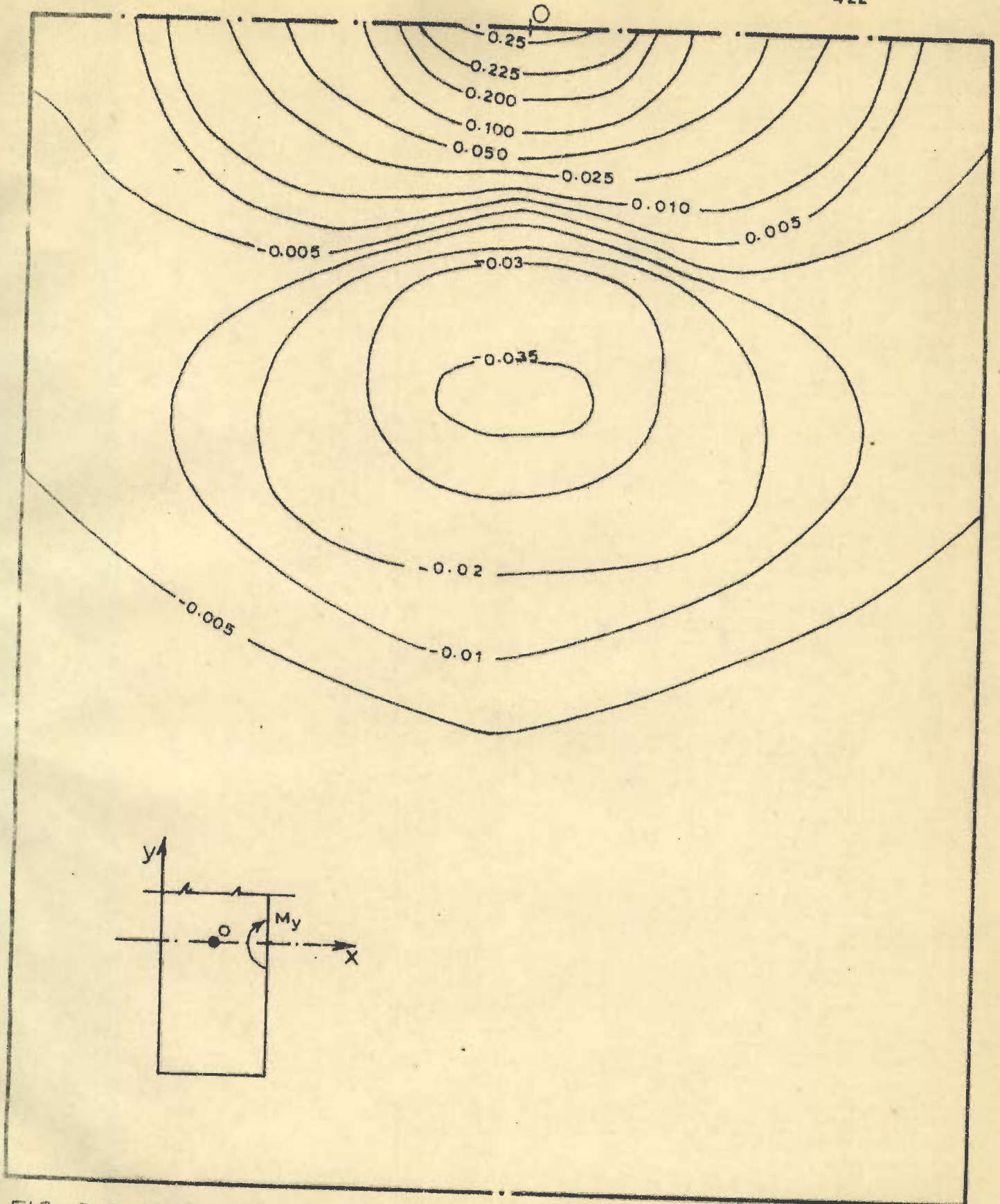
FIG. 9.2 _ INFLUENCE SURFACE FOR MOMENT M_y AT POINT 'O'
IN 20 cm PAVEMENT SLAB
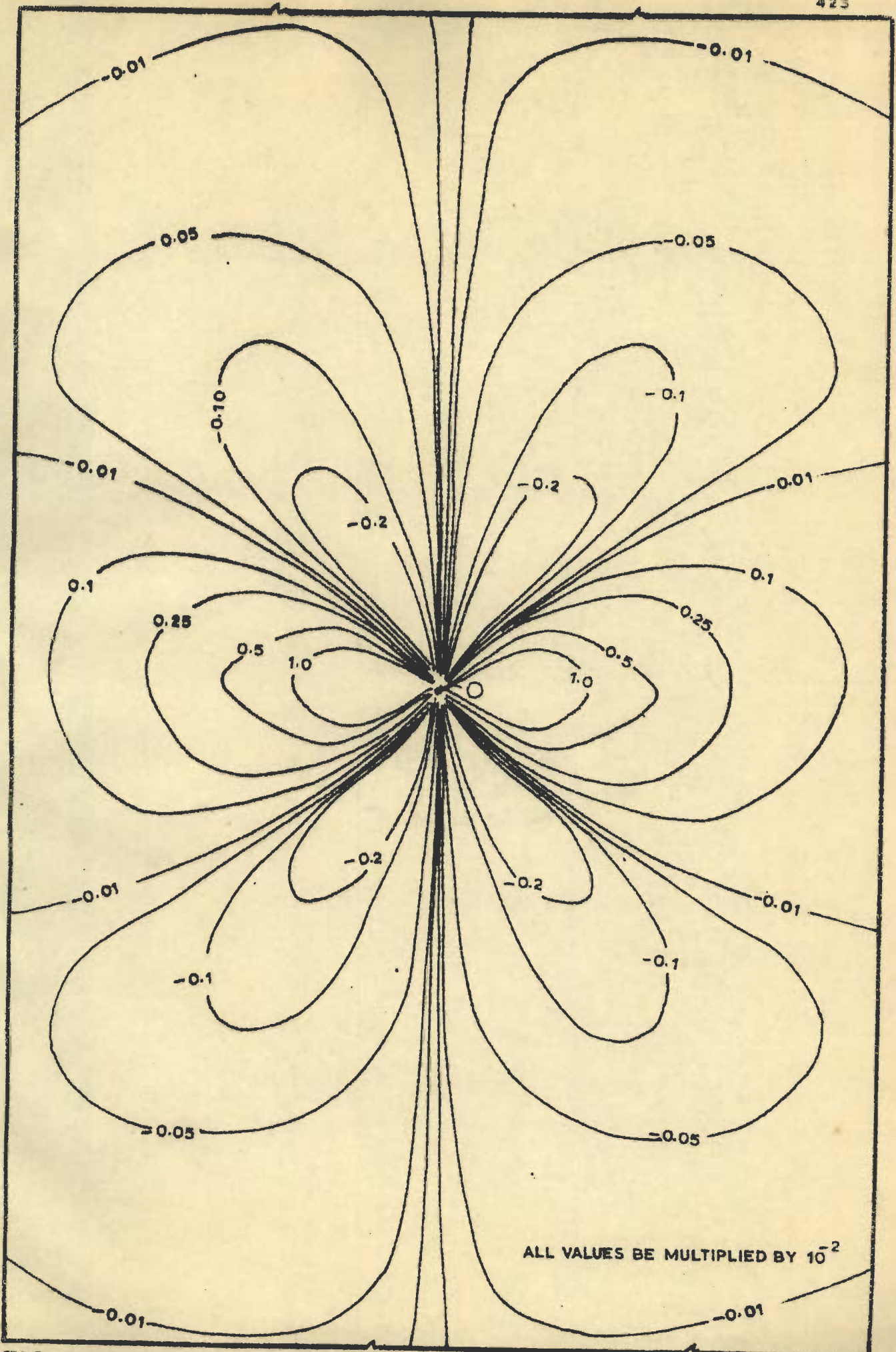
FIG. 9.3 _ INFLUENCE SURFACE FOR MOMENT M$_{xy}$ AT POINT 'O'
IN 20 cm PAVEMENT SLAB

ALL VALUES BE MULTIPLIED BY 10^{-2}
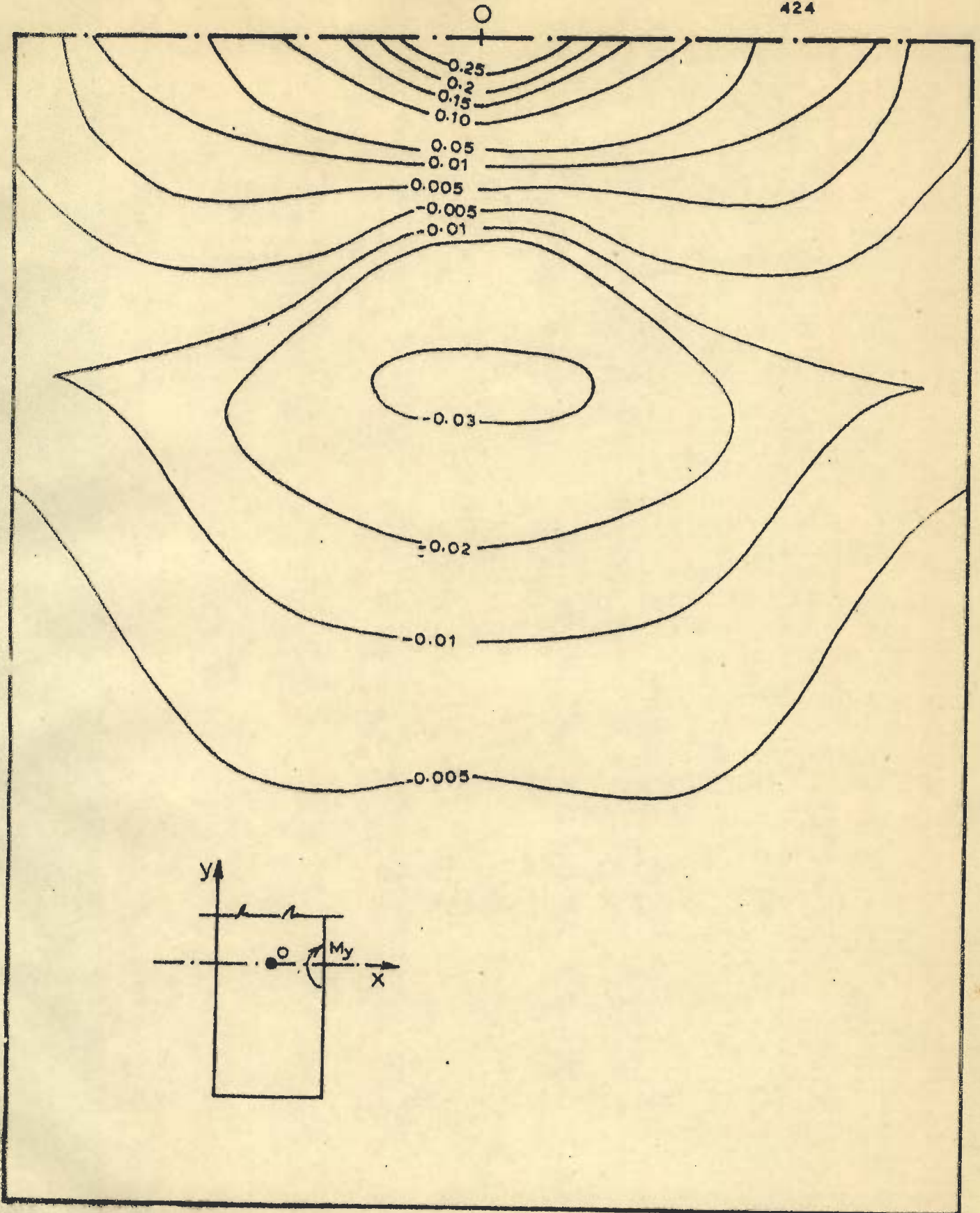
FIG. 9.4 – INFLUENCE SURFACE FOR MOMENT My AT POINT 'O', 10 cm OVERLAY ON 8 cm UNCRACKED BONDED BASE
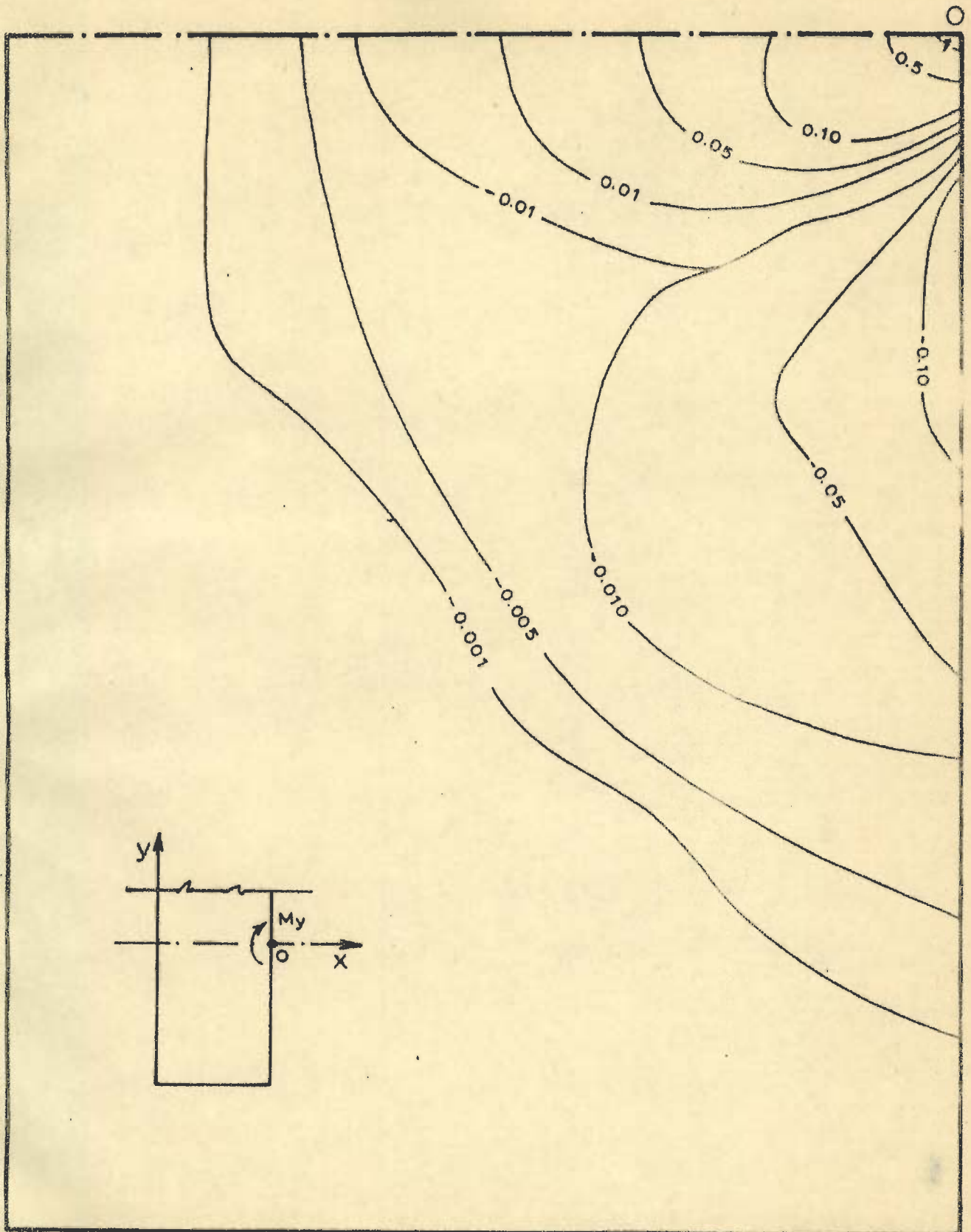
FIG. 9. 5 _ INFLUENCE SURFACE FOR MOMENT M_y AT POINT 'O'
IN PAVEMENT SLAB WITH 10cm OVERLAY ON 8cm
BONDED UNCRACKED BASE
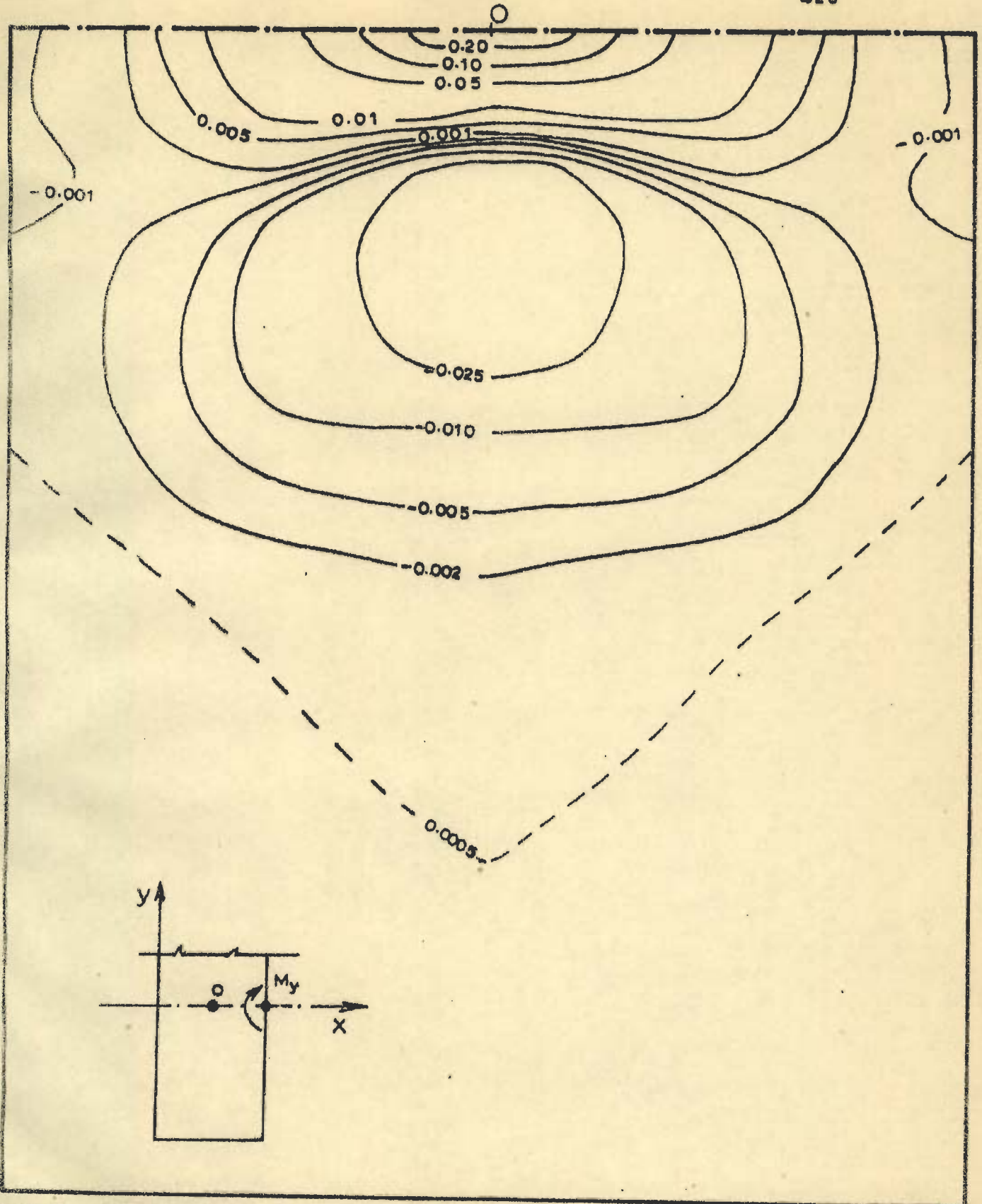
FIG. 9.6 _ INFLUENCE SURFACE FOR MOMENT My' AT POINT 'O'
IN PAVEMENT SLAB WITH 10 cm OVERLAY ON 8 cm
UNBONDED, UNCRACKED BASE .
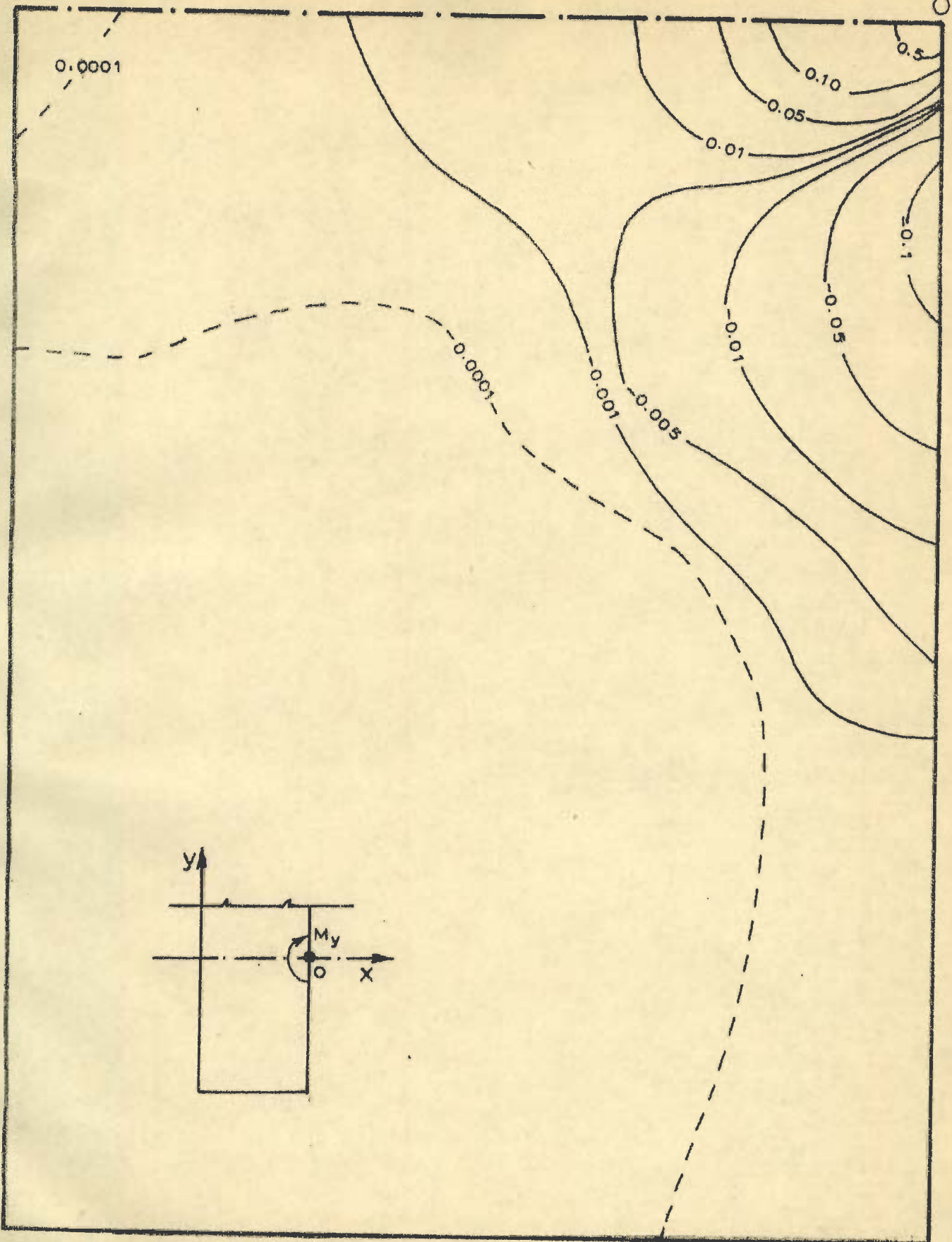
FIG. 9.7 _ INFLUENCE SURFACE FOR MOMENT M_y AT POINT 'O'
IN PAVEMENT SLAB WITH 10cm OVERLAY ON 8cm
UNBONDED, UNCRACKED BASE
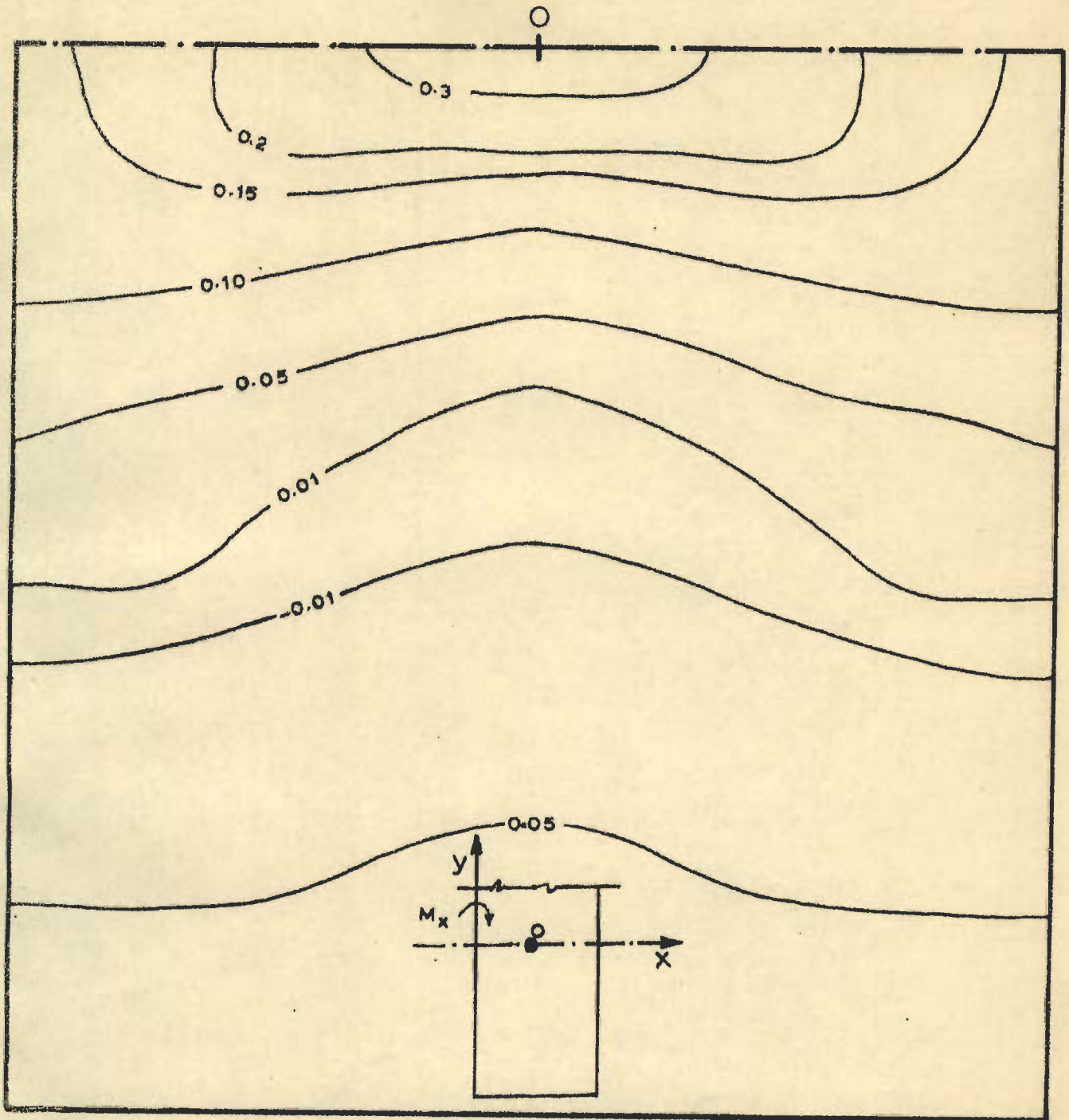
FIG. 9.8 — INFLUENCE SURFACE FOR MOMENT M_X AT POINT 'O' IN PAVEMENT SLAB WITH 10 cm OVERLAY ON 16 cm UNCRACKED BONDED BASE
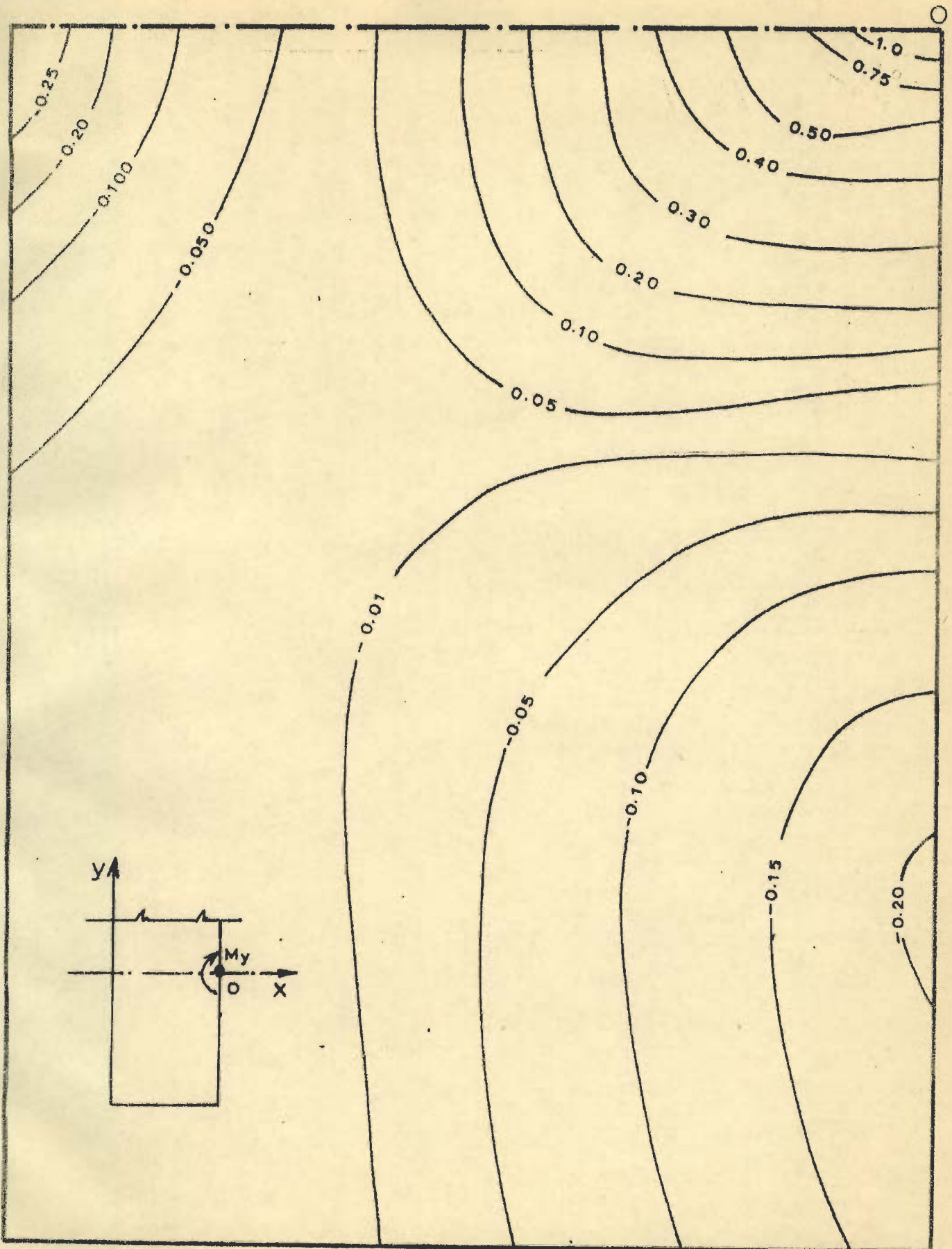
FIG. 9.9 _ INFLUENCE SURFACE FOR MOMENT M_y AT POINT 'o'
IN PAVEMENT SLAB WITH 10 cm OVERLAY ON 16 cm,
UNCRACKED, BONDED BASE
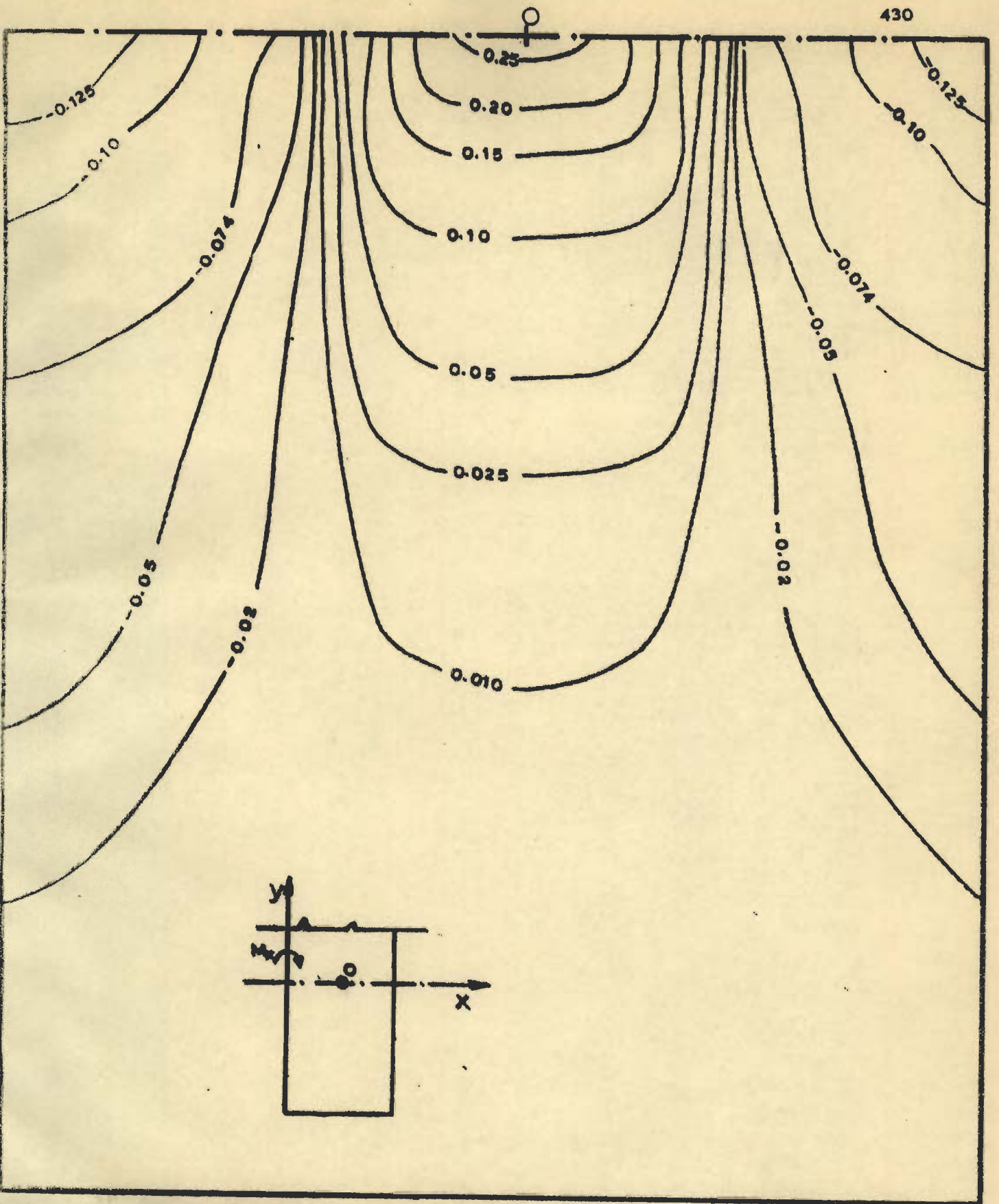
FIG. 9.10 _ INFLUENCE SURFACE FOR MOMENT M$_x$ AT POINT 'O' IN PAVEMENT SLAB WITH 10 cm OVERLAY ON 16 cm CRACKED, BONDED BASE
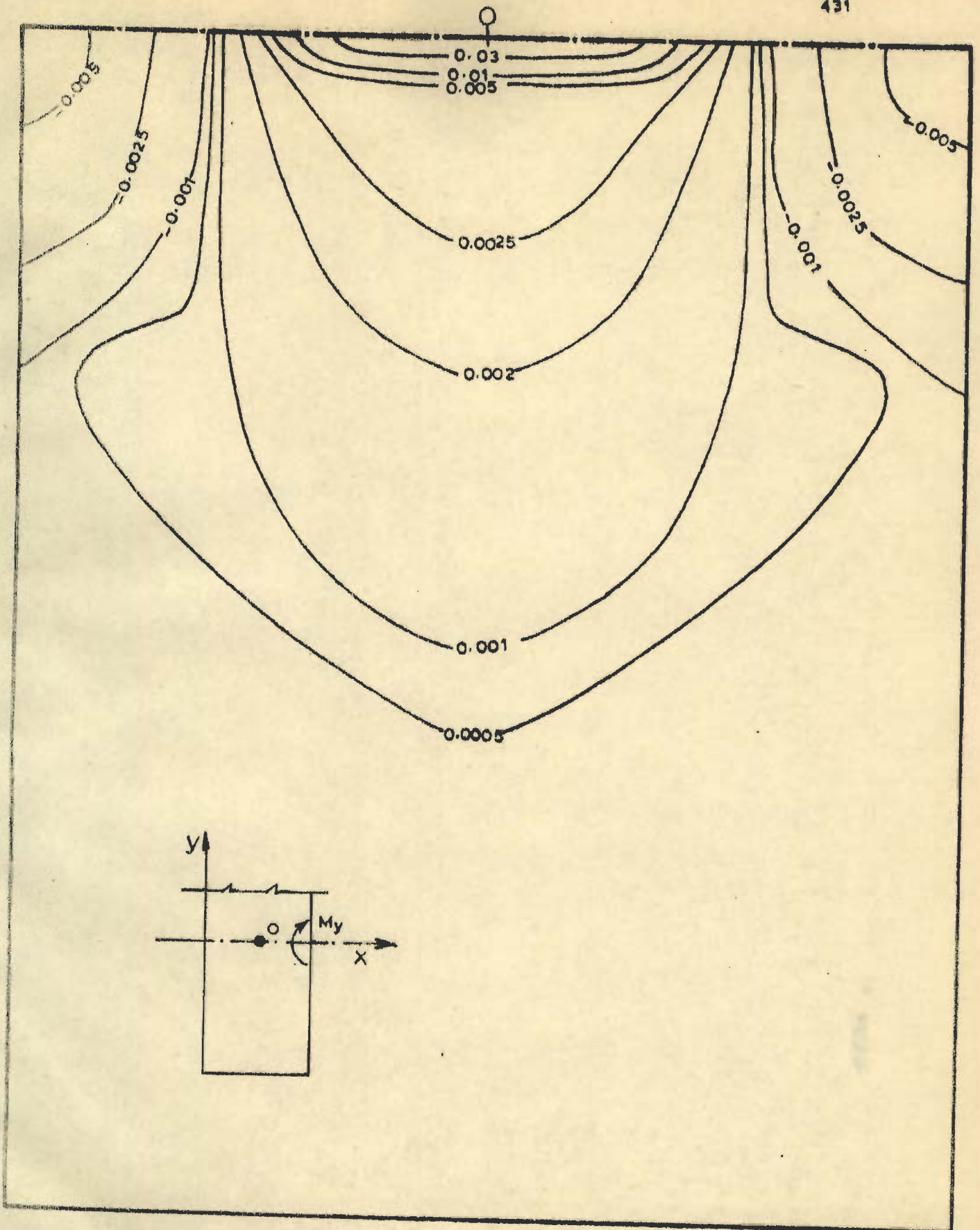
FIG. 9.11 _INFLUENCE SURFACE FOR MOMENT My AT POINT 'O' IN PAVEMENT SLAB WITH 10 cm OVERLAY ON 16 cm CRACKED BONDED BASE
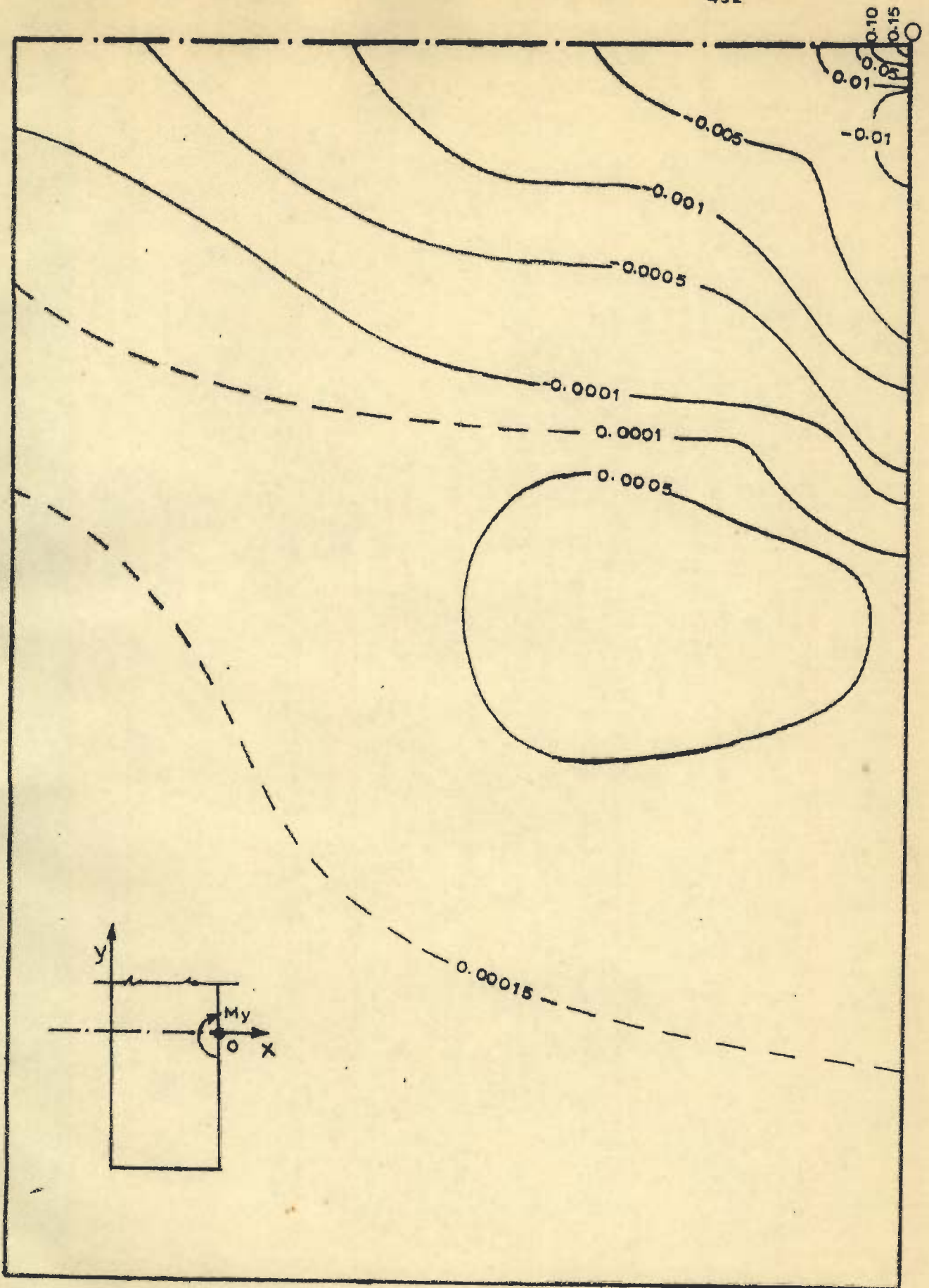
FIG. 9.12 – INFLUENCE SURFACE FOR MOMENT My AT POINT 'O' IN PAVEMENT SLAB WITH 10 cm OVERLAY ON 16 cm CRACKED, BONDED BASE
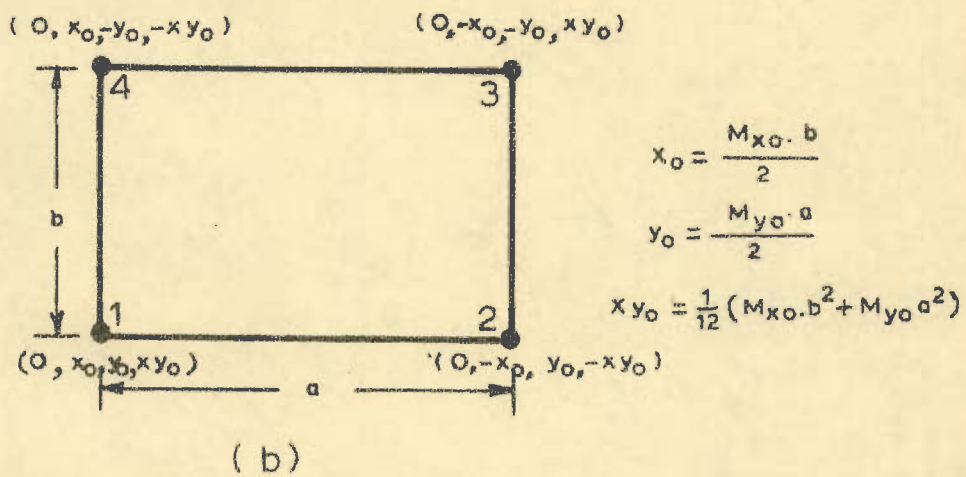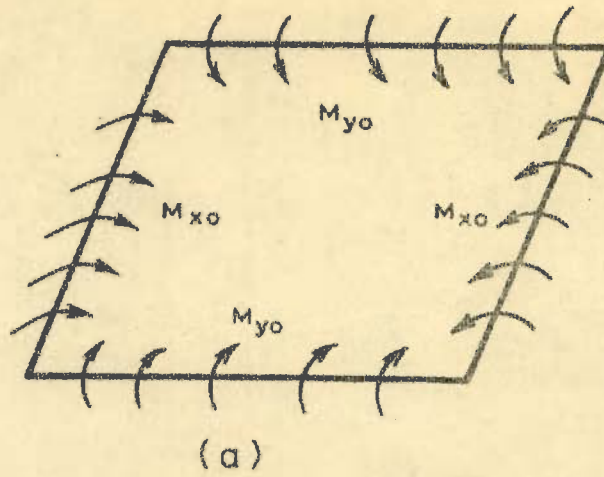
FIG. 9.13 _ EQUIVALENT THERMAL EFFECT

CHAPTER X

C O N C L U S I O N S

Besides the inferences drawn and reported at the end of each chapter, the following are the general conclusions.

10.1 METHOD OF ANALYSIS

A method of analysis is proposed based on finite element technique. A computer program is written so as to develop a system for the pavement analysis due to wheel loads and temperature gradients. The sub-element technique is developed and incorporated to model crack, to evaluate the consistent nodal loads and non-uniformity in subgrade support with a view to achieve economy and accuracy. The program can evaluate stresses and deflections in pavement slabs with subgrade modeled through, Winkler foundation, elastic solid foundation, non-linear foundation model and generalized two parameter foundation model.

The pavement slab in cracked or uncracked condition may have a bonded or unbonded overlay. The program is capable to evaluate stresses and displacements due to wheel loads, hydro-thermal gradients and shrinkage effects of variable nature. Also, the non-uniformity in subgrade can be considered in Winkler and non-linear foundation models.

The results of the model tests show adequacy
of the program for Winkler as well as elastic solid
models.

10.2 OVERLAYS ON UNCRACKED BASES

10.2.1 Unbonded Overlay on Uncracked Base

A stiffer overlay, if provided, normally should
result in reduction of stresses in overlay. But it is
seen that this need not necessarily be true in all cases,
because of the ratio in which the loads are shared bet-
ween base and overlay. This is specially true in cases
where overlay is relatively less stiff as compared to
base. Similarly, some times a thicker base may be subjected
to larger stresses, though in such cases the stresses
in the overlay will be lesser. This is true for wheel
loads as well as for temperature stresses.

The comparison of results of the finite element
analysis with those given by Marcus and Palmer[223]
show general agreement, however the latter analysis
underestimates the stresses in the overlay.

10.2.2 Bonded Overlay on Uncracked Base

Bonding of overlay to the base helps in reducing
the stresses by a substantial amount and greater reduc-
tion can be expected by providing a thicker overlay or
same overlay on a stiffer base. No controversy is found

to exist in this case. Also it is found that the combined interfacial stresses due to wheel loads, temperature gradients and shrinkage effects, which may tend to destroy bond are of low order of magnitude thereby establishing the feasibility of a bonded overlay. Further the magnitude of interfacial stresses due to combined effects, reduce with increasing thickness of base or overlay for the range of parameters studied.

10.3 OVERLAYS ON CRACKED BASES

10.3.1 Bonded Overlay on Cracked Base

The moments in the direction perpendicular to the crack decrease at the crack location whereas, there is a slight increase in the orthogonal direction. However, there is a substantial increase in the overlay fibre stresses in the direction perpendicular to the crack. It is also seen that the interfacial shearing stresses between the overlay and the base due to the effect of wheel load, temperature and shrinkage are significant and the bond, if not securely provided is liable to be damaged. Also, it is seen that the base though cracked may still be an advantage and overlay stresses on a thicker base is less.

Further the failure of bond in the vicinity of the crack results in manifold increase in deflections, slopes and flexural stresses. This is seen to be particularly

disastrous in situation when subgrade is weak. Therefore, enhancing the subgrade quality in the vicinity of the crack is one of the obvious alternatives to improve the stress conditions in overlay due to wheel loads. However, the fundamental principles of fracture mechanics show that stress concentrations are bound to occur at base-overlay interface along the crack resulting in elevated local stresses. Therefore, two conditions are established to prevent reflection cracking,viz. the bond failure must be prevented and the stress concentrations must be avoided. Reinforced key technique' is suggested to fulfil these conditions. Some alternatives to the technique are also put forward to improve and economise the suggested method.

10.3.2 Unbonded Overlay on Cracked Base

It is seen that cracking results in substantial increase in deflections, slopes and moments in overlay slab. A comparison of the stresses in unbonded and bonded overlay of equal thickness on cracked base, shows that stresses are practically twice in unbonded case for the given subgrade property adopted in the analysis. As in case of bonded overlays, the cracked base of larger thickness results in lesser overlay stresses.

10.4 STRESSES IN CRACKED SINGLE SLAB

The stresses and deflections in cracked single slab

have been determined to test the adequacy of the crack
modeling. The comparison of stresses and deflections
determined by modeling a long crack by sub-elements
show agreement with the values given by Niu[42]. The
results of a finite crack of small length can not be
compared by a standard solution but the results indicate
that the stresses increase ahead of crack due to stress
concentrations and therefore a crack once formed
is liable to propagate faster under subsequent loading.

10.5 INFLUENCE OF SUBGRADE MODELS

Limited results of the finite element analysis
in plane strain show that proportinately between deflect-
ion and subgrade reaction does hold in the vicinity of
the load. This validates the model as the property in
this zone is more important and is also the basis of
Winkler's hypothesis. However, whether this constant
of proportionality is same as one given by a standard
plate test remains questionable. But the analytical results
tend to validate the correlation between constants of
Winkler and elastic solid model found by Vesic and
Saxena[30].

A method is developed to determine the second
parameter of two parameter foundation model from the
plate load test results. A method is also developed to
take the second parameter into considerations as well as

to incorporate nonlinear effects due to lifting in pavement slab with overlays on cracked or uncracked bases.

10.6 INFLUENCE SURFACES

The influence surfaces for moments in the pavement are obtained by applying pinch 'loads' a simple modification in the program. The results can be used for estimating the temperature and shrinkage effects even for cases when the temperature or shrinkage effects are occuring in a part of the pavement. Therefore, the method of influence surfaces is the most general one. The utility of influence surfaces can be highlighted when there are numerous cracks in the base and openings in the pavement slab and it is difficult to finalise the critical load positions.The versitility and computational efficiency of the influence surface technique is verified.

10.7 MECHANICS OF REFLECTION CRACKING

It has been observed that interfacial shearing stresses due to wheel loads, temperature differentials and differential shrinkage become very high at the crack location. The bond failure is therefore liable to occur. Thus, this explains the observed field behaviour. The bond failure is liable to increase in deformations and stresses by a substantial amount causing overstressing

of the overlay. This is specially disastrous on weak
subgrades.

10.8 REMEDIAL MEASURES

The fundamental principles of fracture mechanics
indicate that stress concentrations are likely to occur
at crack tip resulting in weakening of the material at
that point. Therefore, reducing stress concentrations
and securing bond are two essential conditions to arrest
crack reflectance. With these in view, the Reinforced
Key Technique is suggested along with some of its
alternatives to achieve economy and efficiency.

10.9 PROPOSED SIMPLIFICATIONS

10.9.1 Bonded and Unbonded Overlays on Uncracked Bases

It is shown that by modifying the procedure for
calculating the value of 'radius of relative stiffness'
it is possible to adopt Westergaard's equation in a
modified form for calculation of stresses and deflections
in case of large pavement slabs with bonded or unbonded
overlays on uncracked base slabs. A similar procedure
can be adopted for calculation of wheel load influences
by Pickett's chart or other formulae.

It is also shown that for calculation of tempera-
ature stresses Bradbury's solution can be used in a

modified form for pavement slabs with bonded or
unbonded overlays. This modification is also princi-
pally based on modifying the radius of relative
stiffness.

10.9.2 Bonded and Unbonded Overlays on
        Cracked Bases

10.9.2.1 Wheel Load Stresses

A formulation based on the theory of beams on
elastic foundation is developed to evaluate the deflect-
ion and stresses in a beam having another bonded or
unbonded beam with or without a crack on a unified basis.
It is shown that this can be used for estimating the
stresses in overlay when base slab is cracked.

10.9.2.2 Temperature and Shrinkage Stresses

It is shown that if the crack is the one as assumed
in this analysis i.e. parallel to one edge but away from
it, then it is still possible to adopt Bradbury's soluti-
on for determination of stresses due to temperature
differentials. Determination of shrinkage stresses is
also possible in such a case by the simplified approach.

10.10 SUGGESTIONS FOR FURTHER WORK

Though many problems pertaining to overlays on
cracked and uncracked bases are solved, several others
are remaining. Also there are question marks that have

come up during the present study.

It is felt that with the availability of the analytical tool as formulated here, a better material characterisation in the form of constitutive laws for paving materials, their characteristics under one face restrained shrinkage and thermal conditions with particular reference to local environmental conditions are essential for realistic assessment and justification of a sophisticated analysis.

In a similar context, as already pointed out, more insight into the stress release mechanism for bonded and unbonded systems on elastic foundation and the relevant properties of material in such cases is infact required for proper modeling the system.

With the availability of the method to analyse pavement slabs on different types of foundation model, fundamental model or full scale studies to establish, their relative merit is warranted.

Field as well as laboratory studies on model or on full scale is required to establish the efficacy of 'Reinforced Key Technique' and similar other suggested alternatives.

Only fundamental principles of fracture mechanics have been applied here to qualitatively judge the behaviour of cracked base-overlay system. For true stress determinations, it is necessary to apply these

principles for anisotropic system as bonded overlay.

Parametric studies incorporating influence of slab dimensions, random crack orientations and other parameters as listed in article 5.8 may be done.

Analysis incorporating non-linear thermal gradients, shrinkage effects and other material properties can be performed with simple modification of the program, on lines similar to those adopted for non-linear analysis incorporating lifting and two parameter foundation model.

With the developed program it is also possible to study the behaviour of pavement slabs which undergo warping and thus nonlinear conditions due to displacement dependent stresses occur under wheel loads.

APPENDIX A

DESCRIPTION OF PROGRAM

INTRODUCTION

The program containing 1500 FORTRAN statements is based on rectangular orthotropic plate elements as described in Chapter IV and has 16 subroutines and 'Phase'. As stated in Chapter IV, V and VI it can solve the problem of a sound or a cracked plate with a bonded or unbonded overlay. It may be assumed to be supported on Winkler foundation, elastic solid, non-linear Winkler or Pasternak type generalised elastic foundation. Also the plate can be assigned its appropriate boundary conditions like simply supported, clamped or free. The loading may be concentrated point loads and couples, distributed surface pressures or body forces. The temperature stresses can be considered and consistent nodal loads can be determined for a part of the element loaded and crack can also be modelled through partly cracked element. Development of influence surface for any desired point for any of the above desired condition for any stress resultant can be obtained as deformations. Stress analysis from moments in desired elements is possible. The function of each subroutine is given below.

DETAILS OF SUBROUTINES

    (i) GDATA   : Reads, stores and prints data regarding nodal coordinates the nodal connections

of elements. Their material proper-
ties and boundary conditions.

(ii) LOAD : Reads data regarding concentrated
loads pressure loads, self weight,
temperature gradient and influence
surface and generates and prints
appropriate consistent nodal loads.

(iii) PARTL(RL) : Reads data and generates load vector
(RL) for an element which is partly
loaded.

(iv) SHAPE : Contains shape functions and their
derivates and generates [N] and [B].

(v) STIFN : Calculates element stiffness for
appropriate conditions and stores in
random access.

(vi) CRACK(N) .: Calculates element stiffness for partly
cracked element 'N' and returns to
'STIFN' to store it on random access.

(vii) GAUSSD : Contains Gaussian data for 2nd to 6th
order Gaussian quadrature to be used
in partly loaded or cracked element,
stiffness calculation and stress comput-
ation.

(viii) MOD(IM) : Calculate the [D] of slab for proper-
ties stored in material no. 'IM', with
due consideration to appropriate
overlay type or single slab. It is
used in 'elastic pinch' calculation,
and equivalent load for temperature
effect in 'LOAD', stiffness calculation
in STIFN and stress calculation in STRESS.

(ix)   MULT   : Multiplies $[B]^T[D][B]$ in cases when direction of crack is other than one of the coordinate axes.

(x)   SOLVE   : Reads element stiffness from appropriate backing storage assenbles global stiffness matrix, applies boundary constrains, stores back partly inverted matrix on another peripheral storage to be used for another load case or subsequent iterations in non-linear or generalised foundation model, and solves for the first load case or iteration using Gaussian elimination process.

(xi)   BSUB   : Performs back-substitution operation in Gaussian elimination procedure to obtain displacements by solving equilibrium equations and writes them.

(xii) RESOLV   : Partly inverted stiffness matrix is read from random access and with the known vector the equations are formed again.

(xiii)SOLVER   : Forms global stiffness matrix for elastic solid foundation and stores its upper triangular part in a linear array. Solves equilibrium equations by Gaussian elimination to obtain displacements. Use of 'OVERLAY' is required if this routine is used, because of the memory limitations, and in such an event subroutines, GDATA, LOAD, SOLVE, RESOLV, BSUB, and PARTL are suppressed.

(xiv) STRESS   : Computes curvatures and moments
                         for each element at all of its
                         Gaussian points and writes them

(xv)   CSTRS(IM)   : Calculates curvatures and moments
                         of a partly cracked element with
                         material properties 'IM' at the
                         Gaussian sampling points.

(xvi) ALAYER(IE)   : Analyses the layers when stresses
                         and strains are desired at the top
                         and bottom of base and overlay in
                         any element 'IE' and prints them
                         out.

    The calling sequence of these routines are indicated
in flow chart shown in FIG.A.1.
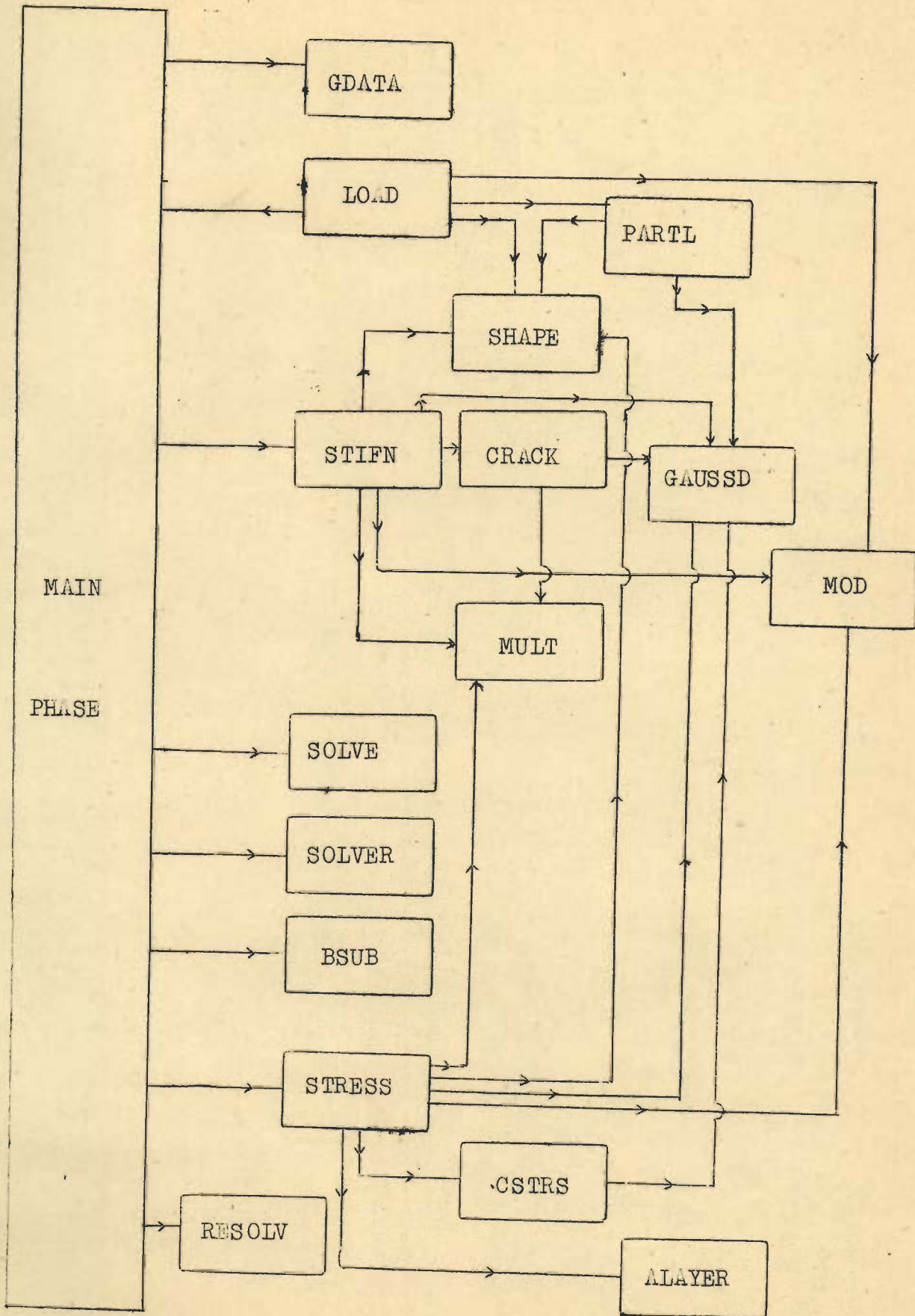
Fig.A.1

REFERENCES

1. Shrivastava, P.N., 'Concrete Roads in Uttar Pradesh' Indian Concrete Journal, October 1968.

2. Borkar, D.S., 'Concrete Roads in Maharashtra State' Indian Concrete Journal, October 1968.

3. Nambiar, K.K., 'Design Aspects of Rigid Pavements and Overlays', Indian Roads Congress, Seminar on Strengthening of Existing Road Pavements, held at Srinagar, 1971.

4. ——— 'Bonded Concrete Overlays for Concrete Roads and Airport Runway Pavements', Indian Concrete Journal, November 1972.

5. Subbaraju, B. and Gokhale, Y.C., 'An Investigation of the Concrete Pavement Failure', Journal Indian Roads Congress, Volume XXIII Part 2, 1958.

6. Gokhale, Y.C., 'Concrete Pavements on Highly Expansive Subgrade Soils', Indian Concrete Journal, July 1964.

7. Reyll, J. and Corkill, J.T., 'Long Term Performance of an Experimental Composite Pavement', Highway Research Record No.434, Highway Research Board, Washington,1973.

8. Ghosh, R.K., Divakaran, M. and Krishnamachari, R., 'Effect of Flexible Overlays on Temperature and Load Stress Variation in Cement Concrete Pavements and their Economics', Seminar, Strengthening of Existing Road Pavements, Srinagar, IRC, 1971.

9. Dhir, M.P. and Mitter, J., 'A Field Study on Strengthening of Thin Cement Concrete Pavements with Flexible Overlays', Seminar, Strengthening of Existing Road Pavements, Srinagar, IRC, 1971.

10. ——— 'Report of the IRC Working Group on Overlays giving Performance Assessment of Overlays on Cement Concrete Road Pavements in India and its Recommendations', 1972.

11. Gillette, Roy, W., 'A 10-Year Report on Performance of Bonded Concrete Resurfacing', Highway Research Record No.94, 1965.

12. Gould, V.G., 'Summarized Committee Report 1948-1960: Salvaging Old Pavements by Resurfacing', HRB Bulletin No.290,1961.

13. Kajfasz, S., Somerville, G. and Rowe, R.E., 'An Investigation of Behaviour of Composite Concrete Beams', Cement and Concrete Association, London, Research Report No.15, Nov.1963.

14. ──── 'Engineering and Design of Rigid Airfield Pavements', Corps of Engineers, U.S.Army, EM 1110-45-303, Office of the Chief of Engineers, 1958.

15. Ghosh, R.K., Phull, Y.R. and Garg, A.K., 'Thin Bonded Resurfacing to Improve the Riding Quality of Rigid Pavements, J.I.R.C. Vol.XXXI No.1, May 1968.

16. Sharma, B.G., 'Laboratory Studies of Concrete Overlays', Thesis submitted to the University of Roorkee, in partial fulfilment of the requirement of M.E. Degree 1963.

17. Felt, Earl, J., 'Repair of Concrete Pavements', Journal A.C.I. Proceedings Vol.57, No.2, August 1960.

18. Bose, S.K., 'Author's reply to the paper, 'Investigation into the Causes of Cracks in Certain Concrete Pavements', J.I.R.C. Vol.24-5, Nov.1960.

19. Taneja, J.R., 'Bonded Concrete Overlays', Paper No.289, J.IRC, Vol.34-2, November 1971.

20. Westall, W.G., 'Discussions on Summarized Committee Report 1948-60, H.R.B. Bulletin No.290,1961.

21. ────'Pavement Rehabilitation, Materials and Techniques' Nat.Coop.Highway, Research Programme, Synthesis of Highway Practice No.9, 1972.

22. Velz, P.G., 'Effect of Pavement Breaker Rolling on Crack Reflectance in Bituminous Overlays', Highway Research Bulletin No.290, 1961.

23. Winkler, E., 'Study of Elasticity and Strength (In German), H.Dominikus, Prague, 1867.

24. Westergaard, H.M., 'Stresses in Concrete Pavements Computed by Theoretical Analysis', Public Roads Vol. 7, No.2, 1926.

25. Biot, M.A., 'Bending of an Infinite Beam on Elastic Foundation',J.Applied Mechanics, Trans.ASME, Vol.59, 1959.

26. Pickett, G. Badruddin, S. and Ganguli, S.C., 'Semi Infinite Pavement Slab Supported by an Elastic Solid Subgrade', Proc. First Indian National Congress on Theoretical and Applied Mechanics, Kharagpur,1955.

27. Holl, D.L., 'Thin Plates on Elastic Foundation', Proceedings 5th Int.Congress on Applied Mechanics, Cambridge,Mass.(U.S.A.),1938.

28. Hogg, A.H.A., 'Equilibrium of a Thin Plate, Symmetrically Loaded, Resting on an Elastic Foundation of Infinite Depth', Phil.Mag.March 1938.

29. Losberg, A., 'Design Methods for Structurally Reinforced Concrete Pavements', Trans.Chalmers University of Technology, Gottenburg, Sweden, No.250, 1961.

30. Vesic, A.S. and Saxena, S.K., 'Analysis of Structural Behaviour of AASHO Road Test, Rigid Pavements', National Cooperative Highway Research Programme(NCHRP), Report No.97, HRB,1970.

31. Meyerhof, G.G., 'Load Carrying Capacity of Concrete Pavements', SMFE Division, Proc. ASCE, June 1962.

32. Ghosh, R.K. and Dinakaran,M., 'Breaking Load for Rigid Pavement', J.Transport Engg.Div.,Proc.ASCE, February 1970.

33. Hudson, W.R. and Matlock, H., 'Cracked Pavement Slabs with Non-Uniform Support', J.Highway Div. Proc. ASCE, April 1967.

34. Desai, C.S. and Abel, J.F., 'Introduction to Finite Element Method, A Numerical Method for Engineering Analysis', Von Nostrand Reinhold Co., New York,1972.

35. Wah, T. and Calcote,L.R., 'Structural Analysis by Finite Difference Calculus', Von Nostrand Reynold Co., New York,1970.

36. Sziland, Rudolph, 'Theory and Analysis of Plates, Classical and Numerical Methods', Civil Engineering and Mechanical Engineering Series, Prentice Hall,1971.

37. Bares, R. and Massonnet, C., 'Analysis of Beam Grids and Orthotropic Plates by the Guyon-Massonnet-Bares Method', Crossby Lockwood and Sons, London, 1968.

38. Saxena, S.K., 'Foundation Mats and Pavement Slabs Resting on an Elastic Foundation-Analysed through a Physical Model', Thesis submitted to the Duke University, Durham, N.C., as a partial requirement for Ph.D.Degree 1971.

39. Agrawal, S.L. and Hudson, W.R., 'Experimental Verification of Discrete Element Solution for Plates and Pavement Slabs', Research Report 56-15, Centre for Highway Research, University of Texas at Austin, April 1970.

40. Abou-Ayyosh, A., Hudson,W.R. and Treybig, H.J., 'Effect of Cracks on Bending Stiffness of Continuous Pavements', HRR No.407, HRB 1972.

41. Ayyash, A.A. and Hudson, W.R., 'Analysis of Bending Stiffness Variation at Cracks in Continuous Pavements', Research Report No.56-22, Centre for Highway Research, University of Texas, April 1972.

42. Niu, H.P., 'Bending of A Cracked Pavement', Doctoral Dissertation, University of Wisconsin, Madison,1967.

43. Ewell, W. and Okubo, S., 'Deflections in Slabs on Elastic Foundation', Proc. HRB, Volume 30,1950.

44. Mounir Badir, 'Bending of Rectangular Plates', J.Struct.Engg.Div.,Proc.ASCE, August 1961.

45. Vlasov, V.Z. and Leontiev, N.N., 'Beams, Plates and Shells on Elastic Foundation', (Translated from Russian) Israel Progress of Science Trans., Jeruslem.

46. Kameshwara Rao, N.S.V., 'Variational Approach to Beams on Elastic Foundation', Thesis submitted to Indian Institute of Technology, Kanpur, India as requirement in partial fulfilment for award of Ph.D. Degree, 1970.

47. Harr, M.E. et al., 'Euler Beams on a Two Parameter Foundation Model', J.SMFE Div.,Proc.ASCE, SM4,1969.

48. Mellinger, F.M., 'Structural Design of Cement Concrete Overlays', J.ACI, February 1963.

49. Huang, Y.H., 'Discussion on Advanced Analysis of Rigid Pavements', by Wang S.K. et al., J.Transport Engg. Div.,Proc. ASCE, TEI 1973.

50. Aziz, A.K., 'The Mathematical Foundations of the Finite Element Method with Application to Partial Differential Equations' Academic Press, New York, 1972.

51. Martin, H.C., and Carey, G.F., 'Introduction to Finite Element Method: Theory and Applications', McGraw Hill Book Co., New York, 1973.

52. Oden, J.T., 'A General Theory of Finite Elements', Int.J.Numerical Methods in Engineering, Vol.1,1969.

53. Holland, I., 'Fundamentals of Finite Element Method', Int.J.Computers and Struct., Pargamon Press, Vol.4, No.1,1974.

54. Zienkiewicz, O.C., 'Finite Element Method in Engineering Science', McGraw Hill, London,1971.

55. Courant, R., 'Variational Methods for the Solution of Problems of Equilibrium and Vibration', Bull. Am. Mathematical Soc., Vol.49, 1943.

56. Prager, W. and Synge, J.L., 'Approximation in Elasticity Based on Concept of Function Space', Quart. Appl.Maths. Vol.5, 1947.

57. Hernikoff, A., 'Solution of Problems of Elasticity by the Frame Work Method', Trans. ASME, Vol.63,1941.

58. McHenry, D., 'A Lattice Analogy for the Solution of Plane Stress Problems', J.Inst.C.E., Vol.21,No.2, 1943.

59. Turner, M.J., Clough, R.W., Martin, H.C. and Topp, L.C. 'Stiffness and Deflection Analysis of Complex Structures', J.Aero.Sc., 1956.

60. Veubeke, B.F., 'Duality Between Displacement and Equilibrium Methods with a view to obtain Upper and Lower Bound to Static Influence Coefficients', Proc.14th Meeting AGARD, Structures and Materials Panel, Paris, July,1962, AGARDograph 72.

61. Taylor, R.L., 'On Completness of Shape Functions for Finite Element Analysis', Int.J.Numerical Methods in Engg. Vol.49, No.1,1972.

62. Timoshenko, S.P. and Goodier, J.N., 'Theory of Elasticity', Engg. Soc. Monograph, McGraw Hill Book Co., New York.

63. Shaw, F.S., 'Virtual Displacements and Analysis of Structures', Civil Engg. and Mech.Engg. Series, Prentice-Hall, Inc., New Jersey, 1972.

64. Ewing, D.J.F., Fawkes, A.J. and Griffiths, J.R., 'Rules Governing the Number of Nodes and Elements in a Finite Element Mesh', Int. J.of Numerical Methods in Engg., Vol.2, No.4, 1970.

65. Turcke, D.J. and McNiece, G.M., 'Guide Lines for Selecting Finite Element Grids based on Optimisation Study', Int. J.Comp. and Struct.Pergamon Press,May, 1974.

66. Sharma, H.D., Nayak, G.C. and Maheshwari, J.B., 'Non-linear Analysis of High Rockfill Dam with Vertical and Inclined Cores', (to be presented)Int.Symp.on Criteria and Assumptions for Numerical Analysis of Dams, Swansea (U.K.), Sept.1975,

67. Melosh, R.J., 'Inherited Errors in the Finite Element Analysis of Structures', J.Comp. and Struct. Paragamon Press, Sept.1973.

68. Argyris, J.H. and Roy, J.R., 'On Reduction of Numerical Error in Matrix Displacement Method', Proc. Conf. on FEM in Engg., The Univ. of New South Wales, Australia, Aug.,1974.

69. Clough, R.W. and Rashid, Y., 'Finite Element Analysis of Axisymmetric Solids', J.Engg. Mech.Div., Proc.ASCE, Vol.91, EM1,1965.

70. Duncan, J.M., Monismith, C.L. and Wilson, E.L.
    'Finite Element Analysis of Pavements', H.R.R.No.228,
    HRB,1968.

71. Burmister, D.M., 'The Theory of Stresses and Dis-
    placements in Layered Systems and Application to
    Design of Airport Runways', Proc. HRB, Vol.23, 1943.

72. Kachroo, P.N., 'Stresses and Deflections in a
    Layered Pavement System', Ph.D.Thesis, University
    of Roorkee, 1971.

73. Wilson, E.L., 'Finite Element Analysis of Two-
    Dimensional Structures', Report No.63-2, Struct.
    and Mat.Res., Deptt. of Civil Engineering, University
    of California, Berkeley, 1963.

74. Cheung, Y.K. and Nag, D.K., 'Plates and Beams on
    Elastic Foundation-Linear and Non-linear Behaviour',
    Geotechnic Vol.18, 1968.

75. Sargious, M. et al., 'Rigid Pavement Stresses Under
    Aircraft Loadings', J.Transp.Engg. Div., Proc., ASCE,
    Nov.1971.

76. Smith, I.M., 'A Finite Element Approach to Elastic
    Soil Structure Interaction', Canadian Geotech.J.,
    May,1970.

77. Wang,S.K., Sargious, M. and Cheung, Y.K., "Advanced
    Analysis of Rigid Pavements', J.Trans. Engg., Div.,
    Proc. ASCE,Feb.1972.

78. Wang, S.K., Sargious,Michel, A. and Cheung, Y.K.
    'Effects of Opening in Stresses in Rigid Pavements',
    J.Transp.Div., Proc. ASCE, Vol.97, No.TE-2 May,
    1973.

79. Huang, Y.H. and Wang, S.T., 'Finite Element Analysis
    for Concrete Slabs and its Implications for Rigid
    Pavement Design', HRR No.466, HRB,1973.

80. Huang, Y.H. and Wang, S.T., 'Finite Element Ana-
    lysis of Rigid Pavements with Partial Subgrade
    Contact', Paper presented to 53th Annual Meeting,
    HRB, 1974.

81. Pitorius, P.C., 'Design Considerations for Pavements containing Soil Cement Bases', Ph.D.Dissertation, University of California, Berkeley 1970.

82. Wilson, E.L., 'Analysis of Prismatic Solids', Rep. Struct. and Mat.Res., Dept. of Civil Engineering Univ. of California Berkeley, 1968.

83. Fossberg, P.E., 'Load Deformation Characteristics of Three Layer Pavements containing Cement-Stabilized Base', Ph.D.Dissertation, University of California, Berkeley, Nov.1970.

84. Hamming, R.W., "Numerical Methods for Scientists and Engineers', McGraw Hill Book Co., 1973.

85. Kaplan, W., 'Advanced Calculus', Addison Wesley Pub.Co.Inc. Mass.1959.

86. Frudenthal, A., 'The Inelastic Behaviour of Engineering Materials and Structures', Wiley, New York,1951.

87. Nayak, G.C. and Jain, V.K., 'Economic Harmonic Analysis of Axisymmetric Bodies with Non-Axisymmetric Loads', Conf.Finite Element Methods in Engineering, University of New South Wales, Australia, August,1974.

88. Dhir, M.P. and Sandhwalia, P.S., 'Investigations for the Strengthening of the Main Runway of a Civil Airport', Paper No.292, J.I.R.C. Vol.34-4, June 1972.

89. Colley, B.E. and Humphrey, H.A., 'Aggregate Interlock at Joints in Concrete Pavements', H.R.R.No.189, HRB, 1967.

90. Moavenzadeh, F. and Kugal, R., 'Fracture of Concrete', J.Materials, Vol.4, No.3,1969.

91. Ergatoudis,J.G., 'Isoparametric Elements in Two and Three Dimensional Analysis', Ph.D.Thesis, University of Wales, Swansea, 1968.

92. Nayak, G.C., 'PSPSAS-Plane Strain, Plain Stress, Axisymmetric-Linear, Parabolic and Cubic Isoparametric Program, Program Report, Civil Engg. Department, University of Roorkee, Nov.1972.

93. —— 'Indian Standards Code of Practice for Plain and Reinforced Concrete for General Building Construction', IS:456-1964, Indian Standards Institution, New Delhi.

94. Jain, K.K., Nautiyal, B.D., and Jain, O.P., 'Compressive Strength and Modulus of Elasticity of Flyash Concrete', Paper to be published in Civil Engineering Div. J.Inst. of Engrs.(India).

95. Orchard, D.F., Walker, J.A. and Stewart, D.T., 'A Study of the Relationship between the Static and Dynamic Modulus of Elasticity and other Properties of Certain Materials', Proc.Australian Road, Res. Board, Vol.3, 1966.

96. Sinno, R. and Furr, H. 'Bonded Concrete Overlays', J.Struct. Div., Proc. ASCE. ST 89, August 1970.

97. Vesic, A.S. and Saxena, S.K., 'Analysis of Structural Behaviour of Road Test Rigid Pavements', HRR No.291, HRB, 1969.

98. McCullough, B.F. and Boedecker, K.J., 'Use of Linear Elastic Layered Theory for Design of CRCP Overlays', HRR No.291, HRB, 1969.

99. —— 'Small Scale Model Study to Determine Minimum Horizontal Dimensions for Infinite Slab Behaviour', Tech.Rep.No.4-32, Ohio River Div.Lab., Cincinnati, July 1964.

100. Lewis, K.H. and Harr, M.E., 'Analysis of Concrete Slabs on Ground Subjected to Warping and Moving Loads', HRR No.291, HRB, 1969.

101. Hetenyi, M., 'Beams on Elastic Foundation', The University of Michigan Press Ann Arbor, 1958.

102. Mahavir Prasad, Sharma, V.P.S. and Jain, R.K., 'Performance of Overlays on Failed Thin Cement Concrete Pavements in U.P.', Seminar on Strengthening of Existing Road Pavements, IRC, Srinagar, Sept.1971.

103. Gillette, Roy, W., 'Performance of Bonded Concrete Overlays', J.ACI, Jan.1963.

104. Beeby A.W., 'Investigation of Cracking in Slab Spanning in One Way', Cement and Concrete Associations, London, Tech.Rep.No.TRA 433, April, 1970.

105. Felt, E.J., 'Resurfacing and Patching Concrete Pavements with Bonded Concrete', Proc. H.R.B., 1956.

106. Holister, G.S. and Thomas, C., 'Fibre Reinforced Materials', Elsevier Publishing Co.Ltd., London, 1966.

107. Singh, K., 'Behaviour of Steel Fibre Reinforced Concrete', Thesis submitted to University of Roorkee in partial fulfilment of the requirement of M.E.Degree, 1974.

108. Hyman, B.I., Nilforoush, J.M. and Packard, W.T., 'Effect of Fiber Distribution on Stress and Strain Concentration at Holes in Composite Plains', Proc. 6th St. Louis Symposium on Composite Materials in Engg. Design, American Society for Metals, Ohio, May 1972.

109. Parratt, N.J., 'Fibre-Reinforced Materials Technology', Von-Nostrand Reinhold Co. London, 1972.

110. ────── 'Steel Fibres in Airport Runways', Concrete, August 1972.

111. Agrawal, S.M. and Khanna, S.K., 'Pavement Subgrade Models', Seminar on Pavement Design and Construction of Roads and Airfields held at College of Military Engg. Pune, Oct.1973.

112. Sokolnikoff, I.S., 'Mathematical Theory of Elasticity', McGraw-Hill Book Co., New York, 1956.

113. 'Road Test One-M.D.', Special Report No.4, H.R.B.1952.

114. Timoshenko, S.P. and Krieger, W., 'Theory of Plates and Shells', McGraw-Hill Book Co., New York.

115. Suidan, M. and Schnobrich, W.C., 'Finite Element Analysis of Reinforced Concrete', J.Struct.Engg.Div., Proc. ASCE, Oct.1973.

116. Bazeley, G.P., Cheung, Y.K., Irons, B.M. and Zienkiewicz, O.C., 'Triangular Elements in Plate Bending Conforming and Non-Conforming Solutions', Proc. Conference Matrix Methods Structure Mechanics, Wright-Patterson Air Force Base, Ohio, 1965.

117. Fraeijs de Veubeke, B., 'Displacement and Equilibrium Models in Finite Element Methods in Stress Analysis, Ch.9., Ed. O.C.Zienkiewicz and G.S.Holister, J.Wiley and Sons, 1965.

118. Fulton, R.E., Eppink, R.T. and Walz, J.E., 'The Accuracy of Finite Element Method in Continuum Problems', Proc. Fifth U.S.Congress. App.Mech., 1966.

119. Dutron, P. and Huberty, J.'Resurfacing and Widening Old Concrete Carriageways with Concrete', 9th National Belgian Roads Conf., 1959.

120. Bogner, F.K., Fox, R.L. and Schmit, L.A., 'The Generalization of Inter Element, Compatible Stiffness and Mass Matrices by the Use of Interpolation Formulae', Proc. Conf.Matrix Methods in Struct. Mech., Wright Patterson Air Force Base, Ohio, 1965.

121. Hamming, R.W., 'Numerical Methods for Scientists and Engineers', McGraw-Hill Book Co., New York,1973.

122. Gallagher, R.H., 'Analysis of Plates and Shell Structures', Key Note Address, ASCE Conf. on Application of Finite Element Method in Civil Engineering, Vanderbilt University, 1969.

123. Argyris, J.H. and William, K.J., 'Some Considerations for Evaluation of Finite Element Models', Nuclear Engineering and Design, North-Holland Publishing Co., Vol.28, No.1, July 1974.

124. Thadani, B.M., 'Structural Mechanics', Asia Publishing House, Bombay,1964.

125. Fabian, G.J., Clark, D.C. and Hutchinson, C.H., 'Preliminary Analysis of Road Loading Mechanics', HRB Bulletin No.250, HRB 1960.

126. Quinn, B.E. and Devries, T.W., 'Highway Characteristics as Related to Vehicle Performance', HRB Bulletin No.250, HRB 1960.

127. 'Dynamic Pavement Loads of Heavy Highway Vehicles', N.C.H.R.P., Report No.105, HRB 1971.

128. Jones, R., Lister, E.N. and Thrower, E.N., 'Dynamic Behaviour of Soils and Foundations'In Vibration in Civil Engineering', Ed. B.O. Skipp, Butterworths, London,1966.

129. Markwick, A.H.D. and Starks, H.J.H., 'Stresses between Tyre and Road', J.Inst.C.E.(London), Vol.16, No.7, 1941.

130. Bones, R.P.H. and Kuhn, S.H., 'Dynamic Forces Exerted by a Moving Vehicle on a Road Surface', HRB Bulletin No.233, HRB 1959.

131. Don, L.I. and Bob, G.H., 'Tyre Pavement Friction: Vital Design Objective', H.R.R.471, HRB, 1973.

132. Freitag, D.R. and Green, A.J., 'Distribution of Stresses on an Unyielding Surface Beneath a Pneumatic Tyre', HRB Bulletin 342, HRB, 1961.

133. Kopal, Z., 'Numerical Analysis', Chapman and Hall Ltd., London,1961.

134. Sargious, M., 'Warping at Edges of Prestressed and Reinforced Concrete Pavements', J.ACI Nov.1968.

135. Westergaard, H.M., 'Analysis of Stresses in Concrete Pavement due to Variation in Temperature', Proc. HRB 1926.

136. Bradbury, R.D., 'Reinforced Concrete Pavements',Wire Reinforcement Inst., Washington, D.C., 1938.

137. Teller, L.W. and Sutherland, E.C., 'The Structural Design of Concrete Pavements', Public Roads, Vol.23, No.8,1943.

138. Bergstrom, S.G.,'Temperature Stresses in Concrete Pavements', Handlinger, N:R 14, Swedish Cement and Concrete Research Institute at Royal Institute of Technology, Stockholm, 1950.

139. Thomlinson, J., 'Temperature Variation and Consequent Stresses Produced by Daily and Seasonal Temperature Cycle in Concrete Slab', Concrete Const.Engg. Vol.35(6 and 7), 1940.

140. Parkus, H., 'Thermo Elasticity', Bails dell Pub. Co., Waltham, Mass, 1968.

141. Bole, B.A. and Weiner, J.H., 'Theory of Thermal Stresses', Wiley and Sons, 1960.

142. Branson, D.E., 'Time Dependent Effects on Composite Concrete Beams', J.A.C.I.Vol.61,1964.

143. Yu, W.W. and Winter, G., 'Instantaneous and Long-term Deflections of Reinforced Concrete Beam Under Working Loads', J., A.C.I., Vol.57, No.1, July 1960.

144. Beeby, A.W., 'An Investigation of Cracking on Side Faces of Beams', Cement and Concrete Association, London, Tech.Report No.42,466, Dec.1971.

145. Bell, J.C. and Elms, D. G., 'Partially Cracked Finite Element', Proc. ASCE, J.Struct. Engg.Div., Vol.97, No.S T.7, July 1971.

146. Mendelson, A., Gross, B. and Srawley, J.E., 'Evaluation of the Use of a Singularity Element in Finite Element Analysis of Centre Cracked Plates', ASCE, National Structural Engg. Meeting, Ohio, April 1972.

147. Bell, J.C. and Elms, D.G., 'Nonlinear Analysis of Reinforced Concrete', J.Struct. Engg. Div.Proc. ASCE, April 1972.

148. Priestley, M.J.N., 'Moment Redistribution in Prestressed Concrete Continuous Beams', Thesis submitted to University of Canterburgy, Christ Church, New Zealand for award of Ph.D., 1966.

149. Valliappan, S. and Doolan, T.F., 'Nonlinear Analysis of Reinforced Concrete', J.Struct.Engg.Div.Proc. ASCE, April 1972.

150. Valliappan, S. and Nath, P., 'Tensile Crack Propagation in Reinforced Concrete B am by Finite Element Technique', International Conf. on Shear, Torsion and Bond in Reinforced Concrete, Coimbatore, India,1969.

151. Ngo, D. and Schordeles, A.C., 'Finite Element Analysis of Reinforced Concrete Beams', J.ACI, March 1967.

152. Nelson, A.H., 'Nonlinear Analysis of Reinforced Concrete by Finite Element Method', J.ACI.Sept.1968.

153. Hand, F.R., Packnold, D.A. and Schnobrich, W.C., 'Nonlinear Layered Analysis of R.C. Plates and Shells', J.Struct.Engg.Div. Proc. ASCE, July 1973.

154. Jofriet, J.C. and McNiece, G.M., 'Finite Element Analysis of Reinforced Concrete Slabs', J.Struct. Engg. Div.,Proc. ASCE, Vol.97, No.ST3, March 1971.

155. Jofriet, J.C., and McNiece, G.M., 'Finite Element Analysis of Reinforced Concrete Slabs', Report No.50, Solid Mech.Div., Unive sity of Waterloo, Canada, 1971.

156. 'Fatigue and Fracture of Concrete',- A Review of Current Knowledge', Editorial, ICJ,June 1971.

157. Post, D., 'Photoelastic Stress Analysis of an Edge Crack in a Tensile Field', Proc. Society of Experimental Stress Analysis, Vol.XII, No.1,1954.

158. Williams, M.L., 'On Stress Distribution at the Base of a Stationary Crack,' J.App.Mech. Trans.ASME, March 1957.

159. Zienkiewicz, O.C., Too, J., Taylor, R.L. 'Reduced Integration Technique in General Analysis of Plates and Shells', International J.Numerical Methods in Engg., Vol.3, 1971.

160. Pawsey, S.F. and Clough, R.W., 'Improved Numerical Integration of Thick Shell Finite Elements', Int. J.Numerical Methods in Engg., Vol.3, 1971.

161. Nayak, G.C., 'Generalized Modulus Matrix in Finite Element Analysis', International Conf. on Finite Element Method, Coimbatore, Dec.1974.

162. Yoder, E.J., 'Principles of Pavement Design', John Wiley and Sons Inc. New York, 1959.

163. Laytton, R.L., 'Analysis for Design of Foundation on Expansive Clays', Geomechanics, J. Inst. of Engrs. Australia, 1970.

164. Hveem, F.N., 'Slab Warping Effects on Pavement Joint Performance', J.ACI, Vol.47, 1950..

165. Nayak, G.C., 'Plasticity and Large Deformation Problems by the Finite Element Method', Ph.D.Thesis, University of Wales Swansea, 1971.

166. Hearmon, R.F.S., 'An Introduction to Applied Anisotropic Elasticity', Oxford University Press, 1961.

167. Lekhnitskii, S.G., 'Theory of Elasticity of an Anisotropic Elastic Body', Holden-day Inc., San Francisco, 1963.

168. Niu, H.P. and Pickett, G., 'Effect of Degree of Continuity Across a Void or Crack on Performance of Concrete Pavements,' HRR No.291, HRB, 1969.

169. Ghosh, R.K., Puri, M.L., Phull, Y.R., Sethi, K.L., and Bhatia, M.L., 'Construction and Performance of Ten Year Old Bonded Rigid Overlay Test Track on N.H.24,', Seminar on Strengthening of Existing Road Pavements, IRC, Srinagar, Sept.1971.

170. Lall, B., Discussion on 'Construction Problems in Bonded Concrete Overlays', by J.R. Taneja, J.IRC Vol.35-5, Aug.1973.

171. Davies, R.E. and Troxell, G.E., 'Modulus of Elasticity and Poisson's Ratio for Concrete and the Influence of Age and other Factors upon These Values', Proc.ASTM, Vol.29, Part II, 1929.

172. Ghosh, R.K., Phull, Y.R. and Garg, A.K., 'Thin Bonded Concrete Resurfacing to Improve the Riding Quality of Rigid Pavements', J.IRC. Vol.31, May 1968.

173. Ghosh, R.K.and Phull, Y.R., 'Bonded Concrete Overlays for Pavements', Civil Engg. and Public Works Review, August 1972.

174. Birkeland, H.W., 'Differential Shrinkage in Composite Beams', J.ACI, Vol.31, 1960.

175. Orchard, D.F., 'Concrete Technology', Applied Science Publishers Ltd., London, 1973.

176. Viest, I.M., Fountain, R.S. and Singleton, R.C., 'Composite Construction in Steel and Concrete', McGraw-Hill Book Co., New York, 1958.

177. Zuk, W., 'Thermal and Shrinkage Stresses in Composite Beams', J.ACI, Vol.58, September 1961.

178. 'General Report on Roads Research in India', J. IRC. Vol.XXXI 1967-68.

179. George, K.P., 'Final Report on Crack Control in Cement Treated Bases', University of Mississippi, School of Engg., Engg. Expt. Station, Mississippi, October 1970.

180. Kaplan, M.F., 'Crack Propagation and Fracture of Concrete', J.ACI, Vol.58, No.5, 1961.

181. Winnie, D.H. and Wundt ,B.M., 'Application of the Griffith-Irwin Theory of Crack Propagation to the Bursting Behaviour of Discs, Including Analytical and Experimental Studies', Trans.ASME, Vol.80,1958.

182. Salam, Y.M. and Monismith, C.L., 'Fracture Characteristics of Asphalt Concrete', Proc.A.A.P.T., Vol.41, 1972.

183. Bueckner, F.H., 'Some Stress Singularities and their Computations by Means of Integral Equations', In Langar, R.E.ed., Boundary Value Problems in Differential Equations, University of Wisconsin Press, Madison, Wisconsin, 1960.

184. Yamamoto, Y. and Tokuda, N., 'Determination of Stress Intensity Factor in Cracked Plates by Finite Element Method',Int.J. Numerical Methods in Engg. Vol.6, No.3, 1973.

185. Dixon, J.R. and Pook, L.P., 'Stress Intensity Factor Calculated Generally by Finite Element Technique', Nature, Vol.224, 1969.

186. Gallagher, R.H., 'A Survey and Evluation of Finite Element Method in Linear Fracture Mechanics Analysis', Proc. Ist International Conf. of Struct. Mech. in Reactor Tech., Berlin, 1971.

187. Salam, Y.M. and Monismith, C.L., 'Distress Characteristics of Asphalt Concrete Mixes', Proc. A.A.P.T., Vol.42 1973.

188. Parker, E.R., 'Brittle Behaviour of Engg. Structures', John Wiley and Sons, New York, 1957.

189. Wiseman, J.F., Harr, M.E. and Leonards, G.A., 'Warping Stresses and Deflections in Concrete Pavements', Part I. Proc. H.R.B., Vol.39, 1960.

190. Peterson, R.E., 'Stress Concentration Factors', John Wiley and Sons, New York, 1974.

191. Neuber,H.,'Theory of Notch Stresses', Edwards, Ann-Arbor, Mich. 1948.

192. Moore, R.R., 'Effect of Grooves, Thread and Corrosion Upon the Fatigue of Metals', Proc.ASTM, Vol.26, Part II, 1966.

193. Kupfer, H., Hilsdorf, H.K. and Rusch, H., 'Behaviour of Concrete Under Biaxial Stresses', Proc. A.C.I., Vol.66, No.8, Aug.1969.

194. Liu, T.C.V., Nelson, A.H. and Slate, F.O., 'Stress-Strain Response and Fracture of Concrete in Uniaxial and Biaxial Compression', Proc. A.C.I., Vol.69, No.4, 1972.

195. Theocaris,P.S. and Prassiankis, J.N., 'The Mohr Envelope of Failure for Concrete: A Study of its Tension-Compression Part', Mag.Concrete Research, June 1974.

196. Harris, A.J., 'The Failure of Concrete Under Compound Stress', Symposium on Strength of Conc. Struct. Cement and Concrete Association,London,1956.

197. Griffith, A.A., 'Theory of Rupture', 1st Int.
     Congress on Applied Mechanics, Delf, 1924.

198. Lott, J. and Kesler, C.E., 'Crack Propagation in
     Plain Concrete', Special Report No.90, HRB, 1966.

199. Taylor, M.A. and Broms, B.B., 'Shear Bond Strength
     between Coarse Aggregate and Cement Paste or
     Mortar', J.ACI, August 1964.

200. Sedov, L.I., 'Elastic and Plastic Solids and Forma-
     tion of Cracks', Wolters-Nordhoff.

201. Knott, J.F., 'Fundamentals of Fracture Mechanics',
     Butterworths, London, 1973.

202. Blight, G.E., 'Fracture of Pavement Materials',
     Proc. J.Transport Engg.Div., ASCE, Nov.1973.

203. Ramsamooj, D.V., ' Prediction of Reflection
     Cracking in Pavement Overlays', H.R.R.No.434, HRB,
     1973.

204. Walsh, P.F., 'Fracture of Plain Concrete', J.I.C.J.,
     1972.

205. Ramsamooj, D.V., 'The Design and Analysis of the
     Flexibility of Pavements, Ohio State University,
     Ph.D. Dissertation, 1970.

206. Glucklich, J., 'Fracture of Plain Concrete', Proc.
     ASCE, J.Engg. Mech. Div., Vol.89, No.EM6, Dec.1963.

207. Naus, D.J. and Lott, J.L., 'Fracture Toughness of
     Portland Cement Concrete', Proc. A.C.I., Vol.66, 1969.

208. Santiago, S.P. and Hillsdorf, H.K., 'Fracture
     Mechanics of Concrete Under Compressive Loads',
     Cement and Concrete Research, Pergamon Press Inc.,
     Vol.5, 1973.

209. George, K.P., 'Theory of Brittle Fracture Applied
     to Soil-Cement,' Proc. ASCE, J.Soil Mech. and Founda-
     tion Div., SM3, Vol.96, 1970.

210. Clyde, D.H., 'On Crack Direction in Relation to Griffith's Biaxial Failure Criterion', Cement and Concrete Research, Pergamon Press Inc.Vol.3, 1973.

211. Schwalbe, K.H., 'Comparison of Several Fatigue Crack Propagation Laws with Experimental Results', J.Engg. Fracture Mech., Sept. 1974.

212. Sih, G.P. and Macdonald, B., 'Fracture Mechanics Applied to Engineering Problems-Strain Energy Fracture Criterion', J.Engg. Fracture Mech., Sept. 1974.

213. Majidzadeh, K.et al., 'Application of Fracture Mechanics in the Analysis of Pavement Fatigue', Authors reply to Prof. J.A.Deacon Proc.A.A.P.T. Vol.40, 1971.

214. Pickett, G., Raville, M.E., James, W.C. and McCormick, F.J., 'Deflections, Moments and Reactive Pressures for Concrete Pavements', Kansas State College Bulletin, Bulletin No.65, Kansas, October,1951.

215. Lall, B., 'Discussion on General Reports on Road Research in India', J.IRC. Vol.34, No.5, August 1973.

216. Lall, B., 'Concrete Overlays of Concrete Pavements', Ph.D.Thesis, University of Birmingham, U.K.1969.

217. 'Heavy Load Test Tracks, Report ofConstruction', Tech.Report No.4-17, U.S.Army, Corps of Engrs., Ohio River Div.Lab., Feb.1961.

218. The Design of Airfield Overlay Pavements', Progress Report of Air Transport Div.Proc. ASCE, Vol.81, Paper No.777, August 1955.

219. Report of Sub-Committee VIII, ACI Committee 325, 'Design of Concrete Overlay for Pavements', J.ACI, Vol.64, August 1967.

220. Bose, S.K., 'The Influence of a Super Imposed Layer in Increasing the Load-Bearing Capacity of a Rigid Pavement.J.IRC. Vol.XIX Part 3 and 4,1955.

221. Reddy, R.S. and Krishnan, S.R., 'Upgrading an Airfield Pavement by Concrete Overlays', ICJ, March 1963.

222. Lemcoe, M.M. and Mahala, C.H., 'Prestressed Overlay Slab for San Antanio Airport', Proc. ACI, Vol.55, July 1959.

223. Arm, L.M., Aaron, H.A., and Palmer, L.A., 'Design of Concrete Overlays for Pavements', Proc.ACI.Vol.55, 1955.

224. Mellinger, F.M. and Carlton, P.F., 'Application of Models to Design Studies of Concrete Airfield Pavements', Proc. HRB Vol.34, 1955.

225. Shackel, B., 'Unbonded Structural Overlays', ICJ. September 1972.

226. Newmark,N.M. et.al., 'Tests and Analysis of Composite Beams with Incomplete Interaction', Proc. Society for Experimental Stress Analysis,1951.

227. Steller, K., 'Composite Construction in Theory and Practice', Structural Engr., Vol.39, No.4, April 1961.

228. Knowles, P.R., 'Composite Steel and Concrete Construction', Butterworths, London, 1973.

229. Ohama, F. and Kobayashi, K., 'On Behaviour at Joint Surfaces of Concrete Composite Beams', Trans.Japan Society of Civil Engrs. Vol.4, 1972.

230. Khanna, S.K., Arora, M.G. and Lohani, L.K., 'Design of Bituminous Overlays by Beam Action Hypothesis', Seminar on Strengthening of Existing Road Pavements, IRC. Srinagar, Sept.1971.

231. Terzaghi, K., 'Evaluation of Coefficient of Sub-grade Reaction', Geotechnic, Vol.5, 1955.

232. Goldbeck, A.T. and Bussard, M.J., 'The Supporting Value of Soil as Influenced by Bearing Area,' Public Roads, Vol.6, No.1,1925.

233. Tsai, N.C. and Westman, B.A., 'Beams on Tensionless Foundation', J.Engg.Mech.Div., Proc. ASCE, Vol.93,EM5, 1967.

234. Geldmacher, R.C., Anderson, R.L., Dunkin, J.W., Partridge, G.R., Harr, M.E. and Wood, L.E., 'Subgrade Support Characteristics as Indicated by Measurement of Deflection and Strains', Proc. HRB. Vol.36, 1957.

235. Leonard, G.A. and Harr, M.E., 'Analysis of Concrete Slabs on Ground', Proc.ASCE, J.Soil Mech. and Found. Div.SM3, June 1959.

236. Larew, H.G. and Leonard, G.A., 'A Strength Criteria for Repeated Loads', Proc. H.R.B.1962.

237. Russam, K. and Dagg, M., 'The Effect of Verge Slope and Cover on Soil-Moisture Distribution Under a Road in Kenya', Moisture Equilibria and Moisture Changes in Soil Beneath Covered Area.Butterworths, Australia, 1965.

238. Williams, A.A.B., 'The Deformation of Road Resulting from Moisture Changes in Expansive Clays', Moisture Equilibria and Moisture Changes in Soil Beneath Covered Areas, Butterworths, Australia, 1965.

239. Richards, B.G., 'An Analysis of Subgrade Condition at   Experimental Road Site Using Two Dimensional Diffusion Equation on a High Speed Digital Computer', Moisture Equilibria and Moisture Changes in Soils beneath Covered Areas Butterworths, Australia, 1965.

240. Richart, F.E. and Zia, P., 'Effect of Local Loss of Support on Foundation Design', Proc. ASCE, J.SM and F.E. Div., SM1, 1962.

241. Brown, P.T., 'The Effect of Local Bearing Failure on Behaviour of Rigid Circular Rafts', Inst. of Engrs. Australia, 1969.

242. Bishop, A.W. and Henkel, D.J., 'The Measurement of Soil Properties in the Triaxial Test', Arnold,1957.

243. Kulhawy, F.H.and Duncan, J.M., 'Stresses and Moments in Oroville Dam', Proc.ASCE.J.S.M.F.E.Div.Vol.98, July 1972.

244. Mednikov, I.A., 'Equivalent Characteristics of Soil for Plates on Elastic Base of a Finite Number of Inhomogeneous Layers,', Soil Mechanics and Foundation Engineering, (Translated from Russian),1969.

245. Poulas, H.G., 'Stresses and Displacements in an Elastic Layer Underlain by a Rough Rigid Base', Geotechnic, Vol.17, 1967.

246. Repnikov, L.N., 'Calculations of Beams on Elastic Base Combining Deformative Properties of a Winkler Base and an Elastic Base', Soil Mech. and Foundation Engg.(Translated from Russian), 1967.

247. Wang, S.K. et al., 'Advanced Analysis of Rigid Pavements', Proc. ASCE, J.Transp.Engg.Div.TE-3, August 1973.

248. Karr, A.D., 'Elastic and Viscoelastic Foundation Models', J.Applied Mech., Trans.ASME, Vol.31,Sept.1964.

249. Pedro, J.O., 'Structural Analysis Including Deformability of Foundations by Finite Element Method', 8th International Conf. of Soil Mech. and Foundation Engg., Moscow, Vol.1.3, 1973.

250. Yang, T.Y., 'A Finite Element Analysis of Plates on Two Parameter Foundation Model', Int.J.Computers and Struct., Vol.2,1972.

251. Mednikov, I.A., 'Coefficient of Subgrade Reaction of a Linear Multilayer Base', Soil Mech. and Foundation Engg. (Translated From Russian), 1967.

252. ———— 'Soil Mechanics for Road Engineers', H.M.S.O., London, 1952.

253. Arora, M.G., 'Strength Characteristics of Puzzolanic Mixtures and Base Courses,' Thesis submitted as requirement for award of Ph.D.Degree, University of Roorkee, Roorkee, 1973.

254. Loof, H.W., 'Theory of Coupled Spring Foundation', Heron, No.3, 1965.

255. Murphy, G., 'Similitude in Engineering', The Ronald Press Co., New York, 1950.

256. Subbaraju, B., 'Model Study of Stresses in Layered System', H.R.R.13, H.R.B.1963.

257. Saran, S., 'Bearing Capacity of Footings Subjected to Moments', Thesis Submitted as Requirement for Award of Ph.D.Degree, University of Roorkee, Roorkee, 1970.

258. Saraf, C.L., 'Investigation of Rigid Pavement Behaviour Under Static Loads by Model Tests', Dissertation Submitted in partial fulfilment for Award of M.E.Degree to University of Roorkee,Roorkee, 1962.

259. Ahlvin, R.G., 'Discussion on Model Study of Stresses in a Layered System', by Subbaraju, B.HRR 13,HRB 1963.

260. Secor, K.E. and Mouismith, C.L., 'Visco-elastic Properties of Asphalt Concrete', Proc. HRB.Vol.41, 1962.

261. Jonker, A. and Nieuwenhuyzen, J.V., 'Controlled Tests of Aircraft Landing Loads at Schiphol Airport,' 5th International Conf.Soil Mechanics and Foundation Engg. Paris, 1961.

262. Tetrior,A.N., 'Foundation Shells(for Tower Shaped Structures', Proc. IA.S.S.Symposium on Tower Shaped Steel and R.C.Structures, Brastilava, June,1966.

263. Roll, F., 'Materials for Structural Models', Proc. ASCE, J.Struct.Engg.Div.Jun, 1968.

264. Carlton, P.F. and Behrmann, Ruth, M., 'A Model Study of Rigid Pavement Behaviour Under Corner and Edge Loadings', Proc.HRB, Vol.35,1956.

265. Shrivastava, S.P., 'Elastic Analysis of Pile Groups Subjected to Vertical and Lateral Loads', Thesis Submitted as a Requirement for award of Ph.D.Degree, University of Roorkee,Roorkee,1971.

266. Wilbur, J.B. and Norris, C.H., 'Structural Model Analysis,'In Handbook of Experimental Stress Analysis Edited by Hetenyi, M., John Wiley and Sons Inc., New York, 1960.

267. Paxon, G.S., 'Factors Influencing the Stress in Concrete Pavements from Applied Loads', Proc. HRB, 1945.

268. Perry, C.C. and Lissner, H.R., 'Strain Gauge Primer', McGraw Hill and Co., New York, 1962.

269. Timoshenko, S.P. and Young, D.H., 'Theory of Structures', McGraw Hill Book Co., N.Y., 1946.

270. Pucher, A., 'Influence Surfaces of Elastic Plates', Springer-Verlag(3rd Ed.), New York, 1964.

271. Krug, S and Stein, P., 'Moment Influence Surfaces of Orthotropic Plates', Springer-Verlag, Berlin,1961.

272. Chen, T.Y., Siess, C.P. and Newmark, N.M., 'Studies of Slab and Beam Highway Bridges,' Part IV, University of Illinois, Research Station Bulletin, 439,1957.

273. Rusch, N., and Hergenroder, A., 'Influence Surface for Moments in Skew Slabs', C. and C.A.Library Translation, 1965.

274. Nayak, G.C. and Davies, J.D., 'Influence Characteristics for Slab Bridges', 2nd Internation l Symposium on Concrete Bridge Design, Chicago, 1969.

275. Davies, J.D. and Nayak, G.C., 'Influence Fields for Stresses in Elasticity Problems', Proc. 3rd Canadian Congress of Applied Mechanics, Calgary, May 1971.